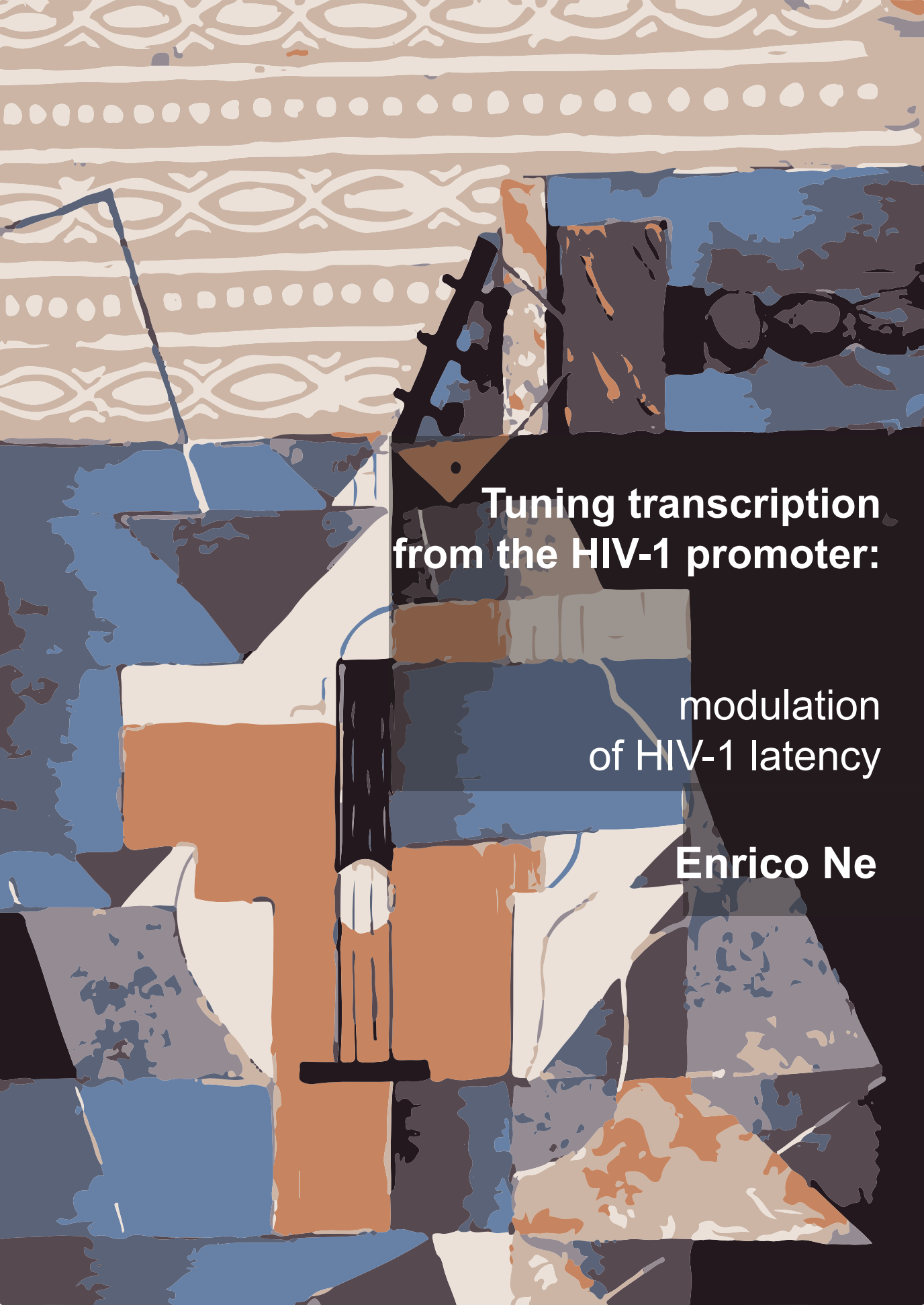

Tuning transcription from the HIV-1 promoter:

modulation of HIV-1 latency

Enrico Ne

TUNING TRANSCRIPTION FROM THE HIV-1 PROMOTER:

modulation of HIV-1 latency

Enrico Ne

ISBN: 978-94-6416-999-7
Cover design and Layout: Enrico Ne
Front cover: modified from “Guitar on the Table”, Juan Gris ,1913
Back cover: modified from “Still life with a guitar”, Juan Gris, 1913

Printed by Riddeprint BV | www.ridderprint.nl

The studies presented in this thesis were performed at the Department of Biochemistry at the Erasmus MC in Rotterdam, the Netherlands

Printing of this thesis was financially supported by Erasmus University Rotterdam, and Department of Biochemistry, Erasmus MC

TUNING TRANSCRIPTION FROM THE HIV-1 PROMOTER:

modulation of HIV-1 latency

Thesis

to obtain the degree of Doctor from the
Erasmus University Rotterdam
by command of the
rector magnificus

Prof.dr. F.A. van der Duijn Schouten

and in accordance with the decision of the Doctorate Board.

The public defence shall be held on

Wednesday the 23rd of June 2021 at 10.30 am

by

Enrico Ne

born in Bergamo, Italy

Erasmus University Rotterdam

DOCTORAL COMMITTEE

Promotor: Prof. Dr. C.P Verrijzer

Other members: Prof. Dr. J. Gribnau

Dr. K.S Wendt

Dr. M. Parra Bola

Copromotor: Dr. T. Mahmoudi

TABLE OF CONTENTS

CHAPTER .1

GENERAL INTRODUCTION

AIM OF THIS THESIS

Transcription: Insights From the HIV-1 Promoter

Enrico Ne, Robert-Jan Palstra, Tokameh Mahmoudi

International Review of Cell and Molecular

http://dx.doi.org/10.1016/bs.ircmb.2017.07.011

Transcription: Insights From the HIV-1 Promoter

Enrico Ne, Robert-Jan Palstra, Tokameh Mahmoudi[1]
Erasmus University Medical Center, Rotterdam, The Netherlands
[1]Corresponding author: e-mail address: t.mahmoudi@erasmusmc.nl

Contents

International Review of Cell and Molecular Biology
ISSN 1937-6448
http://dx.doi.org/10.1016/bs.ircmb.2017.07.011

Abstract

In this review, we cover transcription regulation of human immunodeficiency virus type 1 (HIV-1) gene expression, focusing on the invaluable contributions, made by HIV research over the years, toward the field of transcription. In this context, the HIV promoter can be considered to be a well-studied model promoter, which although a viral promoter, is subject to the same cellular regulatory mechanisms that modulate the transcriptional control of endogenous host cellular genes. The molecular control of HIV-1 transcription has been well studied and considerable knowledge toward development of alternative strategies for therapies aimed at eradicating both active but also latent HIV-1 has been obtained. Additionally, HIV-1 studies have provided insight into fundamental aspects of transcriptional regulation including transcriptional stochasticity, RNA polymerase II pausing, chromatin regulation of transcription, the role of the +1 nucleosome, the use of an RNA enhancer element, i.e., TAR, the discovery, and essential function of P-TEFb, and the super elongation complex in transcription elongation. These findings have been important not only in deciphering the mechanisms used by HIV-1 to regulate its gene expression and to establish and maintain HIV latency for therapeutic advancement, but were at the same time seminal in pushing the transcription field forward.

1. INTRODUCTION

Human immunodeficiency virus type 1 (HIV-1), the causative agent of the acquired immunodeficiency syndrome or AIDS, destroys the immune system by infecting, replicating in, and depleting predominantly CD4+ T lymphocytes (Burger and Poles, 2003; Epstein et al., 1993). HIV-1 is a lentivirus which enters host cells by binding to the CD4 receptor together with the CCR5 or CXCR4 coreceptors and fuses with the target cell, releasing viral RNA into the cytoplasm. The HIV-1 single-stranded RNA genome is then reverse transcribed into dsDNA by the viral enzyme reverse transcriptase (Hu and Hughes, 2012). The dsDNA preintegration complex then enters the nucleus where it integrates into the host genome aided by the activity of the viral integrase (Craigie and Bushman, 2012). The integrated proviral dsDNA then behaves essentially as a cellular gene and directs transcription of the viral genome (De Crignis and Mahmoudi, 2017). Viral transcripts are differentially spliced and translated into viral proteins, which are cleaved by the viral protease enzyme into maturity. Finally, the assembled virus buds from the host cell and is released into the blood stream (Engelman and Cherepanov, 2012; Freed, 2001, 2015).

In the past decade, the advent of effective combination antiretroviral therapy (c-ART), which targets different steps of the viral life cycle, has proven to be extremely successful in suppressing viral replication. However, due to mechanisms that are not clearly understood, a fraction of the integrated transcriptionally competent proviruses become transcriptionally inactive or latent (Siliciano and Greene, 2011). This reservoir of cells infected with latent HIV-1 is indistinguishable from uninfected cells and masked from c-ART. Because it is transcriptionally competent, latent HIV-1 retains the potential to become transcriptionally activated, which as a consequence leads to a rebound of the infection (De Crignis and Mahmoudi, 2017; Finzi et al., 1999; Siliciano et al., 2003) after termination of c-ART. Therefore, although c-ART has changed HIV-1 infection from a lethal to a chronic disease for people with access to the medication, it is not curative and has to be taken life-long (Maartens et al., 2014).

The shock and kill approach is a curative research strategy that aims to target and eliminate the persistent latent HIV-1-infected cell reservoir that presents the main obstacle to development of a cure. This approach aims to transcriptionally activate the latent viruses such that HIV is expressed and replicates, allowing its elimination by viral cytopathic effects or clearance by an effective immune system (Badalà et al., 2008; Dahabieh et al., 2015; Deeks, 2012; Margolis et al., 2016; Rasmussen et al., 2016). The presence of c-ART during shock and kill would safe-guard against new rounds of infection. The first part of the shock and kill approach relies on derepressing and/or activating the transcriptionally silent HIV-1 promoter (De Crignis and Mahmoudi, 2014; Rasmussen et al., 2016). Therefore, molecular mechanisms that govern the establishment and maintenance of transcriptionally silent HIV-1, and molecular mechanisms responsible for reversal of this process, i.e., transcriptional activation of latent virus, continue to be subjects of intense investigation. These studies were not only instrumental for deciphering transcriptional regulation of HIV-1 gene expression but also provided crucial insights into the regulation of transcription of endogenous genes.

Transcription of HIV-1 is controlled by a promoter located within the 5′ long terminal repeat (5′-LTR) of the integrated provirus. The HIV-1 5′-LTR is a long, promiscuous promoter that hijacks the host cell transcriptional apparatus to tightly control transcription of its viral genome. In the immediate-early phase of transcription, HIV promoter activity critically depends on cellular transcription factors (TFs). The presence of a large number of TF consensus binding sites within the 5′-LTR allows the interaction

of a multitude of TFs; transcriptional activators as well as repressors that can modulate promoter activity in a context-dependent manner (Pereira et al., 2000; Rafati et al., 2011; Verdin, 1991; Verdin and Van Lint, 1995). In this way, the HIV-1 5′-LTR has proven to be a useful model promoter system for the identification and characterization of TFs. The context-dependent combinatorial presence of activating and repressive TFs and their associated cofactors creates a balance that determines whether LTR transcription will be silenced, leading to latency, or become active, resulting in a productive infection (Cary et al., 2016; De Crignis and Mahmoudi, 2014; Van Lint et al., 2013).

HIV-1 transcriptional activity is also determined by its chromatin landscape, which provides an additional layer of regulation (Agosto et al., 2015; De Crignis and Mahmoudi, 2017; Lusic and Siliciano, 2017). Within the 5′-LTR, nucleosomes are deposited at specific positions, regardless of the genomic position of virus integration (Mahmoudi, 2012; Verdin et al., 1993). In particular, the nucleosome positioned immediately downstream of the transcription start site (TSS), Nuc-1, which is equivalent to the +1 nucleosome, is repressive to transcription and associated with HIV-1 latency (Rafati et al., 2011; Verdin and Van Lint, 1995). Upon activation, HIV-1 Nuc-1 becomes rapidly and specifically remodeled (Verdin et al., 1993). The well characterized and strict chromatin organization of the HIV 5′-LTR makes it an excellent model system to investigate the role of chromatin structure in transcription regulation. In this context, studies have probed the influence of factors that modulate nucleosome positioning, such as histone-modifying complexes and chromatin remodelers in HIV-1 transcriptional control.

The activity of the HIV-1 promoter is strongly enhanced by the viral transactivator protein Tat. In the absence of Tat, recruitment of cellular TFs to the HIV-1 promoter is sufficient to trigger efficient initiation of transcription. However, very low levels of full-length transcripts are produced at this stage because elongation is terminated prematurely and RNA polymerase II pauses at a region proximal to the TSS (Natarajan et al., 2013; Zhang et al., 2007). Expression of Tat overcomes the block to transcriptional elongation by recruiting the super elongation complex (SEC) to the transactivation response (TAR) region, a short nascent structured mRNA element. This creates a Tat-dependent positive regulatory loop that drastically amplifies HIV-1 transcription, tipping the balance toward productive replication (Flores et al., 1999; Kao et al., 1987; Mousseau et al., 2015b; Ott et al., 2011). In the next sections, we will discuss the factors contributing to transcriptional activation in more detail.

2. STRUCTURE OF THE HIV-1 PROMOTER (5′-LTR)

The integrated HIV-1 provirus, contains two LTRs located, respectively, at the 5′-end and 3′-end of the viral genome. Both LTRs can initiate transcription but the 5′-LTR exerts dominant control and serves as the HIV-1 promoter. Transcriptional interference from the 5′-LTR is likely to repress the promoter activity of the 3′-LTR (Cullen et al., 1984); however, in the presence of a defective 5′-LTR, transcription from the 3′-LTR can be activated (Klaver and Berkhout, 1994).

Like other retroviral LTRs, the HIV-1 LTR is structurally divided into the U3, R, and U5 regions (Fig. 1). Transcription initiates at the beginning of R in the 5′-LTR; the transcripts are then capped and elongated through the U5 region; and the rest of the proviral genome. Transcriptional termination usually occurs within the 3′-LTR, in the R region. At the end of transcription, the polyadenylation signal (poly(A)), encoded by the 3′-LTR U5 region, is added.

The U3 region of the 5′-LTR contains the key regulatory elements for control of transcriptional activity (Gaynor, 1992). The regulatory function of the HIV-1 5′-LTR was probed in early studies that examined the ability of the double-stranded DNA template to act as a promoter for reporter genes. Full-length, mutagenized, and deleted templates of the HIV-1 5′-LTR were fused to chloramphenicol acetyl transferase (CAT) or luciferase reporters and transfected into eukaryotic cell lines and reporter activity was measured (Muesing et al., 1987; Sodroski et al., 1984). These studies identified the main functional regions and *cis*-acting elements in the HIV-1 5′-LTR involved in regulating gene expression and suggested the presence of transacting factors in HIV-infected cells able to enhance the activity of the reporters (Sodroski et al., 1984).

The HIV-1 5′-LTR comprises a region between nucleotides −454 to +188, relative to the TSS, within the approximately 9 kilobases (kb) long viral genome (Fig. 1A) (Ratner et al., 1985; Sanchez-Pescador et al., 1985; Starcich et al., 1985; Wain-Hobson et al., 1985). This region was further divided into four main functional elements based on the effects of each segment on HIV reporter activity or HIV-1 gene expression: the modulatory element (−455, −104), the enhancer region (−109, −79), the core promoter element (−78, −1), and the TAR region (+1, +60) (Fig. 1B). A plethora of (>50) cellular TFs has been reported to bind to the HIV-1 5′-LTR in vitro or predicted to bind the 5′-LTR sequence (Mahmoudi,

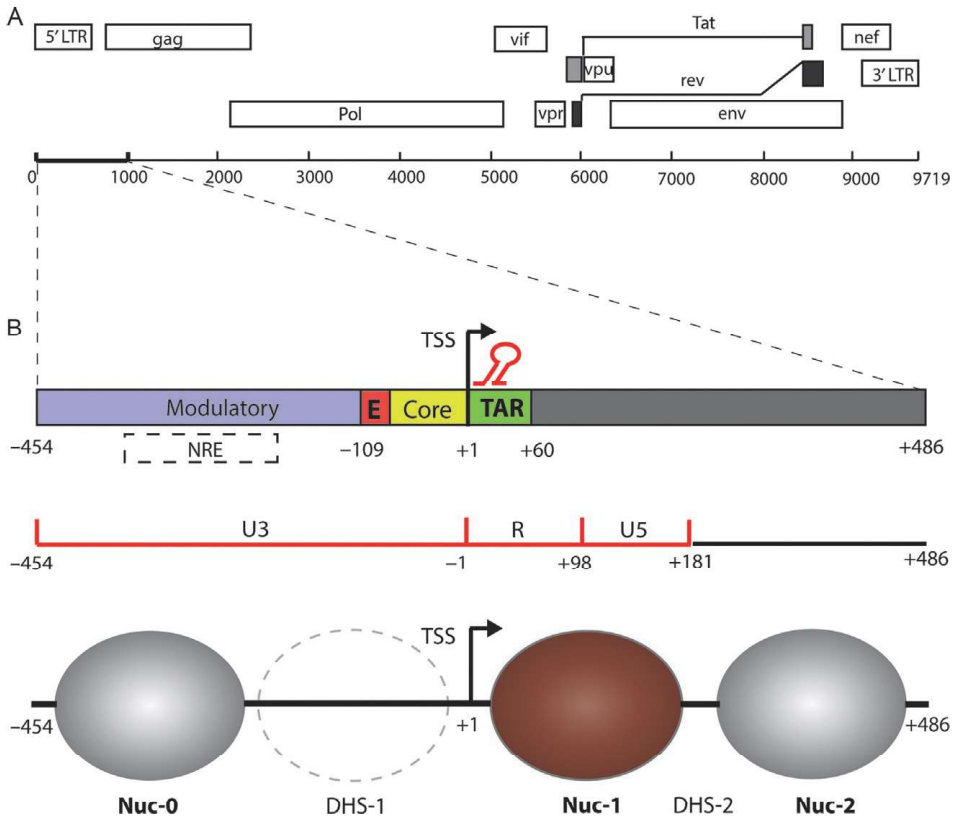

Fig. 1 Schematic representation of the HIV-5′-LTR. (A) Structure of the HIV-1 genome and the 5′-LTR region (~9 kb) that acts as the HIV-1 promoter. The 5′-LTR is divided into the U3, R, and U5 regions. The U3 region can be further divided into the modulatory region (*purple*), enhancer (E) (*red*), basal/core promoter (*yellow*), and TAR (*green*). (B) In vivo observed chromatin landscape of the transcriptionally inactive HIV-1 5′-LTR is defined by the presence of two strictly positioned nucleosomes Nuc-0 and Nuc-1 as indicated connected by a region of accessible DNA, hypersensitive to nucleases, DHS-1 which contains the majority of cellular transcription factor consensus binding sites and which has high propensity for nucleosome formation.

2012; Pereira et al., 2000). However, only a few factors have been shown to be critical for regulation of proviral transcription in vivo: these include nuclear factor (NF)-κB, nuclear factor for activated T cells (NFAT), Sp1, TATA-binding protein (TBP). Other 5′-LTR bound factors are thought to perform a cooperative regulatory function or contribute to the modulation of LTR activity in response to different cellular stimuli. Interestingly, random mutation of the HIV 5′-LTR results in a balance of positive and negative effects on viral fitness, suggesting that the 5′-LTR has not evolved to the most active promoter (van Opijnen et al., 2006).

2.1 The Modulatory Region

Early studies found that deletion of a region between nucleotides −454 to −167 in the HIV 5′-LTR produces a twofold to threefold increase in HIV promoter reporter activity and viral replication (Gaynor, 1992; Lu et al., 1989; Rosen et al., 1985), suggesting that this region behaves as a negative regulatory element. Later this segment was shown to contain multiple *cis*-acting binding sites for activating and repressive factors, supporting a modulatory, rather than repressive function on HIV promoter activity (Pereira et al., 2000) depending on the availability of repressive/activating factors. This region includes three CCAAT/enhancer binding protein (C/EBP) sites (Henderson et al., 1995; Tesmer et al., 1993), an upstream stimulatory factor binding site, the activating transcription factor/cyclic AMP response element binding region (Krebs et al., 1997, 1998), lymphocyte enhancer factor (LEF-1) site, nuclear factor of activated T cells (NF-AT), c-Myb, Ets-1, AP-1, COUP, NF-κB binding sites, and a number of other consensus TF binding sites both shown and predicted to bind (Mahmoudi, 2012; Pereira et al., 2000). Nuclear factor-IB (NF-IB) has also been recently reported to bind to the modulatory region upon HIV-1 infection and to negatively impact viral transcription (Vemula et al., 2015). The 5′-LTR modulatory region is thus thought to regulate the basal activity exerted by the core element and enhancer regions in a context-dependent manner, in response to different cellular signaling pathways. Sequences upstream of the core promoter, between −130 and −201, containing consensus binding sites for LEF-1, NF-AT, and Ets-1 TFs which are highly expressed in T cells, were in particular shown to serve as important elements of regulation of viral expression in peripheral blood lymphocytes and in some T cell lines (Kim et al., 1993).

A recent report using a dCas9 fused to HAT protein p300 has shown that targeting of dCas9-p300 to a segment within the modulatory region that overlaps with Nuc-0 can also drive transcriptional activation supporting a potential regulatory role for this region of the LTR (Limsirichai et al., 2016).

2.2 The Enhancer

Deletion and mutagenesis experiments have identified a region between nucleotides −137 and −17, located directly upstream of the core promoter and the SP binding sites, to be an enhancer element that, irrespective of orientation and distance, is able to activate transcription from a heterologous promoter (Rosen et al., 1985). Consistent with these early studies,

CRISPR/Cas9 studies using a catalytically deficient Cas9 fused to transactivation domains like VP64 (dCas9-VP64), VP64 arrays (dCas9-SunTag) (Bialek et al., 2016; Ji et al., 2016; Saayman et al., 2016), or SAM (dCas9-SAM) (Bialek et al., 2016; Zhang et al., 2015) determined that the HIV-1 enhancer element behaves as the hotspot for dCas9-mediated activation of proviral transcription, in latently infected T cells. These findings also confirm a general rule of transcriptional activation that requires binding of activating complexes at ~100 bases upstream of the TSS.

It is probably not a coincidence that most HIV-1 subtypes have evolved a tandem repeat of the 10 bp consensus binding sites for NF-κB and related factors (Burnett et al., 2010; Nabel and Baltimore, 1987) right in the hotspot, which constitutes the strongest *cis* activator for the promoter. Different NF-κB subunits have been shown to bind to the HIV-1 enhancer in vitro and in vivo and strongly activate HIV-1 transcription (Duckett et al., 1993; Fujita et al., 1992; Kretzschmar et al., 1992; Lin et al., 1995). The NF-κB sites (Kim et al., 1993; Ross et al., 1991) and NF-κB proteins (Qian et al., 1994) play a key role in regulating viral promoter activity in vivo, in PBMCs and activated T-cells. NF-κB is in fact a crucial activator of immune responses and the cellular acute-phase and it is strongly upregulated in activated T-cells. NF-κB binding is conferred by heterodimer formation of p50 and p65 subunits. Most cell types, including T cells, tightly control NF-κB activity by interaction of p65 with the inhibitory protein I-κB that masks the nuclear localization sequence and keeps the complex sequestered in an inactive state in the cytoplasm. Upon T cell activation by mitogens, cytokines, oxygen radicals, and other agents, NF-κB binding activity is restored: I-κB is phosphorylated by mitogen-activated I-κB kinase, ubiquitinated and sent for degradation by the proteasome. Once released from I-κB, the NF-κB subunits are free to translocate into the nucleus and activate transcription.

NF-κB binds to the kB binding sites, and can cooperatively with Sp1 (Li et al., 1994; Perkins et al., 1993, 1994; Sif and Gilmore, 1994) and other TFs (LEF-1, Ets1, and TFE-3) (Sieweke et al., 1998) synergistically activate HIV transcription, even in the presence of a repressive chromatin environment. The ERK1/ERK2 mitogen-activated protein kinase (MAPK) pathway plays a role in mediating the response to external stimuli in HIV-1 latently infected cells via engagement of the NF-κB sites. Upon MAPK activation AP-1 components c-Fos and c-Jun are reportedly induced and physically interact with NF-κB at the NF-κB sites to synergistically activate the HIV-1 promoter (Yang et al., 1999). The two NF-κB binding sites within

the HIV-1 enhancer region can be bound by NFAT factors as well; NFATs were shown to bind the terminal 3′ half of NF-κB motifs located in the U3 region, with similar sequence preference as p50, and modulate HIV promoter activity, increasing infectivity in T-cells (Cron et al., 2000; Kinoshita et al., 1997, 1998; Macian and Rao, 1999), although NFATc2 was shown to also repress transcription in certain contexts via competition with NF-κB for its binding site. Owing to overlap of the consensus sequences, NF-κB–NFAT binding is thought to be mutually exclusive (Chen-Park et al., 2002; Giffin et al., 2003) while binding of NF-κB is enhanced by interactions with Sp1 (Perkins et al., 1993). Although mutation of the NF-κB sites within the HIV-1 enhancer results in only a modest inhibition of viral expression in most cell lines (Liang et al., 1997), the response of the viral enhancer to NF-κB or NF-AT has proven to be essential for reactivation of the latent HIV-1 provirus and to induce viral replication in primary T-cells (Alcamí et al., 1995; Bosque and Planelles, 2009). More recently, HspBP1 was shown to be recruited to the NF-κB sites of the HIV-1 enhancer where it competes with binding of p50/p65 leading to suppression of NF-κB-induced transcription (Chaudhary et al., 2016).

It is important to underline that not all HIV-1 subtypes have two NF-κB sites in their enhancer region. Subtype A/E viruses have a one nucleotide deletion in the upstream NF-κB site that causes a loss of NF-κB binding and increased binding of GABP. The NF-κB to GABP switch in these variants still results in a functional promoter, characterized by an overall reduced basal activity, and enhanced Tat-mediated activation (Verhoef and Berkhout, 1999). Subtype C viruses instead can contain three (Bjorndal et al., 1999; Hunt and Tiemessen, 2000; Naghavi et al., 1999) to four NF-κB sites in their promoter (Bachu et al., 2012b; Hunt and Tiemessen, 2000; Liebert et al., 2002; Papathanasopoulos et al., 2002) and are characterized by moderate enhanced activity (Jeeninga et al., 2000; Montano et al., 1997; Naghavi et al., 1999) and replication fitness (Bachu et al., 2012a).

Upstream of the NF-κB sites, a four-nucleotide AP-1 element was also shown to constitute a latent establishment element as its deletion compromised the ability to establish latent infections, while extension of this site promoted latency (Duverger et al., 2013). c-Jun was shown to suppress HIV-1 promoter activity in the absence of Tat (Duverger et al., 2013). However, c-Jun overexpression also enhances Tat-dependent transcription suggesting that, depending on Tat levels, c-Jun binding to the AP-1 site can mediate repression or enhance HIV-1 promoter activity (van der Sluis et al., 2014).

Interestingly, this AP1 site overlaps with a RBEII binding site, bound by the RBF-2 complex, reported to be necessary for 5′-LTR transcription (Sadowski and Mitchell, 2005), although c-Jun-mediated repression may not solely result from interference with RBF-2 binding (van der Sluis et al., 2014).

2.3 The Core Promoter

The core promoter spans a region of 250 nucleotides and contains the essential elements for HIV-1 promoter basal activity: a TATA box element (Garcia et al., 1989), three tandem GC-rich binding sites for the Sp family of TFs (Jones et al., 1986), and a highly active nonconventional TSS (Zenzie-Gregory et al., 1993). Genetic studies in different HIV-1 subtypes have later revealed that the virus is able to use the overlapping CATA box instead of the canonical TATA box (van Opijnen et al., 2004) and that certain subtypes contain four to five Sp1 sites (Koken et al., 1992; Rosseau et al., 1997).

The TATA box and Sp sites are essential for transcription initiation and basal promoter activity (Jones and Peterlin, 1994) but also necessary for Tat-mediated transactivation as insertions that separate these two regulatory elements compromise transactivation (Huang and Jeang, 1993). HIV-1 basal transcription strictly requires Sp1 and TBP acting together with cellular TAFs (TBP-associated factors) in the general TF complex TFIID (Dynlacht et al., 1991).

Within the complex, Sp1 has been shown to interact directly with TAF-110 (Gill et al., 1994; Hoey et al., 1993). Additionally, Sp1 interacts with additional DNA bound proteins NF-κB (Li et al., 1994; Perkins et al., 1993, 1994; Sif and Gilmore, 1994), YY1 (Seto et al., 1991, 1993), and distal Sp1 monomers (Pascal and Tjian, 1991) and directs the basal machinery to form the preinitiation complex (PIC) via protein–protein interactions (Näär et al., 1998).

TRIM22 was recently reported to interfere with Sp1 binding thereby inhibiting PIC formation and basal proviral transcription (Turrini et al., 2015). Sp1 binding at the core promoter has also been linked to chromatin remodeling as it interacts with histone deacetylases (HDACs) and chromatin modifying factors p300 (Zhao et al., 2003).

The CTGC motifs flanking the TATA box have also been shown to be required for transcription initiation in vitro and Tat-dependent activation in living cells (Wilhelm et al., 2012). Additionally, immediately upstream of

the TSS binding sites for the TF ZASC1, have been shown to have a regulatory role as ZASC1 interacts with Tat and positive transcription elongation factor b (P-TEFb) and cooperatively promotes HIV-1 transcriptional elongation (Bruce et al., 2013).

2.4 The TAR Element

Pioneering studies first led to the observation that expression of viral or reporter genes, under the control of the HIV-1 5′-LTR is greatly enhanced in HIV-infected cells (Sodroski et al., 1984, 1985a) or in cells cotransfected with coding sequences of the viral genome (Sodroski et al., 1985b). It quickly became clear that HIV-infected cells must express HIV-specific transacting TFs. Deletion experiments determined that a sequence between −17 and +44, named the TAR element, as well as the presence of an intact enhancer region (Hauber et al., 1989) were essential for the response to transacting factors (Rosen et al., 1985). Given their crucial nature for the regulation of the HIV promoter, the transacting viral sequences were studied extensively to determine their mechanism of action. Cotransfection (Sodroski et al., 1985b) and functional mapping (Arya et al., 1985) studies resulted in identification of a region between nucleotides 5365 and 5607 of the HIV genome responsible for transactivation activity. This region contains the N-terminal segment of the Tat reading frame, which, depending on the subtype, encodes a protein of 86–104 amino acids. Tat was shown to bind to TAR (Dingwall et al., 1989; Roy et al., 1990), a short RNA transcript containing multiple regulatory elements and two copies of the CTCTCGG repeat sequence thereby mediating recruitment of Tat to the HIV-1 promoter (Hauber et al., 1989; Tong-Starksen et al., 1987). In vitro studies later demonstrated that this RNA element has a hairpin-like structure, which acts as a binding site for Tat and is essential for transactivation (Berkhout et al., 1989; Kao et al., 1987; Muesing et al., 1987; Selby et al., 1989). Different subtypes have acquired mutations in the lower stem region of TAR but most changes in the sequence do not seem to significantly affect its secondary structure or sensitivity to Tat activation (Jeeninga et al., 2000; Montano et al., 1997).

2.5 Region Downstream of TSS

Sequences downstream of TSS have an underappreciated role in regulating transcription (Burke and Kadonaga, 1996, 1997; Emanuel and Gilmour, 1993; He et al., 2002; Pelletier et al., 1997). The HIV-1 5′-LTR contains

several TF binding sites downstream of the TSS, some of which are well conserved within different HIV-1 strains and subtypes (el Kharroubi and Martin, 1996; el Kharroubi and Verdin, 1994). Important downstream HIV-1 regulatory binding sites are: three AP-1 binding sites located in the R/U5 region (+87, +94) (+118, +125) and (+155, +163) (el Kharroubi and Verdin, 1994; Van Lint et al., 1997), NFATc2 and C/EBP sites (+158, +171) (Dahiya et al., 2014), AP-3 like (+162, +177) (el Kharroubi and Verdin, 1994; Van Lint et al., 1997), NFAT (+162, +177) (Van Lint et al., 1997), DBF-1 (+200, +219) (Liang et al., 1997; Sgarbanti et al., 2002, 2004), and Sp sites (+270, +278) (Dahiya et al., 2014) many of which were identified by in vitro foot printing and DNA binding studies (Dahiya et al., 2014; Rabbi et al., 1997; Roebuck et al., 1996).

Some of these factors including AP1, C/EBP, NFAT contribute to transcriptional activation via recruitment of chromatin remodeling and histone-modifying cofactor complexes to improve accessibility of RNA pol II complex to chromatin (Dahiya et al., 2014). Other factors are likely to contribute to transcriptional activation by influencing transcriptional initiation and elongation (Dahiya et al., 2014). Overall, this region may contribute to modulation of the HIV-1 transcriptional response to activating signals in a context-dependent manner (Dahiya et al., 2014).

3. CHROMATIN LANDSCAPE OF THE HIV-1 PROMOTER

In eukaryotic cells, DNA is tightly packaged into nucleosomes, consisting of a histone octamer core wrapped by 147 bp of DNA (Luger and Richmond, 1998). The nucleosomal core comprises two H2A–H2B and two H3–H4 histone heterodimers (Richmond et al., 1997). Histone H1 locks the DNA at the entry and exit sites of the nucleosomal core, acting as a linker (Richmond et al., 1997). Nucleosome positioning throughout the genome is a very dynamic process, tightly linked with transcription that plays a fundamental role in regulating gene expression. The position of nucleosomes can alter the availability of binding sites for TFs and the recruitment of general transcription machinery in vivo (Radman-Livaja and Rando, 2010), thereby influencing expression. Conversely, binding of specific TFs and chromatin remodelers upon transcriptional activation can also result in destabilization or repositioning of nucleosomes at enhancer or promoter regions (Boyle et al., 2011; Henikoff, 2008).

At least three main cellular mechanisms have been described that can regulate nucleosome occupancy and stability. First, chromatin remodeling complexes, large multisubunit complexes containing a core ATPase domain, can actively reposition or remodel nucleosome using ATP hydrolysis as a source of energy (Clapier and Cairns, 2009). Second, histone-modifying enzymes can add several posttranslational modifications (PTMs) to histones to alter their structural configuration or electrostatic charge, thereby influencing their stability or their ability to recruit regulatory cofactors. The N-terminal tails are unstructured and very accessible, as they protrude from the core nucleosome, and can be subjected to PTMs like acetylation, methylation, phosphorylation, ubiquitination, sumoylation, and poly ADP-ribosylation. Combinatorial patterns of PTMs on histone tails have been proposed to generate a "histone code" that directs chromatin templated processes such as replication, repair, and gene expression (Strahl and Allis, 2000). Finally, DNA methylation at CpG motifs has a well-established regulatory function in transposon silencing, genomic imprinting, X-chromosome inactivation, and also influences the chromatin environment at gene regulatory regions (Li and Zhang, 2014).

3.1 Nucleosome Positioning and HIV-1 Expression

As a naked DNA template, the HIV-1 promoter acts as a strong promoter but it is almost silent in vivo when integrated to the host genome, in the absence of activating stimuli (Huang and Jeang, 1993; Pomerantz et al., 1990). This is because the integrated HIV-1 provirus, like endogenous genes, is packaged into nucleosomes, a structure that adds an extra layer of regulation to the activity of the HIV-1 promoter by limiting access to transcription regulators. Assays probing the in vivo chromatin accessibility of the integrated HIV 5′-LTR has provided invaluable insight into the influence of nucleosome positioning on general transcription. The HIV-1 promoter is embedded into three distinct nucleosomes, Nuc-0 (or −1 nucleosome) (−415/−255), Nuc1 (or +1 nucleosome) (+10/+155), and Nuc2 (+256/+412) which are positioned at defined locations with respect to the enhancer and core regions (Fig. 1B) (Steger and Workman, 1997; Verdin, 1991; Verdin et al., 1993) and delimit two regions hypersensitive to nuclease digestion, DHS-1 and DHS-2 (Verdin et al., 1993). The DHS-1 and DHS-2 regions contain consensus binding sites for multiple TFs that have been shown to bind the LTR in vitro and in vivo (Demarchi et al., 1993, 1996; el Kharroubi and Verdin, 1994; Pereira et al., 2000).

In vitro reconstitution studies of HIV-1 transcription demonstrated that incubation of the template with a nucleosome assembly system, purified from Drosophila embryos, strongly represses transcription (Sheridan et al., 1995), likely by inhibiting the formation of the RNA Pol II PIC (reviewed in Owen-Hughes and Workman, 1994). However, chromatin-mediated repression of the HIV promoter activity could be counteracted by preincubating the DNA, before nucleosome incorporation, with the cellular factors LEF-1, Ets-1, TFE-3, and Sp1 (Sheridan et al., 1995). These data suggested that the presence of cellular factors bound to the HIV 5′-LTR is fundamental to the establishment of nucleosome free regions DHS-1 and DHS-2 (Verdin, 1991; Verdin et al., 1993). In agreement, DNA sequences corresponding to the DHS-1 region, even though accessible, were found to have the highest histone binding score within the LTR sequence, indicating higher propensity for nucleosome formation than LTR sequences encompassing Nuc-0 or Nuc-1 (Rafati et al., 2011). The discrepancy between the observed in vivo chromatin structure and its predicted nucleosomal structure is in agreement with the binding and activity of TFs and cofactors within the DHS-1 region, which keep its nucleosomal state disrupted.

3.2 HIV-1 Nuc-1: The +1 Nucleosome

DNase I foot printing and MNase mapping experiments have demonstrated that Nuc-1, located immediately downstream of the TSS is rapidly removed from the LTR upon transcriptional activation (Verdin, 1991; Verdin et al., 1993). This indicates that the presence of Nuc-1 constitutes a block that needs to be moved or rearranged to allow RNA Pol II elongation (el Kharroubi and Verdin, 1994). Only much later, genome-wide nucleosome mapping studies have demonstrated how widespread and conserved this regulatory mechanism is at endogenous protein-coding genes. Pioneering studies in *Saccharomyces cerevisiae* showed that nucleosomes are generally depleted from active regulatory regions (Bernstein et al., 2004; Lee et al., 2004; Sekinger et al., 2005); higher resolution experiments then clarified that upon gene activation there is an additional depletion of nucleosomes at the promoter regions (Guillemette et al., 2005; Schwabish and Struhl, 2004; Zanton and Pugh, 2006; Zhang et al., 2005).

Genome-wide nucleosome mapping in *S. cerevisiae* and metazoans has shown that nucleosomes at the promoter region of most genes are organized exactly as seen in the HIV promoter: a nucleosome free region, hypersensitive

to nuclease digestion which is delimited by −1 and +1 nucleosomes. The gene body instead is packaged by an array of nucleosomes (Barski et al., 2007; Mavrich et al., 2008). Upon transcriptional activation, the +1 nucleosome is evicted but it seems to be rapidly reconstituted after elongation, as highly transcribed genes only show a modest +1 nucleosome depletion (Albert et al., 2007). More recently, genome-wide studies have demonstrated that indeed the +1 nucleosome constitutes a block for RNA pol II transcriptional elongation for essentially all genes, including genes subjected to regulated transcriptional pausing (Weber et al., 2014a).

3.3 Role of ATP-Dependent Chromatin Remodelers

In silico predictions for histone binding point to a lower propensity of the HIV-1 +1 nucleosome Nuc-1 DNA sequence for nucleosome formation, while the DHS-1 region has the highest propensity for nucleosome formation, suggesting that in vivo, the DHS-1 region is kept accessible, while Nuc-1 is positioned at an energetically less favorable position (Rafati et al., 2011). High resolution MNase mapping demonstrated that the BAF complex, an ATP-dependent chromatin remodeling complex containing BAF250a, actively repositions nucleosomes within the 5′-LTR, positioning Nuc-1 over energetically suboptimal DNA sequences, and hence promotes establishment and maintenance of a repressive state for transcription (Rafati et al., 2011). When BAF complex activity is perturbed, either via siRNA depletion of BAF250 or via inhibition with small molecules, the activity of the HIV promoter is significantly derepressed (Rafati et al., 2011; Stoszko et al., 2016). Other chromatin remodeling factors actively maintain a repressed chromatin state at the HIV promoter thereby repressing transcription. The CHD family, like the BAF family, has a centrally located ATPase domain and two additional tandem bromodomains in the N-terminal region (Marfella and Imbalzano, 2007). CHD1 was shown to promote a repressive nucleosomal configuration in a chimeric yeast–HIV transcription model (Vanti et al., 2009) and in latently infected Jurkat cells (Gallastegui et al., 2011), thereby maintaining latency. More recently, an insertional mutagenesis screen identified CHD1 and CHD2 as positive regulators of HIV-1 expression (Rodgers et al., 2014). The NuRD chromatin remodeling complex combines ATPase activity with HDAC activity. One of its subunits, the methyl binding protein MBD2 was also reported to play a role in maintenance of latency (Blazkova et al., 2009; Kauder et al., 2009). Chromatin remodelers are not only crucial for regulation of basal

transcription at the HIV promoter but have also been shown to play a pivotal role in active nucleosome remodeling upon Tat-mediated activation of the promoter (Agbottah et al., 2006; Easley et al., 2010a; Mahmoudi, 2012; Mahmoudi et al., 2006; Tréand et al., 2006; Van Duyne et al., 2011).

3.4 Role of Histone Modifications

PTMs of the N-terminal tail of histones do not only stabilize or destabilize the interaction between DNA and the nucleosomal core but also serve as selective marks, to recruit specific proteins containing specialized domains that can read and bind to the modified histones. These proteins can then act to change chromatin structure, promoting, or repressing transcription. Enzymes that deposit histone marks, referred to as writers, include: histone acetyltransferases (HATs), histone methyltransferases (HMTs/KMTs), protein arginine methyltransferases (PRMTs), histone ubiquitin ligases, and kinases. Proteins containing bromodomains, chromodomains, tudor, PHD fingers, MBT domains, etc., can read the marks (readers) and determine a functional response. PTMs on histone tails are not permanent but can be removed by eraser proteins such as HDACs, lysine demethylases (KDMs), and phosphatases. Acetylation is almost always associated with activation as it masks the positive charge of histones (lowering the affinity for the negatively charged DNA phosphodiester backbone) and helps to loosen the chromatin, thereby facilitating transcription. Methylation can have distinct transcriptional consequences depending on the residue modified. Methylation of H3 lysine residue 4 (H3K4) and 36 (H3K36) is associated with transcriptional activation, while methylation of H3K9 and H3K27 are considered to be repressive.

Reversible acetylation of histones relies on the activity of HATs and HDACs (Tripathy et al., 2011; Van Lint et al., 2013) and represents the best characterized histone modification that regulates HIV-1 promoter activity (Kumar et al., 2015; Van Lint et al., 2013). In the latent state, the HIV-1 promoter is predominantly associated with HDACs (Cary et al., 2016; Donahue et al., 2013; Kouzarides, 2007; Margolis et al., 2016).

Host repressive factors late SV40 factor (LSF), ying-yang 1 (YY1), and NF-κB p50 recruit HDACS to the HIV 5′-LTR thereby causing deacetylation and promoting maintenance of Nuc-1 in a repressive configuration (Williams et al., 2006). The cooperative activity of LSF and YY1 serves to recruit HDAC1 downstream of the TSS (Coull et al., 2000; Romerio et al., 1997), while recruitment to the 5′-LTR is mediated by

the interaction with NF-κB p50 homodimers (Williams et al., 2006), with AP-4 (Imai and Okamoto, 2006), CBF-1 (Tyagi and Karn, 2007), and c-Myc-Sp-1 (Jiang et al., 2007). In monocytes and macrophages, Sp1 recruits COUP-TF interacting protein (CTIP2) which in turn recruits HDAC1 and HDAC2 to promote local deacetylation of histone H3 at the HIV-1 5′-LTR (Marban et al., 2005, 2007). Given the well-described role of HDACs in repressing transcription from the 5′-LTR, HDAC inhibitors have been in the spotlight of strategies aiming to reverse latency. Indeed, treatment of latently infected cell lines or CD4+ T cells isolated from HIV-1-infected patients with HDAC inhibitors results in a significant induction of HIV-1 transcription (Barton et al., 2014; Huber et al., 2011; Margolis, 2011; Palmisano et al., 2012; Reuse et al., 2009; Van Lint et al., 1996). HDAC inhibitor treatment was shown to cause reactivation in a broad range of proviruses, including defective ones (Barton et al., 2016). It has been shown that specifically inhibitors of class I HDACs, but not class II HDACs, induce chromatin derepression and efficiently stimulate transcription (Archin et al., 2009; Keedy et al., 2009). Among class I HDACs, specific depletion of HDAC3, but not HDACs 1 or 2 leads to significant activation of latent HIV-1, suggesting a potentially prominent role for HDAC3 in HIV-1 latency (Huber et al., 2011). Interestingly, the HIV-1 accessory protein Vpr was recently found to indirectly counteract latency by inducing degradation of HDAC3 and HDAC1 at the viral promoter (Romani et al., 2016).

Methylation constitutes another important modification of histones that contributes to silencing of the integrated HIV-1 provirus. In the latent state, the HIV-1 promoter is characterized by a predominance of repressive H3K9 dimethyl (Imai et al., 2010) or trimethyl (du Chéné et al., 2007; Marban et al., 2005, 2007) and H3K27 trimethyl (Pearson et al., 2008) histone marks. The association of these marks with transcriptional repression is well-established genome-wide and constitutes a central mechanism for silencing of the HIV-1 promoter as well. The overall effect of these modifications is to promote stabilization of Nuc-1, establishing a repressive environment for HIV-1 gene expression. In cell line models and PBMCs, chromatin repression of the HIV-1 promoter, via H3K9me3, has been shown to be mediated by the histone methyltransferases (HMTs) Suv39H1 and HP1gamma (du Chéné et al., 2007). In microglial cells, CTIP2 recruits Suv39H1 to the HIV-1 promoter resulting in the formation of an H3K9me3 region, which is recognized by HP1-gamma and promotes the formation of a heterochromatic region (Marban et al., 2005, 2007). Another HMT associated with the HIV-1 promoter transcriptional silencing is G9a which

promotes the formation of a repressive chromatin environment by deposition of the H3K9me2 mark (Imai et al., 2010). Deposition of the H3K27me3 mark is instead mediated by EZH2, a subunit of the polycomb group repressive complex 2 (PRC2), which is also recruited to the HIV-1 5′-LTR (Friedman et al., 2011). Depletion of EZH2 in latently infected cell lines induces HIV-1 transcription (Friedman et al., 2011). PRC2-mediated H3K27 trimethylation then serves as a recognition mark for recruitment of additional repressive complexes including the polycomb group repressive complex 1 (PRC1), other HMTs, DNA methyltransferases, and HDACs. H3K27me3 is thought to be involved in establishment of latency at an early phase of infection and in maintenance of silencing after integration. Depletion of EZH2 reduced the frequency of latently infected cells after new infections, while inhibitors of PRC2 antagonized repression of the promoter activity in latently infected cells (Matsuda et al., 2015).

3.5 Histone Chaperones and Chromatin Assembly Factors

The composition eukaryotic chromatin is not static and the dynamics of nucleosomes is for a large part determined by the incorporation of histone variants (Venkatesh and Workman, 2015). Histone variants can differ from their canonical counterparts by alteration of a few amino acids or addition of larger domains and their presence influences chromatin-mediated processes such as transcription (Venkatesh and Workman, 2015). Exchange of histones is not only mediated by ATP-dependent chromatin remodelers but also by histone chaperones and assembly factors which save guard the formation of proper nucleosomes (Venkatesh and Workman, 2015).

Several histone chaperones have in recent years been implicated in transcriptional regulation of the HIV-1 5′-LTR. The histone chaperone protein nucleosome assembly protein-1 (NAP-1) was identified as an interactor for flag-tagged Tat (Vardabasso et al., 2008) and as a coactivator of the HIV-1 promoter. The mechanism of NAP-1 5′-LTR activation appeared to primarily involve Tat stabilization and potentially NUP-1-assisted removal of H2A–H2B dimers from nucleosomes which results in an open chromatin environment conductive to transcription (Vardabasso et al., 2008). Early genetic screens, using a minimal HIV-1 transcriptional system in yeast, for factors that modify the transcriptional output of the HIV-1 5′-LTR identified the involvement of chromatin reassembly factors Spt6, Chd1, and FACT as well as the histone chaperones ASF1a and HIRA (Gallastegui et al., 2011; Vanti et al., 2009). Curiously it was found that upon

knockdown of these factors the HIV-1 promoter was activated. The authors suggested that chromatin reassembly factors and histone chaperons control the activity of host genes which results in transcriptional interference of the HIV-1 LTR (Gallastegui et al., 2011). A recent functional genomic RNAi screen also identified SUPT16H and SSRP1, both components of the FACT chromatin reassembly complex, as suppressors of HIV-1 transcription (Huang et al., 2015) and demonstrated direct Tat-mediated recruitment of these factors to the viral promoter. This precludes association of the P-TEFb subunit cyclin T1 with the Tat-5′-LTR axis and suggests a direct role for FACT in suppressing the HIV-1 5′-LTR. Two other histone chaperones have been reported to play a role in HIV-1 transcriptional activation: Nucleophosmin (NPM1) and RbAp48 (Gadad et al., 2011; Wang et al., 2016). Acetylated NPM1 is recruited via Tat to DHS-1 of the HIV-1 5′-LTR where it could enhance viral transcription by promoting a dynamic chromatin surrounding. However, NMP1 also regulates the nuclear localization of Tat which potentially significantly contributes to the observed stimulatory effect on HIV-1 transcription (Gadad et al., 2011). RbAp48, a component of several chromatin repressive complexes such as NuRD, NURF, and PRC is also recruited to the 5′-LTR where it represses transcription (Wang et al., 2016). Above studies demonstrate a role for histone chaperones in regulating HIV-1 transcription. Despite the presence of a number of studies implicating a role for histone chaperones in HIV-1 transcription regulation, remains unclear if their mechanism of action involves the deposition of histone variants.

3.6 Role of DNA Methylation

Initial observations for a potential role for DNA methylation in regulation of HIV-1 promoter activity comes from latently infected cell lines, where those harboring heavily methylated promoters were found to be more prone to be highly repressed (Blazkova et al., 2009). The presence of methylation at two CpG islands flanking the TSS was shown to promote HIV promoter binding by the methyl–CpG-binding domain protein (MBD2), where it recruits the repressive NURD complex (Kauder et al., 2009). However, the importance of this regulatory mechanism in vivo is less clear. A role for DNA methylation in maintenance, rather than establishment, of HIV-1 latency was proposed as resting CD4+ T cells isolated from HIV-1-infected patients with undetectable viremia displayed higher levels of DNA methylation at the 5′-LTR compared to cells isolated

from viremic patients (Blazkova et al., 2009). Highly methylated DNA has also been observed in PBMCs infected with HIV-1, suggesting that DNA methylation might be one of the mechanisms employed to achieve transcriptional silencing (Maricato et al., 2015). Several studies though have shown that primary cells obtained from c-ART-treated HIV-1-infected patients have low levels of HIV promoter DNA methylation, questioning the importance of this regulatory mechanism in vivo (Blazkova et al., 2012; Ho et al., 2013; Weber et al., 2014b). Recently it was reported that in the latent reservoir of HIV-1-infected patients under prolonged cART, there is an accumulation of DNA methylation at the HIV-1 5′-LTR. This accumulation may arise as a consequence of repeated cycles of activation of the provirus by cellular stimuli and selection of methylated proviruses less prone to activation or alternatively by de novo methylation induced after cell activation (Trejbalová et al., 2016). Thus, methylation of the HIV 5′-LTR may be regulatory in latency control but further investigation, and larger patient cohorts are needed to derive more significant conclusions.

4. BASAL HIV-1 TRANSCRIPTION

4.1 Transcriptional Initiation

RNA polymerase (Pol) II-dependent transcription of protein-coding genes begins with the recruitment of gene-specific regulatory factors to the core promoter. These factors can act directly by recruiting components of the transcription machinery or can mediate the establishment of a transcriptionally permissive chromatin state by recruiting histone modifiers and chromatin remodelers. At the HIV-1 promoter transcriptional initiation occurs at the junction between the U3 and R regions, where three guanosine residues reside, and efficiently starts when cellular factors Sp1, NF-κB, NFAT are recruited (Karn, 2011; Kinoshita et al., 1997; Nabel and Baltimore, 1987; Perkins et al., 1997). Binding of these factors promotes the recruitment of histone-modifying enzymes that cooperatively establish a transcriptionally permissive chromatin environment, thus facilitating the installment of the transcription machinery at the 5′-LTR (Gerritsen et al., 1997; Kilareski et al., 2009; Kobor and Greenblatt, 2002; Peterlin and Price, 2006; Turk and Stoka, 2007). The HIV-1 core promoter can be regarded as a TATA box containing promoter, the most-extensively studied eukaryotic promoter element, present in about 10%–15% of mammalian genes.

Interestingly, it was recently demonstrated that HIV-1 transcription initiation can occur at each of the three G residues at the start site and that depending on which capped guanosine the transcripts begin with, they can be destined for either translation, or packaging as genomic RNA (Kharytonchyk et al., 2016; Masuda et al., 2015). This is in agreement with previous studies which have shown that RNA Pol II can use multiple TSS within TATA-driven promoters (Kadonaga, 2012). The first step for the assembly of the transcription machinery is the binding of the TFIID complex, containing the TBP subunit, to the TATA box. Upon TFIID binding, five more general TFs (TFIIA, TFIIB, TFIIE, TFIIF, and TFIIH), the mediator complex and RNA pol II are recruited to the TATA box, together forming the PIC (for review, Cramer, 2004; Hirose and Ohkuma, 2007; Sikorski and Buratowski, 2009). RNA pol II contains a C-terminal domain (CTD) composed of multiple heptad repeats of the consensus (Tyr1–Ser2–Pro3–Thr4–Ser5–Pro6–Ser7), whose phosphorylation state is crucial to its activity. In the inactive state, the HIV promoter is occupied with hypophosphorylated RNA pol II, TFIID, and mediator which contains the CDK8 repressive module. Upon activation, interaction with CDK8 is lost and the mediator, TFIIH and RNA pol II is set for activation. Concomitantly, the TFIIH-associated kinase CDK7 catalyzes the phosphorylation of Ser 5 of the heptapeptide repeats at the RNA Pol II CTD, required for transcription initiation (Kim et al., 2006). In this context, TFIIH is also necessary to separate the double-stranded DNA and allow RNA pol II access to the single-stranded DNA template.

4.2 RNA Pol II Pausing

Loading of RNA Pol II to promoters has long been considered the main rate-limiting step in gene transcription. Back in the 1987, pioneering work on HIV-1 transcription began to challenge this view (Kao et al., 1987) but only much later genome-wide approaches that tracked RNA Pol II on the DNA and monitored production of nascent transcripts, have revealed that at the majority of genes transcriptional regulation takes place at the level of RNA pol II pausing and its release into productive elongation (Adelman and Lis, 2012) reviewed in Guo and Price (2013) and Jonkers and Lis (2015). Under basal conditions, transcription is initiated but RNA Pol II elongation is restricted (Fig. 2). Shortly after elongation, RNA Pol II pauses and accumulates on the HIV-1 proximal promoter producing only short

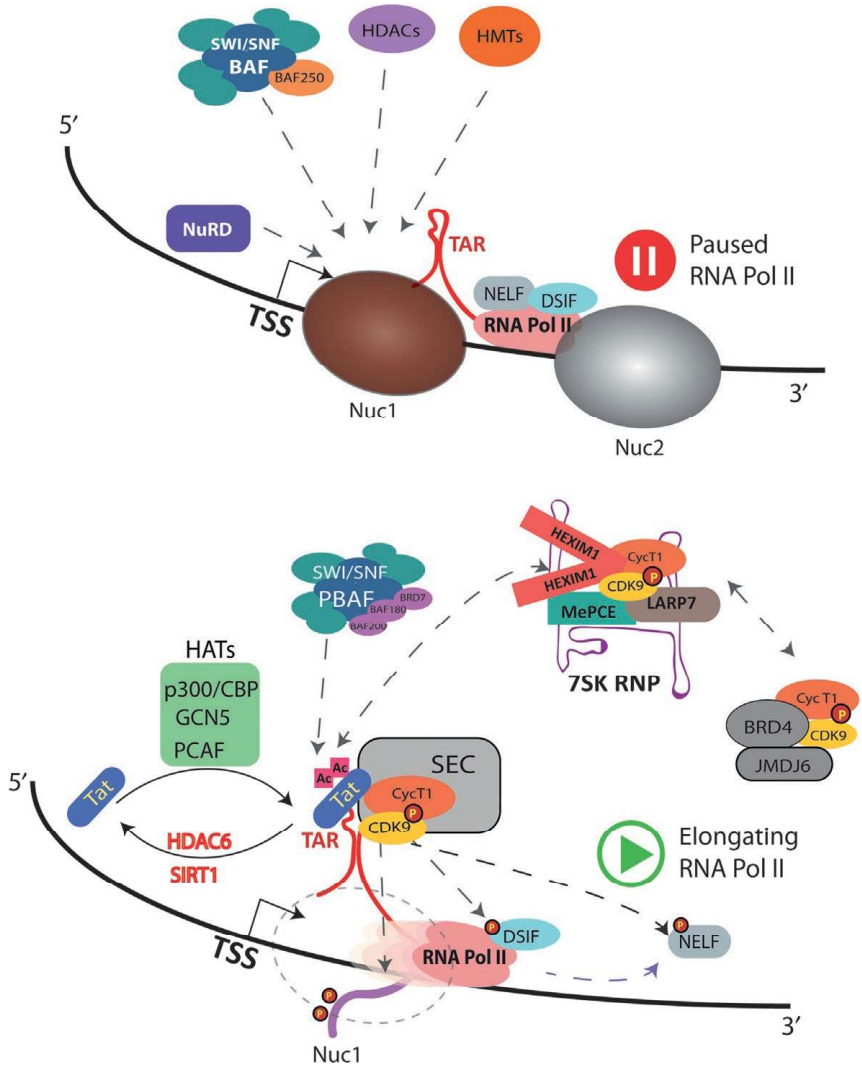

Fig. 2 Regulation of HIV-1 promoter transcriptional activity by Tat and coactivators. HIV-1 Tat recruits pTEFb from its inactive reservoir within the 7SK snRNP–Hexim1 complex to the TAR RNA stem loop structure and together with other components of the SEC phosphorylates the DSIFs and NELFs resulting in release of Pol II pausing and activates transcriptional elongation via phosphorylation of the CTD of RNA Pol II and stimulation of its activity. Tat also associates with various cofactors, which modulate its interaction with TAR and pTEFb via Tat modifications, maintaining its activity and remodeling chromatin to facilitate elongation.

transcripts. Owing to the promoter proximal pausing of RNA pol II, the HIV-1 provirus, is primed for a rapid transcriptional response (Jadlowsky et al., 2014). While RNA pol II pausing initially seemed to be an HIV-1-specific regulatory mechanism it is now known to be common at

inducible cellular genes that require fast or synchronous activation (Adelman and Lis, 2012; Hargreaves et al., 2009). In this process two strong inhibitors of elongation (negative elongation factor) NELF and (DRB sensitivity-inducing factor) DSIF cooperatively stabilize the interaction of RNA pol II with DNA, halting elongation of the transcript (Fig. 2). In latent cells, the 3′-end processing protein Pcf11 is then recruited via a direct interaction with NELF which induces premature dissociation of RNA pol II from the DNA template (Cheng and Price, 2008; Jadlowsky et al., 2014; Natarajan et al., 2013; Yamaguchi et al., 1999; Zhang et al., 2007). DSIF, a heterodimer of Spt4 and Spt5, is recruited to the nascent RNA molecules and promotes capping (Cheng and Price, 2008; Missra and Gilmour, 2010; Wen and Shatkin, 1999). Spt5 binds to nascent RNA and in turn recruits NELF (Yamaguchi et al., 2002), generating a configuration in which the transcription complex has limited chance to escape the proximal promoter site, inducing premature termination of elongation within a range of a few 100 nucleotides (Renner et al., 2001). In agreement, depletion of NELF results in enhanced basal HIV-1 transcription and reduced latency (Jadlowsky et al., 2014; Natarajan et al., 2013; Zhang et al., 2007).

Despite many similarities, this regulatory mechanism has some HIV-1-specific features that distinguish it from regulation at endogenous genes. A prominent characteristic is that transcription elongation control at the HIV-1 promoter is much more efficient than typically observed at cellular promoters (Kim et al., 2011). Additionally, the efficiency of elongation in the presence of Tat is also exceptionally high, much higher than typically observed at endogenous genes (Kim et al., 2011). At the HIV-1 promoter, premature termination of elongation produces an abundant 59 nucleotides transcript (Kao et al., 1987). Such high levels of Pol II promoter proximal pausing are not commonly observed at endogenous genes. The nascent RNA forms a unique stem-loop secondary structure referred as TAR element, which is recognized by the transcriptional transactivating protein (Tat) (Fig. 2). The TAR RNA loop region contains an NBE-like element (CUGGGA) similar to the E binding element (CUGAGGA) associated with transcriptionally paused genes. This element may lead to enhanced recruitment of NELF to the HIV-1 5′-LTR (Pagano et al., 2014). Another peculiarity of HIV-1 5′-LTR transcription is that multiple pausing sites exist downstream of the TSS. These features reinforce the pausing signals to ensure silencing of the promoter by decreasing likelihood of RNA Pol II entering into the elongation phase to produce full-length transcripts (Jadlowsky et al., 2014).

5. TRANSCRIPTIONAL ELONGATION

5.1 P-TEFb and the SEC

In order to establish a productive cycle of viral replication, the transcription elongation block has to be removed. Expression of the viral protein Tat at sufficient levels disrupts the NELF- and DSIF-dependent inhibition, induces the recruitment of coactivating factors, the most critical being the SEC (Fig. 2). These events efficiently remove the block in transcription elongation and establish a Tat positive feedback loop in which Tat is rapidly upregulated and strongly pushes HIV-1 transcription toward activation (Karn, 2011; Mbonye and Karn, 2014; Ott et al., 2011). Once more, transcriptional regulation of the integrated HIV-1 provirus proved to be an excellent model system for studying general transcription and was instrumental in elucidating the molecular mechanisms that control RNA pol II elongation. In vitro reconstitution of RNA Pol II transcription elongation demonstrated that Tat strongly activates HIV-1 expression by recruiting the host P-TEFb complex, a heterodimer kinase composed of CDK9 and its regulatory partner cyclin (primarily cyclin T1 and T2a/T2b), to the TAR region of the HIV promoter (Wei et al., 1998). At the TAR region, Tat and P-TEFb form a protein–RNA complex with the TAR RNA stem-loop located at the 5′-end of all nascent viral transcripts. P-TEFb phosphorylates NELF (Fujinaga et al., 2004), releasing it from the complex, and DSIF (Ping and Rana, 2001), converting it to a positive factor, counteracting the inhibitory activity of the complex on RNA pol II elongation (Fig. 2) (Lu et al., 2013; Ott et al., 2011). Additionally P-TEFb phosphorylates Ser-2 on the CTD of RNA pol II, thereby improving its processivity, promoting the coupling between transcription, and RNA processing and the recruitment of chromatin modifying factors (Barboric and Lenasi, 2010; Bentley, 2014; Ping and Rana, 2001; Schüller et al., 2016; Zhou et al., 2012). These key phosphorylation events cause the release of the paused RNA Pol II and induce the elongation phase of transcription.

Later studies have shown that P-TEFb, although essential for Tat-mediated activation of HIV-1 transcription, is not the only player involved in promoting RNA pol II elongation and it is not sufficient to support full Tat-dependent activation (Lu et al., 2014; Suñé et al., 2000). Affinity purification of P-TEFb and Tat, followed by mass spectrometry analysis led to the identification of a multiprotein complex of cellular elongation factors and coactivators, referred to as SEC, that cooperatively stimulate HIV-1

transcription (He et al., 2010; Sobhian et al., 2010). Tat-mediated recruitment of SEC is a potent mechanism to counteract transcriptional pausing and strongly activate transcriptional elongation (Fig. 2). The SEC consists of the scaffold proteins AFF1 to AFF4 (Lu et al., 2015), the elongation factors ELL1 to ELL3 and several additional partners AF9, ENL, and EAF1/2. AFF4 and AFF1 have short hydrophobic domains distributed along a flexible axis that mediates interaction with the other subunits of the complex (Chou et al., 2013; He et al., 2011). AFF4 makes direct contact with Tat and the surface of cyclin T1 (Schulze-Gahmen et al., 2013, 2014) and the cooperative interaction between those subunits, AFF1 and AFF2, which reside in separate complexes, enhance Tat's affinity for P-TEFb with AFF1-SEC predominantly involved in supporting Tat-mediated transactivation of the HIV promoter (Lu et al., 2015).

5.2 Control of P-TEFb Activity

In order to control transcriptional elongation, the activity of P-TEFb has to be tightly regulated in vivo and this is achieved by PTMs of its components CycT1 and CDK9 (Fig. 2) (Budhiraja et al., 2013; Ramakrishnan et al., 2009; Tyagi et al., 2010). The mTOR complex acts as a repressor of HIV-1 transcription in part by interfering with CDK9 phosphorylation (Besnard et al., 2016). Conversely interaction of CycT1/CDK9 with the 7SK small nuclear ribonucleoprotein complex (7SK snRNP) limits P-TEFb activity and availability at gene promoters (Fig. 2) (He et al., 2008; Nguyen et al., 2001; Van Herreweghe et al., 2007; Yang et al., 2001; Yik et al., 2003). The fraction of P-TEFb molecules bound to the 7SK snRNP varies per cell type: in HeLa cells it is about half in normal growing conditions (Nguyen et al., 2001; Yang et al., 2001) while it can reach 90% in Jurkat T cells or PBMCs (Barboric et al., 2007; Kim et al., 2011). Within the complex, the 7SK snRNA is a scaffold for two molecules of P-TEFb complexed with homo or heterodimers of the inhibitory proteins HEXIM1 or HEXIM2 (Li et al., 2005; Peterlin et al., 2012). LARP7 binds to the 3′ uridine-rich terminus of 7SK-snRNA to protect it from degradation by nucleases, while the enzyme MEPCE stabilizes 7SK snRNA by adding a methyl-phosphate cap to its 5′ terminus (He et al., 2008; Jeronimo et al., 2007; Krueger et al., 2008). More recently it was shown that AFF1 and AFF4 are also partners of P-TEFb in the 7SK snRNP complex (Lu et al., 2014). When sequestered within the 7SK snRNP complex, P-TEFb is activated by phosphorylation of Thr186 in the CDK9 T loop, but its association

with HEXIM1 blocks ATP binding, hence inhibiting its activity (Li et al., 2005). Within the complex, P-TEFb is also physically restrained, which prevents it from participating in the regulation of gene transcription (Chen et al., 2003). Therefore, in this configuration, the activity of P-TEFb is inhibited but kept in a preactivated form, fully ready to promote elongation upon release from the 7SK snRNP complex (Fig. 2).

5.3 Chromatin Association of the 7SK snRNP

As the 7SK snRNP complex is the major reservoir of transcriptionally inactive P-TEFb, significant effort has been made to determine how it engages with the transcriptional machinery to enable the transition into transcriptional elongation. HIV-1 transcription studies were the first to suggest that the 7SK snRNP complex is anchored to chromatin (Barboric and Lenasi, 2010; D'Orso and Frankel, 2010), with the HEXIM1 and LARP7 subunits cooccupying the HIV-1 core promoter with P-TEFb. This finding was later extended to stimulus-dependent primary response genes (McNamara et al., 2013) and verified genome-wide, through chromatin isolation by RNA purification and sequencing (ChIRP-seq) (Flynn et al., 2016; Liu et al., 2013). In murine embryonic stem cells and human cells, the 7SK snRNP complex has been shown to occupy about 3500 active protein-coding genes along the entire transcribed region with peaks, in accordance with RNA pol II occupancy, at the TSSs and transcriptional elongation sites (TESs). The presence of 7SK snRNA has been detected at active enhancers as well, particularly super enhancers. Considering cooccupancy and interaction studies (Das et al., 2007; D'Orso and Frankel, 2010), it was suggested that RNA pol II acts as a recruitment platform for 7SK snRNP at transcribed genes. More recent findings, however, described the different mechanism by which snRNP is likely to be recruited. The repressive chromatin mark H4R3me2 is recognized and bound by the 5′-terminal half of 7SK at a subclass of enhancers cooccupied by Brd4 and JMJD6 (Liu et al., 2013). Also, Kruppel-associated box-interacting protein KAP1 (TRIM28/TIF1β) could be involved in loading 7SK snRNP to promoter proximal regions containing paused Pol II (McNamara et al., 2016). Additionally, a specific subset of 7SK snRNP contains the transcriptional repressor CTIP2 which together with HEXIM1 and the 7SK enhances inhibition of P-TEFb (Cherrier et al., 2013). Recruitment of this subset of highly repressive 7SK snRNPs to HIV-1 and other promoters is suggested to occur via the nonhistone chromatin protein HMGA1 that interacts with CTIP2 and 7SK within the

snRNP complex (Eilebrecht et al., 2013). HIC1 has also recently been shown to be a corepressor of HIV-1 Tat-dependent transcription in complex with HMGA1 and CTIP2 (Le Douce et al., 2016).

5.4 Regulation of P-TEFb Availability

Upon stress-induced response or cellular stimuli that alter cell growth, P-TEFb is rapidly released from 7SK RNP complexes and recruited to active genes. Different signal transduction pathways converge to single components to prevent or disrupt the assembly into 7SK snRNP. In response to T-cell receptor activation, HEXIM1 is phosphorylated at Serine 158 within the 7SK binding region by protein kinase C-ϑ and its ability to bind CycT1 and 7SK is compromised (Fujinaga et al., 2012). Additionally, the unstructured region of HEXIM1 contains Ser/Thr/Tyr target residues, which when phosphorylated, via PI3K/Akt and ERK pathways, abolish HEXIM1–P-TEFb interaction (Contreras et al., 2007; Kim et al., 2011; Mbonye et al., 2015). Expression of HEXIM1 harboring mutations that abrogate phosphorylation of its unstructured C-terminal coiled coil affects the release of P-TEFb from 7SK snRNP and reduces P-TEFb occupancy at the HIV-1 promoter, thereby compromising viral transcription (Contreras et al., 2007; Mbonye et al., 2015). The HAT enzyme p300 also contributes to release of P-TEFb by acetylating lysine residues in the CycT1 coiled-coil domain, inducing dissociation of P-TEFb from HEXIM1 (Cho et al., 2009). Other factors involved in mobilization of P-TEFb, HNRNPA1, HNRNPA2 (Barrandon et al., 2007; Van Herreweghe et al., 2007), SRSF2 (Ji et al., 2013), and DDX21 (Calo et al., 2014) seem to collectively link the release of P-TEFb with elongation and RNA processing.

While the modifications and factors mentioned above contribute to mobilizing P-TEFb without affecting the integrity of the complex, the release of P-TEFb from chromatin-associated 7SK snRNP at enhancers, which are also bound by Brd4-JMJD6, is different. Here, JMJD6 demethylase activity causes the removal of the H4R3me2 repressive chromatin mark and the 5′ 7SK methyl cap, abolishing recruitment of 7SK and alters the stability of 7SK and the 7SK snRNP complex (Liu et al., 2013). Upon release from the 7SK snRNP complex, P-TEFb binds JMJD6 and Brd4 and is loaded on active genes promoters marked by acetylated chromatin, to promote RNA pol II elongation (Fig. 2) (Bisgrove et al., 2007; Chen et al., 2004; Jang et al., 2005; Yang et al., 2005). Formation

of the HIV-1 Tat/P-TEFb complex was found to be restrained by P-TEFb association with chromatin-bound Brd4 as knockdown of Brd4 in latently infected cells or treatment with the bromodomain inhibitor JQ1, resulted in increased release of P-TEFb, and a markedly enhanced Tat-dependent activation of HIV-1 (Bartholomeeusen et al., 2012; Boehm et al., 2013; Mbonye et al., 2013; Zhu et al., 2012). Interestingly, Brd2 has also been reported to repress the activity of the HIV-1 promoter, although the mechanism here seems to be independent of Tat as the effect has also been observed in latently infected cell lines that do not express the HIV-1 transactivator (Boehm et al., 2013).

Tat can also liberate P-TEFb from the 7SK snRNP complex by competing and displacing HEXIM1 binding to CycT1 (Fig. 2) (Barboric et al., 2007; Krueger et al., 2010; Sedore et al., 2007). There is strikingly similarity between the P-TEFb–HEXIM1–7SK binding configuration, within the 7SK RNP complex, and P-TEFb binding to Tat-TAR (Yik et al., 2004). The 7SK binding arginine-rich motif (ARM) of HEXIM1 and the TAR binding ARM of Tat are highly similar (Yik et al., 2004), while 7SK HEXIM1 binding elements are very similar to the minimal consensus structure on TAR (Muniz et al., 2010). Both Tat and HEXIM1 contain a CycT1 binding site and bind CycT1 in a mutually exclusive fashion (Anand et al., 2007; Michels et al., 2004). Tat binding, through its ARM, was shown to displace HEXIM1 from 7SK (Muniz et al., 2010) and via its CycT1 binding domain outcompetes HEXIM1 binding to P-TEFb (Fig. 2) (Barboric et al., 2007). In this process, interaction with AFF1 assists Tat by further increasing its affinity for P-TEFb (Lu et al., 2014).

5.5 Tat Coregulators

In addition to SEC, Tat-dependent transcriptional activation is accompanied by recruitment of transcriptional coactivators and chromatin remodelers which also contribute to strong enhancement of transcription from the HIV-1 promoter (Ott et al., 2011). Tat has been shown to bind and recruit HATs p300/CBP, GCN5, and PCAF to the HIV-1 5′-LTR (Ahmad and Venkatesan, 1988; Benkirane et al., 1998; Col et al., 2001; Deng et al., 2001; Lusic et al., 2003; Marzio et al., 1998; Vendel and Lumb, 2003) which, by acetylation of histone tails, contributes to establishment of a more accessible chromatin environment for transcription (Easley et al., 2010a). Aside from histones, HATs can acetylate and regulate the activity of TFs (Jeng et al., 2015). Upon Tat-dependent recruitment, for example,

p300/CBP acetylates the p50 subunit of NF-κB (Furia et al., 2002), thereby increasing its binding affinity and most likely the ability to enhance HIV-1 transcription in the context of p50–p65 heterodimer (Deng et al., 2003).

Tat itself is modified by PTMs including phosphorylation, acetylation, ubiquitination, and methylation, which generates a "Tat-code" that determines its binding partners, most critically its interaction with P-TEFb and TAR. Tat can be acetylated at lysine residues 28, 50, and 51 (D'Orso and Frankel, 2010; Kiernan et al., 1999; Ott et al., 1999), ubiquitinated (Brès et al., 2003; Zhang et al., 2014), or undergo methylation at lysines 50 and 51 and arginine residues 52 and 53 (Ott et al., 1999; Van Duyne et al., 2011; Xie et al., 2007). Additionally, Tat can undergo CDK2-dependent inhibitory phosphorylation on Serines 16 and 46 (Ammosova et al., 2006). Methyl-transferase Set7/9 methylates Tat at Lys51, enhancing HIV-1 transcription, subsequently Tat is demethylated by LSD1 ensuring the recycling of Tat in an activation cycle (Pagans et al., 2010; Sakane et al., 2011). Polyubiquitination of Tat Lys71, which is Hdm2 dependent, promotes Tat-dependent transactivation (Brès et al., 2003). The acetyl-transferase P300 acetylates Tat at Lys50 and Lys51 inducing dissociation from TAR. PCAF is subsequently recruited to acetylated lys50 and acetylates Tat at Lys 28 which increases its affinity for P-TEFb during transcriptional elongation while HDAC6-dependent deacetylation allows its release from P-TEFb and TAR leading to the beginning of a new cycle of transcription (Brès et al., 2003; Huo et al., 2011; Kiernan et al., 1999; Pagans et al., 2005). Additionally, acetylated Lys50 allows Tat-mediated recruitment of the PBAF chromatin remodeling complex to the LTR (Agbottah et al., 2006; Mahmoudi et al., 2006; Ott et al., 1999; Tréand et al., 2006). This occurs via the PBAF complex subunits BAF180 and BRG1 contain bromodomains that can recognize and bind acetylated Tat (ac-Tat) (Fig. 2) (Agbottah et al., 2006; Easley et al., 2010b; Mahmoudi et al., 2006; Rafati et al., 2011; Van Duyne et al., 2011). Tat-dependent recruitment of the PBAF complex is likely to enhance productive elongation as in the absence of the catalytic subunit BRM prematurely terminated RNA transcripts have been shown to accumulate at the HIV-1 promoter (Mizutani et al., 2009). In line with this model, it has been reported that depletion of the BAF-specific subunit BAF250 does not affect Tat-dependent activation, whereas depletion of BAF200 and BAF180, PBAF-specific subunits, result in impaired HIV-1 transcription (Easley et al., 2010b; Rafati et al., 2011). ChIP experiments have additionally demonstrated that, upon activation, binding of the BAF250

subunit to the HIV-1 5′-LTR is rapidly abrogated while PBAF subunits BAF200 and BAF180 are recruited at the promoter (Rafati et al., 2011; Van Duyne et al., 2011). Moreover, acetylated Tat Lys 50 and 51 allow interaction with bromodomain containing proteins (Dorr et al., 2002; Mujtaba et al., 2002). Among these proteins, BRD4 was shown to diminish P-TEFb availability thus negatively regulating HIV-1 transcription. BRD4, therefore, competes with Tat for interaction and prevents P-TEFb from elongation of transcription (Bartholomeeusen et al., 2012; Bisgrove et al., 2007; Mbonye et al., 2013).

Given the magnitude of the Tat transcriptional feedback loop and Tat-driven epigenetic changes at the viral promoter, strategies aiming at selective inhibition of Tat activity may promote the establishment of a persistent silencing of the HIV-1 promoter, referred as "deep latency" (Mousseau and Valente, 2012; Mousseau et al., 2015a). This alternative approach has been explored in several studies with encouraging results (reviewed in Mousseau and Valente, 2012; Mousseau et al., 2015a). As a proof of concept, recent studies using didehydro-cortistatin A (dCA), a specific inhibitor of Tat-TAR binding, have shown that dCA treatment in the presence of c-ART leads to the establishment of a stronger transcriptional silencing, with lower propensity to reactivation in in vitro and ex vivo models. Importantly, it has been observed in a primary cell model of latency that treatment with dCA has a long lasting inhibitory effect on transcription even after its removal, suggesting that in the absence of Tat activity the HIV-1 promoter may undergo epigenetic changes that promote stronger repression (Mousseau et al., 2015b).

6. STOCHASTICITY IN TRANSCRIPTION

Throughout this review, we have described gene expression and cell fate as a merely deterministic process. Indeed, in the majority of cases, the complex interplay of regulatory mechanisms we have introduced determines the activity of a promoter and ultimately the cell fate. Similarly, for HIV infections, these layers of regulation cooperatively determine latent vs productive infections. There are cases though where cells seem to choose their fate without an apparent cause, stochastically. The main reason is that gene transcription and ultimately expression do not have a perfect "switch" but it is subjected to a certain degree of noise. This phenomenon is clearly revealed for the HIV-1 promoter by the observation that monoclonal Jurkat cell lines

harboring latent HIV-1-derived virus integrated at a single integration site display a nonuniform basal transcriptional state during latency and also in response to activation signals. Thus a population of identical cells shows variability in basal HIV-1 promoter activity as demonstrated by the percentage of cells expressing the GFP reporter gene, and in response to activating stimuli where a percentage but not all of the latent cells undergo transcription elongation to express GFP.

6.1 Noise in Basal Transcription

Noise in transcription originates from transitions between on and off states at the promoter. In the off state, the RNA polymerase II pauses on the HIV-1 proximal promoter but when the block is removed, multiple RNA polymerase units simultaneously read the gene's open reading frame (Tantale et al., 2016), resulting in a burst of RNA transcripts (Dar et al., 2012; Singh et al., 2010). This amplification originates from a mechanism of mediator-dependent reinitiation of transcription. According to this model, after a burst, RNA Pol II molecules rapidly initiate transcription but also can undergo rapid escape from the promoter without fruitful elongation such that the promoter stochastically switches from an on to an off state (Tantale et al., 2016). Oscillations in gene expression also result from random differences in the timing of the process, fluctuations in the availability of RNA polymerases and TFs, differences in cell size, asymmetric distribution, and availability of cellular factors following cell division and other factors (Kaern et al., 2005; Miller-Jensen et al., 2011; Raj and van Oudenaarden, 2008; Raser, 2010; Swain et al., 2002). The chromatin environment at the gene regulatory regions is also considered to be a determinant factor for controlling transcriptional noise (Miller-Jensen et al., 2011). In general, when the gene regulatory regions are accessible and the TSS is free from nucleosomes, transcription can occur relatively freely and more frequently. Conversely, when the chromatin is in a condensed state, transcription is less likely to occur (Raj and van Oudenaarden, 2008). Different studies have suggested that chromatin-related events can alter the grade of stochasticity of gene expression (Dey et al., 2015; Raser and Shea, 2006). It has been observed by electron microscopy in budding yeast that, at the steady state, there is an intrinsically stochastic component that regulates the configurational variation of nucleosomes at gene promoters.

6.2 Modulation of Noise

Transcriptional noise is the driving force of stochastic events but it is not sufficient, per se, to produce an effect. In order for an event to occur stochastically, a mechanism is necessary that stabilizes and possibly amplifies the response to the noise (Losick and Desplan, 2008). HIV-1 has this mechanism. The potent HIV-1 transactivator Tat protein can trigger a positive feedback loop to induce its own expression 50–100-fold (Chavez et al., 2015; Singh and Weinberger, 2009; Weinberger et al., 2005). Even small probabilistic fluctuations in Tat expression can, therefore, by amplification, be determinant and shift the equilibrium from latency to replication. Stochastic fluctuations in the regulatory mechanisms that control HIV-1 transcription can, therefore, influence viral latency. In this light HIV-1 expression is an excellent model system to study the intrinsically stochastic nature of transcription.

A deterministic explanation for the fact that the provirus is more prone to remain silent in resting memory CD4+ T cells, the major reservoir of latently HIV-1-infected cells, is that, due to their resting state, some key cellular TFs such as NF-AT and NF-κB, are sequestered in the cytoplasm and depleted from the nucleus. As a consequence, transcription initiation and elongation do not occur. T cell activation can indeed reverse latency. However, studies show that despite multiple rounds of maximum in vitro activation, latent proviruses remain inactive in a substantial number of cells (Ho et al., 2013) and that the Tat-positive feedback can control latency independently of the cell activation state (Razooky et al., 2015), suggesting that reactivation has a stochastic component. It has been observed in that even in clonal populations of latently infected cell lines there is a probabilistic distribution of cells expressing low to high levels of Tat (Burnett et al., 2009; Miller-Jensen et al., 2013). Transcriptional noise from the HIV-1 promoter is, therefore, likely the cause of stochastic reactivation (Weinberger and Weinberger, 2013). Stochastic variability in HIV expression represents a tremendous obstacle for strategies aiming to reactivate latent HIV to deplete the viral reservoir. It has been estimated that a 10,000-fold depletion of the reservoir is required to prevent viremia rebound in 50% of the patients, after interrupting cART (Hill et al., 2014). An interesting strategy to control HIV-1 expression, taking stochasticity into account, is to look for noise modulating molecules instead of activators only. Transcriptional activators typically activate transcription by improving transcriptional initiation efficiency, hence increasing the frequency of transcriptional events

(Dar et al., 2012; Singh et al., 2010). Noise modulating molecules instead act on elongation, increasing and decreasing the duration of the on state, thereby influencing the magnitude of the burst. Dar et al. have shown that noise enhancing molecules alone, or together with traditional activators, can reactivate latent cells significantly better than existing LRA cocktails while noise suppressing molecules can stabilize latency (Dar et al., 2014).

7. HIV-1 TRANSCRIPTION REGULATION IN THE NUCLEAR 3D ENVIRONMENT

Transcription of genes, and hence the integrated HIV-1 provirus, does not take place on a linear chromatin template but instead involves intricate long range chromatin interactions between regulatory elements (Splinter and de Laat, 2011). At the gene level, the active HIV-1 provirus forms a looped chromatin structure mediated by a direct interaction between the 5′- and 3′-LTRs (Fig. 3) (Perkins et al., 2008). It has long been known that transcription initiation is intimately linked to transcription end processing. The existence of gene loops was first inferred from genetic data obtained from yeast screens. These studies demonstrated a genetic interaction between the promoter bound basal TF TFIIB and Ssu72 (Sun and Hampsey, 1996) that later turned out to be a component of the 3′-end processing complex (He et al., 2003). Similarly, in mammalian cells, a direct interaction between the transcriptional coactivator PC4 and CstF-64, another component of the 3′-end processing complex, was found (Calvo and Manley, 2001). The first promoter–terminator interactions through chromatin looping were described for the yeast FMP27 gene (O'Sullivan et al., 2004) and a direct role for 3′-end processing factors in gene loop formation was demonstrated (Ansari and Hampsey, 2005). The occurrence of gene loops in mammalian cells was first demonstrated for the integrated HIV-1 provirus (Perkins et al., 2008). HIV-1 gene loop formation is linked to transcriptional initiation and elongation since the interaction between the 5′-LTR promoter region and the 3′-LTR polyadenylation signal was induced by activation of the HIV-1 provirus by either TPA treatment or overexpression of the Tat transactivator (Perkins et al., 2008). Conversely, pharmacological inhibition of the P-TEFb with flavopyridol resulted in the collapse of the gene loop suggesting that gene loops are unstable and dependent on ongoing transcription (Perkins et al., 2008). HIV-1 gene loop formation relies on both intact 5′-promoter and 3′-end processing sequences.

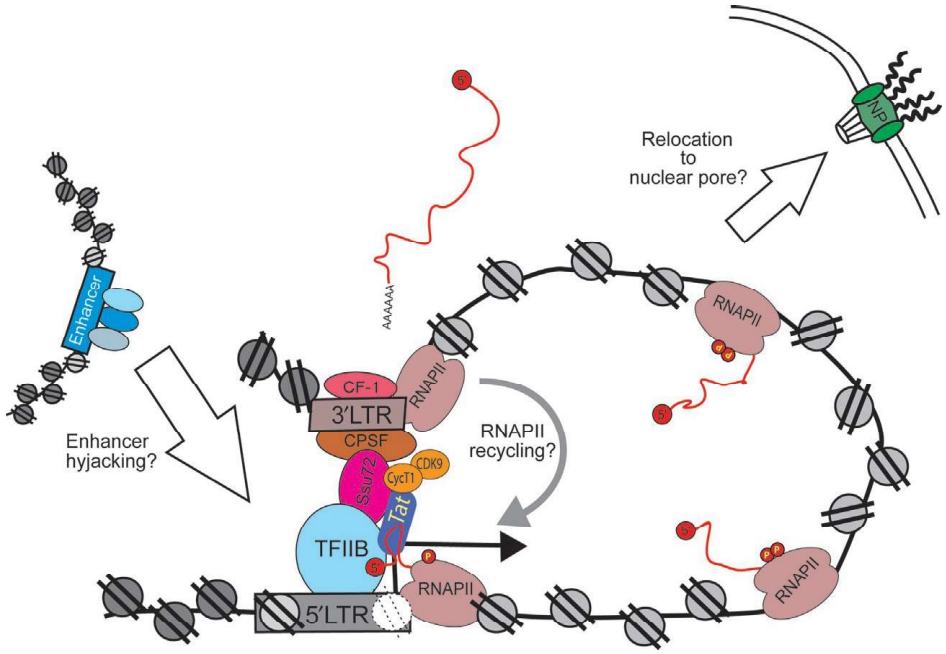

Fig. 3 A model for gene looping of the HIV-1 provirus and its interaction with the 3D nuclear space. The active HIV-1 provirus forms a looped chromatin structure mediated by a direct interaction of factors bound to the 5′- and 3′-LTRs such as the promoter bound basal transcription factor TFIIB and Ssu72 bound to the 3′-LTR. HIV-1 Tat transactivator bound to the TAR sequence also directly interacts with Ssu72 potentially consolidates gene loop formation. Gene looping facilitated RNAPII recycling could aid transcriptional reinitiation and suppress divergent transcription or stochasticity of expression. It has been suggested that HIV-1 gene loop formation induces relocalization of the HIV-1 provirus to nuclear pores which boosts transcriptional output and stability and facilitates nuclear export of HIV-1 proviral RNA. Endogenous enhancer sequences could potentially modulate HIV1 expression if they are hijacked by the HIV-1 provirus.

However, gene loop formation is not a unique feature of HIV-1 proviruses as replacement of viral promoter and end processing sequences with heterologous elements still supported gene looping (Perkins et al., 2008). This observation suggested that gene loop formation is a universal feature of transcription and indeed it was later demonstrated that the endogenous human BRCA1 (Tan-Wong et al., 2008) and CD68 (O'Reilly and Greaves, 2007) genes also form gene loops. Gene looping in yeast is dependent both on factors bound to the promoter and on 3′-end processing complex subunit components like, e.g., Ssu72 (El Kaderi et al., 2009; Medler et al., 2011). Interestingly, the HIV-1 Tat transactivator directly interacts with Ssu72 and stimulates viral gene expression (Fig. 3) (Chen et al., 2014) but a direct role in HIV-1 gene loop formation remains to be demonstrated.

The functional significance of gene loops is currently not clear especially since gene looping appears to depend on transcription. Conversely, loss of looping does not seem to have a major impact on transcription (Hampsey et al., 2011). It has been suggested that gene looping plays a role in suppression of divergent transcription (Grzechnik et al., 2014; Tan-Wong et al., 2012) and provides "transcriptional memory" by targeting the locus to the nuclear pore (Hampsey et al., 2011; Pascual-Garcia et al., 2017; Tan-Wong et al., 2008). Recent research has also revealed that interactions between the nuclear pore complex, chromatin, and the transcriptional machinery regulates transcriptional activation, elongation, and mRNA processing (Ptak et al., 2014). These mechanisms could all potentially influence latency reversal, stochastic expression, and transcriptional output of the HIV-1 provirus (Fig. 3). Interestingly, the HIV-1 virus tends to integrate into the peripheral nuclear compartment presumably in the vicinity of nuclear pores (Lusic and Siliciano, 2017). Integrated HIV-1 proviruses can efficiently be transcribed when located at the nuclear periphery (Dieudonné et al., 2009) and depletion of the nuclear pore component TPR has a strong impact on HIV-1 provirus expression (Lelek et al., 2015). Therefore it is possible that HIV-1 gene loop formation integrates local chromatin organization with the spatial distribution of the HIV-1 provirus to nuclear pores which results in boosted transcriptional output and stability and additionally facilitates nuclear export of HIV-1 proviral RNA (Fig. 3).

Although HIV-1 preferentially integrates into gene-dense regions and active genes, the site of integration still strongly influences viral expression (Lusic and Siliciano, 2017). Integration in or close to heterochromatic regions or a direct interaction in trans with such regions or other repressive compartments leads to clear position effects on the transcriptional output of the HIV-1 provirus and contributes to latency establishment (Dieudonné et al., 2009; Jordan et al., 2001; Lusic and Siliciano, 2017; Lusic et al., 2013). A recent study using barcoded HIV-1 viruses demonstrated that HIV-1 proviruses integrated proximal to endogenous enhancers are expressed at a higher level than those located in other genomic regions (Chen et al., 2016). The same study also found that latent proviruses are integrated further from enhancers than their active counterparts and that distance to these endogenous regulatory elements also determined the response to different latency reversal agents (Chen et al., 2016). These results suggest that HIV1 expression is not only susceptible to the chromatin

environment and availability of TFs but is also subject to regulation by endogenous enhancers (Fig. 3).

The emerging picture is that the 3D chromatin organization and nuclear positioning of the integrated HIV-1 provirus play a crucial part in its transcriptional regulation (Fig. 3). However, direct biophysical evidence supporting a role for gene looping and nuclear positioning in regulation of HIV-1 gene transcription in in vivo-infected patient cells is currently lacking. Also at the mechanistic level questions still remain; e.g., what is the exact role and mechanism of HIV-1 gene loop formation and what is its connection to nuclear positioning? It will also be interesting to know whether the HIV-1 provirus "highjacks" the activity of endogenous regulatory elements by engaging in a direct long range chromatin interaction with enhancers, or do these elements contribute in another way to an increased transcriptional potency of the HIV-1 provirus, e.g., by maintaining a permissive chromatin environment.

8. CONCLUDING REMARKS

The HIV-1 genome does not encode all the factors necessary for its own transcription. Therefore, upon integration into the host cell genome, HIV-1 gene expression, similar to endogenous genes, is regulated by host cellular TFs and the basal transcription machinery. The molecular control of HIV-1 transcription has been intensely studied from a clinical perspective with the aim to cure HIV patients using for example latency reversal therapies. However, the HIV provirus has also been a popular model system to study fundamental aspects of eukaryotic transcriptional regulation. Groundbreaking discoveries related to, e.g., recruitment of TFs, posttranscriptional modification, and remodeling of nucleosomes, recruitment of the basal transcriptional machinery, RNA polymerase II pausing, gene looping, and positioning of gene loci within the nuclear space have been made using this system. It is the unique interplay between clinical driven and fundamental research that has advanced our knowledge of transcriptional regulation and provided valuable insight toward development of alternative strategies for therapies aimed at eradicating both latent and active HIV-1.

ACKNOWLEDGMENTS

This work was supported by two Dutch "Aids Fonds" grants (2014021 and P-12001), the mRACE ErasmusMC grant, and the ERC starting grant (337116—Trxn-PURGE).

REFERENCES

Adelman, K., Lis, J.T., 2012. Promoter-proximal pausing of RNA polymerase II: emerging roles in metazoans. Nat. Rev. Genet. 13 (10), 720–731.

Agbottah, E., et al., 2006. Effect of SWI/SNF chromatin remodeling complex on HIV-1 Tat activated transcription. Retrovirology 3 (1), 48.

Agosto, L., Gagne, M., Henderson, A., 2015. Impact of chromatin on HIV replication. Genes 6 (4), 957–976.

Ahmad, N., Venkatesan, S., 1988. Nef protein of HIV-1 is a transcriptional repressor of HIV-1 LTR. Science (New York, NY) 241 (4872), 1481–1485.

Albert, I., et al., 2007. Translational and rotational settings of H2A.Z nucleosomes across the Saccharomyces cerevisiae genome. Nature 446 (7135), 572–576.

Alcamí, J., et al., 1995. Absolute dependence on kappa B responsive elements for initiation and Tat-mediated amplification of HIV transcription in blood CD4 T lymphocytes. EMBO J. 14 (7), 1552–1560.

Ammosova, T., et al., 2006. Phosphorylation of HIV-1 tat by CDK2 in HIV-1 transcription. Retrovirology 3 (1), 78.

Anand, K., et al., 2007. Cyclin box structure of the P-TEFb subunit cyclin T1 derived from a fusion complex with EIAV Tat. J. Mol. Biol. 370 (5), 826–836.

Ansari, A., Hampsey, M., 2005. A role for the CPF 3′-end processing machinery in RNAP II-dependent gene looping. Genes Dev. 19 (24), 2969–2978.

Archin, N.M., et al., 2009. Expression of latent human immunodeficiency type 1 is induced by novel and selective histone deacetylase inhibitors. AIDS 23 (14), 1799–1806.

Arya, S., et al., 1985. Trans-activator gene of human T-lymphotropic virus type III (HTLV-III). Science 229 (4708), 69–73.

Bachu, M., Mukthey, A.B., et al., 2012a. Sequence insertions in the HIV type 1 subtype C viral promoter predominantly generate an additional NF-κB binding site. AIDS Res. Hum. Retroviruses 28 (10), 1362–1368.

Bachu, M., Yalla, S., et al., 2012b. Multiple NF-κB sites in HIV-1 subtype C long terminal repeat confer superior magnitude of transcription and thereby the enhanced viral predominance. J. Biol. Chem. 287 (53), 44714–44735.

Badalà, F., Nouri-mahdavi, K., Raoof, D.A., 2008. NIH public access. Computer 144 (5), 724–732.

Barboric, M., Lenasi, T., 2010. Kick-sTARting HIV-1 transcription elongation by 7SK snRNP deporTATion. Nat. Struct. Mol. Biol. 17 (8), 928–930.

Barboric, M., et al., 2007. Tat competes with HEXIM1 to increase the active pool of P-TEFb for HIV-1 transcription. Nucleic Acids Res. 35 (6), 2003–2012.

Barrandon, C., et al., 2007. The transcription-dependent dissociation of P-TEFb-HEXIM1-7SK RNA relies upon formation of hnRNP-7SK RNA complexes. Mol. Cell. Biol. 27 (20), 6996–7006.

Barski, A., et al., 2007. High-resolution profiling of histone methylations in the human genome. Cell 129 (4), 823–837.

Bartholomeeusen, K., et al., 2012. Bromodomain and extra-terminal (BET) Bromodomain inhibition activate transcription via transient release of positive transcription elongation factor b (P-TEFb) from 7SK small nuclear ribonucleoprotein. J. Biol. Chem. 287 (43), 36609–36616.

Barton, K.M., et al., 2014. Selective HDAC inhibition for the disruption of latent HIV-1 infection. PLoS One 9 (8), e102684.

Barton, K., et al., 2016. Broad activation of latent HIV-1 in vivo. Nat. Commun. 7, 12731.

Benkirane, M., et al., 1998. Activation of integrated provirus requires histone acetyltransferase: p300 and P/CAF are coactivators for HIV-1 tat. J. Biol. Chem. 273 (38), 24898–24905.

Bentley, D.L., 2014. Coupling mRNA processing with transcription in time and space. Nat. Rev. Genet. 15 (3), 163–175.
Berkhout, B., Silverman, R.H., Jeang, K.T., 1989. Tat trans-activates the human immunodeficiency virus through a nascent RNA target. Cell 59 (2), 273–282.
Bernstein, B.E., et al., 2004. Global nucleosome occupancy in yeast. Genome Biol. 5 (9), R62.
Besnard, E., et al., 2016. The mTOR complex controls HIV latency. Cell Host Microbe 20 (6), 785–797.
Bialek, J.K., et al., 2016. Targeted HIV-1 latency reversal using CRISPR/Cas9-derived transcriptional activator systems. PLoS One 11 (6), e0158294.
Bisgrove, D.A., et al., 2007. Conserved P-TEFb-interacting domain of BRD4 inhibits HIV transcription. Proc. Natl. Acad. Sci. 104 (34), 13690–13695.
Bjorndal, A., et al., 1999. Phenotypic characteristics of human immunodeficiency virus type 1 subtype C isolates of Ethiopian AIDS patients. AIDS Res. Hum. Retroviruses 15 (7), 647–653.
Blazkova, J., et al., 2009. CpG methylation controls reactivation of HIV from latency. PLoS Pathog. 5 (8), e1000554.
Blazkova, J., et al., 2012. Paucity of HIV DNA methylation in latently infected, resting CD4+ T cells from infected individuals receiving antiretroviral therapy. J. Virol. 86 (9), 5390–5392.
Boehm, D., et al., 2013. BET bromodomain-targeting compounds reactivate HIV from latency via a Tat-independent mechanism. Cell Cycle 12 (3), 452–462.
Bosque, A., Planelles, V., 2009. Induction of HIV-1 latency and reactivation in primary memory CD4+ T cells. Blood 113 (1), 58–65.
Boyle, A.P., et al., 2011. High-resolution genome-wide in vivo footprinting of diverse transcription factors in human cells. Genome Res. 21 (3), 456–464.
Brès, V., et al., 2003. A non-proteolytic role for ubiquitin in Tat-mediated transactivation of the HIV-1 promoter. Nat. Cell Biol. 5 (8), 754–761.
Bruce, J.W., et al., 2013. ZASC1 stimulates HIV-1 transcription elongation by recruiting P-TEFb and TAT to the LTR promoter. PLoS Pathog. 9 (10), e1003712.
Budhiraja, S., et al., 2013. Cyclin T1 and CDK9 T-loop phosphorylation are downregulated during establishment of HIV-1 latency in primary resting memory CD4+ T cells. J. Virol. 87 (2), 1211–1220.
Burger, S., Poles, M.A., 2003. Natural history and pathogenesis of human immunodeficiency virus infection. Semin. Liver Dis. 23 (2), 115–124.
Burke, T.W., Kadonaga, J.T., 1996. Drosophila TFIID binds to a conserved downstream basal promoter element that is present in many TATA-box-deficient promoters. Genes Dev. 10 (6), 711–724.
Burke, T.W., Kadonaga, J.T., 1997. The downstream core promoter element, DPE, is conserved from drosophila to humans and is recognized by TAFII60 of drosophila. Genes Dev. 11 (22), 3020–3031.
Burnett, J.C., et al., 2009. Control of stochastic gene expression by host factors at the HIV promoter. PLoS Pathog. 5 (1), e1000260.
Burnett, J.C., et al., 2010. Combinatorial latency reactivation for HIV-1 subtypes and variants. J. Virol. 84 (12), 5958–5974.
Calo, E., et al., 2014. RNA helicase DDX21 coordinates transcription and ribosomal RNA processing. Nature 518 (7538), 249–253.
Calvo, O., Manley, J.L., 2001. Evolutionarily conserved interaction between CstF-64 and PC4 links transcription, polyadenylation, and termination. Mol. Cell 7 (5), 1013–1023.
Cary, D.C., et al., 2016. Molecular mechanisms of HIV latency. J. Clin. Investig. 126 (2), 448–454.
Chaudhary, P., et al., 2016. HSP70 binding protein 1 (HspBP1) suppresses HIV-1 replication by inhibiting NF-κB mediated activation of viral gene expression. Nucleic Acids Res. 44 (4), 1613–1629.

Chavez, L., et al., 2015. HIV latency is established directly and early in both resting and activated primary CD4 T cells. PLoS Pathog. 11 (6), e1004955.
Chen, R., Yang, Z., Zhou, Q., 2003. Phosphorylated positive transcription elongation factor b (P-TEFb) is tagged for inhibition through association with 7SK snRNA. J. Biol. Chem. 279 (6), 4153–4160.
Chen, R., Yang, Z., Zhou, Q., 2004. Phosphorylated positive transcription elongation factor b (P-TEFb) is tagged for inhibition through association with 7SK snRNA. J. Biol. Chem. 279 (6), 4153–4160.
Chen, Y., et al., 2014. A gene-specific role for the Ssu72 RNAPII CTD phosphatase in HIV-1 Tat transactivation. Genes Dev. 28 (20), 2261–2275.
Chen, H.-C., et al., 2016. Position effects influence HIV latency reversal. Nat. Struct. Mol. Biol. 24 (1), 47–54.
Cheng, B., Price, D.H., 2008. Analysis of factor interactions with RNA polymerase II elongation complexes using a new electrophoretic mobility shift assay. Nucleic Acids Res. 36 (20), e135.
Chen-Park, F.E., et al., 2002. The kappa B DNA sequence from the HIV long terminal repeat functions as an allosteric regulator of HIV transcription. J. Biol. Chem. 277 (27), 24701–24708.
Cherrier, T., et al., 2013. CTIP2 is a negative regulator of P-TEFb. Proc. Natl. Acad. Sci. U.S.A. 110 (31), 12655–12660.
Cho, S., et al., 2009. Acetylation of cyclin T1 regulates the equilibrium between active and inactive P-TEFb in cells. EMBO J. 28 (10), 1407–1417.
Chou, S., et al., 2013. HIV-1 Tat recruits transcription elongation factors dispersed along a flexible AFF4 scaffold. Proc. Natl. Acad. Sci. U.S.A. 110 (2), E123–31.
Clapier, C.R., Cairns, B.R., 2009. The biology of chromatin remodeling complexes. Annu. Rev. Biochem. 78 (1), 273–304.
Col, E., et al., 2001. The histone acetyltransferase, hGCN5, interacts with and acetylates the HIV transactivator, Tat. J. Biol. Chem. 276 (30), 28179–28184.
Contreras, X., et al., 2007. HMBA releases P-TEFb from HEXIM1 and 7SK snRNA via PI3K/Akt and activates HIV transcription. PLoS Pathog. 3 (10), e146.
Coull, J.J., et al., 2000. The human factors YY1 and LSF repress the human immunodeficiency virus type 1 long terminal repeat via recruitment of histone deacetylase 1. J. Virol. 74 (15), 6790–6799.
Craigie, R., Bushman, F.D., 2012. HIV DNA integration. Cold Spring Harb. Perspect. Med. 2 (7), a006890.
Cramer, P., 2004. RNA polymerase II structure: from core to functional complexes. Curr. Opin. Genet. Dev. 14 (2), 218–226.
Cron, R.Q., et al., 2000. NFAT1 enhances HIV-1 gene expression in primary human CD4 T cells. Clin. Immunol. 94 (3), 179–191.
Cullen, B.R., Lomedico, P.T., Ju, G., 1984. Transcriptional interference in avian retroviruses—implications for the promoter insertion model of leukaemogenesis. Nature 307 (5948), 241–245.
D'Orso, I., Frankel, A.D., 2010. RNA-mediated displacement of an inhibitory snRNP complex activates transcription elongation. Nat. Struct. Mol. Biol. 17 (7), 815–821.
Dahabieh, M.S., Battivelli, E., Verdin, E., 2015. Understanding HIV latency: the road to an HIV cure. Annu. Rev. Med. 66 (1), 407–421.
Dahiya, S., et al., 2014. CCAAT enhancer binding protein and nuclear factor of activated T cells regulate HIV-1 LTR via a novel conserved downstream site in cells of the monocyte-macrophage lineage. PLoS One 9 (2), e88116.
Dar, R.D., et al., 2012. Transcriptional burst frequency and burst size are equally modulated across the human genome. Proc. Natl. Acad. Sci. 109 (43), 17454–17459.
Dar, R.D., et al., 2014. Screening for noise in gene expression identifies drug synergies. Science 344 (6190), 1392–1396.

Das, R., et al., 2007. SR proteins function in coupling RNAP II transcription to pre-mRNA splicing. Mol. Cell 26 (6), 867–881.
De Crignis, E., Mahmoudi, T., 2014. HIV eradication: combinatorial approaches to activate latent viruses. Virus 6 (11), 4581–4608.
De Crignis, E., Mahmoudi, T., 2017. The multifaceted contributions of chromatin to HIV-1 integration, transcription, and latency. Int. Rev. Cell Mol. Biol. 328, 197–252.
Deeks, S.G., 2012. HIV: Shock and kill. Nature 487 (7408), 439–440.
Demarchi, F., et al., 1993. In vivo footprinting analysis of constitutive and inducible protein-DNA interactions at the long terminal repeat of human immunodeficiency virus type 1. J. Virol. 67 (12), 7450–7460.
Demarchi, F., et al., 1996. Activation of transcription factor NF-kappaB by the Tat protein of human immunodeficiency virus type 1. J. Virol. 70 (7), 4427–4437.
Deng, L., et al., 2001. Enhancement of the p300 HAT activity by HIV-1 Tat on chromatin DNA. Virology 289 (2), 312–326.
Deng, W.-G., Zhu, Y., Wu, K.K., 2003. Up-regulation of p300 binding and p50 acetylation in tumor necrosis factor-alpha-induced cyclooxygenase-2 promoter activation. J. Biol. Chem. 278 (7), 4770–4777.
Dey, S.S., et al., 2015. Orthogonal control of expression mean and variance by epigenetic features at different genomic loci. Mol. Syst. Biol. 5 (5), 806.
Dieudonné, M., et al., 2009. Transcriptional competence of the integrated HIV-1 provirus at the nuclear periphery. EMBO J. 28 (15), 2231–2243.
Dingwall, C., et al., 1989. Human immunodeficiency virus 1 tat protein binds trans-activation-responsive region (TAR) RNA in vitro. Proc. Natl. Acad. Sci. U.S.A. 86 (18), 6925–6929.
Donahue, D.A., et al., 2013. Cellular and molecular mechanisms involved in the establishment of HIV-1 latency. Retrovirology 10 (1), 11.
Dorr, A., et al., 2002. Transcriptional synergy between Tat and PCAF is dependent on the binding of acetylated Tat to the PCAF bromodomain. EMBO J. 21 (11), 2715–2723.
du Chéné, I., et al., 2007. Suv39H1 and HP1gamma are responsible for chromatin-mediated HIV-1 transcriptional silencing and post-integration latency. EMBO J. 26 (2), 424–435.
Duckett, C.S., et al., 1993. Dimerization of NF-KB2 with RelA(p65) regulates DNA binding, transcriptional activation, and inhibition by an I kappa B-alpha (MAD-3). Mol. Cell. Biol. 13 (3), 1315–1322.
Duverger, A., et al., 2013. An AP-1 binding site in the enhancer/core element of the HIV-1 promoter controls the ability of HIV-1 to establish latent infection. J. Virol. 87 (4), 2264–2277.
Dynlacht, B.D., Hoey, T., Tjian, R., 1991. Isolation of coactivators associated with the TATA-binding protein that mediate transcriptional activation. Cell 66 (3), 563–576.
Easley, R., Carpio, L., et al., 2010a. Transcription through the HIV-1 nucleosomes: effects of the PBAF complex in Tat activated transcription. Virology 405 (2), 322–333.
Easley, R., Van Duyne, R., et al., 2010b. Chromatin dynamics associated with HIV-1 Tat-activated transcription. Biochim. Biophys. Acta 1799 (3–4), 275–285.
Eilebrecht, S., et al., 2013. HMGA1 directly interacts with TAR to modulate basal and Tat-dependent HIV transcription. RNA Biol. 10 (3), 436–444.
El Kaderi, B., et al., 2009. Gene looping is conferred by activator-dependent interaction of transcription initiation and termination machineries. J. Biol. Chem. 284 (37), 25015–25025.
el Kharroubi, A., Martin, M.A., 1996. cis-Acting sequences located downstream of the human immunodeficiency virus type 1 promoter affect its chromatin structure and transcriptional activity. Mol. Cell. Biol. 16 (6), 2958–2966.
el Kharroubi, A., Verdin, E., 1994. Protein-DNA interactions within DNase I-hypersensitive sites located downstream of the HIV-1 promoter. J. Biol. Chem. 269 (31), 19916–19924.

Emanuel, P.A., Gilmour, D.S., 1993. Transcription factor TFIID recognizes DNA sequences downstream of the TATA element in the Hsp70 heat shock gene. Proc. Natl. Acad. Sci. U.S.A. 90 (18), 8449–8453.
Engelman, A., Cherepanov, P., 2012. The structural biology of HIV-1: mechanistic and therapeutic insights. Nat. Rev. Microbiol. 10 (4), 279–290.
Epstein, F.H., et al., 1993. The Immunopathogenesis of human immunodeficiency virus infection. N. Engl. J. Med. 328 (5), 327–335.
Finzi, D., et al., 1999. Latent infection of CD4+ T cells provides a mechanism for lifelong persistence of HIV-1, even in patients on effective combination therapy. Nat. Med. 5 (5), 512–517.
Flores, O., et al., 1999. Host-cell positive transcription elongation factor b kinase activity is essential and limiting for HIV type 1 replication. Proc. Natl. Acad. Sci. U.S.A. 96 (13), 7208–7213.
Flynn, R.A., et al., 2016. 7SK-BAF axis controls pervasive transcription at enhancers. Nat. Struct. Mol. Biol. 23 (3), 231–238.
Freed, E.O., 2001. HIV-1 replication. Somat. Cell Mol. Genet. 26 (1–6), 13–33.
Freed, E.O., 2015. HIV-1 assembly, release and maturation. Nat. Rev. Microbiol. 13 (8), 484–496.
Friedman, J., et al., 2011. Epigenetic silencing of HIV-1 by the histone H3 lysine 27 methyltransferase enhancer of Zeste 2. J. Virol. 85 (17), 9078–9089.
Fujinaga, K., et al., 2004. Dynamics of human immunodeficiency virus transcription: P-TEFb phosphorylates RD and dissociates negative effectors from the transactivation response element. Mol. Cell. Biol. 24 (2), 787–795.
Fujinaga, K., et al., 2012. PKC phosphorylates HEXIM1 and regulates P-TEFb activity. Nucleic Acids Res. 40 (18), 9160–9170.
Fujita, T., et al., 1992. Independent modes of transcriptional activation by the p50 and p65 subunits of NF-kappa B. Genes Dev. 6 (5), 775–787.
Furia, B., et al., 2002. Enhancement of nuclear factor-kappa B acetylation by coactivator p300 and HIV-1 Tat proteins. J. Biol. Chem. 277 (7), 4973–4980.
Gadad, S.S., et al., 2011. The multifunctional protein nucleophosmin (NPM1) is a human linker histone H1 chaperone. Biochemistry 50 (14), 2780–2789.
Gallastegui, E., et al., 2011. Chromatin reassembly factors are involved in transcriptional interference promoting HIV latency. J. Virol. 85 (7), 3187–3202.
Garcia, J.A., et al., 1989. Human immunodeficiency virus type 1 LTR TATA and TAR region sequences required for transcriptional regulation. EMBO J. 8 (3), 765–778.
Gaynor, R., 1992. Cellular transcription factors involved in the regulation of HIV-1 gene expression. AIDS (London, England) 6 (4), 347–363.
Gerritsen, M.E., et al., 1997. CREB-binding protein/p300 are transcriptional coactivators of p65. Proc. Natl. Acad. Sci. U.S.A. 94 (7), 2927–2932.
Giffin, M.J., et al., 2003. Structure of NFAT1 bound as a dimer to the HIV-1 LTR κB element. Nat. Struct. Biol. 10 (10), 800–806.
Gill, G., et al., 1994. A glutamine-rich hydrophobic patch in transcription factor Sp1 contacts the dTAFII110 component of the drosophila TFIID complex and mediates transcriptional activation. Proc. Natl. Acad. Sci. U.S.A. 91 (1), 192–196.
Grzechnik, P., Tan-Wong, S.M., Proudfoot, N.J., 2014. Terminate and make a loop: regulation of transcriptional directionality. Trends Biochem. Sci. 39 (7), 319–327.
Guillemette, B., et al., 2005. Variant histone H2A.Z is globally localized to the promoters of inactive yeast genes and regulates nucleosome positioning. PLoS Biol. 3 (12), e384.
Guo, J., Price, D.H., 2013. RNA polymerase II transcription elongation control. Chem. Rev. 113 (11), 8583–8603.
Hampsey, M., et al., 2011. Control of eukaryotic gene expression: gene loops and transcriptional memory. Adv. Enzyme Regul. 51 (1), 118–125.

Hargreaves, D.C., Horng, T., Medzhitov, R., 2009. Control of inducible gene expression by signal-dependent transcriptional elongation. Cell 138 (1), 129–145.
Hauber, J., Malim, M.H., Cullen, B.R., 1989. Mutational analysis of the conserved basic domain of human immunodeficiency virus Tat protein. J. Virol. 63 (3), 1181–1187.
He, X., Fütterer, J., Hohn, T., 2002. Contribution of downstream promoter elements to transcriptional regulation of the rice tungro bacilliform virus promoter. Nucleic Acids Res. 30 (2), 497–506.
He, X., et al., 2003. Functional interactions between the transcription and mRNA 3′ end processing machineries mediated by Ssu72 and Sub1. Genes Dev. 17 (8), 1030–1042.
He, N., et al., 2008. A La-related protein modulates 7SK snRNP integrity to suppress P-TEFb-dependent transcriptional elongation and tumorigenesis. Mol. Cell 29 (5), 588–599.
He, N., et al., 2010. HIV-1 Tat and host AFF4 recruit two transcription elongation factors into a bifunctional complex for coordinated activation of HIV-1 transcription. Mol. Cell 38 (3), 428–438.
He, N., et al., 2011. Human polymerase-associated factor complex (PAFc) connects the super elongation complex (SEC) to RNA polymerase II on chromatin. Proc. Natl. Acad. Sci. 108 (36), E636–E645.
Henderson, A.J., Zou, X., Calame, K.L., 1995. C/EBP proteins activate transcription from the human immunodeficiency virus type 1 long terminal repeat in macrophages/monocytes. J. Virol. 69 (9), 5337–5344.
Henikoff, S., 2008. Nucleosome destabilization in the epigenetic regulation of gene expression. Nat. Rev. Genet. 9 (1), 15–26.
Hill, A.L., et al., 2014. Predicting the outcomes of treatment to eradicate the latent reservoir for HIV-1. Proc. Natl. Acad. Sci. 111 (37), 13475–13480.
Hirose, Y., Ohkuma, Y., 2007. Phosphorylation of the C-terminal domain of RNA polymerase II plays central roles in the integrated events of Eucaryotic gene expression. J. Biochem. 141 (5), 601–608.
Ho, Y.-C., Shan, L., Hosmane, N.N., et al., 2013. Replication-competent noninduced proviruses in the latent reservoir increase barrier to HIV-1 cure. Cell 155, 540–551.
Hoey, T., et al., 1993. Molecular cloning and functional analysis of drosophila TAF110 reveal properties expected of coactivators. Cell 72 (2), 247–260.
Hu, W.-S., Hughes, S.H., 2012. HIV-1 reverse transcription. Cold Spring Harb. Perspect. Med. 2 (10), a006882.
Huang, L.M., Jeang, K.T., 1993. Increased spacing between Sp1 and TATAA renders human immunodeficiency virus type 1 replication defective: implication for Tat function. J. Virol. 67 (12), 6937–6944.
Huang, H., et al., 2015. FACT proteins, SUPT16H and SSRP1, are transcriptional suppressors of HIV-1 and HTLV-1 that facilitate viral latency. J. Biol. Chem. 290 (45), 27297–27310.
Huber, K., et al., 2011. Inhibitors of histone deacetylases: correlation between isoform specificity and reactivation of HIV type 1 (HIV-1) from latently infected cells. J. Biol. Chem. 286 (25), 22211–22218.
Hunt, G., Tiemessen, C.T., 2000. Occurrence of additional NF-kappaB-binding motifs in the long terminal repeat region of south African HIV type 1 subtype C isolates. AIDS Res. Hum. Retroviruses 16 (3), 305–306.
Huo, L., et al., 2011. Regulation of tat acetylation and transactivation activity by the microtubule-associated deacetylase HDAC6. J. Biol. Chem. 286 (11), 9280–9286.
Imai, K., Okamoto, T., 2006. Transcriptional repression of human immunodeficiency virus type 1 by AP-4. J. Biol. Chem. 281 (18), 12495–12505.
Imai, K., Togami, H., Okamoto, T., 2010. Involvement of histone H3 lysine 9 (H3K9) methyltransferase G9a in the maintenance of HIV-1 latency and its reactivation by BIX01294. J. Biol. Chem. 285 (22), 16538–16545.

Jadlowsky, J.K., et al., 2014. Negative elongation factor is required for the maintenance of proviral latency but does not induce promoter-proximal pausing of RNA polymerase II on the HIV long terminal repeat. Mol. Cell. Biol. 34 (11), 1911–1928.
Jang, M.K., et al., 2005. The bromodomain protein Brd4 is a positive regulatory component of P-TEFb and stimulates RNA polymerase II-dependent transcription. Mol. Cell 19 (4), 523–534.
Jeeninga, R.E., et al., 2000. Functional differences between the long terminal repeat transcriptional promoters of human immunodeficiency virus type 1 subtypes A through G. J. Virol. 74 (8), 3740–3751.
Jeng, M.Y., Ali, I., Ott, M., 2015. Manipulation of the host protein acetylation network by human immunodeficiency virus type 1. Crit. Rev. Biochem. Mol. Biol. 50 (4), 314–325.
Jeronimo, C., et al., 2007. Systematic analysis of the protein interaction network for the human transcription machinery reveals the identity of the 7SK capping enzyme. Mol. Cell 27 (2), 262–274.
Ji, X., et al., 2013. SR proteins collaborate with 7SK and promoter-associated nascent RNA to release paused polymerase. Cell 153 (4), 855–868.
Ji, H., et al., 2016. Specific reactivation of latent HIV-1 by dCas9-SunTag-VP64-mediated guide RNA targeting the HIV-1 promoter. Mol. Ther. 24 (3), 508–521.
Jiang, G., et al., 2007. C-Myc and Sp1 contribute to proviral latency by recruiting histone deacetylase 1 to the human immunodeficiency virus type 1 promoter. J. Virol. 81 (20), 10914–10923.
Jones, K.A., Peterlin, M.B., 1994. Control of RNA initiation and elongation at the HIV-1 promoter. Annu. Rev. Biochem. 63 (1), 717–743.
Jones, K.a., et al., 1986. Activation of the AIDS retrovirus promoter by the cellular transcription factor, Sp1. Science (New York, NY) 232 (1966), 755–759.
Jonkers, I., Lis, J.T., 2015. Getting up to speed with transcription elongation by RNA polymerase II. Nat. Rev. Mol. Cell Biol. 16 (3), 167–177.
Jordan, A., Defechereux, P., Verdin, E., 2001. The site of HIV-1 integration in the human genome determines basal transcriptional activity and response to Tat transactivation. EMBO J. 20 (7), 1726–1738.
Kadonaga, J.T., 2012. Perspectives on the RNA polymerase II core promoter. Wiley Interdiscip. Rev. Dev. Biol. 1 (1), 40–51.
Kaern, M., et al., 2005. Stochasticity in gene expression: from theories to phenotypes. Nat. Rev. Genet. 6 (6), 451–464.
Kao, S.-Y.Y., et al., 1987. Anti-termination of transcription within the long terminal repeat of HIV-1 by tat gene product. Nature 330 (6147), 489–493.
Karn, J., 2011. The molecular biology of HIV latency: breaking and restoring the Tat-dependent transcriptional circuit. Curr. Opin. HIV AIDS 6 (1), 4–11.
Kauder, S.E., et al., 2009. Epigenetic regulation of HIV-1 latency by cytosine methylation. PLoS Pathog. 5 (6), e1000495.
Keedy, K.S., et al., 2009. A limited group of class I histone deacetylases acts to repress human immunodeficiency virus type 1 expression. J. Virol. 83 (10), 4749–4756.
Kharytonchyk, S., et al., 2016. Transcriptional start site heterogeneity modulates the structure and function of the HIV-1 genome. Proc. Natl. Acad. Sci. 113 (47), 13378–13383.
Kiernan, R.E., et al., 1999. HIV-1 tat transcriptional activity is regulated by acetylation. EMBO J. 18 (21), 6106–6118.
Kilareski, E.M., et al., 2009. Regulation of HIV-1 transcription in cells of the monocyte-macrophage lineage. Retrovirology 6 (1), 118.
Kim, J.Y., et al., 1993. Replication of type 1 human immunodeficiency viruses containing linker substitution mutations in the −201 to −130 region of the long terminal repeat. J. Virol. 67 (3), 1658–1662.

Kim, M., et al., 2006. Distinct pathways for sno RNA and mRNA termination. Mol. Cell 24 (5), 723–734.
Kim, Y.K., et al., 2011. T-cell receptor signaling enhances transcriptional elongation from latent HIV proviruses by activating P-TEFb through an ERK-dependent pathway. J. Mol. Biol. 410 (5), 896–916.
Kinoshita, S., et al., 1997. The T cell activation factor NF-ATc positively regulates HIV-1 replication and gene expression in T cells. Immunity 6 (3), 235–244.
Kinoshita, S., et al., 1998. Host control of HIV-1 parasitism in T cells by the nuclear factor of activated T cells. Cell 95 (5), 595–604.
Klaver, B., Berkhout, B., 1994. Comparison of 5′ and 3′ long terminal repeat promoter function in human immunodeficiency virus. J. Virol. 68 (6), 3830–3840.
Kobor, M.S., Greenblatt, J., 2002. Regulation of transcription elongation by phosphorylation. Biochim. Biophys. Acta 1577 (2), 261–275.
Koken, S.E., et al., 1992. Natural variants of the HIV-1 long terminal repeat: analysis of promoters with duplicated DNA regulatory motifs. Virology 191 (2), 968–972.
Kouzarides, T., 2007. Chromatin modifications and their function. Cell 128 (4), 693–705.
Krebs, F.C., Goodenow, M.M., Wigdahl, B., 1997. Neuroglial ATF/CREB factors interact with the human immunodeficiency virus type 1 long terminal repeat. J. Neurovirol. 3 (Suppl. 1), S28–32.
Krebs, F.C., et al., 1998. Human immunodeficiency virus type 1 long terminal repeat quasispecies differ in basal transcription and nuclear factor recruitment in human glial cells and lymphocytes. J. Biomed. Sci. 5 (1), 31–44.
Kretzschmar, M., et al., 1992. Transcriptional regulation of the HIV-1 promoter by NF-kappaB in vitro. Genes Dev. 6, 761–774.
Krueger, B.J., et al., 2008. LARP7 is a stable component of the 7SK snRNP while P-TEFb, HEXIM1 and hnRNP A1 are reversibly associated. Nucleic Acids Res. 36 (7), 2219–2229.
Krueger, B.J., et al., 2010. The mechanism of release of P-TEFb and HEXIM1 from the 7SK snRNP by viral and cellular activators includes a conformational change in 7SK. PLoS One 5 (8), e12335.
Kumar, A., et al., 2015. Epigenetic control of HIV-1 post integration latency: implications for therapy. Clin. Epigenetics 7 (1), 103.
Le Douce, V., et al., 2016. HIC1 controls cellular- and HIV-1-gene transcription via interactions with CTIP2 and HMGA1. Sci. Rep. 6, 34920.
Lee, C.-K., et al., 2004. Evidence for nucleosome depletion at active regulatory regions genome-wide. Nat. Genet. 36 (8), 900–905.
Lelek, M., et al., 2015. Chromatin organization at the nuclear pore favours HIV replication. Nat. Commun. 6, 6483.
Li, E., Zhang, Y., 2014. DNA methylation in mammals. Cold Spring Harb. Perspect. Biol. 6 (5), a019133.
Li, Y., Mak, G., Franza, B.R. 1994. In vitro study of functional involvement of Sp1, NF-κB/Rel, and AP1 in phorbol 12-myristate 13-acetate-mediated HIV-1 long terminal repeat activation. J. Biol. Chem., 269 (48), 30616–30619.
Li, Q., et al., 2005. Analysis of the large inactive P-TEFb complex indicates that it contains one 7SK molecule, a dimer of HEXIM1 or HEXIM2, and two P-TEFb molecules containing Cdk9 phosphorylated at threonine 186. J. Biol. Chem. 280 (31), 28819–28826.
Liang, C., et al., 1997. Sequence elements downstream of the human immunodeficiency virus type 1 long terminal repeat are required for efficient viral gene transcription. J. Mol. Biol. 272 (2), 167–177.
Liebert, M.A., et al., 2002. Characterization of the south African HIV type 1 subtype C complete 59 long terminal repeat, nef, and regulatory genes. AIDS Res. Hum. Retroviruses 18 (2), 149–159.

Limsirichai, P., Gaj, T., Schaffer, D.V., 2016. CRISPR-mediated activation of latent HIV-1 expression. Mol. Ther. 24 (3), 499–507.
Lin, R., Gewert, D., Hiscott, J., 1995. Differential transcriptional activation in vitro by NF-kappa B/Rel proteins. J. Biol. Chem. 270 (7), 3123–3131.
Liu, W., et al., 2013. Brd4 and JMJD6-associated anti-pause enhancers in regulation of transcriptional pause release. Cell 155 (7), 1581–1595.
Losick, R., Desplan, C., 2008. Stochasticity and cell fate. Science (New York, NY) 320 (5872), 65–68.
Lu, Y., et al., 1989. Effects of long terminal repeat mutations on human immunodeficiency virus type 1 replication. J. Virol. 63 (9), 4115–4119.
Lu, H., et al., 2013. Viral–host interactions that control HIV-1 transcriptional elongation. Chem. Rev. 113 (11), 8567–8582.
Lu, H., et al., 2014. AFF1 is a ubiquitous P-TEFb partner to enable Tat extraction of P-TEFb from 7SK snRNP and formation of SECs for HIV transactivation. Proc. Natl. Acad. Sci. U.S.A. 111 (1), E15–24.
Lu, H., et al., 2015. Gene target specificity of the super elongation complex (SEC) family: how HIV-1 Tat employs selected SEC members to activate viral transcription. Nucleic Acids Res. 43 (12), 5868–5879.
Luger, K., Richmond, T.J., 1998. The histone tails of the nucleosome. Curr. Opin. Genet. Dev. 8 (2), 140–146.
Lusic, M., Siliciano, R.F., 2017. Nuclear landscape of HIV-1 infection and integration. Nat. Rev. Microbiol. 15 (2), 69–82.
Lusic, M., et al., 2003. Regulation of HIV-1 gene expression by histone acetylation and factor recruitment at the LTR promoter. EMBO J. 22 (24), 6550–6561.
Lusic, M., et al., 2013. Proximity to PML nuclear bodies regulates HIV-1 latency in CD4+ T cells. Cell Host Microbe 13 (6), 665–677.
Maartens, G., Celum, C., Lewin, S.R., 2014. HIV infection: epidemiology, pathogenesis, treatment, and prevention. Lancet 384 (9939), 258–271.
Macian, F., Rao, A., 1999. Reciprocal modulatory interaction between human immunodeficiency virus type 1 Tat and transcription factor NFAT1. Mol. Cell. Biol. 19 (5), 3645–3653.
Mahmoudi, T., 2012. The BAF complex and HIV latency. Transcription 3 (4), 171–176.
Mahmoudi, T., et al., 2006. The SWI/SNF chromatin-remodeling complex is a cofactor for Tat transactivation of the HIV promoter. J. Biol. Chem. 281 (29), 19960–19968.
Marban, C., et al., 2005. COUP-TF interacting protein 2 represses the initial phase of HIV-1 gene transcription in human microglial cells. Nucleic Acids Res. 33 (7), 2318–2331.
Marban, C., et al., 2007. Recruitment of chromatin-modifying enzymes by CTIP2 promotes HIV-1 transcriptional silencing. EMBO J. 26 (2), 412–423.
Marfella, C.G.A., Imbalzano, A.N., 2007. The Chd family of chromatin remodelers. Mutat. Res. 618 (1–2), 30–40.
Margolis, D.M., 2011. Histone deacetylase inhibitors and HIV latency. Curr. Opin. HIV AIDS 6 (1), 25–29.
Margolis, D.M., et al., 2016. Latency reversal and viral clearance to cure HIV-1. Science (New York, NY) 353 (6297), aaf6517.
Maricato, J.T., et al., 2015. Epigenetic modulations in activated cells early after HIV-1 infection and their possible functional consequences. PLoS One 10 (4), e0119234.
Marzio, G., et al., 1998. HIV-1 Tat transactivator recruits p300 and CREB-binding protein histone acetyltransferases to the viral promoter. Proc. Natl. Acad. Sci. U.S.A. 95 (23), 13519–13524.
Masuda, A., et al., 2015. Position-specific binding of FUS to nascent RNA regulates mRNA length. Genes Dev. 29 (10), 1045–1057.

Matsuda, Y., et al., 2015. Epigenetic heterogeneity in HIV-1 latency establishment. Sci. Rep. 5, 7701.
Mavrich, T.N., et al., 2008. A barrier nucleosome model for statistical positioning of nucleosomes throughout the yeast genome. Genome Res. 18 (7), 1073–1083.
Mbonye, U., Karn, J., 2014. Transcriptional control of HIV latency: cellular signaling pathways, epigenetics, happenstance and the hope for a cure. Virology 454–455, 328–339.
Mbonye, U.R., et al., 2013. Phosphorylation of CDK9 at Ser175 enhances HIV transcription and is a marker of activated P-TEFb in CD4+ T lymphocytes. PLoS Pathog. 9 (5), e1003338.
Mbonye, U.R., et al., 2015. Phosphorylation of HEXIM1 at Tyr271 and Tyr274 promotes release of P-TEFb from the 7SK snRNP complex and enhances proviral HIV gene expression. Proteomics 15 (12), 2078–2086.
McNamara, R.P., et al., 2013. Transcription factors mediate the enzymatic disassembly of promoter-bound 7SK snRNP to locally recruit P-TEFb for transcription elongation. Cell Rep. 5 (5), 1256–1268.
McNamara, R.P., et al., 2016. KAP1 recruitment of the 7SK snRNP complex to promoters enables transcription elongation by RNA polymerase II. Mol. Cell 61 (1), 39–53.
Medler, S., et al., 2011. Evidence for a complex of transcription factor IIB (TFIIB) with poly(a) polymerase and cleavage factor 1 subunits required for gene looping. J. Biol. Chem. 286 (39), 33709–33718.
Michels, A.A., et al., 2004. Binding of the 7SK snRNA turns the HEXIM1 protein into a P-TEFb (CDK9/cyclin T) inhibitor. EMBO J. 23 (13), 2608–2619.
Miller-Jensen, K., et al., 2011. Varying virulence: epigenetic control of expression noise and disease processes. Trends Biotechnol. 29 (10), 517–525.
Miller-Jensen, K., et al., 2013. Genetic selection for context-dependent stochastic phenotypes: Sp1 and TATA mutations increase phenotypic noise in HIV-1 gene expression. PLoS Comput. Biol. 9 (7), e1003135.
Missra, A., Gilmour, D.S., 2010. Interactions between DSIF (DRB sensitivity inducing factor), NELF (negative elongation factor), and the Drosophila RNA polymerase II transcription elongation complex. Proc. Natl. Acad. Sci. 107 (25), 11301–11306.
Mizutani, T., et al., 2009. Loss of the Brm-type SWI/SNF chromatin remodeling complex is a strong barrier to the Tat-independent transcriptional elongation of human immunodeficiency virus type 1 transcripts. J. Virol. 83 (22), 11569–11580.
Montano, M.A., et al., 1997. Divergent transcriptional regulation among expanding human immunodeficiency virus type 1 subtypes. J. Virol. 71 (11), 8657–8665.
Mousseau, G., Valente, S., 2012. Strategies to block HIV transcription: focus on small molecule tat inhibitors. Biology 1 (3), 668–697.
Mousseau, G., Kessing, C.F., et al., 2015a. The Tat inhibitor didehydro-cortistatin A prevents HIV-1 reactivation from latency. mBio 6 (4), e00465.
Mousseau, G., Mediouni, S., Valente, S.T., 2015b. Targeting HIV transcription: the quest for a functional cure. Curr. Top. Microbiol. Immunol. 389, 121–145.
Muesing, M.a., Smith, D.H., Capon, D.J., 1987. Regulation of mRNA accumulation by a human immunodeficiency virus trans-activator protein. Cell 48 (4), 691–701.
Mujtaba, S., et al., 2002. Structural basis of lysine-acetylated HIV-1 Tat recognition by PCAF bromodomain. Mol. Cell 9 (3), 575–586.
Muniz, L., et al., 2010. Controlling cellular P-TEFb activity by the HIV-1 transcriptional transactivator Tat. PLoS Pathog. 6 (10), e1001152.
Näär, A.M., Ryu, S., Tjian, R., 1998. Cofactor requirements for transcriptional activation by Sp1. Cold Spring Harb. Symp. Quant. Biol. 63, 189–199.
Nabel, G., Baltimore, D., 1987. An inducible transcription factor activates expression of human immunodeficiency virus in T cells. Nature 326 (6114), 711–713.

Naghavi, M.H., et al., 1999. DNA sequence of the long terminal repeat of human immunodeficiency virus type 1 subtype a through G. AIDS Res. Hum. Retroviruses 15 (5), 485–488.
Natarajan, M., et al., 2013. Negative elongation factor (NELF) coordinates RNA polymerase II pausing, premature termination, and chromatin remodeling to regulate HIV transcription. J. Biol. Chem. 288 (36), 25995–26003.
Nguyen, V.T., et al., 2001. 7SK small nuclear RNA binds to and inhibits the activity of CDK9/cyclin T complexes. Nature 414 (6861), 322–325.
O'Reilly, D., Greaves, D.R., 2007. Cell-type-specific expression of the human CD68 gene is associated with changes in pol II phosphorylation and short-range intrachromosomal gene looping. Genomics 90 (3), 407–415.
O'Sullivan, J.M., et al., 2004. Gene loops juxtapose promoters and terminators in yeast. Nat. Genet. 36 (9), 1014–1018.
Ott, M., et al., 1999. Acetylation of the HIV-1 tat protein by p300 is important for its transcriptional activity. Curr. Biol. 9 (24), 1489–1492.
Ott, M., Geyer, M., Zhou, Q., 2011. The control of HIV transcription: keeping RNA polymerase II on track. Cell Host Microbe 10 (5), 426–435.
Owen-Hughes, T., Workman, J.L., 1994. Experimental analysis of chromatin function in transcription control. Crit. Rev. Eukaryot. Gene Expr. 4 (4), 403–441.
Pagano, J.M., et al., 2014. Defining NELF-E RNA binding in HIV-1 and promoter-proximal pause regions. PLoS Genet. 10 (1), e1004090.
Pagans, S., et al., 2005. SIRT1 regulates HIV transcription via Tat deacetylation. PLoS Biol. 3 (2), e41.
Pagans, S., et al., 2010. The cellular lysine methyltransferase Set7/9-KMT7 binds HIV-1 TAR RNA, monomethylates the viral transactivator Tat, and enhances HIV transcription. Cell Host Microbe 7 (3), 234–244.
Palmisano, I., et al., 2012. Amino acid starvation induces reactivation of silenced transgenes and latent HIV-1 provirus via down-regulation of histone deacetylase 4 (HDAC4). Proc. Natl. Acad. Sci. U.S.A. 109 (34), E2284–93.
Papathanasopoulos, M.A., et al., 2002. Full-length genome analysis of HIV-1 subtype C utilizing CXCR4 and intersubtype recombinants isolated in South Africa. AIDS Res. Hum. Retroviruses 18 (12), 879–886.
Pascal, E., Tjian, R., 1991. Different activation domains of Sp1 govern formation of multimers and mediate transcriptional synergism. Genes Dev. 5 (9), 1646–1656.
Pascual-Garcia, P., et al., 2017. Metazoan nuclear pores provide a scaffold for poised genes and mediate induced enhancer–promoter contacts. Mol. Cell 66 (1). 63–76.e6.
Pearson, R., et al., 2008. Epigenetic silencing of human immunodeficiency virus (HIV) transcription by formation of restrictive chromatin structures at the viral long terminal repeat drives the progressive entry of HIV into latency. J. Virol. 82 (24), 12291–12303.
Pelletier, M.R., et al., 1997. Efficient transcription of an immunoglobulin kappa promoter requires specific sequence elements overlapping with and downstream of the transcriptional start site. Nucleic Acids Res. 25 (20), 3995–4003.
Pereira, L.A., et al., 2000. A compilation of cellular transcription factor interactions with the HIV-1 LTR promoter. Nucleic Acids Res. 28 (3), 663–668.
Perkins, N.D., et al., 1993. A cooperative interaction between NF-kappa B and Sp1 is required for HIV-1 enhancer activation. EMBO J. 12 (9), 3551–3558.
Perkins, N.D., et al., 1994. An interaction between the DNA-binding domains of RelA(p65) and Sp1 mediates human immunodeficiency virus gene activation. Mol. Cell. Biol. 14 (10), 6570–6583.
Perkins, N.D., et al., 1997. Regulation of NF-kappaB by cyclin-dependent kinases associated with the p300 coactivator. Science (New York, NY) 275 (5299), 523–527.

Perkins, K.J., et al., 2008. Transcription-dependent gene looping of the HIV-1 provirus is dictated by recognition of pre-mRNA processing signals. Mol. Cell 29 (1), 56–68.
Peterlin, B.M., Price, D.H., 2006. Controlling the elongation phase of transcription with P-TEFb. Mol. Cell 23 (3), 297–305.
Peterlin, B.M., Brogie, J.E., Price, D.H., 2012. 7SK snRNA: a noncoding RNA that plays a major role in regulating eukaryotic transcription. Wiley Interdiscip. Rev. RNA 3 (1), 92–103.
Ping, Y.H., Rana, T.M., 2001. DSIF and NELF interact with RNA polymerase II elongation complex and HIV-1 Tat stimulates P-TEFb-mediated phosphorylation of RNA polymerase II and DSIF during transcription elongation. J. Biol. Chem. 276 (16), 12951–12958.
Pomerantz, R.J., et al., 1990. Cells nonproductively infected with HIV-1 exhibit an aberrant pattern of viral RNA expression: a molecular model for latency. Cell 61 (7), 1271–1276.
Ptak, C., Aitchison, J.D., Wozniak, R.W., 2014. The multifunctional nuclear pore complex: a platform for controlling gene expression. Curr. Opin. Cell Biol. 28, 46–53.
Qian, J., et al., 1994. Chemically selected subclones of the CEM cell line demonstrate resistance to HIV-1 infection resulting from a selective loss of NF-kappa B DNA binding proteins. J. Immunol. 152 (8), 4183–4191.
Rabbi, M.F., et al., 1997. U5 region of the human immunodeficiency virus type 1 long terminal repeat contains TRE-like cAMP-responsive elements that bind both AP-1 and CREB/ATF proteins. Virology 233 (1), 235–245.
Radman-Livaja, M., Rando, O.J., 2010. Nucleosome positioning: how is it established, and why does it matter? Dev. Biol. 339 (2), 258–266.
Rafati, H., et al., 2011. Repressive LTR nucleosome positioning by the BAF complex is required for HIV latency. PLoS Biol. 9 (11), e1001206.
Raj, A., van Oudenaarden, A., 2008. Nature, nurture, or chance: stochastic gene expression and its consequences. Cell 135 (2), 216–226.
Ramakrishnan, R., Dow, E.C., Rice, A.P., 2009. Characterization of Cdk9 T-loop phosphorylation in resting and activated CD4(+) T lymphocytes. J. Leukoc. Biol. 86 (6), 1345–1350.
Raser, J.M., 2010. Noise in gene expression. Science 2010 (2005), 2010–2014.
Raser, J.M., Shea, E.K.O., 2006. Control of stochasticity in eukaryotic gene expression Jonathan. Science 304 (5678), 1811–1814.
Rasmussen, T.A., Tolstrup, M., Søgaard, O.S., 2016. Reversal of latency as part of a cure for HIV-1. Trends Microbiol. 24 (2), 90–97.
Ratner, L., et al., 1985. Complete nucleotide sequence of the AIDS virus, HTLV-III. Nature 313 (6000), 277–284.
Razooky, B.S., et al., 2015. A hardwired HIV latency program. Cell 160 (5), 990–1001.
Renner, D.B., et al., 2001. A highly purified RNA polymerase II elongation control system. J. Biol. Chem. 276 (45), 42601–42609.
Reuse, S., et al., 2009. Synergistic activation of HIV-1 expression by deacetylase inhibitors and prostratin: implications for treatment of latent infection. PLoS One 4 (6), e6093.
Richmond, T.J., et al., 1997. Crystal structure of the nucleosome core particle at 2.8 |[thinsp]||[Aring]| resolution. Nature 389 (6648), 251–260.
Rodgers, M.J., et al., 2014. CHD1 and CHD2 are positive regulators of HIV-1 gene expression. Virol. J. 11 (1), 180.
Roebuck, K.A., Gu, D.S., Kagnoff, M.F., 1996. Activating protein-1 cooperates with phorbol ester activation signals to increase HIV-1 expression. AIDS (London, England) 10 (8), 819–826.
Romani, B., et al., 2016. HIV-1 Vpr reactivates latent HIV-1 provirus by inducing depletion of class I HDACs on chromatin. Sci. Rep. 6, 31924.

Romerio, F., Gabriel, M.N., Margolis, D.M., 1997. Repression of human immunodeficiency virus type 1 through the novel cooperation of human factors YY1 and LSF. J. Virol. 71 (12), 9375–9382.
Rosen, C.A., Sodroski, J.G., Haseltine, W.A., 1985. The location of cis-acting regulatory sequences in the human T cell lymphotropic virus type III (HTLV-III/LAV) long terminal repeat. Cell 41 (3), 813–823.
Ross, E.K., et al., 1991. Contribution of NF-kappa B and Sp1 binding motifs to the replicative capacity of human immunodeficiency virus type 1: distinct patterns of viral growth are determined by T-cell types. J. Virol. 65 (8), 4350–4358.
Rosseau, C., et al., 1997. Long terminal repeat and *nef* gene variants of human immunodeficiency virus type 1 in perinatally infected long-term survivors and rapid progressors. AIDS Res. Hum. Retroviruses 13 (18), 1611–1623.
Roy, S., et al., 1990. A bulge structure in HIV-1 TAR RNA is required for Tat binding and Tat-mediated trans-activation. Genes Dev. 4 (8), 1365–1373.
Saayman, S.M., et al., 2016. Potent and targeted activation of latent HIV-1 using the CRISPR/dCas9 activator complex. Mol. Ther. 24 (3), 488–498.
Sadowski, I., Mitchell, D.A., 2005. TFII-I and USF (RBF-2) regulate Ras/MAPK-responsive HIV-1 transcription in T cells. Eur. J. Cancer 41 (16), 2528–2536.
Sakane, N., et al., 2011. Activation of HIV transcription by the viral Tat protein requires a demethylation step mediated by lysine-specific demethylase 1 (LSD1/KDM1). PLoS Pathog. 7 (8), e1002184.
Sanchez-Pescador, R., et al., 1985. Nucleotide sequence and expression of an AIDS-associated retrovirus (ARV-2). Science (New York, NY) 227 (4686), 484–492.
Schüller, R., et al., 2016. Heptad-specific phosphorylation of RNA polymerase II CTD. Mol. Cell 61 (2), 305–314.
Schulze-Gahmen, U., et al., 2013. The AFF4 scaffold binds human P-TEFb adjacent to HIV Tat. eLife 2013 (2), 10–12.
Schulze-Gahmen, U., et al., 2014. AFF4 binding to TAT-P-TEFb indirectly stimulates TAR recognition of super elongation complexes at the HIV promoter. eLife 2014 (3), 1–13.
Schwabish, M.A., Struhl, K., 2004. Evidence for eviction and rapid deposition of histones upon transcriptional elongation by RNA polymerase II. Mol. Cell. Biol. 24 (23), 10111–10117.
Sedore, S.C., et al., 2007. Manipulation of P-TEFb control machinery by HIV: recruitment of P-TEFb from the large form by Tat and binding of HEXIM1 to TAR. Nucleic Acids Res. 35 (13), 4347–4358.
Sekinger, E.A., Moqtaderi, Z., Struhl, K., 2005. Intrinsic histone–DNA interactions and low nucleosome density are important for preferential accessibility of promoter regions in yeast. Mol. Cell 18 (6), 735–748.
Selby, M.J., et al., 1989. Structure, sequence, and position of the stem-loop in tar determine transcriptional elongation by tat through the HIV-1 long terminal repeat. Genes Dev. 3 (4), 547–558.
Seto, E., Shi, Y., Shenk, T., 1991. YY1 is an initiator sequence-binding protein that directs and activates transcription in vitro. Nature 354 (6350), 241–245.
Seto, E., Lewist, B., Shenk, T., 1993. Interaction between transcription factors Spl and YY1. Nature 365 (6445), 462–464.
Sgarbanti, M., et al., 2002. Modulation of human immunodeficiency virus 1 replication by interferon regulatory factors. J. Exp. Med. 195 (10), 1359–1370.
Sgarbanti, M., et al., 2004. Analysis of the signal transduction pathway leading to human immunodeficiency virus-1-induced interferon regulatory factor-1 upregulation. Ann. N.Y. Acad. Sci. 1030 (1), 187–195.
Sheridan, P.L., et al., 1995. Activation of the HIV-1 enhancer by the LEF-1 HMG protein on nucleosome-assembled DNA in vitro. Genes Dev. 9 (17), 2090–2104.

Sieweke, M.H., et al., 1998. Cooperative interaction of Ets-1 with USF-1 required for HIV-1 enhancer activity in T cells. EMBO J. 17 (6), 1728–1739.
Sif, S., Gilmore, T.D., 1994. Interaction of the v-Rel oncoprotein with cellular transcription factor Sp1. J. Virol. 68 (11), 7131–7138.
Sikorski, T.W., Buratowski, S., 2009. The basal initiation machinery: beyond the general transcription factors. Curr. Opin. Cell Biol. 21 (3), 344–351.
Siliciano, R.F., Greene, W.C., 2011. HIV latency. Cold Spring Harb. Perspect. Med. 1 (1), a007096.
Siliciano, J.D., et al., 2003. Long-term follow-up studies confirm the stability of the latent reservoir for HIV-1 in resting CD4+ T cells. Nat. Med. 9 (6), 727–728.
Singh, A., Weinberger, L.S., 2009. Stochastic gene expression as a molecular switch for viral latency. Curr. Opin. Microbiol. 12 (4), 460–466.
Singh, A., et al., 2010. Transcriptional bursting from the HIV-1 promoter is a significant source of stochastic noise in HIV-1 gene expression. Biophys. J. 98 (8), L32–L34.
Sobhian, B., et al., 2010. HIV-1 Tat assembles a multifunctional transcription elongation complex and stably associates with the 7SK snRNP. Mol. Cell 38 (3), 439–451.
Sodroski, J.G., Rosen, C.A., Haseltine, W.A., 1984. Trans-acting transcriptional activation of the long terminal repeat of human T lymphotropic viruses in infected cells. Science (New York, NY) 225 (4660), 381–385.
Sodroski, J., Patarca, R., et al., 1985a. Location of the trans-activating region on the genome of human T-cell lymphotropic virus type III. Science 229 (4708), 74–77.
Sodroski, J., Rosen, C., et al., 1985b. Trans-acting transcriptional regulation of human T-cell leukemia virus type III long terminal repeat. Science (New York, NY) 227 (4683), 171–173.
Splinter, E., de Laat, W., 2011. The complex transcription regulatory landscape of our genome: control in three dimensions. EMBO J. 30 (21), 4345–4355.
Starcich, B., et al., 1985. Characterization of long terminal repeat sequences of HTLV-III. Science (New York, NY) 227 (4686), 538–540.
Steger, D.J., Workman, J.L., 1997. Stable co-occupancy of transcription factors and histones at the HIV-1 enhancer. EMBO J. 16 (9), 2463–2472.
Stoszko, M., et al., 2016. Small molecule inhibitors of BAF; a promising family of compounds in HIV-1 latency reversal. eBioMedicine 3, 108–121.
Strahl, B.D., Allis, C.D., 2000. The language of covalent histone modifications. Nature 403 (6765), 41–45.
Sun, Z.W., Hampsey, M., 1996. Synthetic enhancement of a TFIIB defect by a mutation in SSU72, an essential yeast gene encoding a novel protein that affects transcription start site selection in vivo. Mol. Cell. Biol. 16 (4), 1557–1566.
Suñé, C., et al., 2000. An in vitro transcription system that recapitulates equine infectious anemia virus tat-mediated inhibition of human immunodeficiency virus type 1 Tat activity demonstrates a role for positive transcription elongation factor b and associated proteins in the mechanism of tat activation. Virology 274 (2), 356–366.
Swain, P.S., Elowitz, M.B., Siggia, E.D., 2002. Intrinsic and extrinsic contributions to stochasticity in gene expression. Proc. Natl. Acad. Sci. U.S.A. 99 (20), 12795–12800.
Tantale, K., et al., 2016. A single-molecule view of transcription reveals convoys of RNA polymerases and multi-scale bursting. Nat. Commun. 7, 12248.
Tan-Wong, S.M., et al., 2008. Dynamic interactions between the promoter and terminator regions of the mammalian BRCA1 gene. Proc. Natl. Acad. Sci. U.S.A. 105 (13), 5160–5165.
Tan-Wong, S.M., et al., 2012. Gene loops enhance transcriptional directionality. Science 338 (6107), 671–675.
Tesmer, V.M., et al., 1993. NF-IL6-mediated transcriptional activation of the long terminal repeat of the human immunodeficiency virus type 1. Proc. Natl. Acad. Sci. U.S.A. 90 (15), 7298–7302.

Tong-Starksen, S.E., Luciw, P.a., Peterlin, B.M., 1987. Human immunodeficiency virus long terminal repeat responds to T-cell activation signals. Proc. Natl. Acad. Sci. U.S.A. 84 (19), 6845–6849.
Tréand, C., et al., 2006. Requirement for SWI/SNF chromatin-remodeling complex in Tat-mediated activation of the HIV-1 promoter. EMBO J. 25 (8), 1690–1699.
Trejbalová, K., et al., 2016. Development of 5′ LTR DNA methylation of latent HIV-1 provirus in cell line models and in long-term-infected individuals. Clin. Epigenetics 8, 19.
Tripathy, M.K., Abbas, W., Herbein, G., 2011. Epigenetic regulation of HIV-1 transcription. Epigenomics 3 (4), 487–502.
Turk, B., Stoka, V., 2007. Protease signalling in cell death: caspases versus cysteine cathepsins. FEBS Lett. 581 (15), 2761–2767.
Turrini, F., et al., 2015. HIV-1 transcriptional silencing caused by TRIM22 inhibition of Sp1 binding to the viral promoter. Retrovirology 12 (1), 104.
Tyagi, M., Karn, J., 2007. CBF-1 promotes transcriptional silencing during the establishment of HIV-1 latency. EMBO J. 26 (24), 4985–4995.
Tyagi, M., Pearson, R.J., Karn, J., 2010. Establishment of HIV latency in primary CD4+ cells is due to epigenetic transcriptional silencing and P-TEFb restriction. J. Virol. 84 (13), 6425–6437.
van der Sluis, R.M., et al., 2014. Interplay between viral Tat protein and c-Jun transcription factor in controlling LTR promoter activity in different human immunodeficiency virus type I subtypes. J. Gen. Virol. 95 (Pt. 4), 968–979.
Van Duyne, R., et al., 2011. Varying modulation of HIV-1 LTR activity by BAF complexes. J. Mol. Biol. 411 (3), 581–596.
Van Herreweghe, E., et al., 2007. Dynamic remodelling of human 7SK snRNP controls the nuclear level of active P-TEFb. EMBO J. 26 (15), 3570–3580.
Van Lint, C., et al., 1996. Transcriptional activation and chromatin remodeling of the HIV-1 promoter in response to histone acetylation. EMBO J. 15 (5), 1112–1120.
Van Lint, C., et al., 1997. Transcription factor binding sites downstream of the human immunodeficiency virus type 1 transcription start site are important for virus infectivity. J. Virol. 71 (8), 6113–6127.
Van Lint, C., Bouchat, S., Marcello, A., 2013. HIV-1 transcription and latency: an update. Retrovirology 10 (1), 67.
van Opijnen, T., et al., 2004. The human immunodeficiency virus type 1 promoter contains a CATA box instead of a TATA box for optimal transcription and replication. J. Virol. 78 (13), 6883–6890.
van Opijnen, T., Boerlijst, M.C., Berkhout, B., 2006. Effects of random mutations in the human immunodeficiency virus type 1 transcriptional promoter on viral fitness in different host cell environments. J. Virol. 80 (13), 6678–6685.
Vanti, M., et al., 2009. Yeast genetic analysis reveals the involvement of chromatin reassembly factors in repressing HIV-1 basal transcription. PLoS Genet. 5 (1), e1000339.
Vardabasso, C., et al., 2008. The histone chaperone protein nucleosome assembly protein-1 (hNAP-1) binds HIV-1 Tat and promotes viral transcription. Retrovirology 5 (1), 8.
Vemula, S., et al., 2015. HIV-1 induced nuclear factor I-B (NF-IB) expression negatively regulates HIV-1 replication through interaction with the long terminal repeat region. Virus 7 (2), 543–558.
Vendel, A.C., Lumb, K.J., 2003. Molecular recognition of the human coactivator CBP by the HIV-1 transcriptional activator tat. Biochemistry 42 (4), 910–916.
Venkatesh, S., Workman, J.L., 2015. Histone exchange, chromatin structure and the regulation of transcription. Nat. Rev. Mol. Cell Biol. 16 (3), 178–189.
Verdin, E., 1991. DNase I-hypersensitive sites are associated with both long terminal repeats and with the intragenic enhancer of integrated human immunodeficiency virus type 1. J. Virol. 65, 6790–6799.

Verdin, E., Van Lint, C., 1995. Internal transcriptional regulatory elements in HIV-1 and other retroviruses. Cell. Mol. Biol. (Noisy-le-Grand) 41 (3), 365–369.
Verdin, E., Paras, P., Van Lint, C., 1993. Chromatin disruption in the promoter of human immunodeficiency virus type 1 during transcriptional activation. EMBO J. 12 (8), 3249–3259.
Verhoef, K., Berkhout, B., 1999. A second-site mutation that restores replication of a Tat-defective human immunodeficiency virus. J. Virol. 73 (4), 2781–2789.
Wain-Hobson, S., et al., 1985. Nucleotide sequence of the AIDS virus, LAV. Cell 40 (1), 9–17.
Wang, J., et al., 2016. RbAp48, a novel inhibitory factor that regulates the transcription of human immunodeficiency virus type 1. Int. J. Mol. Med. 38 (1), 267–274.
Weber, C.M., Ramachandran, S., Henikoff, S., 2014a. Nucleosomes are context-specific, H2A.Z-modulated barriers to RNA polymerase. Mol. Cell 53 (5), 819–830.
Weber, et al., 2014b. Epigenetic analysis of HIV-1 proviral genomes from infected individuals: Predominance of unmethylated CpG's. Virology 449, 181–189.
Wei, P., et al., 1998. A novel CDK9-associated C-type cyclin interacts directly with HIV-1 Tat and mediates its high-affinity, loop-specific binding to TAR RNA. Cell 92 (4), 451–462.
Weinberger, A.D., Weinberger, L.S., 2013. Stochastic fate selection in HIV-infected patients. Cell 155 (3), 497–499.
Weinberger, L.S., et al., 2005. Stochastic gene expression in a lentiviral positive-feedback loop: HIV-1 Tat fluctuations drive phenotypic diversity. Cell 122 (2), 169–182.
Wen, Y., Shatkin, A.J., 1999. Transcription elongation factor hSPT5 stimulates mRNA capping. Genes Dev. 13 (14), 1774–1779.
Wilhelm, E., et al., 2012. CTGC motifs within the HIV core promoter specify Tat-responsive pre-initiation complexes. Retrovirology 9, 62.
Williams, S.A., et al., 2006. NF-kappaB p50 promotes HIV latency through HDAC recruitment and repression of transcriptional initiation. EMBO J. 25 (1), 139–149.
Xie, B., et al., 2007. Arginine methylation of the human immunodeficiency virus type 1 Tat protein by PRMT6 negatively affects Tat interactions with both cyclin T1 and the Tat transactivation region. J. Virol. 81 (8), 4226–4234.
Yamaguchi, Y.Y., et al., 1999. NELF, a multisubunit complex containing RD, cooperates with DSIF to repress RNA polymerase II elongation. Cell 97 (1), 11.
Yamaguchi, Y., et al., 2002. Evidence that negative elongation factor represses transcription elongation through binding to a DRB sensitivity-inducing factor/RNA polymerase II complex and RNA. Mol. Cell. Biol. 22 (9), 2918–2927.
Yang, X., Chen, Y., Gabuzda, D., 1999. ERK MAP kinase links cytokine signals to activation of latent HIV-1 infection by stimulating a cooperative interaction of AP-1 and NF-kappaB. J. Biol. Chem. 274 (39), 27981–27988.
Yang, Z., et al., 2001. The 7SK small nuclear RNA inhibits the CDK9/cyclin T1 kinase to control transcription. Nature 414 (6861), 317–322.
Yang, Z., et al., 2005. Recruitment of P-TEFb for stimulation of transcriptional elongation by the bromodomain protein Brd4. Mol. Cell 19 (4), 535–545.
Yik, J.H.N., et al., 2003. Inhibition of P-TEFb (CDK9/Cyclin T) kinase and RNA polymerase II transcription by the coordinated actions of HEXIM1 and 7SK snRNA. Mol. Cell 12 (4), 971–982.
Yik, J.H.N., et al., 2004. A human immunodeficiency virus type 1 Tat-like arginine-rich RNA-binding domain is essential for HEXIM1 to inhibit RNA polymerase II transcription through 7SK snRNA-mediated inactivation of P-TEFb. Mol. Cell. Biol. 24 (12), 5094–5105.
Zanton, S.J., Pugh, B.F., 2006. Full and partial genome-wide assembly and disassembly of the yeast transcription machinery in response to heat shock. Genes Dev. 20 (16), 2250–2265.

Zenzie-Gregory, B., et al., 1993. HIV-1 core promoter lacks a simple initiator element but contains a bipartite activator at the transcription start site. J. Biol. Chem. 268 (21), 15823–15832.
Zhang, H., Roberts, D.N., Cairns, B.R., 2005. Genome-wide dynamics of Htz1, a histone H2A variant that poises repressed/basal promoters for activation through histone loss. Cell 123 (2), 219–231.
Zhang, Z., et al., 2007. Negative elongation factor NELF represses human immunodeficiency virus transcription by pausing the RNA polymerase II complex. J. Biol. Chem. 282 (23), 16981–16988.
Zhang, L., et al., 2014. Modulation of the stability and activities of HIV-1 Tat by its ubiquitination and carboxyl-terminal region. Cell Biosci. 4 (1), 61.
Zhang, Y., et al., 2015. CRISPR/gRNA-directed synergistic activation mediator (SAM) induces specific, persistent and robust reactivation of the HIV-1 latent reservoirs. Sci. Rep. 5, 16277.
Zhao, S., et al., 2003. Requirement of a specific Sp1 site for histone deacetylase-mediated repression of transforming growth factor beta type II receptor expression in human pancreatic cancer cells. Cancer Res. 63 (10), 2624–2630.
Zhou, Q., Li, T., Price, D.H., 2012. RNA polymerase II elongation control. Annu. Rev. Biochem. 81 (1), 119–143.
Zhu, J., et al., 2012. Reactivation of latent HIV-1 by inhibition of BRD4. Cell Rep. 2 (4), 807–816.

FURTHER READING

Satinder Dahiya, Y.L., et al., 2014. Role of downstream elements in transcriptional regulation of the HIV-1 promoter. J. Hum. Virol. Retrovirol. 1 (2), 1–7.

AIM OF THIS THESIS

Significant advances have been made in the identification and characterization of regulatory mechanisms that play a role in the maintenance, establishment, and resolution of HIV-1 latency. Although this has led to a growing list of molecular factors and cellular pathways that determine viral latency, this list is far from complete, halting the development of successful latency reversal strategies. As a first step toward an HIV-1 cure strategy, re-activation of the latent HIV-1 cellular reservoir is considered to be crucial to promote its elimination.

This thesis aims to gain a better understanding of the cellular pathways and molecular mechanisms contributing to HIV-1 latency: a critical prerequisite for the successful development of novel therapeutic interventions for latency re-activation.

In the experimental chapters presented in this thesis (**Chapter 2**, **Chapter 3**, and **Chapter 4**) we set out to develop three different discovery tools that aim to identify, in an unbiased way, novel cellular pathways and molecular effectors, required for HIV-1 latency. Each of these chapters has led to the discovery of previously unknown mechanisms of latency and resulted in the identification of novel small molecule inhibitors with latency reversal properties.

The general introduction to this thesis (**Chapter 1**) (Ne, Palstra, and Mahmoudi 2018) offers a detailed review of the chromatin and transcriptional regulation of HIV-1 expression, highlighting some key determinants of latency. Much of the research described in this chapter relies on the identification and characterization of sequence-specific transcription factors (TFs) whose consensus binding sites are present within the 5'LTR. This candidate approach has led to the identification of a plethora of cellular pathways, their transcriptional effectors, and associated cofactors, whose activity can then be modulated to induce chromatin de-repression of the HIV-1 promoter region and favor RNA Pol II-mediated transcriptional initiation.

However, due to the complex nature of viral latency, the pharmacological interventions developed so far to disrupt latency present some limitations. It has been shown that current latency reversal agents

(LRAs) are incapable to achieve robust latency reversal in a significant portion of latently infected cells (Battivelli et al. 2018), have limited capacity to induce viral protein expression (Grau-Expósito et al. 2017; 2019), and have failed to significantly reduce the size of the latent reservoir in patients (Kim, Anderson, and Lewin 2018). Additionally, current interventions target cellular pathways and factors with broad functions and are therefore prone to non-specific and toxic side effects.

We believe that a thorough understanding of the molecular effectors and cellular pathways that regulate HIV-1 gene expression is critical to the development of a more specific combination of therapeutics, that can achieve a potent and robust latency reversal. However, due to technical limitations, comprehensive and unbiased identification of the molecular determinants and cellular pathways of latency has remained a long-term endeavor.

In **Chapter 2** (Ne et al. 2021) of this thesis, we set out to establish a locus-specific proteomic strategy to identify, in an unbiased way, host proteins physically associated with the latent and active integrated proviral promoter. We designed a reverse chromatin immunoprecipitation strategy (reverse-ChIP) that makes use of a nuclease deficient and multiple epitopes tagged Cas9 bait (HA-V5-FLAG-dCas9) to purify the region of interest. Next to an affinity-based capture of the dCas9 bait, we introduced a histone enrichment step in the purification pipeline that enables specific enrichment of the chromatin-bound fraction of the dCas9 associated complexes, allows reduced sample complexity, and increases the sensitivity of the mass spectrometry detection. Importantly, this work resulted in the establishment of a locus-specific proteomic purification pipeline that we named "dCas9 targeted chromatin and histone enrichment for mass spectrometry'' (Catchet-MS), which can be of great interest in the field of chromatin regulation. Catchet-MS is a novel and versatile technique easily applicable and scalable to study the chromatin composition of other single genomic loci in live cells, without the need to modify the region of interest.

Catchet-MS resulted in the identification of multiple novel (and several previously characterized) host factors, physically associated with

the latent and active HIV-1 promoter and represent an invaluable resource of putative molecular targets not only for latency reversal strategies but also for complementary strategies aiming at boosting viral expression or latency promoting strategies, further discussed in **Chapter 5** (Stoszko et al. 2019).

Here we show that IKZF1, one factor identified using Catchet-MS, is a novel HIV-1 5'LTR bound transcriptional repressor required for the recruitment of the Polycomb repressive complex 2 (PRC2) to the region, and the establishment of a repressive chromatin environment characterized by the H3K27me3 mark. The chromatin mark is then read by PRC1 members such as CBX8, in an IKZF1 dependent manner. Of therapeutic interest, we also show that the thalidomide-derived drug iberdomide, by targeting IKZF1 for CBRN mediated degradation, can revert latency in ex vivo HIV-1 infected primary CD4+ T cells and cells isolated from cART suppressed, HIV-1 infected participants.

In **Chapter 3** (Roling et al. 2021) we present an alternative and unique approach by which, using a two-color insertional mutagenesis screening in pseudo-haploid KBM7 cells, we were able to identify previously unknown genes whose disruption leads to upregulation of HIV-1 expression. Forward genetics in mammalian cells is normally hampered by the fact that in diploid cells, mutagenesis often produces heterozygous knockout cells which may not necessarily show a phenotype, resulting in false negatives. The KBM7 cell line used in this study, derived from chronic myelogenous leukemia, is near-haploid for most of its chromosomes and has given us the unique opportunity of conducting forward genetics, for non-essential genes, in mammalian cells. As a cellular platform for the screening, we generated a latently infected KBM7 cell line (Hap-Lat) harboring an integrated transcriptionally silent HIV-1 5'LTR that controls expression of a GFP reporter gene. Hap-Lat cells were then subjected to gene trap (GT) insertional mutagenesis using an mCherry reporter GT virus. Upon mutagenesis, Hap-Lat cells expressing GFP as a reporter of HIV-1 reactivation, and mCherry, confirming the presence of a GT virus, were then selected by multiple rounds of fluorescence activated cell sorting (FACS) and subjected to NGS mapping of the integration sites. The advantage of using this system is that identification

of the candidate targets does not require a-priori knowledge of the molecular determinants of latency and it is completely unbiased. Additionally, being a genetic screen, gene-trap insertional mutagenesis has allowed us to identify previously unappreciated genes and cellular pathways of latency that modulate latency indirectly, through genetic interaction, rather than physical association, with the HIV-1 promoter.

In this study we have first identified a list of 69 candidate gene of which we could confirm 10 to be required for HIV latency in different cellular models of latency, thus representing an important resource for future studies. Importantly, for three of the novel candidates identified we tested different small molecule inhibitors. We found Topiramate, inhibitor of the glutamate ionotropic receptor kainate type subunit 5 (GRIK5) to have potential clinical relevance. Among the factors identified we also identified CHD9 to be a 5'LTR bound chromatin-associated factor that is removed upon viral reactivation in cellular models of latency.

In **Chapter 4** we present a cell-based drug screening approach that has also led to the identification of a novel LRA, for which we then determined the molecular target. While in Chapters 2 and 3 the goal was to expand the known repertoire of molecular determinants of latency, to be used as potential targets for novel HIV-1 latency reversal strategies. Here, without any a priori knowledge of the targeted molecular effector, we screened a library of growth supernatants from selected fungal species in search of novel compounds capable of reversing HIV-1 latency. Having identified the candidate LRA, we then reverse-engineered the procedure to identify its molecular target.

As a cellular readout for the screening, we used latent HIV-1 infected J-Lat 11.1 and A2 cells harboring GFP as a reporter for LTR activity. We identified the supernatant from the species Aspergillus Fumigatus to display latency reversal activity. Coupling our bioassay to orthogonal mass spectrometry (MS) and fractionation of the Aspergillus Fumigatus growth supernatant, we identified Gliotoxin (GTX), as a novel candidate LRA. Experiments on primary cells subsequently confirmed that GTX is a novel LRA capable of inducing HIV-1 activation in ex vivo infected CD4+ T cells and cells isolated from cART suppressed HIV-1 infected participants, with limited toxicity. We then used transcriptome analysis, biochemical assays, and molecular modeling to unravel the

molecular mechanism of GTX mediated HIV-1 induction.

Our data support a model in which, GTX targets the LARP7 component of the 7SK snRNP complex, which sequesters P-TEFb and disrupts it, causing the release of P-TEFb. This results in enhanced availability of the free or active P-TEFb fraction, which then is recruited by the Tat-TAR axis to phosphorylate RNA pol II in its C-terminal domain (CTD). Phosphorylation of RNA pol II in its CTD stabilizes transcriptional elongation and leads to an increased rate of productive HIV-1 transcription.

In **Chapter 5**, we present the state-of-the-art therapeutic interventions available to attack, mobilize, and even permanently silence a reservoir of HIV-1 latently infected cells that has proven to be strenuous and very persistent in infected individuals. Importantly, this review also offers new perspectives on HIV-1 cure strategies.
Emerging evidence shows that while much of the past research efforts have focused on modulating the chromatin regulation and transcriptional activity at the HIV-1 5'LTR, co-transcriptional and post-transcriptional processes are also crucial determinants of latency (Yukl et al. 2018). Research efforts to ameliorate latency reversal strategies should likely further investigate and exploit these regulatory steps. Additionally, while research thus far has mainly focused on reactivation from latency, little has been done to identify interventions capable of promoting apoptosis and clearance of the infected cells. Emerging interventions going into this direction are explored in this chapter and further addressed in the general discussion of the thesis.

The different pipelines of interventions described in this chapter, due to the complexity of the reservoir, are not necessarily mutually exclusive and may need to be examined in a patient-specific context to identify personalized treatments or a robust treatment that can overrule individual variability. An attractive possibility is to combine some of the interventions mentioned in this chapter with immune-boosting strategies that can promote control or full clearance of the reservoir.

In the general discussion of the thesis (**Chapter 6**) we cover the strengths and limitations of the research tools used, offering potential

improvements. We then review our findings and put them in a broader context, examining the implications and future directions in the development of unbiased screens for the identification of molecular targets and putative latency reversal agents. Lastly, we thoroughly discuss the limitations of latency reversal followed by elimination of the latent HIV-1 reservoir, propose a revision to the strategy, and discuss the opportunities for the development of combinatory interventions towards an HIV-1 cure.

REFERENCES

Battivelli, Emilie, Matthew S. Dahabieh, Mohamed Abdel-Mohsen, J. Peter Svensson, Israel Tojal Da Silva, Lillian B. Cohn, Andrea Gramatica, et al. 2018. "Distinct Chromatin Functional States Correlate with HIV Latency Reactivation in Infected Primary CD4+ T Cells." *ELife* 7 (May). https://doi.org/10.7554/eLife.34655.

Grau-Expósito, Judith, Laura Luque-Ballesteros, Jordi Navarro, Adrian Curran, Joaquin Burgos, Esteban Ribera, Ariadna Torrella, et al. 2019. "Latency Reversal Agents Affect Differently the Latent Reservoir Present in Distinct CD4+ T Subpopulations." *PLOS Pathogens* 15 (8): e1007991. https://doi.org/10.1371/journal.ppat.1007991.

Grau-Expósito, Judith, Carla Serra-Peinado, Lucia Miguel, Jordi Navarro, Adrià Curran, Joaquin Burgos, Imma Ocaña, et al. 2017. "A Novel Single-Cell FISH-Flow Assay Identifies Effector Memory CD4+ T Cells as a Major Niche for HIV-1 Transcription in HIV-Infected Patients." *MBio* 8 (4). https://doi.org/10.1128/mBio.00876-17.

Kim, Youry, Jenny L. Anderson, and Sharon R. Lewin. 2018. "Getting the 'Kill' into 'Shock and Kill': Strategies to Eliminate Latent HIV." *Cell Host & Microbe* 23 (1): 14–26. https://doi.org/10.1016/j.chom.2017.12.004.

Ne, Enrico, Raquel Crespo, Ray Izquierdo-Lara, Selin Kocer, Alicja Gorszka, Thomas van Staveren, Tsung Wai Kan, et al. 2020. "DCas9 Targeted Chromatin and Histone Enrichment for Mass Spectrometry (Catchet-MS) Identifies IKZF1 as a Novel Drug-Able Target for HIV-1 Latency Reversal." SSRN Scholarly Paper ID 3553972. Rochester, NY: Social Science Research Network. https://doi.org/10.2139/ssrn.3553972.

Ne, Enrico, Robert-Jan Palstra, and Tokameh Mahmoudi. 2018. "Transcription: Insights From the HIV-1 Promoter." *International Review of Cell and Molecular Biology* 335: 191–243. https://doi.org/10.1016/bs.ircmb.2017.07.011.

Stoszko, Mateusz, Abdullah M. S. Al-Hatmi, Anton Skriba, Michael Roling, Enrico Ne, Raquel Crespo, Yvonne M. Mueller, et al. 2020. "Gliotoxin, identified from a Screen of Fungal Metabolites, Disrupts 7SK SnRNP, Releases P-TEFb, and Reverses HIV-1 Latency." *Science Advances* 6 (33): eaba6617. https://doi.org/10.1126/sciadv.aba6617.

Stoszko, Mateusz, Enrico Ne, Erik Abner, and Tokameh Mahmoudi. 2019. "A Broad Drug Arsenal to Attack a Strenuous Latent HIV Reservoir." *Current Opinion in Virology* 38: 37–53. https://doi.org/10.1016/j.coviro.2019.06.001.

Yukl, Steven A., Philipp Kaiser, Peggy Kim, Sushama Telwatte, Sunil K. Joshi, Mai Vu, Harry Lampiris, and Joseph K. Wong. 2018. "HIV Latency in Isolated Patient

CD4+ T Cells May Be Due to Blocks in HIV Transcriptional Elongation, Completion, and Splicing." *Science Translational Medicine* 10 (430). https://doi.org/10.1126/scitranslmed.aap9927.

CHAPTER .2

dCas9 Targeted Chromatin and Histone Enrichment for Mass Spectrometry (Catchet-MS) Identifies IKZF1 as a novel druggable target for HIV-1 latency reversal

Enrico Ne, Raquel Crespo, Ray Izquierdo-Lara, Selin Kocer, Alicja Gorszka, Thomas van Staveren, Tsung Wai Kan, Dick Dekkers, Casper Rokx, Panagiotis Moulos, Pantelis Hatzis, Robert-Jan Palstra, Jeroen Demmers, Tokameh Mahmoudi

Ne et al., 2021, preprint

https://www.biorxiv.org/content/10.1101/2021.03.19.436149v1

dCas9 targeted chromatin and histone enrichment for mass spectrometry (Catchet-MS) identifies IKZF1 as a novel drug-able target for HIV-1 latency reversal

Authors:

Enrico Ne[1], Raquel Crespo[1], Ray Izquierdo-Lara[1], Selin Kocer[1], Alicja Gorszka[1], Thomas van Staveren[1], Tsung Wai Kan[1], Dick Dekkers[2], Casper Rokx[3], Panagiotis Moulos[4], Pantelis Hatzis[4], Robert-Jan Palstra[1], Jeroen Demmers[2], Tokameh Mahmoudi[1]*

Affiliations:

1 Department of Biochemistry, Erasmus University Medical Center, Ee622 PO Box 2040

3000CA Rotterdam, The Netherlands

2 Proteomics Center, Erasmus University Medical Center, Ee679a PO Box 2040

3000CA Rotterdam, The Netherlands

3 Department of Internal Medicine, Section of Infectious Diseases, Erasmus University Medical Center, Rg-530, PO BOC 2040 3000CA Rotterdam, The Netherlands

4 Fleming Genomics Facility, Biomedical Sciences Research Center "Alexander Fleming", 16672, Vari, Greece

*Correspondence to Tokameh Mahmoudi, t.mahmoudi@erasmusmc.nl

Summary

A major pharmacological strategy toward HIV cure aims to reverse latency in infected cells as a first step leading to their elimination. While the unbiased identification of molecular targets physically associated with the latent HIV-1 provirus would be highly valuable to unravel the molecular correlates of HIV-1 transcriptional repression and latency reversal, due to technical limitations, this has not been possible. Here we use dCas9 targeted chromatin and histone enrichment strategy coupled to mass spectrometry (Catchet-MS) to isolate the latent and activated HIV-1 5'LTR, followed by MS identification of the differentially locus-bound proteins. Catchet-MS identified known and novel latent 5'LTR-associated host factors. Among these, IKZF1 is a novel HIV-1 transcriptional repressor, required for Polycomb Repressive Complex 2 recruitment to the LTR. We find the drug iberdomide, which targets IKZF1 for degradation, to be a clinically advanced novel LRA that reverses HIV-1 latency in CD4+T-cells isolated from virally suppressed HIV-1 infected participants.

INTRODUCTION

Combination antiretroviral therapy (cART) effectively halts HIV replication and has significantly reduced AIDS-associated mortality. However, cART is not curative, it has side effects, and apart from the costs of lifelong therapy, the global roll-out of cART, particularly in resource-limited countries, remains an ongoing challenge (UNAIDS fact sheet 2019). HIV persists because subsequent to stable integration into the CD4+ T cell host genome, the provirus can remain in a nonproductive latent state, defined by the absence of HIV-1 gene expression. Because of this reservoir of latently HIV-1 infected cells, interruption of cART leads to a rapid rebound of unrestricted viral replication, necessitating life-long treatment (Siliciano and Siliciano, 2015).

Therapeutic strategies for HIV cure aim to eliminate, inactivate, or reduce the pool of latently infected cells such that the patient's immune system can control viral replication upon cessation of cART. As quiescent memory CD4+ T cells, which constitute the main cellular reservoir of latent HIV infected cells, have a long half-life (Siliciano et al., 2003), pharmacological approaches aim to speed up the decay rate of this infected reservoir. One such strategy is to induce viral expression in latently infected cells using latency reversal agents (LRAs) to increase the viral transcriptional output and viral protein production, rendering the infected cell recognizable to the immune system or susceptible to viral cytopathic effects for elimination.

At the molecular level, the expression of the HIV-1 genome is determined by the activity of the HIV-1 promoter or 5'LTR, which is controlled by the LTR chromatin landscape (Rafati et al., 2011), the engagement of sequence-specific host transcription factors (TFs) and associated cofactors (Ne et al., 2018; Pereira et al., 2000), the recruitment of RNA polymerase II (Pol II) and its efficient transcriptional elongation (Mousseau and Valente, 2017; Ott et al., 2011). Co-transcriptionally recruited host factors then mediate post-transcriptional processing of the nascent HIV-1 RNA template for its efficient splicing, export, and translation (Chun et al., 2003; Karn and Stoltzfus, 2012; Lassen et al., 2006; Rojas-Araya et al., 2015). Host factors mediating these regulatory steps that control HIV-1 gene expression are thus the main targets of

ongoing pharmacological strategies to reverse latency (Stoszko et al., 2019). However, due to the complex and heterogeneous nature of latency, the currently available LRAs are incapable of reactivating a significant portion of cells carrying a latent provirus (Battivelli et al., 2018), have limited capacity to induce viral protein expression (Grau-Exposito et al., 2019; Grau-Exposito et al., 2017), and thus have failed to significantly impact the reservoir in patients (Kim et al., 2018). Additionally, LRAs target host molecular complexes with widespread regulatory functions and are therefore prone to non-specific pleiotropic effects. The identification of the full repertoire of regulatory factors and cofactors involved in silencing the latent HIV 5'LTR would be critical for a better understanding of the molecular determinants of proviral latency and for the development of a more specific and effective combination of therapeutics to deplete the HIV reservoir. However, due to technical limitations, unbiased proteomic analysis of host proteins associated with the latent or active HIV promoter, in infected cells, has never been conducted.

Locus-specific strategies to identify in vivo chromatin-bound protein complexes, at a single genomic location, are largely based on a reverse chromatin immunoprecipitation (reverse-ChIP) protocol which relies on the introduction of an affinity bait at the chromatin region of interest, followed by purification of the bait and proteomic analysis of the protein complexes that co-purify with it (Byrum et al., 2012; Pourfarzad et al., 2013). A related approach, Proteomics of isolated chromatin fragments (PICh), uses biotinylated oligonucleotides that hybridize with the region of interest to specifically purify the target DNA and associated proteins (Dejardin and Kingston, 2009; Ide and Dejardin, 2015). With the introduction of CRISPR-based methods and nuclease-deficient cas9 (dCas9) fusion constructs, reverse-ChIP strategies have become less labor-intensive and more versatile, as introduction of an artificial consensus sequence for targeting of the bait to the region of interest is no longer required (Liu et al., 2017; Waldrip et al., 2014). Additionally, CRISPR-dCas9 strategies can also be combined with, biotin-based, proximity labeling techniques, such as Bio-ID (Roux et al., 2012; Schmidtmann et al., 2016) and APEX enzyme fusion constructs (Myers et al., 2018), that, by relying on the capture of in vivo biotin-labeled proteins, located in the proximity of the dCas9 construct, do not require cell crosslinking.

Locus-specific isolation techniques represent an enormous challenge in protein biochemistry and proteomics, due to the fact that, in each cell, the number of proteins bound at a specific regulatory region is exceedingly lower than the number of proteins bound to the rest of the genome. Consequently, the minimum amount of input required for mass spectrometry identification of proteins that bind to a specific genomic locus of interest, in a single copy, as would be the case for the integrated latent HIV-1 promoter, is estimated to be of at least half-a-billion cells, (Gauchier et al., 2020; Vermeulen and Dejardin, 2020). As our cellular platform to study latency harbors only one copy of the integrated HIV-1 5'LTR per cell, in this study we used 3 billion cells per condition; thus representing an enormous experimental undertaking both in technical complexity and costs.

While conventional reverse-ChIP approaches for locus-specific proteomics allow the identification of some locus-specific factors, many of these strategies suffer from high signal to noise ratio and low abundance of single loci, rendering the identification of proteins bound to the region of interest challenging (Byrum et al., 2012; Chalkley and Verrijzer, 2004; Hamperl et al., 2014; Pourfarzad et al., 2013; Tsui et al., 2018; Waldrip et al., 2014) (Gauchier et al., 2020). Another caveat in locus-specific proteomics techniques is that there is typically a large fraction of the exogenously expressed bait that is present diffusely in the cells and that is not exclusively bound to the locus of interest. This fraction of the bait, which is inevitably captured during the purification pipeline, likely accumulates in the RNA rich nucleolar compartment, significantly contributing to the background signal and affecting sensitivity (Chen et al., 2013; Ma et al., 2016). A well-established strategy for background elimination is subtraction from the final dataset using a robust set of negative controls and multiple replicates (Gauchier et al., 2020; Liu et al., 2017). This approach effectively eliminates some background and has successfully led to the identification of several locus-specific proteins (Gauchier et al., 2020; Liu et al., 2017). We reasoned, however, that a biochemical strategy designed to eliminate this source of background may greatly improve the sensitivity of the technique and push the field forward.

Here, we combined a CRISPR-dCas9 based reverse-ChIP approach with a sequential purification step, targeting histones to

biochemically remove the unwanted background, prior to semi-quantitative Mass Spectrometry identification; a purification pipeline we refer to as "dCas9 targeted chromatin and histone enrichment for mass spectrometry'' (Catchet-MS). Addition of histone affinity purification as the last step in Catchet-MS enabled specific enrichment and identification of the chromatin-bound fraction of the dCas9 bait proteins bound to the target region, while non-localized bait complexes in the cytoplasm and nucleoplasm were eliminated.

Using Catchet-MS we identify proteins preferentially associated with the latent or active HIV-1 promoter that represent potential key regulators of HIV-1 gene expression. Among these regulators, we demonstrate that the transcription factor IKZF1 is a novel transcriptional repressor of the HIV-1 promoter, required for the sequential recruitment of the polycomb repressive complex 2 (PRC2) and critical for maintenance of a repressive LTR chromatin environment which is characterized by the presence of the H3K27me3 chromatin mark. Additionally, we demonstrate that iberdomide (CC-220), a therapeutically advanced drug, which targets the IKZF1 protein for degradation through modulation of CRBN dependent ubiquitination, leads to HIV-1 latency reversal in both ex vivo infected primary CD4+ T cells and cells isolated from HIV-1 infected aviremic individuals on cART. We demonstrate that Catchet-MS provides a powerful approach towards enrichment and mass spec identification of molecular effectors bound to a single DNA locus. Our data suggest that modulation of IKZF1 protein expression with iberdomide, or other thalidomide derived drugs, represents a viable target for therapeutic intervention to reverse latency in context of HIV-1 cure strategies.

RESULTS

Catchet-MS, a method to isolate and identify locus-bound protein complexes at the latent and activated HIV-1 LTR in vivo

We established a CRISPR/dCas9-based proteomics strategy to identify a comprehensive repertoire of protein complexes associated in vivo with the latent and active HIV promoter (**Figure 1A-C**). As a cellular

platform for latency we used J-Lat 11.1, a Jurkat derived T cell line, which harbors a single latent copy of the integrated full-length HIV-1 proviral genome, defective in *env*, and in which GFP replaces the *nef* coding sequence as a reporter for viral activation (Jordan et al., 2003) (**Figure 1A**). J-Lat 11.1 cells were first modified to stably express a multiple epitopes (V5, HA, FLAG)-tagged dCas9 bait, and an 18 nucleotide single guide-RNA, targeting the hypersensitive site 2 (HS2) region of the HIV-1 promoter, downstream of the Transcription Start Site (TSS) (**Figure 1C**). We confirmed the expression of the tagged dCas9 bait construct by Western blotting, using antibodies specifically recognizing dCas9 and the construct tags HA, V5, and FLAG (**Figure 1D**). We chose to target our dCas9 bait to the HS2 region downstream of Nuc-1, as recent evidence pointed to transcription elongation and RNA processing as critical steps involved in HIV-1 latency in vivo (Yukl et al., 2018). As a negative control, we generated cells expressing HA-V5-FLAG-dCas9 and a non-targeting control gRNA (nt-gRNA). We validated HIV-1 promoter targeting of the gRNA (HS2-gRNA) sequence in a functional assay, by co-transfection of J-Lat 11.1 cells together with a dCas9-VP64-p65-Rta (dCas9-VPR) fusion construct containing the VPR transcriptional activation domain. Confirming correct targeting of the dCas9-VPR construct to the HIV-1 promoter, co-transfection of the HS2 gRNA, but not the nt-gRNA, resulted in an increase in HIV-1 promoter-driven GFP positive cells (**Supplementary Figure 1A**). We additionally examined the specific binding of the HA-V5-FLAG-dCas9 bait at the HS2 region of the HIV-1 promoter in latent J-Lat 11.1 cells by ChIP-qPCR analysis using a V5 epitope-based IP. As shown in **Figure 1E**, enrichment of the HA-V5-FLAG-dCas9 bait was observed specifically over HIV-1 LTR sequences spanning Nuc-1 and Nuc-2, only in the HS2-gRNA guided cells and not in those expressing the non-targeting control gRNA (nt-gRNA) (**Figure 1E**).

To determine the optimal HA-V5-FLAG-dCas9 bait IP enrichment strategy, we examined specific enrichment of the locus in ChIP-qPCR experiments comparing antibodies directed against the HA, V5, and FLAG epitopes (**Supplementary Figure 1B and C**). While antibodies directed against each tag resulted in efficient and specific enrichment of the targeted HIV-1 DNA region, we chose to use anti V5 affinity beads

targeting the V5 epitope as the first step in the large-scale locus enrichment strategy as it demonstrated both optimal purification yield as well as the highest signal to noise ratio (**Supplementary Figure 1C**). To ensure that targeting of the HA-V5-FLAG-dCas9 bait downstream of the HIV-1 promoter would not interfere functionally with viral reactivation, we examined LTR activity in the latent and PMA activated HA-V5-FLAG-dCas9 HS2-gRNA guided J-Lat 11.1 cells. As shown by Flow cytometry and fluorescence microscopy, J-Lat 11.1 cells or those harboring HS2-gRNA guided or non-targeted HA-V5-FLAG-dCas9 bait displayed low basal GFP expression and a similar increase in GFP positive cells in response to PMA treatment (**Figure 1F and Supplementary Figure 1D**). Thus, the targeted dCas9 bait does not interfere with the maintenance of latency or capacity for reactivation. From this, we infer that binding of 5'LTR associated transcription regulatory factors bound in the repressed or activated states is unaltered by dCas9 targeting. We also confirmed that the binding capacity of the HA-V5-FLAG-dCas9 bait is not affected by the transcriptional state of the 5'LTR by ChIP-qPCR in latent and PMA stimulated cells (**Figure 1G**); HA-V5-FLAG-dCas9 was similarly enriched over the sequences spanning LTR Nuc-1 and Nuc-2 in both the transcriptionally repressed and active states, confirming that the established platform is suitable for purification of the locus.

The large number of non-localized bait molecules (e.g. dCas9) present a caveat in reverse-ChIP approaches for single locus chromatin proteomics, as they are also captured through the purification pipeline, thus preventing reliable identification of the locus associated bait interactome within the background signal from purified unspecific complexes. It has been shown that Cas9 molecules, when non-efficiently guided are diffusely present in the nucleus and tend to accumulate in the RNA-rich nucleolar compartment (Chen et al., 2013; Ma et al., 2016). In our experimental system, cell fractionation followed by western blotting demonstrated a large fraction of the HA-V5-FLAG-dCas9 bait molecules to be present in the cytoplasmic fraction, despite the presence of a nuclear localization sequence (NLS) within the bait construct (**Figure 2A, 2B**). To obtain a purer chromatin fraction, we modified our in-house ChIP protocol to include 10 cycles of low-efficiency sonication after nuclear isolation followed by denaturation in the presence of strong denaturing buffers

(adapted from Chromatin enrichment for proteomics protocol (CheP) (Kustatscher et al., 2014). We named the modified protocol Chromatin enrichment for immunoprecipitation (CheIP). Mass spectrometry analysis of individual steps of our purification pipeline demonstrated progressive removal of membrane, cytoplasmic and organelle associated proteins as well as, in part, non-chromatin bound nuclear proteins by CheIP, resulting in the enrichment of chromatin and associated proteins within the insoluble nuclear material (**Supplementary Figure 2A, 2B**). While this biochemical procedure enables a more stringent purification of the chromatin fraction, a substantial amount of non-chromatin associated dCas9 bait complexes remain within the precipitated chromatin fraction, presenting substantial background.

To improve the specificity of the purification, we took advantage of the fact that what distinguishes cross-linked chromatin-associated complexes from non-chromatin associated complexes is the presence of histones within the complex. Therefore we introduced a histone enrichment step into our purification pipeline; given the high abundance of histones within the purified chromatin fraction, we opted to perform histone affinity purification following the V5 epitope-based purification of the HA-V5-FLAG-dCas9 bait-containing cross-linked complexes (**Figure 2C),** thus eliminating the need for large amounts of histone antibodies. We tested this pipeline in a sequential (V5/histone) ChIP experiment, followed by qPCR and western blotting. As shown in **Figure 2D** (top panel), ChIP, using anti V5 affinity beads efficiently enriched for the HIV-1 promoter region targeted by the HA-V5-FLAG-dCas9. Western blotting of the ChIP decrosslinked eluate confirmed efficient bait recovery by immunoprecipitation **Supplementary Figure 3A**. The second sequential immunoprecipitation, using anti H3- anti H2B antibodies conjugated beads, while retaining the HIV-1 target locus of interest (**Figure 2D)** (bottom panel), results in a concomitant loss of HA-V5-FLAG-dCas9 bait at the protein level (**Supplementary Figure 3A**). Relative abundance of histone proteins is reduced during the V5 enrichment step while, as expected, they are retained after the histone H3/H2B enrichment step (**Supplementary Figure 3B**).

The specificity of the guided dCas9 is a critical point for locus purification. We, therefore, performed ChIP-sequencing experiments to

comprehensively investigate the locus specificity of our bait, which is guided and predicted to specifically bind to the integrated HIV-1 5'LTR. ChIP-sequencing was performed using the sequentially purified chromatin, first immunoprecipitated using V5 affinity beads, eluted and re-immunoprecipitated using Histone H3-H2B affinity purification. Both in ChIP-seq (**Figure 2 E**) and its confirmation by ChIP qPCR (**Figure 2F**) we observe a strong enrichment on the HIV-1 5' LTR while enrichment at human chromosomes, aside from centromeric artifacts common to ChIP-seq and a few minor off-target peaks (**Supplementary Table 1**), is low. Next, we specifically monitored the recovery of the top potential dCas9 off-target binding sites as predicted for the HS2 gRNA sequence (5'-GAAGCGCGCACGGCAAG-3') by the online tool http://www.rgenome.net/cas-offinder/. The top predicted off-target, located at chr1:42,957,793 , allows 2 mismatches in the sequence, while all subsequent off-targed locations predicted allow 3 or more mismatches in the sequence. Zooming in on these predicted off-target regions in the ChIP-seq data (**Figure 2E, G**) and by ChIP qPCR (**Figure 2F**) demonstrated the absence of traceable peaks or any substantial PCR signal for these chromosomal loci. Our results demonstrate a highly specific enrichment of the targeted HIV-1 5'LTR at the DNA level, whose protein content was subjected to mass spectrometry, within the Catchet-MS pipeline.

Cachet-MS identifies known and novel host factors associated with the latent and active HIV-1 promoter

We scaled up the Catchet-MS workflow (**Figure 2C)**, to approximately 3 billion cells as starting material in the unstimulated and PMA stimulated conditions to model J-Lat 11.1 HIV-1 latency and activation. **Figure 3A** presents a heatmap of the mass spectrometry analysis performed at different steps of the Catchet-MS purification pipeline. To assess sample complexity prior to bait enrichment, 1% of the input chromatin material, prepared using the optimized CheIP protocol in both latent and activated states, was analyzed by mass spectrometry. As shown in **Figure 3A** the corresponding lanes in the heatmap show high sample complexity, characterized by a large number of high protein

intensity values. The samples are enriched for nuclear and chromatin-associated proteins but also contain numerous cellular contaminants, resulting from carryover precipitation of insoluble, non-chromatin associated complexes (deposited Supplementary raw data). As expected, the abundance of the HA-V5-FLAG-dCas9 bait is low, in these input samples (**Figure 3B and C)**. By contrast, the assessment of sample complexity following the anti-V5 affinity purification step shows efficient enrichment for the HA-V5-FLAG-dCas9 bait-containing complexes. This stage of the purification, shown in the third and fourth lanes of **Figure 3A,** results in a marked reduction in sample complexity caused by the elimination of protein complexes that do not contain the HA-V5-FLAG-dCas9 bait concomitant with high enrichment of the HA-V5-FLAG-dCas9 bait (**Figure 3B and C**). Finally, re-immunoprecipitation using Histone H2B and H3 conjugated affinity beads leads to a clear difference in protein abundances between the unstimulated and PMA stimulated samples, as shown in the last two lanes of **Figure 3A**. Concomitantly, at this stage, we observe a loss in HA-V5-FLAG-dCas9 as well as, presumably, the corresponding bait-associated complexes not associated with histones (**Figure 3B**). As expected, given the known accumulation of non-locus bound Cas9 at the RNA-rich nucleolar compartment (Chen et al., 2013; Ma et al., 2016), V5 affinity purification resulted in an increase in the number of nucleolar proteins detected, followed by their loss following the subsequent histone affinity purification step (**Supplementary Figure 3C**).

Analysis of the MS data from the final locus enrichment step resulted in a list of 678 proteins, identified with high confidence, Mascot score > 100. We then applied two stringent and unbiased selection criteria, Illustrated in **Figure 3D**, to narrow down the list of candidates by removing potential contaminants. First, we filtered out frequent contaminants using the Crapome database https://www.crapome.org/, a comprehensive database of contaminants commonly present in affinity purification coupled to mass spectrometry (AP-MS) experiments. As a second filter, we applied a GO cellular compartment and function analysis (GO-terms nucleus, chromatin-associated, histones bound, bound to transcription factors, DNA associated, or RNA associated) to include only nuclear proteins in our further analysis. Applying these criteria, we compiled a stringent list (n=38) of proteins predominantly associated with

the HIV-1 promoter in the latent state (**Figure 3E and F**), a list (n=122) of common proteins, including the dCas9 bait and potential contaminants, found to associate with the HIV-1 5'LTR under both conditions (**Figure 3E and Supplementary Table 2**), and a list (n=84) of factors predominantly associated with the activated HIV-1 promoter following treatment with PMA (**Figure 3E and Supplementary Table 3).** Previously, it was reported that the latent provirus associates with the nuclear periphery (Dieudonne et al., 2009). Therefore, we re-analyzed our unfiltered data and selected the hits belonging to the "nuclear periphery" GO category (GO:0034399), which includes the subcategories "nuclear matrix" and "nuclear lamina" and indeed find Lamin B1 (LMNB1) among other nuclear body proteins to be more predominantly associated with the latent state (**Supplementary Figure 4**).

Functional validation of proteins identified to associate with the latent promoter

In search of putative molecular targets for therapeutic inhibition and HIV-1 latency reversal, we focused on the 38 proteins presented in the table in **Figure 3F** comprising factors distinctly associated with the latent HIV-1 LTR in vivo. Of these latent HIV-1 LTR-associated candidates, a significant number (n=11) were previously reported to restrict viral expression (**Figure 3F** referenced in the table) and serve as positive controls that validate the quality of the experimental approach, providing confidence towards the veracity of the candidate list. We evaluated the effect of shRNA mediated knockdown of a selection of the novel factors we identified, on the HIV-1 5'LTR-driven GFP reporter by flow cytometry and on the expression of HIV-1 genes Gag, pol, and Tat by RT-PCR in J-Lat 11.1 cells (**Figure 3F; Supplementary Figure 5**). Depletion of a number of the selected candidates (n=5 out of 10), namely HP1BP3, IKZF1, CDC73, DKC1, and PNN, resulted in significant ($p < 0.05$) upregulation of HIV-1 genes and an increase in the percentage of GFP positive cells (green boxes, **Figure 3F** and **Supplementary figure 5**), while for a small number of factors tested (N=3 out of 10), we did not observe a significant change in HIV-1 expression (yellow boxes, **Figure 3F**) and the remaining factors were found to be essential for cell viability

(x mark, **Figure 3F**). Our data suggested that the selected n=5 candidates are required for repression of HIV-1 expression in J-Lat 11.1 cells.

IKZF1 binds to the latent HIV-1 promoter and is repressive to HIV-1 transcription

Catchet-MS identified the IKAROS Family Zinc Finger 1 protein (IKZF1) as one of the factors to be exclusively associated with the repressed HIV-1 promoter (**Figure 3F**). IKZF1, a critical factor required for normal T cell development that can act both as a transcriptional repressor and activator (Geimer Le Lay et al., 2014; Ng et al., 2009; Zhang et al., 2011) has been reported to regulate gene expression through its association with the nucleosome remodeling and deacetylase complex (NuRD) and the positive transcription elongation factor (P-TEFb) (Bottardi et al., 2015; Davis, 2011; Marke et al., 2018; Schwickert et al., 2014; Zhang et al., 2011). Additionally, IKZF1 mediated gene silencing in T cells has been shown to be facilitated by its interaction with the Polycomb repressive complex 2 (PRC2), which promotes histone H3 lysine 27 trimethylation, a mark of transcriptionally silent chromatin (Oravecz et al., 2015). Consistent with its role as a repressive factor in T cells, depletion of IKZF1 in our functional testing screen using independent shRNA clones led to the strongest reactivation of HIV-1 expression (5 to 10 fold), as measured by the increase of GFP positive cells in flow cytometry and qRT-PCR for HIV-1 genes (**Figure 4A-C**). To ensure that the observed latency reversal is not subject to clonal effects in J-Lat 11.1 cells, we depleted IKZF1 in J-Lat A2 cells, harboring an integrated HIV 5' LTR driven GFP reporter and observed similar reversal of HIV-1 latency (**Supplementary Figure 9A**).

The IKZF family consists of several family members (Marke et al., 2018; Powell et al., 2019), although IKZF1 is the only family member detected in our mass spectrometry data. We assessed the expression of the other IKZF family members in Jurkat cells (RNA sequencing (Palstra et al., 2018)) and proceeded with shRNA mediated depletion of IKZF2 and 5, which are expressed in Jurkat cells (**Supplementary Figure 6A**). Depletion of IKZF2 and IKZF5 also resulted in HIV-1 latency reversal, although modestly compared to IKZF1 (**Supplementary Figure 6B**). These results are consistent with the lower levels of expression of IKZF2

and IKZF5 in T cells, compared to IKZF1, and with the well-established heterodimeric interactions among IKZF family members (Boutboul et al., 2018; Mullighan et al., 2009; Sun et al., 1996). We next sought to confirm and examine the association of IKZF1 with the latent HIV-1 LTR. Downstream of the 5'LTR, at position +818/+864 we identified a putative IKZF binding site, which is composed of a consensus TGGGAA/T sequence and two extra GGGA core sites (Li et al., 2011), (**Figure 4D)**. To assess IKZF1 binding at the predicted sites, we performed ChIP-qPCR experiments in latent and PMA treated J-Lat 11.1 cells using antibodies specific for IKZF1 (**Figure 4E**). In agreement with the Catchet-MS data, ChIP experiments in latent J-Lat 11.1 cells demonstrated IKZF1 enrichment between HIV-1 HS2 and Nuc2, (**Figure 4E**). Importantly, activation of HIV-1 transcription by PMA treatment abrogated IKZF1 binding (**Figure 4E and Supplementary Figure 7A**), consistent with the notion that IKZF1 may be important for maintenance of HIV-1 transcriptional repression. To confirm the specificity of IKZF1 binding, we also performed ChIP in control J-Lat 11.1 cells, infected with a scramble shRNA vector (Sh Control), and in cells infected with an shRNA vector targeting the IKZF1 mRNA (sh IKZF1). Our data show clear enrichment of IKZF1 binding over its predicted binding region in the sh Control cell line together with a dramatic loss of binding upon shRNA mediated depletion in the IKZF1 depleted cells (**Figure 4F and Supplementary Figure 8A**), thus confirming the specificity of the antibody. To further control for the specificity of the IKZF1 signal we also monitored enrichment of IKZF1 at endogenous IKZF1 targets previously reported to be enriched for IKZF1 binding in B cells (Song et al., 2016) (**Supplementary Figure 8C**).

We then examined the effect of IKZF1 depletion on the chromatin state of the region by histone ChIP-qPCR experiments using antibodies against the active chromatin modification H3 lysine 4 trimethylation (H3K4me3), the repressive chromatin modifications H3 lysine 27 trimethylation (H3K27me3) and H3 lysine 9 trimethylation (H3K9me3), using the total histone H3 signal (**Figure 4G**) for normalization.

Upon IKZF1 depletion the chromatin state is characterized by a drastic loss of enrichment for the H3K27me3 mark (**Figure 4H; Supplementary Figure 8E**), a moderate increase of the H3K4me3 mark

(**Figure 4I; Supplementary Figure S8F**) and a concomitant decrease in the repressive chromatin mark H3K9me3 (**Supplementary Figure 8G**). Similar data were obtained upon IKZF1 depletion in J-Lat A2 cells (**Supplementary Figure 9C-G**), thus confirming that the effects on chromatin are not subjected to clonal effects.

We compared the histone modification profile observed, with those obtained in latent J-lat 11.1 cells and upon PMA stimulation (**Supplementary Figure 7B-E**). Upon treatment with PMA, the chromatin state is also characterized by increased H3K4me3 (**Supplementary Figure 7C**) and a concomitant decrease in the repressive chromatin marks H3K27me3 (**Supplementary Figure S7D**) and H3K9me3 (**Supplementary Figure 7E**). IKZF1 depletion, however, led to a more prominent loss of enrichment for the H3K27me3 mark (**Figure 4H**).

In T cells, IKZF1 is necessary for mediating gene silencing through the recruitment of the Polycomb repressive complex 2 (PRC2) and the deposition of the H3K27me3 mark (Oravecz et al., 2015). Interestingly, our Catchet-MS experiment identified SUZ12, a core subunit of the PRC2 complex, and CBX8, a subunit of the Polycomb repressive complex 1 (PRC1) that acts as a reader of the H3K27me3 modification (Bracken et al., 2006; Malik and Hemenway, 2013; Vidal and Starowicz, 2017) to be also associated with the HIV-1 5'LTR in its latent state. We therefore conducted ChIP experiments for probing the IKZF-1 mediated binding of SUZ12 to the region to verify the hypothesis that IKZF1 may be necessary for recruitment of PRC2 complex to the HIV-1 5'LTR. We additionally examined the recruitment of CBX8 to check whether, the reduction in H3K27me3 mark deposition observed in absence of IKZF1, affects CBX8 binding. Consistent with this hypothesis, our data shows that depletion of IKZF1 leads to reduced enrichment of SUZ12 (**Figure 4J and Supplementary Figure 8B**) and CBX8 (**Figure 4K**) over the HS2 5'LTR region. Importantly, as shown by western blotting, depletion of IKZF1 does not lead to decreased levels of expression of SUZ12 and CBX8, suggesting that the effects observed are exclusively consequence of the absence of IKZF1 recruitment to the region (**Figure 4L**).

Targeting IKZF1 by iberdomide treatment reverses HIV-1 latency in ex vivo infected primary CD4+ T cells without

significant effects on effector function, inducing T cell activation, or toxicity,

Iberdomide (CC-220) and other thalidomide-derived, immunomodulatory drugs (IMIDs), have been shown to cause selective ubiquitination and degradation of IKZF1 and its related family member IKZF3 (Kronke et al., 2014; Schafer et al., 2018). Thalidomide and its analogs, lenalidomide, and pomalidomide, are FDA approved drugs employed in the treatment for multiple myeloma (MM) leading to improved patient survival rates. The mechanism of action for IMIDs activity lies in their affinity for cereblon (CRBN) which is part of the cullin-ring finger ligase-4 cereblon ($CRL4^{CRBN}$) E3 ubiquitin ligase complex. Other members of the complex include cullin 4A (*CUL4A*), the DNA damage binding protein 1 (*DDB1*) and regulator of cullin 1 (*ROC1*). Iberdomide is a novel compound with higher affinity for CRBN and currently under clinical development for the treatment of systemic lupus erythematosus (SLE) and relapsed/refractory multiple myeloma (RRMM). Binding of iberdomide to CRBN modulates the E3 ubiquitin ligase activity of the complex, increasing its affinity for IKZF1 and IKZF3, and leads to their ubiquitination and proteasome-dependent degradation. We, therefore, set out to establish if iberdomide treatment in latent HIV-1 infected cells would induce degradation of IKZF1 and lead to HIV-1 latency reversal.

As the main reservoir of latent HIV-1 in infected individuals is resting CD4+ T cells, we ex vivo infected, without prior activation, CD4+ T cells obtained from healthy donors, with a defective full-length HIV-1 virus harboring a luciferase reporter to establish latent infections as shown in **Supplementary Figure 10A** (Lassen et al., 2012). Treatment of latent HIV-1 infected primary CD4+ T cells with iberdomide for 48 hours, resulted in moderate but significant ($p < 0.05$) reversal of latency, as observed by an increase in the mean luciferase activity compared to the untreated control (**Figure 5A**) in all 6 donor CD4+ T cells examined. Bromodomain end extra-terminal domain (BET) inhibitors were reported to act synergistically with the activity of IMIDs in treatment of refractory forms of multiple myeloma (Diaz et al., 2017; Moros et al., 2014). We, therefore, examined whether these compounds also synergize in context of

HIV-1 latency reversal. Indeed, co-treatment of Iberdomide and JQ1 resulted in a robust and synergistic HIV-1 latency reversal (**Figure 5A**). To confirm that treatment with iberdomide results in degradation of IKZF1at the protein level, we performed western blot analysis of primary cells treated for 48hours with iberdomide. As expected, treatment with iberdomide, alone or in combination with JQ1, resulted in degradation of IKZF1 as shown in **figure 5B** and **Supplementary figure 10B.** Importantly, treatment with iberdomide did not affect IKZF1 expression at the level of transcription (**Figure 5C),** consistent with the known post-transcriptional mechanism by which IMIDs target IKZF1 for CRBN mediated degradation. Conversely, mRNA levels of the endogenous IKZF1 targets, p21 and cMyc (Bjorklund et al., 2020; Fecteau et al., 2014) were significantly affected by the treatment (**Figure 5C)**.

Confounding factors for potential clinical use of candidate LRAs is toxicity and the possibility that they induce unwanted immunomodulatory effects or global immune activation, thus leading to serious adverse effects. Besides, HIV reactivation strategies that aim for a cure will require an intact cytotoxic compartment that promotes viral clearance. Potential toxicity of iberdomide treatment of primary CD4+ T cells was determined by Annexin V staining, followed by flow-cytometry. As shown in **Figure 5D and Supplementary Figure 10C and E**, CD4+T cell viability quantitated as percentage of Annexin V positive cells 24 and 48 hours following iberdomide treatment was not significantly affected.

Given the known immunomodulatory role of Iberdomide and Thalidomide-derived drugs, we investigated the effects of Iberdomide treatment alone or in combination with JQ-1 in T cell activation, proliferation and functionality. Our results, as shown by extracellular CD69 staining followed by flow-cytometry, demonstrate that Iberdomide treatment alone, or in combination with JQ-1, does not result in global activation of primary CD4+ T cells (**Figure 5E and F**) (**Supplementary Figure 10D and E**).

We then examined proliferation potential upon iberdomide treatment alone or in combination with JQ-1. As previously reported in the literature, and consistent with their anti-lymphoproliferative capacity (Fuchs, 2019), we observed decreased proliferation capacity upon

treatment of CD4+ and CD8+ primary T cells (**Figure 5G and H**; **Supplementary Figure 10F and G**). Lastly, we assessed the effect of iberdomide on T cells functionality, by measuring cytokines IFNγ and IL-2 in CD4+ and CD8+ primary T cells. Iberdomide treatment alone or in combination with JQ-1 does not hamper the production of cytokines IFNγ (**Figure 5 I and J; Supplementary Figure 11A and B**) and IL-2 (**Supplementary Figure 11 C-F**) upon stimulation of CD4+ or CD8+ T cells and therefore does not diminish T cell functionality. On the contrary, and consistent with the literature (Gandhi et al., 2014), we observe an increase in the production of IL-2 upon treatment with the LRAs (**Supplementary Figure 11 C-F**).

Targeting IKZF1 by iberdomide treatment reverses latency in ex vivo infected primary CD4+ T cells and cells obtained from cART suppressed HIV-1 infected patients

To validate our findings in a more relevant setting, we tested the efficacy of Iberdomide in CD4+ T cells obtained from virologically suppressed HIV-1 patients. 5 aviremic patients with maintained viremia below 50 copies/mL for at least one year were selected for the study (**Figure 6A**). CD4+ T cells were isolated from PBMCs by negative selection and were left untreated or treated as indicated with Iberdomide, JQ1, or PMA/Ionomycin as a positive control (**Figure 6B**). Treatment with iberdomide alone resulted in a significant increase in cell-associated HIV-1 gag copies in all 5 donors (mean gag copies 42.68) compared to control (mean gag copies 5.262), and was comparable to that observed after treatment of cells with the BET inhibitor JQ1 (mean gag copies 67.72). Due to the low frequency of reservoir cells, we were unable to detect HIV-1 gag copies above the limit of detection for three donors in the untreated control, which we display as 1 copy for representation purposes. PMA/Ionomycin treatment, as expected, resulted in the highest increase in HIV-1 transcription (mean gag copies 758.1). As also observed in primary CD4+ T cells from healthy donors (**Figure 5C**), treatmenent with iberdomide resulted in a modest downregulation of c-Myc, significant when in combination with JQ1, and a significant upregulation of p21 mRNA levels (**Figure 6C**) in cells isolated from aviremic, HIV-1 infected, partecipants.

Importantly, the latency reversal properties of iberdomide treatment in CD4+ T cells obtained from cART suppressed, HIV-1 infected patients, closely match our observations in ex vivo infected primary CD4+ T cells. Remarkably, also in cells derived from HIV-1 infected, aviremic participants we observe a modest but significant increase upon Iberdomide treatment and a robust, synergistic increase in cell-associated HIV-1 RNA upon co-treatment with JQ-1 (mean gag copies 254.72) (**Figure 6B**).

DISCUSSION

Here we identify regulatory protein complexes distinctly bound to the HIV-1 promoter in the latent and active states in vivo. For this we set-up Catchet-MS, a reverse-ChIP strategy which couples CRISPR/dCas9 targeting and purification of a genomic locus to an additional biochemical histone affinity step to enrich for chromatin-associated dCas9 locus-bound complexes. Using targeted dCas9 as bait makes the system versatile and renders Catchet-MS applicable to study other single genomic loci in live cells, without the need to modify the site of interest. Additionally, the introduction of a second, histone based, affinity purification step ensures that Catchet-MS effectively removes unwanted background originating from cellular contaminants and non-localized bait molecules from the mass spectrometry analysis. Catchet-MS can thus be considered a discovery tool to identify proteins distinctively associated with a genomic region of interest in two functionally disparate states, including transcriptional on-off state, as with the latent and active HIV-5'LTR here, states of differentiation, or distinct genomic SNPs.

As Locus-specific proteomics is a developing field that still represents tremendous biochemical challenges, we acknowledge that our strategy also presents limitations common to locus-specific strategies. The high signal to noise ratio together with the low abundance of single-loci, represent a significant hurdle to overcome in locus-specific strategies to identify the complete repertoire of factors bound to a single locus in vivo (Gauchier et al., 2020). Aware of these limitations, we verified the locus specificity of our dCas9 bait targeting by ChIP sequencing, made use of a large input (~3 billion cells) and introduced a two-step (V5/histones) affinity purification, increasing sensitivity and specificity over a single-step affinity purification, and used stringent filtering and exclusive selection of MS hits detected with high confidence. Importantly, we

describe the distinct proteome of latent versus activated HIV-1 5'LTR bound factors and not that of the total HIV 5'LTR bound proteome. In our analysis, the chromatin obtained from cells containing an activated HIV-1 5'LTR serves as a control for the chromatin obtained from cells harbouring latent HIV-1 5'LTR, and vice versa. Using this approach, the majority of the proteins common to both conditions, including the dCas9 bait, potential non-specific contaminants, but also well-established functionally relevant factors such as EED (Nguyen et al., 2017; Turner et al., 2020), MTA2 (Cismasiu et al., 2008) and UCHL5 (Rathore et al., 2020), are excluded from further analysis, thus confirming the stringency of the approach. A point of concern with the use of dCas9 based bait guided to the HIV-1 promoter was the potential displacement of or interference with binding of putatively important interactors biasing our candidate list. Although we cannot formally exclude this possibility, dCas9 targeting to the 5'LTR did not appear to interfere, functionally, with viral latency or reactivation (Figure 1F and Supplementary Figure 1D), suggesting that any such interference would have been minor. Thus, despite some limitations, we are confident that Catchet-MS has identified bona fide interactors of the HIV-1 5' LTR and thus represents an effective discovery tool. The validity of our approach is justified by the identification of previously identified and characterized interactors serving as positive controls as well as our extensive functional validation of several candidate proteins with a special focus on IKZF1.

Among the list of interactors bound to the HIV-1 5'LTR locus, in addition to the well-established candidates, we find a number of novel interactors of the HIV-1 promoter (5'LTR) in its latent and active states as shown in Figure 3F and Supplementary Table 3. Among the latent 5'LTR associated factors, we find proteins belonging to chromatin remodeling complexes with well-established roles in HIV-1 latency including the Polycomb repressive complex1 (PRC1), Polycomb repressive complex 2 (PRC2), the SWItch/Sucrose Non-Fermentable complex (SWI/SNF) and the Nucleosome Remodeling Deacetylase (NuRD) complexes (Khan et al., 2018; Ne et al., 2018). Sequence-specific transcription factors are another class of proteins we identify enriched on the latent HIV-1 LTR, with YY1 (Coull et al., 2000) and POU2F1 (Goffin et al., 2005) previously reported to repress HIV-1 transcription. We additionally identify proteins

structurally bound to chromatin such as the DNA topoisomerase 2-alpha enzyme (TOP2A) and the Sister chromatid cohesion protein PDS5 homolog A (PDS5A) and B (PDS5B). As expected, the majority of chromatin structural components were enriched in both the activated and repressed states (Supplementary Table 2). Associated with the repressed locus, we also find the facilitates chromatin transcription (FACT) complex component, SUPT16H, previously described to promote viral latency by interfering with Tat-mediated recruitment of P-TEFb (Huang et al., 2015).Dyskerin pseudouridine synthase 1 (DKC1) is another interesting latent LTR-bound candidate, previously described to promote latency by catalyzing the pseudouridylation and stabilization of the 7SK snRNP complex, inhibiting the release of P-TEFb (Zhao et al., 2016). Moreover, given that HIV-1 preferentially integrates in the nuclear periphery and is essentially regulated by proximity to the PML nuclear bodies (Lusic and Giacca, 2015), we re-analysed our unfiltered data for hits belonging to the "nuclear periphery" GO category (GO:0034399). Interestingly, we find that many factors in this category are associated with the HIV-1 5'LTR (Supplementary Figure S4) and that Lamin B1 (LMNB1) is more predomaninantly associated with the latent state consistent with a previous report that the latent provirus associates with the nuclear periphery (Dieudonne et al., 2009). Interestingly in this context, the HIV-1 LTR binding repressor YY-1, has also been reported to interact with and mediate H3K27me3 -dependent formation of lamina-associated domains (LADs), and is more strongly associated with the latent state (Harr et al., 2015). As expected, upon PMA stimulation and HIV-1 transcriptional activation, a much larger number of ribonucleoproteins, splicing factors as well as proteins involved in mRNA processing and nuclear-cytoplasmic transport are identified by Catchet-MS, most likely recruited to the locus following transcriptional activation (Supplementary Table 3).

In search of putative novel molecular targets for HIV-1 latency reversal, we focused on factors identified to be significantly enriched or uniquely bound to the latent and not activated HIV-1 LTR. Using shRNA-mediated depletion, we functionally validated the activity of a number of novel putative candidates in J-Lat 11.1 cells. Of the 10 putative candidates tested, shRNA depletion of 5 factors (HP1BP3, IKZF1, CDC73, DKC1, PNN) resulted in HIV-1 latency reversal as observed by a significant increase in

the percentage of GFP positive cells and expression of HIV-1 genes. One of the strongest observed latency reversals upon depletion was due to the sequence-specific transcription factor IKZF1, an attractive candidate for which pharmacological drug targeting is also available (Kronke et al., 2014; Schafer et al., 2018). IKZF1, a critical factor for lymphoid lineage specification in hematopoietic stem cells, suppresses the stem cell and myeloid programs and primes for the expression of lymphoid specific genes (Ng et al., 2009). IKZF1 is also an important regulator of T cell function (Georgopoulos, 2017; Powell et al., 2019). Mechanistically, IKZF1 has a dual role in transcription, acting, depending on the context, both as a repressor and an activator (Geimer Le Lay et al., 2014; Ng et al., 2009; Zhang et al., 2011). In an activating capacity, IKZF1 can restrict the activity of the NuRD complex, promoting chromatin accessibility (Davis, 2011; Marke et al., 2018; Schwickert et al., 2014; Zhang et al., 2011). IKZF1 has also been proposed to act as an adaptor protein for the local recruitment of p-TEFb and the protein phosphatase 1α at IKZF1 target genes, facilitating transcription elongation (Bottardi et al., 2015). In T cells, however, IKZF1 has been shown to associate with PRC2 and is required for repression of Notch target genes and the hematopoietic stem cell program (Oravecz et al., 2015). IKZF1-mediated gene silencing may also depend on its interaction with the co-repressors CtBP, CtIP and SWI/SNF-related complex and HDAC-containing Sin3 complexes (Marke et al., 2018).

Consistent with its described repressive mechanisms and functions, depletion of IKZF1 led to a strong reactivation of HIV-1 expression in J-Lat 11.1 cells and J-Lat A2. Upon PMA-induced transcription, IKZF1 binding downstream of the HIV-1 promoter is abrogated, indicating that IKZF1 binding is required for transcriptional repression. Remarkably, depletion of IKZF1 in J-Lat 11.1 cells and J-Lat A2, reveals that IKZF1 is required for the establishment of a repressive chromatin environment, characterized by the presence of the repressive chromatin marks H3K9me3 and H3K27me3. Upon IKZF1 depletion the region becomes de-repressed, displaying a drastic loss of enrichment for the H3K27me3 mark which is even more robust than what is observed following PMA induced activation. Evidence points to a model in which, in T-cells, IKZF1 regulates the epigenetic silencing of IKZF1 target genes

via recruitment of the PRC2 complex (Oravecz et al., 2015). The role of PRC2 as a regulatory complex, enriched on the latent HIV-1 promoter with a critical role in compaction of chromatin, recruitment of PRC1 and repression of HIV-1 transcription is well established (Bracken et al., 2006; Khan et al., 2018; Marke et al., 2018). Consistent with these reports our Catchet-MS data identified SUZ12, a core subunit of the PRC2 complex, and CBX8, a subunit of the PRC1 complex, to be also associated with the HIV-1 5'LTR in its latent state, pointing to a possible role for these complexes in regulating the chromatin landscape of this region (Figure 3F). We investigated the potential IKZF1-dependent recruitment of the PRC2 subunit SUZ12 to the HIV-1 5'LTR by ChiP-qPCR; depletion of IKZF1 led to reduced SUZ12 enrichment over the HS2 region. Interestingly, we find that upon IKZF1 depletion, enrichment of the PRC1 component CBX8 at these regions was also reduced. Our results are consistent with a model in which IKZF1 directly recruits PRC2 to the HIV-1 5'LTR, as previously described at endogenous target genes in T cells (Oravecz et al., 2015). The PRC2-modified, H3K27 trimethylated region subsequently serves as a docking site for and results in rectruitment of PRC1 (Figure 6 D).

Expression of IKZF1 and related family member IKZF3 at the protein level can be controlled by modulating ubiquitination levels. IMIDs such as thalidomide, lenalidomide, pomalidomide and iberdomide promote ubiquitin-dependent proteasomal degradation of IKZF1 and IKZF3 by redirecting the substrate specificity of the CRL4CRBN ubiquitin ligase complex (Kronke et al., 2014; Lu et al., 2014). Among these drugs, iberdomide (CC-220), is a novel compound with the highest reported specificity for CRBN and the lowest IC50, currently in phase 2 Clinical trial for Systhemic lupus erythematosus (SLE) and Multiple Myeloma (MM). Due to its high potency we selected iberdomide for treatment of primary ex vivo HIV-1 infected CD4+ T cells and those obtained from cART suppressed aviremic participants. Iberdomide mediated depletion of IKZF1 was accompanied by a significant reversal of HIV-1 latency, with no significant associated toxicity. A class of compounds previously reported to synergize with the activity of IMIDs in inhibiting the growth of refractory forms of MM are BET inhibitors such as JQ1 (Diaz et al., 2017; Moros et al., 2014). As BET inhibitors are also

a well-established class of HIV-1 LRAs, we examined the latency reversal effect of combination treatment with iberdomide and JQ1. Remarkably, co-treatment of latently infected primary CD4+ T cells results in strong and synergistic induction of HIV-1 transcription in cells obtained from HIV infected cART suppressed aviremic patients, quantitated as increase in cell-associated HIV-1 Gag RNA. Thus, similar to what was observed in the treatment of resistant MM, and of therapeutic interest, combination of these two classes of compounds also leads to synergism in context of HIV-1 latency reversal.

Crucial to the potential applicability of Iberdomide treatment alone or in combination with other LRAs in future clinical studies is the absence of detrimental effects on the overall T cell biology and the preservation of a functional cytotoxic compartment. Interestingly, and consistent with its role as an immunomodulatory treatment for lymphoid and myeloid malignancies (Fuchs, 2019), we observed a reduction of T cell proliferative capacity after treatment with Iberdomide alone or in combination with JQ-1. Importantly, we demonstrate that the use of Iberdomide does not affect T cell functionality, as measured by cytokine expression in CD4+ and CD8+ T cells, and does not cause global immune activation. Together, our results support the potential use of Iberdomide as a novel LRA as it reactivates HIV-1 latency without significant toxicity, global T cell activation or impaired T cell functionality. Still, future studies including Iberdomide or other thalidomide class comopunds as LRA alone or in combination with other LRAs should take into consideration the anti-proliferative activity of these compounds and their direct effects on T cell biology.

Our data is consistent with a model in which iberdomide treatment of latent HIV-1 infected cells leads to IKZF1 degradation through CRBN and as consequence inhibits IKZF1 mediated recruitment of the PRC2 and PRC1 complexes downstream of the HIV-1 promoter (Figure 6D). Thus, iberdomide and other FDA/EMA approved IMID family compounds that target IKZF1 for degradation represent attractive candidates for inclusion in proof of concept clinical studies aiming to reduce the latent HIV-1 reservoir. The specificity of the IMID/IKZF1-targeting pharmacological strategy for HIV-1 latency reversal may also be enhanced by combination

treatment with other LRA class compounds such as BET inhibitors, which as our data demonstrates leads to synergistic latency reversal.

FIGURES AND FIGURES LEGENDS

Figure 1

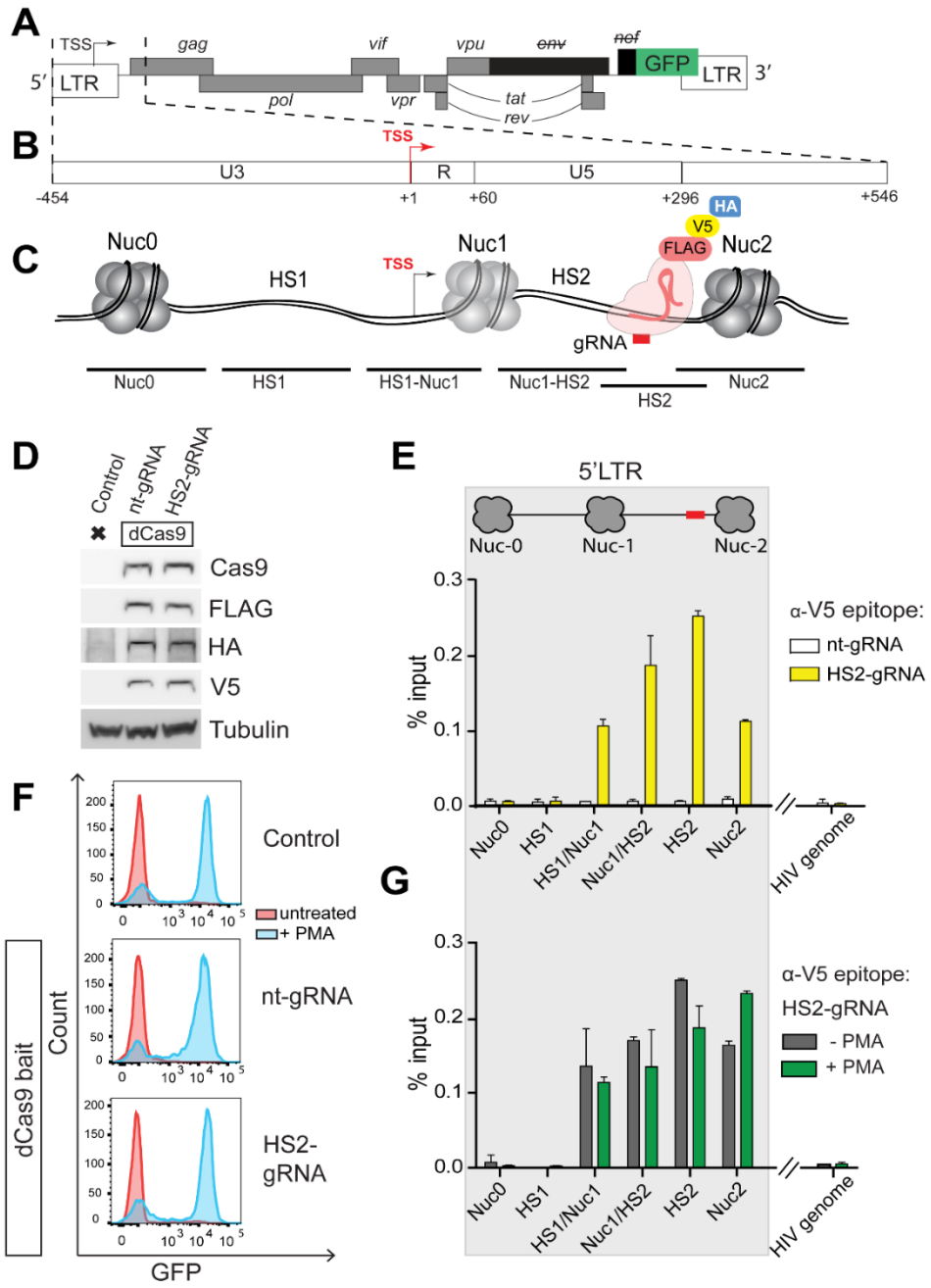

Figure 1. Generation and characterization of J-Lat 11.1 polyclonal cell line expressing a multiple epitope-tagged HA-V5-FLAG-dCas9 bait, guided to the 5'HIV-1 LTR HS2 region.

(A) Schematic representation of the genomic organization of the integrated HIV-1 provirus in J-Lat 11.1 cells, encoding GFP and containing a frameshift mutation in *env* and a partial deletion of *nef*.
(B) The 5' LTR region is further segmented into the U3, R, and U5 regions.
(C) Three strictly positioned nucleosomes, Nuc-0, Nuc-1 and Nuc-2, delimit the nucleosome-free regions HS1 and HS2, hypersensitive to nuclease digestion, as indicated. The HS2 region, to which the multiple epitope-tagged HA-V5-FLAG-dCas9 bait is guided, is indicated. The amplicons used to scan the chromatin region in ChIP-qPCR are shown.
(D) Western blot analysis indicates expression of multiple epitope-tagged HA-V5-FLAG-dCas9 bait in modified J-Lat 11.1 cells using antibodies specific for Cas9, V5, FLAG and HA as indicated. Parental J-Lat 11.1 cell lysate is used as a negative control and α-Tubulin is used as a loading control.
(E) Flow cytometry histograms show the distribution of GFP positive cells in unstimulated and PMA stimulated control J-Lat 11.1 cells, cells expressing the dCas9 bait and a non-targeting gRNA (nt-gRNA) and cells expressing the bait and the HS2 targeting gRNA (HS2-gRNA).
(F) ChIP-qPCR analysis with anti V5 epitope affinity beads indicate specific enrichment of the HA-V5-FLAG-dCas9 bait over the guided HIV-1 LTR region. White bars represent data generated in cells expressing the dCas9 bait together with a non-targeting gRNA (nt-gRNA), yellow bars represent data generated in cells expressing the bait and the single guide RNA targeting the HS2 region of the HIV-1 5'LTR (HS2-gRNA). Data show a representative experiment, error bars represent the standard deviation (±SD) of two separate real-time PCR measurements. HIV-1 5'LTR sequences recovery is calculated as a percentage of the input.
(G) ChIP-qPCR analysis with anti V5 epitope affinity beads in latent (-PMA; grey bars) and PMA treated cells (+PMA; green bars) expressing the dCas9 bait and the HS2-gRNA. Data are the mean of 2 independent experiments (±SD). HIV-1 5'LTR sequences recovery is calculated as a percentage of the input.

Figure 2

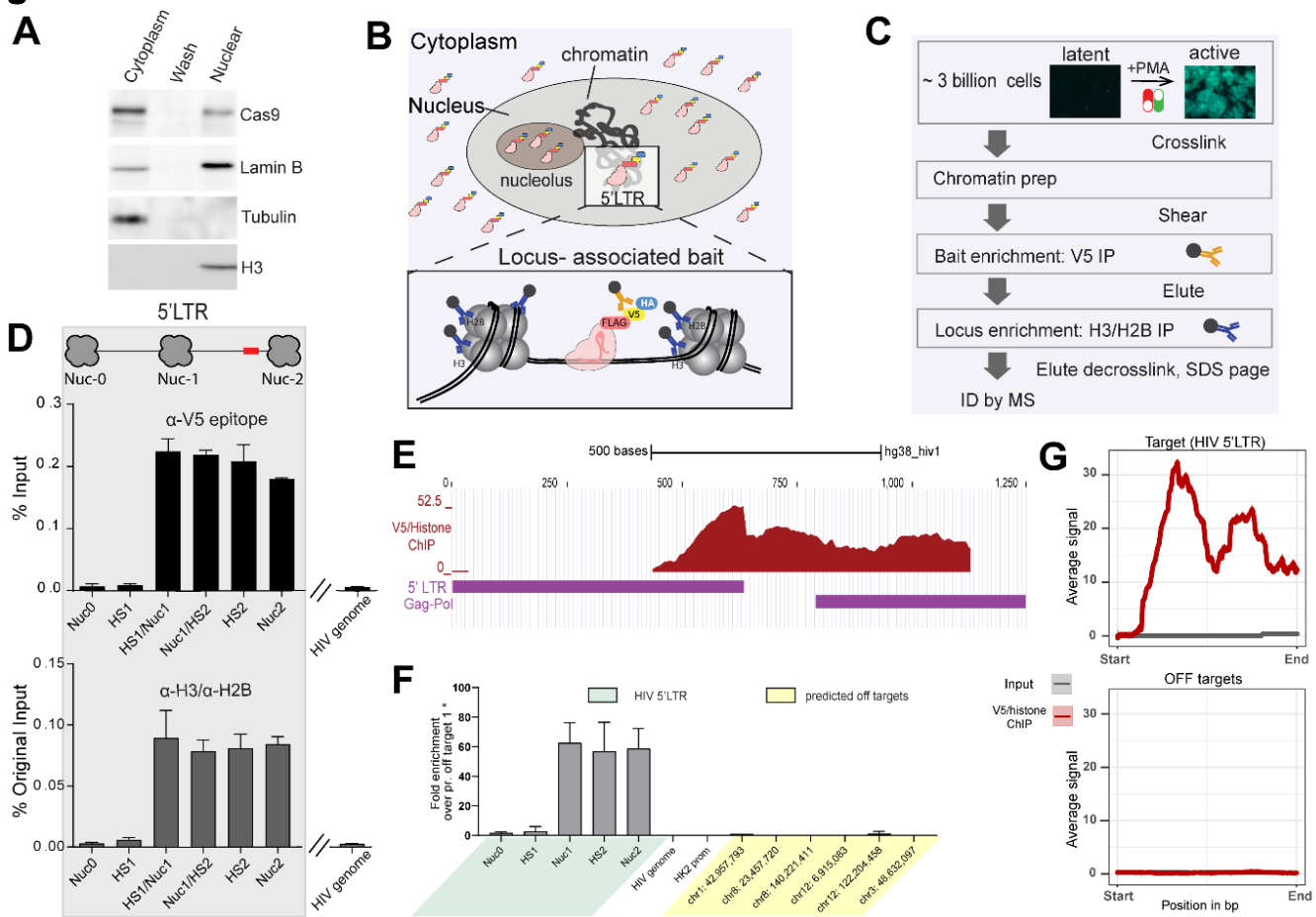
A
Cytoplasm
Wash
Nuclear
Cas9
Lamin B
Tubulin
H3
B
Cytoplasm
chromatin
Nucleus
nucleolus
5'LTR
Locus- associated bait
C
~ 3 billion cells
latent
+PMA
active
Crosslink
Chromatin prep
Shear
Bait enrichment: V5 IP
Elute
Locus enrichment: H3/H2B IP
Elute decrosslink, SDS page
ID by MS
D
5'LTR
Nuc-0
Nuc-1
Nuc-2
α-V5 epitope
% Input
Nuc0
HS1
HS1/Nuc1
Nuc1/HS2
HS2
Nuc2
HIV genome
α-H3/α-H2B
% Original Input
E
500 bases
hg38_hiv1
V5/Histone ChIP
5' LTR
Gag-Pol
F
HIV 5'LTR
predicted off targets
Fold enrichment over pr. off target 1 *
HK2 prom
chr1: 42,957,793
chr8: 23,457,720
chr8: 140,221,411
chr12: 6,915,083
chr12: 122,204,458
chr3: 48,632,097
G
Target (HIV 5'LTR)
Average signal
Start
End
Input
V5/histone ChIP
OFF targets
Position in bp

Figure 2. dCas9 targeted chromatin and histone enrichment for mass spectrometry (Catchet-MS), a method to isolate and identify locus-bound protein complexes in vivo.

A) Western blot analysis using antibody specific for dCas9 indicates localization of HA-V5-FLAG-dCas9 bait following a nuclear and nucleolar fractionation protocol. α-Tubulin is used as a cytoplasmic marker, Histone H3 is used as a chromatin marker while Lamin Bis used as a nuclear marker.
(B) Schematic representation of the dCas9 bait cellular localization.
(C) Schematic representation of the Catchet-MS workflow. Approximately 3 billion cells per condition are cross-linked with formaldehyde to stabilize the protein-protein and protein DNA interaction. Following a stringent chromatin enrichment protocol, the cross-linked chromatin is isolated and fragmented by ultrasound sonication. The dCas9 containing complexes are immunoprecipitated using anti V5 antibody conjugated affinity beads, eluted from the beads, and used as input material for a second round of purification with anti-histones (H3, H2B) antibody-conjugated beads, in order to remove the non-chromatin bound fraction of the HA-V5-FLAG-dCas9 bait complexes and to enrich for the locus associated bait complexes. Immunoprecipitated material is finally decrosslinked, resolved on an SDS-page and prepared for mass spectrometry analysis.
(D) (Top-panel) ChIP-qPCR analysis with anti V5 epitope affinity beads in chromatin fraction prepared from unstimulated cells indicates specific enrichment of HA-V5-FLAG-dCas9 over the HIV-1 5'LTR. Data show a representative experiment, error bars represent the standard deviation (SD) of two separate real-time PCR measurements, HIV-1 5'LTR levels are calculated as percentages of the input. The V5 affinity-purified chromatin (represented in top panel) was eluted and used as input for a sequential immunoprecipitation with a mix of histone H2B and H3 conjugated affinity beads and the isolated material was analyzed by qPCR (Bottom panel). ChIP-qPCR with anti H3/H2B conjugated affinity beads indicates 5'LTR enrichment of HA-V5-FLAG-dCas9 bait after sequential V5/histone affinity purification.Data show a representative experiment, error bars represent the standard deviation (SD) of two separate real-time PCR measurements, HIV-1 5'LTR levels in both the V5 and histone affinity purification are calculated as percentages of the same original input.
(E) ChIP-sequencing tracks of the V5/histone (H3/H2B) sequentially purified chromatin over the HIV-1 5' LTR.
(F) Average coverage profiles using ChIP sequencing reads mapped 500bp upstream and downstream of the peak center at the 5'LTR region of the HIV genome ('Targets') to the respective coverage around the predicted off targets ('OffTargets'). 'Start' denotes the starting base pair of the aforementioned 1kb region around the peak centers and 'End' the ending base pair respectively.
(G) ChIP-qPCR confirmation analysis of the V5/histone (H3/H2B) sequentially purified chromatin at the HIV-1 5'LTR and at dCas9 bait predicted off target regions. Predicted off-target regions were calculated allowing 2 to 3 mismatches

in the gRNA sequence. Data are presented as fold enrichment over the predicted off-target region on genomic location chr1: 42,957,793 and indicated with *.

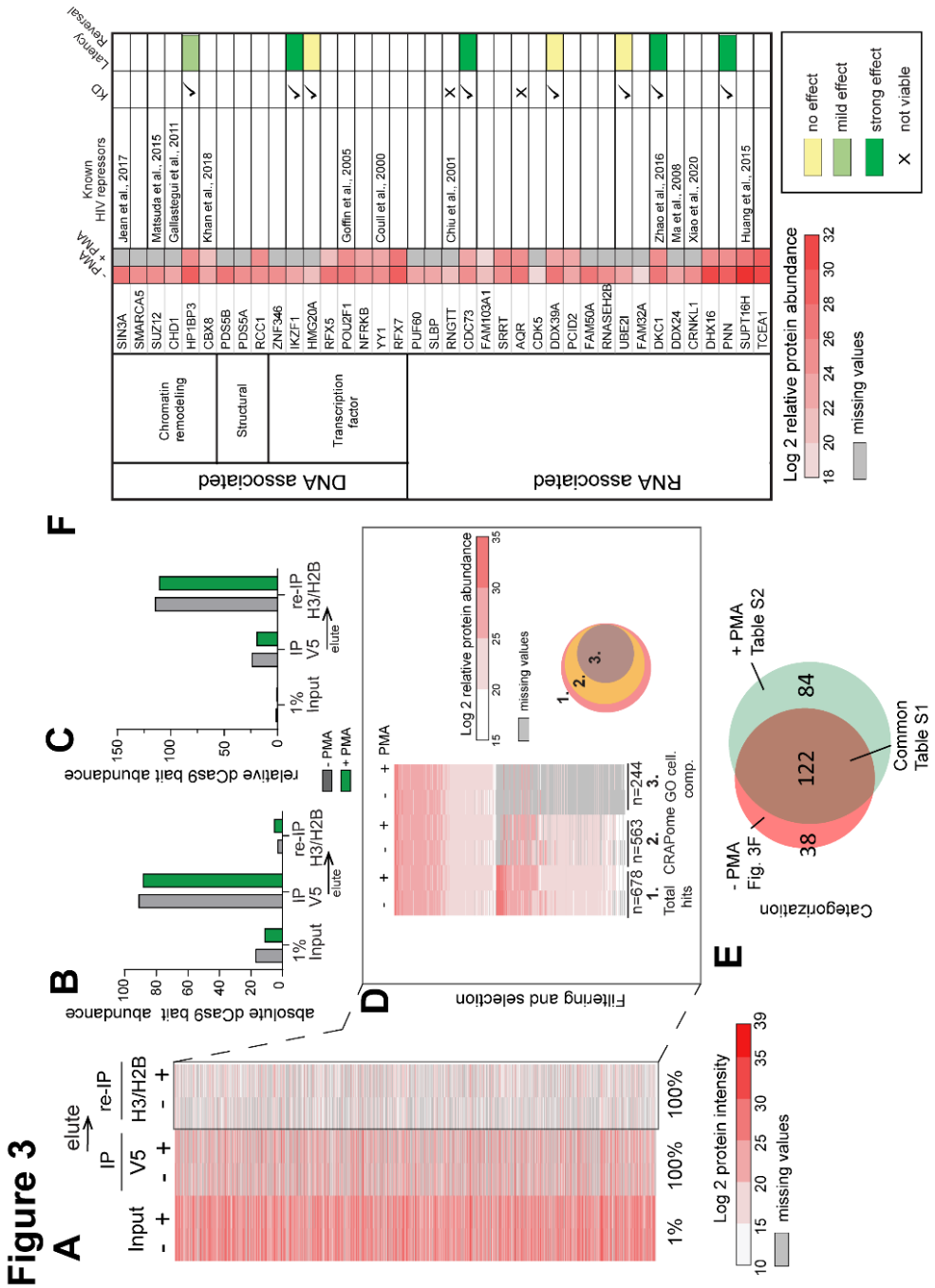

Figure 3. Cachet-MS identifies known and novel host factors associated with the latent and active HIV-1 promoter

(A) Heatmap displays the protein content at each step of the Catchet-MS purification pipeline. The colors represents the Log2 transformation of the protein intensities scores. Values corresponding to the V5 based immunopurification are adjusted to 100% as only a fraction (1:40) of the material that went into the second, histone based (H2B/H3) immunopurification, was analyzed by mass spectrometry. For the V5/histone experiment, 100% of the material was subjected to mass spectrometry. Missing values are represented by grey lines. The heatmap represents data from one Catchet-MS experiment, input material for the experiment corresponds to chromatin generated from a starting material of 3 billion cells per condition.
(B) Bar plots showing the absolute HA-V5-FLAG-dCas9 bait abundance at each step of the purification pipeline. The absolute abundance was calculated based on protein/peptide spectral intensity values and adjusted to the fraction of material analyzed by mass spectrometry. The values are displayed in arbitrary units.
(C) Bar plots showing the relative HA-V5-FLAG-dCas9 bait abundance at each step of the purification pipeline. The relative abundance was calculated based on protein/peptide spectral intensity values and normalized to the total protein content. The values are displayed in arbitrary units.
(D) Filtering criteria applied to Catchet-MS data. Hits are filtered by comparison with the Crapome repository for contaminants of affinity purification experiments . as well as through GO categorization to select hits present in the cell nucleus and classified to be RNA bound, DNA bound or alternatively bound to histones, transcription factors or associated to chromatin. Colors represent the Log2 transformation of the protein relative abundance. The protein relative abundance was calculated based on protein/peptide spectral intensity values and normalized to the total protein content. Missing values are represented by grey lines.
(E) Venn diagram graphically summarizing the overlap between the hits identified to be exclusively, or more abundantly, associated with the unstimulated state (-PMA) and the hits associated with the activated state (+PMA).
(F) Selection and functional classification of hits associated with the unstimulated state and considered for a potential role in the maintenance of HIV-1 latency. The first columns of the table summarize in a heatmap the Log2 trasfomation of the protein relative abundance values in the unstimulated (–PMA) sample and the activated (+PMA) sample. Missing values are represented by grey lines. Candidates previously reported to restrict HIV-1 expression are referenced in the third column. Checkmarks indicate the hits functionally validated by shRNA mediated depletion experiments (Supplementary Figure 3C). Colored boxes (yellow to dark green) summarize the effect of the target depletion on HIV- 1 expression and refers to the effects summarized in S5A.

Figure 4

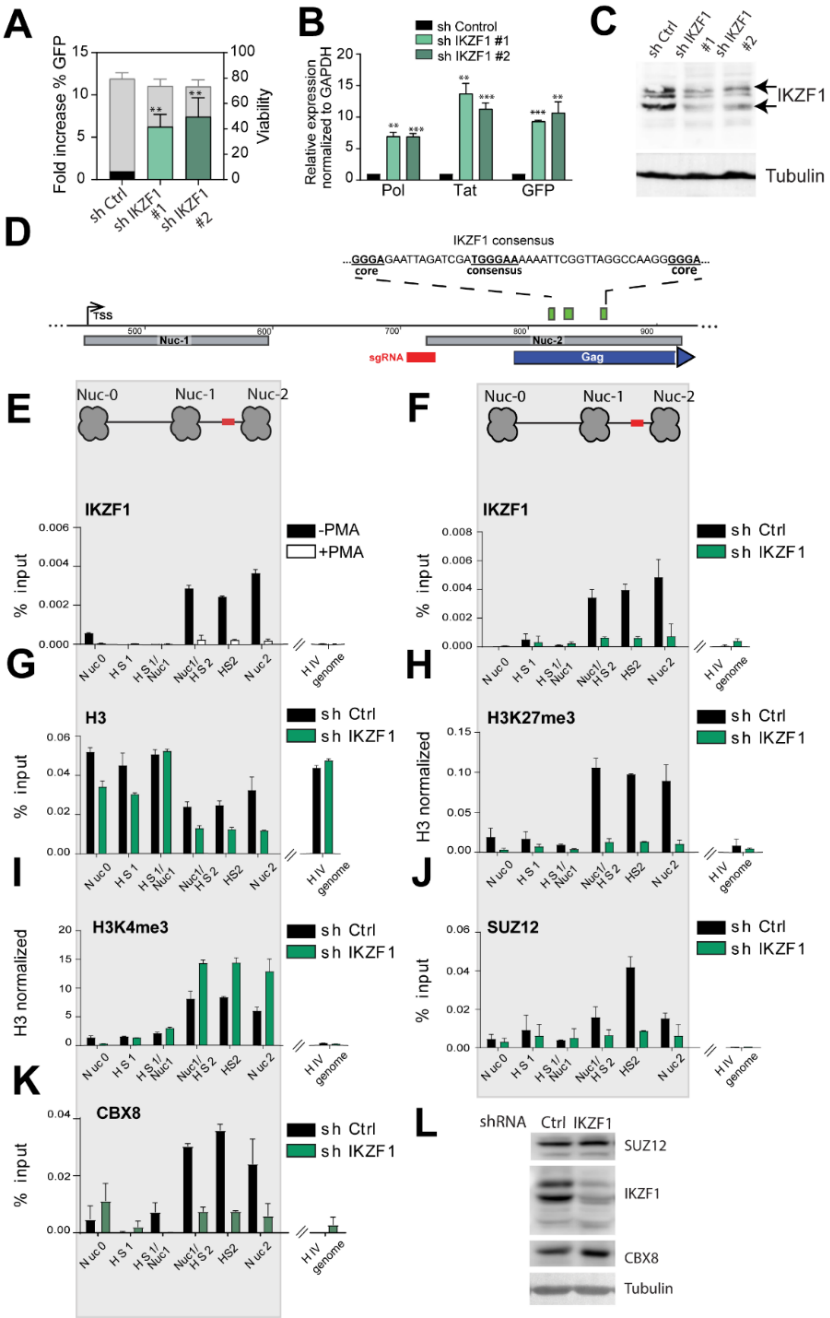
A
Fold increase % GFP
Viability
sh Ctrl
sh IKZF1 #1
sh IKZF1 #2
B
sh Control
sh IKZF1 #1
sh IKZF1 #2
Relative expression normalized to GAPDH
Pol
Tat
GFP
C
sh Ctrl
sh IKZF1 #1
sh IKZF1 #2
IKZF1
Tubulin
D
IKZF1 consensus
GGGAGAATTAGATCGATGGGAAAAAATTCGGTTAGGCCAAGGGGGA
core
consensus
core
TSS
Nuc-1
Nuc-2
sgRNA
Gag
E
Nuc-0
Nuc-1
Nuc-2
IKZF1
% input
-PMA
+PMA
F
IKZF1
% input
sh Ctrl
sh IKZF1
G
H3
% input
H
H3K27me3
H3 normalized
I
H3K4me3
H3 normalized
J
SUZ12
% input
K
CBX8
% input
L
shRNA
Ctrl
IKZF1
SUZ12
IKZF1
CBX8
Tubulin

Figure 4. IKZF1, required for maintenance of HIV-1 latency, binds downstream of the latent HIV-1 5'LTR to promote PRC2/PRC1 recruitment and establish a repressive chromatin environment.

(A) Bar plot showing the fold increase in % GFP positive cells (left y axes) measured by FACS analysis, following IKZF1 depletion in J-Lat 11.1 with two different shRNA constructs (#1 and #2). Data are the mean of three independent experiments (±SD). The right y axis represents the percentage of live cells.
(B) qRT-PCR analysis measuring expression of HIV genes (pol, GFP, tat) in J-lat 11 transduced with scramble shRNA (sh Control) and sh IKZF1 #1 and #2. Data, normalized to GAPDH are represented as fold enrichment over sh Control and are the mean of three independent experiments (±SEM). Statistical significance was calculated using a ratio paired t test, * – p<0,05; **– p<0,01– ***p<0,001.
(C) Western blotting for IKZF1 in J-lat 11 transduced with scramble shRNA (sh Control) and shIKZF1 #1 and #2 iondicates depletion of IKZF1. α-Tubulin is used as a loading control.
(D) Putative IKZF1 binding site (835-840) downstream of the HIV-1 5'-LTR in the proximity of the sequence targeted by the gRNA. The IKZF1 binding site is composed of a consensus sequence (TGGGAA/T) and at least one more extra core site (GGGA) in a 40 bp range (Li et al., 2011).
(E) ChIP-qPCR analysis with IKZF1 antibody in latent cells and PMA stimulated J-Lat 11.1 cells as indicated.
(F) ChIP qPCR analysis with IKZF1 antibody in J-Lat 11. 1 cells transduced with scramble shRNA (shControl) and shIKZF1. Data in (E) and (F) are presented as % input, error bars represent the standard deviation (SD) of two separate real-time PCR measurements.
(G, H, I) ChIP-qPCR using antibodies specific for distinct histone marks in J-Lat 11. 1 cells transduced with scramble shRNA (shControl) and shIKZF1. Total histone H3 (G), H3K27me3 (H), H3K4me3 (I). Total histone H3 data (G) are represented as % input mean (±SD), histone marks data (H)(I) are expressed as fold change over H3 signal (±SD).
(J) ChIP-qPCR analysis with SUZ12 in J-Lat 11. 1 cells transduced with scramble shRNA (shControl) and shIKZF1.
(K) ChIP-qPCR analysis with CBX8 in J-Lat 11. 1 cells transduced with scramble shRNA (shControl) and shIKZF1. Data in (J) and (K) are presented as % input, error bars represent the standard deviation (SD) of two separate real-time PCR measurements. The ChIP analysis presented (E-K) are a representative experiment, biological replicate experiments are shown in S8.
(L) Western blotting for SUZ12, IKZF1, CBX in J-lat 11 transduced with scramble shRNA (sh Control) and shIKZF1. α-Tubulin is used as a loading control.

Figure 5

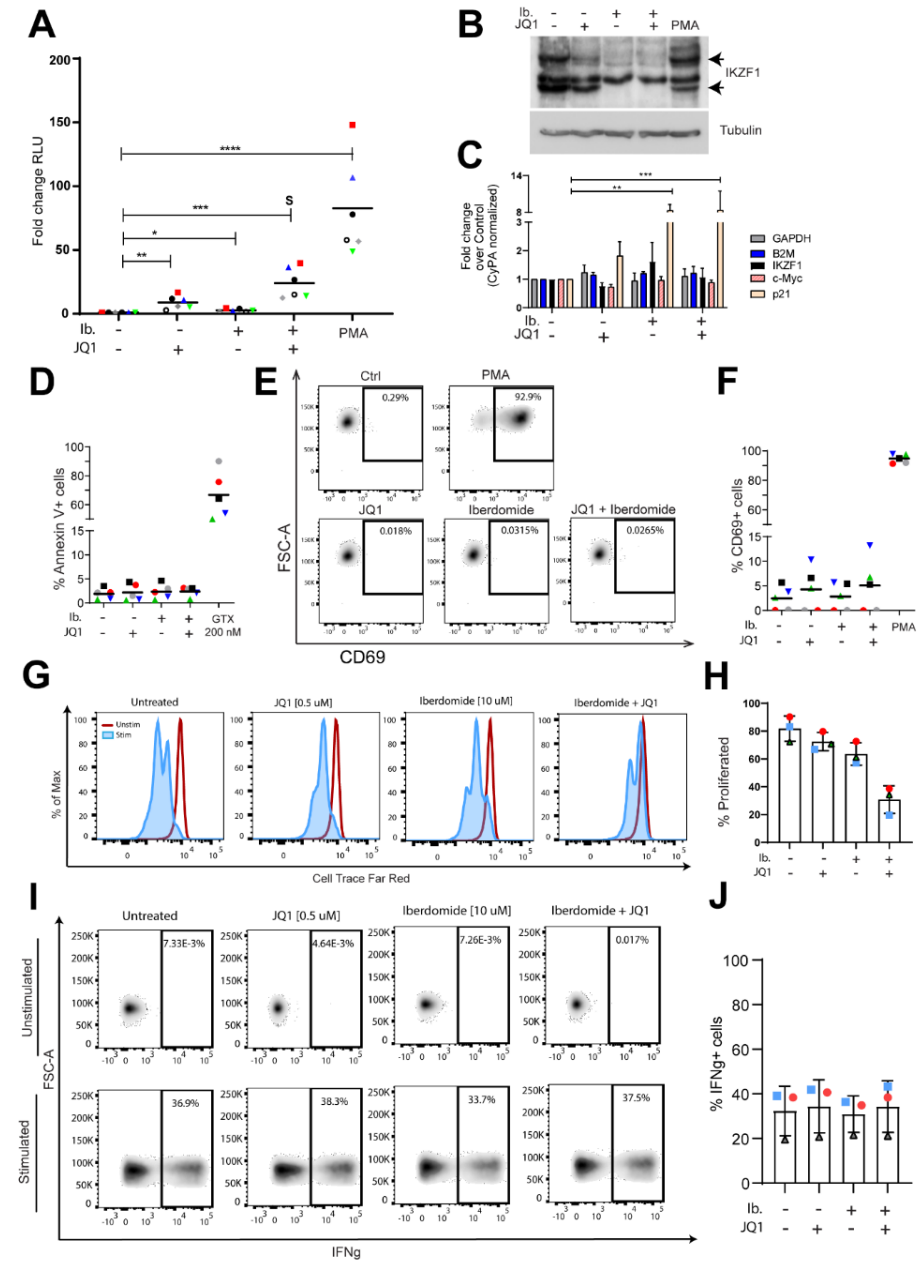
A
Fold change RLU
Ib.
JQ1
PMA
B
IKZF1
Tubulin
C
Fold change over Control (CyPA normalized)
GAPDH
B2M
IKZF1
c-Myc
p21
D
% Annexin V+ cells
GTX 200 nM
E
Ctrl
PMA
JQ1
Iberdomide
JQ1 + Iberdomide
0.29%
92.9%
0.018%
0.0315%
0.0265%
FSC-A
CD69
F
% CD69+ cells
G
Untreated
JQ1 [0.5 uM]
Iberdomide [10 uM]
Iberdomide + JQ1
Unstim
Stim
% of Max
Cell Trace Far Red
H
% Proliferated
I
Unstimulated
Stimulated
7.33E-3%
4.64E-3%
7.26E-3%
0.017%
36.9%
38.3%
33.7%
37.5%
IFNg
J
% IFNg+ cells

Figure 5. Targeting IKZF1 by iberdomide treatment reverses latency in ex vivo infected primary CD4+ T cells with minimal effect on toxicity and effector function

(A) The latency reversal activity of iberdomide alone (10uM) and in combination with JQ1 (500nM) was tested, in primary human CD4+ T cells ex vivo infected to harbour latent HIV-1. The dot plot in panel A shows the fold increase in luciferase activity after treatment as indicated. Each dot represents a single measurement while the black horizontal lines represent the average fold increase for each treatment in the pool of donors. Experiments were performed in duplicate using cells obtained from 6 healthy donors. Statistical significance was determined by repeated measures one-way ANOVA on the log-transformed fold changes followed by Tukey's multiple comparison test * – $p < 0,05$, ** – $p < 0,01$, *** – $p < 0,001$, ****– $p < 0,0001$.
(B) Western blotting shows protein levels of IKZF1 after 24 hours following treatment with Iberdomide, JQ1, and their combination in primary CD4+ T cells. α-Tubulin is used as a loading control.
(C) qRT-PCR analysis of IKZF1 and IKZF1 targets p21 and c-myc upon treatment with JQ1, iberdomide, and their combination. RT-PCR was performed in primary CD4+ T cells isolated from three healthy donors. Data are represented as fold change (±SEM) over untreated and are normalized to Cyclophilin A (CyPA). B2M and GAPDH are used as housekeeping genes. Statistical significance was calculated using ratio-paired t-test * – $p < 0,05$, ** – $p < 0,01$, *** – $p < 0,001$,
(D) Iberdomide treatment is not cytotoxic in primary CD4+ T cells. Percentage of cells expressing the Annexin V marker of apoptosis in primary CD4+ T cells treated with iberdomide, JQ1 and the combination of both compounds for 48 hours. Treatment with a toxic concentration of Gliotoxin (GTX) 200nM was used as a positive control. Experiments were performed in uninfected cells obtained from five healthy donors, represented by the dots.
(E) Iberdomide treatment does not activate CD4+ T cells. Representative flow cytometry plot of extracellular CD69 marker staining analysis in primary CD4+ T cells, upon treatment with JQ1, iberdomide, or a combination of both compunds for 48 hours. CD69 expression was assessed by extracellular staining and analyzed by flow cytometry
(F) Percentage of cells expressing the CD69 marker of cell activation in primary CD4+ T cells from 5 healthy donors as described in E. Treatment with PMA was used as a positive control.
(G) Representantive histogram of proliferative capacity of unstimulated or aCD3/CD28 stimulated CD4+ T cells in the presence or absence of LRAs. Cells were stained with a proliferation dye and analyzed 72 hours later by flow cytometry. Dividing cells show decreased intensity of prolifertion dye as it becomes diluted upon cell division.
(H) Percentage of proliferated CD4+ T cells from 3 healthy donors as described in G.
(I) Representative flow cytometry plots of IFNg production analysis in unstimulated and stimulated primary CD8+ T cells after treatment with LRAs. Cells were treated as indicated for 18 hours followed by PMA/Ionomycin stimulation for 7 hours in the presence of a protein transport inhibitor or remained unstimulated. IFN-g production was assessed by intracellular staining and

analyzed by flow cytometry. Numbers in the plot show percentage of IL-2 producing cells.
(J) Percentage of INFg producing CD8+ T cells from 3 healthy donors as described in I

Figure 6

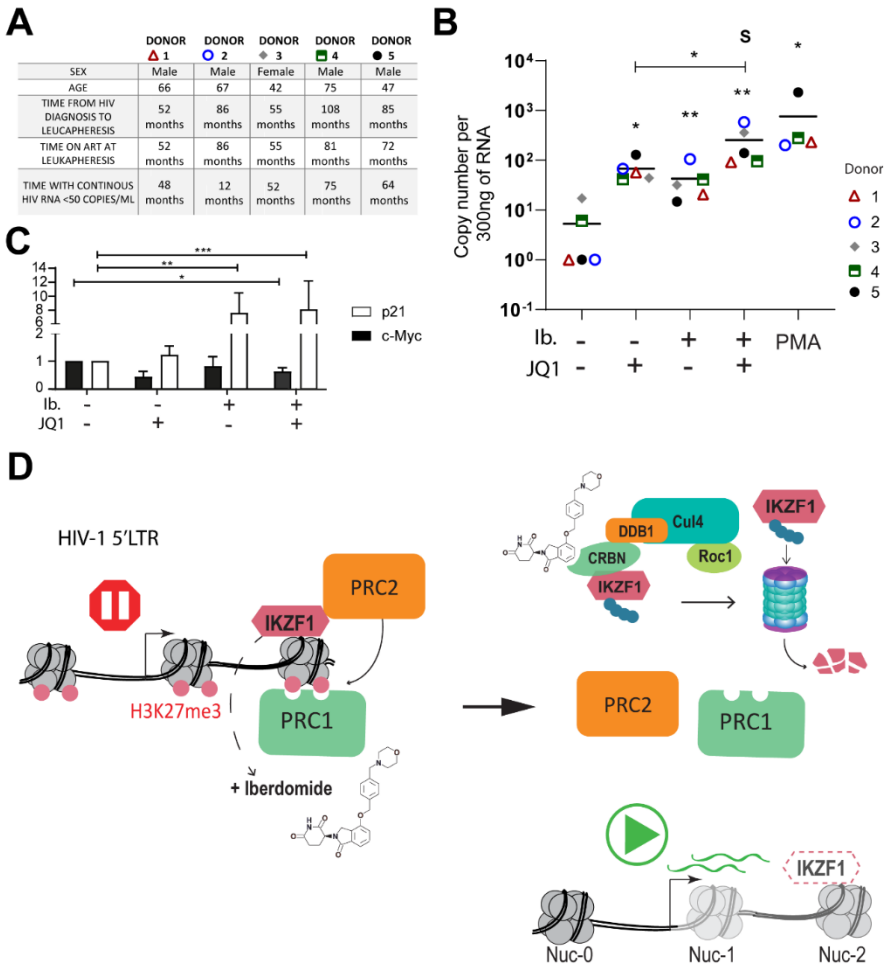

Figure 6 Targeting IKZF1 by iberdomide treatment reverses latency in primary CD4+ T cells obtained from cART suppressed HIV-1 infected patients.

(A) Clinical Information Table corresponding to the HIV-1 infected study participants.
(B) Iberdomide treatment causes significant increase in cell-associated HIV-1 RNA levels and synergistically enhances JQ1-mediated HIV-1 latency reversal in CD4+ T cells obtained from c-ART suppressed HIV-1 infected patient volunteers. Graph panel showing the average levels of cell-associated HIV-1 RNA in CD4+ T cells isolated from five infected, aviremic participants. Statistical significance was calculated using unpaired Mann-Whitney test, * – $p < 0,05$, ** – $p < 0,01$.
(C) qRT-PCR analysis of IKZF1 targets p21 and c-myc upon treatment with JQ1, iberdomide, or both compounds. RT-PCR was performed in primary CD4+ T cells isolated from 5 aviremic HIV-1 infected study partecipants. Data are represented as fold change mean (±SD) over untreated and are normalized with Cyclophilin A (CyPA). Statistical significance was calculated using ratio-paired t test * – $p < 0,05$, ** – $p < 0,01$, *** – $p < 0,001$.
(D) Proposed model for iberdomide mediated latency reversal. Iberdomide binds to CRBN, a subunit of the CRL^{CRBN} E3 ubiquitin ligase complex that acts as a substrate adaptor. Iberdomide biding induces recruitment of IKZF1 and its ubiquitination by the ligase. In latently infected cells, ubiquitination of IKZF1 and its degradation by the proteasome results in a decrease in IKZF1 levels, impaired LTR recruitment of PRC2 and PRC1, leading to chromatin derepression and latency reversal.

Figure S1

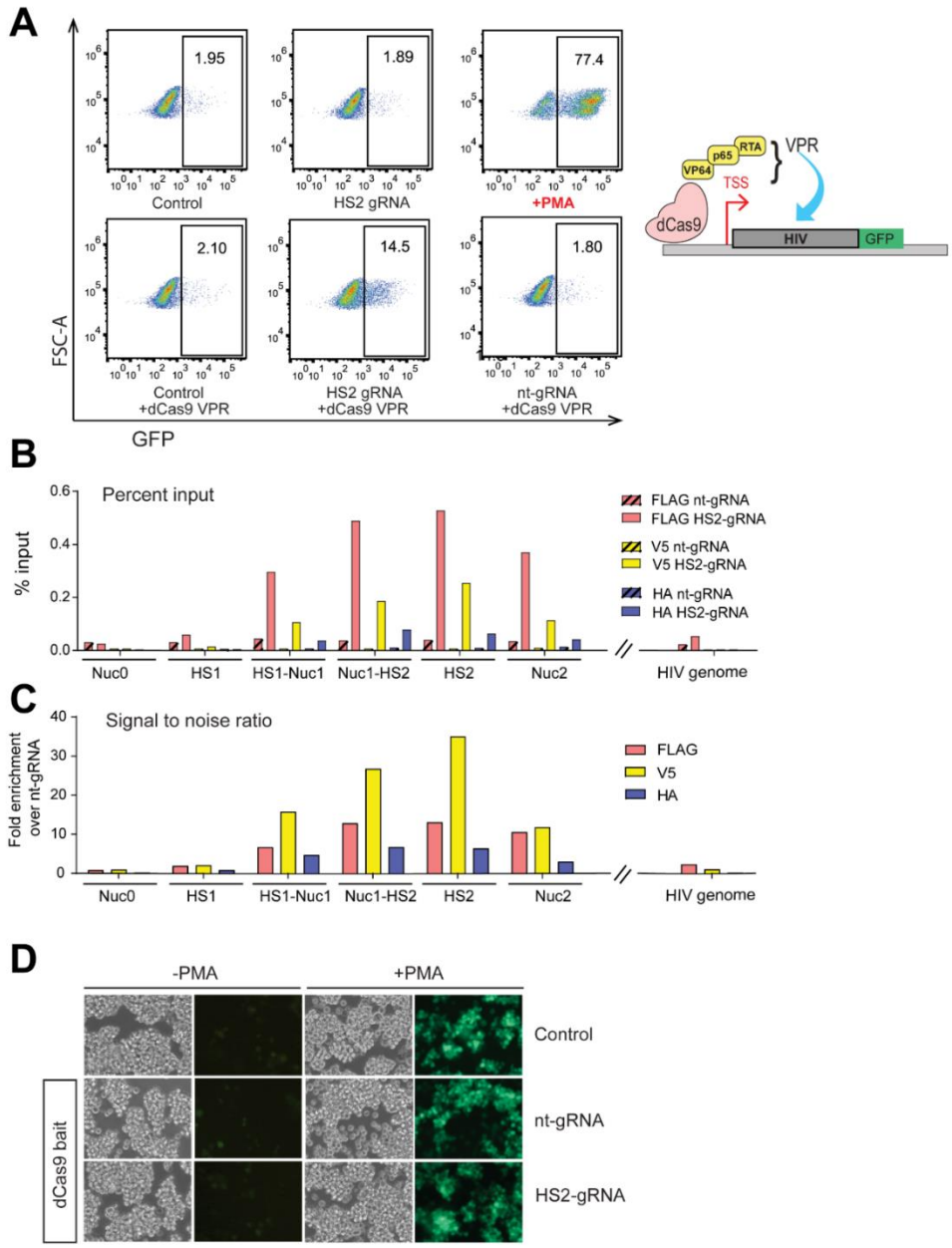
A
1.95
1.89
77.4
Control
HS2 gRNA
+PMA
2.10
14.5
1.80
Control
+dCas9 VPR
HS2 gRNA
+dCas9 VPR
nt-gRNA
+dCas9 VPR
FSC-A
GFP
VPR
RTA
p65
VP64
TSS
dCas9
HIV
GFP
B
Percent input
% input
FLAG nt-gRNA
FLAG HS2-gRNA
V5 nt-gRNA
V5 HS2-gRNA
HA nt-gRNA
HA HS2-gRNA
Nuc0
HS1
HS1-Nuc1
Nuc1-HS2
HS2
Nuc2
HIV genome
C
Signal to noise ratio
Fold enrichment over nt-gRNA
FLAG
V5
HA
Nuc0
HS1
HS1-Nuc1
Nuc1-HS2
HS2
Nuc2
HIV genome
D
-PMA
+PMA
Control
nt-gRNA
HS2-gRNA
dCas9 bait

Supplementary Figure 1. Characterization of the experimental system.
(A) Functional validation of the gRNA designed against the HIV-1 5'LTR HS2 region (HS2-gRNA). The FACSs plots show J-Lat 11.1 cells examined by flow-cytometry at 72 hours after nucleofection with a dCas9 VPR construct to check for HIV-1 LTR dependent GFP expression, measured as % GFP positive cells. (B) ChIP-qPCR experiments performed using different antibodies, conjugated to affinity beads, against the different synthetic tags (FLAG, V5, HA) of the dCas9 construct. Cells expressing the HS2 gRNA and control cells expressing a non-targeting gRNA (nt-gRNA) are compared. HIV-1 5'LTR sequences recovery is calculated as a percentage of the input. (C) From the experiment shown in (B), the signal to noise ratio of the experiment is calculated by dividing the ChIP-qPCR signal obtained in the HS2 gRNA expressing pool with the signal obtained in the nt-gRNA expressing pool. Data are represented as fold enrichment over the non-targeting gRNA signal. (D) Microscopy pictures (bright field and fluorescence) of control J-lat 11.1 cells, cells expressing dCas9 bait and a non-targeting gRNA, cells expressing the bait and a gRNA targeting the HS2 region. Cells have been examined in unstimulated (-PMA) and in the presence of 20nM PMA (+PMA) to assess reactivation capacity.

Figure S2

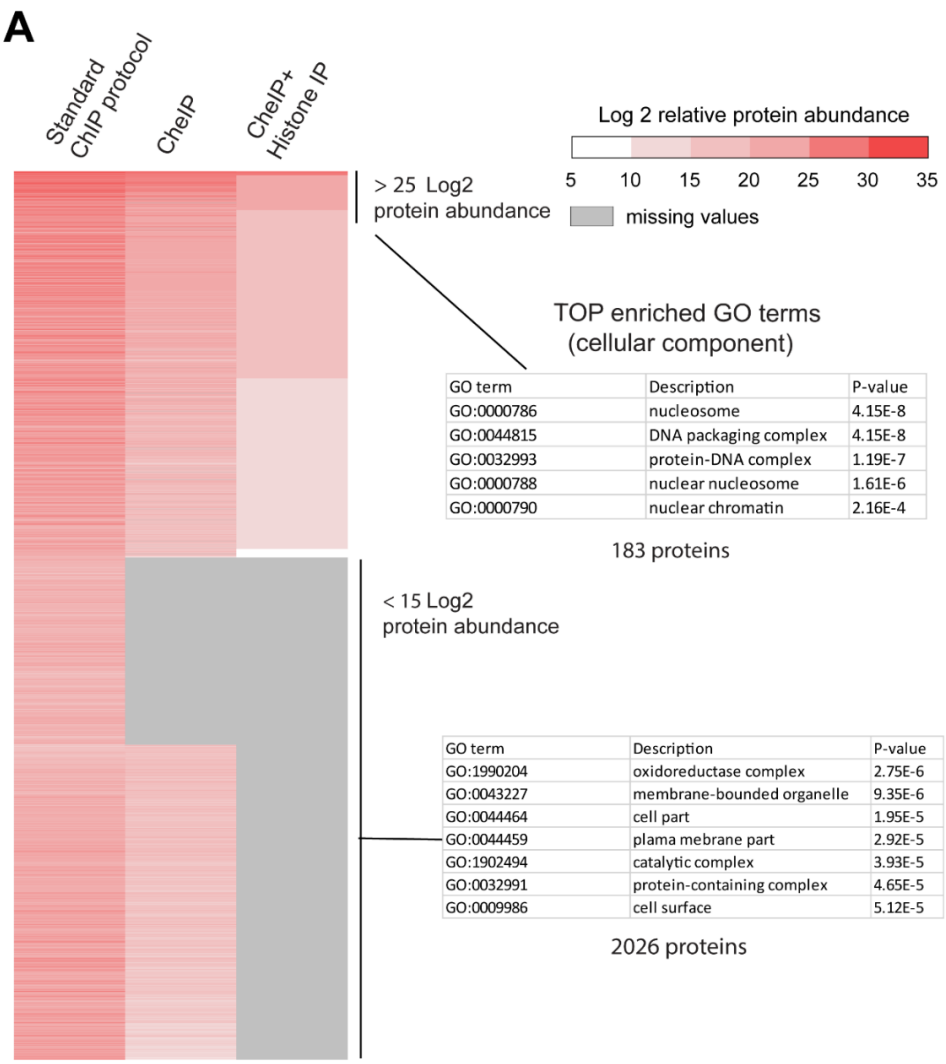
A
Standard ChIP protocol
ChIP
ChIP+ Histone IP
Log 2 relative protein abundance
5 10 15 20 25 30 35
missing values
> 25 Log2 protein abundance
TOP enriched GO terms (cellular component)
GO term | Description | P-value
GO:0000786 | nucleosome | 4.15E-8
GO:0044815 | DNA packaging complex | 4.15E-8
GO:0032993 | protein-DNA complex | 1.19E-7
GO:0000788 | nuclear nucleosome | 1.61E-6
GO:0000790 | nuclear chromatin | 2.16E-4
183 proteins
< 15 Log2 protein abundance
GO term | Description | P-value
GO:1990204 | oxidoreductase complex | 2.75E-6
GO:0043227 | membrane-bounded organelle | 9.35E-6
GO:0044464 | cell part | 1.95E-5
GO:0044459 | plama mebrane part | 2.92E-5
GO:1902494 | catalytic complex | 3.93E-5
GO:0032991 | protein-containing complex | 4.65E-5
GO:0009986 | cell surface | 5.12E-5
2026 proteins
B
1. Standard ChIP
2. ChIP
3. ChIP + Histone IP

Supplementary Figure 2. Characterization of the chromatin preparation protocol by mass spectrometry. (A) The heatmap shows a comparison between the protein content of a standard ChIP protocol, CheIP, and CheIP followed by a histone enrichment step (CheIP + histone IP) with H2B and H3 conjugated affinity beads. The colors represent the Log2 transformation of the proteins relative abundance. The protein relative abundance was calculated based on protein/peptide spectral intensity values and normalized to the total protein content (B) Venn diagram showing the proportion of the number of hits identified in the different protocols

Figure S3

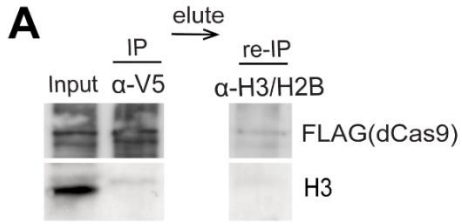
A
elute
IP
re-IP
Input
α-V5
α-H3/H2B
FLAG(dCas9)
H3

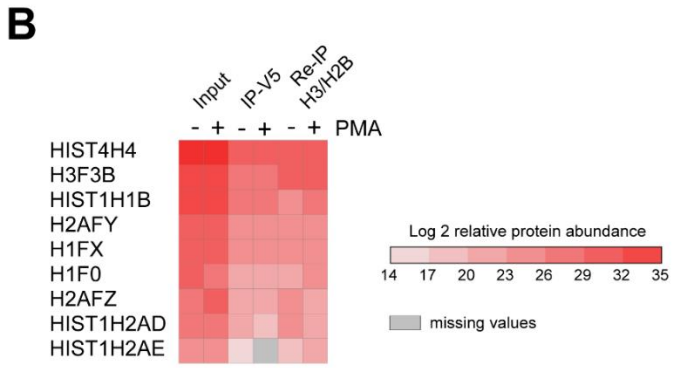
B
Input
IP-V5
Re-IP H3/H2B
- + - + - + PMA
HIST4H4
H3F3B
HIST1H1B
H2AFY
H1FX
H1F0
H2AFZ
HIST1H2AD
HIST1H2AE
Log 2 relative protein abundance
14 17 20 23 26 29 32 35
missing values

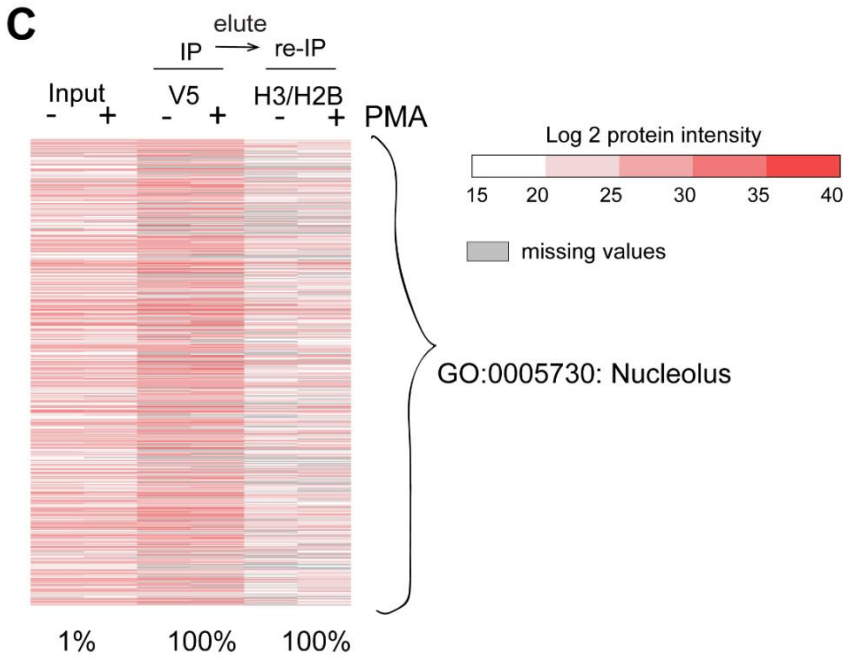
C
elute
IP
re-IP
Input
V5
H3/H2B
- + - + - + PMA
Log 2 protein intensity
15 20 25 30 35 40
missing values
GO:0005730: Nucleolus
1%
100%
100%

Supplementary Figure 3. Depletion of non-localized bait and nucleolar proteins

(A) Western blotting with anti Cas9 and anti-V5 antibody indicates relative presence of HA-V5-FLAG-dCas9 bait in the fractions used in the sequential ChIP experiments in Figure 2D. (B) Detection of histones. The heatmap summarizes the relative abundance of histone proteins, detected by Catchet-MS. The colors represents the Log2 transformation of the proteins relative abundance. The protein relative abundance was calculated based on protein/peptide spectral intensity values and normalized to the total protein content. Missing values are represented by grey lines. (C) Heatmap displaying the content of nucleolar proteins (GO cellular compartment category GO:005730; nucleolus) at each step of the Catchet-MS purification pipeline used for isolation of the HIV-1 5'LTR. The colors range represents the represents the Log2 transformation of the proteins intensities scores. Values corresponding to the V5 based immunopurification are adjusted to the fraction of material analyzed by mass spectrometry, corresponding to 1:40 of the material used for the second, histone based (H2B/H3) immunopurification. Missing values are represented by grey lines.

Figure S4

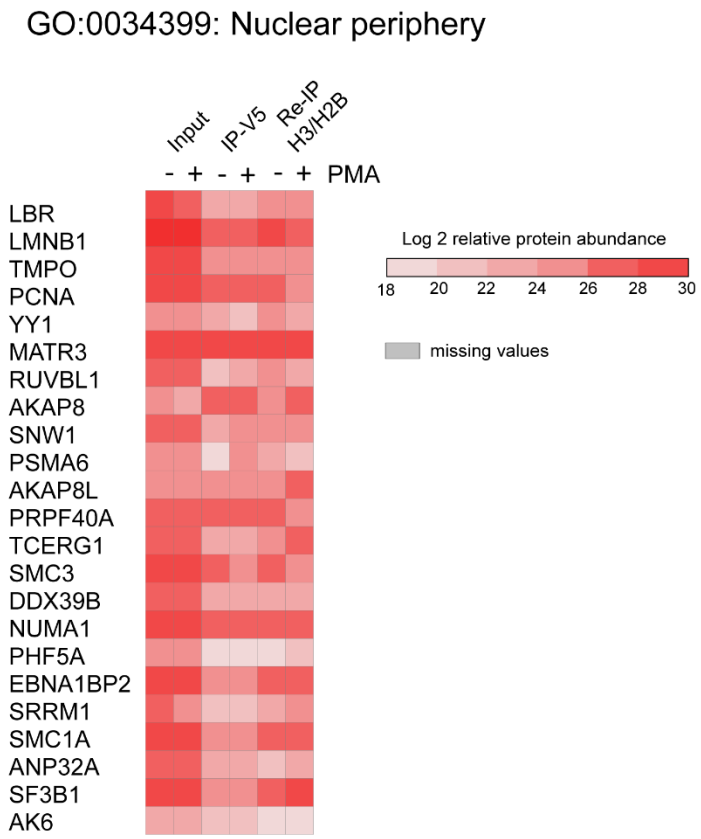

Supplementary Figure 4. Identification of nuclear body and nuclear periphery associated proteins with the latent HIV-1 LTR.
The heatmap summarizes the relative abundance of proteins associated with the nuclear periphery (GO:0034399), detected by Catchet-MS. The colors represent the Log2 transformation of the proteins relative abundance. The protein relative abundance was calculated based on protein/peptide spectral intensity values and normalized to the total protein content. Missing values are represented by grey lines.

Figure S5

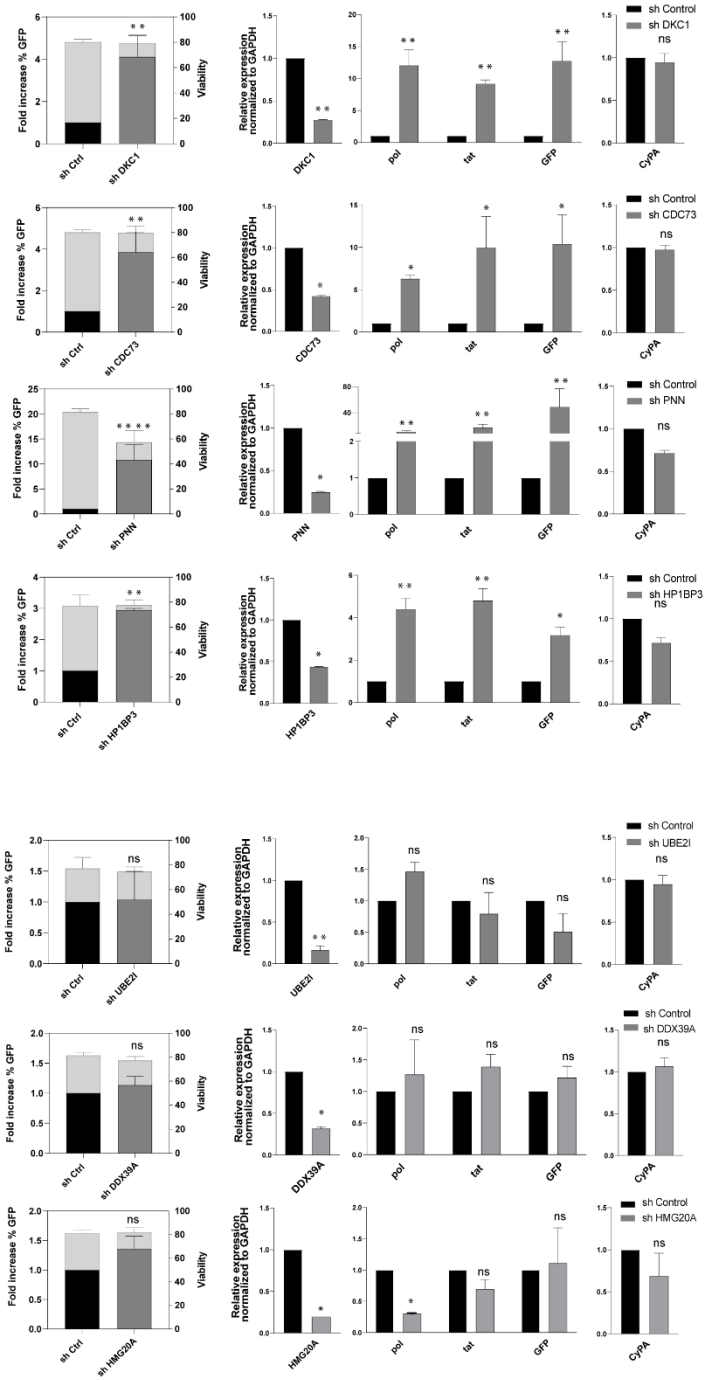
Fold increase % GFP
Viability
sh Ctrl
sh DKC1
Relative expression normalized to GAPDH
DKC1
pol
tat
GFP
CyPA
sh Control
sh DKC1
sh CDC73
sh PNN
sh HP1BP3
sh UBE2I
sh DDX39A
sh HMG20A
ns

Supplementary Figure 5. Functional validation of a selection of proteins bound downstream of the latent HIV-1 promoter.
Functional validation of the hits associated with the repressed HIV-1 LTR. shRNA mediated depletion followed by Flow cytometry and RT-PCR. Statistical significance was calculated using ratio-paired t-test and multiple comparison t-test on Log2 transforment fold changes * – p < 0,05, ** – p < 0,01 , *** – p < 0,001, ****– p < 0,0001 .

Figure S6

A

RNA seq, Jurkat cells

Target	Total reads
IKZF1	5202,5
IKZF2	3303
IKZF3	49
IKZF4	1
IKZF5	701,5

B

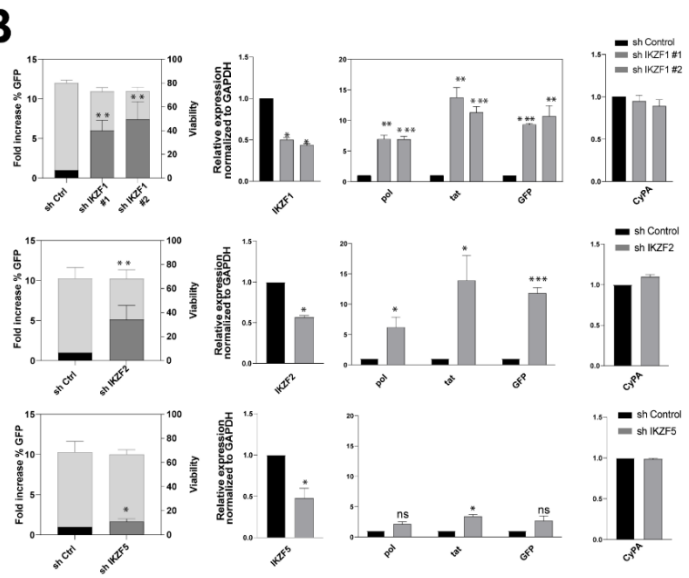

Supplementary Figure 6. IKZF family members expression and role in HIV-1 latency in J-Lat 11.1 cells. (A) Expression of IKZF family members in Jurkat cells. The panel shows the number of RNA seq reads in Jurkat cells. The data are published and available in Palstra et al., Science advances, 2018).
(B) IKZF2 and IKZF5, the two prominent Jurkat cells expressed IKZF members were depleted from J-Lat 11.1 cells following shRNA-mediated transduction and

GFP expression was examined by Flow cytometry and RT-PCR. Statistical significance was calculated using ratio-paired t-test and multiple comparison t-test * – p < 0,05, ** – p < 0,01 , *** – p < 0,001, ****– p < 0,0001 .

Figure S7

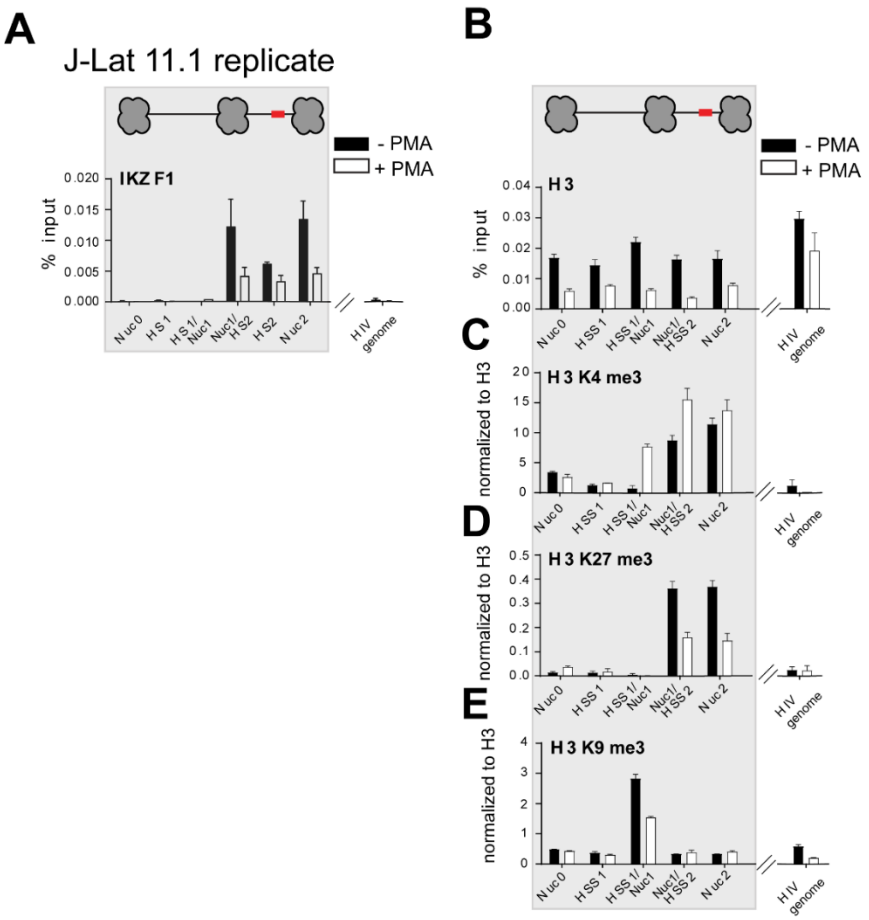

Supplementary Figure 7. Carachterization of IKZF1 binding and chromatin state at the 5'LTR following treatment with PMA in J-Lat 11.1 cells. (A) Replicate ChIP-qPCR analysis with IKZF1 antibody in latent and PMA stimulated

J-Lat 11.1 cells as indicated. Data are presented as % input, error bars represent the standard deviation (SD) of two separate real-time PCR measurements. (B-C) ChIP-qPCR using antibodies specific for distinct histone marks in latent and PMA stimulated J-Lat 11.1 cells as indicated; total histone H3 (B), H3K4me3 (C), H3K27me3 (D), H3K9me3 (E). Total histone H3 data (G) are presented as % input mean (±SD), data corresponding to histone marks (C-E) are expressed as fold change over H3 signal. Error bars represent the standard deviation (SD) of two separate real-time PCR measurements.

Figure S8

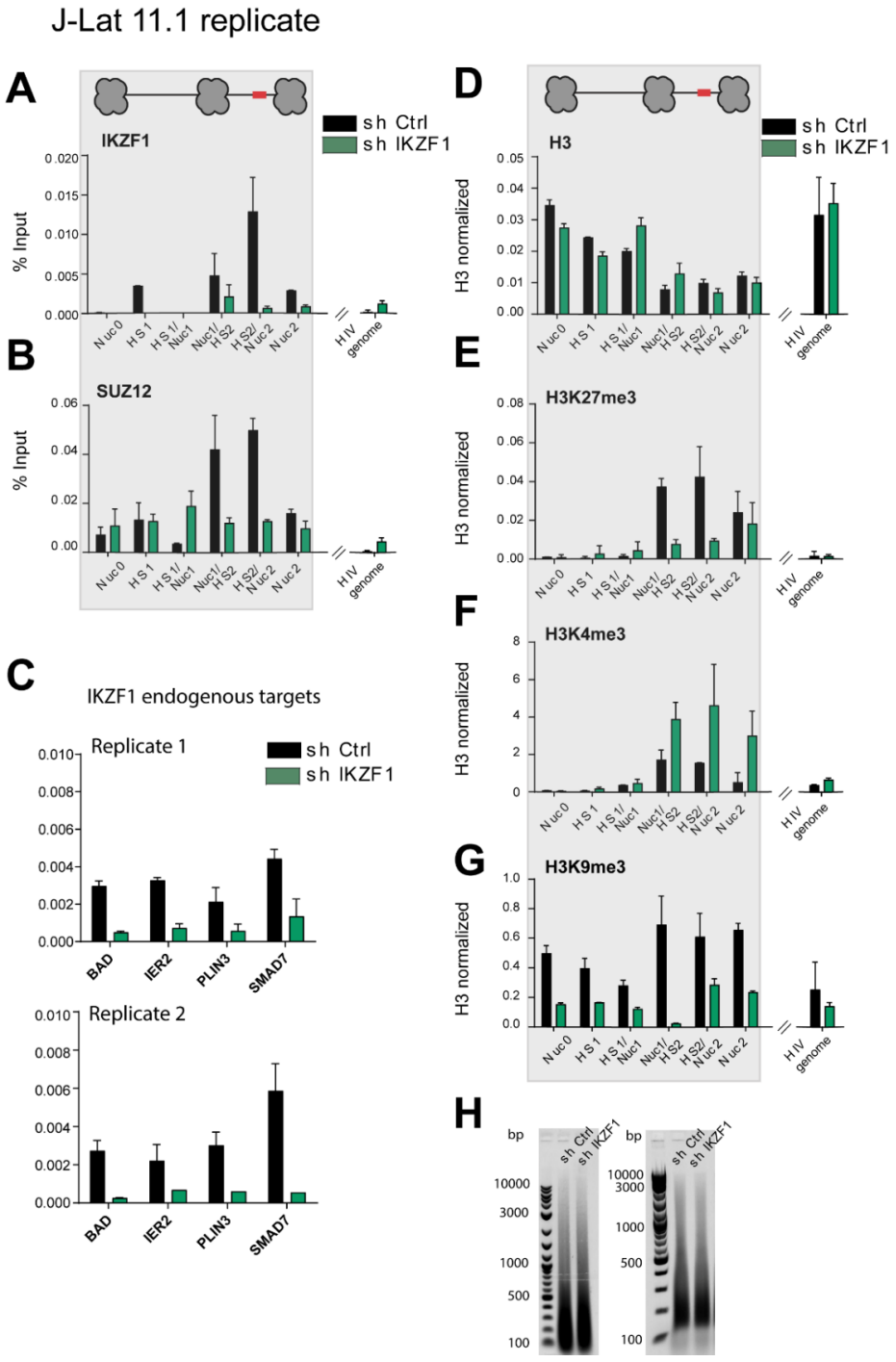
J-Lat 11.1 replicate
A
IKZF1
sh Ctrl
sh IKZF1
% Input
B
SUZ12
C
IKZF1 endogenous targets
Replicate 1
Replicate 2
BAD
IER2
PLIN3
SMAD7
D
H3
H3 normalized
E
H3K27me3
F
H3K4me3
G
H3K9me3
Nuc0
HS1
HS1/ Nuc1
Nuc1/ HS2
HS2/ Nuc2
Nuc2
HIV genome
H
bp
10000
3000
1000
500
100

Supplementary Figure 8. IKZF1, required for maintenance of HIV-1 latency in J-Lat 11.1 cells, binds downstream of the latent HIV-1 5'LTR to promote PRC2/PRC1 recruitement and the establishment of a repressive chromatin environment. (A) ChIP qPCR analysis using antibody against IKZF1 in J-Lat 11.1 cells transduced with scramble shRNA (shControl) and shIKZF1 probing binding to the HIV-1 5'LTR. (B) ChIP-qPCR analysis with SUZ12 in J-Lat 11.1 cells transduced with scramble shRNA (shControl) and shIKZF1 at the HIV-1 5'LTR. Data in (A) and (B) are presented as % input, error bars represent the standard deviation (SD) of two separate real-time PCR measurements. (C) ChIP qPCR analysis using antibody against IKZF1 in J-Lat 11.1 cells transduced with scramble shRNA (shControl) and shIKZF1 probing binding of IKZF1 to endogenous IKZF target genes BAD, IER2, PLIN3 and SMAD7 (Song et al., 2016). (D-G) ChIP-qPCR using antibodies specific for distinct histone marks in J-Lat 11.1 cells transduced with scramble shRNA (shControl) and shIKZF1; total histone H3 (D), H3K27me3 (E), H3K4me3 (F), H3K9me3 (G). Total histone H3 data (D) are represented as % input mean (±SD), histone marks data (E-G) are expressed as fold change over H3 signal. Error bars represent the standard deviation (SD) of two separate real-time PCR measurements. (H) Representative agarose gels demonstrating range of DNA size resulting from sonication of chromatin used in the ChIP experiments presented in the manuscript.

Figure S9

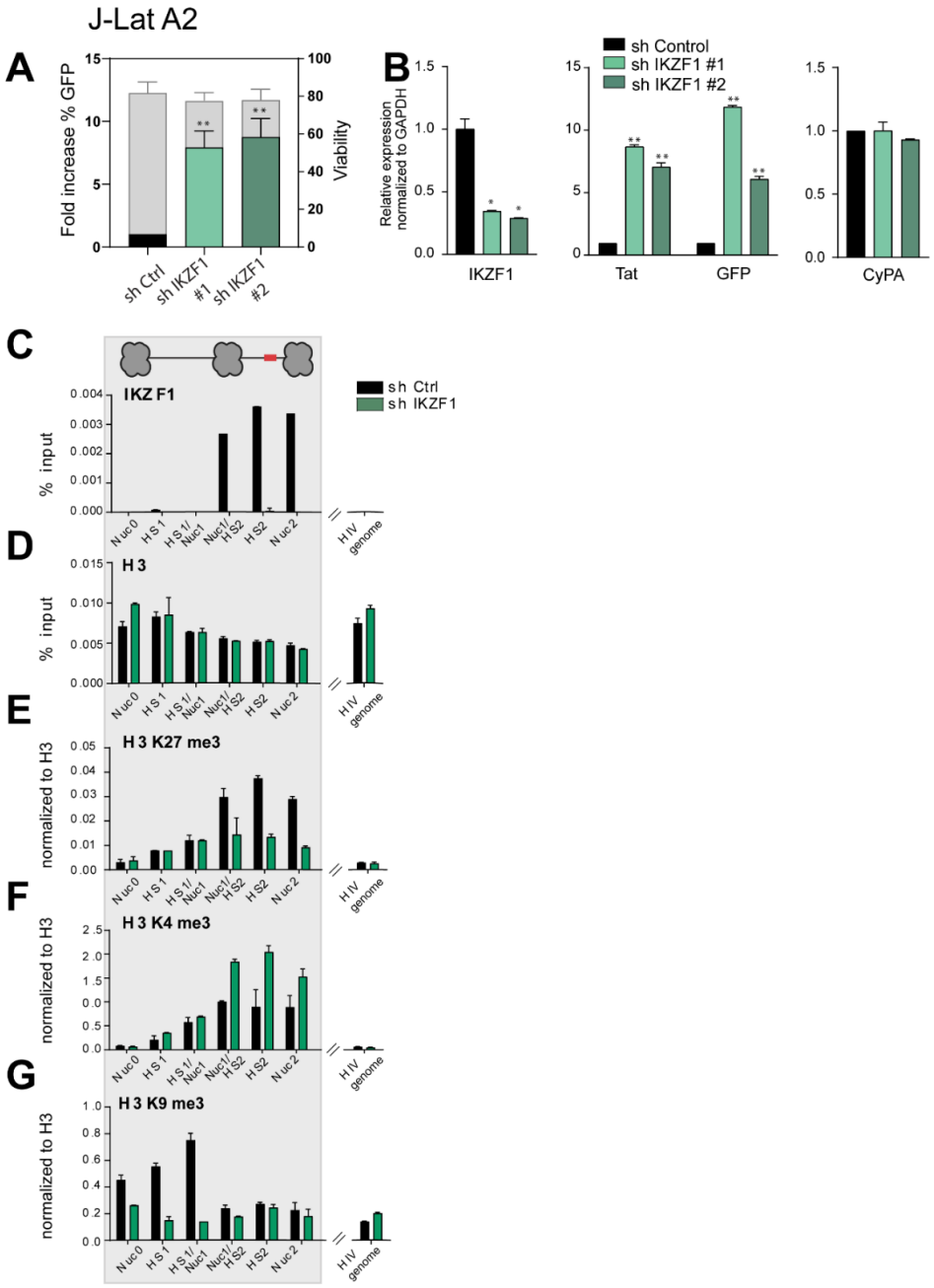
J-Lat A2
A
Fold increase % GFP
Viability
sh Ctrl
sh IKZF1 #1
sh IKZF1 #2
B
Relative expression normalized to GAPDH
sh Control
sh IKZF1 #1
sh IKZF1 #2
IKZF1
Tat
GFP
CyPA
C
IKZ F1
% input
sh Ctrl
sh IKZF1
D
H 3
E
H 3 K27 me3
F
H 3 K4 me3
G
H 3 K9 me3
normalized to H3
Nuc 0
HS 1
HS 1/ Nuc1
Nuc1/ HS2
HS 2
Nuc 2
HIV genome

Supplementary figure 9. IKZF1, required for maintenance of HIV-1 latency in J-Lat A2 cells, binds downstream of the latent HIV-1 5'LTR to promote PRC2 recruitment

(A) Bar plot showing the fold increase in % GFP positive cells (left y-axes) measured by FACS analysis, following IKZF1 depletion in J-Lat A2 cells with two different shRNA constructs (#1 and #2). The right y-axis represents the percentage of live cells. Data are the mean of two independent experiments (±SD).

(B) qRT-PCR analysis measuring expression of HIV genes (pol, GFP, tat) in J-lat A2 cells transduced with scramble shRNA (sh Control) and sh IKZF1 #1 and #2. Data, normalized to GAPDH are represented as fold enrichment over sh Control and are the mean of three independent experiments (±SEM). Statistical significance was calculated using a ratio paired t test, * – p<0,05; **– p<0,01– ***p<0,001.

(C) ChIP qPCR analysis with IKZF1 antibody in J-Lat A2 cells transduced with scramble shRNA (shControl) and shIKZF1. Data are presented as % input, error bars represent the standard deviation (SD) of two separate real-time PCR measurements. (D-E) Histone marks ChIP qPCR analysis of the HIV-1 5' LTR in J-Lat A2 cells transduced with scramble shRNA (shControl) and shIKZF1; (D) Total histone H3 (E) H3K27me3 (F) H3K4me3 (G) H3K9me3. Total histone H3 data (D) are presented as % input mean (±SD), histone marks data (E-G) are expressed as fold change over H3 signal. Error bars represent the standard deviation (SD) of two separate real-time PCR measurements.

Figure S10

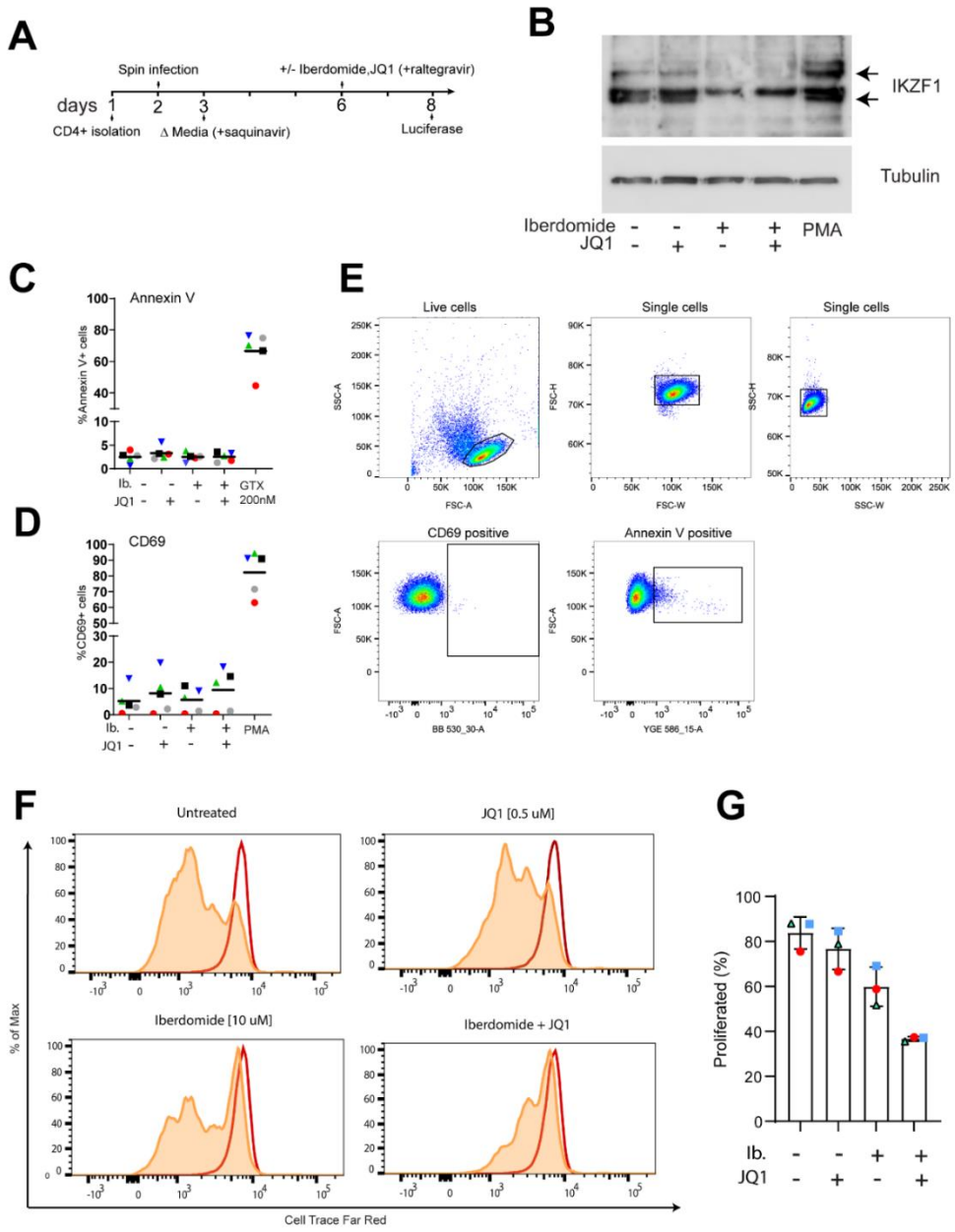
A
Spin infection
+/- Iberdomide,JQ1 (+raltegravir)
days 1 2 3 6 8
CD4+ isolation
Δ Media (+saquinavir)
Luciferase
B
IKZF1
Tubulin
Iberdomide - - + + PMA
JQ1 - + - +
C
Annexin V
%Annexin V+ cells
Ib. - - + + GTX
JQ1 - + - + 200nM
D
CD69
%CD69+ cells
Ib. - - + + PMA
JQ1 - + - +
E
Live cells
Single cells
Single cells
SSC-A
FSC-A
FSC-H
FSC-W
SSC-H
SSC-W
CD69 positive
Annexin V positive
BB 530_30-A
YGE 586_15-A
F
Untreated
JQ1 [0.5 uM]
Iberdomide [10 uM]
Iberdomide + JQ1
% of Max
Cell Trace Far Red
G
Proliferated (%)
Ib. - - + +
JQ1 - + - +

Supplementary figure 10 Iberdomide treatment of primary CD4+ T cells causes depletion of IKZF1 at the protein levels, reduces proliferation but does not cause cytotoxicity or induce T cell activation.

(A) schematic representation of the protocol for HIV-1 latency establishment in primary human CD4+ T cells.

(B) Western blot analysis using an antibody specific for IKZF1 indicates depletion of IKZF1 at the protein level in CD4+ T cells, upon treatment with iberdomide, JQ1 or a combination of both compounds as indicated. PMA is used as a control LRA. α-Tubulin is used as a loading control.

(C) Percentage of cells expressing the Annexin V marker of apoptosis in primary CD4+ T cells treated with iberdomide for 24 hours, JQ1 and the combination of both compounds. Treatment with a toxic concentration of Gliotoxin (GTX) 200nM was used as a positive control

(D) Percentage of cells expressing the CD69 marker of cell activation in primary CD4+ T cells treated with iberdomide for 24 hours, JQ1 and the combination of both compounds.

Experiments were performed in uninfected cells obtained from 5 healthy donors. Treatment with PMA was used as a positive control. Bars represent the average of experiments performed on samples deriving from two healthy donors.

(E) Representative flow cytometry plots and gating strategy for annexin V and CD69 staining.

(F) Representantive histogram of proliferative capacity of unstimulated or aCD3/CD28 stimulated CD8+ T cells in the presence or absence of LRAs. Cells were stained with a proliferation dye and analyzed 72 hours later by flow cytometry. Dividing cells show decreased intensity of proliferaiton dye as it becomes diluted upon cell division.

(G) Percentage of proliferated CD8+ T cells from 3 healthy donors as described in C.

Figure S11

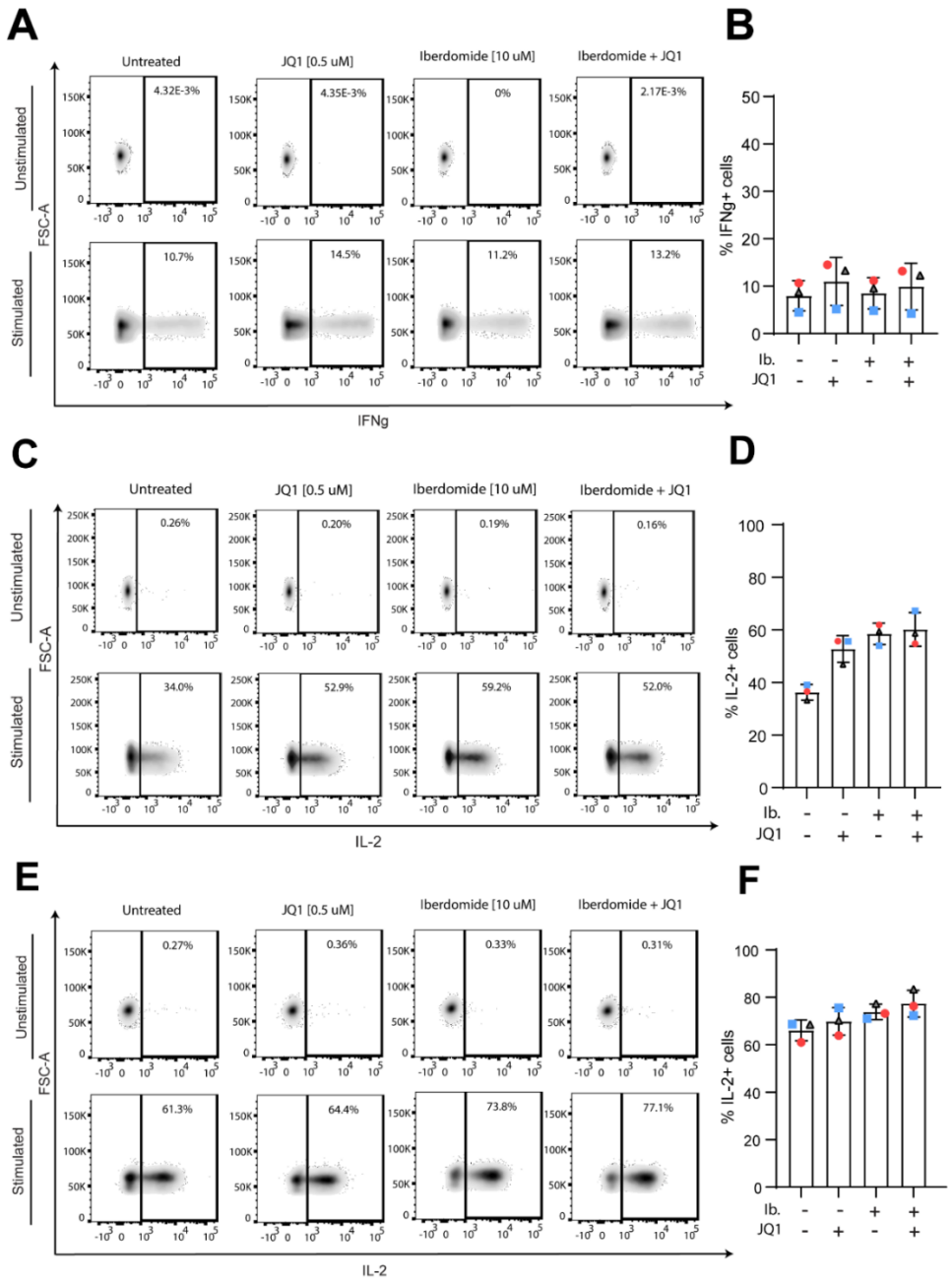
A
Untreated
JQ1 [0.5 uM]
Iberdomide [10 uM]
Iberdomide + JQ1
Unstimulated
Stimulated
FSC-A
IFNg
4.32E-3%
4.35E-3%
0%
2.17E-3%
10.7%
14.5%
11.2%
13.2%
B
% IFNg+ cells
Ib.
JQ1
C
IL-2
0.26%
0.20%
0.19%
0.16%
34.0%
52.9%
59.2%
52.0%
D
% IL-2+ cells
E
0.27%
0.36%
0.33%
0.31%
61.3%
64.4%
73.8%
77.1%
F

Supplementary figure 11 Effect of iberdomide treatment alone and in combination with JQ1 on T cell toxicity, activation, proliferation capacity and effector function

(A) Representative flow cytometry plots (left panel) of INF-g production analysis in unstimulated and stimulated primary CD8+ T cells. . Cells were treated as indicated for 18 hours followed by PMA/Ionomycin stimulation for 7 hours in the presence of a protein transport inhibitor or remained unstimulated. IL-2 production was assessed by intracellular staining and analyzed by flow cytometry.
(B) Percentage of INF-g producing CD8+ T cells from 3 healthy donors as described in B.
(C) Representative flow cytometry plots (left panel) of IL2 production analysis in unstimulated and stimulated primary CD8+ T cells. Cells were treated as indicated for 18 hours followed by PMA/Ionomycin stimulation for 7 hours in the presence of a protein transport inhibitor or remained unstimulated. IL-2 production was assessed by intracellular staining and analyzed by flow cytometry.
(D) Percentage of IL-2 producing CD8+ T cells from 3 healthy donors as described in C
(E) Representative flow cytometry plots (left panel) of IL2 production analysis in unstimulated and stimulated primary CD8+ T cells. . Cells were treated as indicated for 18 hours followed by PMA/Ionomycin stimulation for 7 hours in the presence of a protein transport inhibitor or remained unstimulated. IL-2 production was assessed by intracellular staining and analyzed by flow cytometry.
(F) Percentage of IL-2 producing CD8+ T cells from 3 healthy donors as described in E

Supplementary Table 1 dCas9 V5/Histone ChIP sequencing peak calling summary

Table S1

Location coordinates	Reads V5/Histone	Reads_INPUT	avg_reads_V5/Histone	avg_reads_INPUT	avg_reads_V5/Histone	avg_reads_INPUT	fold_enrichment	fold_enrichment_norm	significance	fdr	qc_flag	pileup	saturation_treatment	saturation_control	MACS_fe
K03455.1:324-1353	163	0	15.8252	0.09709	15.8252	0	7.34873	7.34873	125.021	120.338	33	68	0.17952	0.0011	48.8854
K03455.1:7469-7950	58	1	12.0332	0.20747	12.0332	0.20747	5.85798	5.85798	59.4773	55.3671	33	44	0.16111	0.00278	24.244
chr1:163642157-163642744	52	0	8.84354	0.17007	8.84354	0	5.70044	5.70044	69.5395	65.3325	33	42	0.11159	0.00215	30.4648
chr13:106929710-106930148	35	0	7.97267	0	7.97267	0	5.12928	5.12928	40.4553	36.5264	33	27	0.11041	0	19.8376
chr18:69452480-69452979	32	0	6.4	0.2	6.4	0	5	5	42.3036	38.3524	33	28	0.08466	0.00265	20.546
chr10:10107793-10108316	30	0	5.72519	0	5.72519	0	4.90689	4.90689	36.4838	32.6128	33	25	0.07463	0	18.2645
K03455.1:4591-5133	29	0	5.3407	0	5.3407	0	4.85798	4.85798	31.4541	27.6399	33	22	0.06888	0	16.2951
chrX:79904028-79904440	25	0	6.05327	0	6.05327	0	4.64386	4.64386	33.2202	29.3807	33	23	0.08591	0	17.0036
chr10:81712946-81713497	49	0	8.87681	0.36232	8.87681	0	4.61471	5.61471	81.8569	77.5484	33	48	0.11395	0.00465	34.7157
chr10:42527461-42527960	47	1	9.4	0.4	9.4	0.2	4.55459	5.55459	65.5112	61.3377	33	40	0.12434	0.00529	29.0479
chr14:27677712-27678319	46	1	7.56579	0.32895	7.56579	0.16447	4.52356	5.52356	54.3442	50.2743	33	41	0.09465	0.00412	22.6278
chr10:67391032-67391407	21	0	5.58511	0.26596	5.58511	0	4.39232	4.39232	24.5825	20.8832	33	18	0.08268	0.00394	13.4612
chr8:83440464-83441020	53	0	9.51526	0.5386	9.51526	0	4.14296	5.72792	88.1367	83.7771	33	51	0.12184	0.0069	36.8412
chr5:45664104-45664588	35	0	7.21649	0.41237	7.21649	0	4.12928	5.12928	49.8391	45.809	33	32	0.09642	0.00551	23.38
chr11:33625473-33625961	35	0	7.15746	0.409	7.15746	0	4.12928	5.12928	42.3036	38.3524	33	28	0.09537	0.00545	20.546
chr2:42995018-42995354	17	1	5.04451	0.29674	5.04451	0.29674	4.08746	4.08746	21.2761	17.6472	33	16	0.07907	0.00465	12.0442
chr4:120251096-120251584	32	0	6.54397	0.409	6.54397	0	4	5	46.0438	42.0515	33	30	0.08719	0.00545	21.963
chr13:67564368-67564889	38	0	7.27969	0.57471	7.27969	0	3.66297	5.24793	53.4639	49.4081	33	35	0.095	0.0075	24.4341
chr5:164248717-164249084	67	1	18.2065	1.63043	18.2065	0.27174	3.48113	6.06609	101.348	96.8835	33	67	0.27236	0.02439	36.6354
chr2:117593970-117594523	44	0	7.94224	0.72202	7.94224	0	3.45943	5.45943	65.5112	61.3377	33	40	0.10185	0.00926	29.0479
chr2:167082840-167083383	31	1	5.69853	0.55147	5.69853	0.18382	3.36923	4.9542	31.4541	27.6399	33	22	0.07346	0.00711	16.2951
chr10:115327573-115327989	49	0	11.7506	1.19904	11.7506	0	3.29278	5.61471	83.9417	79.6163	33	49	0.1661	0.01695	35.4242
chr4:57790810-57791142	19	1	5.70571	0.6006	5.70571	0.3003	3.24793	4.24793	22.9176	19.2508	33	17	0.09005	0.00948	12.7527
chr7:57945316-57945811	37	0	7.45968	0.80645	7.45968	0	3.20945	5.20945	46.0438	42.0515	33	30	0.09893	0.0107	21.963

Table S2

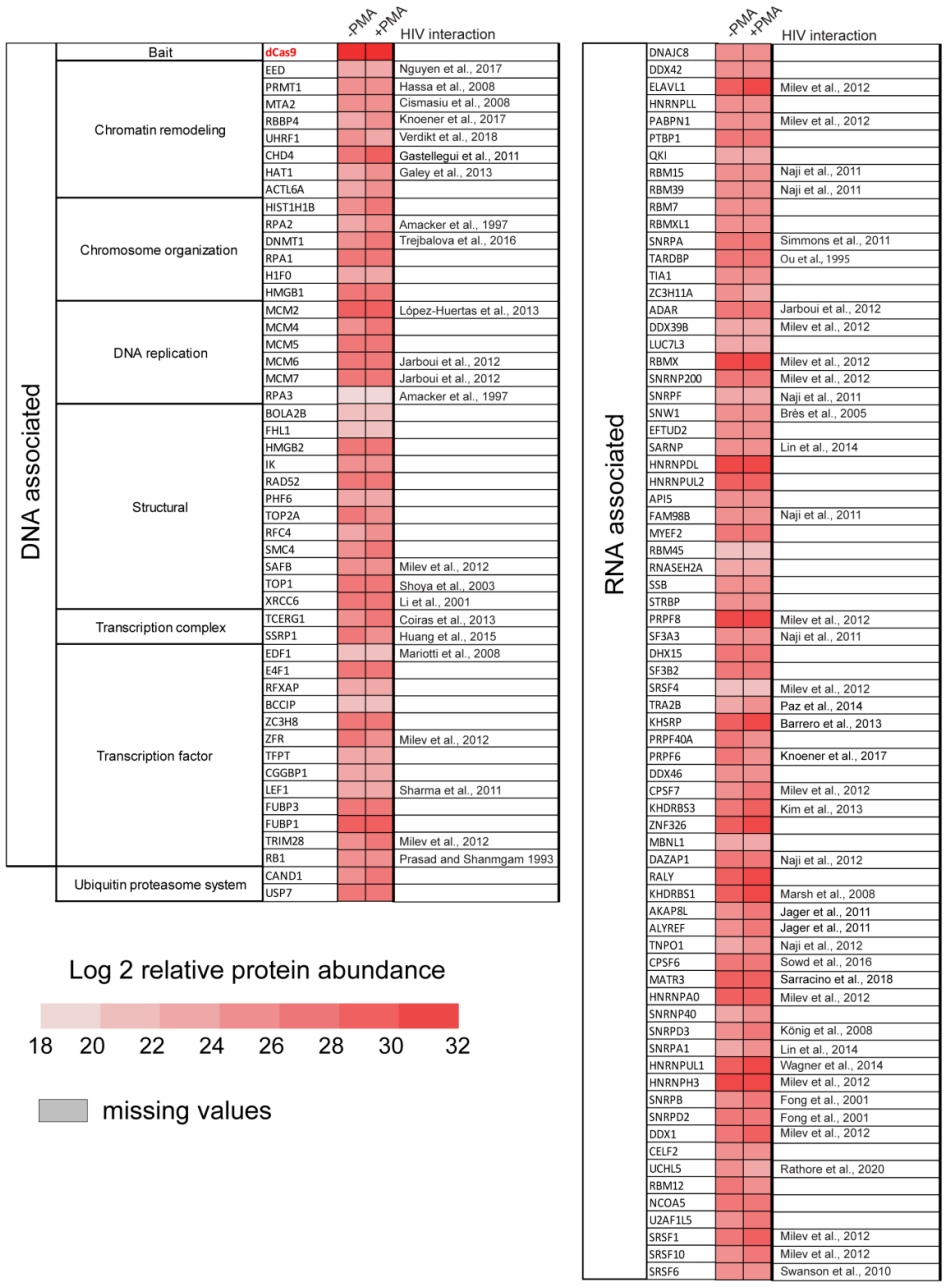
-PMA
+PMA
HIV interaction
DNA associated
Bait
dCas9
Chromatin remodeling
EED
PRMT1
MTA2
RBBP4
UHRF1
CHD4
HAT1
ACTL6A
Chromosome organization
HIST1H1B
RPA2
DNMT1
RPA1
H1F0
HMGB1
DNA replication
MCM2
MCM4
MCM5
MCM6
MCM7
RPA3
Structural
BOLA2B
FHL1
HMGB2
IK
RAD52
PHF6
TOP2A
RFC4
SMC4
SAFB
TOP1
XRCC6
Transcription complex
TCERG1
SSRP1
Transcription factor
EDF1
E4F1
RFXAP
BCCIP
ZC3H8
ZFR
TFPT
CGGBP1
LEF1
FUBP3
FUBP1
TRIM28
RB1
Ubiquitin proteasome system
CAND1
USP7
Nguyen et al., 2017
Hassa et al., 2008
Cismasiu et al., 2008
Knoener et al., 2017
Verdikt et al., 2018
Gastellegui et al., 2011
Galey et al., 2013
Amacker et al., 1997
Trejbalova et al., 2016
López-Huertas et al., 2013
Jarboui et al., 2012
Jarboui et al., 2012
Amacker et al., 1997
Milev et al., 2012
Shoya et al., 2003
Li et al., 2001
Coiras et al., 2013
Huang et al., 2015
Mariotti et al., 2008
Milev et al., 2012
Sharma et al., 2011
Milev et al., 2012
Prasad and Shanmgam 1993
Log 2 relative protein abundance
18 20 22 24 26 28 30 32
missing values
RNA associated
DNAJC8
DDX42
ELAVL1
HNRNPLL
PABPN1
PTBP1
QKI
RBM15
RBM39
RBM7
RBMXL1
SNRPA
TARDBP
TIA1
ZC3H11A
ADAR
DDX39B
LUC7L3
RBMX
SNRNP200
SNRPF
SNW1
EFTUD2
SARNP
HNRNPDL
HNRNPUL2
API5
FAM98B
MYEF2
RBM45
RNASEH2A
SSB
STRBP
PRPF8
SF3A3
DHX15
SF3B2
SRSF4
TRA2B
KHSRP
PRPF40A
PRPF6
DDX46
CPSF7
KHDRBS3
ZNF326
MBNL1
DAZAP1
RALY
KHDRBS1
AKAP8L
ALYREF
TNPO1
CPSF6
MATR3
HNRNPA0
SNRNP40
SNRPD3
SNRPA1
HNRNPUL1
HNRNPH3
SNRPB
SNRPD2
DDX1
CELF2
UCHL5
RBM12
NCOA5
U2AF1L5
SRSF1
SRSF10
SRSF6
Naji et al., 2011
Naji et al., 2011
Milev et al., 2012
Milev et al., 2012
Naji et al., 2011
Brès et al., 2005
Lin et al., 2014
Naji et al., 2011
Milev et al., 2012
Barrero et al., 2013
Knoener et al., 2017
Milev et al., 2012
Kim et al., 2013
Naji et al., 2012
Marsh et al., 2008
Jager et al., 2011
Jager et al., 2011
Naji et al., 2012
Sowd et al., 2016
Sarracino et al., 2018
Milev et al., 2012
König et al., 2008
Lin et al., 2014
Wagner et al., 2014
Milev et al., 2012
Fong et al., 2001
Fong et al., 2001
Milev et al., 2012
Rathore et al., 2020
Milev et al., 2012
Milev et al., 2012
Swanson et al., 2010

Supplementary Table 2 List of factors enriched on both the latent and active state of the HIV-1 promoter. The table displays selected and functionally classified hits (n=122) identified in both experimental conditions with similar scores, including the HA-V5-FLAG-dCas9 bait and potential non-specific binding contaminants.

Table S3

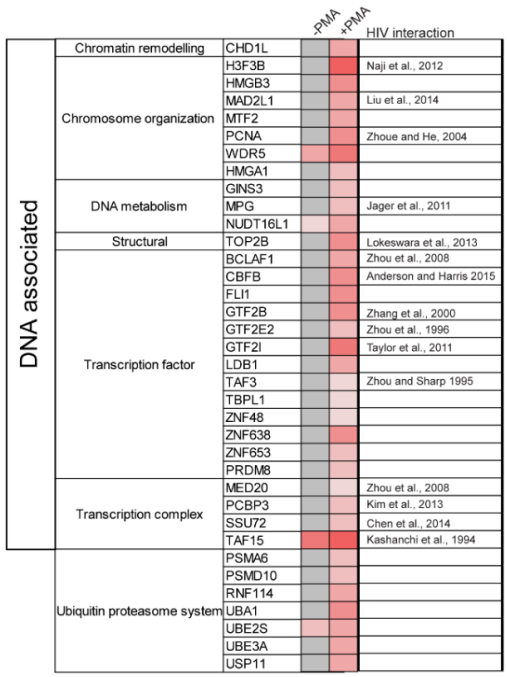
DNA associated
-PMA
+PMA
HIV interaction
Chromatin remodelling
CHD1L
Chromosome organization
H3F3B
Naji et al., 2012
HMGB3
MAD2L1
Liu et al., 2014
MTF2
PCNA
Zhoue and He, 2004
WDR5
HMGA1
DNA metabolism
GINS3
MPG
Jager et al., 2011
NUDT16L1
Structural
TOP2B
Lokeswara et al., 2013
Transcription factor
BCLAF1
Zhou et al., 2008
CBFB
Anderson and Harris 2015
FLI1
GTF2B
Zhang et al., 2000
GTF2E2
Zhou et al., 1996
GTF2I
Taylor et al., 2011
LDB1
TAF3
Zhou and Sharp 1995
TBPL1
ZNF48
ZNF638
ZNF653
PRDM8
Transcription complex
MED20
Zhou et al., 2008
PCBP3
Kim et al., 2013
SSU72
Chen et al., 2014
TAF15
Kashanchi et al., 1994
Ubiquitin proteasome system
PSMA6
PSMD10
RNF114
UBA1
UBE2S
UBE3A
USP11

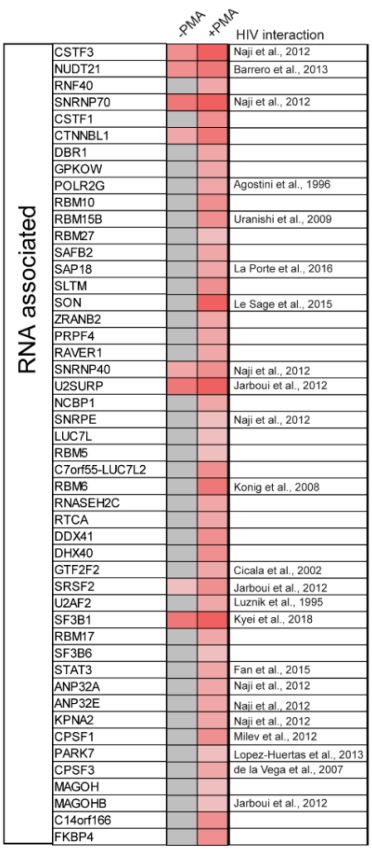
RNA associated
-PMA
+PMA
HIV interaction
CSTF3
Naji et al., 2012
NUDT21
Barrero et al., 2013
RNF40
SNRNP70
Naji et al., 2012
CSTF1
CTNNBL1
DBR1
GPKOW
POLR2G
Agostini et al., 1996
RBM10
RBM15B
Uranishi et al., 2009
RBM27
SAFB2
SAP18
La Porte et al., 2016
SLTM
SON
Le Sage et al., 2015
ZRANB2
PRPF4
RAVER1
SNRNP40
Naji et al., 2012
U2SURP
Jarboui et al., 2012
NCBP1
SNRPE
Naji et al., 2012
LUC7L
RBM5
C7orf55-LUC7L2
RBM6
Konig et al., 2008
RNASEH2C
RTCA
DDX41
DHX40
GTF2F2
Cicala et al., 2002
SRSF2
Jarboui et al., 2012
U2AF2
Luznik et al., 1995
SF3B1
Kyei et al., 2018
RBM17
SF3B6
STAT3
Fan et al., 2015
ANP32A
Naji et al., 2012
ANP32E
Naji et al., 2012
KPNA2
Naji et al., 2012
CPSF1
Milev et al., 2012
PARK7
Lopez-Huertas et al., 2013
CPSF3
de la Vega et al., 2007
MAGOH
MAGOHB
Jarboui et al., 2012
C14orf166
FKBP4

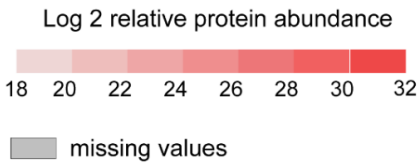
Log 2 relative protein abundance
18
20
22
24
26
28
30
32
missing values

Supplementary Table 3 List of putative factors enriched on the active (+PMA) HIV-1 promoter. The table displays selected and functionally classified hits (n=84) identified by Catchet-MS in the +PMA state

Table S4

Name	Arithmetic Mean	Median	SD	IQR	CV	Sum	Minimum	Maximum	Count
Proteins - # AAs	625.9015755	449	763.2457635	472.5	1.219434163	3694697	18	34350	5903
Proteins - # Peptides	7.049974589	3	9.941955035	8	1.410211471	41616	1	167	5903
Proteins - # Peptides (by Search Engine): A4 Mascot	7.049974589	3	9.941955035	8	1.410211471	41616	1	167	5903
Proteins - # Protein Groups	1.075385397	1	0.804874751	0	0.748452372	6348	0	11	5903
Proteins - # Protein Unique Peptides	5.691004574	2	9.409635432	6	1.653422574	33594	0	166	5903
Proteins - # PSMs	85.45383703	12	238.3124063	52	2.78878532	504434	1	3565	5903
Proteins - # PSMs (by Search Engine): A4 Mascot	85.45383703	12	238.3124063	52	2.78878532	504434	1	3565	5903
Proteins - # Unique Peptides	6.197187871	3	9.440269279	7	1.523315006	36582	0	166	5903
Proteins - Abundance Ratio (log2): (F27) / (F1)	-3.645077669	-4.022450988	3.256357008	5.050406102	-0.893357372	-18706.5386	-6.64385619	6.64385619	5132
Proteins - Abundance Ratio (log2): (F28) / (F2)	-3.080770486	-3.058825361	3.274785095	5.829354752	-1.062976002	-15810.51413	-6.64385619	6.64385619	5132
Proteins - Abundance Ratio (log2): (F29) / (F1)	-3.489604345	-4.214873516	3.490343712	5.662728971	-1.000211877	-17908.6495	-6.64385619	6.64385619	5132
Proteins - Abundance Ratio (log2): (F3) / (F1)	-3.7296844	-4.124734329	3.018716311	4.452048224	-0.809375804	-19140.74034	-6.64385619	6.64385619	5132
Proteins - Abundance Ratio (log2): (F30) / (F2)	-3.339627058	-3.54799393	3.405717493	5.870080586	-1.019789765	-17138.96606	-6.64385619	6.64385619	5132
Proteins - Abundance Ratio (log2): (F4) / (F2)	-3.658679244	-4.105673663	3.098987039	4.64434842	-0.847023429	-18776.34188	-6.64385619	6.64385619	5132
Proteins - Abundance Ratio: (F27) / (F1)	2.625520118	0.049843132	13.37986578	0.269872962	5.096081985	13474.16925	0	100	5132
Proteins - Abundance Ratio: (F28) / (F2)	2.531365802	0.100205681	12.73420222	0.472421481	5.030565796	12990.96929	0	100	5132
Proteins - Abundance Ratio: (F29) / (F1)	2.841371373	0.0364059	13.46780769	0.415348333	4.739897015	14581.91789	0	100	5132
Proteins - Abundance Ratio: (F3) / (F1)	2.387959743	0.050110282	13.29634644	0.183140747	5.568078139	12255.0094	0	100	5132
Proteins - Abundance Ratio: (F30) / (F2)	2.226408549	0.060088502	11.05184387	0.45543572	4.963978365	11425.92867	0	100	5132
Proteins - Abundance Ratio: (F4) / (F2)	2.611594288	0.051448102	13.91148538	0.205106275	5.326817202	13402.70189	0	100	5132
Proteins - Abundance: F1: Sample, control	59131448.73	1996852.621	569381322.9	13897669.05	9.629077845	3.03463E+11	0	35892627283	5132
Proteins - Abundance: F2: Sample, PMA	59208972.49	1739722.451	941523815.1	12793741.41	15.9017084	3.0386E+11	0	64933805348	5132
Proteins - Abundance: F27: Sample, control	1896039.707	5601.295166	34358041.65	92306.19226	18.12095048	9730475779	0	1684339964	5132
Proteins - Abundance: F28: Sample, PMA	3097478.294	16661.19287	51491849.94	178842.3175	16.62379686	15896258606	0	2854568181	5132
Proteins - Abundance: F29: Sample, control	864449.2629	2883.788208	14068899.68	60276.5614	16.27498603	4436353617	0	623270265.7	5132
Proteins - Abundance: F3: Sample, control	6563848.329	17273.24548	227245221.5	179896.2858	34.62073012	33685669625	0	15861526519	5132
Proteins - Abundance: F30: Sample, PMA	919751.1687	3881.058167	14206434.72	60436.61716	15.44595452	4720162998	0	740924934.1	5132
Proteins - Abundance: F4: Sample, PMA	7890541.895	19108.25586	273278590.4	203837.4481	34.63369107	40494261008	0	19132853673	5132
Proteins - Abundances (Grouped) Count: F1	0.96745908	1	0.17744899	0	0.183417566	4965	0	1	5132
Proteins - Abundances (Grouped) Count: F2	0.964925955	1	0.183984925	0	0.190672584	4952	0	1	5132
Proteins - Abundances (Grouped) Count: F27	0.585931411	1	0.492608442	1	0.840727144	3007	0	1	5132
Proteins - Abundances (Grouped) Count: F28	0.656664069	1	0.474868729	1	0.72315321	3370	0	1	5132
Proteins - Abundances (Grouped) Count: F29	0.538776306	1	0.498542705	1	0.925324109	2765	0	1	5132
Proteins - Abundances (Grouped) Count: F3	0.684333593	1	0.464826019	1	0.679238932	3512	0	1	5132
Proteins - Abundances (Grouped) Count: F30	0.55806703	1	0.496665165	1	0.889974032	2864	0	1	5132
Proteins - Abundances (Grouped) Count: F4	0.679462198	1	0.466728793	1	0.686909138	3487	0	1	5132
Proteins - Abundances (Grouped) CV [%]: F1	0	0	0	0		0	0	0	5132
Proteins - Abundances (Grouped) CV [%]: F2	0	0	0	0		0	0	0	5132
Proteins - Abundances (Grouped) CV [%]: F27	0	0	0	0		0	0	0	5132
Proteins - Abundances (Grouped) CV [%]: F28	0	0	0	0		0	0	0	5132
Proteins - Abundances (Grouped) CV [%]: F29	0	0	0	0		0	0	0	5132
Proteins - Abundances (Grouped) CV [%]: F3	0	0	0	0		0	0	0	5132
Proteins - Abundances (Grouped) CV [%]: F30	0	0	0	0		0	0	0	5132
Proteins - Abundances (Grouped) CV [%]: F4	0	0	0	0		0	0	0	5132
Proteins - Abundances (Grouped): F1	61325236.83	2070936.237	590505479.3	14413275.24	9.629077845	3.14721E+11	0	37224250649	5132
Proteins - Abundances (Grouped): F2	59208972.49	1739722.451	941523815.1	12793741.41	15.9017084	3.0386E+11	0	64933805348	5132
Proteins - Abundances (Grouped): F27	69605376.47	205628.7414	1261315580	3388645.943	18.12095048	3.57215E+11	0	61833682499	5132
Proteins - Abundances (Grouped): F28	65854165.71	354226.5198	1094746273	3802290.282	16.62379686	3.37964E+11	0	60689757327	5132
Proteins - Abundances (Grouped): F29	71814646.11	239572.4521	1168782362	5007511.848	16.27498603	3.68553E+11	0	51778554837	5132
Proteins - Abundances (Grouped): F3	69886905.22	183912.4869	2419535684	1915399.937	34.62073012	3.5866E+11	0	1.68882E+11	5132
Proteins - Abundances (Grouped): F30	67935838.7	286667.6885	1049333874	4464046.814	15.44595452	3.48647E+11	0	54727146342	5132
Proteins - Abundances (Grouped): F4	70339478.96	170338.7142	2436115784	1817089.381	34.63369107	3.60982E+11	0	1.70558E+11	5132
Proteins - Abundances (Normalized): F1: Sample, control	61325236.83	2070936.237	590505479.3	14413275.24	9.629077845	3.14721E+11	0	37224250649	5132
Proteins - Abundances (Normalized): F2: Sample, PMA	59208972.49	1739722.451	941523815.1	12793741.41	15.9017084	3.0386E+11	0	64933805348	5132
Proteins - Abundances (Normalized): F27: Sample, control	69605376.47	205628.7414	1261315580	3388645.943	18.12095048	3.57215E+11	0	61833682499	5132
Proteins - Abundances (Normalized): F28: Sample, PMA	65854165.71	354226.5198	1094746273	3802290.282	16.62379686	3.37964E+11	0	60689757327	5132
Proteins - Abundances (Normalized): F29: Sample, control	71814646.11	239572.4521	1168782362	5007511.848	16.27498603	3.68553E+11	0	51778554837	5132
Proteins - Abundances (Normalized): F3: Sample, control	69886905.22	183912.4869	2419535684	1915399.937	34.62073012	3.5866E+11	0	1.68882E+11	5132
Proteins - Abundances (Normalized): F30: Sample, PMA	67935838.7	286667.6885	1049333874	4464046.814	15.44595452	3.48647E+11	0	54727146342	5132
Proteins - Abundances (Normalized): F4: Sample, PMA	70339478.96	170338.7142	2436115784	1817089.381	34.63369107	3.60982E+11	0	1.70558E+11	5132
Proteins - Abundances Count: F1: Sample, control	6.950701481	3	10.45416281	7	1.504044281	35671	0	192	5132
Proteins - Abundances Count: F2: Sample, PMA	6.980904131	3	10.55383253	7	1.511814564	35826	0	193	5132
Proteins - Abundances Count: F27: Sample, control	2.914848012	1	6.213724014	3	2.13174889	14959	0	136	5132
Proteins - Abundances Count: F28: Sample, PMA	3.46745908	1	6.650409091	4	1.917948831	17795	0	143	5132
Proteins - Abundances Count: F29: Sample, control	2.273967264	1	4.790582305	2	2.106706803	11670	0	107	5132
Proteins - Abundances Count: F3: Sample, control	3.694466095	1	7.060157504	4	1.911008877	18960	0	137	5132
Proteins - Abundances Count: F30: Sample, PMA	2.677123928	1	5.843138828	3	2.182617983	13739	0	130	5132
Proteins - Abundances Count: F4: Sample, PMA	3.604247857	1	6.883036344	4	1.909701169	18497	0	135	5132
Proteins - calc. pI	7.21698289	7.01	1.629887877	2.65	0.225840618	42601.85	3.78	12.41	5903
Proteins - Coverage [%]	16.39207976	9.803921569	16.71646786	23.27724859	1.019789319	96762.44682	0.061135371	94.59854015	5903
Proteins - Coverage [%] (by Search Engine): A4 Mascot	16.39207976	9.803921569	16.71646786	23.27724859	1.019789319	96762.44682	0.061135371	94.59854015	5903
Proteins - MW [kDa]	69.923392	50.114	85.01040993	53.1425	1.215764961	412757.783	2.172	3813.652	5903
Proteins - Score Mascot: A4 Mascot	1992.34036	241.3936976	5841.714586	1166.60379	2.932086658	11760785.14	0	111969.5972	5903
Protein Groups - # Peptides	8.097394276	4	10.65309734	8	1.31562043	37912	1	167	4682
Protein Groups - # Proteins	1.355830842	1	1.94064817	0	1.431335024	6348	1	44	4682
Protein Groups - # PSMs	89.42994447	15	239.6488314	62	2.679738121	418711	1	3565	4682
Protein Groups - # Unique Peptides	7.451089278	4	10.14664217	8	1.361766285	34886	1	166	4682
Peptide Groups - # Missed Cleavages	0.211967266	0	0.456436943	0	2.15333693	8470	0	2	39959
Peptide Groups - # Protein Groups	1.046072224	1	0.314178563	0	0.300341177	41800	0	11	39959
Peptide Groups - # Proteins	1.147751445	1	0.963569809	0	0.839528291	45863	1	53	39959
Peptide Groups - # PSMs	9.256287695	4	18.45459183	9	1.993735765	369872	1	1016	39959
Peptide Groups - Abundance Ratio (log2): (F27) / (F1)	-4.427275803	-6.64385619	3.201323989	4.184645862	-0.723091158	-162768.7949	-6.64385619	6.64385619	36765
Peptide Groups - Abundance Ratio (log2): (F28) / (F2)	-3.96321723	-6.64385619	3.417120885	5.089851971	-0.862208828	-145707.6814	-6.64385619	6.64385619	36765
Peptide Groups - Abundance Ratio (log2): (F29) / (F1)	-4.616874934	-6.64385619	3.327400265	3.949680358	-0.720704007	-169739.4069	-6.64385619	6.64385619	36765
Peptide Groups - Abundance Ratio (log2): (F3) / (F1)	-4.380463896	-6.385266372	3.039468743	3.908941314	-0.693869146	-161047.7551	-6.64385619	6.64385619	36765
Peptide Groups - Abundance Ratio (log2): (F30) / (F2)	-4.250586005	-6.64385619	3.45884849	4.848126938	-0.813734503	-156272.7945	-6.64385619	6.64385619	36765
Peptide Groups - Abundance Ratio (log2): (F4) / (F2)	-4.383447925	-6.64385619	3.08928167	3.945770081	-0.704760664	-161157.463	-6.64385619	6.64385619	36765
Peptide Groups - Abundance Ratio: (F27) / (F1)	2.138980967	0.01	12.34151993	0.127078462	5.76981288	78639.63525	0	100	36765
Peptide Groups - Abundance Ratio: (F28) / (F2)	2.487092839	0.01	12.73635452	0.260723468	5.120980739	91437.96821	0	100	36765
Peptide Groups - Abundance Ratio: (F29) / (F1)	2.203438043	0.01	12.12087239	0.074909761	5.500890949	81009.39967	0	100	36765
Peptide Groups - Abundance Ratio: (F3) / (F1)	1.888389535	0.01	11.74717175	0.110001574	6.22073546	69426.64127	0	100	36765
Peptide Groups - Abundance Ratio: (F30) / (F2)	2.299673368	0.01	11.85249127	0.205131313	5.153989014	84547.49137	0	100	36765
Peptide Groups - Abundance Ratio: (F4) / (F2)	1.945044238	0.01	11.77744248	0.114117072	6.05510263	71509.55141	0	100	36765
Peptide Groups - Abundance: F1: Sample, control	9768077.383	1002071.805	133899705.8	3782878.344	13.70788749	3.59123E+11	0	14225552205	36765
Peptide Groups - Abundance: F2: Sample, PMA	10130474.93	860133.4023	191378462	3147426.527	18.8913613	3.72447E+11	0	17123692824	36765
Peptide Groups - Abundance: F27: Sample, control	275952.5729	0	7670051.194	12220.73145	27.79481674	10145396342	0	1009310882	36765
Peptide Groups - Abundance: F28: Sample, PMA	476491.1356	0	9768870.495	25158.16406	20.50168359	17518196601	0	979450692.5	36765

Peptide Groups - Abundance: F29: Sample, control	121942.8356	0	3009821.78	4152.288574	24.68223545	4483228352	0	419899557.7	36765
Peptide Groups - Abundance: F3: Sample, control	951464.38	1966.508301	84377961.21	28388.42505	88.68220711	34980587931	0	15861501896	36765
Peptide Groups - Abundance: F30: Sample, PMA	137151.7057	0	3343645.749	7889.714355	24.37917728	5042382461	0	462384751.1	36765
Peptide Groups - Abundance: F4: Sample, PMA	1136416.391	1308.020508	101585114	28943.14844	89.39075045	41780348630	0	19132837467	36765
Peptide Groups - Abundances (Grouped) Count: F1	0.96496668	1	0.183866543	0	0.190541857	35477	0	1	36765
Peptide Groups - Abundances (Grouped) Count: F2	0.969862641	1	0.170967522	0	0.17628014	35657	0	1	36765
Peptide Groups - Abundances (Grouped) Count: F27	0.408459132	0	0.491555533	1	1.203438713	15017	0	1	36765
Peptide Groups - Abundances (Grouped) Count: F28	0.484292126	0	0.499759999	1	1.031939138	17805	0	1	36765
Peptide Groups - Abundances (Grouped) Count: F29	0.317149463	0	0.465372509	1	1.46736023	11660	0	1	36765
Peptide Groups - Abundances (Grouped) Count: F3	0.515735074	1	0.499759143	1	0.969022989	18961	0	1	36765
Peptide Groups - Abundances (Grouped) Count: F30	0.375492996	0	0.484256528	1	1.289655287	13805	0	1	36765
Peptide Groups - Abundances (Grouped) Count: F4	0.503386373	1	0.499995332	1	0.993263543	18507	0	1	36765
Peptide Groups - Abundances (Grouped) CV [%]: F1	0	0	0	0		0	0	0	36765
Peptide Groups - Abundances (Grouped) CV [%]: F2	0	0	0	0		0	0	0	36765
Peptide Groups - Abundances (Grouped) CV [%]: F27	0	0	0	0		0	0	0	36765
Peptide Groups - Abundances (Grouped) CV [%]: F28	0	0	0	0		0	0	0	36765
Peptide Groups - Abundances (Grouped) CV [%]: F29	0	0	0	0		0	0	0	36765
Peptide Groups - Abundances (Grouped) CV [%]: F3	0	0	0	0		0	0	0	36765
Peptide Groups - Abundances (Grouped) CV [%]: F30	0	0	0	0		0	0	0	36765
Peptide Groups - Abundances (Grouped) CV [%]: F4	0	0	0	0		0	0	0	36765
Peptide Groups - Abundances (Grouped): F1	10130474.93	1039248.861	138867410.6	3923223.857	13.70788749	3.72447E+11	0	14753322925	36765
Peptide Groups - Abundances (Grouped): F2	10130474.93	860133.4023	191378462	3147426.527	18.8913613	3.72447E+11	0	17123692824	36765
Peptide Groups - Abundances (Grouped): F27	10130474.93	0	281574694.2	448634.3876	27.79481674	3.72447E+11	0	37052738731	36765
Peptide Groups - Abundances (Grouped): F28	10130474.93	0	207691791.6	534877.0025	20.50168359	3.72447E+11	0	20823683683	36765
Peptide Groups - Abundances (Grouped): F29	10130474.93	0	250042767.5	344953.8883	24.68223545	3.72447E+11	0	34883410091	36765
Peptide Groups - Abundances (Grouped): F3	10130474.93	20937.89685	898392875.9	302258.5336	88.68220711	3.72447E+11	0	1.68881E+11	36765
Peptide Groups - Abundances (Grouped): F30	10130474.93	0	246972644.3	582760.1856	24.37917728	3.72447E+11	0	34153254636	36765
Peptide Groups - Abundances (Grouped): F4	10130474.93	11660.22337	905570756.4	258010.9209	89.39075045	3.72447E+11	0	1.70558E+11	36765
Peptide Groups - Abundances (Normalized): F1: Sample, control	10130474.93	1039248.861	138867410.6	3923223.857	13.70788749	3.72447E+11	0	14753322925	36765
Peptide Groups - Abundances (Normalized): F2: Sample, PMA	10130474.93	860133.4023	191378462	3147426.527	18.8913613	3.72447E+11	0	17123692824	36765
Peptide Groups - Abundances (Normalized): F27: Sample, control	10130474.93	0	281574694.2	448634.3876	27.79481674	3.72447E+11	0	37052738731	36765
Peptide Groups - Abundances (Normalized): F28: Sample, PMA	10130474.93	0	207691791.6	534877.0025	20.50168359	3.72447E+11	0	20823683683	36765
Peptide Groups - Abundances (Normalized): F29: Sample, control	10130474.93	0	250042767.5	344953.8883	24.68223545	3.72447E+11	0	34883410091	36765
Peptide Groups - Abundances (Normalized): F3: Sample, control	10130474.93	20937.89685	898392875.9	302258.5336	88.68220711	3.72447E+11	0	1.68881E+11	36765
Peptide Groups - Abundances (Normalized): F30: Sample, PMA	10130474.93	0	246972644.3	582760.1856	24.37917728	3.72447E+11	0	34153254636	36765
Peptide Groups - Abundances (Normalized): F4: Sample, PMA	10130474.93	11660.22337	905570756.4	258010.9209	89.39075045	3.72447E+11	0	1.70558E+11	36765
Peptide Groups - Abundances Count: F1: Sample, control	4.479722562	2	5.67021581	5	1.265751557	164697	0	213	36765
Peptide Groups - Abundances Count: F2: Sample, PMA	4.473167415	2	5.75199837	5	1.285889357	164456	0	221	36765
Peptide Groups - Abundances Count: F27: Sample, control	1.062341901	0	2.420654201	1	2.27860183	39057	0	139	36765
Peptide Groups - Abundances Count: F28: Sample, PMA	1.401332789	0	3.020985854	2	2.155794738	51520	0	142	36765
Peptide Groups - Abundances Count: F29: Sample, control	0.753189174	0	2.029354528	1	2.694349038	27691	0	105	36765
Peptide Groups - Abundances Count: F3: Sample, control	1.63244934	1	3.639521693	2	2.22948523	60017	0	234	36765
Peptide Groups - Abundances Count: F30: Sample, PMA	1.020563035	0	2.502313446	1	2.451895041	37521	0	139	36765
Peptide Groups - Abundances Count: F4: Sample, PMA	1.579355365	1	3.661589668	2	2.318407718	58065	0	249	36765
Peptide Groups - Charge (by Search Engine): A4 Mascot	2.27760955	2	0.515622043	0	0.226387373	91011	2	6	39959
Peptide Groups - Concatenated Rank (by Search Engine): A4 Mascot	1.006306464	1	0.09549788	0	0.0948994	40211	1	6	39959
Peptide Groups - Ions Score (by Search Engine): A4 Mascot	48.26798994	44.03	19.5713523	25.11	0.405472702	1928740.61	13.06	189.06	39959
Peptide Groups - m/z [Da] (by Search Engine): A4 Mascot	615.8574228	592.2871094	160.9139442	235.5726624	0.261284411	24609046.76	374.204	1368.588257	39959
Peptide Groups - Rank (by Search Engine): A4 Mascot	1.006306464	1	0.09549788	0	0.0948994	40211	1	6	39959
Peptide Groups - RT [min] (by Search Engine): A4 Mascot	27.42003655	27.33202667	11.91351497	19.89909226	0.434482097	1095677.24	6.371940223	58.84110185	39959
Peptide Groups - Search Engine Rank (by Search Engine): A4 Mascot	1.006306464	1	0.09549788	0	0.0948994	40211	1	6	39959
Peptide Groups - Sequence Length	12.26459621	12	4.285822242	5	0.349446665	490081	6	49	39959
Peptide Groups - Theo. MH+ [Da]	1390.766984	1314.701204	444.3190626	557.3550343	0.319477718	55573657.92	747.4610811	4852.389837	39959
Peptide Groups - Top Apex RT [min]	34.91930421	34.84970565	11.98924577	19.88060326	0.343341485	1299696.503	7.332193851	65.35504679	37220
Peptide Groups - ΔCn (by Search Engine): A4 Mascot	7.4136E-05	0	0.001667698	0	22.49511887	2.9624	0	0.05	39959
Peptide Groups - ΔM [ppm] (by Search Engine): A4 Mascot	-0.335248381	-0.600007916	1.699005782	1.398146383	-5.067901533	-13396.19004	-10.00784576	9.95517133	39959
Peptide Groups - Δm/z [Da] (by Search Engine): A4 Mascot	-0.000179905	-0.000338092	0.001148927	0.000782437	-6.386301978	-7.188822863	-0.008193627	0.009014794	39959
Peptide Groups - ΔScore (by Search Engine): A4 Mascot	0.858403769	0.9231	0.194457775	0.1935	0.226534159	34300.9562	0	1	39959
PSMs - # Missed Cleavages	0.189973829	0	0.432670676	0	2.2775278	70266	0	2	369872
PSMs - # Protein Groups	1.132042977	1	0.563864963	0	0.498095015	418711	0	11	369872
PSMs - # Proteins	1.363806939	1	1.772538808	0	1.299699215	504434	1	53	369872
PSMs - Aligned m/z [Da]	610.9495306	592.848056	150.1197701	216.8768911	0.245715501	225973124.8	374.204	1368.588922	369872
PSMs - Apex RT [min]	34.82322869	34.91168594	11.78910601	19.04831871	0.338541441	11923438.68	7.063932419	68.82004149	342399
PSMs - Charge	2.302956158	2	0.531473438	1	0.230778791	851799	2	6	369872
PSMs - Concatenated Rank	1.01650571	1	0.145332399	0	0.142972536	375977	1	7	369872
PSMs - Expectation Value	0.008506321	0.001787946	0.013216423	0.010966158	1.553717836	3146.250091	1.36582E-19	0.062900933	369872
PSMs - First Scan	18628.62877	17656	11138.85506	17818	0.597942833	6890208179	37	47149	369872
PSMs - Homology Threshold	17.84616825	17	3.198909224	5	0.179249079	5240795	13	28	293665
PSMs - Identity Relaxed	23.63392201	25	3.248101016	4	0.137433855	8741526	13	29	369872
PSMs - Identity Strict	30.57488266	32	3.44780049	4	0.11276578	11308793	13	36	369872
PSMs - Intensity	411994.6241	161245.08	4049520.624	276167.2513	9.829061806	1.52385E+11	497.5424387	472309873.8	369872
PSMs - Ion Inject Time [ms]	50.05243485	50	46.32631629	23.6732502	0.925555698	18512994.18	0.01	405	369872
PSMs - Ions Score	42.3708514	38.63	16.0202789	19.55	0.378096696	15671791.55	13	189.06	369872
PSMs - Isolation Interference [%]	24.21034591	21.41119003	20.29280653	33.34288645	0.838187385	8952719.605	0	100	369789
PSMs - Last Scan	18628.62877	17656	11138.85506	17818	0.597942833	6890208179	37	47149	369872
PSMs - m/z [Da]	610.9493594	592.8479004	150.1197229	216.8767548	0.245715493	225973061.5	374.204	1368.588257	369872
PSMs - Matched Ions	8.940644331	8	3.653160233	4	0.40860145	3306894	3	47	369872
PSMs - MH+ [Da]	1387.947643	1332.702867	398.5069065	507.2485013	0.287119553	513362970.5	747.4601234	4852.38817	369872
PSMs - Original Precursor Charge	2.302956158	2	0.531473438	1	0.230778791	851799	2	6	369872
PSMs - Peptides Matched	315.2430219	332	151.7696314	247	0.481436926	116599567	1	926	369872
PSMs - Precursor Abundance	3770530.128	347015.5625	48778663.1	996942.2813	12.93681828	1.29103E+12	1319.942261	3558978048	342399
PSMs - Rank	1.003947312	1	0.076458628	0	0.076158008	371332	1	6	369872
PSMs - RT [min]	35.12487057	35.21066658	12.02516657	19.57748062	0.342354758	12991706.13	7.075704602	69.06229308	369872
PSMs - Search Engine Rank	1.01650571	1	0.145332399	0	0.142972536	375977	1	7	369872
PSMs - Theo. MH+ [Da]	1387.947993	1332.700536	398.5067833	507.247517	0.287119392	513363100.2	747.4610811	4852.389837	369872
PSMs - Total Ions	114.6922611	108	48.09247484	60	0.419317523	42421456	40	564	369872
PSMs - ΔCn	4.23541E-05	0	0.001265631	0	29.88212821	15.6656	0	0.05	369872
PSMs - ΔM [ppm]	-0.307557476	-0.584566922	1.679606174	1.499008222	-5.461113139	-113756.8988	-10.01231837	9.984084329	369872
PSMs - Δm/z [Da]	-0.000152428	-0.000325844	0.001143479	0.000842563	-7.501760949	-56.37888414	-0.009015198	0.010827309	369872
PSMs - ΔScore	0.864610257	0.9286	0.187494838	0.1905	0.216854747	315244.6811	0	1	364609
MS/MS Spectrum Info - # PSMs	0.192323832	0	0.402099916	0	2.090744099	369872	0	7	1923173
MS/MS Spectrum Info - First Scan	15231.46535	13295	10567.79198	15300	0.693813217	29292742918	3	47710	1923173
MS/MS Spectrum Info - Ion Inject Time [ms]	70.26806714	50	64.70516652	20.95400238	0.920833163	135137649.5	0.01	405	1923173
MS/MS Spectrum Info - Isolation Interference [%]	29.51677465	26.44338799	24.75437571	41.43119109	0.838654494	56369011.02	0	100	1909728
MS/MS Spectrum Info - Last Scan	15231.46535	13295	10567.79198	15300	0.693813217	29292742918	3	47710	1923173
MS/MS Spectrum Info - Original Mass	652.3559541	626.8167114	177.9248498	238.1844482	0.272741973	1254593357	370.1434	1399.947998	1923173
MS/MS Spectrum Info - Original Precursor Charge	2.376992085	2	0.600460824	1	0.252613725	4571367	2	6	1923173
MS/MS Spectrum Info - Precursor Charge	2.376992085	2	0.600460824	1	0.252613725	4571367	2	6	1923173

MS/MS Spectrum Info - Precursor Intensity	213557.8148	46452.89755	2334027.242	151371.0227	10.92925232	4.10709E+11	21.61298144	472309673.8	1923173
MS/MS Spectrum Info - Precursor m/z [Da]	652.3559541	626.8167114	177.9248498	238.1844482	0.272741973	1254593357	370.1434	1399.947998	1923173
MS/MS Spectrum Info - Precursor MH+ [Da]	1538.281566	1428.227848	551.2313513	581.1628149	0.358342298	2958381575	739.2795234	4999.598776	1923173
MS/MS Spectrum Info - RT [min]	33.45201969	33.14864308	12.60194188	19.59304474	0.376716922	64334021.07	6.012299866	69.09696422	1923173
Consensus Features - # Isotopes	2.828294601	2	1.073049029	1	0.379397899	6367696	1	11	2251426
Consensus Features - # PSMs	0.151898397	0	0.606765537	0	3.994548653	341988	0	28	2251426
Consensus Features - Abundances (Normalized): F1	314833.9195	1424.515476	8869282.148	65200.24473	28.1713043	7.08825E+11	0	2565607859	2251426
Consensus Features - Abundances (Normalized): F2	308451.6701	1634.985413	12021096.99	57789.875	38.97238418	6.94456E+11	0	3558978048	2251426
Consensus Features - Abundances (Normalized): F27	1592416.602	0	99125250.65	0	62.24831525	3.58521E+12	0	31240017314	2251426
Consensus Features - Abundances (Normalized): F28	1170373.197	0	62065790.36	61398.46206	53.03076873	2.63501E+12	0	21653060950	2251426
Consensus Features - Abundances (Normalized): F29	2857699.299	0	210421347.8	0	73.63313134	6.4339E+12	0	92229373061	2251426
Consensus Features - Abundances (Normalized): F3	1142345.686	0	62942361.17	49136.51464	55.09922432	2.57191E+12	0	22181353259	2251426
Consensus Features - Abundances (Normalized): F30	2926949.378	0	200681879.1	97307.62522	68.56349502	6.58981E+12	0	70348920112	2251426
Consensus Features - Abundances (Normalized): F4	1050457.155	0	56942597.8	41397.52739	54.20744437	2.36503E+12	0	18410173385	2251426
Consensus Features - Abundances (per File): F1	303571.3636	1373.556274	8552001.259	62867.83594	28.1713043	6.83468E+11	0	2473828352	2251426
Consensus Features - Abundances (per File): F2	308451.6701	1634.985413	12021096.99	57789.875	38.97238418	6.94456E+11	0	3558978048	2251426
Consensus Features - Abundances (per File): F27	43377.18236	0	2700156.522	0	62.24831525	97660516171	0	850973248	2251426
Consensus Features - Abundances (per File): F28	55048.99403	0	2919290.471	2887.902405	53.03076873	1.23939E+11	0	1018460800	2251426
Consensus Features - Abundances (per File): F29	34398.77777	0	2532889.722	0	73.63313134	77446302640	0	1110185984	2251426
Consensus Features - Abundances (per File): F3	107290.2541	0	5911609.778	4614.950806	55.09922432	2.41556E+11	0	2083294976	2251426
Consensus Features - Abundances (per File): F30	39626.58241	0	2716936.986	1317.401886	68.56349502	89216317936	0	952420736	2251426
Consensus Features - Abundances (per File): F4	117838.1801	0	6387706.594	4643.891724	54.20744437	2.65304E+11	0	2065216384	2251426
Consensus Features - Abundances Count: F1	0.512485865	1	0.51957881	1	1.013840275	1153824	0	7	2251426
Consensus Features - Abundances Count: F2	0.513884978	1	0.517792059	1	1.007603027	1156974	0	7	2251426
Consensus Features - Abundances Count: F27	0.248284421	0	0.449655857	0	1.811051439	558994	0	6	2251426
Consensus Features - Abundances Count: F28	0.287191762	0	0.469100232	1	1.633404207	646591	0	6	2251426
Consensus Features - Abundances Count: F29	0.226378748	0	0.430265863	0	1.900645999	509675	0	7	2251426
Consensus Features - Abundances Count: F3	0.351991138	0	0.49598871	1	1.409094312	792482	0	5	2251426
Consensus Features - Abundances Count: F30	0.266895292	0	0.465703721	1	1.744892976	600895	0	6	2251426
Consensus Features - Abundances Count: F4	0.33983351	0	0.491769307	1	1.44708892	765110	0	5	2251426
Consensus Features - Avg. Apex RT [min]	34.15686315	32.67115726	14.79300682	22.84614764	0.433090321	76901649.77	6.042416096	69.54751187	2251426
Consensus Features - Avg. m/z [Da]	588.5644275	552.9387608	162.0658118	223.1567236	0.27535781	1325109255	375.0216788	1399.732844	2251426
Consensus Features - Charge	2.37724269	2	1.45475301	1	0.611949725	5352186	0	12	2251426
Consensus Features - Fraction No.	6.61378433	7	3.358662346	6	0.507827619	14890446	1	12	2251426
Consensus Features - Left RT [min]	33.75953003	32.20213839	14.80070439	22.86659648	0.438415593	76007083.66	6.000916958	69.49367123	2251426
Consensus Features - Max. Apex S/N	71.5143955	12.54756069	527.2665243	21.86564887	7.372872562	161009369.4	5	45418.12109	2251426
Consensus Features - Right RT [min]	34.58304349	33.15800289	14.79615169	22.86233732	0.427844117	77861163.26	6.086333752	69.59352475	2251426
LCMS Features - # Isotopes	2.129449163	2	1.107326312	2	0.520005986	15177634	1	11	7127493
LCMS Features - Aligned m/z [Da]	585.6580588	552.9435201	156.3686768	220.63798	0.266996543	4174273714	375.0213422	1399.732844	7127493
LCMS Features - Apex RT [min]	33.87854927	32.43117868	14.57580316	21.84757997	0.430236934	241469122.8	6.025818825	69.54971676	7127493
LCMS Features - Apex S/N	39.10979803	6.544229984	352.3536005	11.05107164	9.009343395	278754811.7	1.000031114	45418.12109	7127493
LCMS Features - Area	3749613.925	117245.5938	174610615.8	463043.6094	46.56762518	2.67253E+13	172.289093	93029072896	7127493
LCMS Features - Charge	2.472280646	2	1.631848322	1	0.66005788	17621163	0	12	7127493
LCMS Features - Intensity	330111.2665	14159.41797	10547387.41	54186.26904	31.95100708	2.35287E+12	59.92860031	3558978048	7127493
LCMS Features - Intensity (aligned)	1620190.163	61683.59919	74967646.15	199591.2197	46.27089329	1.15479E+13	0.785402608	32437220452	7127493
LCMS Features - Left RT [min]	33.72749859	32.27890015	14.56616046	21.82295609	0.431877876	240392510.1	6.000916958	69.49367123	7127493
LCMS Features - m/z [Da]	585.6575936	552.9435493	156.3684233	220.6374607	0.266996322	4174270399	375.02105	1399.729259	7127493
LCMS Features - Right RT [min]	34.04627201	32.61019488	14.58636863	21.87874245	0.428427777	242664565.4	6.048110485	69.59352475	7127493

Supplementary Table 4. Mass spectrometry statistics

EXPERIMENTAL MODEL AND SUBJECT DETAILS

Cell lines

Latent HIV-1 infected Jurkat cells (clone J-Lat 11.1 and clone J-Lat A2) were cultured in RPMI-1640 media supplemented with 7% FBS and 100 µg/ml penicillin-streptomycin at 37°C in a humidified 95% air, 5% CO_2 incubator. Primary CD4+ T cells were cultured in RPMI-1640 media supplemented with 7% FBS and 100 µg/ml penicillin-streptomycin at 37°C in a humidified 95%-air-5%CO2 incubator. HEK 293T cells were cultured in DMEM supplemented with 10% FBS and 100 µg/ml penicillin-streptomycin at 37 ºC in a humidified 95% air 5% CO2 incubator and used exclusively for the production of lentiviral shRNA vectors.

Establishment of J-lat 11.1 cells expressing the HA-V5-FLAG-dCas9 bait

In order to generate J-Lat 11.1 cells expressing the triple tagged (HA, V5, 3xFLAG) dCas9 construct, cells were then nucleofected with a modified version of the PX462 plasmid (AddGene) and selected for resistance to puromycin. pSpCas9n(BB)-2A-Puro (PX462) V2.0 was a gift from Feng Zhang (Addgene plasmid # 62987 ; http://n2t.net/addgene:62987 ; RRID:Addgene_62987). The original plasmid encodes for a Cas9 D10A nickase mutant, we modified the original sequence by introducing an H841A mutation that renders the Cas9 fully catalytically inactive (dCas9). Additionally, we introduced a triple FLAG epitope sequence (3xFLAG), a V5 epitope sequence and an HA epitope sequence at the N-terminal region of the dCas9. The plasmid contains a chicken β-actin promoter that drives the expression of the dCas9 bait and a U6 promoter that drives the expression of the gRNA scaffold. The sequence of the gRNA is 5'-GAAGCGCGCACGGCAAG-3' and is located between nucleotides 708 and 724 on the HIV-1 5' LTR, downstream the transcriptional start site (TSS) and in-between Nuc-1 and Nuc-2 (Figure 1A). Within the plasmid, the dCas9 open reading frame (ORF) sequence additionally contains an IRES sequence that is followed by a puromycin resistance cassette, allowing for puromycin selection of dCas9 expressing cells. The plasmid

sequence information is available upon request. 48 hours after nucleofection the cells were selected for a week with 1μg/ml puromycin and expanded in a polyclonal population. Unstimulated J-Lat 11.1 cells were used to model the latent, repressed, promoter while cells stimulated with 10 μm of phorbol 12 myristate 13-acetate (PMA) (Sigma), a potent PKC agonist, were used to model the transcriptionally active promoter.

Plasmids nucleofection

The expression plasmids for the HA-V5-FLAG-dCas9 bait and the dCas9-VPR were delivered to J-Lat 11.1 cells by nucleofection using Amaxa Nucleofector (Lonza) as previously described (Rafati et al., 2011) and the Cell Line Nucleofector Kit R (Lonza). Briefly, cells were split to 4×10^5 cells/ml one day before nucleofection, 8 million cells were centrifuged at 600rcf for 5 min at room temperature, resuspended in 100 μl of solution R, and nucleofected with 2 μgs of plasmid, using program O28 and the Cell line nucleofector Kit R. Nucleofected cells were then resuspended in 500 μl of pre-warmed, serum-free antibiotic-free RPMI at 37 °C for 15 min and then plated in 5 ml of pre-warmed complete media. Seventy-two hours post-nucleofection cells nucleofected with the dCas9 VPR plasmid were analyzed with flow cytometry while cells nucleofected with the dCas9 construct for purification (HA, V5, FLAG) were selected for 10 days in puromycin 0.5μg/ml and expanded as a polyclonal population.

Bacterial strains

DH5α and Stable3 bacterial cells were used to propagate the plasmids used in the study.

METHOD DETAILS

Western Blotting

$10x10^6$ cells were lysed with 100 μl cold lysis buffer containing 150 mM NaCl, 30 mM Tris (pH 7.5), 1 mM EDTA, 1% Triton X-100, 10% Glycerol, 0.5 mM DTT, protease inhibitor cocktail tablets (EDTA-free) (Roche) at 4°C per 30 minutes. Cell lysates were clarified by centrifugation (14,000 rpm for 30 min at 4°C), mixed with 4x sodium

dodecyl sulfate (SDS)-loading buffer with 0.1M DTT and boiled at 95°C per 5 min. Samples were run in a 10% SDS-polyacrylamide gel at 100V. The proteins were then transferred to polyvinylidene difluoride (PVDF) membranes (Immobilion) and the membranes probed with primary antibodies (anti-V5 epitope (Invitrogen), anti-HA epitope (Abcam), anti-FLAG epitope (Sigma) and anti-tubulin (Abcam) overnight at 4 °C. Secondary antibodies were used accordingly to the species reactivity and incubated for 1 hour at room temperature. Proteins were detected by chemical luminescence using the SuperSignal West Pico or SuperSignal West Pico Femto Chemiluminescent Substrate (Thermo Scientific).
For visualization of dCas9 protein enrichment during the ChIP-MS protocol, the protein complexes bound to the beads were decrosslinked and eluted and at 95°C for 30min in 4x sodium dodecyl sulfate (SDS)-loading buffer containing 0.1M DTT. The proteins were then resolved in a 10% polyacrylamide SDS-PAGE gel and western blotting was performed using a mouse anti-FLAG antibody, a secondary anti-mouse HRP antibody, and imaged as above.

Cytoplasmic and nuclear fractionation

Approximately $2x10^7$ J-lat 11.1 cells expressing the HA-V5-FLAG-dCas9 bait were subjected to cellular fractionation to separate the cytoplasmic and nuclear fraction. We adapted the cellular fractionation protocol described in (Ten Have et al., 2012) to cells in suspension. Briefly, the cells were collected by centrifugation at 800rcf for 5 minutes at 4C and washed twice with PBS. The cell pellet was then transferred and resuspended into a pre-chilled 7ml dounce homogenizer, where the cell membrane was broken using 10 strokes of a tight pestle. The dounced cells were then centrifuged for 5 minutes at 4C, 800rcf and the supernatant was retained as cytoplasmic fraction.
The nuclear pellets were then resuspended in 3ml of a solution (S1) containing 0.25M Sucrose and 10mM MgCl2 and layered over a 3ml cushion of a 0.35M Sucrose and 0.5mM MgCl2 solution (S2) by slowly pipetting S1 on top S2. The cell pellets were then centrifuged again for 10 minutes at 4C at 2500rcf and the remaining pellets retained as the nuclear fraction.

Chromatin immunoprecipitation and HIV-1 5'LTR purification using Catchet-MS:

In order to more specifically enrich for chromatin and reduce background from cellular contaminants and from the non-chromatin associated bait, we improved the stringency of our in-house ChIP protocol (Rafati et al., 2011) by incorporating a few steps from the Chromatin enrichment for proteomics (CheP) (Kustatscher et al., 2014) during the preparation of our input material. We have then followed a traditional ChIP protocol in which we have enriched for the dCas9 bait and its associated complexes using an Anti-V5 Agarose Affinity Gel (Sigma). To further eliminate the background originating from the purification of non-chromatin associated bait complexes we have additionally added a histone enrichment step, downstream of the bait enrichment step, using histone H2B (Abcam) and H3 antibodies (Abcam) conjugated to Protein G SepharoseTM 4 Fast flow (GE Healthcare) and Protein A SepharoseTM 4 Fast flow (GE Healthcare) beads by dimethyl pimelimidate cross-linking as described in (Chalkley and Verrijzer, 2004).

Chromatin input preparation using CheIP

Approximately 3 billion cells per condition were collected, cross-linked and processed in batches of 400million cells. After collection, by centrifugation at 800rcf for 5 minutes, each batch was washed two times in 40 ml PBS supplemented with 1mM MgCl2 and 1mM CaCl2, and cross-linked in 40 ml PBS with 1% formaldehyde (Formaldehyde methanol free 16%, Polysciences inc.) at room temperature for 30 min with vertical rotation at 15rpm. The reaction was then quenched with the addition of 1 M glycine to a final concentration of 125 mM. Cross-linked cells pellet were then washed in 20 ml cold buffer B (0.25% Triton x-100, 1mM EDTA, 0.5mM EGTA, 20mM HEPES pH 7.6) and 20 ml cold buffer C (0.15M NaCl, 1mM EDTA, 0.5mM EGTA, 20mM HEPES pH 7.6), resuspended in 2 ml ChIP incubation buffer (1% Triton x-100, 150mM NaCl, 1mM EDTA, ph 8.0, 0.5 mM EGTA, 20mM HEPES pH 7.6, protease inhibitor cocktail tablets (EDTA-free, Roche) and then transferred in 15ml polystyrene Falcon tubes compatible with sonication.

In order to isolate and expose the cross-linked nuclei to the subsequent denaturation steps the samples were sonicated with 15 ml probes at medium intensity for 10 minutes (30' ON/30' OFF intervals; Diogenode Bioruptor) and the cell nuclei were spun at 800rcf for 10 minutes. The pellets were then re-suspended in 2 ml ChIP incubation buffer containing 0.15% SDS and sonicated again for 10 minutes at medium intensity (30' ON/30' OFF intervals; Diogenode Bioruptor). The sonicated nuclei in suspension were then aliquoted (500µls per tube) in 2ml Eppendorf tubes and denatured for 5 minutes at room temperature with 350µls 10% SDS and 1.2 ml 8M Urea buffer (10mM Tris pH 7.4, 1mM EDTA and 8 M urea). The insoluble fraction of the nuclei, enriched for chromatin, was then precipitated by centrifugation at 16200rcf at room temperature for 20minutes. The precipitated pellets were then resuspended and combined (4 into 1) in a single 2ml Falcon tube and denatured again for 5 minutes at room temperature with 500µls of 4% SDS buffer (50mM Tris ph 7.4, 10 mM EDTA, 4% SDS) and 8M Urea buffer and then precipitated again by centrifugation at 16200rcf at room temperature for 20minutes.
The pellets were then resuspended and washed by centrifugation at 16200rcf at room temperature for 20minutes in 2ml 4% SDS buffer and then resuspended in 2.5 ml ChIP incubation buffer containing 1% SDS. The content of each tube was then transferred in a 15ml polystyrene tube and sonicated (3 tubes at the time) at a high intensity (30' ON/30' OFF intervals; Diogenode Bioruptor), using metal probes, to obtain chromatin fragments in a 200-500bp size range. The different chromatin batches were then pulled together concentrated through 100kDa Centricon filters, to buffer exchange with 0.1% SDS ChIP incubation buffer and remove smaller proteins and fragments. The sonicated chromatin (a total of 50 ml per condition) was then spun at max speed (20817 rcf) at 4°C for 30 minutes to remove cellular debris and diluted to 50 ml per condition. The chromatin was then precleared overnight at 4°C with vertical rotation at 15rpm (a total of 5 reactions per condition in 15ml tubes) with 500µls of a mix of Protein G and A Sepharose^{TM} 4 Fast flow (GE Healthcare) beads and then used for immunoprecipitation.

HA-V5-FLAG-dCas9 bait enrichment

Per each condition, dCas9 containing complexes were isolated from the sonicated chromatin using 500µls (a total of 5 reaction where 100µls of affinity beads were used to purify 10ml of chromatin) of Anti-V5 Agarose Affinity Gel (Sigma) and then washed two times per each buffer (5minutes, 15rpm vertical rotation washes) with buffer 1 (0.1% SDS, 0.1% DOC, 1% Triton x-100, 150mM NaCl, 1 mM EDTA pH 8.0, 0.5 mM EGTA, 20mM HEPES pH8.0.), buffer 2 (500mM NaCl: 0.1% SDS, 0.1% DOC, 1% Triton x-100, 500mM NaCl, 1 mM EDTA pH 8.0, 0.5mM EGTA, 20mM HEPES pH8.0), buffer 3 (0.25M LiCL, 0.5%DOC, 0.5% NP-40, 1mM EDTA pH 8.0, 0.5mM EGTA pH 8.0, 20mM HEPES pH 8.0), buffer 4 (1mM EDTA pH8.0, 0.5mM EGTA pH 8.0, 20mM HEPES pH 8.0) to remove unspecific binding and eluted in a total volume of 1 ml elution buffer 1% SDS, 0.1M NaHCO3 per each condition. At this stage a 50µl aliquot of the eluate was taken to be analyzed by qPCR as quality control for dCas9 enrichment over the chromatin input at the desired chromatin locus.

Locus enrichment

The eluate was then diluted 10 times in ChIP incubation buffer without SDS (1% Triton x-100, 150mM NaCl, 1mM EDTA, ph 8.0, 0.5 mM EGTA, 20mM HEPES pH 7.6, protease inhibitor cocktail tablets (EDTA-free) (Roche) and immunoprecipitated again in a single reaction with 100µls of a mix of Protein G and A SepharoseTM 4 Fast flow (GE Healthcare) pre-conjugated with histone H3 and histone H2B antibodies in order to specifically enrich for chromatin-associated dCas9 complexes and eliminate from the purification unspecific non-chromatin associated dCas9 complexes. The immunoprecipitated material, bound to the beads, was then washed again 2 times per each buffer with buffer 1, buffer 2, buffer 3 and buffer 4 to remove unspecific binding and the protein complexes bound to the beads were finally eluted and decrosslinked by boiling the sample for 30min in 100µls of 4x sodium dodecyl sulfate (SDS)-loading buffer, containing 0.1M DTT.

Mass spectrometry

Proteins were resolved in a 15% polyacrylamide SDS-PAGE gel, visualized by Colloidal Blue Staining Kit (ThermoFisher) and prepared for

nanoflow LC-MS/MS analysis. SDS-PAGE gel lanes were cut into 1-mm slices and protein were subjected to in-gel reduction with dithiothreitol, alkylation with iodoacetamide and digested with trypsin (TPCK Trypsin, ThermoScientific, Rockford, IL, USA), as described previously (Schwertman et al., 2012). Peptides were extracted from the gel blocks in 30 % acetonitrile (Biosolve) and 0.5 % formic acid (Biosolve) and dried in a SpeedVac Vacuum Concentrator (ThermoFisher). Samples were analyzed by LC-MS/MS on a 20 cm x 75 µm C18 column (BEH C18, 130 Å, 3.5 µm, Waters) after trapping on a nanoAcquity UPLC Symmetry C18 trapping column (Waters, 100 Å, 5 µm, 180 µm x 20 mm) on an EASY-nLC 1000 coupled to a Fusion Tribrid Orbitrap mass spectrometer (ThermoFisher Scientific), essentially as described in (Sap et al., 2017). Data analysis was performed with the Mascot software suite (Daemon version 2.3.2 and Distiller version 2.3.02, Matrix Science) within the Proteome Discoverer (version 2.2, ThermoFisher Scientific) framework. Spectra were searched against a Uniprot database (version April 2017, taxonomy Homo sapiens) concatenated with a fasta database containing amino acid sequences of the triple tagged dCas9 (HA, V5, 3xFLAG) construct. Protein Mascot scores and peptide numbers were taken directly from the Mascot output and reported. The same procedure was used to analyze input samples for the protocol characterization (Supplementary Figure 3). Heat maps were generated using MORPHEUS (http://software.broadintistute.org/morpheus/index.html).

Chromatin quality control

100µl aliquots of chromatin were taken per each batch of the purification protocol, resuspended in 500µls of ChIP elution buffer and, after addition of 24µl 5M NaCl (200mM final concentration), decrosslinked overnight at 65°C on a heat block. DNA isolation was then performed using phenol-chloroform isoamyl isolation method and ethanol precipitation in the presence of glycogen as a carrier. The DNA pellet was resuspended in 100µls of nuclease-free water. 5µls of DNA was then mixed with sample 4x sample buffer and run on a 1% agarose DNA electrophoreses gel to check for fragmentation between 200 and 500bps.

ChIP- qPCR

Real-time qPCR was used to detect the specific enrichment of the 5'-LTR locus at a DNA level after the ChIP procedure. Reactions of 10 µl were performed with the GoTaq qPCR Master Mix kit (Promega) in a CFX Connect Real-Time PCR thermocycler (Biorad) Relative quantitation was calculated with the 2-ΔCt method where relative enrichment over the adjusted DNA input was used for data representation.

To evaluate IKZF1, CBX8 and SUZ12 binding to the HIV-1 promoter and histone marks profile a smaller scale ChIP experiment (50 million cells) with identical preparation of the chromatin input as for the mass spectrometry experiment. For the immunoprecipitation, protein G-beads or A-beads were used in combination with the anti-IKZF1 antibody (Cell signal technology), anti-SUZ12 (abcam), anti CBX8 (homemade) and histone antibodies: Histone H3 (abcam), histone H3K27me3 (Millipore), H3K4me3 (Millipore), H3K9me3 (Abcam). DNA was PCI extracted and used to evaluate the enrichment of ChIP-Ikaros at the HIV-1 5'LTR by the same primer sets summarized in the key resources table. Antibodies used are summarized in the Key resource table.

ChIP-Sequencing data analysis

In order to align the short reads produced by the ChIP-Seq procedure and also capture reads mapped to the HIV genome, we constructed a custom version of the human genome (UCSC version hg38) where we attached the HIV genome as an additional chromosome. We used the HIV strain K03455.1 (https://www.ncbi.nlm.nih.gov/nuccore/K03455). Subsequently, the resulting genome was indexed and reads were aligned with bwa 0.7.17 (1) and the bwa mem algorithm. In order to compensate for differences in library sizes between ChIP and Input DNA sequencing samples, the total number of reads of each sample was equalized by uniformly downsampling reads relatively to the sample with the lower number of reads. ChIP peaks were then called with MACS2 (2) using default parameters. The peaks returned by MACS2 were further filtered by i) imposing an additional MACS FDR threshold of 0.1%, ii) excluding peaks demonstrating a fold enrichment less than 3 in log2 scale (where fold enrichment is the ratio of normalized reads under a peak area in the

ChIP sample to the respective number of normalized reads in the Input DNA sample). Finally, in order to visualize the ChIP-Seq signals, we constructed a custom UCSC track hub based on the combined hg38-HIV genomes using instructions and tools provided by UCSC (Li and Durbin, 2010; Zhang et al., 2008).

Production of shRNA lentiviral vectors

Lentiviral constructs containing the desired shRNA sequence were amplified from bacterial glycerol stocks obtained in house from the Erasmus Center for Biomics and part of the MISSION® shRNA library (sigma). Briefly, 5.0 x 10^6 HEK293T cells were plated in a 10 cm dish and transfected with 12,5 µg of plasmids mix. 4,5 µg of pCMVΔR8.9 (envelope), 2 µg of pCMV-VSV-G (packaging) and 6ug of shRNA vector were mixed in 500 µL serum-free DMEM and combined with 500 µL DMEM containing 125 µL of 10 mM polyethyleneimine (PEI, Sigma). The resulting 1 mL mixture was applied to HEK293T cells after 15 min incubation at room temperature. The transfection mix was removed after 12 hr and replaced with fresh RPMI medium. Virus-containing medium was harvested twice and replaced with fresh medium at 36 hours 48 hr, 60, 72 hr post-transfection. After each harvest, the collected medium was filtered through a cellulose acetate membrane (0.45 µm pore) and used directly for shRNA infections or stored at -80°C for subsequent use. Lentivaral vectors used in the study are summarized in the summarized the key resources table.

Flow Cytometry of J-lat 11.1

GFP expression in the J-Lat cell lines was analyzed by Flow Cytometry. The live-cell population was defined by using the forward scatter area versus side scatter area profiles (FSC-A, SSC-A). Single cells were then gated by using forward scatter height (FSC-H) versus forward scatter width (FSC-W) and side scatter height (SSC-H) versus side scatter width (SSC-W). GFP intensity to differentiate between GFP-positive and negative cells. Between 2 - 4x105 events were collected per sample on an LSR Fortessa (BD Biosciences) and analyzed using FlowJo software (version 9.7.4, Tree Star).

Fluorescence microscopy

Fluorescence microscopy and bright field pictures of J-Lat 11.1 cells in the absence and presence of PMA were acquired using an Olympus IX70 Fluorescence Phase Contrast inverted Microscope.

Total RNA Isolation and quantitative real-time PCR (RT-qPCR)

Total RNA was isolated from the cells using Trizol (Thermo Fisher) and the Total RNA Zol out kit (A&A Biotechnology) and residual genomic DNA digested with DNAseI (Life technologies). cDNA synthesis reactions were performed with Superscript II Reverse Transcriptase (Life Technologies) kit following with random priming and manufacturer's instructions. RT-qPCR reactions were conducted CFX Connect Real-Time PCR Detection System thermocycler (BioRad) using GoTaq qPCR Master Mix (Promega) following manufacturer protocol. Amplification was performed on the using following thermal program starting with 3 min at 95 °C, followed by 40 cycles of 95 °C for 10 s and 60 °C for 30 s. The specificity of the RT-qPCR products was assessed by melting curve analysis. Primers used for real-time PCR are listed in Table 1. Expression data was calculated using 2-ΔΔCt method by Livak Schmittgen (Schmittgen and Livak, 2008). Cyclophilin A (CyPA), GAPDH and β2 microglobulin (B2M) were used as housekeeping genes for the analysis.

Isolation and ex vivo infection of primary CD4+ T cells

Peripheral blood mononuclear cells (PBMCs) were isolated by Ficoll density gradient sedimentation of buffy coats from healthy donors (GE Healthcare). Total CD4+ T cells were separated by negative selection using EasySep Human CD4+ T Cell Enrichment Cocktail (StemCell Technologies). Primary CD4+ T cells were plated at a concentration of $1{,}5x10^{6}$ cells/mL left overnight for recovery. HIV-1 latency *ex vivo* model was generated by spinoculation according to Lassen and Greene method as described elsewhere (Lassen et al., 2012). Pseudotyped viral particles

were obtained from co-transfecting HEK 293T cells with HXB2 Env and pNL4.3.Luc.R-E- plasmids using PEI. Supernatants were collected at 48 and 72h post-transfection, filtered with a 0.45 µM filter and stored at -80^{o}C. Expression vectors HXB2 Env and pNL4.3.Luc.R-E- were donated by Dr. Nathaniel Landau and Drs. Kathleen Page and Dan Littman, respectively. Antiretroviral drugs Saquinavir Mesylate and Raltegravir were kindly provided by the Centre for AIDS reagents, NIBSC.

Flow cytometry for T cells activation and toxicity assay

Primary CD4+ T cells isolated from buffy coats of healthy volunteers were treated with 10uM of iberdomide, 500nM of JQ1, or both compounds, with PMA/ionomycin used as a positive control. The cells were examined by flow-cytometry at 24 and 48 hours, live cells were gated using forward scatter area versus side scatter area profiles (FSC-A, SSC-A). Cells were then stained for expression of Annexin V to examine the percentage of cells undergoing apoptosis and with the surface receptor CD69 to measure T cells activation. For Annexin V and CD69 staining, 10^6 cells were washed with PBS supplemented with 3% FBS and 2.5 mM CaCl2 followed by staining with Annexin V-PE (Becton and Dickinson), CD69-FITC (eBIOSCIENCE) for 20 minutes at 4C in the presence of 2.5 mM CaCl2. Cells were then washed with PBS/FBS/CaCl2 and analyzed by flow cytometry. Between 2 - 4x10^5 events were collected per sample within 3 hours after staining on an LSRFortessa (BD Biosciences, 4 lasers, 18 parameters) and analyzed using FlowJo software (version 9.7.4, Tree Star).

T cell proliferation and functionality assay

To analyze the effect of the LRA on CD8+ and CD4+ T cells, proliferation and cytokine expression were analyzed by flow cytometry. Primary CD8+ and CD4+ T cells were isolated from buffy coats form healthy donors by Ficoll gradient (GE Healthcare) followed by negative selection with RosetteSep Human CD8+ T Cell Enrichment Cocktail or RosetteSep Human CD4+ T Cell Enrichment Cocktail (StemCell Technologies) respectively. Isolated cells were left overnight for recovery. To analyze T cell proliferation capacity, 1 million CD8+ or CD4+ T cells were stained

with 0,07 uM CellTrace Far Red Cell Proliferation dye (ThermoFisher Scientific) following manufacturer's instructions. Cells were then cultivated for 72 hours with either unstimulated or stimulated conditions in the presence of the LRA, and analyzed by flow cytometry. Stimulation of T cells was performed using Anti-CD3/CD28 coated Dynabeads (ThermoFisher Scientific) following manufacturer's protocol. Proliferation capacity was determined by a decrease in proliferation dye intensity in daughter cells upon cell division. To analyze T cell functionality by means of cytokine expression 1 million CD8+ or CD4+ T cells were left untreated or treated with the LRA for 18 hours. Cells were then left unstimulated or stimulated with 50 ng/mL PMA and 1uM Ionomycin for 7 hours in the presence of a protein transport inhibitor (BD GolgiPlug^{TM}, BD Biosciences). To stain for intracellular cytokines cells were washed with PBS supplemented with 3% FBS followed by a fixation and permeabilization step with FIX & PERM Kit (Invitrogen) following manufacturer's protocol and incubated with 1:25 BV510 anti-IL2 (563265, BD Biosciences) and PE-Cy7 anti-IFNg (27-7319-41, eBioscience) in permeabilization buffer for 45 minutes at 4C. Stained cells were washed with PBS supplemented with 3% FBS and analyzed by flow cytometry.

HIV-1 latency reversal in primary CD4+ T cells isolated from aviremic patients

Primary CD4+ T cells from 5 aviremic patients (maintained viremia below 50 copies/mL for at least two years) were isolated as described previously (Stoszko et al., 2016). Two million CD4+ T cells were plated at the cell density of 10^6/ml and treated as indicated. After 16 hours cells were lysed in TRI reagent and RNA was isolated with Total RNA Zol-out kit (A&A Biotechnology), cDNA synthesis was performed as described above. Absolute quantification of cell-associated HIV-1 gag RNA was performed in a nested PCR as described previously (Pasternak et al., 2008). Briefly, first round of amplification was performed in a final volume of 25 µl using 4 µl of cDNA, 2.5 µl of 10× PCR buffer (Life Technologies), 1 µl of 50mM MgCl2 (Life Technologies), 1 µl of 10 mM dNTPs (Life Technologies), 0.075 µl of 100 µM Gag Forward primer, 0.075 of 100 µM SK437 Reverse

primer, and 0.2 µl Platinum Taq polymerase (Life Technologies). The second round of amplification was performed in a final volume of 25 µl using 2 µl of pre-amplified cDNA, 2.5 µl of 10× PCR buffer (Life Technologies), 1 µl of 50mM MgCl2 (Life Technologies), 1 µl of 10 mM dNTPs (Life Technologies), 0.05 µl of 100 µM Gag Forward primer, 0.05 µl of 100 µM Gag Reverse primer, 0.075 µl of 50 µM Gag Probe and 0.2 µl Platinum Taq polymerase. The absolute number of gag copies in the PCR was calculated using a standard curve ranging from 8 to 512 copies of a plasmid containing the full-length HIV-1 genome (pNL4.3.Luc.R-E-). The amount of HIV-1 cellular associated RNA was expressed as number of copies/µg of input RNA in reverse transcription.

The study was conducted according to the ethical principles of the Declaration of Helsinki. All patients involved in the study gave their written informed consent. The study protocol and any amendment were approved by The Netherlands Medical Ethics Committee (MEC-2012-583).

STATISTICAL ANALYSIS

Statistical analysis was conducted as indicated in the figure legends using Prism version 8.3.0 (GraphPad software).

KEY RESOURCES TABLE

Reagent	Source	Identifier
Antibodies		
Cas9 antibody (mAb)	Active Motif	61577
Monoclonal ANTI-FLAG_ M2 antibody produced in mouse	Sigma	F3165-.2MG
Mouse monoclonal V5 Tag	Invitrogen	46-0705
HA tag antibody	Abcam	ab18181
Anti-Flag M2 affinity gel	Sigma	A-2220

Anti-V5 Agarose Affinity Gel antibody produced in mouse	Sigma	A7345-1ml
Anti-Tubulin antibody [YL1/2]	Abcam	ab6160
Anti-HA Agarose	Pierce	26181
Ikaros (D10E5) Rabbit mAb	Cell Signaling Techn	#CST081119Q
Anti-Ikaros antibody - N-terminal	Abcam	ab229275
anti mouse HRP antibody	Promega	W4021
anti Rabbit HRP antibody	Sigma	A0545
Anti-Histone H2B antibody - ChIP Grade	Abcam	ab1790
Histone H3 antibody - ChIP Grade	Abcam	ab1791-100
Anti-timethyl-Histone H3 (Lys4) Antibody	Millipore	07-030
Anti-Histone H3 (tri methyl K9) antibody - ChIP Grade	Abcam	ab8898
Anti-trimethyl-Histone H3 (Lys27) Antibody	Millipore	07-449
Antibody: donkey anti goat IgG HRP	Promega	V8051
Annexin V-PE	Becton and Dickinson	559763
CD69-FITC	eBIOSCIENCE	11-0699-42
Chemicals, peptides and recombinant proteins		
anhydrous DMSO	Sigma	276855-100ml
Iberdomide	MedChemExpress	HY-101291
JQ1	Cayman Chemical	11187-1
Phorbol 12 myristate 13 acetate (PMA)	Sigma	P8139
Random Primers	Invitrogen	48190-011
DNaseI amplification grade	Invitrogen	18068-015
Superscript II Reverse Transcriptase	Invitrogen	18064-014
Oligo(dT)12-18 Primer	Invitrogen	18418-012
100 mM dNTP Set	Invitrogen	10297-018
Formaldehyde methanol free 16%	Polyscience Inc.	18814

Gliotoxin	ApexBio	A4443
Commercial Assays		
GoTaq qPCR Mastermix	Promega	A6002
Platinum Taq DNA Polymerase	Invitrogen	10966-050
Easy sep human CD4 T-cell enrichment kit	Stem Cell Technologies	19052
Ficoll Paque Plus	GE Healthcare	17-1440-02
Total RNA Zol-Out	A en A	030-100
GenElute plasmid Mini prep kit	Sigma	PLN350
Plasmid Midi AX	A en A	A en A
Pure Link Maxiprep kit	Invitrogen	K210017
Nano-Glo® Luciferase Assay System	Promega	N1120
Supersignal West Pico	Thermo Scientific	345788
Supersignal West Femto	Thermo Scientific	34095
Colloidal Blue Staining Kit	Thermo Scientific	LC6025
Cell Line Nucleofector Kit R	Lonza	VVCA-1001
Deposited Data		
Mass spectrometry	this paper	(link)
Western blot original scans	this paper	(link)
Experimental models: cell lines		
J-Lat A2	(Jordan et al., 2003)	NIH AIDS Reagent Program
J-Lat 11.1	(Jordan et al., 2003)	NIH AIDS Reagent Program
HeK 293T	ATCC	CRL-3216
Experimental Models: Organisms/Strains		
DH5a	Thermo	18265017
Recombinant DNA		
sh IKZF1 #1	Sigma	TRCN0000107874
sh IKZF1 #2	Sigma	TRCN0000107871
sh CDC73	Sigma	TRCN0000008728
sh Control	Sigma	SHC002

sh CTR9	Sigma	TRCN0000008739
sh DKC1	Sigma	TRCN0000352996
sh NFRKB	Sigma	TRCN0000014868
sh HP1BP3	Sigma	TRCN0000180320
sh CHD1	Sigma	TRCN0000021309
sh DDX3Y	Sigma	TRCN0000000020
sh EED	Sigma	TRCN0000021204
sh SIN3A	Sigma	TRCN0000021774
sh SUZ12	Sigma	TRCN0000038724
UBE2I	Sigma	TRCN0000007205
FAM19A2	Sigma	TRCN0000138849
CBX8	Sigma	TRCN0000363282
HMG20A	Sigma	TRCN0000015578
UCHL5	Sigma	TRCN0000234906
RNGTT	Sigma	TRCN0000284836
PRPF6	Sigma	TRCN0000293597
PNN	Sigma	TRCN0000072278
DDX39	Sigma	TRCN0000050668
Lentiviral packaging construct pCMVDR8.91	(Naldini et., 1996)	N/A
VSV-G glycoprotein-expressing vector	(Naldini et., 1996)	N/A
Plasmid: SpCas9n-2A-Puro V2.0	(Ran et al., 2013)	62987
Oligonucleotides		
PCR primers	Integrated DNA Technologies IDT	
Softwares and Algorithms		
Prism version 8.3.0	GraphPad	https://www.graphpad.com/scientific-software/prism/
Morpheus heatmapper	Broad institute	https://software.broadinstitute.org/morpheus/
Proteome Discoverer	ThermoFisher Scientific	https://www.thermofisher.com/order/catalog/product/OPTON-30812
Mascot Daemon	Matrix Science	http://www.matrixscience.com/daemon_install.html

Table of Oligonucleotides

Primer	Application	Forward (5' to 3')	Reverse (5' to 3')
Nuc-0	ChIP-qPCR	CCACACACAAGGCTACTTCC	AACTGGTACTAGCTTGTAGCAC
HS1	ChIP-qPCR	TGTGAGCCTGCATGGGATGG	GAAAGTCCCCAGCGGAAAGT
HS1/Nuc1	ChIP-qPCR	AGTGGCGAGCCCTCAGATG	AGCTTTATTGAGGCTTAAGC
Nuc1/HS2	ChIP-qPCR	CGTCTGTTGTGTGACTCTGGT	TCGAGAGAGCTCCTCTGGTT
Nuc1	ChIP-qPCR	TCTCTGGCTAACTAGGGAACC	AAAGGGTCTGAGGGATCTCTAG
HS2/Nuc2	ChIP-qPCR	GCCCGAACAGGGACTTGAAA	TTGGCGTACTCACCAGTCG
Nuc2/Gag	ChIP-qPCR	GGTGCGAGAGCGTCAGTAT	AGCTCCCTGCTTGCCCATA
HIV-1 genome (Vif)	ChIP-qPCR	GGTCTGCATACAGGAGAAAGAG	TTAGTTGGTCTGCTAGGTCAGG
Cyclophilin A (PPIA)	RT-qPCR	TCATCTGCACTGCCAAGACTG	CATGCCTTCTTTCACTTTGCC
GAPDH	RT-qPCR	CAAGAAGGTGGTGAAGCAG	GCCAAATTCGTTGTCATACC
β2-microglobulin	RT-qPCR	ATGAGTATGCCTGCCGTGTG	CCAAATGCGGCATCTTCAAAC
HIV-1 Pol	RT-qPCR	GGTTTATTACAGGGACAGCAGAGA	ACCTGCCATCTGTTTTCCATA
HIV-1 Tat	RT-qPCR	CAAAAGCCTTAGGCATCTCCT	CCACCTTCTTCTTCGATTCCT
GFP	RT-qPCR	GAAGCAGCACGACTTCTTCAA	GCTTGTCGGCCATGATATAGA
IKZF1	RT-qPCR	GGGTCAAGACATGTCCCAAGT	ACATTACTGGCCACGACTCTG
CDC73	RT-qPCR	GTTTATGTCCGACGTGCAGC	TACTTGCCGATGTTGACGCT
DKC1	RT-qPCR	CACTTACCCTCGGAAGTGGG	TTTTGGCAGACTCACTGTAGTCAA
SUZ12	RT-qPCR	GCCTTTGAGAAGCCAACACAG	AGCTGCAAATGAGCTGACAAG
UBE2I	RT-qPCR	GAAAGGGACTCCGTGGGAAG	GCTTGAGCTGGGTCTTGGAT
PNN	RT-qPCR	AAGAGCGCACACGTAGAGAC	CCAAAAGCCGCAGTTCTGTC
HP1BP3	RT-qPCR	GCCGCCGCCATTACG	ATCTTCTACCTTCTCACCTAACTTG
DDX39A	RT-qPCR	CGGCGGAAAACCGAAGTTGG	GCTGTGGATGGAAACGTAGGA
HMG20A	RT-qPCR	AGCTACACATCACTTGACACCA	ATCTGCAAAAAGGGGCGGTA
IKZF2	RT-qPCR	TTCCTTCCTCCTCCCCTTGA	TGAAAGCTCATTGTCACACGTT
IKZF5	RT-qPCR	GAAGCAGAGGCTCTTCAGGG	TGAGGTTTTTCACCTGTGTGG
p21	RT-qPCR	AGCAGAGGAAGACCATGTGGAC	TTTCGACCCTGAGAGTCTCCAG
c-Myc	RT-qPCR	TCTCCACACATCAGCACAACTACGC	CGCCTCTTGACATTCTCCTCGGTG
Gag1 Fw/ SK437 Rv	Nested PCR	TCAGCCCAGAAGTAATACCCATGT	TGCTATGTCAGTTCCCCTTGGTTCTCT
Gag1 Fw/ Gag2 Rv	Nested PCR	TCAGCCCAGAAGTAATACCCATGT	CACTGTGTTTAGCATGGTGTTT
Gag Taqman probe	[6FAM]ATTATCAGAAGGAGCCACCCCACAAGA[BHQ1]		
U6 promoter	Sequencing,	ACTATCATATGCTTACCGTAAC	

REFERENCES

Battivelli, E., Dahabieh, M.S., Abdel-Mohsen, M., Svensson, J.P., Tojal Da Silva, I., Cohn, L.B., Gramatica, A., Deeks, S., Greene, W.C., Pillai, S.K., et al. (2018). Distinct chromatin functional states correlate with HIV latency reactivation in infected primary CD4(+) T cells. Elife 7.

Bjorklund, C.C., Kang, J., Amatangelo, M., Polonskaia, A., Katz, M., Chiu, H., Couto, S., Wang, M., Ren, Y., Ortiz, M., et al. (2020). Iberdomide (CC-220) is a potent cereblon E3 ligase modulator with antitumor and immunostimulatory activities in lenalidomide- and pomalidomide-resistant multiple myeloma cells with dysregulated CRBN. Leukemia 34, 1197-1201.

Bottardi, S., Mavoungou, L., and Milot, E. (2015). IKAROS: a multifunctional regulator of the polymerase II transcription cycle. Trends Genet 31, 500-508.

Boutboul, D., Kuehn, H.S., Van de Wyngaert, Z., Niemela, J.E., Callebaut, I., Stoddard, J., Lenoir, C., Barlogis, V., Farnarier, C., Vely, F., et al. (2018). Dominant-negative IKZF1 mutations cause a T, B, and myeloid cell combined immunodeficiency. J Clin Invest 128, 3071-3087.

Bracken, A.P., Dietrich, N., Pasini, D., Hansen, K.H., and Helin, K. (2006). Genome-wide mapping of Polycomb target genes unravels their roles in cell fate transitions. Genes Dev 20, 1123-1136.

Byrum, S.D., Raman, A., Taverna, S.D., and Tackett, A.J. (2012). ChAP-MS: a method for identification of proteins and histone posttranslational modifications at a single genomic locus. Cell Rep 2, 198-205.

Chalkley, G.E., and Verrijzer, C.P. (2004). Immuno-depletion and purification strategies to study chromatin-remodeling factors in vitro. Methods Enzymol 377, 421-442.

Chen, B., Gilbert, L.A., Cimini, B.A., Schnitzbauer, J., Zhang, W., Li, G.W., Park, J., Blackburn, E.H., Weissman, J.S., Qi, L.S., et al. (2013). Dynamic imaging of genomic loci in living human cells by an optimized CRISPR/Cas system. Cell 155, 1479-1491.

Chun, T.W., Justement, J.S., Lempicki, R.A., Yang, J., Dennis, G., Jr., Hallahan, C.W., Sanford, C., Pandya, P., Liu, S., McLaughlin, M., et al. (2003). Gene expression and viral prodution in latently infected, resting CD4+ T cells in viremic versus aviremic HIV-infected individuals. Proc Natl Acad Sci U S A 100, 1908-1913.

Cismasiu, V.B., Paskaleva, E., Suman Daya, S., Canki, M., Duus, K., and Avram, D. (2008). BCL11B is a general transcriptional repressor of the HIV-1 long terminal repeat in T lymphocytes through recruitment of the NuRD complex. Virology 380, 173-181.

Coull, J.J., Romerio, F., Sun, J.M., Volker, J.L., Galvin, K.M., Davie, J.R., Shi, Y., Hansen, U., and Margolis, D.M. (2000). The human factors YY1 and LSF repress the human immunodeficiency virus type 1 long terminal repeat via recruitment of histone deacetylase 1. J Virol 74, 6790-6799.

Davis, K.L. (2011). Ikaros: master of hematopoiesis, agent of leukemia. Ther Adv Hematol 2, 359-368.

Dejardin, J., and Kingston, R.E. (2009). Purification of proteins associated with specific genomic Loci. Cell 136, 175-186.

Diaz, T., Rodriguez, V., Lozano, E., Mena, M.P., Calderon, M., Rosinol, L., Martinez, A., Tovar, N., Perez-Galan, P., Blade, J., et al. (2017). The BET bromodomain inhibitor CPI203 improves lenalidomide and dexamethasone activity in in vitro and in vivo models of multiple myeloma by blockade of Ikaros and MYC signaling. Haematologica 102, 1776-1784.

Dieudonne, M., Maiuri, P., Biancotto, C., Knezevich, A., Kula, A., Lusic, M., and Marcello, A. (2009). Transcriptional competence of the integrated HIV-1 provirus at the nuclear periphery. EMBO J 28, 2231-2243.

Fecteau, J.F., Corral, L.G., Ghia, E.M., Gaidarova, S., Futalan, D., Bharati, I.S., Cathers, B., Schwaederle, M., Cui, B., Lopez-Girona, A., et al. (2014). Lenalidomide inhibits the proliferation of CLL cells via a cereblon/p21(WAF1/Cip1)-dependent mechanism independent of functional p53. Blood 124, 1637-1644.

Fuchs, O. (2019). Treatment of Lymphoid and Myeloid Malignancies by Immunomodulatory Drugs. Cardiovasc Hematol Disord Drug Targets 19, 51-78.

Gandhi, A.K., Kang, J., Havens, C.G., Conklin, T., Ning, Y., Wu, L., Ito, T., Ando, H., Waldman, M.F., Thakurta, A., et al. (2014). Immunomodulatory agents lenalidomide and pomalidomide co-stimulate T cells by inducing degradation of T cell repressors Ikaros and Aiolos via modulation of the E3 ubiquitin ligase complex CRL4(CRBN.). Br J Haematol 164, 811-821.

Gauchier, M., van Mierlo, G., Vermeulen, M., and Dejardin, J. (2020). Purification and enrichment of specific chromatin loci. Nat Methods 17, 380-389.

Geimer Le Lay, A.S., Oravecz, A., Mastio, J., Jung, C., Marchal, P., Ebel, C., Dembele, D., Jost, B., Le Gras, S., Thibault, C., et al. (2014). The tumor suppressor Ikaros shapes the repertoire of notch target genes in T cells. Sci Signal 7, ra28.

Georgopoulos, K. (2017). The making of a lymphocyte: the choice among disparate cell fates and the IKAROS enigma. Genes Dev 31, 439-450.

Goffin, V., Demonte, D., Vanhulle, C., de Walque, S., de Launoit, Y., Burny, A., Collette, Y., and Van Lint, C. (2005). Transcription factor binding sites in the pol gene intragenic regulatory region of HIV-1 are important for virus infectivity. Nucleic Acids Res 33, 4285-4310.

Grau-Exposito, J., Luque-Ballesteros, L., Navarro, J., Curran, A., Burgos, J., Ribera, E., Torrella, A., Planas, B., Badia, R., Martin-Castillo, M., et al. (2019). Latency reversal agents affect differently the latent reservoir present in distinct CD4+ T subpopulations. PLoS Pathog 15, e1007991.

Grau-Exposito, J., Serra-Peinado, C., Miguel, L., Navarro, J., Curran, A., Burgos, J., Ocana, I., Ribera, E., Torrella, A., Planas, B., et al. (2017). A Novel Single-Cell FISH-Flow Assay Identifies Effector Memory CD4(+) T cells as a Major Niche for HIV-1 Transcription in HIV-Infected Patients. mBio 8.

Hamperl, S., Brown, C.R., Perez-Fernandez, J., Huber, K., Wittner, M., Babl, V., Stockl, U., Boeger, H., Tschochner, H., Milkereit, P., et al. (2014). Purification of specific chromatin domains from single-copy gene loci in Saccharomyces cerevisiae. Methods Mol Biol 1094, 329-341.

Harr, J.C., Luperchio, T.R., Wong, X., Cohen, E., Wheelan, S.J., and Reddy, K.L. (2015). Directed targeting of chromatin to the nuclear lamina is mediated by chromatin state and A-type lamins. J Cell Biol 208, 33-52.

Huang, H., Santoso, N., Power, D., Simpson, S., Dieringer, M., Miao, H., Gurova, K., Giam, C.Z., Elledge, S.J., and Zhu, J. (2015). FACT Proteins, SUPT16H and SSRP1, Are Transcriptional Suppressors of HIV-1 and HTLV-1 That Facilitate Viral Latency. J Biol Chem 290, 27297-27310.

Ide, S., and Dejardin, J. (2015). End-targeting proteomics of isolated chromatin segments of a mammalian ribosomal RNA gene promoter. Nat Commun 6, 6674.

Jordan, A., Bisgrove, D., and Verdin, E. (2003). HIV reproducibly establishes a latent infection after acute infection of T cells in vitro. EMBO J 22, 1868-1877.

Karn, J., and Stoltzfus, C.M. (2012). Transcriptional and posttranscriptional regulation of HIV-1 gene expression. Cold Spring Harb Perspect Med 2, a006916.
Khan, S., Iqbal, M., Tariq, M., Baig, S.M., and Abbas, W. (2018). Epigenetic regulation of HIV-1 latency: focus on polycomb group (PcG) proteins. Clin Epigenetics 10, 14.
Kim, Y., Anderson, J.L., and Lewin, S.R. (2018). Getting the "Kill" into "Shock and Kill": Strategies to Eliminate Latent HIV. Cell Host Microbe 23, 14-26.
Kronke, J., Udeshi, N.D., Narla, A., Grauman, P., Hurst, S.N., McConkey, M., Svinkina, T., Heckl, D., Comer, E., Li, X., et al. (2014). Lenalidomide causes selective degradation of IKZF1 and IKZF3 in multiple myeloma cells. Science 343, 301-305.
Kustatscher, G., Wills, K.L., Furlan, C., and Rappsilber, J. (2014). Chromatin enrichment for proteomics. Nat Protoc 9, 2090-2099.
Lassen, K.G., Hebbeler, A.M., Bhattacharyya, D., Lobritz, M.A., and Greene, W.C. (2012). A flexible model of HIV-1 latency permitting evaluation of many primary CD4 T-cell reservoirs. PLoS One 7, e30176.
Lassen, K.G., Ramyar, K.X., Bailey, J.R., Zhou, Y., and Siliciano, R.F. (2006). Nuclear retention of multiply spliced HIV-1 RNA in resting CD4+ T cells. PLoS Pathog 2, e68.
Li, H., and Durbin, R. (2010). Fast and accurate long-read alignment with Burrows-Wheeler transform. Bioinformatics 26, 589-595.
Li, Z., Perez-Casellas, L.A., Savic, A., Song, C., and Dovat, S. (2011). Ikaros isoforms: The saga continues. World J Biol Chem 2, 140-145.
Liu, X., Zhang, Y., Chen, Y., Li, M., Zhou, F., Li, K., Cao, H., Ni, M., Liu, Y., Gu, Z., et al. (2017). In Situ Capture of Chromatin Interactions by Biotinylated dCas9. Cell 170, 1028-1043 e1019.
Lu, G., Middleton, R.E., Sun, H., Naniong, M., Ott, C.J., Mitsiades, C.S., Wong, K.K., Bradner, J.E., and Kaelin, W.G., Jr. (2014). The myeloma drug lenalidomide promotes the cereblon-dependent destruction of Ikaros proteins. Science 343, 305-309.
Lusic, M., and Giacca, M. (2015). Regulation of HIV-1 latency by chromatin structure and nuclear architecture. J Mol Biol 427, 688-694.
Ma, H., Tu, L.C., Naseri, A., Huisman, M., Zhang, S., Grunwald, D., and Pederson, T. (2016). CRISPR-Cas9 nuclear dynamics and target recognition in living cells. J Cell Biol 214, 529-537.
Malik, B., and Hemenway, C.S. (2013). CBX8, a component of the Polycomb PRC1 complex, modulates DOT1L-mediated gene expression through AF9/MLLT3. FEBS Lett 587, 3038-3044.
Marke, R., van Leeuwen, F.N., and Scheijen, B. (2018). The many faces of IKZF1 in B-cell precursor acute lymphoblastic leukemia. Haematologica 103, 565-574.
Moros, A., Rodriguez, V., Saborit-Villarroya, I., Montraveta, A., Balsas, P., Sandy, P., Martinez, A., Wiestner, A., Normant, E., Campo, E., et al. (2014). Synergistic antitumor activity of lenalidomide with the BET bromodomain inhibitor CPI203 in bortezomib-resistant mantle cell lymphoma. Leukemia 28, 2049-2059.
Mousseau, G., and Valente, S.T. (2017). Role of Host Factors on the Regulation of Tat-Mediated HIV-1 Transcription. Curr Pharm Des 23, 4079-4090.
Mullighan, C.G., Su, X., Zhang, J., Radtke, I., Phillips, L.A., Miller, C.B., Ma, J., Liu, W., Cheng, C., Schulman, B.A., et al. (2009). Deletion of IKZF1 and prognosis in acute lymphoblastic leukemia. N Engl J Med 360, 470-480.

Myers, S.A., Wright, J., Peckner, R., Kalish, B.T., Zhang, F., and Carr, S.A. (2018). Discovery of proteins associated with a predefined genomic locus via dCas9-APEX-mediated proximity labeling. Nat Methods 15, 437-439.

Ne, E., Palstra, R.J., and Mahmoudi, T. (2018). Transcription: Insights From the HIV-1 Promoter. Int Rev Cell Mol Biol 335, 191-243.

Ng, S.Y., Yoshida, T., Zhang, J., and Georgopoulos, K. (2009). Genome-wide lineage-specific transcriptional networks underscore Ikaros-dependent lymphoid priming in hematopoietic stem cells. Immunity 30, 493-507.

Nguyen, K., Das, B., Dobrowolski, C., and Karn, J. (2017). Multiple Histone Lysine Methyltransferases Are Required for the Establishment and Maintenance of HIV-1 Latency. mBio 8.

Oravecz, A., Apostolov, A., Polak, K., Jost, B., Le Gras, S., Chan, S., and Kastner, P. (2015). Ikaros mediates gene silencing in T cells through Polycomb repressive complex 2. Nat Commun 6, 8823.

Ott, M., Geyer, M., and Zhou, Q. (2011). The control of HIV transcription: keeping RNA polymerase II on track. Cell Host Microbe 10, 426-435.

Palstra, R.J., de Crignis, E., Roling, M.D., van Staveren, T., Kan, T.W., van Ijcken, W., Mueller, Y.M., Katsikis, P.D., and Mahmoudi, T. (2018). Allele-specific long-distance regulation dictates IL-32 isoform switching and mediates susceptibility to HIV-1. Sci Adv 4, e1701729.

Pasternak, A.O., Adema, K.W., Bakker, M., Jurriaans, S., Berkhout, B., Cornelissen, M., and Lukashov, V.V. (2008). Highly sensitive methods based on seminested real-time reverse transcription-PCR for quantitation of human immunodeficiency virus type 1 unspliced and multiply spliced RNA and proviral DNA. J Clin Microbiol 46, 2206-2211.

Pereira, L.A., Bentley, K., Peeters, A., Churchill, M.J., and Deacon, N.J. (2000). A compilation of cellular transcription factor interactions with the HIV-1 LTR promoter. Nucleic Acids Res 28, 663-668.

Pourfarzad, F., Aghajanirefah, A., de Boer, E., Ten Have, S., Bryn van Dijk, T., Kheradmandkia, S., Stadhouders, R., Thongjuea, S., Soler, E., Gillemans, N., et al. (2013). Locus-specific proteomics by TChP: targeted chromatin purification. Cell Rep 4, 589-600.

Powell, M.D., Read, K.A., Sreekumar, B.K., and Oestreich, K.J. (2019). Ikaros Zinc Finger Transcription Factors: Regulators of Cytokine Signaling Pathways and CD4(+) T Helper Cell Differentiation. Front Immunol 10, 1299.

Rafati, H., Parra, M., Hakre, S., Moshkin, Y., Verdin, E., and Mahmoudi, T. (2011). Repressive LTR nucleosome positioning by the BAF complex is required for HIV latency. PLoS Biol 9, e1001206.

Rathore, A., Iketani, S., Wang, P., Jia, M., Sahi, V., and Ho, D.D. (2020). CRISPR-based gene knockout screens reveal deubiquitinases involved in HIV-1 latency in two Jurkat cell models. Sci Rep 10, 5350.

Rojas-Araya, B., Ohlmann, T., and Soto-Rifo, R. (2015). Translational Control of the HIV Unspliced Genomic RNA. Viruses 7, 4326-4351.

Roux, K.J., Kim, D.I., Raida, M., and Burke, B. (2012). A promiscuous biotin ligase fusion protein identifies proximal and interacting proteins in mammalian cells. J Cell Biol 196, 801-810.

Sap, K.A., Bezstarosti, K., Dekkers, D.H.W., Voets, O., and Demmers, J.A.A. (2017). Quantitative Proteomics Reveals Extensive Changes in the Ubiquitinome after Perturbation of the Proteasome by Targeted dsRNA-Mediated Subunit Knockdown in Drosophila. J Proteome Res 16, 2848-2862.

Schafer, P.H., Ye, Y., Wu, L., Kosek, J., Ringheim, G., Yang, Z., Liu, L., Thomas, M., Palmisano, M., and Chopra, R. (2018). Cereblon modulator iberdomide induces degradation of the transcription factors Ikaros and Aiolos: immunomodulation in healthy volunteers and relevance to systemic lupus erythematosus. Ann Rheum Dis 77, 1516-1523.

Schmidtmann, E., Anton, T., Rombaut, P., Herzog, F., and Leonhardt, H. (2016). Determination of local chromatin composition by CasID. Nucleus 7, 476-484.

Schmittgen, T.D., and Livak, K.J. (2008). Analyzing real-time PCR data by the comparative C(T) method. Nat Protoc 3, 1101-1108.

Schwertman, P., Lagarou, A., Dekkers, D.H., Raams, A., van der Hoek, A.C., Laffeber, C., Hoeijmakers, J.H., Demmers, J.A., Fousteri, M., Vermeulen, W., et al. (2012). UV-sensitive syndrome protein UVSSA recruits USP7 to regulate transcription-coupled repair. Nat Genet 44, 598-602.

Schwickert, T.A., Tagoh, H., Gultekin, S., Dakic, A., Axelsson, E., Minnich, M., Ebert, A., Werner, B., Roth, M., Cimmino, L., et al. (2014). Stage-specific control of early B cell development by the transcription factor Ikaros. Nat Immunol 15, 283-293.

Siliciano, J.D., Kajdas, J., Finzi, D., Quinn, T.C., Chadwick, K., Margolick, J.B., Kovacs, C., Gange, S.J., and Siliciano, R.F. (2003). Long-term follow-up studies confirm the stability of the latent reservoir for HIV-1 in resting CD4+ T cells. Nat Med 9, 727-728.

Siliciano, J.M., and Siliciano, R.F. (2015). The Remarkable Stability of the Latent Reservoir for HIV-1 in Resting Memory CD4+ T Cells. J Infect Dis 212, 1345-1347.

Song, C., Pan, X., Ge, Z., Gowda, C., Ding, Y., Li, H., Li, Z., Yochum, G., Muschen, M., Li, Q., et al. (2016). Epigenetic regulation of gene expression by Ikaros, HDAC1 and Casein Kinase II in leukemia. Leukemia 30, 1436-1440.

Stoszko, M., De Crignis, E., Rokx, C., Khalid, M.M., Lungu, C., Palstra, R.J., Kan, T.W., Boucher, C., Verbon, A., Dykhuizen, E.C., et al. (2016). Small Molecule Inhibitors of BAF; A Promising Family of Compounds in HIV-1 Latency Reversal. EBioMedicine 3, 108-121.

Stoszko, M., Ne, E., Abner, E., and Mahmoudi, T. (2019). A broad drug arsenal to attack a strenuous latent HIV reservoir. Curr Opin Virol 38, 37-53.

Sun, L., Liu, A., and Georgopoulos, K. (1996). Zinc finger-mediated protein interactions modulate Ikaros activity, a molecular control of lymphocyte development. EMBO J 15, 5358-5369.

Tsui, C., Inouye, C., Levy, M., Lu, A., Florens, L., Washburn, M.P., and Tjian, R. (2018). dCas9-targeted locus-specific protein isolation method identifies histone gene regulators. Proc Natl Acad Sci U S A 115, E2734-E2741.

Turner, A.W., Dronamraju, R., Potjewyd, F., James, K.S., Winecoff, D.K., Kirchherr, J.L., Archin, N.M., Browne, E.P., Strahl, B.D., Margolis, D.M., et al. (2020). Evaluation of EED Inhibitors as a Class of PRC2-Targeted Small Molecules for HIV Latency Reversal. ACS Infect Dis 6, 1719-1733.

Vermeulen, M., and Dejardin, J. (2020). Locus-specific chromatin isolation. Nat Rev Mol Cell Biol 21, 249-250.

Vidal, M., and Starowicz, K. (2017). Polycomb complexes PRC1 and their function in hematopoiesis. Exp Hematol 48, 12-31.

Waldrip, Z.J., Byrum, S.D., Storey, A.J., Gao, J., Byrd, A.K., Mackintosh, S.G., Wahls, W.P., Taverna, S.D., Raney, K.D., and Tackett, A.J. (2014). A CRISPR-based

approach for proteomic analysis of a single genomic locus. Epigenetics 9, 1207-1211.
Yukl, S.A., Kaiser, P., Kim, P., Telwatte, S., Joshi, S.K., Vu, M., Lampiris, H., and Wong, J.K. (2018). HIV latency in isolated patient CD4(+) T cells may be due to blocks in HIV transcriptional elongation, completion, and splicing. Sci Transl Med 10.
Zhang, J., Jackson, A.F., Naito, T., Dose, M., Seavitt, J., Liu, F., Heller, E.J., Kashiwagi, M., Yoshida, T., Gounari, F., et al. (2011). Harnessing of the nucleosome-remodeling-deacetylase complex controls lymphocyte development and prevents leukemogenesis. Nat Immunol 13, 86-94.
Zhang, Y., Liu, T., Meyer, C.A., Eeckhoute, J., Johnson, D.S., Bernstein, B.E., Nusbaum, C., Myers, R.M., Brown, M., Li, W., et al. (2008). Model-based analysis of ChIP-Seq (MACS). Genome Biol 9, R137.
Zhao, Y., Karijolich, J., Glaunsinger, B., and Zhou, Q. (2016). Pseudouridylation of 7SK snRNA promotes 7SK snRNP formation to suppress HIV-1 transcription and escape from latency. EMBO Rep 17, 1441-1451.

CHAPTER .3

A two-color haploid genetic screen identifies novel and druggable host factors in HIV latency

Michael D Röling, Mahsa Mollapour Sisakht, **Enrico Ne**, Panagiotis Moulos, Mateusz Stoszko, Elisa De Crignis, Helen Bodmer, Tsung Wai Kan, Maryam Akbarzadeh, Vaggelis Harokopos, Thijn Brummelkamp, Pantelis Hatzis, Robert-Jan Palstra, Tokameh Mahmoudi*

Roling et al. 2021, preprint

https://www.biorxiv.org/content/10.1101/2021.01.20.427543v1

A two-color haploid genetic screen identifies novel host factors involved in HIV latency

Authors:

Michael D Röling[1], Mahsa Mollapour Sisakht[1#], **Enrico Ne[1#],** Panagiotis Moulos[2#], Mateusz Stoszko[1], Elisa De Crignis[1], Helen Bodmer[1], Tsung Wai Kan[1], Maryam Akbarzadeh[1], Vaggelis Harokopos[2], Thijn Brummelkamp[3], Pantelis Hatzis[2], Robert-Jan Palstra[1], Tokameh Mahmoudi[1]*

[#] authors contributed equally

Affiliations:

1Department of Biochemistry, Erasmus University Medical Center, Ee634 PO Box 2040 3000CA Rotterdam, the Netherlands

2 Institute for Fundamental Biomedical Research, Biomedical Sciences Research Center, Alexander Fleming', Fleming, Fleming Street 34, 16672, Vari, Greece

3 NKI Amsterdam

* Correspondence to: Tokameh Mahmoudi: t.mahmoudi@erasmusmc.nl

Summary

A reservoir of latent HIV-1-infected cells persists in the presence of combination antiretroviral therapy (cART), representing a major obstacle for viral eradication. Reactivation of the latent HIV-1 provirus is part of curative strategies which aim to promote clearance of the infected cells. To identify novel host factors as putative targets to reverse HIV latency, we performed an insertional mutagenesis two-color genetic screen in a latently HIV-1-infected pseudo-haploid KBM7 cell line (Hap-Lat). Following mutagenesis, re-activated GFP and mCherry double-positive cells harboring gene trap-mediated gene disruption together with HIV LTR-driven transcription, were sorted by flow cytometry and insertions were mapped to the genome by inverse PCR and high-throughput sequencing. Bioinformatic analysis using stringent thresholding resulted in the identification of 69 candidate host genes involved in maintaining HIV-1 latency. We used shRNA mediated depletion in latent HIV-1 infected J-Lat A2 and 11.1 T cell lines to functionally validate a select set of candidate genes and confirmed ADK, CHD9, CMSS1, EVI2B, EXOSC8, FAM19A, GRIK5, IRF2BP2, NF1, and USP15 as novel host factors involved in the maintenance of HIV latency. Chromatin immunoprecipitation assays indicated that CHD9, a Chromodomain Helicase DNA-binding protein, maintains HIV latency via direct association with the HIV 5'LTR, and its depletion results in increased histone acetylation at the HIV-1 promoter, concomitant with HIV-1 latency reversal. As FDA-approved inhibitors are available for three of the validated candidate genes—5-Iodotubercidin, Trametinib, and Topiramate, targeting ADK, NF1, and GRIK5, respectively—we tested their potential as latency reversal agents in J-Lats and a primary CD4+ T cell model of HIV latency. 5-Iodotubercidin exhibited significant cytotoxicity in both J-Lat and primary CD4+ T cells, while Trametinib reversed latency in J-Lat cells but not in latently HIV-1-infected primary CD4+ T cells. In contrast, the GRIK5 inhibitor, Topiramate, reversed latency both in cell-line models as well as in latent HIV-1 infected primary CD4+ T cells, without inducing T cell activation or significant toxicity. Thus, using an adaptation of a haploid forward genetic screen, we have identified novel potentially druggable host factors contributing to HIV-1 latency.

INTRODUCTION

Combination antiretroviral therapy (cART) has proven to effectively abrogate viral replication in HIV-1-infected patients and has substantially reduced AIDS-related mortality. However, cART is not curative and patients must remain on life-long medication regiments, as interruption of the therapy leads to rapid rebound of viral replication (Siliciano and Siliciano 2015). This is due to the persistence of a reservoir of latently infected cells, harboring replication-competent provirus blocked at the level of gene expression, that escape clearance by the immune system (Sengupta and Siliciano 2018). Therapeutic strategies toward HIV-1 cures aim to inactivate, reduce or completely eradicate the latent reservoir, such that, upon cessation of cART, the patient's immune system can effectively control the infection or fully clear it (Sengupta and Siliciano 2018). Strategies aiming to reduce or eliminate the reservoir rely on drugs, termed latency-reversing agents (LRAs), capable of inducing the latent HIV infected cells to express viral genes to render infected cells susceptible to cytopathic effects and/or recognition and clearance by the immune system (Deeks 2012). Much focus has therefore been placed on finding small molecules for activating transcription of the latent HIV-1 provirus, which are not cytotoxic and do not induce harmful T cell activation or proliferation.

The identification of molecules capable of inducing HIV gene expression has been largely accomplished using candidate approaches, which build on existing knowledge of transcription factors and co-factors that bind to and regulate transcription at the HIV LTR (Ne, Palstra, and Mahmoudi 2018; Van Lint, Bouchat, and Marcello 2013; Pereira et al. 2000). One of the most clinically studied classes of molecules in HIV latency reversal, HDAC inhibitors (HDACis) such as SAHA (Nancie M. Archin et al. 2009), valproic acid (Ylisastigui et al. 2004), rhomidepsin (Wei et al. 2014) and M344 (Ying et al. 2012), target HDACs, which have been shown to be recruited to the HIV LTR by multiple transcription factors (Williams et al. 2006; Coull et al. 2000; G. Jiang et al. 2007) to deacetylate histones and repress transcription. Similarly, agonists of the PKC pathway, such as prostratin and bryostratin, have been studied as activators of the HIV LTR, as they induce nuclear localization and LTR binding of the NFκB (p65/p50) heterodimer, a potent activator of HIV

transcription (Williams et al. 2004; Pérez et al. 2010). While this candidate approach has led to the identification of druggable targets or potential candidate LRAs, none of the LRAs currently under clinical investigation are capable of strong latency reversal in patients or lead to a reduction in the size of the latent HIV reservoir (N. M. Archin et al. 2012; Elliott et al. 2014). Thus, to identify more potent and clinically relevant LRAs, it is critical to identify the full repertoire of functionally relevant host factors and pathways that play a role in the maintenance of latency.

Complementary to the approach of targeting candidate LTR-bound transcription factors and complexes for inhibition or activation, other studies have embarked on unbiased screens of small molecule libraries to identify compounds capable of reversing HIV latency (Sadowski and Hashemi 2019). Alternatively, recent large-scale unbiased gene knock-out/knock-down screens have been employed to unravel the molecular mechanisms of latent HIV (Das et al. 2018a; W.-M. Jiang et al. 2014; Besnard et al. 2016; Zhu et al. 2014b, 201; Li, Hajian, and Greene 2020; Yang et al. 2020; Goff 2008; Rathore et al. 2020; Krasnopolsky, Kuzmina, and Taube 2020; Huang et al. 2019). RNA interference methods, which rely on the reduction of mRNA expression levels, have been widely used as screening platforms in mammalian cells (Martin and Caplen 2007). However, this method has been shown to suffer from serious limitations, including the presence of false-positives due to off-target effects and the persistence of residual gene expression, which results in false negatives (Yamamoto-Hino and Goto 2013; Hart et al. 2014). For example, several RNAi screens have been performed to identify host cell factors essential for HIV infection and replication (Besnard et al. 2016; Das et al. 2018b; Zhu et al. 2014a; Boehm et al. 2017); surprisingly, very little overlap was found between the lists of genes identified in these screens, pointing to the need for other screening methods that achieve complete inactivation of genes. Another large-scale unbiased gene disruption approach uses the precision of CRISPR-Cas9 targeting for complete gene knock-outs (Yu and Yusa 2019). A recent screen using a lentiviral sgRNA sub-library targeting nuclear proteins identified MINA53 as a possible latency-promoting gene (LPG) (Huang et al. 2019).

In mammalian cells, functional analysis via forward genetic screens and mutational analysis has largely been hampered due to

diploidy, as, in somatic cells, when one copy of a gene essential for a cellular process is inactivated, the second copy often remains active and compensates for that partial loss. Pseudo-haploid screens are based on KBM7s, a chronic myelogenous leukemia (CML) cell line, which is haploid for all chromosomes except for chromosome 8 and a 30Mb stretch of chromosome 15 (Kotecki, Reddy, and Cochran 1999), allowing for forward genetics in mammalian cells (Carette et al. 2009). Using Gene-Trap (GT) retrovirus-mediated mutagenesis for generating a library of gene knockouts in KBM7 cells enables unbiased loss-of-function screening in mutant cells for the identification of host genes essential to a specific cell function. Haploid screens have proven to be a powerful method to identify genes involved in drug import (Reiling et al. 2011; Birsoy et al. 2013), druggable target genes to treat cancer (Logtenberg et al. 2019; Mezzadra et al. 2019; Heijink et al. 2019), key components of cellular pathways (Mezzadra et al. 2017; Janssen et al. 2018; Raaijmakers et al. 2018; Blomen et al. 2015; Lee et al. 2013), and genes involved in the pathogenesis of various viruses (Carette et al. 2011; Jae et al. 2013; Staring et al. 2017; Hoffmann et al. 2017; Raaben et al. 2017; Staring et al. 2018; Jangra et al. 2018; Qi et al. 2015) and susceptibility to toxins (Carette et al. 2009; Guimaraes et al. 2011; Tafesse et al. 2014).

To identify novel host genes that could potentially serve as molecular targets for HIV latency reversal, we performed insertional mutagenesis in latently HIV-1-infected KBM7 cells. First, using a flow cytometry activated cell sorting-based strategy described previously (Jordan, Bisgrove, and Verdin 2003; Rafati et al. 2011), we generated a latent pseudo-haploid KBM7/(Hap-Lat) cell line that harbors an integrated transcriptionally silent HIV-1 5'LTR controlling the expression of a GFP reporter gene. Hap-Lat cells were then subjected to GT insertional mutagenesis, using a mCherry reporter GT virus, and Hap-Lat cells expressing both GFP (as a reporter of HIV-1 expression) and mCherry (confirming the presence of a GT integration within an active gene) were then sorted using fluorescence-activated cell sorting (FACS). GT integration sites within these two populations were then amplified by inverse PCR and mapped to the genome by high-throughput sequencing. Computational candidate identification resulted in the identification of 69 candidate genes, whose function is required for maintenance of HIV

latency, but which are not essential to cell survival. For functional follow-up experiments, we selected a subset of 16 GT-identified putative HIV latency re-enforcing target genes, which are also expressed in primary CD4+ T cells, and examined the effect of their depletion via shRNA knock-down in maintaining latency in J-Lat T cell lines A2 and 11.1. Functional validation identified 10 putative novel latency promoting genes: ADK, CHD9, CMSS1, GRIK5, USP15, IRF2BP2, EXOSC8, NF1, EVI2B, and FAM19A. Because of the obvious mechanistic potential of CHD9, a Chromodomain Helicase DNA-binding protein, we explored its association with the 5'LTR using ChIP-qPCR analysis. We found CHD9 to be enriched at the 5'LTR in the latent state but to dissociate from the HIV-1 promoter after PMA treatment. Loss of CHD9 enrichment upon re-activation was accompanied by a relative increase in H3 acetylation at the HIV-1 LTR, indicating a functional shift in chromatin organization from repressed to transcriptionally active. We also found three genes in our candidate list, ADK, GRIK5, and NF1 to be targetable by existing small molecule inhibitors. The latency reversal potential of these compounds was evaluated in J-Lat T cell lines A2 and 11.1, and in a primary cell model of HIV latency. We found 5-Iodotubercidin, which inhibits ADK, not to be a viable LRA due to its toxicity in both A2, 11.1, and primary CD4+ T-cells. While the NF1 inhibitor Trametinib reactivated latent HIV in the J-Lat cell lines, it was not effective in the primary cell model of latency. On the other hand, the GRIK5 inhibitor Topiramate reversed HIV-1 latency in both J-Lat T-cell lines as well as in primary CD4+ T cells harboring latent HIV-1, without significant associated cytotoxicity or T cell activation, and thus presents an interesting potential novel LRA.

RESULTS

Establishment of a latent pseudo-haploid cell line

To identify potentially druggable host genes as putative molecular targets for HIV latency reversal, we generated pseudo-haploid latent HIV-1-infected cells in which we performed insertional mutagenesis according to a strategy schematically depicted in Figure 1A. A latent HIV-1-infected pseudo-haploid KBM7 cell line was generated according to a previously described strategy used in Jurkat cells (Jordan, Bisgrove, and Verdin 2003; Rafati et al. 2011) (Figure 1B). Subsequently, haploid latent (Hap-Lat) cells harboring a latent integrated HIV-1-derived virus containing a GFP reporter, were subjected to insertional mutagenesis using gene trap virus carrying an mCherry reporter. Instead of using a lethality-selecting scheme, our system relies on fluorescence activated cell sorting (FACS) to select for reactivated cells, marked by elevated GFP expression resulting from insertional mutagenesis of genes essential for maintenance of HIV latency. Cells expressing both GFP and mCherry were FACS-sorted and expanded for multiple rounds, after which GT insertion sites were mapped and identified by inverse PCR and high-throughput sequencing. To establish a latent HIV infection in the pseudo haploid KBM7 system, near-haploid KBM7 cells were infected at low MOI with the single infectious cycle HIV-derived virus LTR-GFP-LTR, in which GFP reporter expression is controlled by the activity of the HIV-1 promoter or 5'LTR (Figure 1A). After infection, the population of GFP negative cells comprising mainly uninfected cells and putative latently infected cells were sorted by FACS and subsequently stimulated with 5ng/µl TNF-α and 350µM Vorinostat. In response, a small percentage of existing latent HIV-infected cells were transcriptionally reactivated and expressed GFP. These GFP positive cells were -sorted by FACS as single cells and expanded (Figure 1B). The resulting clonal latent KBM7 haploid lines were characterized by flow cytometry to determine GFP expression at basal and stimulated states. From the clonal lines established, Hap-Lat#1 was selected for low basal activity and significant reactivation upon stimulation (Figure 1C). To ensure maintenance of haploidy, Haplat#1 cells were periodically sorted to enrich for the 5% of smallest cells (Supplemental figure 1A).

Gene-trap mutagenesis of Hap-Lat cells

Hap-Lat#1 cells were mutagenized by infection with a murine stem cell virus (MSCV)-derived viral gene-trap (GT) vector containing an inactivated 3' LTR, an adenoviral splice-acceptor site, an mCherry reporter cassette and a polyA terminator tail (Carette et al. 2009). Dendritic and myeloid cells are notoriously refractory to retroviral infection (Goujon et al. 2008; Kaushik et al. 2009). We indeed found that infectivity of KBM7 is poor compared to T-cell-derived cell lines SupT1 and Jurkat, as well as other myeloid-derived cell lines (Supplemental Figure 1B). SAMHD1, a nucleotide scavenger, has been identified as a causative restricting host factor that limits the free available pool of nucleotides for reverse transcription (Laguette et al. 2011). To bypass SAMHD1-mediated restriction, we supplemented cells with 2μM nucleosides (dNs), which increased GT infectivity by approximately two-fold (Supplemental figure 1C). GT preferentially inserts in the 5' regions of genes (J. Hansen et al. 2003), effectively knocking out gene expression by truncating the native transcript (Supplemental figure 1D). For a full-scale mutagenesis experiment, approximately 200 million Hap-Lat #1 cells were mutagenized using two rounds of infection with GT-mCherry in the presence of exogenously supplied nucleosides. Infection of Hap-Lat#1 with GT-mCherry effectively caused reactivation of a subpopulation of latent KBM7 cells (Figure 1D-E). We reasoned that insertional mutagenesis in genes essential for maintenance of HIV latency would result in Hap-Lat#1 cells expressing the GFP reporter. We determined GT integrations in individual GFP/mCherry double-positive clones and estimated that the sequential infection resulted in 1 to 4 GT integrations per cell, with the majority of cells containing one integration (data not shown). By gating conservatively, approximately 1-4% GFP/mCherry double-positive cells were then sorted and expanded (Figure 1E). After expansion, reactivated cells tend to revert to a latent state (Supplemental figure 1E). To enrich for a more stable GFP-expressing, mCherry GT-containing double-positive cell population, cell sorting was repeated for multiple rounds (Figure 1F). Sequential rounds of sorting led to the appearance of a stable subpopulation within the total double-positive population expressing high levels of mCherry (Figure 1F). To examine any potential biological differences between the two, we separately sorted the

total double-positive population and the mCherry-high subpopulation, which we designated GFP^{Total} and GFP^{Sub} respectively, for a final (5^{th}) round (Figure 1F). Genomic DNA extracted from GFP^{Total} and GFP^{Sub} obtained in the 5^{th} round of sorting was used to determine GT integrations, while that of a pool of unsorted GT-infected cells was used as a reference.

Mapping of insertion sites to identify host factors maintaining HIV latency

To determine the host sequences flanking the GT insertion sites, inverse PCR with primers annealing to internal sequences in the gene trap vector followed by amplification was performed. The amplified products were processed for high-throughput sequencing (Figure 1F). For GFP^{Sub} 2 biological replicates, samples A and B, were generated. For GFP^{Total} 3 biological replicates were generated, samples C, D and E. To estimate the sampling depth of our GT, we re-sequenced GFP^{Sub} sample B and GFP^{Total} sample D at greater depth. The resulting NGS datasets were processed for candidate gene identification. A previously described method to analyze GT data, HaSAPPy (Haploid Screen Analysis Package in Python), was rigorously re-implemented, appended with additional steps for quality control, library normalization, and optimized resolution for the selection of integration sites (Minin, Postlmayr, and Wutz 2018). HaSAPPY assigns a Local Outlier Factor (LOF) score to each gene in a sample based on a triplet score derived from the number of putative GT integrations in the sample compared to the reference. For each population, we compiled all genes with an LOF score >3 from each replicate and obtained 686 hits for GFP^{Total} and 382 hits for GFP^{Sub}. 183 genes were common to both populations (Supplementary figure S2A). Next, we investigated any potential biological basis for the difference between GFP^{Total} and GFP^{Sub}. Since expression levels of the integrated mCherry reporter appear to be on average higher in the GFP^{Sub} population than in the GFP^{Total} population, we wondered if expression levels of the targeted genes were higher in GFP^{Sub}. We obtained recently published KBM7 gene expression data (Mayor-Ruiz et al. 2020) and found no substantial difference in the average level of expression between the two populations (Supplementary figure S2B). To determine if there was any difference in the functionality of the GT target genes found in GFP^{Total} and GFP^{Sub}, we performed

enrichment analysis using GO terms and found no substantial differences in enrichment for biological process and molecular function ontologies (Supplementary figure S2C and D). Similarly, both populations contain a comparable fraction (32.7%) of integrations within non-coding or anti-sense genes (Supplementary figure S2E). Finally, we cross-referenced the GT target genes found in GFP^{Total} and GFP^{Sub} populations to the HIV interaction database (https://www.ncbi.nlm.nih.gov/genome/viruses/retroviruses/hiv-1/interactions/) and found that both the GFP^{Total} and the GFP^{Sub} populations contain similar fractions (21.9% and 20.2%, respectively) of genes previously reported to be involved in HIV biology, fractions which are substantially higher than the 7.4% found for the complete list of ENSEMBL genes (Supplementary figure S2F). In order to limit our extensive list of candidate genes for follow up functional validation, we applied more stringent thresholds for each population and defined candidate genes as having an LOF score equal to or greater than 3 in at least 2 biological replicate samples. We thus identified 19 candidate genes in the GFP^{Sub} population and 55 in the GFP^{Total} population (Figures 2A and B and Table 1).

Candidate list validation

Since our bioinformatics analysis did not reveal a defining difference between the GFP^{Total} and the GFP^{Sub} populations, we decided to proceed with functional assays using shRNA-mediated depletion of candidate genes obtained from both populations. To prioritize the candidate genes found in the KBM7 haploid screen for functional validation in the more biologically relevant Jurkat T-cell-based HIV-1 latency models J-Lat A2 and 11.1, we focused on protein-coding genes and took into account LOF scores as well as gene expression in white blood cells (as extracted from the GTEx portal (https://www.gtexportal.org/home/) or Illumina's Human BodyMap 2.0 project (http://www.ensembl.info/2011/05/24/human-bodymap-2-0-data-from-illumina/)) and the Jurkat T-cell model (Palstra et al. 2018) (Table 1). Eight genes from GFP^{Sub} and nine genes from GFP^{Total} were selected as candidates for validation using shRNA-mediated depletion in J-Lat A2 and J-Lat 11.1 cells. These cells contain a latent HIV-derived GFP reporter

driven by the 5'HIV-LTR and are well-established model systems for HIV latency (Jordan, Bisgrove, and Verdin 2003; Jordan, Defechereux, and Verdin 2001). While J-Lat A2 cells contain an integrated latent LTR-Tat-IRES-GFP virus, J-Lat 11.1 cells contain an envelope defective full-length HIV-1 genome expressing GFP in place of Nef. We used flow cytometry to assess reactivation as measured by GFP expression and extracted RNA to assess knockdown of the targeted candidate genes and expression of the HIV genes GAG, POL, and TAT by RT-qPCR (figure 2C-E and Supplemental figure S3 and S4). We observed significant latency reversal upon candidate gene knockdown in 10 of 15 genes depleted by shRNA (ADK, CHD9, CMSS1, EVI2B, EXOSC8, FAM19A, GRIK5, IRF2BP2, NF1, and USP15) in both J-Lat A2 and J-Lat 11.1 cells (Figure 2C-E and Supplemental figure S3 and Table 1). Knockdown of SCN9A, RHOF, SPN, COPS5 and EVL did not result in significant latency reversal in one or both J-Lat models (Supplemental figure S4). These results demonstrate that a significant proportion of the candidate genes found in our myeloid-derived KBM7 haploid screen play a role in maintenance of HIV-1 latency in the more relevant T cell-derived J-Lat A2 and J-Lat 11.1 HIV latency models.

CHD9 is an LTR-associated repressor of HIV-1 transcription

Interestingly, two genes, CIITA and CHD9, from our candidate list are associated with the GO-term DNA binding (GO:0003677). CIITA is a well-established factor involved in HIV expression and has been previously shown to inhibit Tat function and hence viral replication (Forlani et al. 2016; Accolla et al. 2002). The Chromodomain helicase DNA binding protein 9 (CHD9) is a member of an ATP-dependent chromatin remodeler family, the members of which modulate DNA-histone interactions and positioning of nucleosomes and play key roles in stem cell regulation, development, and disease (Mills 2017). Previously, we have shown that chromatin remodeling by another ATP-dependent remodeler, the BAF complex, plays a crucial role in maintenance of HIV-1 latency and its re-activation (Rafati et al. 2011) . We therefore decided to further characterize the role of CHD9 in regulating HIV-1 gene expression. We knocked down CHD9 using a lentivirally transduced shRNA and verified its depletion in both J-Lat A2 and J-Lat 11.1 cells at

the protein level by Western blotting (Figure 3A). Depletion of CHD9 led to a significant reversal of latency, as shown by an increase in the percentages of GFP positive cells (Figure 3B and C). Latency reversal was also confirmed by increased expression of viral genes Gag, Pol, and Tat in J-Lat 11.1 (Figure 3D). To characterize a potential direct association of CHD9 with the latent HIV-1 5'LTR, we performed chromatin immuno-precipitation (ChIP) in latent and PMA-activated 11.1 J-Lat cells. The positions of nucleosomes within the latent HIV-1 LTR are rigid, with positioned nucleosomes Nuc-0, Nuc-1, and Nuc-2 separated by DNAse I-sensitive regions HSS1 and HSS2, respectively, visually summarized in Figure 3E. CHD9 was found to be enriched throughout the HIV-1 LTR in latent 11.1 J-Lat cells, predominantly present over the Nuc0-HSS1 region, and this association was significantly decreased after LTR activation by PMA treatment (Figure 3F and Supplemental figure S5). No significant enrichment was observed at the HIV-1 internal control region (the GFP reporter) or the unrelated gene locus (HK2) (Figure 3F and Supplemental figure S5). As expected, PMA treatment led to an increase in histone H3 acetylation, a mark of active chromatin, over the HIV-1 5'LTR (Figure 3G and Supplemental figure S5). Our data demonstrate a role for CHD9 in the repression of HIV-1 gene expression and maintenance of latency via direct recruitment to and association with the HIV 5'LTR.

Pharmacological targeting of ADK, GRIK5 and NF1

With the aim of identifying potential latency reversing agents (LRAs), we performed a literature search and identified three candidate genes, ADK, GRIK5, and NF1, all present in the GFP^{Sub} list, for which FDA-approved small molecule inhibitors are available. We therefore examined the latency reversal potential of the ADK inhibitor 5-Iodotubercidin, the GRIK5 inhibitor Topiramate, and the NF1 inhibitor Trametinib. Adenosine kinase (ADK) is a phosphotransferase that converts adenosine into 5'-adenosine-monophosphate and thus plays a major role in regulating the intracellular and extracellular concentrations of adenosine, activation of specific signaling pathways, and bioenergetic and epigenetic functions (Park and Gupta 2013; Boison 2013). 5-Iodotubercidin is a purine derivative that inhibits adenosine kinase by competing with adenosine for binding to the enzyme (Zhang et al. 2013).

Glutamate ionotropic receptor kainate type subunit 5 (GRIK5) is a subunit of the tetrameric kainate receptor (KAR), a subgroup of ionotropic glutamate receptors. GRIK5, together with GRIK4, binds glutamate, whereas subunits GRIK1-3 form functional ion-channels (Rojas and Dingledine 2013). Topiramate is an FDA-approved GRIK5 inhibitor employed as an anti-epileptic drug and is used to manage seizures and prevent migraines (Shank et al. 2000). Neurofibromin 1(NF1) is ubiquitously expressed; however, its highest levels are found in cells of the central nervous system and it has been described to function as a negative regulator of the Ras signal transduction pathway (Walker and Upadhyaya 2018; Harrell Stewart and Clark 2020). Trametinib is an NF1 inhibitor which is also known as a mitogen-activated protein kinase (MAPK) kinase (MEK) inhibitor with anticancer activity and is FDA-approved for use in metastatic malignant melanoma (Wright and McCormack 2013).

We examined the effects of treatment with 5-Iodotubercidin, Topiramate, and Trametinib in J-Lat 11.1, J-Lat A2 cells, and a primary CD4+ T cell model of latency, on latency reversal. Treatment with the ADK inhibitor 5-Iodotubercidin resulted in only a moderate induction of latency reversal in both A2 and 11.1 J-Lat cells and was accompanied by significant toxicity, especially at high concentrations [16μM] (Figure 4A & B). Only at a 5-Iodotubercidin concentration of 4μM in 11.1 J-Lat cells was a significant increase in GFP positive cells with acceptable viability observed (Figure 4A & B). Treatment of J-Lat A2 and 11.1 cells with the GRIK5 inhibitor Topiramate or the NF1 inhibitor Trametinib resulted in significant, concentration-dependent latency reversal (Figure 4A & B). Importantly, neither Topiramate nor Trametinib displayed significant toxicity in comparison with the DMSO vehicle control group, as measured by gating for live cells. In particular, treatment of J-Lat 11.1 cells with Trametinib resulted in significant latency reversal at all evaluated concentrations [250nM, 1μM, 4μM and 16μM], with minimal associated toxicity (Figure 4B).

Next, we evaluated the latency reversal potential of the inhibitors in a more clinically relevant primary ex vivo infection latency model, in which CD4+ T cells are infected with a full-length non-replication competent HIV-1 virus driving expression of a luciferase reporter (Figure

4C) (Lassen et al. 2012). After spin infection, cells are allowed to rest for 4 days and are treated with the different compounds, as indicated, for 48 hours, followed by measurement of HIV-1 LTR-driven luciferase activity and staining for Annexin positive cells and T-cell activation markers CD69 and CD25 (Figure 4D- G and Supplemental figure S6). Similar to what was observed for the A2 and 11.1 J-Lat cell-lines, treatment of HIV-1-infected latent primary CD4+ T cells with the ADK-inhibitor 5-Iodotubercidin did not result in significant latency reversal (Figure 4D), while it produced significant toxicity at the highest concentration used, as indicated by Annexin V staining (Figure 4E). Treatment with the GRIK5 inhibitor Topiramate, at a concentration of 16 and 20 µM, resulted in significant ($p < 0.05$) reversal of latency, as measured by a 3-6 fold increases in mean luciferase activity compared to untreated controls (Figure 4D). Topiramate treatment did not significantly affect CD4+ T cell viability after 48 hours, while control treatment with a toxic (200nM) concentration of Gliotoxin (GTX) caused apoptosis of primary CD4+ T-cells, as evidenced by an increase in the percentage of Annexin V-positive cells, as was observed previously (Figure 4E) (Stoszko et al. 2020). In contrast to what was observed in the A2 and 11.1 J-Lat cell-lines, treatment of latently infected CD4+ T-cells with the NF1 inhibitor, Trametinib did not lead to a significant reversal of latency (Figure 4D), while viability was only moderately affected (figure 4E).

For LRA candidates to be viable in a clinical setting, it is crucial that they reactivate latent HIV without inducing activation of CD4+ T-cells. Therefore, we examined the potential of our candidate LRAs to induce expression of the activation markers CD25 and CD69 in treated CD4+T cells. While the ADK inhibitor 5-Iodotubercidin resulted in markedly elevated expression of the activation markers, the GRIK5 inhibitor Topiramate and NF1 inhibitor Trametinib did not induce significant induction of the T cell activation markers CD69 and CD25 (Figure 4F & G and Supplemental figure S6). As expected, PMA/Ionomycin treatment substantially activated T cells (Figure 4F & G and Supplemental figure S6). Taken together, our data indicate that the FDA-approved GRIK5 inhibitor Topiramate reverses HIV-1 latency in a variety of T cell models of latency, without induction of T cell activation

and with limited cytotoxicity, and, therefore, can be considered an attractive LRA for further mechanistic and pre-clinical investigation.

DISCUSSION

In search of potentially novel host factors and pathways that play a role in the maintenance of HIV-1 latency, we performed a two-color haploid genetic screen in latent HIV-1-infected KBM7 cells. An important advantage presented by this approach is that identification of putative functionally relevant candidate latency-promoting host target genes does not require a-priori knowledge of the molecular determinants of latency and is thus completely unbiased. Additionally, gene-trap insertional mutagenesis has enabled identification of previously unappreciated latency genes and cellular pathways, which likely modulate latency not only via direct physical association with the HIV-1 promoter, but also indirectly, through involvement in cellular signaling. We produced a list of 69 candidate genes and proceeded to validate ten candidates, the depletion of which in various in vitro models of latency, including primary CD4+ T-cell models, led to latency reversal.

The haploid KBM7 cell line, while a powerful system for GT-mediated forward genetic screens, is a myeloid cell line (Kotecki, Reddy, and Cochran 1999, 199). HIV can infect and establish latent infection in monocytes and macrophages (Kumar, Abbas, and Herbein 2014; Wong, Jaworowski, and Hearps 2019), but these are not considered to be the prime source of the latent reservoir; this begs the question how relevant the myeloid nuclear environment may be for HIV latency in lymphocytic cells. Nevertheless, when we tested a selected subset of the candidate genes by shRNA-mediated knockdown in a T-cell derived model of HIV latency, we found that knockdown of 67% of candidates (10 out of 15) led to latency reversal, which demonstrates the validity of our approach. Moreover, several of the genes identified in our gene trap screen have previously been implicated in HIV susceptibility: 15 out of 69 genes are listed in the HIV-1 human interaction database (https://www.ncbi.nlm.nih.gov/genome/viruses/retroviruses/hiv-1/interactions/), a detailed database of all known interactions between HIV-1 and the human host. Furthermore, one of the candidates, IRF2BP2, is a potential target of HIV-associated nucleotide polymorphisms within a cluster of regulatory DNA elements (Palstra et al. 2018) which loop to and potentially regulate the IRF2BP2 promoter in CD4+ T-cells (Fishilevich et al. 2017; Lai et al. 2018). In the current study, we demonstrate that

knock-down of IRF2BP2 results in latency reversal. IRF2BP2 has been shown to interact with NFAT1 and to repress transcriptional activity (Carneiro et al. 2011), providing a plausible mechanism for its role in latency maintenance.

Among the candidate gene list, we also identified CHD9, a member of the chromodomain helicase DNA-binding (CHD) family of the ATP dependent chromatin remodelers. Members of this family are involved in various cellular processes and in normal development and disease; however, CHD9 is one of the least-studied members. We found that CHD9 is associated with the latent HIV-1 5'LTR and is displaced upon promoter activation by PMA stimulation, suggesting that it acts as a repressor of HIV transcription. Indeed, depletion of CHD9 by shRNA-mediated knockdown led to de-repression of HIV, as observed by increase in the expression of the HIV-1 LTR-driven reporter GFP as well as the HIV-1 genes Gag, Pol and Tat. Future studies will determine the mode of recruitment of CHD9 to the HIV-1 LTR and the molecular interplay between CHD9 and other chromatin remodeler and modifying complexes associated with the latent HIV-1 5'LTR (Ne, Palstra, and Mahmoudi 2018).

A large subset of the list of 69 candidate genes are non-coding RNAs (N=22); upon closer inspection we found that 16 of those are at least in part oriented in an anti-sense direction with respect to known protein-coding genes. We currently do not know if these non-coding transcripts fulfill a biological function in maintenance of HIV-1 latency, directly through their transcripts, through regulatory effects on other (protein-coding) genes in cis or in trans, through other effects, or if they represent mapping artefacts. Further investigation into these possibilities is ongoing.

An interesting observation emerging from our experimental set-up is the appearance of a sub-population of cells after multiple rounds of sorting that is more stable in its GFP expression. This sub-population is also higher in mCherry expression, as compared to the total double-positive population. The reversal of double-positive cells after sorting may reflect the intrinsically stochastic transcription of HIV-1(Razooky et al. 2015; M. M. K. Hansen, Martin, and Weinberger 2019; Tantale et al. 2020). Latent cell lines are notoriously sensitive to cellular stresses, which cause reactivation (Piette and Legrand-Poels 1994; Vallejo-Gracia et al.

2020; Timmons et al. 2020). It is, therefore, possible that the less stable GFP-positive cells represent cells that are temporarily activated, and which slowly revert back to a latent state. Therefore, we focused our analysis and validation experiments mainly on the stable GFP-high population. Nevertheless, the few candidate genes unique to the total population that we tested in our shRNA knockdown validation experiment had a similar false positive ratio (i.e. 33.3%) as we found for the candidate genes from the stable GFP-positive population.

For our analysis, we set a strict criterion of the LOF score being ≥3 in at least two biological replicates, although a cut-off at lower LOF scores of 2 or above has been used previously (Kriegel et al. 2009). We chose this stringent criteria to confidently identify 69 candidate genes. We believe however that our dataset likely contains additional candidate genes that we miss due to the stringency applied. This is exemplified by our observation that STRING analysis indicates that many of the 598 protein-coding genes with an LOF score of 3 and higher functionally interact (Supplemental Figure S7). Moreover, 32% of these genes (195) appear in the HIV-1 human interaction database, pointing to their potential roles in HIV-1 biology. Importantly, proteins with well-described functions in HIV biology, such as, e.g., IL32 (LOF=9.5; (Palstra et al. 2018), RUNX1 (LOF=12.6; (Klase et al. 2014), and SMARCA4/BRG1 (LOF=8.7; (Rafati et al. 2011), are detected with high LOF scores in at least one of our samples.

Identification of functionally relevant molecular targets and novel compounds effective in latency reversal has proven to be an outstanding challenge in the field (Stoszko et al. 2019). Most clinically investigated LRAs have thus far failed to significantly impact the size of the latent reservoir in patients. From our list of validated host factors we identified three druggable targets, ADK, NF1, and GRIK5. The ADK inhibitor 5-Iodotubercidin displayed cytotoxicity in both J-Lat and primary models of HIV latency. Since knockdown of ADK did not lead to significant toxicity, off target, pleiotropic effects of 5-Iodotubercidin may underlie the observed T cell toxicity. 5-Iodotubercidin is the prototype nucleoside ADK inhibitor, with a relatively high IC_{50}. Novel nucleoside and non-nucleoside ADK inhibitors have been developed with more favorable pharmacological properties that would be attractive to pursue in the

context of HIV-1 latency reversal in future studies (Boison 2013). Trametinib, a small molecule inhibitor of NF1, reactivated HIV-1 in J-Lat cell models with modest effects on viability but displayed significant toxicity in the primary cell models. These results highlight the importance of interrogating the potential effectiveness of candidate LRAs in multiple models of HIV-1 latency to circumvent potential integration-site mediated biases present in cell line models of latency, and, most importantly, to confirm effectiveness in the more relevant primary CD4+ T cells harboring latent HIV-1 in vivo.

Our data point to the GRIK5 inhibitor Topiramate as a potentially promising compound for latency reversal. Topiramate, effectively reversed latency in primary HIV-1-infected CD4+ T cells without inducing significant T cell activation or cytotoxicity; this makes Topiramate a potentially clinically promising LRA and a target for further investigation. GRIK5 (glutamate ionotropic receptor kainate type subunit 5), primarily studied in neurons, is a subunit of the tetrameric kainate receptor (KAR), a subgroup of ionotropic glutamate receptors. GRIK5, together with GRIK4, bind glutamate, whereas subunits GRIK1-3 form functional ion-channels (Rojas and Dingledine 2013). In B-cells, KAR activation by glutamate increases ADAM10 levels, leading to increased B cell proliferation and immunoglobulin production (Sturgill et al. 2011). Topiramate is primarily used as an anticonvulsant or antiepileptic drug. While the exact mechanism by which Topiramate exerts anticonvulsant or antiepileptic properties is unclear, it has been shown to block voltage-dependent sodium and calcium channels (Zhang et al. 2013; Zona, Ciotti, and Avoli 1997), to inhibit the excitatory glutamate pathway and enhance inhibition by GABA (White et al. 2000). Interestingly, Topiramate can induce cytochrome P450 family member CYP3A4 activity and potentially negatively affect the metabolism of many drugs (Nallani et al. 2003), which should be taken into account when considering a potential therapeutic combination of LRAs in future studies.

Acknowledgments

TM received funding from the European Research Council (ERC) under the European Union's Seventh Framework Programme (FP/2007-2013)/ERC STG 337116 Trxn-PURGE, Dutch AIDS Fonds grant

2014021, and Erasmus MC mRACE research grant. RJP received funding from Dutch AIDS Fonds grant 2016014.

Conflicts of interest

The authors have no conflict of interest

Author Contributions

MR, MMS, MS, EN, EDC, TWK, HB, MA and TM carried out experiments and performed data analysis. PM, VH, and PH performed Nextgen sequencing and data analysis. TB provided expertise, material and contributed to the writing of the manuscript. MR, EN, MM, RJP and TM conceived the study and wrote the manuscript. All authors read and approved the final manuscript.

MATERIAL AND METHODS

Cell culture

KBM7 and Hap-Lat (latent HIV infected KBM7-derived cell lines) were cultured in IMDM media (ThermoFisher Scientifc) supplemented with 10% FCS and 2% Pen/Strep. Haploidy of KBM7 cells was maintained by periodically sorting cells for size (5% smallest). Ploidy of cells was determined by propidium iodide staining

Establishment of haploid latent (Hap-Lat) HIV infected cell lines

We used a strategy described previously (Jordan, Bisgrove, and Verdin 2003; Rafati et al. 2011) to generate latently HIV infected KBM7 haploid cell lines. Minimal HIV (LTR-GFP, HIV-658 (Verdin, Paras, and Van Lint 1993) virus was produced by transfection of 293T cells in 15cm culture dishes using polyethylenimine (PEI) Sigma Aldrich) with a mixture of 6.8µg p658, 2µg VSVG and 4.5µg Gag-pol plasmids. Haploid KBM7 cells were infected with HIV-derived virus at low MOI such that approximately

5-10% of cells became productively infected as determined by GFP expression. 5 days after infection, the GFP negative cell population harboring uninfected and potentially latently infected cells were sorted by flow cytometry activated cell sorting (FACS) and stimulated with 350nM SAHA (Selleck Chem), and 5ng/µl TNFα (Sigma-Aldrich). Twenty-four hours post stimulation, GFP positive cells were single cell sorted by FACS into 96 well plates. Clones were expanded and characterized for their basal GFP expression and their potential for re-activation. From the clonal cell lines generated Hap-Lat #1 was selected for low background and relative high reactivation upon stimulation (GFP negative under basal conditions but inducible to express GFP upon activation).

Gene Trap virus production and mutagenesis of Hap-Lat cell lines

We adapted a strategy described previously (Carette et al. 2009) to mutagenize Hap-Lat cells. Briefly, Gene Trap virus was produced by transfection of HEK293T cells in 15cm culture dishes using 180 µl polyethylenimine (PEI) with a mixture of 8 µg pGT-mCherry, 2.1 µg pAdvantage, 3.1 µg CMV-VSVG and 4.8 µg Gag-pol plasmids in at total volume of 1ml serum free RPMI. After 12 hours the growth media was changed to fresh FCS supplemented RPMI. The virus was collected at 12, 24, 36 and 48 hours. For the GT mutagenesis, 192 million Hap-Lat #1 cells were pre-incubated with 100µM dNTPs (Invitrogen) 1hr before transduction. Cells are resuspended in 192ml of undiluted GT virus. Spin infection was performed for 90minutes @ 1500rpm in 24 well plates containing 2 million cells per well and 8µl protamine sulfate per ml. After 24 hours cells were subjected to a second round of infection after which virus was removed, and cells were left to recover in supplemented IMDM. We estimate that this sequential infection resulted in 1 to 4 GT integrations per cell, with the majority of cells containing one integration (data not shown). A first round of sorting was performed 8 days after the second infection. Subsequently, between 500.000 and 1 million GFP-mCherry double positive cells were sorted each day for 5 consecutive days using two cell sorters (BD FACSAriaII SORP and BD FACSAriaIII). Sorted cells were pooled, left to recover and expanded for the next round of sorting. A second round of sorting was performed 17 days after the second

infection. Between 2.6 and 3 million cells were collected each day for 3 consecutive days using two sorters. These cells were pooled and left to recover and expand for a third round of sorting on day 22 after the second infection, yielding 6.1 million cells from 1-day sorting on two machines. On day 29 after the second infection a fourth round of sorting was performed, yielding 7.2 million cells from 1-day sorting on two machines. After the cells of the fourth round of sorting were left to recover and expand a sub-population of highly mCherry and GFP double positive cells were apparent. In a final fifth round of sorting the total GFP-mCherry positive population (10.1 million cells) and the GFP-mCherry positive high sub-population (5.9 million cells) were respectively sorted on day 33 and 35 after the second infection. After recovery, genomic DNA was isolated from the sorted cell populations, as well as from a population of mutagenized unsorted cells.

Mapping insertion sites through inverse PCR

A previously described inverse PCR protocol was adapted to determine host sequences flanking the proviral insertion sites (Carette et al. 2009). Briefly, genomic DNA was isolated from 5 million cells using the DNAeasy kit (Qiagen). 4ug gDNA was digested with NlaIII or MseI. After PCR spin column purification (Qiagen), 50ul of eluted digested DNA was ligated using T4 DNA ligase (Roche) in a volume of 2ml. The reaction mix was purified using spin columns and used in as template in a PCR reaction with primers annealing to internal sequences in the gene trap vector (5'-CTGCAGCATCGTTCTGTGTT-3' and 5'-TCTCCAAATCTCGGTGGAAC-3'). The resulting PCR products were used for library preparation.

High-throughput sequencing and identification of integration sites

Sequencing libraries were created using the Ion Plus Fragment Library Kit (ThermoFisher Scientific) according to manufacturer's instructions, with minor modifications: briefly, 15ng of the PCR products were diluted with ddH2O to a final volume of 39 µl. The samples were end-repaired, adaptor ligated and amplified; this was followed by 2 rounds of purification using

Agencourt AMPure XP beads. Library qualities and quantities were assessed by Bioanalyzer, using the DNA High Sensitivity Kit (Agilent Technologies). The quantified libraries were pooled together in 10plex, at a final concentration of 40pM. Templating, enrichment and chip loading was performed on an Ion Proton Chef system using the Ion PI™ Hi-Q™ Chef Kits (ThermoFisher Scientific); sequencing was performed on an Ion Proton PI™ V3 chip, with the Ion PI™ Hi-Q™ Sequencing 200 Kit, on an Ion Proton instrument (ThermoFisher Scientific), according to manufacturer's instructions.

The resulting FASTQ files were processed to remove the gene trap vector primers. To this end, we used R/Bioconductor packages ShortRead (Morgan et al. 2009) and Biostrings to match primer sequences within the sequenced reads, allowing for two mismatches at maximum for each primer sequence. The identified primers were trimmed and reads shorter than 15bp were discarded. The remaining reads were aligned to the human reference genome version hg19 retrieved from the Illumina iGenomes repository, using bwa mem. The produced aligned reads (BAM files) were then subjected to integration site identification. To this end, we re-implemented the HaSAPPy algorithm (Minin, Postlmayr, and Wutz 2018) in R. The re-implemented version operates on BAM instead of SAM files and was enriched with additional noise filtering steps, which improved the overall process of detecting integration sites using the Local Outlier Method (LOF), as described in the original HaSAPPy implementation. Specifically, we added attributes for i) filtering out read artifacts from introns, based on the overall intronic read distribution for each sample, ii) selecting the fraction of neighboring (Independent Insertions, Disrupting Insertions, Bias) triplets for LOF analysis and iii) library normalization across samples. After the quality control steps, our HaSAPPY re-implementation assigns a Local Outlier Factor (LOF) score to each gene in a sample based on a triplet score derived from the number of putative GT integrations in the sample compared to the reference, additionally taking into account the potential bias arising from unbalanced sense and anti-sense read numbers. LOF is a metric to indicate to what extent a vector measurement deviates from a population of vectors with the same properties. In our case, a triplet vector corresponds to a gene and LOF measures the deviation from the respective population, i.e. a gene is an

outlier based on a distribution of vectorized scores, such as the aforementioned triplet. The re-implemented version can be found in https://github.com/pmoulos/ngs-stone-age/blob/master/R/hasar.R.

ShRNA knock-down of candidate genes in A2 and 11.1 cell lines

Pre-designed shRNA sequences (MISSION® shRNA library (Sigma); Table 2) were purchased as bacterial glycerol stocks from the Erasmus Center for Biomics. Virus was produced as follows, 3×10^5 HEK293T cells/ml were plated in a 10 cm dish cells one day before transfection and transfected with 4,5 μg of pCMVΔR8.9 (envelope), 2 μg of pCMV-VSV-G (packaging) and 6ug of shRNA vector. The transfection mixure was removed after 12 hr and replaced with fresh RPMI medium contain 10% FBS. Virus containing supernatant was collected at 36, 48, 60- and 72-hours post-transfection. Jurkat, J-Lat A2 (LTR-Tat-IRES-GFP) and J-Lat 11.1 (integrated full-length HIV-1 genome mutated in env gene and GFP replacing Nef) cells were cultured in RPMI-1640 medium (Sigma) supplemented with 10% FBS and 100 μg/ml penicillin-streptomycin at 37 °C in a humidified 95% air-5% CO2 atmosphere. A2 and 11.1 cell lines were infected by adding 500 μl of filtered lentivirus to 2.5 ml of cell culture. After 48 hours, medium was refreshed and cells were puromycin selected. 14 days after infection, RNA was harvested to determine knock-down of genes by qPCR and reactivation of latent HIV was measured by flow-cytometry and RT-qPCR for Gag, Pol and Tat.

Flow cytometry for GFP expression in the J-Lat cell lines

Cells were collected in PBS. GFP fluorescent signal indicating latency reversal was monitored using a LSRFortessa (BD Biosciences). Viability was determined using the forward scatter area versus side scatter area profiles (FSC-A, SSC-A). Data was analyzed using FlowJo software (version 9.7.4, Tree Star).

Total RNA Isolation and Quantitative RT-PCR (RT-qPCR)

Total RNA was isolated from tranduced A2 and 11.1 cells using Trizol (Thermo Fisher) on day 14 after infection using Total RNA Zol out kit

(A&A Biotechnology), residual genomic DNA was digested with DNAseI (Life technologies). cDNA was synthesized using superscript II Reverse Transcriptase (Life Technologies) using oligo (dT) primers or random primers (for Gag, Pol and Tat). RT-qPCR reactions were performed on a CFX Connect Real-Time PCR Detection System thermocycler (BioRad) using GoTaq qPCR Master Mix (Promega) (3 min at 95 °C, followed by 40 cycles of 95 °C for 10 s and 60 °C for 30 s). Melting curve analysis was performed to assess specificity of RT-qPCR products. Primers used for real-time PCR are listed in Table2. Expression data was calculated using 2-ΔΔCt method (Schmittgen and Livak 2008). ß-2-microglobulin (B2M) and GAPDH were used as housekeeping genes for the analysis.

Isolation and ex vivo infection of primary CD4+ T cells

HIV-1 latency *ex vivo* model was generated based on Lassen and Greene method by spinoculation (90 min at 1200 g), washed in PBS and cultured in RPMI 1640 containing 10% FBS, 100 µg/ml penicillin-streptomycin, IL2 (5ng/ml) and the antiretroviral drug Saquinavir Mesylate (5µM) (Lassen et al. 2012). HEK 293T cells were transfected with HXB2 Env and pNL4.3.Luc.R-E- plasmids using PEI (Polyethylenimine) as described above. Supernatants containing pseudovirus particles are collected at 24, 48 and 72 h post-transfection. Peripheral blood mononuclear cells (PBMCs) were isolated by Ficoll density gradient sedimentation of buffy coats from healthy donors. Total CD4+ T cells were separated by negative selection using RosetteSep™ Human CD4+ T Cell Enrichment Cocktail (StemCell Technologies). Primary CD4+ T cells were plated at a concentration of $1{,}5x10^{6}$ cells/mL left overnight for recovery and infected. Two days after infection, cells were collected, washed once with PBS and treated with 5-Iodotubercidin, Topiramate or Trametinib. Cells were collected in 48 hr after treating, washed once in PBS and luciferase activity was measured using Luciferase Assay System (Promega).

Flow cytometry for T cells activation and toxicity assay

Primary CD4+ T cells isolated from buffy coats of healthy volunteers were treated with different concentration of 5-Iodotubercidin, Topiramate and Trametinib and PMA/ionomycin as a positive control.

After 24 and 48 hours, cells were stained with Annexin V to examine the percentage of cells undergoing apoptosis and with the surface receptor CD69 and CD25 to measure T cell activation. For staining, 10^6 cells were washed with PBS supplemented with 3% FBS and 2.5 mM CaCl2 followed by staining with Annexin V-PE (Becton and Dickinson), CD69-FITC (eBioscience) and CD25-APC (eBioscience) for 20 minutes at 4C in the presence of 2.5 mM CaCl2. Cells were then washed with PBS/FBS/CaCl2 and analyzed by flow cytometry. Between 2 - $4x10^5$ events were collected per sample within 3 hours after staining on a LSRFortessa (BD Biosciences, 4 lasers, 18 parameters) and analyzed using FlowJo software (version 9.7.4, Tree Star).

Western Blotting

$10x10^6$ cells were lysed for 30 minutes on ice with 200 ul lysis buffer (150 mM NaCl, 30 mM Tris (pH 7.5), 1 mM EDTA, 1% Triton X-100, 10% Glycerol, 0.5 mM DTT, protease inhibitor cocktail tablets (EDTA-free) (Roche). Cell lysates were clarified by centrifugation (14,000 rpm for 30 min at 4°C), mixed with 4x sodium dodecyl sulfate (SDS)-loading buffer containing 0.1M DTT and boiled at 95°C for 5 min. Samples were run in a 10% SDS-polyacrylamide gel at 100V. The proteins were transferred to polyvinylidene difluoride (PVDF) membranes and the membranes were probed with anti-CHD9 (13402-1-AP, Proteintech) and anti- α-tubulin (ab6160, Abcam). The next day, blots were incubated with HRP conjugated secondary antibody and proteins were imaged by chemical luminescence using SuperSignal West Pico (Thermo Scientific).

Chromatin immunoprecipitation (ChIP) and qPCR

Approximately 50 to 100 million J-Lat 11.1 cells per condition were collected and crosslinked with 1% formaldehyde (Polysciences inc.) in 40 ml PBS, supplemented with 1mM $MgCl_2$ and 1mM $CaCl_2$, at RT for 30 min with 15rpm vertical rotation. The reaction was quenched with 125 mM Glycine. Cross-linked cells were pelleted at 800rcf for 5 minutes RT and subjected to chromatin enrichment as described previously (Ne et al.

2020). Briefly: the pellets were re-suspended in 2 ml ChIP incubation buffer (1% SDS, 1% Triton x-100, 150mM NaCl, 1mM EDTA, ph 8.0, 0.5 mM EGTA, 20mM HEPES pH 7.6, protease inhibitor cocktail tablets (EDTA-free, Roche) containing 1% SDS and sonicated (30' ON/30' OFF intervalsDiogenode Bioruptor plus) to obtain chromatin fragments between 300 and 500bp. Sonicated chromatin was spun at 20817 rcf at 4°C for 30 minutes and diluted 10 times in ChIP incubation buffer without SDS. Diluted chromatin corresponding to 30-40 million cells was precleared overnight at 4°C with vertical rotation at 15rpm with 80uls of Protein A SepharoseTM 4 Fast flow (GE Healthcare) beads and immunoprecipitated overnight with 40uls of beads and 5ug of antibody (13402-1-AP, Proteintech). Samples were washed two times per each buffer (5minutes, 15rpm vertical rotation) with buffer 1 (0.1% SDS, 0.1% DOC, 1% Triton x-100, 150mM NaCl, 1 mM EDTA pH 8.0, 0.5 mM EGTA, 20mM HEPES pH8.0.), buffer 2 (500mM NaCl: 0.1% SDS, 0.1% DOC, 1% Triton x-100, 500mM NaCl, 1 mM EDTA pH 8.0, 0.5mM EGTA, 20mM HEPES pH8.0), buffer 3 (0.25M LiCL, 0.5%DOC, 0.5% NP-40, 1mM EDTA pH 8.0, 0.5mM EGTA pH 8.0, 20mM HEPES pH 8.0), buffer 4 (1mM EDTA pH8.0, 0.5mM EGTA pH 8.0, 20mM HEPES pH 8.0) to remove unspecific binding. Finally, each sample was eluted in 400ul elution buffer (1% SDS, 0.1M $NaHCO_3$) de-crosslinked overnight at 65ºC in presence of 200mM NaCl, phenol-chloroform extracted, ethanol precipitated and subjected to qPCR analysis using the primer sets summarized in Table2.

FIGURES AND FIGURES LEGENDS

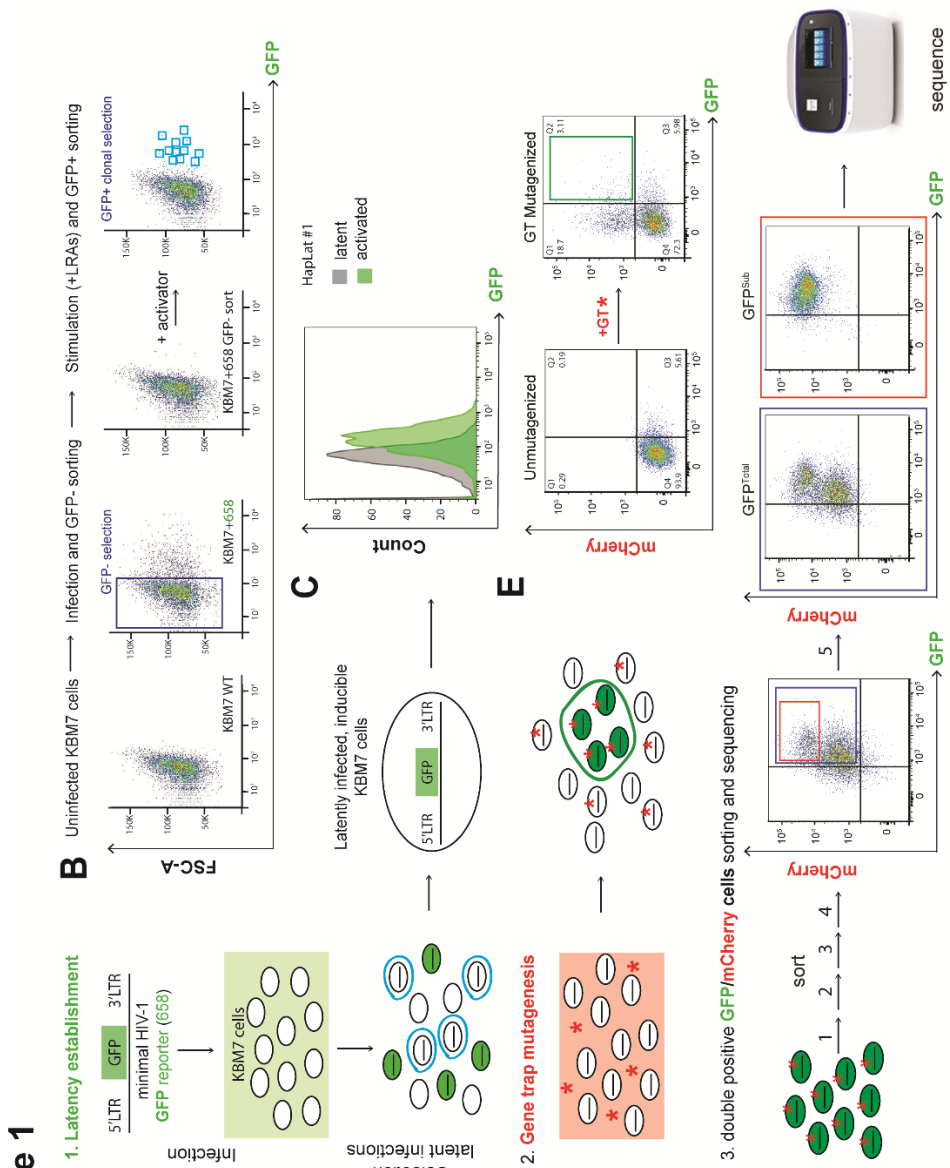

Figure 1 Schematic representation of the two-color haploid screening strategy for identification of novel host factors and cellular pathways involved in the maintenance of HIV latency.

(A) Scheme depicting the generation of a clonal latent haploid KBM7 cell line. To this end, haploid KBM7 cells were infected with a minimal HIV virus harboring GFP (HIV-1 658). After stimulation, reactivated cells were sorted and left to expand and revert to a latent state.

(B) FACS plots depicting the establishment of haploid HIV-1 latently infected KBM7 cell-line (Hap Lat #1). Parental KBM7 cells were infected with a minimal HIV virus carrying a GFP reporter (HIV-1 658). GFP negative cells, consisting of uninfected and latently infected cells, were sorted by FACS. The polyclonal cell pool was stimulated with a cocktail of latency reversal agents (LRAs) and reactivated cells were clonally sorted by FACS and expanded to generate haploid latent cell lines.

(C) Hap-Lat #1 displays low basal activity (GFP expression) but is effectively reactivated using LRAs.

(D) Hap-Lat#1 cells were mutagenized by infection with a Gene Trap (GT) virus infection harboring a mCherry reporter. Cells infected with the GT reporter will be mCherry positive (red asterisk). Latently infected KBM7 cells that reactivate following GT mutagenesis will be double positive for GFP and mCherry (Green cells, red asterisk).(E) Representative FACS plots demonstrating gating strategy for sorting double positive cells (GFP, mCherry).

(F) Double positive cells (GFP, mCherry) are sorted in multiple rounds to eliminate cells stochastically reverting back to a GFP negative state. During these rounds of sorting, a stable and distinct double positive sub-population (GFP Sub) appears which was sorted separately.

Figure 2

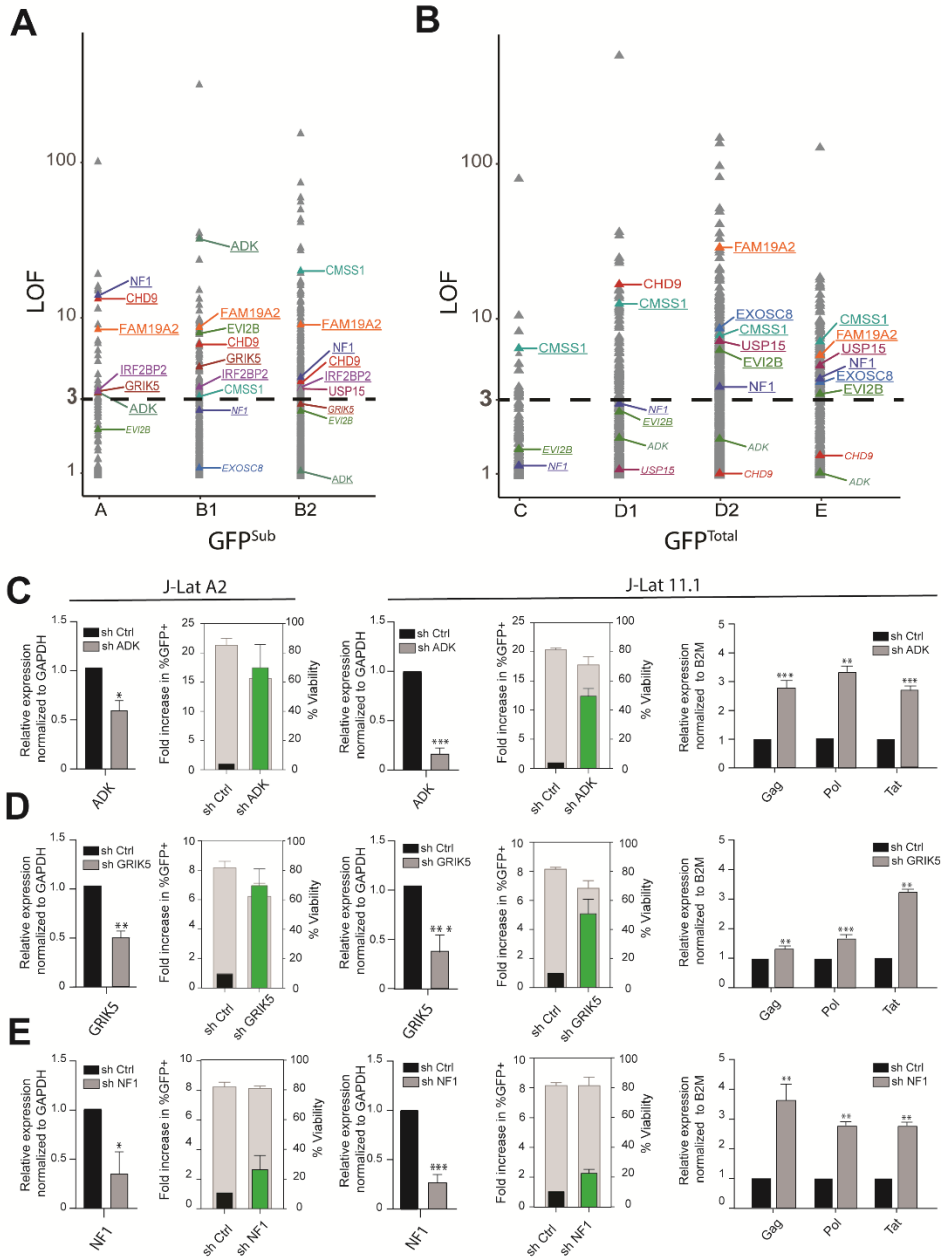
A
B
LOF
100
10
3
1
A
B1
B2
C
D1
D2
E
GFPSub
GFPTotal
NF1
CHD9
FAM19A2
IRF2BP2
GRIK5
ADK
EVI2B
CMSS1
EXOSC8
USP15
C
J-Lat A2
J-Lat 11.1
D
E
sh Ctrl
sh ADK
sh GRIK5
sh NF1
Relative expression normalized to GAPDH
Fold increase in %GFP+
% Viability
Relative expression normalized to B2M
Gag
Pol
Tat

Figure 2 Identification and validation of candidate host factors.
(A) LOF scores of genes in the GFP^{sub} population (samples A, B1 and B2), validated candidates are indicated. Genes with LOF>3 are in large font, underlined genes comply to our candidate gene selection criteria and have a LOF>3 in at least two biological replicates within either the GFP^{sub} or GFP^{total} population while genes with LOF<3 but complying to our selection criteria based on other samples are depicted in small font and italics.
(B) LOF scores of genes in the GFP^{total} population (samples C,D1,D2 and E), Markings as in Figure 2A.
(C) Functional validation of candidate hits ADK, GRIK5, NF1 by shRNA mediated depletion followed by determination of latency reversal by flow-cytometry and RT-PCR in latently infected J-Lat A2 (left panels) and 11.1 cells (right panels). Flow-cytometry bar plots: green bars show the percent of GFP positive cells after knockdown over control (black bar), left y-axis, whereas gray bars show cell viability, right y-axis. Viral reactivation is confirmed by RT-qPCR for viral genes Tat, Gag and Pol in J-Lat 11.1 cells. Statistical significance was calculated using ratio-paired t-test and multiple comparison t-test on Log2 transformed fold changes * – $p < 0,05$, ** – $p < 0,01$, *** – $p < 0,001$,

Figure 3

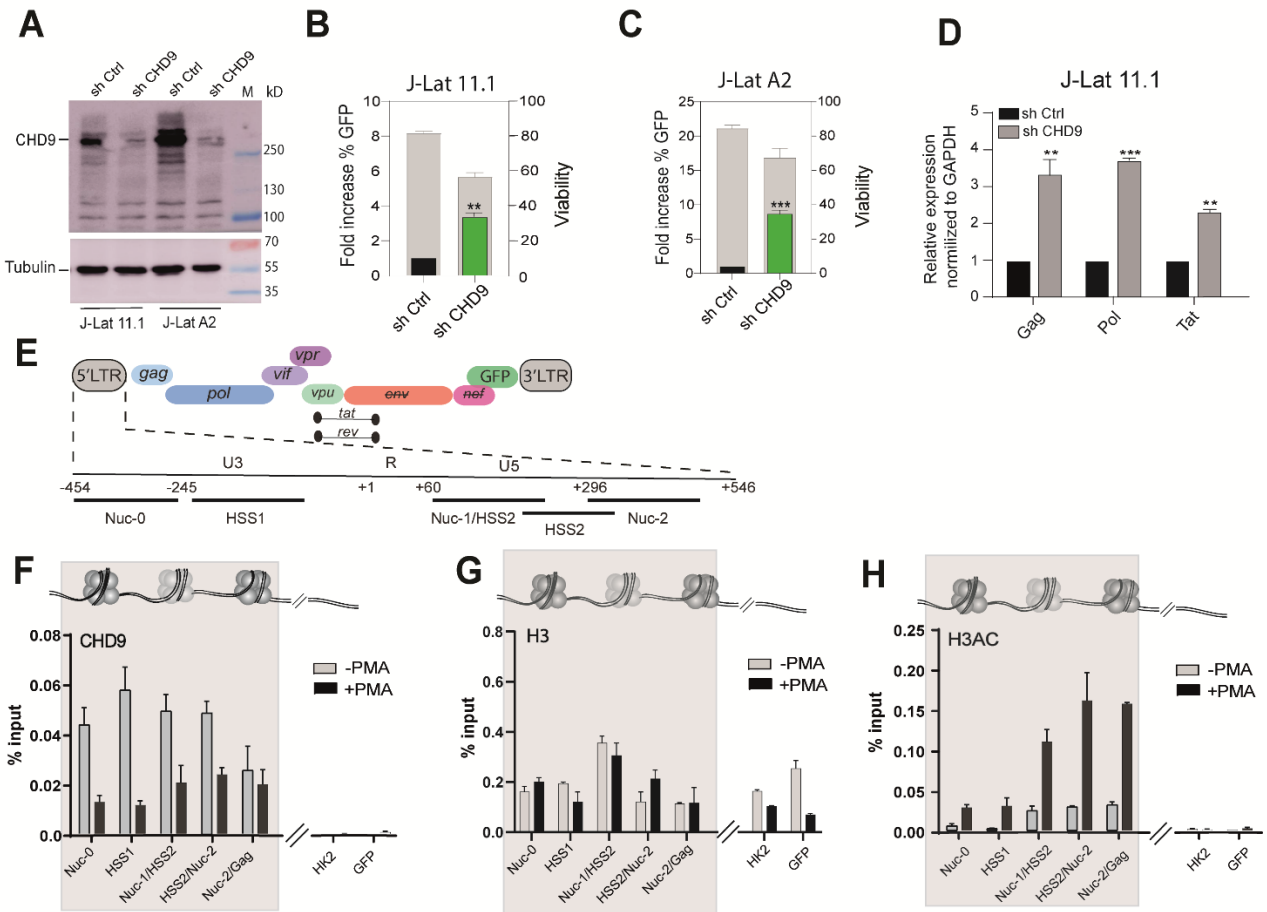
A
sh Ctrl
sh CHD9
sh Ctrl
sh CHD9
M
kD
CHD9
250
130
100
70
55
35
Tubulin
J-Lat 11.1
J-Lat A2
B
J-Lat 11.1
Fold increase % GFP
Viability
sh Ctrl
sh CHD9
C
J-Lat A2
Fold increase % GFP
Viability
sh Ctrl
sh CHD9
D
J-Lat 11.1
sh Ctrl
sh CHD9
Relative expression normlized to GAPDH
Gag
Pol
Tat
E
5'LTR
gag
pol
vpr
vif
vpu
env
rev
tat
rev
GFP
3'LTR
U3
R
U5
-454
-245
+1
+60
+296
+546
Nuc-0
HSS1
Nuc-1/HSS2
HSS2
Nuc-2
F
CHD9
% input
-PMA
+PMA
Nuc-0
HSS1
Nuc-1/HSS2
HSS2/Nuc-2
Nuc-2/Gag
HK2
GFP
G
H3
% input
-PMA
+PMA
H
H3AC
% input
-PMA
+PMA

Figure 3 CHD9 regulates HIV-1latency in J-Lat A2s and J-Lat 11.1 cells.
(A) Western blot for CHD9 in control and CHD9 shRNA depleted J-Lat 11.1 and A2 cells, α-Tubulin as a loading control.
(B) Flow-cytometry bar plots demonstrating latency reversal after CHD9 shRNA depletion in J-Lat 11.1 cells: green bars indicate the percent of GFP positive cells after knockdown over control (black bar), left y-axis, whereas gray bars show cell viability, right y-axis.
(C) Latency reversal after CHD9 shRNA depletion in J-Lat A2 cells.
(D) Viral reactivation is confirmed by RT-qPCR in J-Lat 11.1 cells for the viral genes Tat, Gag and Pol. Data are normalized to GAPDH and represented as fold increase over sh Control. Statistical significance was calculated using ratio-paired t-test and multiple comparison t-test on Log2 transformed fold changes * – $p < 0,05$, ** – $p < 0,01$, *** – $p < 0,001$.
(E) Schematic of HIV genome. 5' LTR region further segmented into the U3, R, and U5 regions. Amplicons used in ChIP-qPCR experiments are indicated.
(F) ChIP-qPCR analysis of CHD9 binding to the HIV-1 5'LTR in untreated and PMA stimulated J-Lat 11.1 cells. Data are represented as percentage of the input.
(G) ChIP-qPCR analysis of Histone H3 occupancy at the HIV-1 5'LTR untreated and PMA stimulated J-Lat 11.1 cells. Data are represented as percentage of the input.
(H) ChIP-qPCR analysis of Histone H3 acetylation at the HIV-1 5'LTR in untreated and PMA stimulated J-Lat 11.1cells. (E-H) Data represent the average (±SD) of two technical replicates.

Figure 4

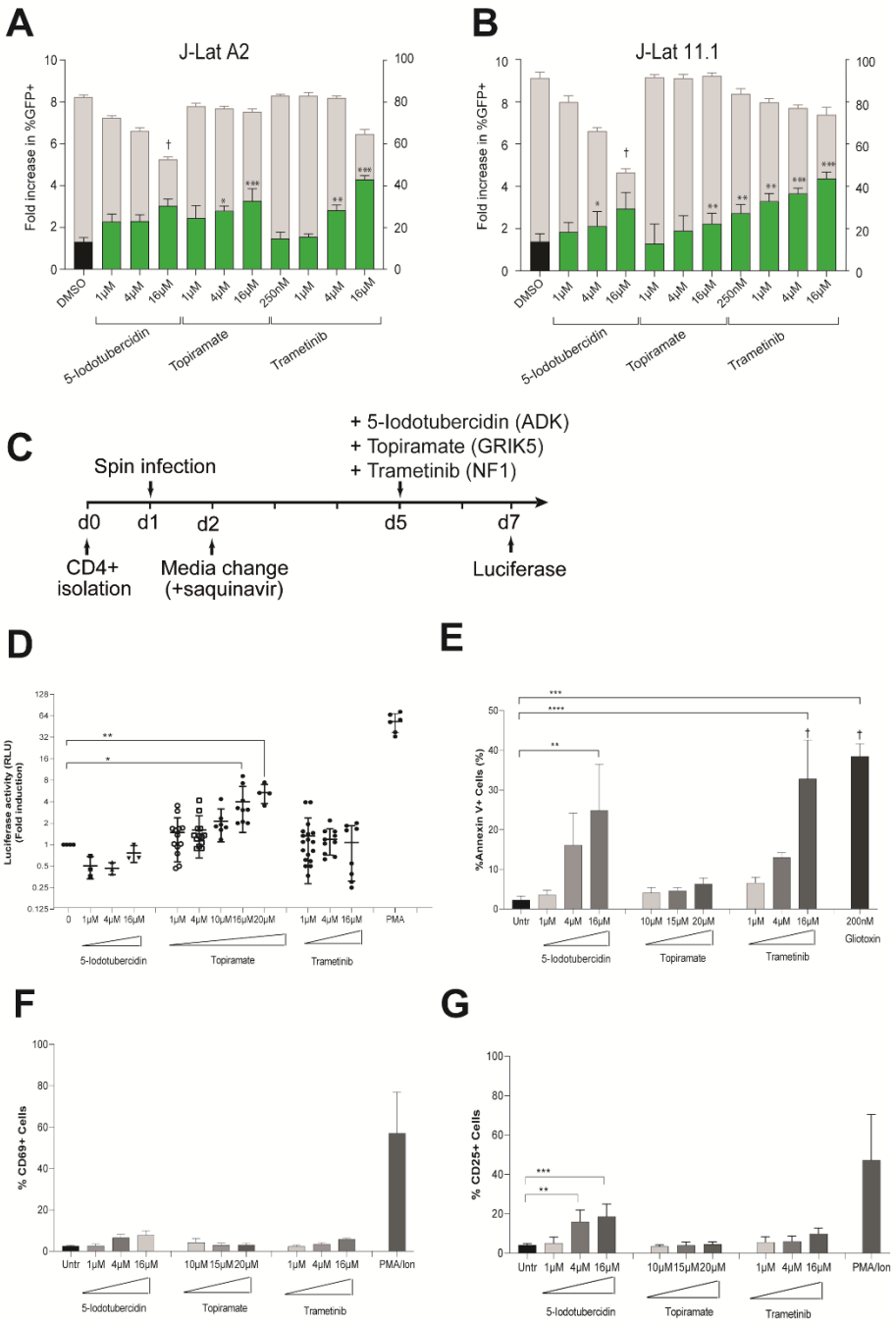

Figure 4 HIV latency reversal by small molecule inhibitors of three candidate genes ADK, GRIK5, NF1.

(A) Latency reversal potential upon 48 h treatment of J-Lat A2 cells with increasing concentrations of 5-iodotubercidin (ADK inhibitor), Topiramate (GRIK5 inhibitor) and Trametinib (NF1 inhibitor) was evaluated by flow-cytometry. Treatment with DMSO (black bar) is used as a negative control. Percent of GFP positive cells is indicated by green bars (left y-axes), cell viability is indicated by grey bars (right y-axis). (B) Latency reversal potential upon 48 h treatment of J-Lat 11.1 cells.(C) Schematic representation of candidate LRAs treatment in a primary cell model of latent HIV-1 infection. CD4+ T-cells are isolated on day 0 and spin infected on day 1. On day 2 virus is removed by media change in presence of saquinavir. Latently infected cells are stimulated with candidate LRAs on day 5 and HIV reactivation is evaluated at day 7. (D) Latency reversal as measured by Luciferase activity in a primary cell model of HIV latency after treatment with 5-Iodotubercidin, Trametinib and Topiramate in different concentrations. Plots show the fold increase in luciferase activity, measured in relative light units (RLU), after treatment with different concentrations of 5-iodotubercidin (ADK inhibitor), Topiramate (GRIK5 inhibitor) and Trametinib (NF1 inhibitor). Each dot represents a single measurement, black horizontal lines show the average fold increase for each treatment. Averaged data of at least 3 independent experiments performed using each time two different donors (totaling at least 6 different donors). PMA was used as a positive control. Statistical significance was calculated using t test, * – p<0,05; ** – p<0,005; *** – p<0,0005.
(E) Percentage of cells expressing apoptosis marker Annexin V in primary CD4+ T cells upon treatment with candidate LRAs for 48 hours. Treatment with a toxic concentration of Gliotoxin (GTX) 200nM was used as a positive control. Experiments were performed in uninfected cells obtained from 6 healthy donors. Data are presented as mean ±SD from three independent experiments. The (†) symbol indicates low viability.(F) Percentage of cells expressing marker of cell activation CD69 in primary CD4+ T cells from 6 healthy donors, data are presented as mean ±SD from three independent experiments of 2 different healthy donors upon treatment with candidate LRAs for 48 hours. Treatment with PMA/Ionomycin PMA is used as a positive control. (G) Percentage of cells expressing marker of cell activation CD25 in primary CD4+ T cells from 6 healthy donors, data are presented as Mean ±SD from three independent experiments of 2 different healthy donors upon treatment with candidate LRAs for 48 hours. Treatment with PMA/Ionomycin is used as a positive control. Statistical significance was calculated using one-way Anova, multiple comparison test. Asterisks indicate the level of significance. (**p < 0.01, ***p < 0.001).

S1

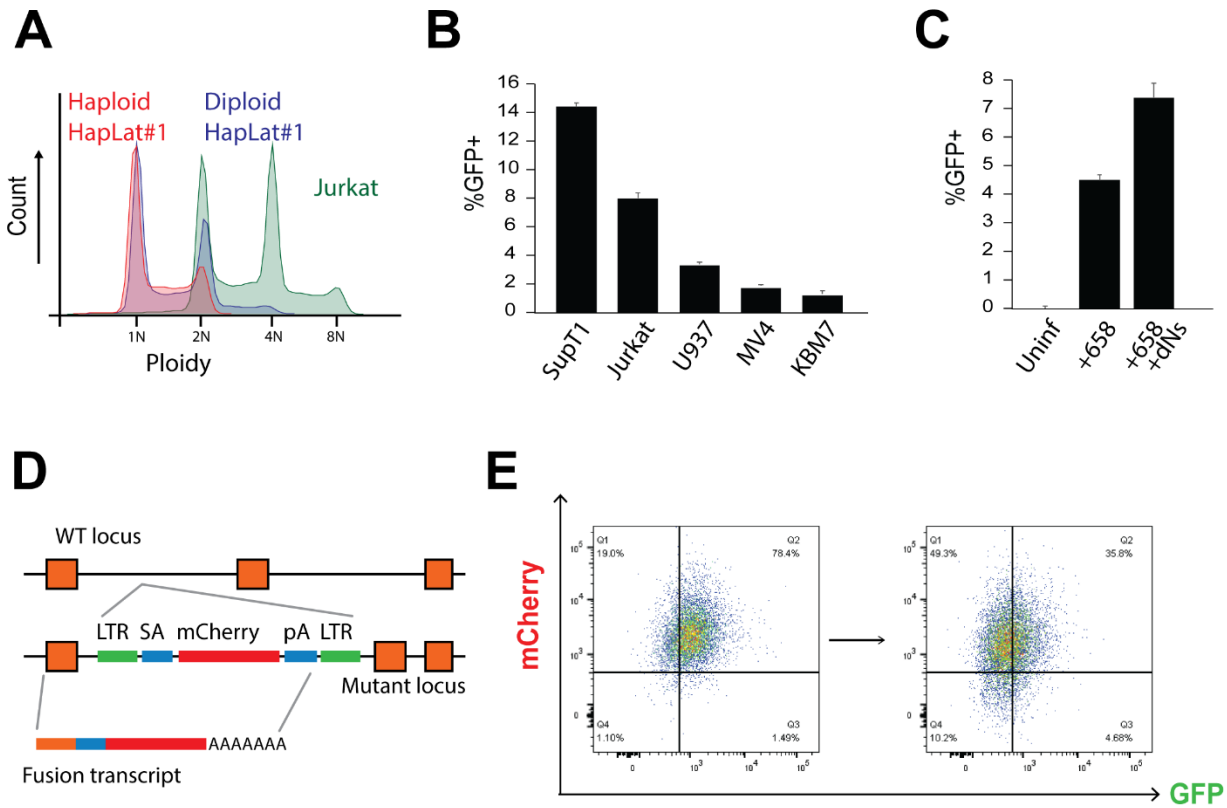
A
Haploid
HapLat#1
Diploid
HapLat#1
Jurkat
Count
1N
2N
4N
8N
Ploidy
B
%GFP+
SupT1
Jurkat
U937
MV4
KBM7
C
%GFP+
Uninf
+658
+658
+dNs
D
WT locus
LTR SA mCherry pA LTR
Mutant locus
AAAAAAA
Fusion transcript
E
mCherry
GFP
Q1
19.0%
Q2
78.4%
Q4
1.10%
Q3
1.49%
Q1
49.3%
Q2
35.8%
Q4
10.2%
Q3
4.68%

Supplemental Figure 1 Generation of haploid latent cell lines.
(A) Ploidy of Hap-Lat #1 compared to Hap-Lat #1 cells cultured over a prolonged period and Jurkat cells. Haploidy of HapLat #1 cells can be maintained over time by periodic cell sorting of small cells.
(B) Infectivity to HIV-1 of KBM7 and other myeloid lineage cell lines, U937 and MV4, is poor compared to lymphocyte derived cell lines (SupT1 and Jurkat) as shown by percentage GFP positive cells after 4 days of infections with minimal HIV (658).
(C) Nucleoside pre-incubation before and after supplementation during infection improves infectivity of KBM7 cells.
(D) Schematic representing the mechanism of GT insertional mutagenesis. The inactive LTRs of MSCV flank a splice acceptor (SA) site, a mCherry reporter and a poly-adenylation (pA) terminator,
(E) After sorting and expansion, sorted double-positive cells tend to revert to a latent state as indicated by a loss of GFP signal. FACS plots obtained 1day (left panel) and 5 days (right panel) after sorting.

S2

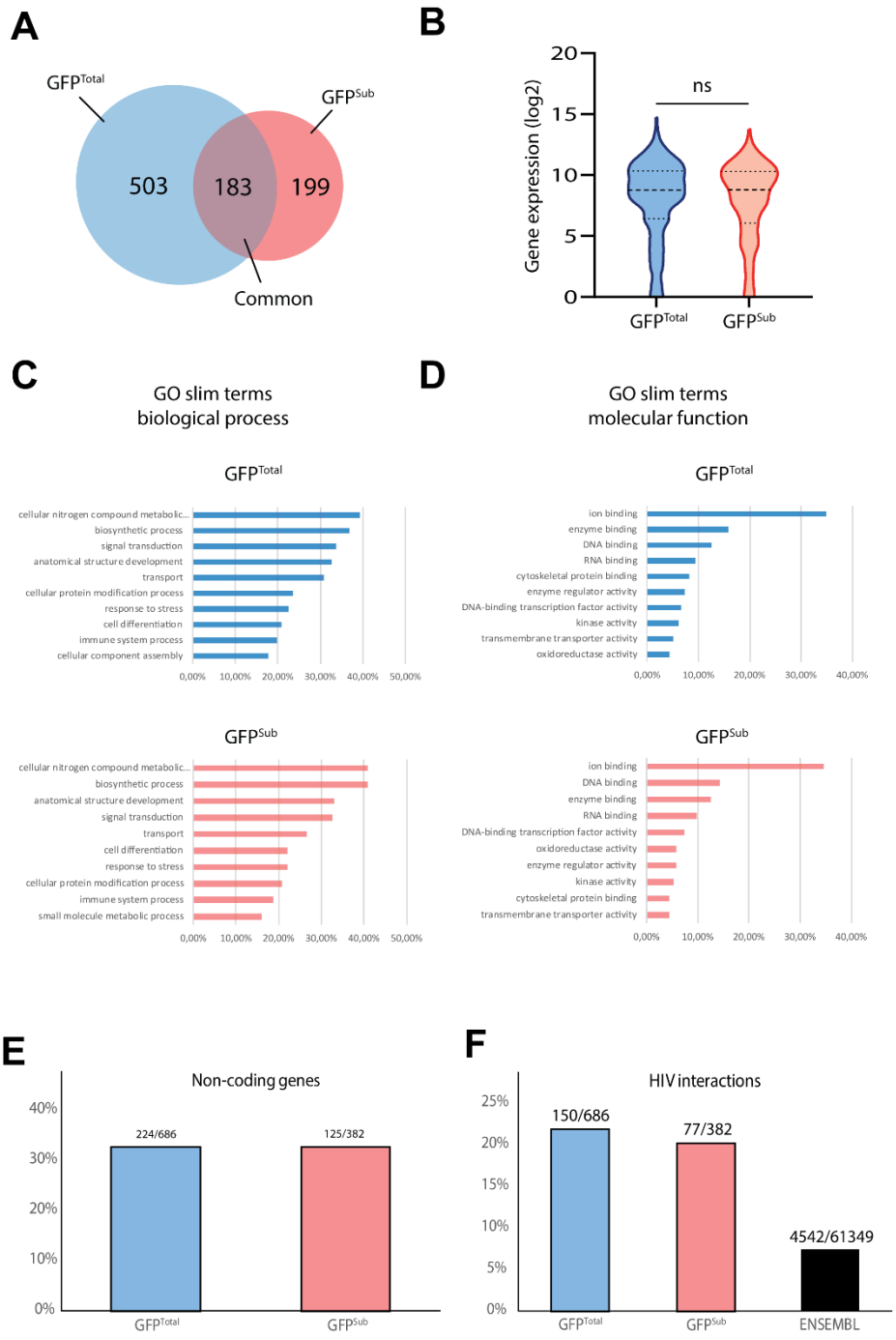
A
GFPTotal
GFPSub
503
183
199
Common
B
Gene expression (log2)
20
15
10
5
0
ns
GFPTotal
GFPSub
C
GO slim terms
biological process
GFPTotal
cellular nitrogen compound metabolic...
biosynthetic process
signal transduction
anatomical structure development
transport
cellular protein modification process
response to stress
cell differentiation
immune system process
cellular component assembly
0,00% 10,00% 20,00% 30,00% 40,00% 50,00%
GFPSub
cellular nitrogen compound metabolic...
biosynthetic process
anatomical structure development
signal transduction
transport
cell differentiation
response to stress
cellular protein modification process
immune system process
small molecule metabolic process
0,00% 10,00% 20,00% 30,00% 40,00% 50,00%
D
GO slim terms
molecular function
GFPTotal
ion binding
enzyme binding
DNA binding
RNA binding
cytoskeletal protein binding
enzyme regulator activity
DNA-binding transcription factor activity
kinase activity
transmembrane transporter activity
oxidoreductase activity
0,00% 10,00% 20,00% 30,00% 40,00%
GFPSub
ion binding
DNA binding
enzyme binding
RNA binding
DNA-binding transcription factor activity
oxidoreductase activity
enzyme regulator activity
kinase activity
cytoskeletal protein binding
transmembrane transporter activity
0,00% 10,00% 20,00% 30,00% 40,00%
E
Non-coding genes
40%
30%
20%
10%
0%
224/686
125/382
GFPTotal
GFPSub
F
HIV interactions
25%
20%
15%
10%
5%
0%
150/686
77/382
4542/61349
GFPTotal
GFPSub
ENSEMBL

Supplemental Figure 2 Characterization of gene trap integration candidate genes.

(A) Venn diagram depicting all genes with an LOF score >3 in one replicate from the GFP^{Total} (686 hits) and the GFP^{Sub} (382 hits) population. 183 genes are common to both populations.

(B) Expression levels of genes in the GFP^{Total} and the GFP^{Sub} populations. No significant differences in the average expression levels of genes between the two populations is found (Mann-Whitney test).

(C) GO-slim term analysis for biological process of genes in the GFP^{Total} and the GFP^{Sub} populations. No substantial differences in GO-slim term enrichment are found.

(D) GO-slim term analysis for molecular function of genes from both populations.

(E) Percentage of non-coding genes present among genes in the GFP^{Total} and the GFP^{Sub} populations are similar.

(F) Percentage of genes present in the HIV interaction database (https://www.ncbi.nlm.nih.gov/genome/viruses/retroviruses/hiv-1/interactions/) among genes in the GFP^{Total} and the GFP^{Sub} populations are similar but higher compared to the total ENSEMBL gene list.

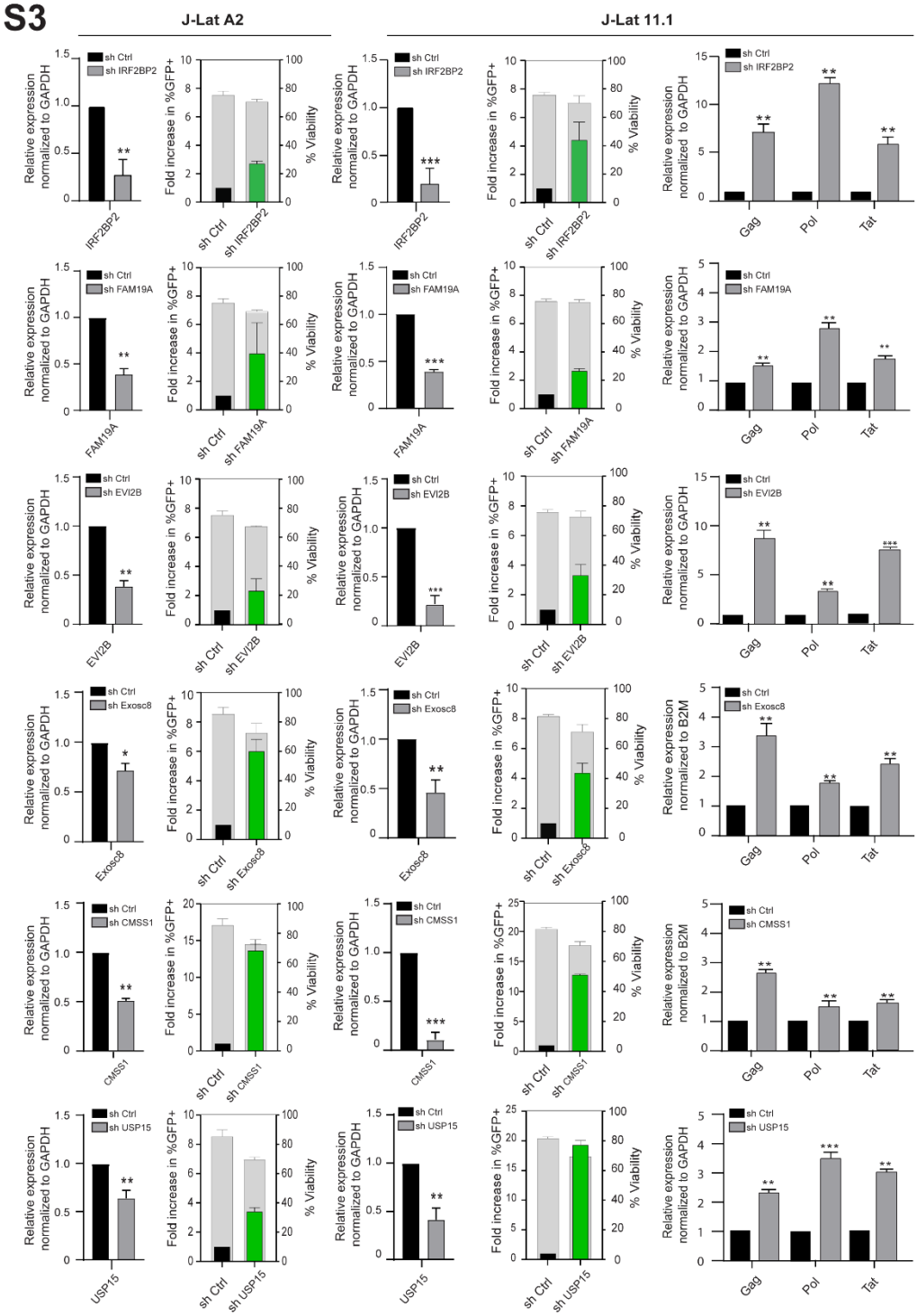
S3
J-Lat A2
J-Lat 11.1
sh Ctrl
sh IRF2BP2
sh FAM19A
sh EVI2B
sh Exosc8
sh CMSS1
sh USP15
Relative expression normalized to GAPDH
Relative expression normalized to B2M
Fold increase in %GFP+
% Viability
IRF2BP2
FAM19A
EVI2B
Exosc8
CMSS1
USP15
Gag
Pol
Tat

Supplemental Figure 3 Functional validation of positive candidates.
Re-activation of HIV-1 in J-Lat A2 and 11.1 cell lines was assessed by measuring the percentage of cells expressing GFP (green bars) and cell viability (gray bars) using flow-cytometry. Efficacy of knockdown by shRNA was quantitated in J-Lat 11.1 cells by RT-qPCR (left panel) as well as expression of viral genes Tat, Pol and Gag. RT-qPCR data (right panel) are presented as mean ± SD normalized to the control. Statistical significance was calculated using ratio-paired t-test and multiple comparison t-test on Log2 transformed fold changes (* – $p < 0,05$, ** – $p < 0,01$, *** – $p < 0,001$).

S4

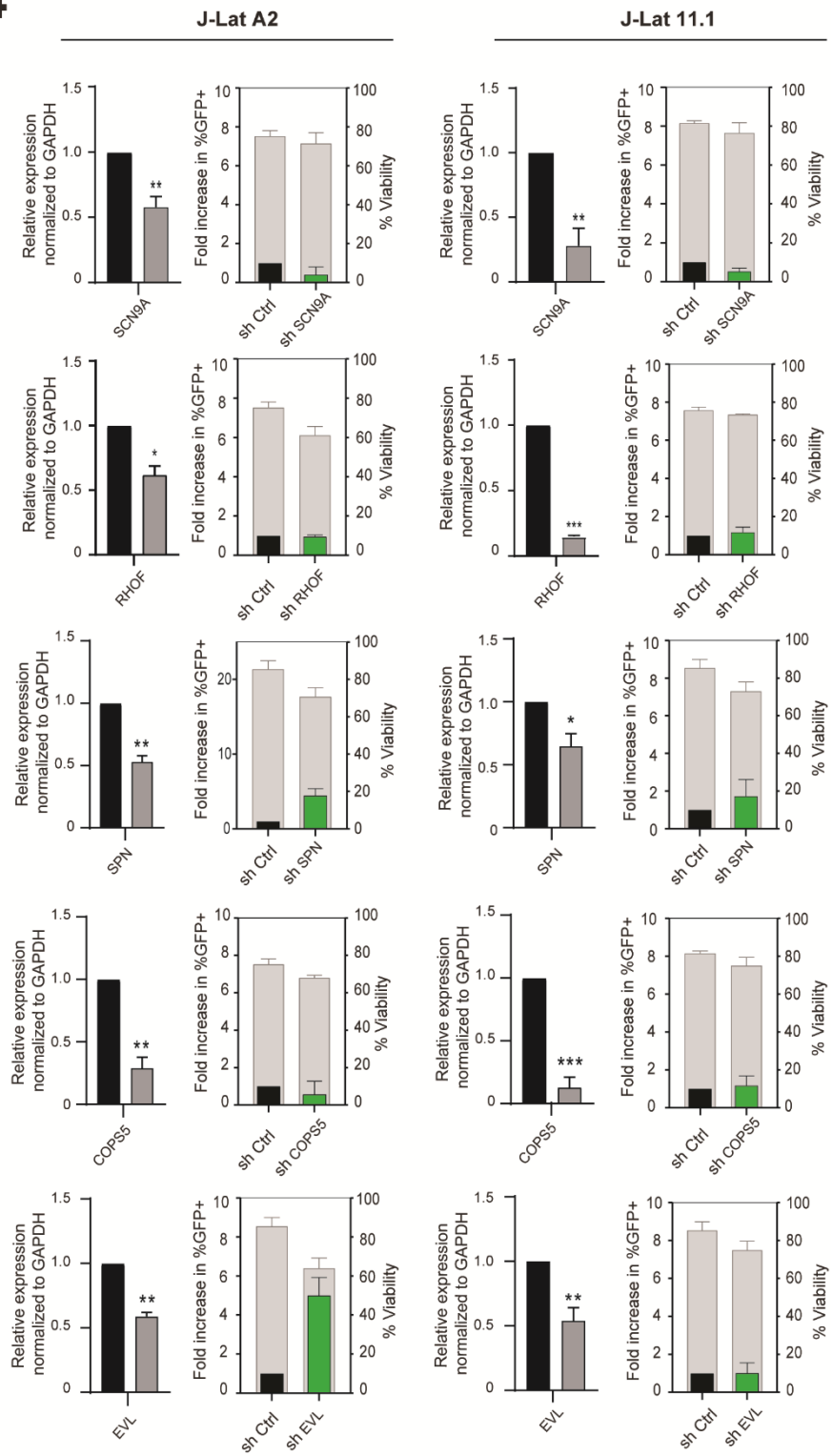
J-Lat A2
J-Lat 11.1
Relative expression normalized to GAPDH
Fold increase in %GFP+
% Viability
SCN9A
sh Ctrl
sh SCN9A
RHOF
sh RHOF
SPN
sh SPN
COPS5
sh COPS5
EVL
sh EVL

Supplemental Figure 4 Functional validation of false positive candidates. Efficacy of knockdown by shRNA was quantitated by RT-qPCR. Re-activation of HIV-1 was assessed by measuring by the percentage of cells expressing GFP (green bars) and cell viability (gray bars). RT-qPCR data are presented as mean ± SD normalized to the control. Statistical significance was calculated using ratio-paired t-test and multiple comparison t-test on Log2 transformed fold changes (* – $p < 0,05$, ** – $p < 0,01$, *** – $p < 0,001$).

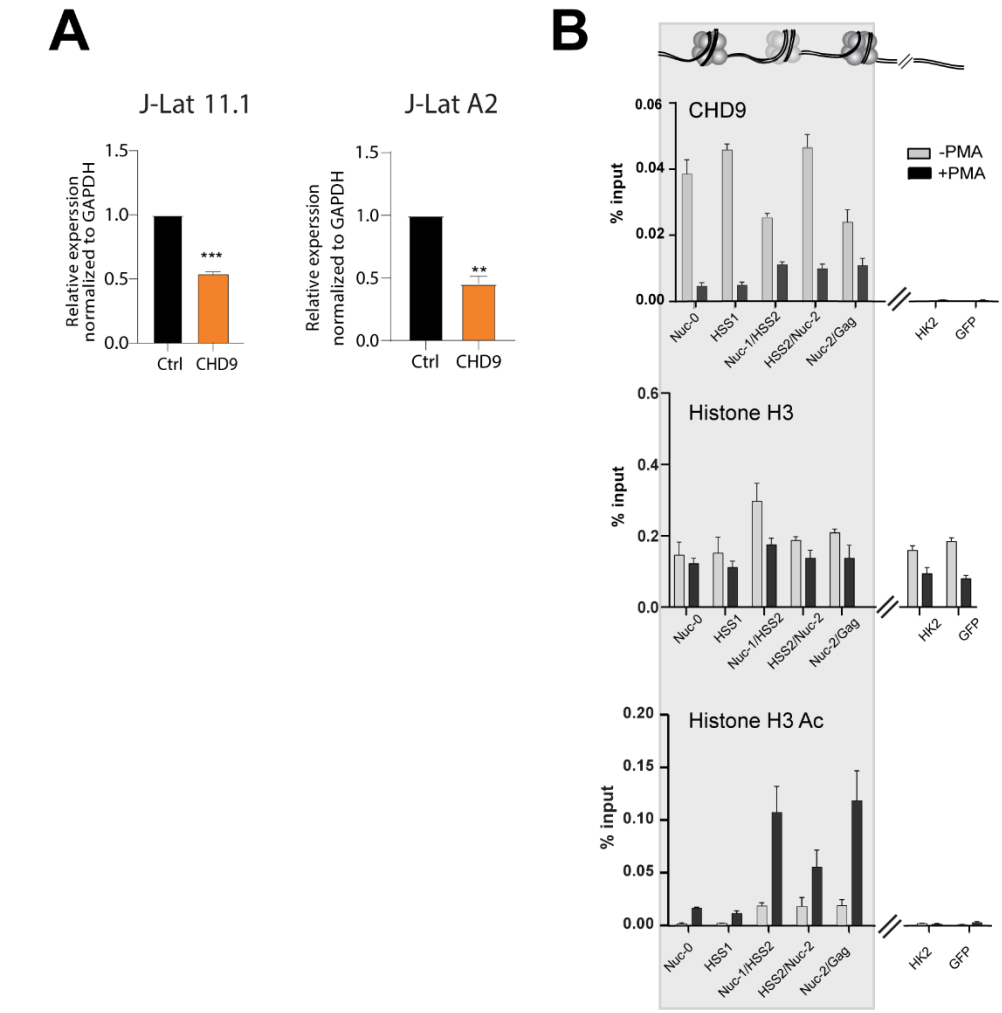

Supplemental Figure 5 Additional data on the functional characterization of CHD9.

(A) Efficacy of CHD9 knockdown in J-Lat A2 cells and J-Lat 11.1 cells by shRNA was quantitated by RT qPCR

(B) Biological replicate of a ChIP-qPCR analysis of CHD9 binding to the HIV-1 5'LTR in untreated J-Lat 11.1 cells and PMA stimulated cells (Similar to data from figure 3G-H). Data are represented as percentage of the input and represent the average (±SD) of two technical replicates.

S6

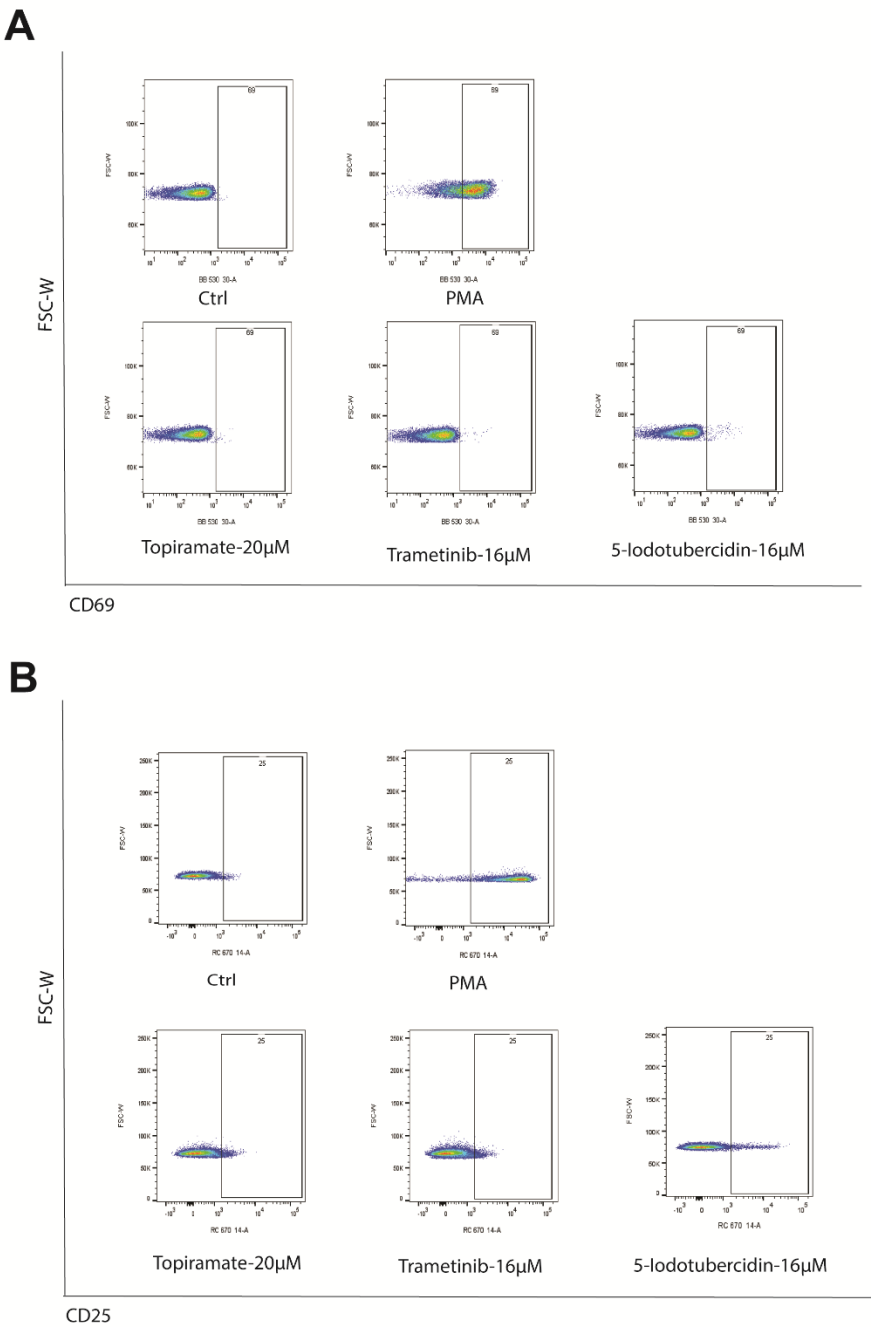

Supplemental Figure 6 Characterization of T-cell activation by candidate LRAs.

(A) FACS plot of staining for T-cell activation marker CD69 after treatment of primary CD4+ T cells from 6 healthy donors with candidate LRAs (5-

Iodotubercidin, Topiramate and Trametinib). Treatment with PMA/Ionomycin PMA is used as a positive control (Plots correspond to data from figure 4F).
(B) FACS plot of staining for T-cell activation marker CD25 after treatment with candidate LRAs (Plots correspond to data from figure 4G).

S7

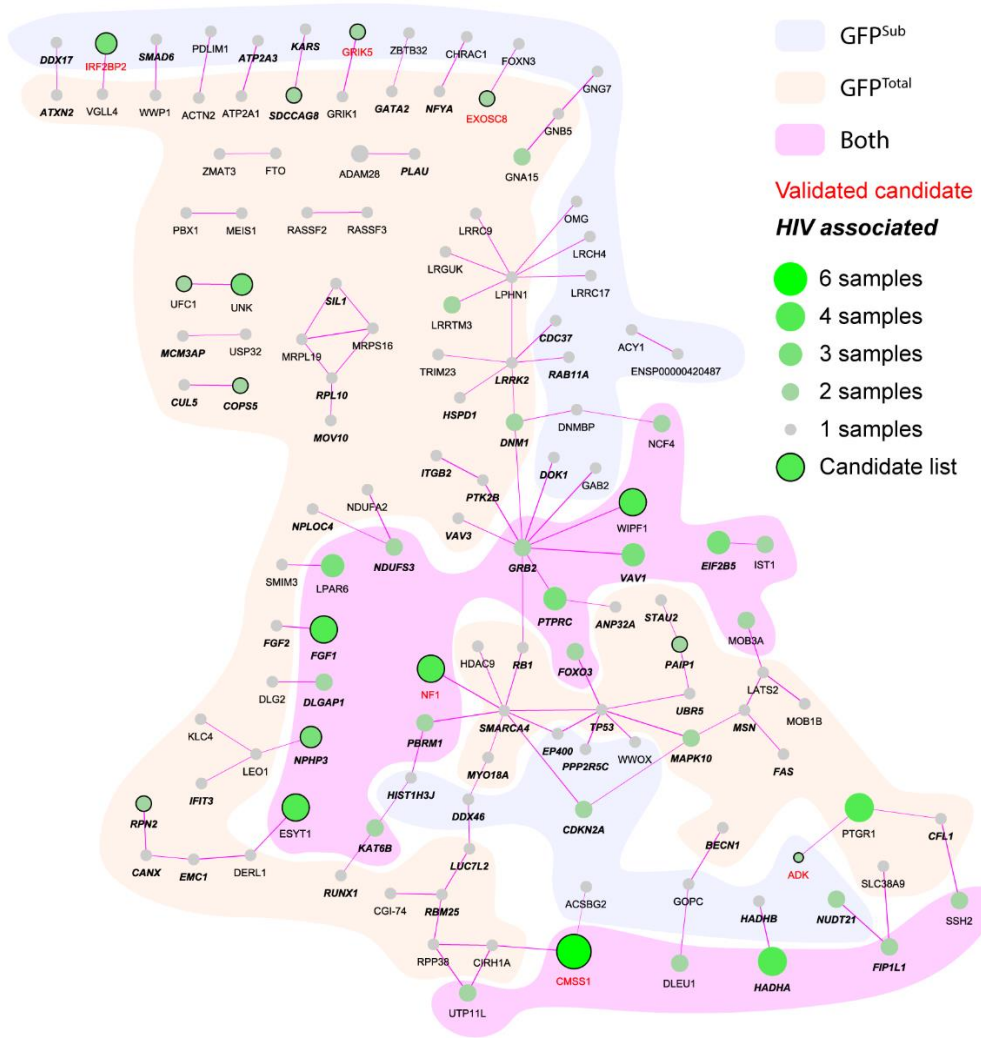

Supplemental Figure 7 STRING analysis of protein coding candidate genes. STRING analysis indicates that many of the 598 protein coding candidate genes with an LOF score of 3 and higher from the GFP^{Total} and the GFP^{Sub} populations functionally interact. Validated candidate genes are indicated in red. Circle size

and green shade indicate the number of samples the Gene Trap target gene is found in. Circled genes are part of our candidate genes list. Background color indicates if the Gene Trap target gene is found in the GFP^{Total}, in the GFP^{Sub} or in both populations.

Table 1

Candidate gene list GFP^{Sub}

	Sub population			Total population				Expr (100*FPKM)1/2		Knock Down		GFP-FACS		HIV genes expression			Full name	HIV-1
Gene name	A	B1	B2	C	D1	D2	E	WBC	Jurkat	A2	11.1	A2	11.1	GAG	POL	TAT		Interactions
AC005616.1	3,4	3,7	3,4	0,0	1,9	0,0	3,4	0,58	Na								Non-coding mRNA	
AC079466.1	3,4	3,5	2,2	0,0	1,6	4,3	9,7	NA	NA								Non-coding mRNA	
ADK	3,3	32,2	1,0	0,0	1,7	1,7	1,0	16	469.5	√	√	√	√	√	√	√	Adenosine Kinase	
CAPN9	3,3	0,0	4,0	0,0	0,0	0,0	0,0	0.8	3								Calpain 9	√
CHD9	13,3	6,8	3,9	0,0	10,3	1,0	1,3	15	672	√	√	√	√	√	√	√	Chromodomain Helicase DNA Binding Protein 9	
CTD-2066I21.3	3,7	4,1	74,0	3,6	0,0	27,7	5,1	NA	NA								Non-coding mRNA	
ESYT1	3,5	3,5	0,0	0,0	4,5	6,1	0,0	81	2328								Extended Synaptotagmin 1	
FAM19A2	8,4	8,7	9,0	0,0	0,0	28,9	5,8	NA	24.5	√	√	√	√	√	√	√	Family With Sequence Similarity 19 Member A2	
FGF1	3,7	4,1	1,2	0,0	4,3	4,3	0,0	3	0								Fibroblast Growth Factor 1	√
GRIK5	3,3	4,8	2,8	0,0	0,0	0,0	0,0	4	9	√	√	√	√	√	√	√	Glutamate Ionotropic Receptor Kainate Type Subunit 5	
IRF2BP2	3,4	3,6	3,5	0,0	0,0	0,0	0,0	9	2205	√	√	√	√	√	√	√	Interferon Regulatory Factor 2 Binding Protein 2	
NF1	14,0	2,5	4,1	1,1	2,8	3,6	4,1	10	1452	√	√	√	√	√	√	√	Neurofibromin 1	
RP11-355N15.1	19,1	9,2	9,2	4,7	3,2	6,4	0,0	NA	NA								Non-coding mRNA	
RP11-755B10.4	3,3	1,0	6,8	0,0	4,4	1,0	0,0	NA	NA								Non-coding mRNA	
RP4-569M23.2	3,0	0,0	4,8	0,0	0,0	3,3	0,0	NA	NA								Non-coding mRNA	
RP4-613B23.1	6,8	4,6	0,0	0,0	4,2	0,0	0,0	NA	NA								Non-coding mRNA	
SCN9A	3,5	3,1	1,7	0,0	0,0	0,0	0,0	4	2.5	√	√	X	X				Sodium Voltage-Gated Channel Alpha Subunit 9	
SPN	11,5	2,8	6,0	0,0	0,0	1,0	0,0	60	8743	√	√	X	X				Sialophorin	√
ZNF385D	3,9	4,1	1,0	0,0	0,0	1,1	0,0	7	3								Zinc Finger Protein 385D	

Candidate gene list GFP^{Total}

	Sub population			Total population				Expr (100*FPKM)1/2		Knock Down		GFP-FACS		HIV genes expression			FullName	HIV-1
Gene name	A	B1	B2	C	D1	D2	E	WBC	Jurkat	A2	11.1	A2	11.1	GAG	POL	TAT		Interactions
AC004381.7	0,0	1,2	0,0	0,0	0,0	3,0	5,8	NA	NA								Non-coding mRNA	
AC018890.6	0,0	6,8	4,3	0,0	4,0	9,4	3,6	NA	NA								Non-coding mRNA	
AC079466.1	3,4	3,5	2,2	0,0	1,6	4,3	9,7	NA	NA								Non-coding mRNA	
AC084018.1	0,0	2,5	2,8	0,0	0,0	5,4	4,1	NA	NA								Non-coding mRNA	
ACSM3	1,1	3,2	8,5	0,0	1,3	11,5	3,4	5	9								Acyl-CoA Synthetase Medium Chain Family Member 3	
ALDH1A2	9,0	1,2	2,2	4,6	3,7	3,3	0,0	6	833								Aldehyde Dehydrogenase 1 Family Member A2	
AVL9	0,0	3,5	1,3	3,4	3,1	2,3	0,0	15	420								AVL9 Cell Migration Associated	
C17orf64	0,0	8,6	16,7	0,0	15,3	13,8	5,4	2	0								Chromosome 17 Open Reading Frame 64	
C9orf139	1,1	2,4	2,1	8,3	3,0	10,6	1,0	NA	12								Chromosome 9 Open Reading Frame 139	
CCDC26	1,0	1,6	1,2	0,0	4,1	2,0	9,6	6	NA								CCDC26 Long Non-Coding RNA	
CDH23	0,0	13,1	3,5	2,2	4,1	3,4	4,2	15	57								Cadherin Related 23	√
CIITA	0,0	1,8	6,0	3,3	2,7	2,9	4,2	26	1								Class II Major Histocompatibility Complex Transactivator	√
CMSS1	0,0	3,1	20,0	6,4	12,5	7,8	7,1	8	1066	√	√	√	√	√	√	√	Cms1 Ribosomal Small Subunit Homolog	
COPS5	0,0	0,0	1,0	0,0	5,5	1,1	6,6	52	1337	√	√	X	X				COP9 Signalosome Subunit 5	√
CTD-2066I21.3	3,7	4,1	74,0	3,6	0,0	27,7	5,1	NA	NA								Non-coding mRNA	
CTD-2260A17.2	3,7	0,0	1,7	0,0	0,0	5,2	4,5	NA	NA								Non-coding mRNA	
CTD-2370N5.3	2,7	13,2	3,7	2,3	6,0	8,8	3,0	NA	NA								Non-coding mRNA	
CTD-2376I20.1	0,0	3,5	0,0	0,0	4,5	0,0	5,0	NA	NA								Non-coding mRNA	
CTD-3187F8.14	0,0	0,0	1,1	3,5	4,6	0,0	0,0	NA	NA								Non-coding mRNA	
CYP2F2P	0,0	5,3	10,0	1,3	0,0	8,2	5,2	4	NA								Cytochrome P450 Family 2 Subfamily F Member 2, Pseudogene	
DEF6	0,0	0,0	1,0	5,8	4,2	0,0	0,0	78	1336								DEF6 Guanine Nucleotide Exchange Factor	
DOCK11	0,0	0,0	1,0	0,0	1,6	14,9	5,8	53	635.5								Dedicator Of Cytokinesis 11	
EGFL7	0,0	0,0	3,9	3,4	5,4	1,5	0,0	11	79								EGF Like Domain Multiple 7	√
EVI2B	1,9	8,0	2,5	1,4	2,5	6,3	3,3	234	207.5	√	√	√	√	√	√	√	Ecotropic Viral Integration Site 2B	√
EVL	0,0	3,1	8,1	0,0	7,1	8,7	4,9	42	2656.5	√	√	√	X				Enah/Vasp-like	√
EXOSC8	0,0	1,1	0,0	0,0	0,0	8,7	3,9	37	1068.5	√	√	√	√	√	√	√	Exosome component 8	
FAM19A2	8,4	8,7	9,0	0,0	0,0	28,9	5,8	NA	24.5	√	√	√	√	√	√	√	Family With Sequence Similarity 19 Member A2	
GSG1	0,0	0,0	3,8	0,0	1,5	3,1	4,2	NA	20								Germ Cell Associated 1	
LINC00922	1,2	0,0	1,0	3,2	0,0	1,1	5,6	5	NA								Non-coding mRNA	
LY86-AS1	0,0	8,9	6,8	0,0	6,6	9,5	8,2	2	8.5								LY86 Antisense RNA 1	
NF1	14,0	2,5	4,1	1,1	2,8	3,6	4,1	10	1452	√	√	√	√	√	√	√	Neurofibromin 1	
NINJ2	0,0	2,6	4,5	0,0	0,0	9,1	5,2	35	9.5								Ninjurin 2	
NPHP3	0,0	3,6	1,0	3,4	0,0	6,4	0,0	13	64.5								Nephrocystin 3	√
OXR1	0,0	2,3	1,0	0,0	1,1	3,6	5,8	38	563.5								Oxidation Resistance 1	
PAIP1	0,0	0,0	1,0	0,0	2,7	7,2	5,5	39	809								Poly(A) Binding Protein Interacting Protein 1	√
RHOF	0,0	6,7	41,2	0,0	0,0	14,8	5,5	21	343.5	√	√	X	X				Ras Homolog Family Member F, Filopodia Associated	√
RP11-297K8.2	0,0	3,2	0,0	10,5	22,9	0,0	0,0	NA	NA								Non-coding mRNA	
RP11-336K24.12	0,0	1,3	2,4	0,0	4,4	5,6	3,8	NA	NA								Non-coding mRNA	
RP11-355N15.1	19,1	9,2	9,2	4,7	3,2	6,4	0,0	NA	NA								Non-coding mRNA	
RP11-681I3.2	0,0	4,5	2,5	0,0	5,0	0,0	3,6	NA	NA								Non-coding mRNA	
RP11-691H4.4	0,0	3,5	6,7	3,2	0,0	3,7	0,0	NA	NA								Non-coding mRNA	
RPN2	0,0	0,0	1,5	3,1	0,0	4,3	0,0	94	5373.5								Ribophorin II	√
SDCCAG8	0,0	0,0	1,0	0,0	1,0	5,6	3,4	35	210.5								Serologically Defined Colon Cancer Antigen 8	√
SERTAD2	0,0	1,1	10,8	0,0	1,6	4,3	6,4	39	837								SERTA Domain Containing 2	
SLC7A6	0,0	1,2	1,3	0,0	3,9	6,5	7,4	28	1480								Solute Carrier Family 7 Member 6	
SPESP1	0,0	1,4	1,5	0,0	0,0	3,1	4,9	10	0								Sperm Equatorial Segment Protein 1	
ST3GAL3	0,0	0,0	1,2	1,0	1,0	4,6	3,2	24	294								ST3 Beta-Galactoside Alpha-2,3-Sialyltransferase 3	√
STRADB	0,0	2,1	7,6	0,0	3,2	3,8	6,1	28	659.5								STE20 Related Adaptor Beta	
TBC1D1	0,0	0,0	1,0	0,0	0,0	4,7	14,3	74	1437								TBC1 Domain Family Member 1	
TRAK2	0,0	4,7	1,7	0,0	4,1	2,9	5,9	39	672								Trafficking Kinesin Protein 2	
TRAPPC6A	0,0	0,0	0,0	0,0	3,9	3,8	9,8	41	218								Trafficking Protein Particle Complex 6A	
UFC1	0,0	1,3	0,0	0,0	2,8	15,9	3,2	88	1380.5								Ubiquitin-Fold Modifier Conjugating Enzyme 1	
UNK	2,9	2,1	0,0	0,0	3,8	4,0	6,1	17	633.5								Unkempt homolog(drosophila)	
USP15	0,0	0,0	3,4	0,0	1,1	7,2	5,0	81	816.5	√	√	√	√	√	√	√	Ubiquitin Specific Peptidase 15	
WIPF1	0,0	1,8	3,1	0,0	3,0	3,4	5,5	146	1356								WAS/WASL Interacting Protein Family Member 1	

Table 1 Prioritized candidate list for the GFP^{Total} and the GFP^{Sub} populations.

Prioritized candidate genes are defined as having an LOF equal to or greater than 3 in at least 2 independent samples. Overlapping genes are underlined in both lists. Results of shRNA mediated knockdown validation experiments of selected candidate genes in A2 and 11.1 J-Lat cell models are indicated.

Table 2 List of RT-qPCR primers and recombinant DNA.

List of RT-qPCR primers		
Name of gene	Forward Primer	Reverse Primer
ADK	GACACAAGCCCTGCCAAAGAT	TCAGAGACCAGTTGAGACAGAA
CMSS1	GCCAATGATTTGACTCACAGTCT	CTGAATGCTGTCATCGACCTAAT
IRF2BP2	CCCATGACTCCTACATCCTCTT	GAGGGCGGACTGTTGCTATTC
NF1	AGATGAAACGATGCTGGTCAAA	CCTGTAACCTGGTAGAAATGCGA
CHD9	GAAATGCTAGAAAGGTTGGAGG	CGGGACCAGTGAGAATACGTT
FAM19A	TGTTAAAACGGGAACTTGTGAGG	AAGCATCCACACATGATGGAG
SCN9A	ATTCGTGGCTCCTTGTTTTCTG	CTACTGGCTTGGCTGATGTTAC
RHOF	CCCCATCGGTGTTCGAGAAG	GGCCGTGTCGTAGAGGTTC
GRIK5	CCACCGTGAGCCATATCTGTG	CGCGAAGCGAAGGTACTGAA
USP15	CGACGCTGCTCAAAACCTC	TCCCATCTGGTATTTGTCCCAA
EVL	CTTCCGTGATGGTCTACGATG	TGCAACTTGACTCCAACGACT
EXOSC8	CGGTTCAATTAGTACCGCAGAT	ACGTATCCTTTATCAGGGGCAT
COPS5	TGGGTCTGATGCTAGGAAAGG	CTATGATACCACCCGATTGCATT
SLC7A6	CGGGCTTTCAGTTGTTAGACC	ACACAGTCAATCGCTCACGG
EVI2B	ACCAACACAATTCAGCGACAC	GTTGTAGGCAAGTGGTTGTCC
SPN	GCTGGTGGTAAGCCCAGAC	GGCTCGCTAGTAGAGACCAAA
POL	GGTTTATTACAGGGACAGCAGAGA	ACCTGCCATCTGTTTTCCATA
GAG	AGTAGTGTGTGCCCGTCTGT	TCGCTTTCAGGTCCCTGTTCG
TAT	CAAAAGCCTTAGGCATCTCCT	CCACCTTCTTCTTCGATTCCT
β2M	AGCGTACTCCAAAGATTCAGGTT	ATGATGCTGCTTACATGTCTCGAT
GAPDH	CAAGAAGGTGGTGAAGCAG	GCCAAATTCGTTGTCATACC
Nuc 0	CCACACACAAGGCTACTTCC	AACTGGTACTAGCTTGTAGCAC
HSS1	TGTGAGCCTGCATGGGATGG	GAAAGTCCCCAGCGGAAAGT
Nuc1/HSS2	CGTCTGTTGTGTGACTCTGGT	TCGAGAGAGCTCCTCTGGTT
HSS2/Nuc2	GCCCGAACAGGGACTTGAAA	TTGGCGTACTCACCAGTCG
Nuc2/Gag	GGTGCGAGAGCGTCAGTAT	AGCTCCCTGCTTGCCCATA
Hk2	GCCGACTCTTGTATTGCCTG	TATTGTAGCACGGCCGGAAA
GFP	GGAGTGGTCCCAGTTCTTGTTG	ACAGGTAGCTTCCCAGTAGTGC

Recombinant DNA		
sh ADK	MISSION® shRNA library (Sigma)	TRCN000011535
sh GRIK5	MISSION® shRNA library (Sigma)	TRCN000011537
sh SPN	MISSION® shRNA library (Sigma)	TRCN000011539
sh Control	MISSION® shRNA library (Sigma)	SHC002
sh CMSS1	MISSION® shRNA library (Sigma)	TRCN000011541
sh EVL	MISSION® shRNA library (Sigma)	TRCN000011542
sh COPS5	MISSION® shRNA library (Sigma)	TRCN000011543
sh EXOSC8	MISSION® shRNA library (Sigma)	TRCN000011544
sh SLC7A6	MISSION® shRNA library (Sigma)	TRCN000011545
sh USP15	MISSION® shRNA library (Sigma)	TRCN000011547
sh NF1	MISSION® shRNA library (Sigma)	TRCN000011638
sh IRF2BP2	MISSION® shRNA library (Sigma)	TRCN000011635
sh RHOF	MISSION® shRNA library (Sigma)	TRCN000011642
sh EVI2B	MISSION® shRNA library (Sigma)	TRCN000011644
sh CHD9	MISSION® shRNA library (Sigma)	TRCN0000230236
sh FAM19A	MISSION® shRNA library (Sigma)	TRCN000011641

REFERENCES

Accolla, Roberto S., Stefania Mazza, Andrea De Lerma Barbaro, Andrea De Maria, and Giovanna Tosi. 2002. "The HLA Class II Transcriptional Activator Blocks the Function of HIV-1 Tat and Inhibits Viral Replication." *European Journal of Immunology* 32 (10): 2783–91. https://doi.org/10.1002/1521-4141(2002010)32:10<2783::AID-IMMU2783>3.0.CO;2-E.

Archin, N. M., A. L. Liberty, A. D. Kashuba, S. K. Choudhary, J. D. Kuruc, A. M. Crooks, D. C. Parker, et al. 2012. "Administration of Vorinostat Disrupts HIV-1 Latency in Patients on Antiretroviral Therapy." *Nature* 487 (7408): 482–85. https://doi.org/10.1038/nature11286.

Archin, Nancie M., Amy Espeseth, Daniel Parker, Manzoor Cheema, Daria Hazuda, and David M. Margolis. 2009. "Expression of Latent HIV Induced by the Potent HDAC Inhibitor Suberoylanilide Hydroxamic Acid." *AIDS Research and Human Retroviruses* 25 (2): 207–12. https://doi.org/10.1089/aid.2008.0191.

Besnard, Emilie, Shweta Hakre, Martin Kampmann, Hyung W. Lim, Nina N. Hosmane, Alyssa Martin, Michael C. Bassik, et al. 2016. "The MTOR Complex Controls HIV Latency." *Cell Host & Microbe* 20 (6): 785–97. https://doi.org/10.1016/j.chom.2016.11.001.

Birsoy, Kivanç, Tim Wang, Richard Possemato, Omer H. Yilmaz, Catherine E. Koch, Walter W. Chen, Amanda W. Hutchins, et al. 2013. "MCT1-Mediated Transport of a Toxic Molecule Is an Effective Strategy for Targeting Glycolytic Tumors." *Nature Genetics* 45 (1): 104–8. https://doi.org/10.1038/ng.2471.

Blomen, Vincent A., Peter Májek, Lucas T. Jae, Johannes W. Bigenzahn, Joppe Nieuwenhuis, Jacqueline Staring, Roberto Sacco, et al. 2015. "Gene Essentiality and Synthetic Lethality in Haploid Human Cells." *Science* 350 (6264): 1092–96. https://doi.org/10.1126/science.aac7557.

Boehm, Daniela, Mark Jeng, Gregory Camus, Andrea Gramatica, Roland Schwarzer, Jeffrey R. Johnson, Philip A. Hull, et al. 2017. "SMYD2-Mediated Histone Methylation Contributes to HIV-1 Latency." *Cell Host and Microbe* 21 (5): 569-579.e6. https://doi.org/10.1016/j.chom.2017.04.011.

Boison, Detlev. 2013. "Adenosine Kinase: Exploitation for Therapeutic Gain." *Pharmacological Reviews* 65 (3): 906–43. https://doi.org/10.1124/pr.112.006361.

Carette, Jan E., Carla P. Guimaraes, Malini Varadarajan, Annie S. Park, Irene Wuethrich, Alzbeta Godarova, Maciej Kotecki, et al. 2009. "Haploid Genetic Screens in Human Cells Identify Host Factors Used by Pathogens." *Science (New York, N.Y.)* 326 (5957): 1231–35. https://doi.org/10.1126/science.1178955.

Carette, Jan E., Matthijs Raaben, Anthony C. Wong, Andrew S. Herbert, Gregor Obernosterer, Nirupama Mulherkar, Ana I. Kuehne, et al. 2011. "Ebola Virus Entry Requires the Cholesterol Transporter Niemann-Pick C1." *Nature* 477 (7364): 340–43. https://doi.org/10.1038/nature10348.

Carneiro, Flávia R. G., Renata Ramalho-Oliveira, Giuliana P. Mognol, and João P. B. Viola. 2011. "Interferon Regulatory Factor 2 Binding Protein 2 Is a New NFAT1 Partner and Represses Its Transcriptional Activity ▿ ." *Molecular and Cellular Biology* 31 (14): 2889–2901. https://doi.org/10.1128/MCB.00974-10.

Coull, J. J., F. Romerio, J. M. Sun, J. L. Volker, K. M. Galvin, J. R. Davie, Y. Shi, U. Hansen, and D. M. Margolis. 2000. "The Human Factors YY1 and LSF Repress

the Human Immunodeficiency Virus Type 1 Long Terminal Repeat via Recruitment of Histone Deacetylase 1." *Journal of Virology* 74 (15): 6790–99. https://doi.org/10.1128/jvi.74.15.6790-6799.2000.

Das, Biswajit, Curtis Dobrowolski, Benjamin Luttge, Saba Valadkhan, Nicolas Chomont, Rowena Johnston, Peter Bacchetti, et al. 2018a. "Estrogen Receptor-1 Is a Key Regulator of HIV-1 Latency That Imparts Gender-Specific Restrictions on the Latent Reservoir." *Proceedings of the National Academy of Sciences of the United States of America* 115 (33): E7795–7804. https://doi.org/10.1073/pnas.1803468115.

Deeks, Steven G. 2012. "HIV: Shock and Kill." *Nature* 487 (7408): 439–40. https://doi.org/10.1038/487439a.

Elliott, Julian H., Fiona Wightman, Ajantha Solomon, Khader Ghneim, Jeffrey Ahlers, Mark J. Cameron, Miranda Z. Smith, et al. 2014. "Activation of HIV Transcription with Short-Course Vorinostat in HIV-Infected Patients on Suppressive Antiretroviral Therapy." *PLOS Pathogens* 10 (11): e1004473. https://doi.org/10.1371/journal.ppat.1004473.

Fishilevich, Simon, Ron Nudel, Noa Rappaport, Rotem Hadar, Inbar Plaschkes, Tsippi Iny Stein, Naomi Rosen, et al. 2017. "GeneHancer: Genome-Wide Integration of Enhancers and Target Genes in GeneCards." *Database: The Journal of Biological Databases and Curation* 2017 (January). https://doi.org/10.1093/database/bax028.

Forlani, Greta, Filippo Turrini, Silvia Ghezzi, Alessandra Tedeschi, Guido Poli, Roberto S. Accolla, and Giovanna Tosi. 2016. "The MHC-II Transactivator CIITA Inhibits Tat Function and HIV-1 Replication in Human Myeloid Cells." *Journal of Translational Medicine* 14 (April): 94. https://doi.org/10.1186/s12967-016-0853-5.

Goff, Stephen P. 2008. "Knockdown Screens to Knockout HIV-1." *Cell* 135 (3): 417–20. https://doi.org/10.1016/j.cell.2008.10.007.

Goujon, C., V. Arfi, T. Pertel, J. Luban, J. Lienard, D. Rigal, J.-L. Darlix, and A. Cimarelli. 2008. "Characterization of Simian Immunodeficiency Virus SIVSM/Human Immunodeficiency Virus Type 2 Vpx Function in Human Myeloid Cells." *Journal of Virology* 82 (24): 12335–45. https://doi.org/10.1128/jvi.01181-08.

Guimaraes, Carla P., Jan E. Carette, Malini Varadarajan, John Antos, Maximilian W. Popp, Eric Spooner, Thijn R. Brummelkamp, and Hidde L. Ploegh. 2011. "Identification of Host Cell Factors Required for Intoxication through Use of Modified Cholera Toxin." *Journal of Cell Biology* 195 (5): 751–64. https://doi.org/10.1083/jcb.201108103.

Hansen, Jens, Thomas Floss, Petra Van Sloun, Ernst Martin Füchtbauer, Franz Vauti, Hans Hennig Arnold, Frank Schnütgen, Wolfgang Wurst, Harald Von Melchnert, and Patricia Ruiz. 2003. "A Large-Scale, Gene-Driven Mutagenesis Approach for the Functional Analysis of the Mouse Genome." *Proceedings of the National Academy of Sciences of the United States of America* 100 (17): 9918–22. https://doi.org/10.1073/pnas.1633296100.

Hansen, Maike M. K., Benjamin Martin, and Leor S. Weinberger. 2019. "HIV Latency: Stochastic across Multiple Scales." *Cell Host & Microbe* 26 (6): 703–5. https://doi.org/10.1016/j.chom.2019.11.010.

Harrell Stewart, Desmond R., and Geoffrey J. Clark. 2020. "Pumping the Brakes on RAS - Negative Regulators and Death Effectors of RAS." *Journal of Cell Science* 133 (3). https://doi.org/10.1242/jcs.238865.

Hart, Traver, Kevin R. Brown, Fabrice Sircoulomb, Robert Rottapel, and Jason Moffat. 2014. “Measuring Error Rates in Genomic Perturbation Screens: Gold Standards for Human Functional Genomics.” *Molecular Systems Biology* 10 (7). https://doi.org/10.15252/msb.20145216.

Heijink, Anne Margriet, Francien Talens, Lucas T. Jae, Stephanie E. van Gijn, Rudolf S.N. Fehrmann, Thijn R. Brummelkamp, and Marcel A.T.M. van Vugt. 2019. “BRCA2 Deficiency Instigates CGAS-Mediated Inflammatory Signaling and Confers Sensitivity to Tumor Necrosis Factor-Alpha-Mediated Cytotoxicity.” *Nature Communications* 10 (1). https://doi.org/10.1038/s41467-018-07927-y.

Hoffmann, H. Heinrich, William M. Schneider, Vincent A. Blomen, Margaret A. Scull, Alain Hovnanian, Thijn R. Brummelkamp, and Charles M. Rice. 2017. “Diverse Viruses Require the Calcium Transporter SPCA1 for Maturation and Spread.” *Cell Host and Microbe* 22 (4): 460-470.e5. https://doi.org/10.1016/j.chom.2017.09.002.

Huang, Huachao, Weili Kong, Maxime Jean, Guillaume Fiches, Dawei Zhou, Tsuyoshi Hayashi, Jianwen Que, Netty Santoso, and Jian Zhu. 2019. “A CRISPR/Cas9 Screen Identifies the Histone Demethylase MINA53 as a Novel HIV-1 Latency-Promoting Gene (LPG).” *Nucleic Acids Research* 47 (14): 7333–47. https://doi.org/10.1093/nar/gkz493.

Jae, Lucas T., Matthijs Raaben, Moniek Riemersma, Ellen Van Beusekom, Vincent A. Blomen, Arno Velds, Ron M. Kerkhoven, et al. 2013. “Deciphering the Glycosylome of Dystroglycanopathies Using Haploid Screens for Lassa Virus Entry.” *Science* 340 (6131): 479–83. https://doi.org/10.1126/science.1233675.

Jangra, Rohit K., Andrew S. Herbert, Rong Li, Lucas T. Jae, Lara M. Kleinfelter, Megan M. Slough, Sarah L. Barker, et al. 2018. “Protocadherin-1 Is Essential for Cell Entry by New World Hantaviruses.” *Nature*. Nature Publishing Group. https://doi.org/10.1038/s41586-018-0702-1.

Janssen, Louise M.E., Tessa V. Averink, Vincent A. Blomen, Thijn R. Brummelkamp, René H. Medema, and Jonne A. Raaijmakers. 2018. “Loss of Kif18A Results in Spindle Assembly Checkpoint Activation at Microtubule-Attached Kinetochores.” *Current Biology* 28 (17): 2685-2696.e4. https://doi.org/10.1016/j.cub.2018.06.026.

Jiang, G., A. Espeseth, D. J. Hazuda, and D. M. Margolis. 2007. “C-Myc and Sp1 Contribute to Proviral Latency by Recruiting Histone Deacetylase 1 to the Human Immunodeficiency Virus Type 1 Promoter.” *Journal of Virology* 81 (20): 10914–23. https://doi.org/10.1128/jvi.01208-07.

Jiang, Wei-Min, Xin-Yun Zhang, Yun-Zhi Zhang, Li Liu, and Hong-Zhou Lu. 2014. “A High Throughput RNAi Screen Reveals Determinants of HIV-1 Activity in Host Kinases.” *International Journal of Clinical and Experimental Pathology* 7 (5): 2229–37.

Jordan, Albert, Dwayne Bisgrove, and Eric Verdin. 2003. “HIV Reproducibly Establishes a Latent Infection after Acute Infection of T Cells in Vitro.” *The EMBO Journal* 22 (8): 1868–77. https://doi.org/10.1093/emboj/cdg188.

Jordan, Albert, Patricia Defechereux, and Eric Verdin. 2001. “The Site of HIV-1 Integration in the Human Genome Determines Basal Transcriptional Activity and Response to Tat Transactivation.” *The EMBO Journal* 20 (7): 1726–38. https://doi.org/10.1093/emboj/20.7.1726.

Kaushik, Rajnish, Xiaonan Zhu, Ruzena Stranska, Yuanfei Wu, and Mario Stevenson. 2009. “A Cellular Restriction Dictates the Permissivity of Nondividing Monocytes/Macrophages to Lentivirus and Gammaretrovirus Infection.” *Cell*

Host and Microbe 6 (1): 68–80. https://doi.org/10.1016/j.chom.2009.05.022.
Klase, Zachary, Venkat S. R. K. Yedavalli, Laurent Houzet, Molly Perkins, Frank Maldarelli, Jason Brenchley, Klaus Strebel, Paul Liu, and Kuan-Teh Jeang. 2014. "Activation of HIV-1 from Latent Infection via Synergy of RUNX1 Inhibitor Ro5-3335 and SAHA." *PLoS Pathogens* 10 (3): e1003997. https://doi.org/10.1371/journal.ppat.1003997.
Kotecki, M., P. S. Reddy, and B. H. Cochran. 1999. "Isolation and Characterization of a Near-Haploid Human Cell Line." *Experimental Cell Research* 252 (2): 273–80. https://doi.org/10.1006/excr.1999.4656.
Krasnopolsky, Simona, Alona Kuzmina, and Ran Taube. 2020. "Genome-Wide CRISPR Knockout Screen Identifies ZNF304 as a Silencer of HIV Transcription That Promotes Viral Latency." *PLoS Pathogens* 16 (9): e1008834. https://doi.org/10.1371/journal.ppat.1008834.
Kriegel, Hans-Peter, Peer Kröger, Erich Schubert, and Arthur Zimek. 2009. "LoOP: Local Outlier Probabilities." In *Proceedings of the 18th ACM Conference on Information and Knowledge Management*, 1649–52. CIKM '09. New York, NY, USA: Association for Computing Machinery. https://doi.org/10.1145/1645953.1646195.
Kumar, Amit, Wasim Abbas, and Georges Herbein. 2014. "HIV-1 Latency in Monocytes/Macrophages." *Viruses* 6 (4): 1837–60. https://doi.org/10.3390/v6041837.
Laguette, Nadine, Bijan Sobhian, Nicoletta Casartelli, Mathieu Ringeard, Christine Chable-Bessia, Emmanuel Ségéral, Ahmad Yatim, Stéphane Emiliani, Olivier Schwartz, and Monsef Benkirane. 2011. "SAMHD1 Is the Dendritic- and Myeloid-Cell-Specific HIV-1 Restriction Factor Counteracted by Vpx." *Nature* 474 (7353): 654–57. https://doi.org/10.1038/nature10117.
Lai, Binbin, Qingsong Tang, Wenfei Jin, Gangqing Hu, Darawalee Wangsa, Kairong Cui, Benjamin Z. Stanton, et al. 2018. "Trac-Looping Measures Genome Structure and Chromatin Accessibility." *Nature Methods* 15 (9): 741–47. https://doi.org/10.1038/s41592-018-0107-y.
Lassen, Kara G., Andrew M. Hebbeler, Darshana Bhattacharyya, Michael A. Lobritz, and Warner C. Greene. 2012. "A Flexible Model of HIV-1 Latency Permitting Evaluation of Many Primary CD4 T-Cell Reservoirs." *PloS One* 7 (1): e30176. https://doi.org/10.1371/journal.pone.0030176.
Lee, Clarissa C, Jan E Carette, Thijn R Brummelkamp, and Hidde L Ploegh. 2013. "A Reporter Screen in a Human Haploid Cell Line Identifies CYLD as a Constitutive Inhibitor of NF-KB." *PloS One* 8 (7): e70339. https://doi.org/10.1371/journal.pone.0070339.
Li, Zichong, Cyrus Hajian, and Warner C. Greene. 2020. "Identification of Unrecognized Host Factors Promoting HIV-1 Latency." *PLOS Pathogens* 16 (12): e1009055. https://doi.org/10.1371/journal.ppat.1009055.
Logtenberg, Meike E.W., J. H.Marco Jansen, Matthijs Raaben, Mireille Toebes, Katka Franke, Arianne M. Brandsma, Hanke L. Matlung, et al. 2019. "Glutaminyl Cyclase Is an Enzymatic Modifier of the CD47- SIRPα Axis and a Target for Cancer Immunotherapy." *Nature Medicine*. Nature Publishing Group. https://doi.org/10.1038/s41591-019-0356-z.
Martin, Scott E., and Natasha J. Caplen. 2007. "Applications of RNA Interference in Mammalian Systems." *Annual Review of Genomics and Human Genetics* 8 (1): 81–108. https://doi.org/10.1146/annurev.genom.8.080706.092424.
Mayor-Ruiz, Cristina, Sophie Bauer, Matthias Brand, Zuzanna Kozicka, Marton Siklos,

Hana Imrichova, Ines H. Kaltheuner, et al. 2020. “Rational Discovery of Molecular Glue Degraders via Scalable Chemical Profiling.” *Nature Chemical Biology* 16 (11): 1199–1207. https://doi.org/10.1038/s41589-020-0594-x.

Mezzadra, Riccardo, Marjolein De Bruijn, Lucas T. Jae, Raquel Gomez-Eerland, Anja Duursma, Ferenc A. Scheeren, Thijn R. Brummelkamp, and Ton N. Schumacher. 2019. “SLFN11 Can Sensitize Tumor Cells towards IFN-γ-Mediated T Cell Killing.” *PLoS ONE* 14 (2). https://doi.org/10.1371/journal.pone.0212053

Mezzadra, Riccardo, Chong Sun, Lucas T. Jae, Raquel Gomez-Eerland, Evert De Vries, Wei Wu, Meike E.W. Logtenberg, et al. 2017. “Identification of CMTM6 and CMTM4 as PD-L1 Protein Regulators.” *Nature* 549 (7670): 106–10. https://doi.org/10.1038/nature23669.

Mills, Alea A. 2017. “The Chromodomain Helicase DNA-Binding Chromatin Remodelers: Family Traits That Protect from and Promote Cancer.” *Cold Spring Harbor Perspectives in Medicine* 7 (4). https://doi.org/10.1101/cshperspect.a026450.

Minin, Giulio Di, Andreas Postlmayr, and Anton Wutz. 2018. “HaSAPPy: A Tool for Candidate Identification in Pooled Forward Genetic Screens of Haploid Mammalian Cells.” *PLOS Computational Biology* 14 (1): e1005950. https://doi.org/10.1371/journal.pcbi.1005950.

Morgan, Martin, Simon Anders, Michael Lawrence, Patrick Aboyoun, Hervé Pagès, and Robert Gentleman. 2009. “ShortRead: A Bioconductor Package for Input, Quality Assessment and Exploration of High-Throughput Sequence Data.” *Bioinformatics (Oxford, England)* 25 (19): 2607–8. https://doi.org/10.1093/bioinformatics/btp450.

Nallani, Srikanth C., Tracy A. Glauser, Niresh Hariparsad, Kenneth Setchell, Donna J. Buckley, Arthur R. Buckley, and Pankaj B. Desai. 2003. “Dose-Dependent Induction of Cytochrome P450 (CYP) 3A4 and Activation of Pregnane X Receptor by Topiramate.” *Epilepsia* 44 (12): 1521–28. https://doi.org/10.1111/j.0013-9580.2003.06203.x.

Ne, Enrico, Raquel Crespo, Ray Izquierdo-Lara, Selin Kocer, Alicja Gorszka, Thomas van Staveren, Tsung Wai Kan, et al. 2020. “DCas9 Targeted Chromatin and Histone Enrichment for Mass Spectrometry (Catchet-MS) Identifies IKZF1 as a Novel Drug-Able Target for HIV-1 Latency Reversal.” SSRN Scholarly Paper ID 3553972. Rochester, NY: Social Science Research Network. https://doi.org/10.2139/ssrn.3553972.

Ne, Enrico, Robert-Jan Palstra, and Tokameh Mahmoudi. 2018. “Transcription: Insights From the HIV-1 Promoter.” *International Review of Cell and Molecular Biology* 335: 191–243. https://doi.org/10.1016/bs.ircmb.2017.07.011.

Palstra, Robert-Jan, Elisa de Crignis, Michael D. Röling, Thomas van Staveren, Tsung Wai Kan, Wilfred van Ijcken, Yvonne M. Mueller, Peter D. Katsikis, and Tokameh Mahmoudi. 2018. “Allele-Specific Long-Distance Regulation Dictates IL-32 Isoform Switching and Mediates Susceptibility to HIV-1.” *Science Advances* 4 (2): e1701729. https://doi.org/10.1126/sciadv.1701729.

Park, Jaoek, and Radhey S. Gupta. 2013. “Adenosine Metabolism, Adenosine Kinase, and Evolution.” In *Adenosine: A Key Link between Metabolism and Brain Activity*, edited by Susan Masino and Detlev Boison, 23–54. New York, NY: Springer. https://doi.org/10.1007/978-1-4614-3903-5_2.

Pereira, L. A., K. Bentley, A. Peeters, M. J. Churchill, and N. J. Deacon. 2000. “A Compilation of Cellular Transcription Factor Interactions with the HIV-1 LTR

Promoter." *Nucleic Acids Research* 28 (3): 663–68. https://doi.org/10.1093/nar/28.3.663.

Pérez, Moisés, Amaya García de Vinuesa, Gonzalo Sanchez-Duffhues, Nieves Marquez, M. Luz Bellido, M. Angeles Muñoz-Fernandez, Santiago Moreno, Trevor P. Castor, Marco A. Calzado, and Eduardo Muñoz. 2010. "Bryostatin-1 Synergizes with Histone Deacetylase Inhibitors to Reactivate HIV-1 from Latency." *Current HIV Research* 8 (6): 418–29. https://doi.org/10.2174/157016210793499312.

Piette, Jacques, and Sylvie Legrand-Poels. 1994. "HIV-1 Reactivation after an Oxidative Stress Mediated by Different Reactive Oxygen Species." *Chemico-Biological Interactions*, Special Issue: The place of oxygen free radicals in HIV infections, 91 (2): 79–89. https://doi.org/10.1016/0009-2797(94)90028-0.

Qi, Wenjing, Ruoxi Wang, Hongyu Chen, Xiaolin Wang, Ting Xiao, Istvan Boldogh, Xueqing Ba, et al. 2015. "BRG1 Promotes the Repair of DNA Double-Strand Breaks by Facilitating the Replacement of RPA with RAD51." *Journal of Cell Science* 128 (2): 317–30. https://doi.org/10.1242/jcs.159103.

Raaben, Matthijs, Lucas T. Jae, Andrew S. Herbert, Ana I. Kuehne, Sarah H. Stubbs, Yi ying Chou, Vincent A. Blomen, et al. 2017. "NRP2 and CD63 Are Host Factors for Lujo Virus Cell Entry." *Cell Host and Microbe* 22 (5): 688-696.e5. https://doi.org/10.1016/j.chom.2017.10.002.

Raaijmakers, Jonne A., Roy G.H.P. van Heesbeen, Vincent A. Blomen, Louise M.E. Janssen, Ferdy van Diemen, Thijn R. Brummelkamp, and René H. Medema. 2018. "BUB1 Is Essential for the Viability of Human Cells in Which the Spindle Assembly Checkpoint Is Compromised." *Cell Reports* 22 (6): 1424–38. https://doi.org/10.1016/j.celrep.2018.01.034.

Rafati, Haleh, Maribel Parra, Shweta Hakre, Yuri Moshkin, Eric Verdin, and Tokameh Mahmoudi. 2011. "Repressive LTR Nucleosome Positioning by the BAF Complex Is Required for HIV Latency." *PLoS Biology* 9 (11): e1001206. https://doi.org/10.1371/journal.pbio.1001206.

Rathore, Anurag, Sho Iketani, Pengfei Wang, Manxue Jia, Vincent Sahi, and David D. Ho. 2020. "CRISPR-Based Gene Knockout Screens Reveal Deubiquitinases Involved in HIV-1 Latency in Two Jurkat Cell Models." *Scientific Reports* 10 (1): 5350. https://doi.org/10.1038/s41598-020-62375-3.

Razooky, Brandon S., Anand Pai, Katherine Aull, Igor M. Rouzine, and Leor S. Weinberger. 2015. "A Hardwired HIV Latency Program." *Cell* 160 (5): 990–1001. https://doi.org/10.1016/j.cell.2015.02.009.

Reiling, Jan H., Clary B. Clish, Jan E. Carette, Malini Varadarajan, Thijn R. Brummelkamp, and David M. Sabatini. 2011. "A Haploid Genetic Screen Identifies the Major Facilitator Domain Containing 2A (MFSD2A) Transporter as a Key Mediator in the Response to Tunicamycin." *Proceedings of the National Academy of Sciences* 108 (29): 11756–65. https://doi.org/10.1073/pnas.1018098108.

Rojas, Asheebo, and Raymond Dingledine. 2013. "Ionotropic Glutamate Receptors: Regulation by G-Protein-Coupled Receptors." *Molecular Pharmacology* 83 (4): 746–52. https://doi.org/10.1124/mol.112.083352.

Sadowski, Ivan, and Farhad B. Hashemi. 2019. "Strategies to Eradicate HIV from Infected Patients: Elimination of Latent Provirus Reservoirs." *Cellular and Molecular Life Sciences: CMLS* 76 (18): 3583–3600. https://doi.org/10.1007/s00018-019-03156-8.

Schmittgen, Thomas D., and Kenneth J. Livak. 2008. "Analyzing Real-Time PCR Data

by the Comparative C(T) Method." *Nature Protocols* 3 (6): 1101–8. https://doi.org/10.1038/nprot.2008.73.

Sengupta, Srona, and Robert F. Siliciano. 2018. "Targeting the Latent Reservoir for HIV-1." *Immunity* 48 (5): 872–95. https://doi.org/10.1016/j.immuni.2018.04.030.

Shank, R. P., J. F. Gardocki, A. J. Streeter, and B. E. Maryanoff. 2000. "An Overview of the Preclinical Aspects of Topiramate: Pharmacology, Pharmacokinetics, and Mechanism of Action." *Epilepsia* 41 (S1): 3–9.

Siliciano, Janet M., and Robert F. Siliciano. 2015. "The Remarkable Stability of the Latent Reservoir for HIV-1 in Resting Memory CD4+ T Cells." *The Journal of Infectious Diseases* 212 (9): 1345–47. https://doi.org/10.1093/infdis/jiv219.

Staring, Jacqueline, Eleonore Von Castelmur, Vincent A. Blomen, Lisa G. Van Den Hengel, Markus Brockmann, Jim Baggen, Hendrik Jan Thibaut, et al. 2017. "PLA2G16 Represents a Switch between Entry and Clearance of Picornaviridae." *Nature* 541 (7637): 412–16. https://doi.org/10.1038/nature21032.

Staring, Jacqueline, Lisa G. van den Hengel, Matthijs Raaben, Vincent A. Blomen, Jan E. Carette, and Thijn R. Brummelkamp. 2018. "KREMEN1 Is a Host Entry Receptor for a Major Group of Enteroviruses." *Cell Host and Microbe* 23 (5): 636-643.e5. https://doi.org/10.1016/j.chom.2018.03.019.

Stoszko, Mateusz, Abdullah M. S. Al-Hatmi, Anton Skriba, Michael Roling, Enrico Ne, Raquel Crespo, Yvonne M. Mueller, et al. 2020. "Gliotoxin, Identified from a Screen of Fungal Metabolites, Disrupts 7SK SnRNP, Releases P-TEFb, and Reverses HIV-1 Latency." *Science Advances* 6 (33): eaba6617. https://doi.org/10.1126/sciadv.aba6617.

Stoszko, Mateusz, Enrico Ne, Erik Abner, and Tokameh Mahmoudi. 2019. "A Broad Drug Arsenal to Attack a Strenuous Latent HIV Reservoir." *Current Opinion in Virology* 38: 37–53. https://doi.org/10.1016/j.coviro.2019.06.001.

Sturgill, Jamie L., Joel Mathews, Peggy Scherle, and Daniel H. Conrad. 2011. "Glutamate Signaling through the Kainate Receptor Enhances Human Immunoglobulin Production." *Journal of Neuroimmunology* 233 (1–2): 80–89. https://doi.org/10.1016/j.jneuroim.2010.11.014.

Tafesse, Fikadu G., Carla P. Guimaraes, Takeshi Maruyama, Jan E. Carette, Stephen Lory, Thijn R. Brummelkamp, and Hidde L. Ploegh. 2014. "GPR107, a G-Protein-Coupled Receptor Essential for Intoxication by Pseudomonas Aeruginosa Exotoxin a, Localizes to the Golgi and Is Cleaved by Furin." *Journal of Biological Chemistry* 289 (35): 24005–18. https://doi.org/10.1074/jbc.M114.589275.

Tantale, Katiana, Encarnation Garcia-Oliver, Adèle L'Hostis, Yueyuxio Yang, Marie-Cécile Robert, Thierry Gostan, Meenakshi Basu, et al. 2020. "Stochastic Pausing at Latent HIV-1 Promoters Generates Transcriptional Bursting." *BioRxiv*, August, 2020.08.25.265413. https://doi.org/10.1101/2020.08.25.265413.

Timmons, Andrew, Emily Fray, Mithra Kumar, Fengting Wu, Weiwei Dai, Cynthia Korin Bullen, Peggy Kim, et al. 2020. "HSF1 Inhibition Attenuates HIV-1 Latency Reversal Mediated by Several Candidate LRAs In Vitro and Ex Vivo." *Proceedings of the National Academy of Sciences* 117 (27): 15763–71. https://doi.org/10.1073/pnas.1916290117.

Vallejo-Gracia, Albert, Irene P. Chen, Rosalba Perrone, Emilie Besnard, Daniela Boehm, Emilie Battivelli, Tugsan Tezil, et al. 2020. "FOXO1 Promotes HIV Latency by Suppressing ER Stress in T Cells." *Nature Microbiology* 5 (9): 1144–57. https://doi.org/10.1038/s41564-020-0742-9.

Van Lint, Carine, Sophie Bouchat, and Alessandro Marcello. 2013. “HIV-1 Transcription and Latency: An Update.” *Retrovirology* 10 (June): 67. https://doi.org/10.1186/1742-4690-10-67.

Verdin, E., P. Paras, and C. Van Lint. 1993. “Chromatin Disruption in the Promoter of Human Immunodeficiency Virus Type 1 during Transcriptional Activation.” *The EMBO Journal* 12 (8): 3249–59.

Walker, James A., and Meena Upadhyaya. 2018. “Emerging Therapeutic Targets for Neurofibromatosis Type 1.” *Expert Opinion on Therapeutic Targets* 22 (5): 419–37. https://doi.org/10.1080/14728222.2018.1465931.

Wei, Datsen George, Vicki Chiang, Elizabeth Fyne, Mini Balakrishnan, Tiffany Barnes, Michael Graupe, Joseph Hesselgesser, et al. 2014. “Histone Deacetylase Inhibitor Romidepsin Induces HIV Expression in CD4 T Cells from Patients on Suppressive Antiretroviral Therapy at Concentrations Achieved by Clinical Dosing.” Edited by Ronald C Desrosiers. *PLoS Pathogens* 10 (4): e1004071. https://doi.org/10.1371/journal.ppat.1004071.

White, H. S., S. D. Brown, J. H. Woodhead, G. A. Skeen, and H. H. Wolf. 2000. “Topiramate Modulates GABA-Evoked Currents in Murine Cortical Neurons by a Nonbenzodiazepine Mechanism.” *Epilepsia* 41 (S1): 17–20.

Williams, Samuel A., Lin-Feng Chen, Hakju Kwon, David Fenard, Dwayne Bisgrove, Eric Verdin, and Warner C. Greene. 2004. “Prostratin Antagonizes HIV Latency by Activating NF-KappaB.” *The Journal of Biological Chemistry* 279 (40): 42008–17. https://doi.org/10.1074/jbc.M402124200.

Williams, Samuel A, Lin-Feng Chen, Hakju Kwon, Carmen M Ruiz-Jarabo, Eric Verdin, and Warner C Greene. 2006. “NF-KB P50 Promotes HIV Latency through HDAC Recruitment and Repression of Transcriptional Initiation.” *The EMBO Journal* 25 (1): 139–49. https://doi.org/10.1038/sj.emboj.7600900.

Wong, Michelle E., Anthony Jaworowski, and Anna C. Hearps. 2019. “The HIV Reservoir in Monocytes and Macrophages.” *Frontiers in Immunology* 10 (June). https://doi.org/10.3389/fimmu.2019.01435.

Wright, Cameron J. M., and Paul L. McCormack. 2013. “Trametinib: First Global Approval.” *Drugs* 73 (11): 1245–54. https://doi.org/10.1007/s40265-013-0096-1.

Yamamoto-Hino, Miki, and Satoshi Goto. 2013. “In Vivo RNAi-Based Screens: Studies in Model Organisms.” *Genes* 4 (4): 646–65. https://doi.org/10.3390/genes4040646.

Yang, Xinyi, Yanan Wang, Panpan Lu, Yinzhong Shen, Xiaying Zhao, Yuqi Zhu, Zhengtao Jiang, et al. 2020. “PEBP1 Suppresses HIV Transcription and Induces Latency by Inactivating MAPK/NF-KB Signaling.” *EMBO Reports* 21 (11): e49305. https://doi.org/10.15252/embr.201949305.

Ying, Hao, Yuhao Zhang, Xin Zhou, Xiying Qu, Pengfei Wang, Sijie Liu, Daru Lu, and Huanzhang Zhu. 2012. “Selective Histonedeacetylase Inhibitor M344 Intervenes in HIV-1 Latency through Increasing Histone Acetylation and Activation of NF-KappaB.” *PLoS ONE* 7 (11). https://doi.org/10.1371/journal.pone.0048832.

Ylisastigui, Loyda, Nancie M. Archin, Ginger Lehrman, Ronald J. Bosch, and David M. Margolis. 2004. “Coaxing HIV-1 from Resting CD4 T Cells: Histone Deacetylase Inhibition Allows Latent Viral Expression.” *AIDS (London, England)* 18 (8): 1101–8. https://doi.org/10.1097/00002030-200405210-00003.

Yu, Jason S. L., and Kosuke Yusa. 2019. “Genome-Wide CRISPR-Cas9 Screening in Mammalian Cells.” *Methods (San Diego, Calif.)* 164–165 (July): 29–35.

https://doi.org/10.1016/j.ymeth.2019.04.015.
Zhang, Xin, Deyong Jia, Huijuan Liu, Na Zhu, Wei Zhang, Jun Feng, Jun Yin, et al. 2013. "Identification of 5-Iodotubercidin as a Genotoxic Drug with Anti-Cancer Potential." *PloS One* 8 (5): e62527. https://doi.org/10.1371/journal.pone.0062527.
Zhu, Jian, Teresa Davoli, Jill M. Perriera, Christopher R. Chin, Gaurav D. Gaiha, Sinu P. John, Frederic D. Sigiollot, et al. 2014a. "Comprehensive Identification of Host Modulators of HIV-1 Replication Using Multiple Orthologous RNAi Reagents." *Cell Reports* 9 (2): 752–66. https://doi.org/10.1016/j.celrep.2014.09.031.
Zona, C., M. T. Ciotti, and M. Avoli. 1997. "Topiramate Attenuates Voltage-Gated Sodium Currents in Rat Cerebellar Granule Cells." *Neuroscience Letters* 231 (3): 123–26. https://doi.org/10.1016/s0304-3940(97)00543-0.

CHAPTER .4

Gliotoxin, identified from a screen of fungal metabolites, disrupts 7SK snRNP, releases PTEFb and reverses HIV-1 latency.

Mateusz Stoszko, Abdullah M. S. Al-Hatmi, Anton Skriba, Michael Roling, **Enrico Ne**, Raquel Crespo, Yvonne M. Mueller, Mohammad Javad Najafzadeh, Joyce Kang, Renata Ptackova, Elizabeth LeMasters, Pritha Biswas, Alessia Bertoldi, Tsung Wai Kan, Elisa de Crignis, Miroslav Sulc, Joyce H.G. Lebbink, Casper Rokx, Annelies Verbon, Wilfred van Ijcken, Peter D. Katsikis, Robert-Jan Palstra, Vladimir Havlicek, Sybren de Hoog, Tokameh Mahmoudi

Stoszko et al., Science Advances 2019

https://doi.org/10.1126/sciadv.aba6617

MOLECULAR BIOLOGY

Gliotoxin, identified from a screen of fungal metabolites, disrupts 7SK snRNP, releases P-TEFb, and reverses HIV-1 latency

Mateusz Stoszko[1], Abdullah M. S. Al-Hatmi[2,3,4]*, Anton Skriba[5]*, Michael Roling[1]*, Enrico Ne[1]*, Raquel Crespo[1]*, Yvonne M. Mueller[6]*, Mohammad Javad Najafzadeh[2,7]*, Joyce Kang[8], Renata Ptackova[5], Elizabeth LeMasters[1], Pritha Biswas[1], Alessia Bertoldi[1,9], Tsung Wai Kan[1], Elisa de Crignis[1], Miroslav Sulc[5], Joyce H.G. Lebbink[10], Casper Rokx[11], Annelies Verbon[11], Wilfred van Ijcken[12], Peter D. Katsikis[6], Robert-Jan Palstra[1], Vladimir Havlicek[5], Sybren de Hoog[2,3], Tokameh Mahmoudi[1†]

A leading pharmacological strategy toward HIV cure requires "shock" or activation of HIV gene expression in latently infected cells with latency reversal agents (LRAs) followed by their subsequent clearance. In a screen for novel LRAs, we used fungal secondary metabolites as a source of bioactive molecules. Using orthogonal mass spectrometry (MS) coupled to latency reversal bioassays, we identified gliotoxin (GTX) as a novel LRA. GTX significantly induced HIV-1 gene expression in latent ex vivo infected primary cells and in CD4$^+$ T cells from all aviremic HIV-1$^+$ participants. RNA sequencing identified 7SK RNA, the scaffold of the positive transcription elongation factor b (P-TEFb) inhibitory 7SK small nuclear ribonucleoprotein (snRNP) complex, to be significantly reduced upon GTX treatment of CD4$^+$ T cells. GTX directly disrupted 7SK snRNP by targeting La-related protein 7 (LARP7), releasing active P-TEFb, which phosphorylated RNA polymerase II (Pol II) C-terminal domain (CTD), inducing HIV transcription.

INTRODUCTION

Combination antiretroviral therapy (cART) causes a drastic and immediate viral decrease by targeting distinct steps in the HIV-1 life cycle, effectively blocking replication and halting disease progression (*1*–*3*). However, cART does not target or eliminate HIV that persists in a latent state in cellular reservoirs. Because some of the proviruses are replication competent, latent HIV-infected cells inevitably rebound once cART is interrupted, leading to necessity for lifelong therapy (*4*). Particularly in resource-limited countries, which are also disproportionally affected, this is translated into an insurmountable medical, social, and financial burden. To achieve a scalable cure for HIV infection, it will be necessary to reduce or eliminate the latent HIV-infected reservoir of cells and/or equip the immune system with the robustness and effectiveness necessary to prevent viral rebound such that cART can be safely discontinued.

An important breakthrough in HIV-1 cure was the unequivocal proof that it is possible to mobilize the latent patient HIV reservoir by treatment with agents that activate HIV gene expression [latency reversal agents (LRAs)] (*5*). However, clinical studies thus far have shown little to no reduction in the latent reservoir in patients (*6*, *7*). This is consistent with limited potency and specificity of currently tested drugs, which appear to be unable to reach a significant proportion of latently infected cells or to induce HIV-1 expression in latent reservoir at sufficient levels to produce viral proteins for recognition by the immune system (*8*). Furthermore, transcriptional stochasticity and heterogeneity of latent HIV integrations (*9*) may pose additional barriers to reactivation of the latent reservoir as a whole; sequential rounds of stimulation yield new infectious particles (*10*), while certain LRA combinations result in more efficient latency reversal when administered in intervals rather than at once (*11*). In addition, pleiotropic functions and toxic effects of LRAs may compromise the ability of CD8$^+$ T cells to eliminate HIV protein–expressing cells (*12*, *13*). Therefore, it is critical to identify and develop novel therapeutics, which strongly induce HIV-1 gene expression to effectively disrupt HIV latency without dampening the immune response.

The pharmaceutical industry is highly equipped for high-throughput screens using defined synthetic libraries. While this is an effective approach, it is important to record that approximately half of the novel small molecules introduced to the market between 1981 and 2014 are natural or nature-derived (*14*). Biological systems represent an invaluable source of functional molecules with high chemical diversity and biochemical specificity, evolved during millions of years of adaptation. In particular, fungi represent a largely unexplored source of compounds with potential therapeutic use. Fungi secrete a gamut

[1]Department of Biochemistry, Erasmus MC University Medical Center Rotterdam, PO Box 2040, 3000 CA Rotterdam, Netherlands. [2]Westerdijk Fungal Biodiversity Institute, Utrecht, Netherlands. [3]Center of Expertise in Mycology of Radboud UMC/CWZ, Nijmegen, Netherlands. [4]Ministry of Health, Directorate General of Health Services, Ibri, Oman. [5]Institute of Microbiology of the Czech Academy of Sciences, Videnska 1083, CZ 14220 Prague 4, Czech Republic. [6]Department of Immunology, Erasmus MC University Medical Center Rotterdam, PO Box 2040, 3000 CA Rotterdam, Netherlands. [7]Department of Parasitology and Mycology, Faculty of Medicine, Mashhad University of Medical Sciences, Mashhad, Iran. [8]Key Laboratory of Environmental Pollution Monitoring/Disease Control, Ministry of Education and Guizhou Talent Base of Microbes and Human Health, School of Basic Medicine, Guizhou Medical University, Guiyang 550025, P. R. China. [9]Microbiology Section, Department of Experimental, Diagnostic and Specialty Medicine, School of Medicine, University of Bologna, Bologna, Italy. [10]Departments of Molecular Genetics and Radiation Oncology, Erasmus University Medical Center, PO Box 2040, 3000 CA Rotterdam, Netherlands. [11]Department of Internal Medicine, Section of Infectious Diseases, Erasmus University Medical Center, PO Box 2040, 3000 CA, Rotterdam, Netherlands. [12]Erasmus MC Genomics Core Facility, Department of Cell Biology, Erasmus University Medical Center, PO Box 2040, 3000 CA, Rotterdam, Netherlands.
*These authors contributed equally to this work.
†Corresponding author. Email: t.mahmoudi@erasmusmc.nl

of extracellular compounds and other small molecular extrolites (*15*). While some of these compounds have been shown to have antibiotic (ex. penicillin) or carcinogenic (ex. aflatoxin) properties, little is known in general about their biological activities and possible molecular targets. In addition, a single fungal strain often produces a wide array of secondary metabolites that are not essential for its growth but are exuded as a consequence of specific environment, such as nutrient-rich versus minimal growth conditions (*16*, *17*). Fungal extrolites might target various signaling pathways in mammalian cells, such as those influencing HIV-1 gene expression. Fungal supernatants are an ideal source for an expert academic setting, where low- and medium-throughput biological screening systems, academic knowledge of evolutionary mycology, and state-of-the-art fractionation and purification techniques are routinely combined. Studies of regulation of HIV-1 gene expression have identified distinct molecular mechanisms and cellular pathways at play, which can be targeted pharmacologically to activate expression of latent HIV (*18*, *19*). The rich diversity of fungal extrolites therefore may prove an untapped source of new compounds that target HIV for reactivation. In search of novel LRAs, here, we have performed an unbiased medium-throughput screen of fungal extrolites, coupled to HIV latency reversal bioassays and orthagonal fractionation and mass spectrometry (MS)/nuclear magnetic resonance (NMR), and identified gliotoxin (GTX). GTX potently reversed HIV-1 latency in multiple in vitro latency models as well as ex vivo in cells obtained from all aviremic HIV-1–infected patients examined without associated cytotoxicity. We demonstrate that GTX disrupts the positive transcription elongation factor (P-TEFb)–sequestering 7SK small nuclear ribonucleoprotein (snRNP) complex by targeting the La-related protein 7 (LARP7) component, leading to degradation of its scaffold 7SK RNA and release of active P-TEFb, which is then recruited by Tat to phosphorylate the Ser^2 residue of the RNA polymerase II (Pol II) C-terminal domain (CTD) and activate HIV transcription elongation. Our data highlight the power of combining a medium-throughput bioassay, mycology, and orthogonal MS to identify novel potentially therapeutic compounds.

RESULTS

Growth supernatant of *Aspergillus fumigatus* identified in a medium-throughput screen of fungal secondary metabolite has HIV-1 latency reversal activity

We screened 115 species of filamentous fungi for their ability to induce HIV-1 proviral expression; of the species that appeared promising, 2 to 4 additional strains were tested (table S1). The species belonged to 28 orders (43 families) of the fungal kingdom (Fig. 1A) and were chosen on the basis of their evolutionary position, ecological trends, and known active production of extracellular compounds. The majority of fungi were of ascomycetous affinity, four species were of basidiomycetous affinity, and two belonged to the lower fungi. Selected fungi were grown in both complete yeast media and minimal media (RPMI 1640), as they are known to produce distinct extrolites depending on their growth conditions (fig. S1). Culture supernatants were then screened for latency reversal activity using Jurkat-derived 11.1 and A2 cell line models of HIV-1 latency (J-Lat) in a low-medium throughput assay setup, in which expression of green fluorescent protein (GFP) is controlled by the HIV-1 promoter and indicates latency reversal. We identified the supernatant of *Aspergillus fumigatus* CBS 542.75 to strongly activate the latent HIV-1 5′ long terminal repeat (LTR) (Fig. 1B). We also compared other *Aspergillus* species growth supernatants indicated for their potential to induce HIV-1 expression (Fig. 1C) and observed that only strains of *A. fumigatus* (CBS 542.75, CBS 113.26, and CBS 100074) had latency reversal activity (Fig. 1C).

Orthogonal liquid chromatography–MS/NMR strategy coupled to latency reversal bioassays identifies GTX from growth supernatant of *A. fumigatus* as a putative LRA

Because of the chemical complexity of the positive fungal supernatants, direct MS analysis of their constituents proved to be impossible. Therefore, *A. fumigatus* CBS 100074 growth supernatant was fractionated several times by means of orthogonal MS (Fig. 1D). We selected this particular supernatant as it showed the highest potency to reverse latency in the J-Lat models. After each round of fractionation, all samples/fractions were again tested in latency reversal bioassays, followed by quantitation of the GFP expression and identification of fractions retaining latency reversal activity. As expected, originally less active fractions became more active during the fractionation/enrichment process (Fig. 1E). The most active 7B/7C fractions were further fractioned on a hydrophilic-lipophilic balance (HLB) cartridge (11 samples) and components of 7B/7C and 11C fractions dereplicated by CycloBranch software (Fig. 1E and fig. S2, A and B) (*20*). Compound matching against the annotated database of *Aspergillus* secondary metabolites revealed a set of candidate compounds further selected for latency reversal testing (fig. S2C and table S2). Among the candidate molecules identified, GTX, obtained from a commercially available synthetic source, was able to induce expression of the latent provirus in a concentration-dependent manner (Fig. 1F). Notably, GTX was found in all positive fractions (table S2). While GTX isolated from supernatant of CBS 100074 showed strong induction of HIV-1 transcription, supernatant of *Aspergillus flavus* (CBS 625.66), a close relative of *A. fumigatus* that was inactive in latency reversal (Fig. 1C), did not contain GTX (fig. S2, D and E), providing further support that GTX is the main mediator of LRA activity in *A. fumigatus* supernatants.

GTX reverses latency in ex vivo infected primary $CD4^+$ T cells without associated cytotoxicity

To examine the latency reversal potential of GTX in a more clinically relevant system, we used a modified primary ex vivo infected latency model, in which primary $CD4^+$ T cells are infected with a full-length replication-incompetent HIV-1 virus driving expression of the luciferase reporter (fig. S3A) (*21*). Treatment of latently infected $CD4^+$ T cells with GTX resulted in significant, concentration-dependent latency reversal at lower concentrations than necessary to achieve reactivation in latently infected cell lines (Fig. 2, A to C). GTX (20 nM) treatment resulted in more than 20-fold induction of HIV-1 expression (Fig. 2A), which translated into more than 10% latency reversal of that observed upon maximal stimulation with phorbol 12-myristate 13-acetate (PMA)/ionomycin (Fig. 2B). Similar to the latency reversal observed using commercially available synthetic GTX (Fig. 2, A and B), treatment of HIV-1–infected latent primary $CD4^+$ T cells with GTX isolated from growth supernatant of *A. fumigatus* CBS 100074, estimated at 20 nM by NMR in comparison to commercially available GTX, resulted in significant latency reversal, approximately 10% of maximal PMA/ionomycin stimulation (Fig. 2C). At high concentrations, GTX is known to be toxic to immune cells (*22*–*24*), ascribed to its unusual disulfide

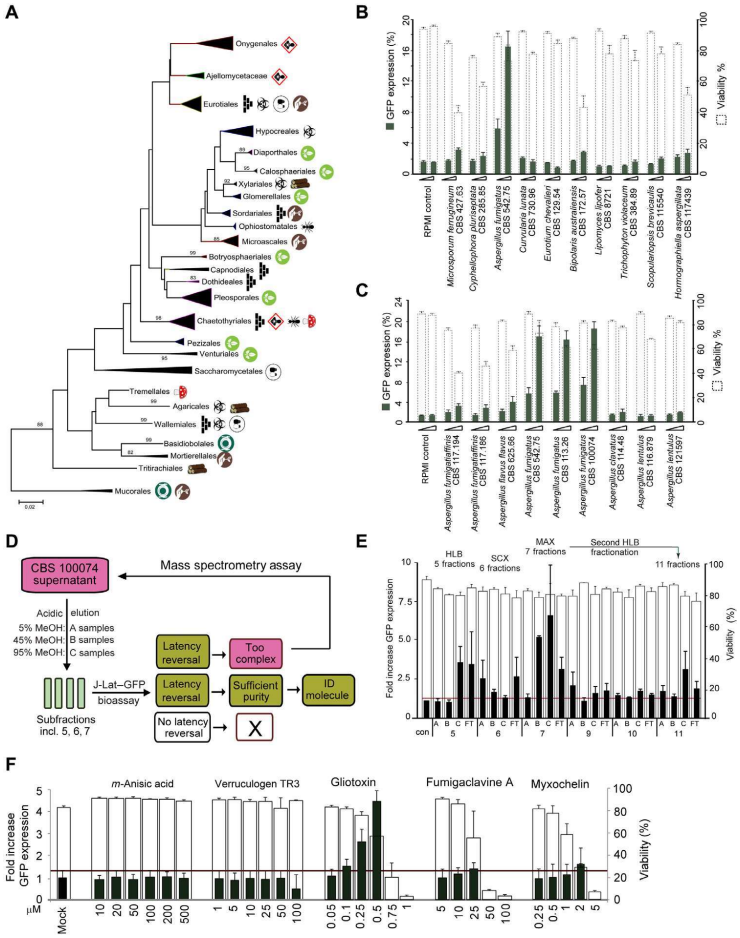

Fig. 1. Medium-throughput screen of fungal secondary metabolites combined with orthogonal fractionation and MS strategy coupled to latency reversal bioassays identifies GTX from growth supernatant of *A. fumigatus* to reverse HIV-1 latency. (**A**) Phylogenetic tree representing the main orders of the fungal kingdom with strains used in the current study, collapsed per order. Orders selected from the tree published (*57*), with some of the lower orders included for structural reasons. Approximate ecological trends in the orders are summarized by symbols, as follows: vertebrate pathogenicity prevalent, climatic extremotolerance prevalent, frequent production of extracellular metabolites or mycotoxins, frequent osmotolerance or growth in sugary fluids, numerous members with soilborne lifestyle, numerous members inhabiting decaying wood rich in hydrocarbons, frequent insect association, frequent mushroom decomposition or hyperparasitism on fungi or lichens, and frequent inhabitants of foodstuffs or vertebrate intestinal tracts. (**B**) Latency reversal bioassay performed by treatment of J-Lat A2 cells with increasing volumes of growth [normalized by O.D. (optical density)] supernatants obtained from selected fungal strains. (**C**) Latency reversal bioassay in J-Lat A2 cells with growth supernatants obtained from members of the *Aspergillus* genus. Cells were treated as in (B). (**D**) Schematic representation of the orthogonal MS strategy coupled to latency reversal bioassays used to identify putative LRA. See main text for full description. (**E**) Three preconcentration cartridges (HLC, SCX, and MAX) were combined with variable content of extracting solvent (A: 5% MeOH, B: 45% MeOH, and C: 95% MeOH; FT, flowthrough). Latency reversal potential of fractionated secondary fungal metabolites was tested via treatment of J-Lat A2 cells. Latency reversal (fold increase percentage of GFP, left axis, black bars) and cell viability (percentage of viability, right axis, empty bars) were assessed by flow cytometry analysis. (**F**) Commercially obtained versions of five common molecules identified in active fractions were tested for LRA activity in J-Lat A2 cells. Data are presented as fold increase percentage of GFP expression and percentage of viability as indicated, ±SD from at least three independent experiments.

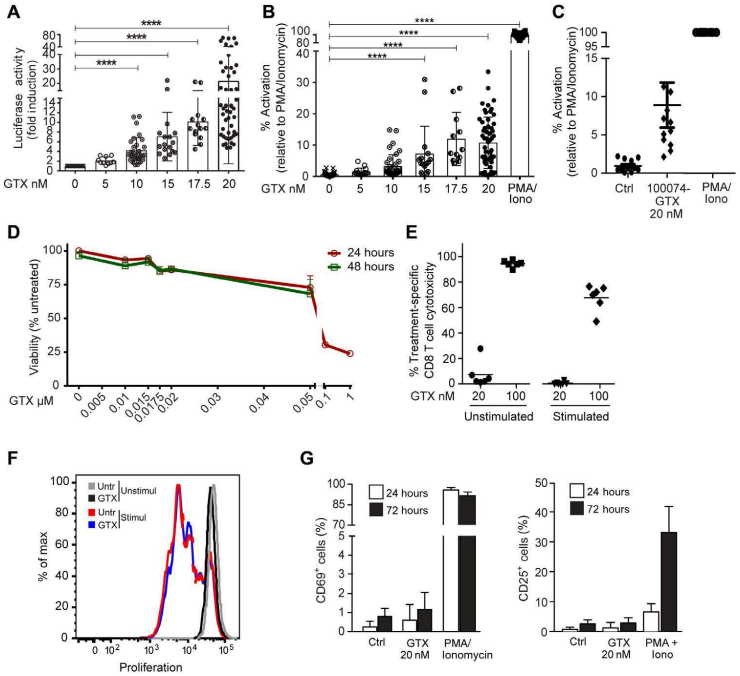

Fig. 2. GTX (20 nM) reverses HIV-1 latency in ex vivo infected primary CD4$^+$ T cells without associated cytotoxicity, T cell activation, or inhibition of proliferative capacity. (**A**) Latency reversal after treatment of latently infected primary CD4$^+$ T cells with increasing concentrations of GTX for 24 hours as indicated, shown as fold induction over untreated control luciferase activity. Statistical analysis was calculated using Kruskal-Wallis one-way analysis of variance (ANOVA) (****$P < 0.0001$). (**B**) Data presented in (A) normalized and shown as percent latency reversal activity relative to treatment with PMA/Ionomycin. (**C**) Latency reversal after treatment of HIV-1–infected latent primary CD4$^+$ T cells with 20 nM GTX isolated from growth supernatant of *A. fumigatus* CBS 100074, measured as increased luciferase activity normalized to and shown as percentage of activation of PMA/ionomycin ($n = 6$). Wide horizontal lines represent average, and shorter horizontal lines represent SD. (**D**) Viability of the primary CD4$^+$ T cells treated for 24 (red line) and 48 (green line) hours with indicated increasing concentrations of GTX, assessed by flow. (**E**) Unstimulated or αCD3/αCD28-stimulated PBMCs were treated with 20 and 100 nM GTX for 72 hours, stained with AnnexinV, and cell death (AnnexinV$^+$ CD3$^+$CD8$^+$) was determined by flow cytometry. Treatment-specific cell cytotoxicity was calculated as indicated in the Materials and Methods section. Each symbol represents one healthy donor ($n = 6$), and horizontal lines depict means. (**F**) Representative fluorescence-activated cell sorting (FACS) plot overlay showing the proliferation of unstimulated or αCD3/CD28-stimulated CD8$^+$ T cells in the presence or absence of GTX. Cells were stained with a proliferation dye and analyzed 72 hours later by flow cytometry to define nonproliferating cells (proliferation dye undiluted, bright stain intensity) and dividing cells (proliferation dye diluted, reduced stain intensity). (**G**) Activation status of primary CD4$^+$ T cells upon GTX treatment as indicated ($n = 6$).

bridge, and responsible for pleiotropic effects on cellular and viral systems (*25*).

Consistent with the literature, GTX concentrations upward of 100 nM induced significant toxicity as indicated by annexin V staining (Fig. 2D and fig. S3B). However, primary CD4$^+$ T cell viability was not significantly affected after GTX treatment at concentrations up to 20 nM, with moderate toxicity observed at 50 nM (Fig. 2D and fig. S3B). Thus, at lower concentrations in which GTX did not show toxicity on CD4$^+$ T cells, strong latency reversal was induced (Fig. 2, A to D, and fig. S3B). CD8$^+$ T cells play a central role in eliminating HIV-infected cells (*26*). Therefore, it is of utmost importance to evaluate the potential toxicity of newly developed LRAs on CD8$^+$ T cells (*13*). GTX at a low concentration of 20 nM did not reduce the viability or proliferation capacity of CD8$^+$ T cells whether unstimulated or αCD3/αCD28-stimulated peripheral blood mononuclear cells (PBMCs) were examined (Fig. 2, E and F, and fig. S4, A and B). Consistent with the literature (*22*–*25*), treatment with higher concentrations of GTX at 100 nM and 1 µM caused apoptosis and death of primary CD4$^+$ and CD8$^+$ T cells as well as B cells, natural killer (NK) cells, and monocytes, as shown by annexin V staining followed by flow cytometry (Figs. 2, D and E, and 3C and figs. S3B and S4, A to C). Potential for clinical applicability of a candidate LRA also requires that it does not induce global T cell activation nor should it interfere with CD8$^+$ T cell activation. Treatment of unstimulated primary CD4$^+$ T cells and CD8$^+$ T cells with GTX (20 nM), which significantly reversed latency, did not induce expression of the T cell activation markers CD69 and CD25 (Figs. 2G and 3D and fig. S5, A and B), nor did it induce proliferation of resting CD4$^+$ and CD8$^+$ T cells (fig. S5, C and D), while, as expected, PMA/ionomycin treatment activated T cells (Fig. 2G). Conversely, GTX treatment of activated PBMCs also did

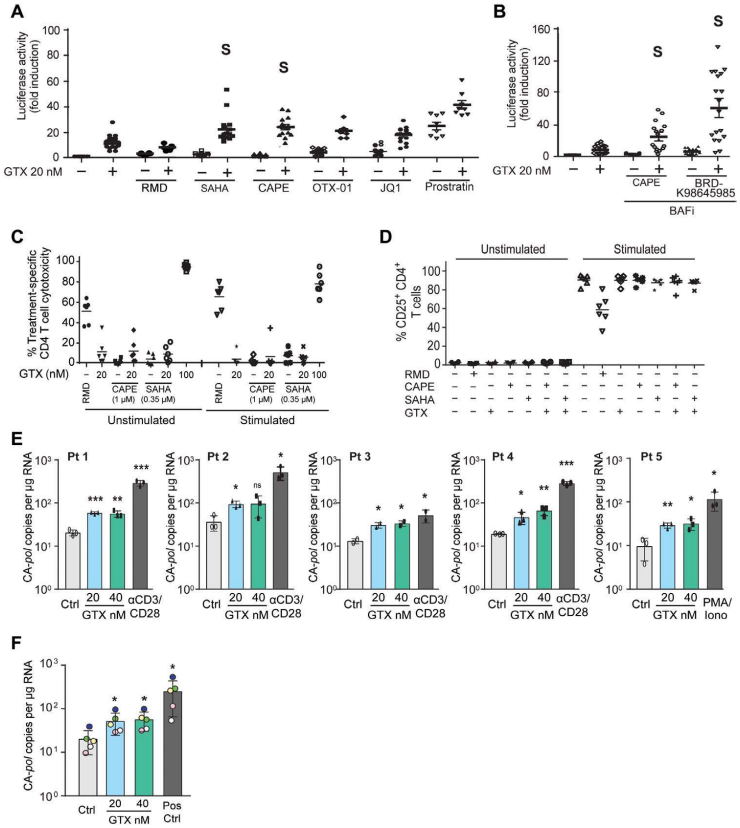

Fig. 3. GTX strongly synergizes with HDAC and BAF inhibitors and reverses latency in primary CD4$^+$ T cells obtained from all tested aviremic participants. (**A** and **B**) HIV-1 latency reversal in latent ex vivo HIV-1–infected primary CD4$^+$ T cells in response to 24-hour cotreatment with 20 nM GTX and distinct LRA class compounds [2 nM RMD, 350 nM SAHA, 1 μM CAPE, 2 μM OTX-01, 0.5 μM JQ-1, and 0.2 μM prostratin (A) and 1 μM CAPE and 5 μM BRD-K98645985 (B)] and shown as fold increase in luciferase activity. S indicates compound synergism in latency reversal according to the Bliss independence score. (**C**) Cytotoxicity of GTX alone and combined with indicated LRAs in CD4$^+$ T cells. Unstimulated or αCD3/αCD28-stimulated PBMCs were cotreated as indicated for 72 hours followed by annexin V staining, and cell death (AnnexinV$^+$ CD3$^+$CD4$^+$) was determined by flow cytometry. (**D**) GTX (20 nM) does not alter activation of CD4$^+$ T cells. PBMCs from healthy donors were incubated with the indicated LRAs for 72 hours, either unstimulated or stimulated with αCD3/αCD28 antibodies. Panels depict pooled data showing the frequency of CD25$^+$ cells within CD4$^+$ T cells. (**E**) Absolute, cell-associated (CA) *pol* copy number in CD4$^+$ T cells isolated from five aviremic participants that were treated in vitro with vehicle control (Untr), GTX (20 and 40 nM), or positive control for 24 hours as indicated. Statistical significance was calculated using *t* test (*$P < 0.05$; **$P < 0.005$; ***$P < 0.0005$). ns, not significant. (**F**) Data presented in (D) had been averaged and plotted together. Each symbol represents aviremic participant: green, participant 1; blue, participant 2; white, participant 3; yellow, participant 4; and pink, participant 5. Statistical significance was calculated using unpaired Mann-Whitney test (*$P < 0.05$).

not inhibit CD25 expression (Fig. 3D and fig. S5, A and B) or proliferation of activated CD4$^+$ or CD8$^+$ T cells (fig. S5, C and D).

GTX enhances activity of other LRA class molecules and synergizes strongly with histone deacetylase and BAF inhibitors

To investigate possible synergies, we tested the latency reversal potential of GTX (20 nM) in combination with a panel of known LRAs in the J-Lat A2 and 11.1 models of latency (fig. S6) as well as in ex vivo infected primary CD4$^+$ T cells (Fig. 3, A and B). GTX cotreatment enhanced the latency reversal activity observed after single treatments with all compounds (Fig. 3, A and B). When latent HIV-1–infected primary CD4$^+$ T cells were cotreated with GTX (20 nM) and either the histone deacetylase (HDAC) inhibitor suberoylanilide hydroxamic acid (SAHA) or BAF (BRG1- or BRM-associated factors) inhibitors caffeic acid phenethyl ester (CAPE) [at 1 μM concentration in which it does not inhibit nuclear factor κB (NF-κB)] (*27*) or BRD-K98645985 (*28*), synergistic reversal of HIV-1 latency was observed (Fig. 3, A and B). Cotreatments with BET (bromodomain and extra-terminal proteins) inhibitors JQ-1 and OTX-015, as well

as prostratin, resulted in an additive effect on HIV-1 provirus expression. In the primary $CD4^+$ T cell model of HIV-1 latency, GTX treatment alone showed more potent latency reversal activity than SAHA, CAPE, OTX-015, JQ-1, or romidepsin (RMD) alone at tested noncytotoxic concentrations (Fig. 3, A and B). RMD treatment showed modest latency reversal activity (Fig. 3A) and, consistent with the literature (*13*), significant $CD4^+$ and $CD8^+$ T cell cytotoxicity (Fig. 3C and fig. S4, A and B). With the exception of RMD, we did not observe any negative impact of these cotreatments on viability and proliferation of $CD4^+$ T cells (Fig. 3C and fig. S5C), $CD8^+$ T cells (figs. S4, A and B, and S5D), and other immune subpopulations, including $CD19^+$ B cells, $CD56^+$ NK cells, and $CD14^+$ monocytes (fig. S4C). Moreover, none of the cotreatments altered the activation status of either resting or activated $CD4^+$ and $CD8^+$ T cells (Fig. 3D and fig. S5, A and B). Our observed synergistic effects upon GTX cotreatment with BAF inhibitors and the HDAC inhibitor SAHA suggested that GTX may target a different pathway for HIV-1 latency reversal, as targeting the same pathway with different molecules would more likely result in additive effects. Unlike SAHA, GTX treatment of $CD4^+$ T cells did not result in increased histone acetylation (fig. S7A). Similarly, we excluded that GTX behaves as a protein kinase C (PKC) agonist, as treatment with GTX did not induce T cell activation or the expression of PKC pathway target genes (Fig. 2G and fig. S7B).

GTX reverses HIV-1 latency after ex vivo treatment of $CD4^+$ T cells from all aviremic HIV-1–infected study participants

We next examined the potential of GTX to reverse latency after ex vivo treatment of $CD4^+$ T cells obtained from people living with HIV-1. All five participants enrolled were treated with cART and maintained HIV-1 viremia below 50 copies/ml for at least 2 years. Despite differences in the size of the latent pool, assessed by maximal stimulation of the cells with α-CD3/CD28 beads or PMA/ionomycin, GTX treatment at noncytotoxic 20 and 40 nM concentrations significantly increased the levels of cell-associated HIV-1 *pol* RNA copies (CA-*pol* copies) in $CD4^+$ T cells obtained from aviremic HIV-1^+ participants (Fig. 3, E and F). Notably, the observed GTX effect is systematic, as latency reversal was uniformly observed in cells of all tested participants after 24 hours of stimulation (Fig. 3, E and F). This observed latency reversal at the RNA level is the first step consistent with induction of protein expression, although this is not formally examined here. In addition, we observed no increase in expression of genes related to T cell–specific responses, reactive oxygen species, or apoptosis, previously reported pleiotropic effects of GTX observed at significantly higher concentrations (fig. S7C). These results therefore indicate that GTX treatment at nontoxic concentrations reverses latency without inducing immune cell toxicity or activation and without affecting T cell proliferation, rendering GTX a promising potential candidate for further clinical investigation in context of HIV-1 latency reversal and inclusion in "shock and kill" strategies.

GTX reverses HIV-1 latency via disruption of 7SK snRNP, leading to release of active P-TEFb

To gain insight into the molecular mechanism by which GTX reverses latency, we performed RNA sequencing of primary resting $CD4^+$ T cells isolated from healthy blood donors that were treated for 4 hours with 20 nM GTX. This short incubation time was chosen to focus on primary effects of GTX on the global transcriptome, decreasing the presence and likelihood of secondary transcriptional effects. We observed a very good correlation between treatments of two independent healthy blood donors (Fig. 4A, top). Moreover, less than 700 genes showed an altered differential expression pattern (Fig. 4A, bottom). Small nuclear RNA 7SK was the most decreased (more than ninefold) transcript after GTX treatment in $CD4^+$ T cells from the independent donors (Fig. 4, A and B). 7SK RNA serves as a scaffold for the 7SK snRNP complex that sequesters the P-TEFb and inhibits its activity (*29*–*33*). Among all components of the 7SK snRNP complex and its close interactors, only the 7SK transcript was affected by treatment with GTX (Fig. 4B and fig. S9A). Consistent with our observations after treatment of $CD4^+$ T cells obtained from aviremic participants (fig. S7C), we did not detect significant change in expression of NF-κB, oxidative stress, apoptosis, and T cell effector function-related genes after GTX treatment (figs. S7B and S8), indicating that GTX (20 nM) treatment does not influence these pathways after 4 or 24 hours of stimulation. As P-TEFb is an essential cofactor for Tat-mediated HIV-1 transcription elongation (*34*, *35*), we examined whether GTX treatment affects P-TEFb activity. Phosphorylation of Ser^2 residues within the CTD of RNA Pol II is a prerequisite for activation of transcription elongation and is mediated by the kinase activity of cyclin-dependent kinase 9 (CDK9), a component of P-TEFb (*36*). To examine whether GTX treatment resulted in Ser^2 RNA Pol II phosphorylation, we treated resting $CD4^+$ T cells with GTX, the CDK9 inhibitor flavopiridol (FPD), and PMA or αCD3/αCD28 as positive control (Fig. 4C and fig. S9B). As expected, FPD treatment abrogated RNA Pol II phosphorylation, while PMA stimulation led to strong Ser^2 RNA Pol II phosphorylation. Treatment with GTX caused an increase in phosphorylation of the CDK9 target RNA Pol II Ser^2 in three independent donors tested (Fig. 4, C and D, and fig. S9B). We also examined potential Tat-independent effects of GTX on basal HIV-1 transcription by comparing GTX-induced reactivation in J-Lat A72 cells, which lack Tat, with that in J-Lat A2 cells (fig. S9C). While GTX robustly reactivated transcription in Tat-containing A2 cells, in comparison, A72 cells were not significantly reactivated. These results support a Tat-dependent mechanism of GTX function consistent with a role in enhancing Tat–P-TEFb–mediated HIV-1 transcription.

The fact that short-term GTX treatment enhanced P-TEFb activity in resting $CD4^+$ T cells without cellular activation (Figs. 2G, 3D, and 4C) led us to hypothesize that GTX treatment may cause destabilization of the 7SK snRNP complex, leading to the release of free (active) P-TEFb. Active P-TEFb would then become available for transcription elongation at the latent HIV-1 LTR, a critical step required for HIV-1 latency reversal (*37*–*39*). To test this, we performed glycerol gradient sedimentation experiments after treatment of resting $CD4^+$ T cells with GTX (Fig. 4, E to G, and fig. S9D). GTX treatment (20 nM) of $CD4^+$ T cells for 4 hours resulted in release of free P-TEFb from its inhibitory higher–molecular weight 7SK snRNP complex, as shown by Western blot analysis depicting distribution of the P-TEFb component CDK9 over high– and low–molecular weight fractions (Fig. 4F and fig. S9D). As expected, control treatment of $CD4^+$ T cell lysates with ribonuclease A (RNase A), which digests the 7SK RNA scaffold, resulted in release of free P-TEFb, which eluted at lower–molecular weight fractions (Fig. 4F and fig. S9D). Quantification of free versus 7SK snRNP–sequestered P-TEFb demonstrates a significant GTX-induced release of free P-TEFb from the 7SK snRNP complex in $CD4^+$ T cells from three independent donors (Fig. 4G). CDK9 T-loop phosphorylation at Thr^{186} is critical for the kinase

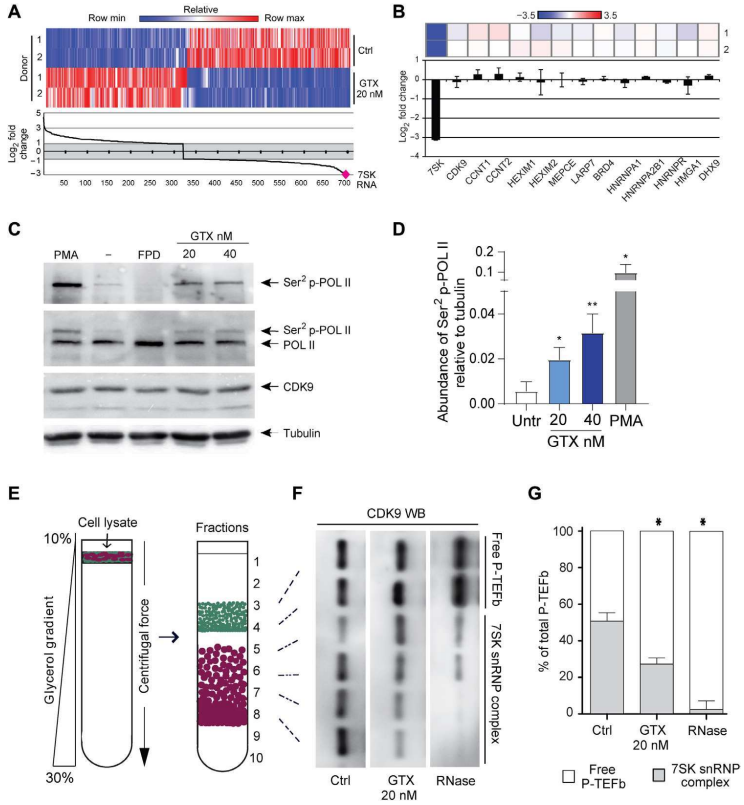

Fig. 4. GTX treatment of resting CD4$^+$ T cells causes decrease in 7SK RNA and activation of P-TEFb activity. (**A**) Heatmap of differentially expressed genes obtained from RNA sequencing analysis of primary CD4$^+$ T cells treated as indicated for 4 hours (top). RNA sequencing indicates 7SK RNA to be the most differentially decreased gene in response to GTX treatment of CD4$^+$ T cells in two independent donors (bottom). (**B**) GTX treatment of primary CD4$^+$ T cells for 4 hours leads to specific depletion of 7SK RNA levels and not mRNA levels of other components of the 7SK snRNP complex. (**C**) Representative Western blot (WB) analysis of CTD Ser^2 phosphorylation of RNA Pol II mediated by CDK9 in primary CD4$^+$ T cells treated for 6 hours with GTX as indicated. PMA was used as a positive control, and FPD was used as a negative control. (**D**) Quantification of bands representing phosphorylated RNA Pol II normalized to tubulin and relative to untreated control from three independent experiments (C; fig. S9C). Statistical significance was calculated using unpaired *t* test (*$P < 0.05$; **$P < 0.01$). (**E** and **F**) GTX treatment causes release of P-TEFb from sequestration within the 7SK snRNP complex. (E) Schematic of glycerol gradient experiments, in which cell lysates (from GTX-treated or untreated cells) are loaded on top of generated glycerol gradients (10 to 30%) and ultracentrifuged, followed by collection of fractions, trichloroacetic acid protein precipitation, and subsequent analysis by SDS–polyacrylamide gel electrophoresis Western blotting. (F) Representative Western blot analysis of glycerol gradient sedimentation of lysates from primary CD4$^+$ T cell, which were treated (6 hours) with GTX (20 nM) or vehicle control as indicated using antibodies specific for the P-TEFb component CDK9. As control, untreated lysates were treated with RNase for 1 hour to digest 7SK RNA and release P-TEFb. (**G**) Quantification of free versus total CDK9 in primary CD4$^+$ T cells treated as indicated, as shown in (F) and fig. S9E, from three independent donors. Statistical significance was calculated using unpaired *t* test (*$P < 0.05$).

activation and its dissociation from the 7SK snRNP (*40*). In resting CD4$^+$ T cells, cyclin T1 levels are low, as are the levels of CDK9 T-loop phosphorylation (*39*). To check whether GTX-induced release of P-TEFb involves increased CDK9 T-loop phosphorylation or increase in cyclin T1 levels, we treated primary CD4$^+$ T cells with increasing concentrations of GTX for 6 hours and used PMA as positive control. At 6 hours after treatment, at a time point in which we observe phosphorylation of RNA Pol II CTD (Fig. 4, C and D), GTX treatment does not cause phosphorylation of CDK9 at Thr^{186}, nor does it lead to increased cyclin T1 levels (fig. S9, E and F), demonstrating that these mechanisms are not involved in GTX-induced latency reversal at this early time point.

To understand better which component of the 7SK snRNP complex may be targeted by GTX, we performed in silico docking experiments using two independent software packages, Chimera and Achilles. We modeled GTX against all essential components of the complex separately, as complete crystal structure of 7SK snRNP is not yet available. Notably, we observed preferential binding of GTX

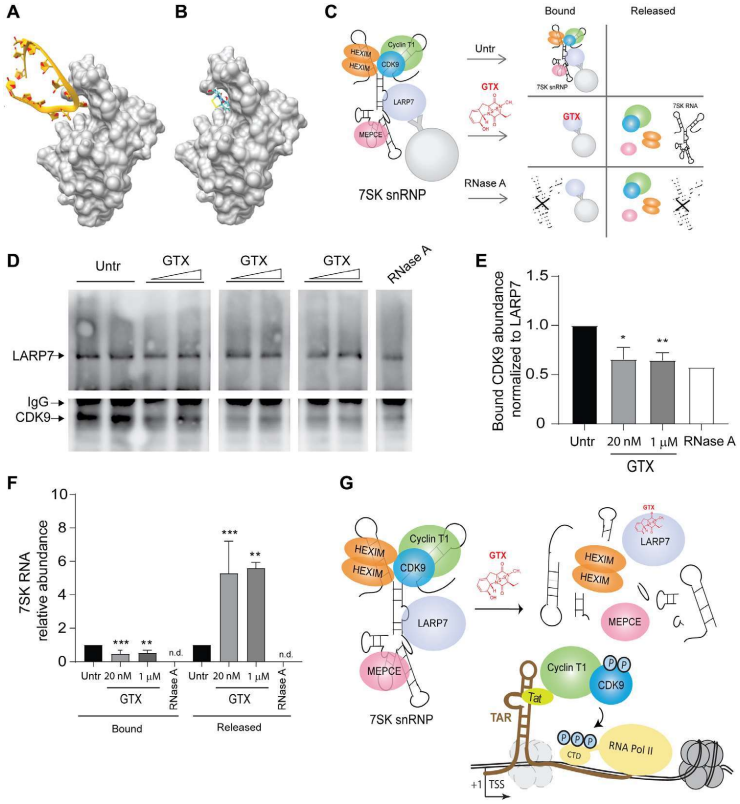

Fig. 5. GTX disrupts 7SK snRNP, causing release of P-TEFb and enhanced HIV-1 transcription. (**A**) Crystal structure of human LARP7 CTD in complex with 7SK RNA SL4 (Protein Data Bank ID code 6D12). LARP7 is shown in space-filling representation (gray) with bound RNA as yellow cartoon representation with bases indicated as flat rings (oxygen in red). (**B**) Proposed binding mode of GTX into the deep pocket on the surface of LARP7 as predicted by Chimera's AutoDock Vina function and the Achilles Blind Docking server. Color code for GTX: carbon (turquoise), oxygen (red), sulfur (yellow), hydrogen (white), and nitrogen (blue). (**C**) Schematic representation of the 7SK snRNP coimmunoprecipitation CDK9 release experiment. (**D**) 7SK snRNP complex is immunoprecipitated using beads coated with anti-LARP7. Beads are divided and left either untreated or treated with GTX 20 nM or 1 μM or RNase A as indicated. Bead-bound fractions are separated and subjected to Western blot analysis to detect presence of LARP7 and CDK9. IgG, immunoglobulin G. (**E**) Quantification of CDK9 abundance normalized to immunoprecipitated LARP7 and relative to untreated control ($n = 3$). Statistical significance was calculated using unpaired t test (*$P < 0.05$; **$P < 0.01$). (**F**) 7SK RNA release assay from immunoprecipitated 7SK snRNP complex, as represented in (C). Bound and released fractions are subjected to reverse transcription quantitative polymerase chain reaction to quantitate the levels of bead-bound and released 7SK RNA in reaction supernatant. Input 7SK RNA (prereaction beads) was used for normalization. Statistical significance was calculated with unpaired t test ($n = 3$, **$P < 0.01$; ***$P < 0.001$; n.d., not detected). (**G**) Proposed model for GTX-mediated transcription activation of the latent HIV-1 LTR via degradation of 7SK RNA and release of CDK9 from the 7SK snRNP complex. Free P-TEFb is then recruited to the HIV-1 Tat-TAR axis, leading to phosphorylation of RNA Pol II at Ser^2 and subsequent stimulation of transcription elongation.

into the hydrophobic pocket of LARP7, which, in physiological conditions, is responsible for binding stem loop 4 (SL4) of the 7SK RNA (Fig. 5, A and B, and fig. S10). LARP7 is a critical component, responsible for stabilization of the 7SK snRNP complex, as its depletion has been shown to lead to decreased levels of 7SK RNA with concomitant increase in free P-TEFb levels (*41*). To test whether GTX interferes with LARP7-7SK RNA binding, we performed a 7SK RNA release assay (Fig. 5, C to F). 75K snRNP complex was immunoprecipitated and immobilized on protein G beads using a LARP7 antibody. 7SK snRNP–bound beads were then either left untreated or treated with GTX or RNase A as indicated, and the presence of LARP7-bound CDK9 was examined by Western blot analysis of the bead-bound fraction (Fig. 5, D and E). As expected, RNase A treatment resulted in direct disruption of the 75K snRNP complex as measured by release of the CDK9 component into the supernatant and its separation from the bead-bound LARP7 component (Fig. 5, D and E). GTX treatment also resulted in release of CDK9 as observed in relative decrease in LARP7-bound

CDK9 as determined by Western blot analysis (Fig. 5, D and E). In agreement, treatment with GTX resulted in a concomitant significant decrease in abundance of scaffold 7SK RNA from the bead-bound 7SK snRNP fraction as well as an approximately sixfold increase in levels of 7SK RNA in the released fraction (Fig. 5F).

Our experimental data, together with this modeling exercise and previously published data, are consistent with a model in which GTX interferes with the binding of SL4 of 7SK RNA into the hydrophobic pocket of LARP7, which results in destabilization of the complex and subsequent release of P-TEFb and 7SK RNA (Fig. 5, D to G). In resting $CD4^+$ T cells, 7SK RNA is then degraded and free P-TEFb made available for recruitment to the paused RNA Pol II at the latent HIV LTR by the Tat-TAR (trans-activation response element) axis. CDK9 then phosphorylates CTD of RNA Pol II, leading to activation of proviral transcription elongation (Fig. 5G).

DISCUSSION

Distinct classes of LRAs have been shown to target different subpopulations of proviruses (*9*, *19*, *42*, *43*). Thus far, none of the clinically tested LRAs have been able to induce strong viral expression or to significantly deplete the latent reservoir in patients, pointing to potential limitations of single treatments (*6*, *7*). The heterogeneous nature of latent HIV integrations and the complex molecular mechanisms that contribute to maintaining HIV latency, together with individual genetic variability, dictate that a cocktail of stimulatory compounds targeting distinct cellular and HIV gene regulatory pathways would be most effective to activate the latent reservoir in HIV-1–infected patients (*19*). Preclinical studies demonstrate that combination treatments can result in synergism and lead to stronger HIV-1 latency reversal (*11*, *19*, *27*, *28*, *44*–*48*). Here, we found that GTX, a molecule that targets the HIV-1 transcription elongation step, strongly synergized with LRAs that derepress chromatin structure, namely, BAF and HDAC inhibitors, which respectively target complexes that position the latent LTR chromatin in a repressive configuration (*49*) or deacetylate histones compacting LTR chromatin. Cotreatment of primary latently infected $CD4^+$ T cells with GTX and BET inhibitors resulted in additive and not synergistic increase in HIV transcription. This observation is consistent with the fact that these compounds target the same mechanistic step: transcription elongation at the HIV-1 LTR. Our data highlight the attractiveness of simultaneous pharmacological targeting of mechanistically distinct steps in HIV-1 transcription regulation, namely, at the level of chromatin structure, transcription factor–induced activation and transcription elongation. We postulate that more robust latency reversal will be observed when compounds targeting these three mechanistic steps are combined, and further optimized by interventions that address blocks occurring posttranscriptionally, at the polyadenylation and splicing stages, which may hinder translation of HIV-1 genes (*38*). In addition, consistent with the importance of targeting transcription elongation, shown recently to be a major rate-limiting step in HIV-1 latency reversal in patient $CD4^+$ T cells (*38*), ex vivo GTX treatment of $CD4^+$ T cells obtained from cART-suppressed aviremic HIV-1–infected patients demonstrated significant increase in levels of cell-associated HIV-1 RNA in all patients examined.

GTX causes disruption of the 7SK snRNP complex with subsequent release of active P-TEFb by directly targeting LARP7. Other molecules including HMBA (hexamethylene bisacetamide) (*50*) and DRB (5,6-Dichloro-1-β-d ribofuranosylbenzimidazole) and actinomycin D (*30*, *32*) have also previously been shown to cause 7SK snRNP disruption although through indirect mechanisms. Given the significance of P-TEFb in HIV transcription elongation and the current lack of available molecules able to mediate its release from the inhibitory 7SK snRNP complex, GTX may be a promising candidate not only in the context of HIV-1 latency reversal but also in other diseases in which P-TEFb plays a prominent regulatory role (*51*). Our modeling exercises provide insight toward a mechanism where GTX competes with 7SK RNA for the hydrophobic pocket of LARP7, causing destabilization and disassembly of the 7SK snRNP complex, leading to the release of P-TEFb and subsequent degradation of the 7SK RNA scaffold as observed in our experiments (Figs. 4 and 5 and figs. S9 and S10). LARP7 has been shown to be a critical scaffold required for the stability of the 7SK snRNP complex; consistent with our observations, RNA interference–mediated depletion of LARP7 resulted in elevated levels of free P-TEFb and increased Tat-mediated HIV-1 expression, concomitant with degradation of 7SK RNA (*41*).

Thus far, GTX has been regarded as a toxin and a virulence factor of *Aspergillus* spp. fungi, shown to function as an immunosuppressant that inhibits phagocytosis, blocks NF-κB signaling and cytokine production, and induces reactive oxygen species formation (*22*, *24*, *25*, *52*–*55*). These properties are ascribed to the molecule's unusual disulfide bridge, which may mediate the activity of GTX by cycling between a reduced and oxidized state (*25*). However, it is important to note that all of the above-mentioned effects of GTX were observed at high concentrations in the 100 nM to 5 μM range, concentrations at which we also observed significant toxicity and cell death (Fig. 2 and figs. S3, S4, and S6). Serum concentrations of GTX reported in patients with aspergillosis are found to be between 200 nM and 2.4 μM (*56*), more than 10 to 100 orders of magnitude higher than concentrations that we have shown to effectively reverse HIV-1 latency in primary T cells and cells of cART-suppressed HIV-1–infected participants (Figs. 3 and 4). Together, these observations suggest that lower GTX concentrations in the 20 nM range, at which effective HIV-1 latency reversal is observed in primary $CD4^+$ T cells without associated toxicity, global T cell activation, or interference with capacity for $CD8^+$ T cells activation, will be physiologically achievable in a therapeutic context. Our data therefore support the potential of GTX for inclusion in combination latency reversal therapeutic approaches in a safe concentration range. Last, our data underlie the power of coupling a screen of fungal extrolites, which comprise a largely unexplored plethora of bioactive chemical entities, with bioassays and state-of-the-art fractionation and MS/NMR as a strategy to identify and characterize novel compounds with therapeutic potential.

MATERIALS AND METHODS

Cells and culture conditions

Jurkat latent (J-Lat) cell lines A2 and 11.1 were cultured in RPMI 1640 media supplemented with 10% fetal bovine serum (FBS) and penicillin-streptomycin (100 μg/ml) at 37°C in a humidified 95% air–5% CO_2 incubator. Primary $CD4^+$ T cells were cultured in RPMI 1640 media supplemented with 7% FBS and penicillin-streptomycin (100 μg/ml) at 37°C in a humidified 95% air–5% CO_2 incubator.

Preparation of fungal supernatants

We screened 115 species of filamentous fungi (table S1 and fig. S1A). The species belonged to 28 orders (43 families) of the fungal kingdom.

The majority were of ascomycetous affinity including ascomycetous yeasts (Saccharomycetales: 4 species), 12 were of basidiomycetous affinity including 3 basidiomycetous yeasts (Trichosporonales and Tremellales) and 3 species of lower fungi (Mucorales) (*57*). Rationale for choice was the expected production of a wide array of metabolites, which are known to be more pronounced in fungi living in habitats with environmental stress or microbial competition. Particularly versatile nutrient scavengers in Eurotiales and Hypocreales are established metabolite and toxin producers. Onygenales are cellulose and keratin degraders and contain a large cluster of mammal pathogens with alternating environmental life cycles. Members of Capnodiales are saprobes in environments with stressful microclimates such as rock, glass, and indoor. Identity of all strains was verified by recombinant DNA internal transcribed spacer and partial nucLSU (D1/D2 of large subunit) sequencing. Strains were derived from lyophilized storage in the reference collection of the Centraalbureau voor Schimmelcultures (housed at the Westerdijk Fungal Biodiversity Institute, Utrecht, The Netherlands). After opening, contents of vials were taken up in 1 ml of malt peptone and distributed on Malt Extract Agar (MEA; Oxoid) culture plates. Strains were maintained on MEA slants and subcultured regularly until use. Mycelial fragments of 1-week-old colonies grown on MEA at 25°C were used as inocula for 500-ml flasks containing 150 ml of RPMI 1640 (with glutamine), shaken at 180 rpm and incubated at 25°C for 7 days, with one negative control. Flasks were checked daily until biomass reached one-third to one-fourth of the volume and then harvested by centrifugation at 14,000*g* and filtered using 0.2-μm metal filters. Supernatants were transferred to Falcon tubes and used for latency screens. One strain per genus was used in a first round; additional isolates, some of which were close relatives and others located at larger phylogenetic distance, were tested in case of positive response. Positive tests of strain *A. fumigatus* CBS 113.26 was thus followed by *A. fumigatus* CBS 154.89, CBS 117884, and CBS 100074, *Aspergillus lentulus* CBS 117884, and *A. flavus* CBS 625.66.

Fractionation and MS characterization of active components

Complex fungal supernatants (3.3 ml) were twice extracted with ethylacetate (3 ml) in glass tubes (5-min vortex) and centrifuged at 3000 rpm. Water phase was discarded and organic extract dried in a vacuum concentrator. Lipids were removed by consequent hexane/water extraction [50/50 (v/v), 4-ml total volume], and aqueous phase was collected and dried. The dried material was reconstituted in 50% methanol (MeOH) and such a solution loaded onto HLB, MCX (Mixed-mode, strong Cation-eXchange), and MAX (Mixed-mode, strong Anion-eXchange) cartridges (Fig. 2, A and B) obtained from Waters Corporation (Prague, Czech Republic). The adsorbed compounds were desalted and stepwise eluted with increasing (5, 45, and 95%) organic solvent (MeOH) gradient (1% HCOOH), providing A, B, and C sample variants, respectively (Fig. 2B). HLB was based on *N*-vinylpyrrolidone–divinylbenzene copolymer and provided 5 fractions. MCX was a cation-exchange sorbent that represented the HLB material modified with SO_3H^- groups (6 fractions). The best performance was provided by anion-exchange MAX cartridge, providing 7 fractions. After each round of fractionation, all samples were tested in J-Lat/S-Lat latency models, followed by quantitation GFP/luciferase expression and identification of fraction-retaining activating component. As expected, originally less active fractions have become positive, as the active components became populated during the enrichment process. The same phenomenon was observed when working with less or more active *Aspergillus* strains (fig. S2B). The most active 7B/7C fractions were further fractioned on HLB cartridge (11 samples) and components dereplicated by CycloBranch software (*20*). Compound matching against the annotated database of *Aspergillus* secondary metabolites has revealed a set of candidate compounds further selected for latency reversal testing. GTX was present in active fractions (Fig. 2B and fig. S2B). Detailed examination of commercial (GTX, Cayman and ApexBio) and natural GTXs was performed by high-performance liquid chromatography and Fourier transform ion cyclotron resonance (FTICR) MS. A solariX XR 12T FTICR instrument (Bruker Daltonics, Billerica, USA) was operated in a positive ion mode with electrospray ionization. Separation of GTX components was performed on an Acquity UPLC HSS T3 analytical column (Waters, Prague, Czech Republic) with 1.0 mm by 150 mm dimensions and 1.8-μm particle size. The analysis was carried out at 30°C and a 30 μl/min flow rate with the following A/B gradient: 0 min, 30% B; 30 min, 95% B; 40 min, 95% B; 50 min, 30% B; 60 min, 30% B. The gradient components A and B were represented by 0.1% formic acid in water or acetonitrile (ACN), respectively. One-minute time windows around S2 and S3/S4 GTXs were used for fraction isolation. The preparative chromatography was performed both with commercial GTX and with *A. fumigatus* 100074 strain.

Flow cytometry and annexin V staining

GFP expression of cell lines J-Lat A2 and 11.1 and phenotype of spin-infected primary $CD4^+$ T cells at the moment of reactivation were analyzed by fluorescence-activated cell sorting (FACS) as described previously (*27*). For annexin V staining, 10^6 cells were washed with phosphate-buffered saline (PBS) supplemented with 3% FBS and 2.5 mM $CaCl_2$ and stained with annexin V–PE (phycoerythrin) (Becton and Dickinson) for 20 min at 4°C in the dark in the presence of 2.5 mM $CaCl_2$. Stained cells were washed with PBS/FBS/$CaCl_2$, fixed with 1% formaldehyde, and analyzed by FACS.

Primary $CD4^+$ T cell isolation and infection

Primary $CD4^+$ T cells were isolated from buffy coats from healthy donors by Ficoll gradient (GE Healthcare) followed by negative selection with RosetteSep Human $CD4^+$ T Cell Enrichment Cocktail (STEMCELL Technologies). Isolated cells were left overnight for recovery and used for spin infection according to Lassen and Greene method as described previously (*27*, *58*). Briefly, $CD4^+$ T cells were infected with the pNL4.3.Luc.R-E- virus by spinoculation (120 min at 1200*g*) and cultured for 3 days in RPMI 1640, 10% FBS, and penicillin-streptomycin (100 μg/ml) in the presence of saquinavir mesylate (5 μM). Three days after infection, cells were treated as indicated in the presence of raltegravir (30 μM). Cells were harvested 24 hours after treatment, and luciferase activity was measured using the Luciferase Assay System (Promega, Leiden, The Netherlands). Infections were performed using pseudotyped particles obtained by cotransfecting HXB2-Env with pNL4.3.Luc.R-E- plasmid into human embryonic kidney 293T cells using polyethylenimine 48 and 72 hours after transfection, and supernatants containing pseudotyped virus were collected, filtered with a 0.45-μm filter, and stored at −80°C. Molecular clones pNL4.3.Luc.R-E- and HIV-1 HXB2-Env and antiretroviral drugs saquinavir mesylate and raltegravir were provided by the Centre for AIDS Reagents, National Institute for Biological Standards and Control. HIV-1 molecular

clone pNL4.3.Luc.R-E- and HIV-1 HXB2-Env expression vectors were donated by N. Landau and by K. Page and D. Littman, respectively.

HIV-1 latency reversal in primary CD4$^+$ T cells isolated from aviremic patients

Primary CD4$^+$ T cells were isolated as described previously (*27*). Three million CD4$^+$ T cells were plated in triplicate at a cell density of 10^6/ml and treated as indicated. After 24 hours, cells were lysed, and total RNA was isolated as described below. Written informed consent was obtained from all patients involved in the study. The study was conducted in accordance with ethical principles of the Declaration of Helsinki. The study protocol and any amendment were approved by The Netherlands Medical Ethics Committee (MEC-2012-583).

Total RNA isolation and quantitative reverse transcription polymerase chain reaction

Cells were lysed in TRI reagent, and RNA was isolated with the Total RNA Zol-Out kit (A&A Biotechnology); complementary DNA (cDNA) synthesis and quantitative polymerase chain reaction (qPCR) was performed as described previously (*27*). Gene expression was calculated using the $2^{-\Delta\Delta Ct}$ method (*59*), and expression of glyceraldehyde phosphate dehydrogenase (GAPDH) was used for normalization. Absolute quantification of cell-associated *pol* RNA was performed as described previously (*27*). Briefly, qPCR was performed in a final volume of 25 µl using 4 µl of cDNA, 2.5 µl of 10× PCR buffer (Life Technologies), 1.75 µl of 50 mM $MgCl_2$ (Life Technologies), 1 µl of 10 mM deoxynucleotide triphosphates (Life Technologies), 0.125 µl of 100 µM Pol forward primer (HXB2 genome 4901 → 4924), 0.125 of 100 µM Pol reverse primer (HXB2 genome 5060 → 5040), 0.075 µl of 50 µM of Pol probe, and 0.2 µl of Platinum Taq polymerase (Life Technologies). The lower limit of detection of this method was of 20 copies of HIV-1 RNA in1 µg of total RNA. The absolute number of pol copies in PCR was calculated using standard curves ranging from 7 to 480 copies of a plasmid containing the full-length HIV-1 genome (pNL4.3.Luc.R-E-). The amount of HIV-1 cell-associated RNA was expressed as the number of copies per microgram of input RNA in reverse transcription. Preparations of cell-associated RNA were tested for potential contamination with HIV-1 DNA and/or host DNA by performing the PCR amplification in the presence and absence of reverse transcriptase.

Primers used for reverse transcription (RT)–qPCR were as follows: pol forward, 5′GGTTTATTACAGGGACAGCAGAGA3′ and pol reverse, 5′ACCTGCCATCTGTTTTCCATA3′; pol probe, [6FAM] AAA ATT CGG TTA AGG CCA GGG GGA AAG AA[BHQ1]; tumor necrosis factor–α (TNFα) forward, 5′TAGGCTGTTCCCATGTAGCC3′ and TNFα reverse, 5′CAGAGGCTCAGCAATGAGTG3′; interleukin-2 (IL-2) forward, 5′ACCTCAACTCCTGCCACAAT3′ and IL-2 reverse, 5′GCACTTCCTCCAGAGGTTTG3′; IFNγ forward, 5′ATAATGCAGAGCCAAATTGTCTCC3′ and IFNγ reverse, 5′ATGTCTTCCTTGATGGTCTCCAC3′; CD25 forward, 5′ATCAGTGCGTCCAGGGATAC3′ and CD25 reverse, 5′GACGAGGCAGGAAGTCTCAC3′; BAK1 (Brassinosteroid Insensitive 1-associated receptor kinase 1) forward, 5′GGTTTTCCGCAGCTACGTTTTT3′ and BAK1 reverse, 5′GCAGAGGTAAGGTGACCATCTC3′; BAX (BCL-2-associated X protein) forward, 5′CCCGAGAGGTCTTTTCCGAG3′ and BAX reverse, 5′CCAGCCCATGATGGTTCTGAT3′; BCL2 (B-Cell lymphoma 2 protein) forward, 5′GGTGGGGTCATGTGTGTGG3′ and BCL2 reverse, 5′CGGTTCAGGTACTCAGTCATCC3′; CASP-3 (Caspase-3 protein) forward, 5′CATGGAAGCGAATCAATGGACT3′ and CASP-3 reverse, 5′CTGTACCAGACCGAGATGTCA3′; AKT1 (RAC-alpha serine/threonine-protein kinase) forward, 5′AGCGACGTGGCTATTGTGAAG3′ and AKT1 reverse, 5′GCCATCATTCTTGAGGAGGAAGT3′; NRF2 (NFE2-related factor 2 protein) forward, 5′TTCCCGGTCACATCGAGAG3′ and NRF2 reverse, 5′TCCTGTTGCATACCGTCTAAATC3′; FOXO3a forward, 5′CGGACAAACGGCTCACTCT3′ and FOXO3a reverse, 5′GGACCCGCATGAATCGACTAT3′; KEAP1 (Kelch-like ECH-associated protein 1) forward, 5′GCAATGAACACCATCCGAAGC3′ and KEAP1 reverse, 5′ACCATCATAGCCTCCAAGGAC3′; CYCT1 (Cyclin T 1 protein) forward, 5′GGCGTGGACCCAGATAAAG3′ and CYCT1 reverse, 5′CTGTGTGAAGGACTGAATCAT3′; CDK9 forward, 5′ATGGCAAAGCAGTACGACTCG3′ and CDK9 reverse, 5′GCAAGGCTGTAATGGGGAAC3′; GAPDH forward, 5′CAAGAAGGTGGTGAAGCAG3′ and GAPDH reverse, 5′GCCAAATTCGTTGTCATACC3′; and B2M forward, 5′ATGAGTATGCCTGCCGTGTG3′ and B2M reverse, 5′CCAAATGCGGCATCTTCAAAC3′.

Glycerol gradient sedimentation

Glycerol gradients were prepared as described previously (*50*). Briefly, around 40×10^6 primary CD4$^+$ T cells isolated from healthy donors were either untreated or treated with GTX (20 nM) for 4 hours for RNase A treatment. Cells were lysed for 30 min in buffer A supplemented either with RNasin (100 U/ml; Promega) for untreated and GTX conditions or with RNase A (100 µg/ml). RNase-supplemented lysates were incubated for 10 min at room temperature to ensure efficient degradation of RNA. Lysates were fractionated by centrifugation in a SW41 Ti rotor at 38,000 rpm for 20 hours. Fractions (1 ml) were collected in 2-ml tubes and subjected to trichloroacetic acid (TCA) precipitation of proteins as described previously (*60*). Briefly, to each 1 ml of fraction, 110 µl of ice-cold 100% TCA was added and incubated on ice for 10 min. Then, 500 µl of ice-cold 10% TCA was added to each sample and incubated on ice for 20 min, followed by centrifugation at 20,000*g* for 30 min. Supernatants were carefully removed, and precipitates were gently washed with 500 µl of ice-cold acetone followed by centrifugation at 20,000*g* for 10 min. Supernatants were gently removed and dried at room temperature for about 10 min. Protein precipitates were then resuspended in 50 µl of Laemmli loading buffer and subjected to 10% SDS–polyacrylamide gel electrophoresis (SDS-PAGE) separation and detection of CDK9 (C-20, sc-484, Santa Cruz Biotechnology).

RNA Pol II and CDK9 T-loop phosphorylation

For RNA Pol II phosphorylation, 10 million primary CD4$^+$ T cells were either untreated or treated with GTX, OTX-015 (1 µM), FPD (500 nM), PMA (10 nM), or αCD3/CD28 beads (cell:bead ratio of 1:1) for 6 hours. For CDK9 phosphorylation, 5 million primary CD4$^+$ T cells were either untreated or treated with GTX (20 and 40 nm) or PMA (10 nM) for 6 hours. Four million cells were lysed for 30 min on ice with immunoprecipitation buffer [25 mM Hepes (pH 7.9), 150 mM KCl, 1 mM EDTA, 5 mM $MgCl_2$, 5% glycerol, 1% NP-40, 0.5 mM dithiothreitol (DTT), PhosSTOP phosphatase inhibitor (Sigma-Aldrich), and a cOmplete protease inhibitor cocktail (Sigma-Aldrich)] and subjected to Western blot analysis using the following antibodies: total RNA Pol II (N-20, sc-899, Santa Cruz Biotechnology), phospho-Ser^2 RNA Pol II (H5, ab-24758, Abcam), CDK9 (C-20, sc-484,

Santa Cruz Biotechnology) (Fig. 4C and fig. S9B), total CDK9 (D7, sc-13130, Santa Cruz Biotechnology) (fig. S9E), cyclinT1 (H-245, sc-10750, Santa Cruz Biotechnology), α-tubulin (ab6160, Abcam), and phospho-CDK9 Thr^{186} (#2549, Cell Signaling Technology).

7SK snRNP complex immunoprecipitation and 7SK RNA / CDK9 release assay

Fifty million Jurkat cells were lysed in 5 ml of immunoprecipitation buffer [1% NP-40, 25 mM tris (pH 7.4), 150 mM NaCl, 1 mM EDTA, 5% glycerol, and EDTA-free protease inhibitor cocktail (1 U/ml; Roche)] for 30 min on ice and centrifuged for 10 min at 14,000 rpm. Protein G Sepharose beads (200 μl) were washed two times with lysis buffer. Lysates were incubated with beads and 2 μg of antibody against human LARP7 (A303-723A, Bethyl Laboratories) at 4°C overnight. Next day, the beads were washed two times with lysis buffer, resuspended in 400 μl of lysis buffer containing 1 mM DTT, and divided in four reactions of 100 μl each. The presence of DTT is critical to the activity of GTX in agreement with its lability and known unusual disulfide bridge. Aliquotes were left untreated or treated with GTX for 1 hour or with RNase A for 15 min at room temperature. Next, supernatant was discarded, and beads were washed twice with lysis buffer. Beads were resuspended in 100 μl of Laemmli loading buffer and subjected to 12% SDS-PAGE separation and detection of CDK9 (sc-484, Santa Cruz Biotechnology) and LARP7 by Western blot. Ten microliters of beads suspension before and after treatment and 10 μl of supernatant after treatment were taken and resuspended in TRI reagent (Sigma) for subsequent RNA isolation (Total RNA Zol-Out kit, A&A Biotechnology). cDNA was synthetized using 10 μl of RNA solution as described above and diluted 560 times for quantitative RT-PCR. 7SK RNA was amplified using specific primers described elsewhere (*61*). qPCR was performed as described above. Values were normalized to the input RNA (post-treatment bead suspension).

Histone acetylation

Ten million primary CD4$^+$ T cells were treated with GTX concentration gradient, SAHA, or left untreated for 4 hours and then washed twice in PBS. Cells were lysed for 10 min at 4°C in TBE (Tris-borate-EDTA) buffer [PBS, 0.5% Triton X-100 (v/v), 2 mM phenylmethylsulfonyl fluoride, and 0.02% (w/v) NaN_3] at a density of 10^7 cells per 1 ml of the buffer. Samples were centrifuged at 425*g* for 10 min at 4°C. Supernatants were discarded, and cell pellets were washed in half the volume of TEB buffer used for lysis and centrifuged as before. Supernatants were discarded, and pellets were resuspended in 0.2 N HCl at a density of 4×10^7 cells/ml. Histones were extracted overnight at 4°C and then centrifuged at 425*g* for 10 min at 4°C. Supernatants were collected, protein concentration was determined by Bradford assay, and samples were subjected to SDS-PAGE Western blot. The following antibodies were used in Western blot analysis: anti–acetyl-histone H4 (06-598, Millipore) and anti-histone H2B (ab52484, Abcam).

RNA sequencing and data analysis

Ten million primary CD4$^+$ T cells were stimulated with 20 nM GTX or left unstimulated for 4 hours. Experiment was performed in duplicate on cells isolated from two buffy coats from healthy donors as described above. RNA was isolated as described above. cDNA libraries were generated using the Illumina TruSeq Stranded mRNA Library Prep kit (Illumina). The resulting DNA libraries were sequenced according to the Illumina TruSeq Rapid v2 protocol on an Illumina HiSeq 2500 sequencer. Reads were generated of 50 base pairs in length. Reads were mapped against the GRCh38 human reference using HiSat2 (version 2.0.4). We calculated gene expression values using htseq-count (version 0.6.1) using Ensembl transcript annotation. Heatmaps were generated using MORPHEUS (https://software.broadinstitute.org/morpheus/index.html).

Toxicity assay

PBMCs were isolated by density gradient centrifugation (Ficoll-Hypaque, GE Healthcare Life Sciences) from buffy coats from healthy donors (Sanquin, Amsterdam) and either used immediately or frozen in freezing media [90% FBS/10% dimethyl sulfoxide (DMSO] and stored short term at −80°C. For cytotoxicity testing, cells were cultivated in culture media RPMI 1640 (Life Technologies) supplemented with 10% FBS, 2 mM L-glutamine, penicillin (100 U/ml), and streptomycin-sulfate (100 g/ml) at a concentration of 1×10^6 cells/ml in 24-well plates (Thermo Scientific) that were either uncoated (unstimulated cells) or coated with anti-human CD3 (1 μg/ml; clone UCHT1, no azide/low endotoxin, BD Biosciences) and anti-CD28 (10 μg/ml; clone CD28.2, no azide/low endotoxin, BD Biosciences) monoclonal antibodies (stimulated cells). PMA/ionomycin was added at 50 ng/ml and 1 μg/ml, respectively, and cells were exposed for 16 hours. The following LRAs were added at the concentrations indicated in figures: GTX (ApexBio), SAHA-Vorinostat (Selleck Chemicals), CAPE (MP Biomedicals), and RMD (Sigma-Aldrich). LRAs at indicated concentrations were added to the cultures, and cells were continuously exposed for 72 hours. Since GTX was reconstituted in ACN and all other LRAs in DMSO, both solvents were added to the DMSO/ACN control culture (ACN, 1:10000; DMSO, 1:2500) to control for the effect that these solvents may have on cell viability.

Flow cytometry for cytotoxicity assay

To examine the effects the LRAs have on immune cell subpopulations, cell viability, activation, and proliferation were analyzed by flow cytometry. To determine the cytotoxic effect of the LRAs on cells, AnnexinV staining was used to define apoptotic and dead cells. Surface antigens were detected by incubating 0.8 to 1.0×10^6 cells with predetermined optimal concentrations of monoclonal antibody mixes in FACS wash [FW; Hank's Balanced Salt Solution (Life Technologies), 3% FBS (Life Technologies), 0.02% NaN_3, and 2.5 mM $CaCl_2$] for 20 min at 4°C, washed one time with FW, and fixed with 1% paraformaldehyde. To determine proliferation, cells were stained with 0.07 μM CellTrace Far Red Cell Proliferation dye according to the manufacturer's protocol (Thermo Fisher Scientific) before cultivating for 72 hours with either unstimulated or stimulated conditions in the presence of LRA. Upon cell division, the proliferation dye intensity decreases in daughter cells, and this was measured by flow cytometry. The following directly conjugated monoclonal anti-human antibodies were used to analyze CD8$^+$ T cells (CD3$^+$CD8$^+$), CD4$^+$ T cells (CD3$^+$CD4$^+$), B cells (CD3$^-$CD19$^+$), monocytes (CD14$^+$), and NK cells (CD3$^-$CD56$^+$): CD3-BV421 (clone UCHT1), CD4-BV650 (SK3), CD8-BV786 (RPA-T8), CD14-PE-Cy7 (61D3, eBioscience), CD19-PerCP-Cy5.5 (HIB19, eBioscience), CD56-PE-Cy5.5 (CMSSB, eBioscience), annexin V–PE, and CD25$^-$ Super Bright 600 (BC96, eBioscience). All antibodies were purchased from BD Biosciences unless otherwise indicated. Between 2×10^5 and 4×10^5 events were collected per sample within 24 hours after staining on a LSRFortessa (BD Biosciences, 4 lasers, 18 parameters) and analyzed using FlowJo

software (version 9.7.4, Tree Star). Data are represented as frequency within a defined population. Treatment-specific cell cytotoxicity was calculated using the following formula: [(% drug-induced cell death − % cell death in DMSO/ACN only)/(100 − % cell death in DMSO/ACN only)]*100.

Molecular docking

Molecular docking was used to predict the most likely binding mode of GTX to LARP7 CTD. The crystal structure of human LARP7 CTD in complex with 7SK RNA SL4 [Protein Data Bank (PDB) ID code 6D12] was optimized using PDB-REDO (*62*) and used as a template to define the receptor for the docking simulation. The resulting pdb file was manually adapted for input into the docking procedure by elimination of protein chain B and RNA domain C and replacement of selenium atoms (present as selenomethionin, incorporated for phasing purposes) (*63*) by sulfur. GTX ligand structure was built and energy minimized using the program Chimera (*64*). Molecular docking of GTX to LARP7 CTD was performed using the Achilles Blind Docking server (https://bio-hpc.ucam.edu/achilles/) and Chimera's AutoDock Vina function (*65*). The resulting solutions were ranked on the basis of the highest binding affinity (or lowest binding energy). Figures were created using PyMol software (*66*).

Quantification and statistical analysis

Western blot quantification

Differential band density was quantified by ImageQuant TL software using area and profile-based toolbox. For glycerol gradient Western blot quantification, an area frame was defined for all bands (total CDK9 protein content in all fractions), and complex-bound CDK9 bands (heavy fractions) or free CDK9 bands (light fractions) were defined. The three area frames were measured for total density after background subtraction (local average). Relative complex-bound CDK9 or free CDK9 percentage was calculated regarding the untreated control (total CDK9 abundance). For RNAPII Ser^2 phosphorylation, CDK9 T-loop phosphorylation, or immunoprecipitation Western blot quantification, an area for each respective band and loading controls were defined, and total density was measured after background subtraction (local average). LARP7 abundance was first normalized to total CDK9 abundance for each lane, and relative abundance was calculated regarding untreated control. RNAPII Ser^2 abundance was first normalized to tubulin abundance for each lane, and relative abundance was calculated with respect to untreated control. Thr^{186} P-CDK9 and cyclin T1 band density was normalized to total CDK9 abundance, and relative abundance was calculated with respect to untreated control.

Statistical significance

Statistical significance was calculated as indicated in the figure legends. Analyses were performed using Prism version 7.03 (GraphPad software).

Data and code availability

Sequencing data that support the findings of this study were deposited in Gene Expression Omnibus and are available under the accession code GSE135184.

SUPPLEMENTARY MATERIALS

Supplementary material for this article is available at http://advances.sciencemag.org/cgi/content/full/6/33/eaba6617/DC1

View/request a protocol for this paper from *Bio-protocol*.

REFERENCES AND NOTES

1. D. D. Ho, A. U. Neumann, A. S. Perelson, W. Chen, J. M. Leonard, M. Markowitz, Rapid turnover of plasma virions and CD4 lymphocytes in HIV-1 infection. *Nature* **373**, 123–126 (1995).
2. A. S. Perelson, P. Essunger, Y. Cao, M. Vesanen, A. Hurley, K. Saksela, M. Markowitz, D. D. Ho, Decay characteristics of HIV-1-infected compartments during combination therapy. *Nature* **387**, 188–191 (1997).
3. X. Wei, S. K. Ghosh, M. E. Taylor, V. A. Johnson, E. A. Emini, P. Deutsch, J. D. Lifson, S. Bonhoeffer, M. A. Nowak, B. H. Hahn, M. S. Saag, G. M. Shaw, Viral dynamics in human immunodeficiency virus type 1 infection. *Nature* **373**, 117–122 (1995).
4. J. M. Siliciano, R. F. Siliciano, The Remarkable Stability of the Latent Reservoir for HIV-1 in Resting Memory $CD4^+$ T Cells. *J. Infect. Dis.* **212**, 1345–1347 (2015).
5. N. M. Archin, A. L. Liberty, A. D. Kashuba, S. K. Choudhary, J. D. Kuruc, A. M. Crooks, D. C. Parker, E. M. Anderson, M. F. Kearney, M. C. Strain, D. D. Richman, M. G. Hudgens, R. J. Bosch, J. M. Coffin, J. J. Eron, D. J. Hazuda, D. M. Margolis, Administration of vorinostat disrupts HIV-1 latency in patients on antiretroviral therapy. *Nature* **487**, 482–485 (2012).
6. T. A. Rasmussen, O. S. Søgaard, Clinical interventions in HIV cure research. *Adv. Exp. Med. Biol.* **1075**, 285–318 (2018).
7. A. M. Spivak, V. Planelles, Novel latency reversal agents for HIV-1 cure. *Annu. Rev. Med.* **69**, 421–436 (2018).
8. Y. Kim, J. L. Anderson, S. R. Lewin, Getting the "Kill" into "Shock and Kill": Strategies to eliminate latent HIV. *Cell Host Microbe* **23**, 14–26 (2018).
9. E. Battivelli, M. S. Dahabieh, M. Abdel-Mohsen, J. P. Svensson, I. T. D. Silva, L. B. Cohn, A. Gramatica, S. Deeks, W. C. Greene, S. K. Pillai, E. Verdin, Distinct chromatin functional states correlate with HIV latency reactivation in infected primary $CD4^+$ T cells. *eLife* **7**, e34655 (2018).
10. Y.-C. Ho, L. Shan, N. N. Hosmane, J. Wang, S. B. Laskey, D. I. S. Rosenbloom, J. Lai, J. N. Blankson, J. D. Siliciano, R. F. Siliciano, Replication-competent noninduced proviruses in the latent reservoir increase barrier to HIV-1 cure. *Cell* **155**, 540–551 (2013).
11. S. Bouchat, N. Delacourt, A. Kula, G. Darcis, B. Van Driessche, F. Corazza, J.-S. Gatot, A. Melard, C. Vanhulle, K. Kabeya, M. Pardons, V. Avettand-Fenoel, N. Clumeck, S. De Wit, O. Rohr, C. Rouzioux, C. Van Lint, Sequential treatment with 5-aza-2′-deoxycytidine and deacetylase inhibitors reactivates HIV-1. *EMBO Mol. Med.* **8**, 117–138 (2016).
12. R. B. Jones, R. O'Connor, S. Mueller, M. Foley, G. L. Szeto, D. Karel, M. Lichterfeld, C. Kovacs, M. A. Ostrowski, A. Trocha, D. J. Irvine, B. D. Walker, Histone deacetylase inhibitors impair the elimination of HIV-infected cells by cytotoxic T-lymphocytes. *PLOS Pathog.* **10**, e1004287 (2014).
13. M. Zhao, E. De Crignis, C. Rokx, A. Verbon, T. van Gelder, T. Mahmoudi, P. D. Katsikis, Y. M. Mueller, T cell toxicity of HIV latency reversing agents. *Pharmacol. Res.* **139**, 524–534 (2019).
14. D. J. Newman, G. M. Cragg, Natural products as sources of new drugs from 1981 to 2014. *J. Nat. Prod.* **79**, 629–661 (2016).
15. J. F. Sanchez, A. D. Somoza, N. P. Keller, C. C. C. Wang, Advances in *Aspergillus* secondary metabolite research in the post-genomic era. *Nat. Prod. Rep.* **29**, 351–371 (2012).
16. A. A. Brakhage, Regulation of fungal secondary metabolism. *Nat. Rev. Microbiol.* **11**, 21–32 (2013).
17. J. Přichystal, K. A. Schug, K. Lemr, J. Novák, V. Havlíček, Structural analysis of natural products. *Anal. Chem.* **88**, 10338–10346 (2016).
18. E. Ne, R.-J. Palstra, T. Mahmoudi, Transcription: Insights from the HIV-1 promoter. *Int. Rev. Cell Mol. Biol.* **335**, 191–243 (2018).
19. M. Stoszko, E. Ne, E. Abner, T. Mahmoudi, A broad drug arsenal to attack a strenuous latent HIV reservoir. *Curr. Opin. Virol.* **38**, 37–53 (2019).
20. J. Novák, L. Sokolová, K. Lemr, T. Pluháček, A. Palyzová, V. Havlíček, Batch-processing of imaging or liquid-chromatography mass spectrometry datasets and *De Novo* sequencing of polyketide siderophores. *Biochim. Biophys. Acta. Proteins Proteom.* **1865**, 768–775 (2017).
21. K. G. Lassen, A. M. Hebbeler, D. Bhattacharyya, M. A. Lobritz, W. C. Greene, A flexible model of HIV-1 latency permitting evaluation of many primary CD4 T-cell reservoirs. *PLOS ONE.* **7**, e30176 (2012).
22. M. Stanzani, E. Orciuolo, R. Lewis, D. P. Kontoyiannis, S. L. R. Martins, L. S. S. John, K. V. Komanduri, *Aspergillus fumigatus* suppresses the human cellular immune response via gliotoxin-mediated apoptosis of monocytes. *Blood* **105**, 2258–2265 (2005).
23. Y. K. Suen, K. P. Fung, C. Y. Lee, S. K. Kong, Gliotoxin induces apoptosis in cultured macrophages via production of reactive oxygen species and cytochrome c release without mitochondrial depolarization. *Free Radic. Res.* **35**, 1–10 (2001).
24. A. Yamada, T. Kataoka, K. Nagai, The fungal metabolite gliotoxin: Immunosuppressive activity on CTL-mediated cytotoxicity. *Immunol. Lett.* **71**, 27–32 (2000).
25. D. H. Scharf, A. A. Brakhage, P. K. Mukherjee, Gliotoxin--bane or boon? *Environ. Microbiol.* **18**, 1096–1109 (2016).
26. L. Trautmann, Kill: Boosting HIV-specific immune responses. *Curr. Opin. HIV AIDS* **11**, 409–416 (2016).
27. M. Stoszko, E. De Crignis, C. Rokx, M. M. Khalid, C. Lungu, R.-J. Palstra, T. W. Kan, C. Boucher, A. Verbon, E. C. Dykhuizen, T. Mahmoudi, Small molecule inhibitors of BAF: A promising family of compounds in HIV-1 latency reversal. *EBioMedicine* **3**, 108–121 (2016).

28. C. A. Marian, M. Stoszko, L. Wang, M. W. Leighty, E. de Crignis, C. A. Maschinot, J. Gatchalian, B. C. Carter, B. Chowdhury, D. C. Hargreaves, J. R. Duvall, G. R. Crabtree, T. Mahmoudi, E. C. Dykhuizen, Small molecule targeting of specific BAF (mSWI/SNF) complexes for HIV latency reversal. *Cell Chem. Biol.* **25**, 1443–55.e14 (2018).
29. A. J. C. Quaresma, A. Bugai, M. Barboric, Cracking the control of RNA polymerase II elongation by 7SK snRNP and P-TEFb. *Nucleic Acids Res.* **44**, 7527–7539 (2016).
30. V. T. Nguyen, T. Kiss, A. A. Michels, O. Bensaude, 7SK small nuclear RNA binds to and inhibits the activity of CDK9/cyclin T complexes. *Nature* **414**, 322–325 (2001).
31. E. Uchikawa, K. S. Natchiar, X. Han, F. Proux, P. Roblin, E. Zhang, A. Durand, B. P. Klaholz, A.-C. Dock-Bregeon, Structural insight into the mechanism of stabilization of the 7SK small nuclear RNA by LARP7. *Nucleic Acids Res.* **43**, 3373–3388 (2015).
32. Z. Yang, Q. Zhu, K. Luo, Q. Zhou, The 7SK small nuclear RNA inhibits the CDK9/cyclin T1 kinase to control transcription. *Nature* **414**, 317–322 (2001).
33. J. H. N. Yik, R. Chen, R. Nishimura, J. L. Jennings, A. J. Link, Q. Zhou, Inhibition of P-TEFb (CDK9/Cyclin T) kinase and RNA polymerase II transcription by the coordinated actions of HEXIM1 and 7SK snRNA. *Mol. Cell* **12**, 971–982 (2003).
34. M. Ott, M. Geyer, Q. Zhou, The control of HIV transcription: Keeping RNA polymerase II on track. *Cell Host Microbe* **10**, 426–435 (2011).
35. G. Mousseau, S. T. Valente, Role of host factors on the regulation of Tat-Mediated HIV-1 transcription. *Curr. Pharm. Des.* **23**, 4079–4090 (2017).
36. B. M. Peterlin, D. H. Price, Controlling the elongation phase of transcription with P-TEFb. *Mol. Cell* **23**, 297–305 (2006).
37. I. Jonkers, J. T. Lis, Getting up to speed with transcription elongation by RNA polymerase II. *Nat. Rev. Mol. Cell Biol.* **16**, 167–177 (2015).
38. S. A. Yukl, P. Kaiser, P. Kim, S. Telwatte, S. K. Joshi, M. Vu, H. Lampiris, J. K. Wong, HIV latency in isolated patient $CD4^+$ T cells may be due to blocks in HIV transcriptional elongation, completion, and splicing. *Sci. Transl. Med.* **10**, eaap9927 (2018).
39. U. Mbonye, J. Karn, The molecular basis for human immunodeficiency virus latency. *Annu. Rev. Virol.* **4**, 261–285 (2017).
40. R. Ramakrishnan, E. C. Dow, A. P. Rice, Characterization of Cdk9 T-loop phosphorylation in resting and activated $CD4^+$ T lymphocytes. *J. Leukoc. Biol.* **86**, 1345–1350 (2009).
41. B. J. Krueger, C. Jeronimo, B. B. Roy, A. Bouchard, C. Barrandon, S. A. Byers, C. E. Searcey, J. J. Cooper, O. Bensaude, E. A. Cohen, B. Coulombe, D. H. Price, LARP7 is a stable component of the 7SK snRNP while P-TEFb, HEXIM1 and hnRNP A1 are reversibly associated. *Nucleic Acids Res.* **36**, 2219–2229 (2008).
42. E. Abner, M. Stoszko, L. Zeng, H.-C. Chen, A. Izquierdo-Bouldstridge, T. Konuma, E. Zorita, E. Fanunza, Q. Zhang, T. Mahmoudi, M.-M. Zhou, G. J. Filion, A. Jordan, A new quinoline BRD4 inhibitor targets a distinct latent HIV-1 reservoir for reactivation from other "Shock" drugs. *J. Virol.* **92**, (2018).
43. H.-C. Chen, J. P. Martinez, E. Zorita, A. Meyerhans, G. J. Filion, Position effects influence HIV latency reversal. *Nat. Struct. Mol. Biol.* **24**, 47–54 (2017).
44. E. Abner, A. Jordan, HIV "shock and kill" therapy: In need of revision. *Antiviral Res.* **166**, 19–34 (2019).
45. G. Darcis, A. Kula, S. Bouchat, K. Fujinaga, F. Corazza, A. Ait-Ammar, N. Delacourt, A. Melard, K. Kabeya, C. Vanhulle, B. Van Driessche, J.-S. Gatot, T. Cherrier, L. F. Pianowski, L. Gama, C. Schwartz, J. Vila, A. Burny, N. Clumeck, M. Moutschen, S. De Wit, B. M. Peterlin, C. Rouzioux, O. Rohr, C. Van Lint, An in-depth comparison of latency-reversing agent combinations in various *In Vitro* and *Ex Vivo* HIV-1 Latency Models Identified Bryostatin-1+JQ1 and Ingenol-B+JQ1 to Potently Reactivate Viral Gene Expression. *PLOS Pathog.* **11**, e1005063 (2015).
46. P. Hashemi, K. Barreto, W. Bernhard, A. Lomness, N. Honson, T. A. Pfeifer, P. R. Harrigan, I. Sadowski, Compounds producing an effective combinatorial regimen for disruption of HIV-1 latency. *EMBO Mol. Med.* **10**, 160–174 (2018).
47. G. M. Laird, C. K. Bullen, D. I. S. Rosenbloom, A. R. Martin, A. L. Hill, C. M. Durand, J. D. Siliciano, R. F. Siliciano, Ex vivo analysis identifies effective HIV-1 latency-reversing drug combinations. *J. Clin. Invest.* **125**, 1901–1912 (2015).
48. T. A. Rasmussen, S. R. Lewin, Shocking HIV out of hiding: Where are we with clinical trials of latency reversing agents? *Curr. Opin. HIV AIDS* **11**, 394–401 (2016).
49. H. Rafati, M. Parra, S. Hakre, Y. Moshkin, E. Verdin, T. Mahmoudi, Repressive LTR nucleosome positioning by the BAF complex is required for HIV latency. *PLOS Biol.* **9**, e1001206 (2011).
50. X. Contreras, M. Barboric, T. Lenasi, B. M. Peterlin, HMBA releases P-TEFb from HEXIM1 and 7SK snRNA via PI3K/Akt and activates HIV transcription. *PLOS Pathog.* **3**, 1459–1469 (2007).
51. J. Kohoutek, P-TEFb- the final frontier. *Cell Div.* **4**, 19 (2009).
52. H. S. Choi, J. S. Shim, J.-A. Kim, S. W. Kang, H. J. Kwon, Discovery of gliotoxin as a new small molecule targeting thioredoxin redox system. *Biochem. Biophys. Res. Commun.* **359**, 523–528 (2007).
53. K. J. Kwon-Chung, J. A. Sugui, What do we know about the role of gliotoxin in the pathobiology of *Aspergillus fumigatus*? *Med. Mycol.* **47**, (suppl. 1), S97–S103 (2009).
54. H. Sakamoto, S. Egashira, N. Saito, T. Kirisako, S. Miller, Y. Sasaki, T. Matsumoto, M. Shimonishi, T. Komatsu, T. Terai, T. Ueno, K. Hanaoka, H. Kojima, T. Okabe, S. Wakatsuki, K. Iwai, T. Nagano, Gliotoxin suppresses NF-κB activation by selectively inhibiting linear ubiquitin chain assembly complex (LUBAC). *ACS Chem. Biol.* **10**, 675–681 (2015).
55. G. Wichmann, O. Herbarth, I. Lehmann, The mycotoxins citrinin, gliotoxin, and patulin affect interferon-γ rather than interleukin-4 production in human blood cells. *Environ. Toxicol.* **17**, 211–218 (2002).
56. R. E. Lewis, N. P. Wiederhold, J. Chi, X. Y. Han, K. V. Komanduri, D. P. Kontoyiannis, R. A. Prince, Detection of gliotoxin in experimental and human aspergillosis. *Infect. Immun.* **73**, 635–637 (2005).
57. C. Gostinčar, J. Zajc, M. Lenassi, A. Plemenitaš, S. de Hoog, A. M. S. Al-Hatmi, N. Gunde-Cimerman, Fungi between extremotolerance and opportunistic pathogenicity on humans. *Fungal Diversity.* **93**, 195–213 (2018).
58. C. A. Spina, J. Anderson, N. M. Archin, A. Bosque, J. Chan, M. Famiglietti, W. C. Greene, A. Kashuba, S. R. Lewin, D. M. Margolis, M. Mau, D. Ruelas, S. Saleh, K. Shirakawa, R. F. Siliciano, A. Singhania, P. C. Soto, V. H. Terry, E. Verdin, C. Woelk, S. Wooden, S. Xing, V. Planelles, An in-depth comparison of latent HIV-1 reactivation in multiple cell model systems and resting CD4+ T cells from aviremic patients. *PLOS Pathog.* **9**, e1003834 (2013).
59. T. D. Schmittgen, K. J. Livak, Analyzing real-time PCR data by the comparative C_T method. *Nat. Protoc.* **3**, 1101–1108 (2008).
60. A. J. Link, J. LaBaer, Trichloroacetic acid (TCA) precipitation of proteins. *Cold Spring Harb. Protoc.* **2011**, 993–994 (2011).
61. K. Bartholomeeusen, Y. Xiang, K. Fujinaga, B. M. Peterlin, Bromodomain and extra-terminal (BET) bromodomain inhibition activate transcription via transient release of positive transcription elongation factor b (P-TEFb) from 7SK small nuclear ribonucleoprotein. *J. Biol. Chem.* **287**, 36609–36616 (2012).
62. R. P. Joosten, F. Long, G. N. Murshudov, A. Perrakis, The *PDB_REDO* server for macromolecular structure model optimization. *IUCrJ.* **1**, (Pt. 4), 213–220 (2014).
63. C. D. Eichhorn, Y. Yang, L. Repeta, J. Feigon, Structural basis for recognition of human 7SK long noncoding RNA by the La-related protein Larp7. *Proc. Natl. Acad. Sci. U.S.A.* **115**, E6457–E6466 (2018).
64. E. F. Pettersen, T. D. Goddard, C. C. Huang, G. S. Couch, D. M. Greenblatt, E. C. Meng, T. E. Ferrin, UCSF Chimera--a visualization system for exploratory research and analysis. *J. Comput. Chem.* **25**, 1605–1612 (2004).
65. O. Trott, A. J. Olson, AutoDock Vina: Improving the speed and accuracy of docking with a new scoring function, efficient optimization, and multithreading. *J. Comput. Chem.* **31**, 455–461 (2010).
66. L. Schrödinger, The {PyMOL} Molecular Graphics System, Version 1.8 (2015).

Acknowledgments

Funding: T.M. received funding from the European Research Council (ERC) under the European Union's Seventh Framework Programme (FP/2007-2013)/ERC STG 337116 Trxn-PURGE, the Dutch AIDS Fonds grant 2014021, and Erasmus MC mRACE research grant. J.K. was supported by the Technology Innovation Team Project of Guiyang [20161001]005; Guiyang Science and Technology Project (2017) No.5-19. V.H. was supported by the Ministry of Education, Youth, and Sports of the Czech Republic (LO 1509). R.P. was supported by the Dutch AIDS Fonds grant. 2016014. J.H.G.L. is supported by the gravitation program CancerGenomiCs.nl from the Netherlands Organization for Scientific Research (NWO). P.D.K. was supported in part by a grant awarded by Worldwide Cancer Research. **Author contributions:** M.St., A.M.S.A.-H., A.S., M.R., E.N., Y.M.M., M.J.N., R.C., J.K., R.P., E.L., P.B., A.B., T.W.K., E.d.C., R.-J.P., M.Su., C.R., and W.v.I. conducted the experiments. M.St., Y.M.M., R.-J.P., J.H.G.L., A.V., P.D.K., V.H., S.d.H., and T.M. designed the experiments and wrote the paper. **Competing interests:** The authors declare that they have no competing interests. **Data and materials availability:** All data needed to evaluate the conclusions in the paper are present in the paper and/or the Supplementary Materials. Additional data related to this paper may be requested from the authors.

Submitted 20 December 2019
Accepted 1 July 2020
Published 12 August 2020
10.1126/sciadv.aba6617

Citation: M. Stoszko, A. M. S. Al-Hatmi, A. Skriba, M. Roling, E. Ne, R. Crespo, Y. M. Mueller, M. J. Najafzadeh, J. Kang, R. Ptackova, E. LeMasters, P. Biswas, A. Bertoldi, T. W. Kan, E. de Crignis, M. Sulc, J. H. Lebbink, C. Rokx, A. Verbon, W. van Ijcken, P. D. Katsikis, R.-J. Palstra, V. Havlicek, S. de Hoog, T. Mahmoudi, Gliotoxin, identified from a screen of fungal metabolites, disrupts 7SK snRNP, releases P-TEFb, and reverses HIV-1 latency. *Sci. Adv.* **6**, eaba6617 (2020).

ScienceAdvances

Gliotoxin, identified from a screen of fungal metabolites, disrupts 7SK snRNP, releases P-TEFb, and reverses HIV-1 latency

Mateusz Stoszko, Abdullah M. S. Al-Hatmi, Anton Skriba, Michael Roling, Enrico Ne, Raquel Crespo, Yvonne M. Mueller, Mohammad Javad Najafzadeh, Joyce Kang, Renata Ptackova, Elizabeth LeMasters, Pritha Biswas, Alessia Bertoldi, Tsung Wai Kan, Elisa de Crignis, Miroslav Sulc, Joyce H.G. Lebbink, Casper Rokx, Annelies Verbon, Wilfred van Ijcken, Peter D. Katsikis, Robert-Jan Palstra, Vladimir Havlicek, Sybren de Hoog and Tokameh Mahmoudi

Sci Adv **6** (33), eaba6617.
DOI: 10.1126/sciadv.aba6617

CHAPTER .5

A broad drug arsenal to attack a strenuous latent HIV reservoir.

Mateusz Stoszko, **Enrico Ne**, Tokameh Mahmoudi

Stoszko M, Ne E, Mahmoudi T, Curr Opin Virology, 2019

https://doi.org/10.1016/j.coviro.2019.06.001

Available online at www.sciencedirect.com

ScienceDirect

Current Opinion in Virology

A broad drug arsenal to attack a strenuous latent HIV reservoir

Mateusz Stoszko[1,3], Enrico Ne[1,3], Erik Abner[2] and Tokameh Mahmoudi[1]

HIV cure is impeded by the persistence of a strenuous reservoir of latent but replication competent infected cells, which remain unsusceptible to c-ART and unrecognized by the immune system for elimination. Ongoing progress in understanding the molecular mechanisms that control HIV transcription and latency has led to the development of strategies to either permanently inactivate the latent HIV infected reservoir of cells or to stimulate the virus to emerge out of latency, coupled to either induction of death in the infected reactivated cell or its clearance by the immune system. This review focuses on the currently explored and non-exclusive pharmacological strategies and their molecular targets that 1. stimulate reversal of HIV latency in infected cells by targeting distinct steps in the HIV-1 gene expression cycle, 2. exploit mechanisms that promote cell death and apoptosis to render the infected cell harboring reactivated virus more susceptible to death and/or elimination by the immune system, and 3. permanently inactivate any remaining latently infected cells such that c-ART can be safely discontinued.

Addresses
[1] Department of Biochemistry, Erasmus University Medical Center, Ee634 PO Box 2040, 3000CA, Rotterdam, The Netherlands
[2] Institute of Genomics, University of Tartu, Tartu, Estonia

Corresponding author:
Mahmoudi, Tokameh (t.mahmoudi@erasmusmc.nl)
[3] These authors contributed equally.

Current Opinion in Virology 2019, **38**:37–53

This review comes from a themed issue on **Engineering for viral resistance**

Edited by **Chen Liang** and **Ben Berkhout**

For a complete overview see the Issue and the Editorial

Available online 16th July 2019

https://doi.org/10.1016/j.coviro.2019.06.001

Introduction

Millions worldwide are infected with HIV and depend on daily antiretrovirals for survival. Combination antiretroviral therapy (cART) suppresses HIV replication and halts disease progression. However, a small reservoir of replication-competent virus lingers in long-lived resting memory CD4+T cells, which, because the virus is in a latent state, are not targeted by cART [1]. Persistence of these cells leads to inevitable rebound of viral replication once cART is interrupted and constitutes a roadblock to cure. Viable HIV cure dictates either elimination of the latent reservoir or its permanent containment such that cART can be safely discontinued. Ongoing progress in molecular understanding of HIV latency has led to development of pharmacological strategies that target the latent HIV infected cell reservoir (Figure 1). While 'block and lock' [2•] relies on permanent suppression of latent virus, other approaches aim to reverse HIV-1 latency in infected cells via latency reversal agents (LRAs) [3] such that either cell death is induced, or HIV infected cells are 'seen' and eliminated by an immune response. This review focuses on the arsenal of pharmacological agents and mechanisms they exploit to target the reservoir for latency reversal, permanent inactivation, and/or cell death. Other important strategies not discussed include the breadth of interventions to boost HIV-specific immunity for viral elimination [4–7].

Pipeline of latency reversal agents (LRAs)

Following integration, transcription at the proviral promoter or 5′ long terminal repeat (5′LTR) is controlled by the host transcription machinery and influenced by surrounding chromatin landscape [8]. Regardless of genomic position, 5′LTR latent structure is defined by Nucleosome-0 (Nuc0) connected by a stretch of accessible DNA (HSS1) to the strictly positioned repressive Nuc1 downstream of the transcription start site (TSS), which is remodeled upon activation (Figure 2a) [8,12,15]. HIV-1 transcription is initiated by engagement of inducible sequence-specific transcription factors (TFs) and associated cofactors at the 5′LTR, controlling accessibility to RNA Polymerase II (Pol II) and permissiveness to transcription (Figure 2). Under basal conditions transcription is initiated but Pol II pauses, producing short transcripts [9,12,15]. The HIV transactivator Tat, a major determinant of reactivation from latency, when expressed, recruits the positive transcription elongation factor (PTEFb) to the nascent TAR RNA, releases Pol II pausing, activating transcription elongation [8,12,15]. HIV-1 expression is also restricted post-transcriptionally via previously underappreciated mechanisms that can also be explored pharmacologically to modulate latency [10,11].

De-repressors: pharmacological interventions that counter repressive chromatin

Targeting PTMs

A broad category of LRAs affect post-translational modifications (PTMs) of N-terminal histone tails, modulating

Figure 1

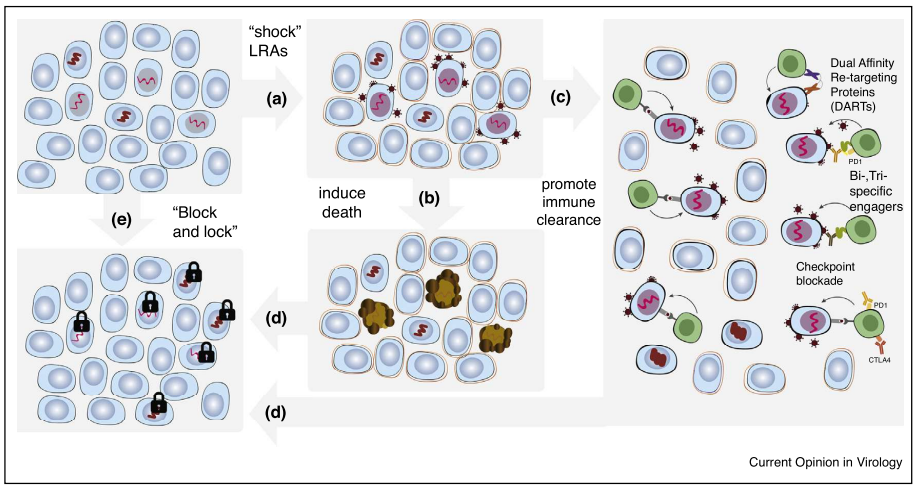

Pharmacological strategies to target the latent HIV-1 reservoir. **(a)** The inducible fraction of the HIV-1 latent reservoir is 'shocked' with LRAs to induce expression of the provirus. **(b)** Cells expressing viral particles die due to the associated cytotoxicity and via pharmacological interventions that sensitize HIV reactivated cells toward cell death. **(c)** Reactivated cells are also recognized and killed by the immune system which can be strengthened and boosted via a number of strategies including small molecule checkpoint inhibitors that enhance T cell function, bi/tri-specific T cell engagers (BI/TRIES) and dual-affinity re-targeting proteins (DARTs). **(d)** In case of inefficient activation and insufficient clearance of latently infected cells, a deeper state of latency is pharmacologically promoted in the remaining fraction of the reservoir ('block and lock'). **(e)** Efficient 'block and lock' strategies, capable of driving the whole reservoir into a deep latency state, could also, in principle, be used alone without the need of additional interventions.

the strength of DNA-nucleosomal core interaction and can serve as marks for recruitment of protein complexes that regulate chromatin structure [12,13]. The best-characterized modification, histone acetylation is deposited by histone acetyltransferases (HATs) and removed by histone deacetylases (HDACs), which are associated with the latent HIV-1 promoter and can be targeted with HDAC inhibitors (HDACis) for derepression [13]. The repressed HIV-1 promoter is also characterized by latency-associated H3K27me3, deposited by polycomb group repressive complex 2 (PRC2) histone methyltransferase (HMT) EZH2, and serves as a mark to recruit other repressors including HDACs, PRC1 and DNA methyltransferases (DNMTs) [14–16]. As well, heterochromatin associated HMTs G9a and Suv39H1-deposited H3K9di/tri-methyl marks [14–16] occupy the latent LTR. A previously underappreciated modification, H4K3 Crotonylation, found to be associated with latency reversal, can be enhanced by sodium crotonate as substrate [17].

HDACis Romidepsin, Panobinostat, Vorinostat, and Valproic acid have been extensively studied for their latency reversal potential [18–21]. The metabolite acetate, highly concentrated in the gut and blood, inhibits HDAC activity and boosted HIV replication [22]. Clinical trials and *in vitro* data have confirmed their sufficient clinical tolerance and effectiveness as LRAs that mechanistically enhance transcriptional noise and synergize with signal-dependent HIV-1 activation [23,8], inducing viral RNA and protein [24]. But clinically, no significant reservoir depletion with HDACis has been observed [18–22]. A multitude of HDACis, targeting all or specific HDAC classes have been developed (Table 1). Class I appear to play a prominent role in latency with Class I HDACis inducing stronger HIV-1 derepression [25,26•]. A recent comparison of HDACis pointed to benzamide moiety and pyridyl cap group molecules, such as Chidamide to be most active with least associated cytoxicity [27].

HMTis. The potential of HMTIs as LRAs has more recently emerged. Inhibition of SUV39H1 with Chaetocin, or targeting G9a with the quinazoline BIX-01294 and more recently UNC-0638, a BIX-01294 derivative with better toxicity profile, reversed latency in CD4+T cells of suppressed patients [14–16,28•]. H4K20 monomethylation, deposited by SMYD2, was linked to HIV-1 latency and its inhibition by AZ391 led to increased cell associated HIV-1 RNA in c-ART treated patient CD4+T cells [29]. Wide spectrum EZH2 HMTis including

Figure 2

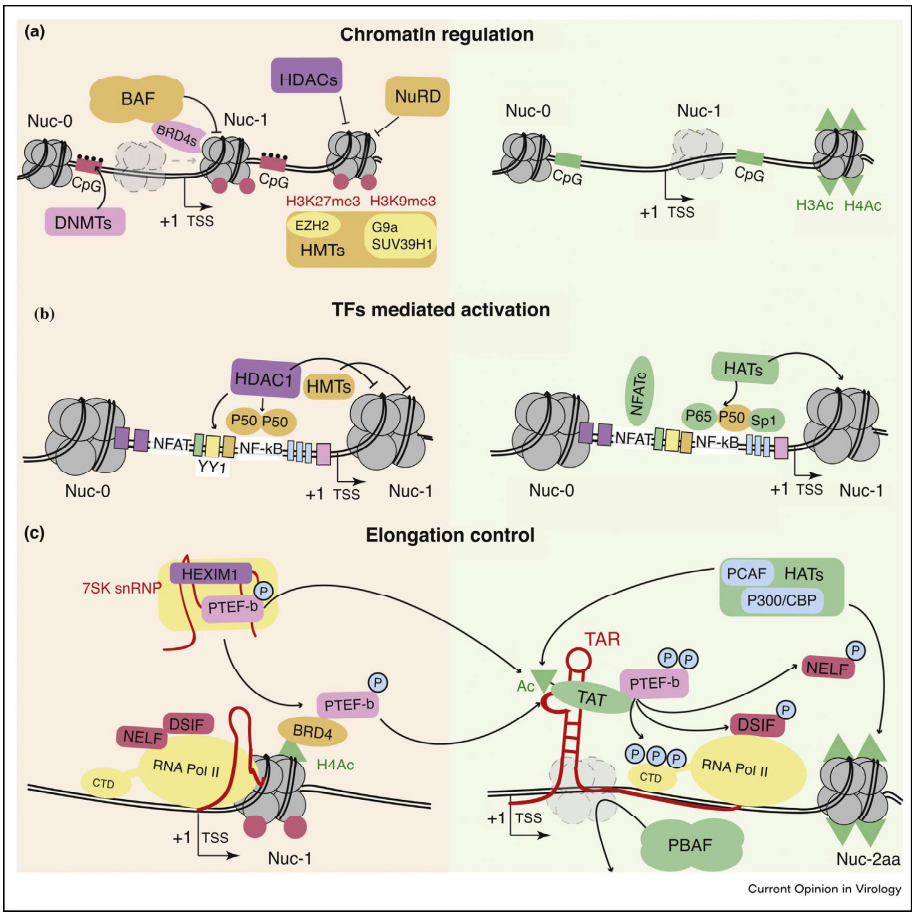

Distinct steps in control of the HIV-1 LTR transcription cycle represented in the latent and active states, simplified overview. **(a)** The chromatin architecture of the HIV-1 promoter consists of three strictly positioned nucleosomes (Nuc-0, Nuc-1 and Nuc-2) separated by nucleosome free regions. In the repressed state (left panel), the BAF complex is recruited to the LTR tethered by BRD4S and mediates the positioning of the repressive Nuc-1, downstream of the transcriptional start site (TSS). The latent HIV-1 promoter is also characterized by the presence of repressive cofactors, including HDACs, HMTs and the NuRD complex. **(b)** Upon signal-dependent activation, sequence-specific TFs bind their consensus sites at the HIV-1 5′ LTR and mediate the recruitment of RNA Pol II, required for transcription initiation, and HATs, rendering the chromatin more permissive to transcription. **(c)** In basal conditions RNA Pol II processivity is restricted by the activity of negative elongation factors NELF and DSIF which promote the early dissociation of RNA Pol II from the DNA template, and inhibit the production of full length viral RNAs. Additionally, the availability of P-TEFb is restricted by sequestration within the 7SK snRNP complex and by BRD4-dependent chromatin recruitment. Productive infection requires sufficient expression of the viral transactivator Tat that dramatically potentiates transcription elongation. Tat binds TAR, a hairpin loop RNA structure of the nascent transcript, and recruits P-TEFb to the 5′ LTR. Within P-TEFb, the kinase activity of CDK9 promotes phosphorylation of NELF, DSIF and the RNA Pol II CTD, hence increasing RNA Pol II processivity. Tat PTMs modulates its association with cellular cofactors including HATs and PBAF, remodeling chromatin and enhancing transcription.

DZNep reactivated latent HIV in cell lines, although with substantial toxicity, while recently, specific EZH2 inhibitors EPZ-6438, GSK-343 more effectively reversed latency in resting CD4+T cells from infected individuals [14–16,28•].

DNMTis. HIV 5′LTR CpG methylation promotes binding of methyl–CpG-binding protein (MBD2) and recruitment of the repressive NuRD complex [8]. While the importance of this mechanism *in vivo* has been questioned [8,12,15], sequential treatment with DNMTis and

Table 1

Pharmacologic interventions to target the latent HIV-1 reservoir

Class	Subclass	Function/Target	Compounds	Experimental system	References (Fully listed in reference list)
Chromatin modulators		ACSS2 agonist	Sodium crotonate (Na-Cro)	A, F	Jiang *et al.*, 2018
		HMT (SMYD2 inhibitor)	AZ391	A, F	Boehm *et al.*, 2017
			BIX-01294	A	Imai *et al.*, 2010
		HMT (G9a inhibitor)	UNC-0638	D, F	Nguyen *et al.*, 2017
		Polycomb (L3MBTL1 inhibitor)	UNC-926	A, F	Boehm *et al.*, 2017
	Histone methyl transferases inhibitors (HMTis)	Polycomb (SUV39H1 inhibitor)	Chaetocin	A	Bernhard *et al.*, 2011
		Polycomb (EZH1/EZH2 inhibitor)	UNC-1999	D	Kobayashi *et al.*, 2017
		Polycomb (EZH2 inhibitor)	3-deazaneplanocin A (DZNep)	A	Friedman *et al.*, 2011
			EPZ-6438; GSK-343	A, F	Nguyen *et al.*, 2017
			CG05; CG06	A	Choi *et al.*, 2010
			Thiophenyl benzamide (TPB)	A, F	Huang *et al.*, 2018
			Chidamide	A, F, G (NCT02902185, NCT02513901)	Yang *et al.*, 2018
			Entinostat	A, F	Wightman *et al.*, 2013
			Largazoles (SDL148; JMF1080; SDL256)	A, D	Albert *et al.*, 2017
			Mocetinostat	C	Zaikos *et al.*, 2018
		HDAC Class I	Romidepsin	D; G (NCT02092116, NCT01933594, NCT02850016, NCT03041012, NCT03619278, NCT02616874, NCT01933594)	Wei *et al.*, 2014
	Histone deacetylases inhibitors (HDACis)		Pimelic diphenylamide 106, Pyroxamide	D	Kobayashi *et al.*, 2017
		HDAC3/6	Apicidin	A	Lin *et al.*, 2011
		HDAC3	BRD3308	A, F	Barton *et al.*, 2014
		HDAC3/6/8	Droxinostat		
			Belinostat	A	Matalon *et al.*, 2011
			Givinostat	A	Matalon *et al.*, 2010
			KD5170, Pracinostat (SB939)	D	Kobayashi *et al.*, 2017
			M344	A	Ying *et al.*, 2012
		(pan)HDAC	Metacept-1; Metacept-2; Oxamflatin	A	Shehu-Xhilaga *et al.*, 2009
			Panobinostat	F, G (NCT02471430, NCT01680094)	Bullen *et al.*, 2014

Table 1 (*Continued*)

Class	Subclass	Function/Target	Compounds	Experimental system	References (Fully listed in reference list)
Chromatin modulators			Psammaplin A	A, E	Richard K *et al.*, 2018
			Scrpitaid	A	Ying *et al.*, 2010
			Sodium butyrate (Na-But)	A	Reuse *et al.*, 2009
			ST7612AA1	E	Badia *et al.*, 2015
		(pan)HDAC	Trichostatin A (TSA); Trapoxin A (TPX)	A	Van Lint *et al.*, 1996
			Valproic Acid (VPA)	G (NCT03525730, NCT00614458)	Lehrman *et al.*, 2005
	Histone deacetylases inhibitors (HDACis)		Vorinostat (SAHA)	D, F, G (NCT02336074, NCT03198559, NCT03803605, NCT03212989, NCT03382834, NCT02475915, NCT02707900, NCT01319383)	Contreras *et al.*, 2009
		SIRT2 inhibitor	AGK2	D	Kobayashi *et al.*, 2017
		HDACI/II	acetate	E	Bolduc *et al.*, 2017
	BRG-1-associated factors complex inhibitors (BAFis)	BAF complex	CAPE; MGD-486; Pyrimethamine	D, F, G (NCT03525730)	Stoszko *et al.*, 2016
		ARID1A subunit of BAF	Macrolactams	D, F	Marian *et al.*, 2018
	DNA methyltransferases inhibitors (DNMTis)		Decitabine (5-aza-2′-deoxycytidine)	A, D	Kauder *et al.*, 2009
			Zebularine	A, F	Blazkova *et al.*, 2009
Activators of Transcription		CD122/CD132	ALT-803 (IL-15 superagonist complex)	D, E (NCT02191098)	Jones *et al.*, 2016
		CD122/CD132	IL-2, Il-6, TNFα	F, G (NCT03382834)	Tae-Wook Chun *et al.*, 1998
		CD127/CD132	CYT107 (recombinant IL-7)	F, G (NCT01019551)	Wang *et al.*, J 2005; Katlama *et al.*, 2016
		CD28	αCD28	A, D	Tong-Starkesen *et al.*, 1989; Spina *et al.*, 2013
	Extracellular stimulators	Surface glycans	rGal9 (recombinant Gal9)	A, F	Abdel-Mohsen *et al.*, 2016
			Phytohemagglutinin (PHA)	A, D	Spina *et al.*, 2013
		EGFR inhibitor	AG555	A	Calvanese *et al.*, 2013
		TCR agonist	αCD3	A, D	Spina *et al.*, 2013
		S1P1	S1P1 agonists	C,	Duquenne *et al.*, 2017
		αPD1 antibodies	Pembrolizumab	E, G (NCT02595866, NCT03239899)	Fromentin *et al.*, 2019

Table 1 (*Continued*)

Class	Subclass	Function/Target	Compounds	Experimental system	References (Fully listed in reference list)
Activators of transcription			12-deoxyphorbol 13-phenylacetate (DPP)	A	Bocklandt *et al.*, 2003
			3-(2-Naphthoyl)ingenol	A	Liu *et al.*, 2018
			Aplysiatoxin; Debromoaplysiatoxin	A, E	Richard *et al.*, 2018
			Bryologs	A, D	Marsden *et al.*, 2018
			Bryostatin-1	G (NCT02269605)	Gutiérrez *et al.*, 2016
			C3-esterified ingenol derivatives	A, F	Spivak *et al.*, 2018
			EK-16A	A, F	Wang *et al.*, 2017
			Euphoria Kansui extract	D, E, G (NCT02531295)	Cary *et al.*, 2016
			Gnidimacrin	A, E	Huang *et al.*, 2011; Lai *et al.*, 2015
	Protein kinase C agonists (PKC agonists)		IDB (ingenol 3, 20-dibenzoate)	F	Spivak *et al.*, 2015
			Ingenol-B (ingenol-3-hexanoate)	D, F	Jiang *et al.*, 2014; Pandeló José *et al.*, 2014
			LMC03; LMC07	F	Hamer *et al.*, 2003
			Namushen-1; Namushen-2	A	Tietjen *et al.*, 2018
			PEP005 (ingenol-3- angelate)	A, F,	Jiang *et al.*, 2015
			Phorbol 12-myristate 13-acetate (PMA)	A, D	Folks *et al.*, 1988; Spina *et al.*, 2013
			Prostratin	A, E	Gulatosky *et al.*, 1997; Kulkosky *et al.*, 2001
			Sesterterpenoids	A	Wang *et al.*, 2016
			SJ23B	A	Bedoya *et al.*, 2009
		TLR1/2	Pam2CSK4, Pam3CSK4; Imiquimod	D, E	Novis *et al.*, 2013, Macedo *et al.*, 2018
		TLR2	HKLM	A	Alvarez-Carbonell *et al.*, 2017
			PIM6	D	Rodriguez *et al.*, 2013
		TLR3	Poly-ICLC	A, G (NCT02071095)	Alvarez-Carbonell *et al.*, 2017
	Toll-like receptor agonists	TLR2/7	CL413	D, E	Macedo *et al.*, 2018
		TLR5	Flagellin	A	Thibault *et al.*, 2009
		TLR7/8	R-848	A, C (productive infection)	Schlaepfer *et al.*, 2006
			vesatolimod (GS- 9620)	E, G (NCT03060447, NCT02858401)	Tsai *et al.*, 2017
		TLR7	GS-986	H	Lim *et al.*, 2018
		TLR8	3M-002	A, F	Schlaepfer and Speck, J, 2011; Rochat *et al.*, 2017

Table 1 (*Continued*)

Class	Subclass	Function/Target	Compounds	Experimental system	References (Fully listed in reference list)
Activators of transcription	**Toll-like receptor agonists**	TLR9	CPG-7909	G (NCT00562939)	Winckelmann *et al.*, 2013
			MGN1703	A, E, G (NCT02443935)	Offersen *et al.*, 2016
			CpG oligonucleotides: ODN-2006; ODN-2040	A	Scheller *et al.*, 2004
		NF-κB - CCR5	Maraviroc	D, G (NCT02486510, NCT02475915, NCT00935480, NCT00808002)	López-Huertas *et al.*, 2017; Madrid-Elena *et al.*, 2018
		NF-κB	Juglone (5HN)	A, D	Yang *et al.*, 2009
		NF-κB and MSK1 activation	Cocaine	A	Sahu *et al.*, 2015
		NF-κB activation	As2O3 (Aresenic trioxide; FDA-approved drug)	A	Wang *et al.*, 2013
		STAT5 sumoylation inhibitors	Benzotriazoles (HODHBt, HBt, HOBt, HOAt)	F	Bosque *et al.*, 2017
		NFAT activator	AV6	D	Micheva-Viteva *et al.*, 2011
		RUNX1 inhibitor	Ro5-3335	E	Klase *et al.*, 2014
		SRC agonist	MCB-613	A, B	Nikolai *et al.*, 2017 (8th HIV Persistence during Therapy Workshop)
	Activators of transcription factors	HSF-1 stimulators	Resveratrol; Triacetyl resveratrol	A	Pan *et al.*, 2016; Zeng *et al.*, 2017
		PTEN dysregulation	Disulfiram	D, G (NCT03198559; NCT01286259; NCT01944371, NCT01571466)	Elliott *et al.*, HIV 2015; Spivak *et al.*, 2014
		PKA agonist	Bucladesine (dibutyryl-cAMP)	A	Lin *et al.*, 2018
		PI3K agonist	Oxoglaucine (57704)	A, E	Doyon *et al.*, 2014
		Heme oxygenase-1 agonist	Heme arginate	A	Shankaran *et al.*, 2011
		GSK3 inhibitors	SB-216763; Tideglusib	F	Gramatica *et al.*, 2017 (8th HIV Persistence during Therapy Workshop)
		GADD34 / PP1 inhibitor	Salubrinal	A, F	Pan *et al.*, 2016
		Calcineurin agonist	Ionomycin	A, D	Slekevitz *et al.*, 1988; Spina *et al.*, 2013
		BTK inhibitor	Terreic acid	A	Calvanese *et al.*, 2013
		Sp1	Hydroxyurea	A	Oguariri *et al.*, 2007
	Inhibitors of apoptosis (IAPs)		Debio 1143	B, F	Bobardt, Kuo, Gallay, 2019
		BIRC2	Birinapant; SBI-0637142; LCL-161	F	Pache *et al.*, 2015

Table 1 (*Continued*)

Class	Subclass	Function/Target	Compounds	Experimental system	References (Fully listed in reference list)
Transcription elongation control		KAT5 inhibitor	MG-149	D, F	Li *et al.*, 2018
			8-methoxy-6- methylquinolin-4-ol (MMQO)	D, E	Abner *et al.*, 2018; Gallastegui *et al.*, 2012
			Apabetalone (RVX-208), PFI-1	A, F	Lu *et al.*, 2017
	Inhibition of BET		I-BET; I-BET-151; MS-417	A, D	Nilsson *et al.*, 2016
		BET inhibitors	JQ1	D, F	Banerjee *et al.*, 2012
			OTX-015	A, F	Lu *et al.*, 2016
			UMB-136	D, F	Huang *et al.*, 2017
			Hexamethylene bisacetamide (HMBA)	C, F	Vlach and Pitha, 1993; Klichko *et al.*, 2005
		HEXIM	HMBA	A C, D	Contreras *et al.*, 2009; Spina *et al.*, Pathogens 2013
	7SK snRNP	7SK RNA	Gliotoxin	D, F	Stoszko *et al.*, 8th HIV Persistence during therapy workshop, Miami 2017
	Tat	TAR-LTR	TatR5M4	A, D, F	Geng *et al.*, 2016
			EXO-Tat	A, D, F	Tang *et al.*, 2018
	Immune checkpoint inhibitors		Durvalumab (anti-PD1)	G	NCT03094286
			Cemiplimab (anti-PD1)	G	NCT03787095
			Nivolumab (anti-PD1)	G	NCT02408861
			BMS-936559 (anti-PD1)	G	NCT02028403
			Pembrolizumab	F, G case study, $N = 1$	Fromentin *et al.*, 2019, NCT02595866
			Ipilimumab (anti- CTLA-4)	E (case study, $N = 1$); G (NCT02408861, NCT03407105)	Wightman *et al.*, 2015
Post transcriptional control		SF3B1 inhibitor	sudemycin D6	A, D	Kyei *et al.*, 2018
		SR protein family: SRp20/ SRSF3	Digoxin	C, E	Wong *et al.*, 2013
			Cardiac glycoside/aglycones	A, C, E	Wong *et al.*, 2018
		SR protein family: SF-2	DHA-type compound 9 (1C8)	A	Cheung *et al.*, 2016
			Clomifene	A	Prado *et al.* 2016
		Rev-RRE formation	8-Azaguanine, 2-(2-[5-Nitro-2-thienyl]vinyl)quinolone	C, E	Wong *et al.*, 2013
		CRM1 inhibitors	LMB, ratjadone A	A	Fleta-Soriano *et al.*, 2014
			PKF050-638	A	Daelemans *et al.*, 2002
		CBC inhibitor	ABX464	D, G (NCT02735863, NCT02990325)	Vautrin *et al.*, 2019; Steens *et al.*, 2017
Miscellaneous		Deoxyhypusyl hydroxylase	Deferiprone	C, G (NCT02191657)	Saxena *et al.*, 2016

Table 1 (*Continued*)

Class	Subclass	Function/Target	Compounds	Experimental system	References (Fully listed in reference list)
Miscellaneous		Adenosine reuptake inhibitor	Dilazep	A	Calvanese *et al.*, 2013
			Carfilzomib (CFZ)	A, F	Pan *et al.*, JBC 2016
		Proteasome inhibitors	MG-132 (ONX-0914/PR-957); Velcade; CLBL	A, D	Miller *et al.*, 2013
			PR-957 (ONX-0914/MG-132)	A, F	Li *et al.*, 2018
			Abyssomicin-2	D, F	Leon *et al.*, 2015
			HHODC	A, E	Kapewangolo *et al.*, 2017
			Piceatannol	A	Elbezanti *et al.*, 2017 (oral presentation); Zeng *et al.*, JAFC 2017
		Unknown	PH01; PH02; PH03; PH04; PH05	A, F	Hashemi *et al.*, 2018
			Quinolin-8-ol derivatives	A, D	Xing *et al.*, J 2011
			Radicicol; Pochonin B; Pochonin C	D	Mejia *et al.*, J 2014
Block and Lock approaches		Kinase inhibitors	Danusertib, PF-3758309	D	Vargas *et al.*, 2018
		mTOR inhibitors	Torin1, pp242 and rapamycin (Sirolimus)	F, G (NCT02440789)	Besnard *et al.*, 2017
			Didehydro-cortistatin A (dCA)	A, B, F	Mosseau *et al.*, 2015; Kessing *et al.*, 2017
		Tat inhibitor	Triptolide wilfordii	A, G (NCT02219672)	Wan and Chen, 2014
		JAK-STAT inhibitors	Tofacitinib and ruxolitinib	D, F	Gavegnano *et al.*, 2017
		LEDGF/p75 inhibitors	LEDGINs	D	Vranckx *et al.*, 2016
		FACT complex, elongation	curaxin 100 (CBL0100)	D, E	Jean *et al.*, 2017
		Inhibition of NFKB activation, through Hsp90 inhibition	GV1001	A	Kim *et al.*, 2016
		calcineurin inhibitor	cyclosporin A	A, D	Chan *et al.*, 2013
			F07#13	B	Van Duyne *et al.*, 2013
			FIT-039	A	Okamoto *et al.*, 2015
		CDK9 inhibitors	Panel of inhibitors	A	Nemeth *et al.*, 2011
			2-fluorophenyl (12 d), flavopiridol analogue	A	Ali *et al.*, 2009
		PKC	Benzolactam derivative, BL-V8-310	A, E	Matsuda *et al.*, 2019
Induction of cell death		BET inhibitor	Apabetalone	A, F	Xuan-xuan Zhang *et al.*, 2019
		Bcl-2 agonists	Venetoclax, Navitoclax	F	Campbell *et al.*, 2015, CROI, conference
		PI3K/Akt inhibitors	Edelfosine, Perifosine, Miltefosine	A	Lucas *et al.*, 2010
			Lancemaside A, Compound K, Arctigenin	A	Kim *et al.*, 2016
Induction of cell death			Birinapant, GDC- 0152, Embelin	F	Campbell *et al.*, 2018, Hattori, 2018
		SMAC mimetics	AZD5582; AT406; BV6; SM164; GDC0152	A, F	Sampey *et al.*, 2018
			SM-AEG40730, SM-LCL161	A, C	Ashok Kumar *et al.*, 2019
		RIG-I	Acitretin	F	Li *et al.*, 2016; Garcia-Vidal *et al.* [90]

Table 1 (*Continued*)

Class	Subclass	Function/Target	Compounds	Experimental system	References (Fully listed in reference list)
Promote cell killing		Bispecific T-cell engaging (BiTE) antibodies	B12; VRC01; CD4(1+2)L17b	C	Brozy *et al.*, 2018
			MGD014	G	NCT03570918
		Dual-affinity re- targeting (DART)	HIVxCD3	A, D, F	Sung *et al.*, 2015
			HIVxCD3	D, E	Sloan *et al.*, 2015

Model systems:
A – cell lines.
B – mouse models.
C – *ex vivo* infected PBMCs.
D – *ex vivo* infected primary CD4+ T cells.
E – PBMCs from aviremic participants.
F – CD4+ T cells from aviremic participants.
G – aviremic participants (*in vivo*).

HDACis synergized to reactivate HIV-1 in cART treated patient cells [30].

Targeting chromatin structure

A major determinant of HIV latency, chromatin, is restructured by the activity of ATP-dependent remodelers. The CHD3 containing NuRD remodeller and related CHD1 repress HIV-1 [8,9]. The INI-1 containing ATP-dependent BAF remodeller is associated with the 5′LTR and represses HIV-1 by actively positioning Nuc-1 [8]. Interestingly, BRD4S, a short isoform of the bromodomain protein BRD4, tethers BAF to the 5′LTR, silencing HIV-1 [31•]. Such enforced chromatin structure represents a mechanical block for HIV-1 transcription, subject to pharmacological intervention for reversal [8,31•,32,33•,34].

BAF inhibitors (BAFis). Small molecule BAFis re-activated latent HIV-1 in a spectrum of *in vitro* latency models and in c-ART suppressed HIV-1 infected patient CD4+T cells [32]. BAFis CAPE and Pyrimethamine enhance transcriptional noise [34]. When combined with PKC agonists showed significantly increased potency than single treatments, pointing, similar to HDACis, to their potential in combinatorial LRA approaches. Recently, a screen of almost 350 000 compounds led to identification of ARID1A targeting macrolactam scaffold BAFis, which reversed HIV-1 latency in primary CD4+T cells with limited cytoxicity, representing promising LRAs for clinical investigation [33•].

BET inhibitors (BETis), in addition to enhancing HIV-1 transcription elongation (Section 'Enhancing HIV-1 transcriptional elongation'), act as derepressors of HIV-1 transcription in a Tat independent manner [8]. BETis inhibited 5′LTR-bound BRD2, and BRD4S, inducing LTR chromatin derepression in a BAF-dependent manner [8,31•]. Small molecule BETis are under development with differing potency and specificity to circumvent clinical limitations of JQ1 (Table 1).

Inducing HIV-1 transcription activation

The 5′LTR contains a plethora of consensus sequences for TFs whose binding leads to HIV-1 5′LTR recruitment of Pol II and basal TFs [8,12,15] (Figure 2b). NF-κB/p65, arguably the strongest activator of HIV-1 transcription initiation, and molecular effectors that facilitate its binding such as those in the protein kinase C (PKC), TLR, and TNFα signaling pathways, are high potential pharmacological targets for latency reversal [9,35]. AP-1, STAT5 and NFAT are also among important HIV-1 transcription activators [8,9,36].

Targeting NFkB

In latent HIV-1 infected resting CD4+T cells, p65 is sequestered in the cytoplasm while the 5′LTR is repressed by p50 homodimers. Upon canonical NFκB

activation, p65 translocates to the nucleus, binds 5′LTR as a p65/p50 heterodimer and recruits Pol II, HATs, as well as PTEFb, leading to initiation and elongation of HIV transcription [8,9,35]. While an attractive pathway for LRA-based interventions, NFkB signaling is a master regulator of immune and other functions and its pharmacological modulation exposes risks of serious side effects [35]. Interestingly, small molecule mimetics of mitochondria-derived activator of caspases (SMAC mimetics) (Section 'Inhibitors of IAPs'), activated non-canonical NF-κB and binding of RELB/p52 heterodimers to the 5′LTR resulting in latency reversal (Table 1) without causing T cell activation, pointing to non-canonical NFκB as an interesting avenue for further exploration [27,37,38].

PKC agonists. A spectrum of drugs targeting the PKC pathway, including Prostratin, Bryostatin-1 and Ingenols activate NFAT, NFκB and AP-1 binding to the 5′LTR (Table 1), leading to strong proviral transcription initiation [18,39–45]. While PKCα and PKCθ stimulation targets HIV-1 [46], most currently available PKC agonists target many PKC isoforms resulting in pleiotropic and consequent toxic effects, highlighting need for novel more specific PKC agonists [18,45,46].

Maraviroc, a CCR5 antagonist HIV entry blocker was shown to also reverse latency via NFkB activation [47,48]. Maraviroc induced NFκB phosphorylation and HIV transcription as shown by increased cell associated HIV-1 RNA in patient CD4+ T cells [48]. Maraviroc is attractive for inclusion in pharmacological LRA strategies because of its mechanistic versatility as an LRA and antiviral.

TLR agonists have gained much attention due to their multifactorial effects on the HIV-1 reservoir [49••,50–54]. At least ten TLRs are described that function as first line of pathogen recognition and induce innate and adaptive immune defenses. Dual TLR agonists such as CL413 showed potent HIV-1 reactivation via complementary targeting of TLR2 and TLR7, leading to NFkB activation concomitant with TNFα production [49••]. MGN1703, a TLR9 agonist induced HIV plasma RNA in 6 of 15 study participants concomitant with increased activation of NK and CD8+T cells, although no reduction in latent reservoir was observed [50]. The TLR7 agonists GS-986 and GS-9620, suggested to also enhance anti-HIV immune effector function, reversed latency in patient cells [51]. These TLR7 agonists also increased plasma HIV-1 RNA concominant with decreased HIV-1 DNA in the infected rhesus model, where two of nine animals have remained aviremic [52]. Because of this functional versatility, TLR agonists show much promise in reservoir elimination strategies.

Other TFs

LRAs can reduce or enhance HIV-1 5′LTR binding of repressive/activating TFs [8,12,15]. Resveratrol promotes histone acetylation and activation of HSF1, an HIV-1 transcription activator [55]. Benzotriazoles were recently shown to stabilize the active form of STAT5 and reactivate HIV-1 [36].

Enhancing HIV-1 transcriptional elongation

Inefficient transcription elongation via promoter-proximal Pol II 5′LTR pausing is a major rate-limiting step in latency reversal [56••] (Figure 2c), which is released by Tat; when expressed at sufficient levels, Tat orchestrates a strong positive transcriptional feedback loop [8]. Tat binds TAR and recruits PTEFb, whose CDK9 component phosphorylates the Pol II C-terminal domain (CTD) as well as NELF and DSIF (which promote Pol II dissociation when unphosphorylated), enhancing Pol II processivity. In latent cells, PTEFb is predominantly sequestered within the 7SKsnRNP complex, a ribonucleoprotein scaffold in which PTEFb activity is inhibited [8]. Tat also competes for PTEFb with BRD4, which binds and sequesters PTEFb [9]. To enhance transcription elongation, in addition to PTEFb, Tat recruits a number of other interactors, including chromatin modifiers, whose binding is regulated by deposition and removal of PTMs and these can also be exploited pharmacologically [8,57–59].

BETis. Inhibition of BRD4 releases PTEFb, increasing its availability for binding Tat. BETis activate latent HIV in a spectrum of latency models and after treatment of cells from HIV infected patients [60–63] (Table 1). Interestingly, inhibition of the lysine acetyltransferase KAT5 reduced 5′LTR histone H4 acetylation and impaired BRD4 recruitment, similar to BETis, resulting in increased PTEFb pool for Tat reactivation of latent HIV-1 [64]. Thus BETis are promising LRAs that act via a dual mechanism, relieving BRD4S-BAF-mediated LTR repression as well as increasing availability of PTEFb for Tat.

Compounds disrupting 7SK snRNP. In resting CD4+T cells the majority of PTEFb is sequestered in an inactive form within the 7SK snRNP complex [8]. Inhibition of the HEXIM subunit of 7SK snRNP by HMBA enhanced PTEFb activity and latency reversal [9,63,65]. We recently found Gliotoxin, a small molecule secreted by *Aspergillus fumigatus* reversed latency in HIV infected patient CD4+T cells by disrupting 7SK snRNP causing PTEFb release and transcription elongation at the HIV LTR (submitted).

Tat has remarkable specificity for the HIV 5′LTR and can penetrate cell membranes. In an attenuated form [66], or exosomally delivered [67], Tat activated HIV-1 in CD4 +T cells obtained from c-ART suppressed infected individuals and significantly increased the potency of other LRAs. The potential of Tat as a therapeutic vaccine

candidate has also been explored [68] and may play a role in efforts toward reservoir depletion.

Immune checkpoint (IC) blockers. PD-1 has been suggested to confer persistence of HIV-1 latency during c-ART, likely via inhibition of signaling pathways that lead to PTEFb activity [69,70]. IC blockers reversed latency in cells obtained from suppressed patients [71], although another study found less robust effects [72]. Further investigation will determine effectiveness of IC blockers as LRAs and/or in alleviating CD8+T cell exhaustion.

Targeting post transcriptional regulation

Viral proteins were shown to be produced in a small fraction of LRA-reactivated cells which transcribed viral RNA [73••]. This points to the presence of post-transcriptional blocks in viral reactivation [56••], where HIV-1 RNA is subjected to splicing and polyadenylation and RNA surveillance proteins influence viral RNA metabolism. Lack of polyadenylated mRNA compromises transcript stability, export and HIV-1 protein production while block in splicing decreases HIV-1 expression [10,11,56••,74–77]. The significant contribution of post-transcriptional and transcription elongation blocks to efficient HIV latency reversal have only recently come to light. Although these regulatory mechanisms have not been extensively explored in the context of HIV reactivation, effective latency reversal may require interventions that improve viral RNA stability, splicing, export and translation in order to boost viral protein production.

Pipeline of block and lock agents

On the flip side of reversing latency as a stepping stone to viral elimination, 'block and lock' [2•] is a functional cure strategy to permanently shut down viral expression, eliminating the need for continued antiviral therapy.

Tat inhibition

The HIV-1 Tat inhibitor Didehydro-Cortistatin A (dCA) binds Tat and effectively disrupts Tat/TAR axis [78], restricting HIV-1 transcription and replication. dCA treatment was shown to restrict PBAF recruitment while enhancing BAF 5'LTR occupancy and Nuc-1 mediated repression [79]. Consistently, *ex vivo* dCA treatment of CD4+T cells from HIV-1 infected individuals both improved c-ART suppression of infection and led to strengthened 5′LTR chromatin and epigenetic repression, restricting viral reactivation in latently infected cells and leading to a delayed viral rebound after c-ART interruption [2•].

Targeting host factors to reinforce latency

In line with block and lock, compounds targeting host factors DDX3, DDX5, Matrin3, Mov10, splicing factors, UPF proteins, involved in HIV-1 post-transcriptional processing, including inhibitors of mTOR, cardiotonic steroids, SR proteins, inhibit HIV-1 latency reversal and lead to a block in translation [74–81]. Inhibition of HIV-1 Rev and Rev response element (RRE) association on the viral RNA or the cellular factor CRM1 can block nuclear export of unspliced viral mRNA [82]. ABX464-mediated inhibition of the cap binding complex increased viral splicing, halting production of unspliced RNA required for viral assembly [83]. LEDGINs, molecules that inhibit HIV-1 integrase-LEDGF interaction were described to shift preferential sites of HIV-1 integration out of active transcription units, and retarget HIV into regions refractory to reactivation [84]. Block and lock strategies, similarly to LRAs, can in principle work most effectively in combination; dCA, LEDGINs, compounds that strengthen proviral epigenetic repression, and ultimately modulators of splicing and viral export, may act synergistically to induce a deeper state of latency to delay or permanently suppress viral rebound.

Inducing cell death

An attractive approach to eliminate HIV-1 emerging out of latency is to pharmacologically target danger sensing, stress and apoptotic pathways in order to induce cell death in LRA-reactivated HIV expressing cells [85]. This would bypass necessity for an anti-HIV immune response to eliminate reactivated cells. To this end, coupling LRA-induced HIV activation with inhibitors of inhibitors of apoptosis (IAPs), stimulation of danger sensing pathways, and indirect triggering of stress by blocking the cell's physiological processes have drawn much attention as a way to eliminate latently infected cells.

Inhibitors of IAPs

SMAC mimetics (SMs), molecules which target cell survival factors XIAP and cIAP1/BIRC2 have shown much promise as both LRAs that act through noncanonical NFkB activation as well as compounds that induce apoptosis in HIV-1 infected cells through proteasomal degradation of IAPs. SMs SBI-0637142 and LCL161 down-regulated BIRC2/IAP, leading to proviral transcription [37]. Debio 1143 targets BIRC2 for degradation inducing non-canonical NFκB with subsequent HIV-1 latency reversal in resting CD4+T cell from aviremic participants [86]. SMs birinapant [38], GDC-0152, and embelin induced apoptosis selectively in HIV-1 infected (but not uninfected) central memory CD4+Tcells, leading to their elimination [87••]. Benzolactam related compound BL-V8-310 induced apoptosis in HIV infected cells reactivated in a PKC induced manner [44]. Interestingly, *in vitro* treatment with the pro-apoptotic drug Venetoclax, which blocks Bcl-2, followed by anti-CD3/CD28 stimulation resulted in fast decay of productively infected primary T cells *in vitro* and reduction of the latent reservoir *in vitro* [88].

Stimulation of TLRs and RIG-I-like receptors (RLRs)

When latent HIV is reactivated, TLRs, RLRs and their molecular effectors, act as sensors that trigger NFkB,

MAP kinase and interferon signaling and initiate an innate immune response. Subsequent to detection of viral RNA, RIG-1 induces apoptosis. Interestingly, retinoic acid (RA) induces expression of RIG-I and p300, which in turn stimulates HIV-1. Acitretin a derivative of RA reversed HIV-1 latency and induced apoptosis in infected cells [89,90]. When combined with Vorinostat even higher depletion of proviral DNA was observed. A later study however challenged these findings showing only weak latency reversal and cell death, pointing to need for further evaluation. TLRs may also play multiple roles, as LRAs, and mediators of HIV-infected cell death [51,54]. A remaining question is whether and which TLRs become activated by HIV-1 transcripts and proteins upon latency reversal.

Combination, synergism and scalable therapy

Current LRAs reactivate only 5% of latently infected cells [91••], of which only an approximated 2–10% produce viral protein in addition to expressing viral RNA [73••]. Administration of certain LRA combinations in intervals, rather than at once [19,30], stimulated higher proviral expression, while sequential treatment rounds yielded new infecious particles. These observations point to a limitation in potency of current LRAs as well as transcriptional stochasticity of a diverse and strenuous latent reservoir. The heterogeneous nature of molecular mechanisms controlling HIV latency predicts that a combination of compounds targeting distinct regulatory pathways will be most effective to activate the reservoir. Synergistic effects of LRAs have been shown ex vivo [8,9,30,32,33•,40,43,63]. While ongoing and future clinical trials will shed more light on which mechanisms of latency should be targeted in concert for most roboust reversal, mechanistic and preclinical observations point to combinations that include derepressors (eg. Vorinostat, BAFis), activators of NFkB (eg. dual TLR agonists or SMAC mimetics) and activators of transcription elongation (eg. BETis, Gliotoxin) to have high potential. The use of LRAs in combination allows for lower concentrations of each molecule to induce HIV activation. Hence, combinatorial approaches emerge not only as a way to improve the activation efficacy of individual LRAs, but also as a way to govern a level of specificity towards HIV-1 latency reversal, limiting the pleiotropic and toxic effects of each intervention (Figure 3).

Figure 3

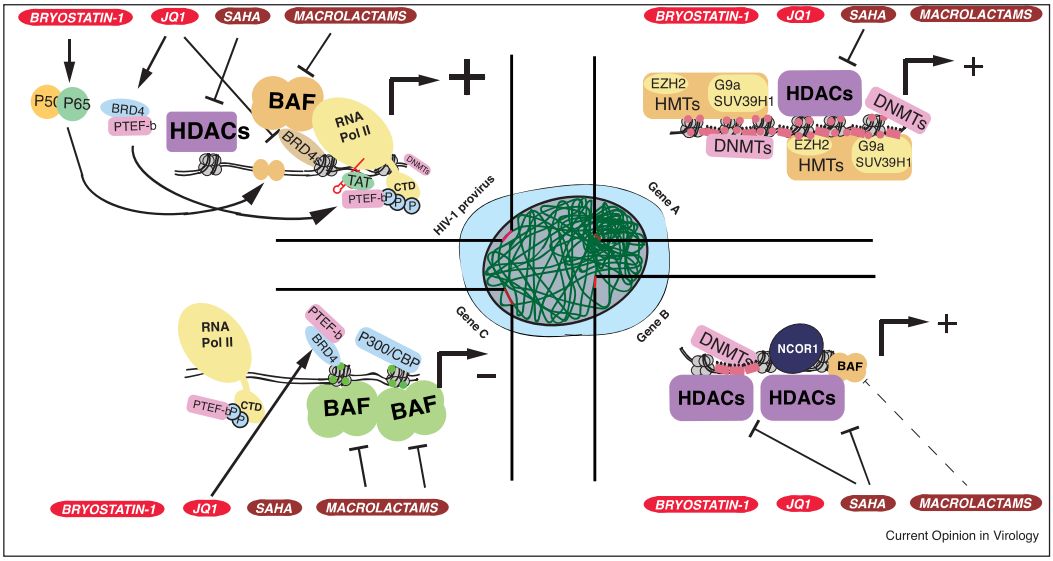

Combinatorial targeting to obtain synergism and selectivity for the HIV promoter to achieve HIV latency reversal with minimal associated pleiotropic effects and cytotoxicity. Combinatorial use of different classes of LRAs (e.g. bryostatin-1, JQ1, Vorinostat and macrolactam scaffold BAFis shown here) may confer specificity for transcriptional reactivation at the latent HIV-1 promoter relative to endogenous genes. The HIV-1 promoter is targeted by the activity of each LRA, which together strongly synergize to re-activate HIV-1 transcription. Gene A, is highly repressed and targeted only by Vorinostat for re-activation, with limited effect. Gene B, predominantly repressed by NCOR1, histone hypoacetylation and DNA methylation, and partially by the repressive BAF is moderately re-activated by the combination of LRAs. Gene C is an actively transcribed gene, dependent on p300, BAF and BRD4 and undergoes partial repression as result of the combination LRAs.

In contrast to antivirals, which target HIV, pharmacological interventions to eliminate the HIV reservoir (Table 1), with the exception of Tat and Tat and Rev-RRE inhibitors, all target host molecular effectors, harbor inherent pleiotropic effects and are subject to variability in response. In this context, pharmacogenetics to investigate the patient-specific response to distinct molecules may identify robust treatments, which synergize at sufficient magnitudes to overrule individual variability, paving the way for scalable therapy options. Importantly, the complex nature of the latent reservoir points to the likelihood of future combinations of nonexclusive pipelines of interventions. For example, potent latency reversal and cell death promoting combination regimens could be used, in presence of c-ART, to activate and eliminate a more reactivatable fraction of the reservoir. Here promoting clearance of latent cells via apoptosis and immune boosting strategies could be used concomitantly to improve reservoir elimination. Upon clearance of this more labile latent reservoir, 'block and lock' regimens may be employed to lock the remaining reservoir in a permanently repressed state. A strengthened immune system would then control the latent virus in case of escape from the blocked state, in combination allowing cessation of c-ART.

Conflict of interest statement

Nothing declared.

Acknowledgements

TM received funding from the European Research Council (ERC) under the European Union's Seventh Framework Programme(FP/2007-2013)/ ERC STG 337116 Trxn-PURGE, the Dutch AIDS Fonds grant 2014021 and Erasmus MC mRACE research grant.

References and recommended reading

Papers of particular interest, published within the period of review, have been highlighted as:

- • of special interest
- •• of outstanding interest

1. Siliciano JM, Siliciano RF: **The remarkable stability of the latent reservoir for HIV-1 in resting memory CD4 + T cells**. *J Infect Dis* 2015, **212**:1345-1347.

2. • Kessing CF, Nixon CC, Li C, Tsai P, Takata H, Mousseau G, Ho PT, Honeycutt JB, Fallahi M, Trautmann L *et al.*: **In vivo suppression of HIV rebound by Didehydro-Cortistatin A, a "Block-and-Lock" strategy for HIV-1 treatment**. *Cell Rep* 2017, **17**:600-611.
The authors describe the use of dCA, an inhibitor of Tat-TAR in the 'Block and lock' approach which aims to induce a deep and stable state of HIV-1 latency whereby c-ART could be discontinued.

3. Deeks SG: **HIV: shock and kill**. *Nature* 2012, **25**:439-40.6.

4. Kuhlmann A-S, Peterson CW, Kiem H-P: **Chimeric antigen receptor T-cell approaches to HIV cure**. *Curr Opin HIV AIDS* 2018:446-453.

5. Gao Y, McKay PF, Mann JFS: **Advances in HIV-1 vaccine development**. *Viruses* 2018, **10**.

6. Jones RB, Walker BD: **HIV-specific CD8$^+$T cells and HIV eradication**. *J Clin Invest* 2016, **126**:455-463.

7. Kumar R, Qureshi H, Deshpande S, Bhattacharya J: **Broadly neutralizing antibodies in HIV-1 treatment and prevention**. *Ther Adv Vaccines Immunother* 2018, **6**:61-68.

8. Ne E, Palstra RJ, Mahmoudi T: **Transcription: insights from the HIV-1 promoter**. *Int Rev Cell Mol Biol* 2018, **335**:191-243.

9. De Crignis E, Mahmoudi T: **The multifaceted contributions of chromatin to HIV-1 integration, transcription, and latency**. *Int Rev Cell Mol Biol* 2017, **328**:197-252.11.

10. Sarracino A, Marcello A: **The relevance of post-transcriptional mechanisms in HIV latency reversal**. *Curr Pharm Des* 2017, **23**.

11. Baxter AE, O'Doherty U, Kaufmann DE: **Beyond the replication-competent HIV reservoir: transcription and translation-competent reservoirs**. *Retrovirology* 2018, **15**:18.

12. Cary DC, Fujinaga K, Peterlin BM, Barre-Sinoussi F, Alizon M, Sanchez-Pescador R *et al.*: **Molecular mechanisms of HIV latency**. *J Clin Invest* 2016, **126**:448-454.

13. Margolis DM, Archin NM: **Proviral latency, persistent human immunodeficiency virus infection, and the development of latency reversing agents**. *J Infect Dis* 2017, **215**:S111-S118.

14. Khan S, Iqbal M, Tariq M, Baig SM, Abbas W: **Epigenetic regulation of HIV-1 latency: focus on polycomb group (PcG) proteins**. *Clin Epigenet* 2018, **5**:14.

15. Mbonye U, Karn J: **The molecular basis for human immunodeficiency virus latency**. *Annu Rev Virol* 2017, **29**:261-285.

16. Boehm D, Ott M: **Host methyltransferases and demethylases: potential new epigenetic targets for HIV cure strategies and beyond**. *AIDS Res Hum Retroviruse* 2017, **33**:S8-S22.

17. Jiang G, Nguyen D, Archin NM, Yukl SA, Méndez-Lagares G, Tang Y, Elsheikh MM, Thompson GR 3rd, Hartigan-O'Connor DJ, Margolis DM *et al.*: **HIV latency is reversed by ACSS2-driven histone crotonylation**. *J Clin Invest* 2018, **128**:1190-1198.

18. Rasmussen TA, Søgaard OS: **Clinical interventions in HIV cure research**. *Adv Exp Med Biol* 2018, **1075**:285-318.

19. Archin NM, Kirchherr JL, Sung JA, Clutton G, Sholtis K, Xu Y, Allard B, Stuelke E, Kashuba AD, Kuruc JD *et al.*: **Interval dosing with the HDAC inhibitor vorinostat effectively reverses HIV latency**. *J Clin Invest* 2017, **1**:3126-3135.

20. Brinkmann CR, Højen JF, Rasmussen TA, Kjær AS, Olesen R, Denton PW, Østergaard L, Ouyang Z, Lichterfeld M, Yu X *et al.*: **Treatment of HIV-infected individuals with the histone deacetylase inhibitor panobinostat results in increased numbers of regulatory T cells and limits ex vivo lipopolysaccharide-induced inflammatory responses**. *mSphere* 2018, **14** pii: e00616-17.

21. Spivak AM, Planelles V: **Novel latency reversal agents for HIV-1 cure**. *Annu Rev Med* 2017, **69** annurev-med-052716-031710.

22. Bolduc JF, Hany L, Barat C, Ouellet M, Tremblay MJ: **Epigenetic metabolite acetate inhibits class I/II histone deacetylases, promotes histone acetylation, and increases HIV-1 integration in CD4+ T cells**. *J Virol* 2017, **91** e01943-16.

23. Dar RD, Hosmane NN, Arkin MR, Siliciano RF, Weinberger LS: **Screening for noise in gene expression identifies drug synergies**. *Science* 2014, **344**:1392-1396.

24. Wu G, Swanson M, Talla A, Graham D, Strizki J, Gorman D, Barnard RJO, Blair W, Søgaard OS, Tolstrup M *et al.*: **HDAC inhibition induces HIV-1 protein and enables immune-based clearance following latency reversal**. *JCI Insight* 2017, **2**: e92901.

25. Albert BJ, Niu A, Ramani R, Marshall GR, Wender PA, Williams RM, Ratner L, Barnes AB, Kyei GB: **Combinations of isoform-targeted histone deacetylase inhibitors and bryostatin analogues display remarkable potency to activate latent HIV without global T-cell activation**. *Sci Rep* 2017, **7** 7456.38.

26. • Zaikos TD, Painter MM, Sebastian Kettinger NT, Terry VH, Collins KL: **Class 1-Selective Histone Deacetylase (HDAC) inhibitors enhance HIV latency reversal while preserving the**

activity of HDAC isoforms necessary for maximal HIV gene expression. *J Virol* 2018, **92** e02110-17.
The authors demonstrate that specific class I HDACis more potently reverse latency, alone or in synergy with other LRAs, than pan-HDACIs. They provide evidence that certain non-class 1 HDACs support the activity of factors required for proviral activation thus explaining the limited potency of pan-HDACis.

27. Kobayashi Y, Gélinas C, Dougherty JP: **HDAC inhibitors containing a benzamide functional group and a Pyridyl cap are preferentially effective HIV-1 latency reversing agents in primary resting CD4+ T cells**. *J Gen Virol* 2017:799-809.

28. • Nguyen K, Das B, Dobrowolski C, Karn J: **Multiple histone lysine methyltransferases are required for the establishment and maintenance of HIV-1 latency**. *mBio* 2017, **28** e00133-17.
The authors provide a thorough characterization of the histone lysine methyltransferases implicated in HIV-1 latency establishment and maintenance and propose novel epigenetic drugs for use in latency reversal strategies.

29. Boehm D, Jeng M, Camus G, Gramatica A, Schwarzer R, Johnson JR, Hull PA, Montano M, Sakane N, Pagans S *et al.*: **SMYD2-mediated histone methylation contributes to HIV-1 latency**. *Cell Host Microbe* 2017, **21**:569-579.e6.

30. Bouchat S, Delacourt N, Kula A, Darcis G, Van Driessche B, Corazza F, Gatot JS, Melard A, Vanhulle C, Kabeya K *et al.*: **Sequential treatment with 5-aza-2'-deoxycytidine and deacetylase inhibitors reactivates HIV-1**. *EMBO Mol Med* 2016, **8**:117-138.

31. • Conrad RJ, Fozouni P, Thomas S, Sy H, Zhang Q, Zhou MM, Ott M: **The short isoform of BRD4 promotes HIV-1 latency by engaging repressive SWI/SNF chromatin-remodeling complexes**. *Mol Cell* 2017, **67**:1001-1012.e6.
The authors show that a short BRD4 isoform tethers the repressive BAF complex to the LTR, and that JQ1 leads to a BAF-dependent remodeling of the latent HIV LTR.

32. Stoszko M, De Crignis E, Rokx C, Khalid MM, Lungu C, Palstra RJ, Kan TW, Boucher C, Verbon A, Dykhuizen EC, Mahmoudi T: **Small molecule inhibitors of BAF; a promising family of compounds in HIV-1 latency reversal**. *BioMedicine* 2015, **27**:108-121.

33. • Marian CA, Stoszko M, Wang L, Leighty MW, de Crignis E, Maschinot CA, Gatchalian J, Carter BC, Chowdhury B, Hargreaves DC *et al.*: **Small molecule targeting of specific BAF (mSWI/SNF) complexes for HIV latency reversal**. *Cell Chem Biol* 2018, **25**:1443-1455.e14.
The authors describe identification, from a screen of 350 000 molecules, a macrolactam scaffold class of small molecules that target and inhibit the ARID1a subunit of the BAF complex and reverse HIV latency with less associated cytotoxicity.

34. Megaridis MR, Lu Y, Tevonian EN, Junger KM, Moy JM, Bohn-Wippert K, Dar RD: **Fine-tuning of noise in gene expression with nucleosome remodeling**. *APL Bioeng* 2018, **2**:026106.

35. Jiang G, Dandekar S: **Targeting NF-κB signaling with protein kinase C agonists as an emerging strategy for combating HIV latency**. *AIDS Res Hum Retroviruses* 2015, **31**:4-12.

36. Bosque A, Nilson KA, Macedo AB, Spivak AM, Archin NM, Van Wagoner RM, Martins LJ, Novis CL, Szaniawski MA, Ireland CM *et al.*: **Benzotriazoles reactivate latent HIV-1 through inactivation of STAT5 SUMOylation**. *Cell Rep* 2017, **18**:1324-1334.

37. Pache L, Dutra MS, Spivak AM, Marlett JM, Murry JP, Hwang Y, Maestre AM, Manganaro L, Vamos M, Teriete P *et al.*: **BIRC2/cIAP1 is a negative regulator of HIV-1 transcription and can be targeted by Smac mimetics to promote reversal of viral latency**. *Cell Host Microbe* 2015, **18**:345-353.

38. Hattori SI, Matsuda K, Tsuchiya K, Gatanaga H, Oka S, Yoshimura K, Mitsuya H, Maeda K: **Combination of a latency-reversing agent with a Smac mimetic minimizes secondary HIV-1 infection in vitro**. *Front Microbiol* 2018, **9**:2022.

39. Brogdon J, Ziani W, Wang X, Veazey RS, Xu H: **In vitro effects of the small-molecule protein kinase C agonists on HIV latency reactivation**. *Sci Rep* 2016, **6**:39032.

40. Spivak AM, Nell RA, Petersen M, Martins L, Sebahar P, Looper RE, Planelles V: **Synthetic ingenols maximize protein kinase C-induced HIV-1 latency reversal**. *Antimicrob Agents Chemother* 2018, **62** e01361-18.

41. Marsden MD, Loy BA, Wu X, Ramirez CM, Schrier AJ, Murray D, Shimizu A, Ryckbosch SM, Near KE, Chun TW *et al.*: **In vivo activation of latent HIV with a synthetic bryostatin analog effects both latent cell "kick" and "kill" in strategy for virus eradication**. *PLoS Pathog* 2017, **13**:e1006575.

42. Marsden MD, Wu X, Navab SM, Loy BA, Schrier AJ, De Christopher BA, Shimizu AJ, Hardman CT, Ho S, Ramirez CM *et al.*: **Characterization of designed, synthetically accessible bryostatin analog HIV latency reversing agents**. *Virology* 2018, **520**:83-93.

43. Hashemi P, Barreto K, Bernhard W, Lomness A, Honson N, Pfeifer TA, Harrigan PR, Sadowski I: **Compounds producing an effective combinatorial regimen for disruption of HIV-1 latency**. *EMBO Mol Med* 2018, **10**:160-174.

44. Matsuda K, Kobayakawa T, Tsuchiya K, Hattori SI, Nomura W, Gatanaga H, Yoshimura K, Oka S, Endo Y, Tamamura H *et al.*: **Benzolactam-related compounds promote apoptosis of HIV-infected human cells via protein kinase C-induced HIV latency reversal**. *J Biol Chem* 2019, **294**:116-129.

45. Gutiérrez C, Serrano-Villar S, Madrid-Elena N, Pérez-Elías MJ, Martín ME, Barbas C, Ruipérez J, Muñoz E, Muñoz-Fernández MA, Castor T, Moreno S: **Bryostatin-1 for latent virus reactivation in HIV-infected patients on antiretroviral therapy**. *AIDS* 2016, **30**:1385-1392.

46. Phetsouphanh C, Kelleher AD: **The role of PKC-θ in CD4+ T cells and HIV infection: to the nucleus and back again**. *Front Immunol* 2015, **30**:391.

47. López-Huertas MR, Jiménez-Tormo L, Madrid-Elena N, Gutiérrez C, Rodríguez-Mora S, Coiras M, Alcamí J, Moreno S: **The CCR5-antagonist maraviroc reverses HIV-1 latency in vitro alone or in combination with the PKC-agonist Bryostatin-1**. *Sci Rep* 2017, **7**:2385.

48. Madrid-Elena N, García-Bermejo ML, Serrano-Villar S, Díaz-de Santiago A, Sastre B, Gutiérrez C, Dronda F, Coronel Díaz M, Domínguez E, López-Huertas MR *et al.*: **Maraviroc is associated with latent HIV-1 reactivation through NF-κB activation in resting CD4+ T cells from HIV-infected individuals on suppressive antiretroviral therapy**. *J Virol* 2018, **92**.

49. •• Macedo AB, Novis CL, De Assis CM, Sorensen ES, Moszczynski P, Huang SH, Ren Y, Spivak AM, Jones RB, Planelles V, Bosq ue A: **Dual TLR2 and TLR7 agonists as HIV latency-reversing agents**. *JCI Insight* 2018, **3** pii: 122673.
The authors describe dual TLR2/7 agonists that reverse latency in a complementary manner via both inducing NFkB in CD4+ T cells via the TLR2 component and TLR7 mediated production of TNFa by monocytes and dendritic cells.

50. Vibholm L, Schleimann MH, Højen JF, Benfield T, Offersen R, Rasmussen K, Olesen R, Dige A, Agnholt J, Grau J *et al.*: **Short-course toll-like receptor 9 agonist treatment impacts innate immunity and plasma viremia in individuals with human immunodeficiency virus infection**. *Clin Infect Dis* 2017, **64**:1686-1695.

51. Tsai A, Irrinki A, Kaur J, Cihlar T, Kukolj G, Sloan DD, Murry JP: **Toll-like receptor 7 agonist GS-9620 induces HIV expression and HIV-specific immunity in cells from HIV-infected individuals on suppressive antiretroviral therapy**. *J Virol* 2017, **91** e02166-16.

52. Lim SY, Osuna CE, Hraber PT, Hesselgesser J, Gerold JM, Barnes TL, Sanisetty S, Seaman MS, Lewis MG, Geleziunas R *et al.*: **TLR7 agonists induce transient viremia and reduce the viral reservoir in SIV-infected rhesus macaques on antiretroviral therapy**. *Sci Transl Med* 2018, **10** pii: eaao4521.119.

53. Rochat MA, Schlaepfer E, Speck RF: **Promising role of toll-like receptor 8 agonist in concert with prostratin for activation of silent HIV**. *J Virol* 2017, **91** e02084-16.

54. Cheng L, Wang Q, Li G, Banga R, Ma J, Yu H, Yasui F, Zhang Z, Pantaleo G, Perreau M *et al.*: **TLR3 agonist and CD40-targeting vaccination induces immune responses and reduces HIV-1 reservoirs**. *J Clin Invest* 2018, **128**:4387-4396.

55. Zeng X, Pan X, Xu X, Lin J, Que F, Tian Y, Li L, Liu S: **Resveratrol reactivates latent HIV through increasing histone acetylation and activating heat shock factor 1**. *J Agric Food Chem* 2017, **65**:4384-4394.

56. •• Yukl SA, Kaiser P, Kim P, Telwatte S, Joshi SK, Vu M, Lampiris H, Wong JK: **HIV latency in isolated patient CD4+ T cells may be due to blocks in HIV transcriptional elongation, completion, and splicing**. *Sci Transl Med* 2018, **10** pii: eaap9927.
The authors use RT-ddPCR to demonstrate that major blocks to transcription of the HIV virus occur beyond the level of transcription initiation, at the transcription elongation, polyadenylation and splicing stages, and that LRAs showed differing effects on these distinct blocks.

57. Jean M, Power D, Kong W, Huang H, Santoso N, Zhu J: **Identification of HIV-1 Tat-associated proteins contributing to HIV-1 transcription and latency**. *Viruses* 2017, **9**:67.

58. Khoury G, Mota TM, Li S, Tumpach C, Lee MY, Jacobson J, Harty L, Anderson JL, Lewin SR, Purcell DFJ: **HIV latency reversing agents act through Tat post translational modifications**. *Retrovirology* 2018, **15** 36.146.

59. Mousseau G, Valente ST: **Role of host factors on the regulation of Tat-mediated HIV-1 transcription**. *Curr Pharm Des* 2017, **23**:4079-4090.

60. Abner E, Stoszko M, Zeng L, Chen HC, Izquierdo-Bouldstridge A, Konuma T, Zorita E, Fanunza E, Zhang Q, Mahmoudi T *et al.*: **A new quinoline BRD4 inhibitor targets a distinct latent HIV-1 reservoir for reactivation from other "Shock" drugs**. *J Virol* 2018, **92** e02056-17.

61. Lu P, Qu X, Shen Y, Jiang Z, Wang P, Zeng H, Ji H, Deng J, Yang X, Li X *et al.*: **The BET inhibitor OTX015 reactivates latent HIV-1 through P-TEFb**. *Sci Rep* 2016, **12**:24100.

62. Huang H, Liu S, Jean M, Simpson S, Huang H, Merkley M, Hayashi T, Kong W, Rodríguez-Sánchez I, Zhang X *et al.*: **A novel bromodomain inhibitor reverses HIV-1 latency through specific binding with BRD4 to promote Tat and P-TEFb association**. *Front Microbiol* 2017, **7**:1035.

63. Darcis G, Kula A, Bouchat S, Fujinaga K, Corazza F, Ait-Ammar A, Delacourt N, Melard A, Kabeya K, Vanhulle C *et al.*: **An in-depth comparison of latency-reversing agent combinations in various in vitro and ex vivo HIV-1 latency models identified bryostatin-1+JQ1 and ingenol-B+JQ1 to potently reactivate viral gene expression**. *PLoS Pathog* 2015, **11**:e1005063.

64. Li Z, Mbonye U, Feng Z, Wang X, Gao X, Karn J, Zhou Q: **The KAT5-Acetyl-Histone4-Brd4 axis silences HIV-1 transcription and promotes viral latency**. *PLoS Pathog* 2018, **14**:e1007012.

65. Chen D, Wang H, Aweya JJ, Chen Y, Chen M, Wu X, Chen X, Lu J, Chen R, Liu M: **HMBA enhances prostratin-induced activation of latent HIV-1 via suppressing the expression of negative feedback regulator A20/TNFAIP3 in NF-κB signaling**. *Biomed Res Int* 2016, **2016**:5173205.

66. Geng G, Liu B, Chen C, Wu K, Liu J, Zhang Y, Pan T, Li J, Yin Y, Zhang J *et al.*: **Development of an attenuated Tat protein as a highly-effective agent to specifically activate HIV-1 latency**. *Mol Ther* 2016, **24**:1528-1537.

67. Tang X, Lu H, Dooner M, Chapman S, Quesenberry PJ, Ramratnam B: **Exosomal Tat protein activates latent HIV-1 in primary, resting CD4+ T lymphocytes**. *JCI Insight* 2018, **3** pii: 95676.

68. Sgadari C, Monini P, Tripiciano A, Picconi O, Casabianca A, Orlandi C, Moretti S, Francavilla V, Arancio A, Paniccia G *et al.*: **Continued decay of HIV proviral DNA upon vaccination with HIV-1 Tat of subjects on long-term ART: an 8-year follow-up study**. *Front Immunol* 2019, **10** 233.156.

69. Boyer Z, Palmer S: **Targeting immune checkpoint molecules to eliminate latent HIV**. *Front Immunol* 2018, **9**:2339.

70. Evans VA, van der Sluis RM, Solomon A, Dantanarayana A, McNeil C, Garsia R, Palmer S, Fromentin R, Chomont N, Sékaly RP *et al.*: **Programmed cell death-1 contributes to the establishment and maintenance of HIV-1 latency**. *AIDS* 2018, **32**:1491-1497.

71. Fromentin R, DaFonseca S, Costiniuk CT, El-Far M, Procopio FA, Hecht FM, Hoh R, Deeks SG, Hazuda DJ, Lewin SR *et al.*: **PD-1 blockade potentiates HIV latency reversal ex vivo in CD4+ T cells from ART-suppressed individuals**. *Nat Commun* 2019, **10**:814.

72. Bui JK, Cyktor JC, Fyne E, Campellone S, Mason SW, Mellors JW: **Blockade of the PD-1 axis alone is not sufficient to activate HIV-1 virion production from CD4+ T cells of individuals on suppressive ART**. *PLoS One* 2019, **25**:e0211112.

73. •• Grau-Expósito J, Serra-Peinado C, Miguel L, Navarro J, Curran A, Burgos J, Ocaña I, Ribera E, Torrella A, Planas B *et al.*: **A novel single-cell FISH-Flow assay identifies effector memory CD4+ T cells as a major niche for HIV-1 transcription in HIV-infected patients**. *mBio* 2017, **8** e00876-17.
The authors show, using FISH-Flow technology, that effector memory CD4 T cells are the main population that harbor HIV transcription in infected patients, and that after reactivation, only up to 10% of cells that express viral RNA also express gag (protein).

74. Rao S, Amorim R, Niu M, Temzi A, Mouland AJ: **The RNA surveillance proteins UPF1, UPF2 and SMG6 affect HIV-1 reactivation at a post-transcriptional level**. *Retrovirology* 2018, **28**:42.

75. Sarracino A, Gharu L, Kula A, Pasternak AO, Avettand-Fenoel V, Rouzioux C, Bardina M, De Wit S, Benkirane M, Berkhout B *et al.*: **Posttranscriptional regulation of HIV-1 gene expression during replication and reactivation from latency by nuclear matrix protein MATR3**. *mBio* 2018, **9** e02158-18.

76. Cheung PK, Horhant D, Bandy LE, Zamiri M, Rabea SM, Karagiosov SK, Matloobi M, McArthur S, Harrigan PR, Chabot B, Grierson DS: **Parallel synthesis approach to the identification of novel diheteroarylamide-based compounds blocking HIV replication: potential inhibitors of HIV-1 Pre-mRNA alternative splicing**. *J Med Chem* 2016, **59**:1869-1879.

77. Kyei GB, Meng S, Ramani R, Niu A, Lagisetti C, Webb TR, Ratner L: **Splicing factor 3B subunit 1 interacts with HIV Tat and plays a role in viral transcription and reactivation from latency**. *mBio* 2018, **9** e01423-18.

78. Mediouni S, Chinthalapudi K, Ekka MK, Usui I, Jablonski JA, Clementz MA, Mousseau G, Nowak J, Macherla VR, Beverage JN *et al.*: **Didehydro-Cortistatin A inhibits HIV-1 by specifically binding to the unstructured basic region of Tat**. *mBio* 2019, **10**: e02662-1.

79. Li C, Mousseau G, Valente ST: **Tat inhibition by didehydro-Cortistatin A promotes heterochromatin formation at the HIV-1 long terminal repeat**. *Epigenetics Chromatin* 2019, **12**:23.

80. Besnard E, Hakre S, Kampmann M, Lim HW, Hosmane NN, Martin A, Bassik MC, Verschueren E, Battivelli E, Chan J: **The mTOR complex controls HIV latency**. *Cell Host Microbe* 2016, **20**:785-797.

81. Wong RW, Lingwood CA, Ostrowski MA, Cabral T, Cochrane A: **Cardiac glycoside/aglycones inhibit HIV-1 gene expression by a mechanism requiring MEK1/2-ERK1/2 signaling**. *Sci Rep* 2018, **8**:850.

82. Balachandran A, Wong R, Stoilov P, Pan S, Blencowe B, Cheung P, Harrigan PR, Cochrane A: **Identification of small molecule modulators of HIV-1 Tat and Rev protein accumulation**. *Retrovirology* 2017, **14**:7.

83. Vautrin A, Manchon L, Garcel A, Campos N, Lapasset L, Laaref AM, Bruno R, Gislard M, Dubois E, Scherrer D *et al.*: **Both anti-inflammatory and antiviral properties of novel drug candidate ABX464 are mediated by modulation of RNA splicing**. *Sci Rep* 2019, **9**.

84. Debyser Z, Vansant G, Bruggemans A, Janssens J, Christ F: **Insight in HIV integration site selection provides a block-and-lock strategy for a functional cure of HIV infection**. *Viruses* 2018, **11** pii: E12.

85. Kim Y, Anderson JL, Lewin SR: **Getting the "kill" into "shock and kill": strategies to eliminate latent HIV**. *Cell Host Microbe* 2018, **23**:14-26.

86. Bobardt M, Kuo J, Chatterji U, Chanda S, Little SJ, Wiedemann N, Vuagniaux G, Gallay PA: **The inhibitor apoptosis protein**

antagonist Debio 1143 Is an attractive HIV-1 latency reversal candidate. *PLoS One* 2019, **14**:e0211746.

87. •• Campbell GR, Bruckman RS, Chu YL, Trout RN, Spector SA: **SMAC mimetics induce autophagy-dependent apoptosis of HIV-1-infected resting memory CD4+ T cells**. *Cell Host Microbe* 2018, **24**:689-702.e7.
The authors show selective elimination of HIV infected and not uninfected TCM by SMAC mimetic molecules, which degrade inhibitors of apoptosis (IAPs), inducing autophagy and apoptosis in infected cells.

88. Cummins NW, Sainski-Nguyen AM, Natesampillai S, Aboulnasr F, Kaufmann S, Badley AD: **Maintenance of the HIV reservoir is antagonized by selective BCL2 inhibition**. *J Virol* 2017, **91** e00012-17.

89. Li P, Kaiser P, Lampiris HW, Kim P, Yukl SA, Havlir DV, Greene WC, Wong JK: **Stimulating the RIG-I pathway to kill cells in the latent HIV reservoir following viral reactivation**. *Nat Med* 2016, **22**:807-811.

90. Garcia-Vidal E, Castellví M, Pujantell M, Badia R, Jou A, Gomez L, Puig T, Clotet B, Ballana E, Riveira-Muñoz E, Esté JA: **Evaluation of the innate immune modulator acitretin as a strategy to clear the HIV reservoir**. *Antimicrob Agents Chemother* 2017, **61** e01368-17.

91. •• Battivelli E, Dahabieh MS, Abdel-Mohsen M, Svensson JP, Tojal Da Silva I, Cohn LB, Gramatica A, Deeks S, Greene WC, Pillai SK, Verdin E: **Distinct chromatin functional states correlate with HIV latency reactivation in infected primary CD4+ T cells**. *eLife* 2018, **7** pii: e34655.
The authors show that transcription competent latent viruses exist in distinct chromatin domains with differing reactivation potential in primary latently infected CD4+ T cells, and that LRAs reactivate a small fraction, which are integrated in more accessible, reactivatable chromatin domains.

CHAPTER .6

GENERAL DISCUSSION

Concluding remarks and future perspectives

GENERAL DISCUSSION

For almost four decades the scientific community has been searching for a strategy to completely eradicate HIV-1, the causative agent of AIDS, and put an end to this devastating infectious disease. The most recent data from UNAIDS (2020 fact sheet) report that since the start of the pandemic approximately 32.7 million people have died from AIDS-related illnesses, with this number unfortunately still rising. It is estimated that 1.7 million people became infected with HIV in 2019 and that approximately 700 000 people have died from AIDS-related illnesses in the same year. Currently, approximately 38 million people worldwide are living with HIV-1.

Significant progress has been made over the years in understanding the molecular pathogenesis of the infection and this has been crucial for the development of the current treatments. However, the virus constantly mutating nature has made it impossible, so far, to develop an effective vaccine. The introduction of combination antiretroviral therapy (cART) has allowed to effectively halt HIV-1 replication, decrease viral loads, restore immune T cell function, and prevent transmission to uninfected individuals. While cART has significantly reduced AIDS-associated mortality, however, it is not curative, has side effects, and must be taken lifelong. Additionally, the global roll-out of cART, particularly in resource-limited countries, remains an ongoing challenge, with only about half of the people currently living with HIV-1 receiving the therapy. Curing HIV-1 is therefore a global priority.

HIV-1 persists because, following infection and integration into the host genome, the provirus can establish latent infections, defined by the absence of viral expression, in resting CD4+ T cells and other long-lived immune cell populations. Due to this reservoir of long-lived latently HIV-1 infected cells, interruption of cART leads to a rapid rebound of unrestricted viral replication, necessitating life-long treatment (Siliciano and Siliciano 2015).

Therapeutic strategies for HIV-1 cure aim to eliminate, inactivate, or reduce the pool of latently infected cells such that the patient's immune system can control viral replication upon cessation of cART. A popular strategy is to induce viral production in latently infected cells, using drug interventions referred to as latency reversal agents (LRAs), to render the

infected cell recognizable to the immune system or susceptible to viral cytopathic effects for elimination. Crucial for successful latency reversal in infected cells is the identification of the right combination of LRAs that can effectively trigger viral reactivation, to then promote cytolysis and/or immune-mediated clearance of the infected cells.

In this thesis, we presented three different and complementary discovery strategies (**Chapter 2, Chapter 3, Chapter 4**) that have led to the unbiased identification of novel molecular targets and drug candidates for latency reversal, with potential relevance for ameliorating current reactivation strategies. This work further expands the known repertoire of factors and cellular pathways that determine viral latency (described in **Chapter 1**), contributing to a better understanding of the mechanisms and routes that can be targeted by latency reversal strategies. Additionally, the novel drug interventions examined in these chapters extend the available drug arsenal that can be exploited to reactivate, attack, and hopefully mobilize the latent HIV-1 cellular reservoir (described in **Chapter 5**).

In **Chapter 2** of this thesis, in search of novel determinants of HIV-1 latency, we have zoomed in on the HIV-1 5'LTR (or viral promoter) by setting up a biochemical purification strategy, coupled to proteomics, to identify its chromatin-bound regulators. This attempt is extremely important as the identification of the complete repertoire of LTR-bound factors, implicated in latency, would represent an invaluable resource for fully understanding their molecular function and moving the field forward. Before our study, due to technical limitations, a comprehensive and unbiased description of the molecular factors bound to the HIV-1 promoter in its latent and active conditions, was never conducted and our investigation is unique in the field.

The strategy we designed is a locus-specific purification pipeline, coupled to proteomics, that is based on a reverse-ChIP approach and the antibody-based affinity purification of a multiple epitopes tagged HA-V5-FLAG-dCas9 bait, bound to the 5'LTR. It is well established that locus-specific strategies present tremendous biochemical challenges and, not surprisingly, to date only less than 30 articles have been published that deal with the isolation and characterization of specific genomic locations

(Vermeulen and Déjardin 2020). The high signal to noise ratio and the low abundance of single-loci represent a significant barrier to identify the complete repertoire of factors bound to a single locus in vivo (Gauchier et al. 2020). Additionally, the fold enrichment required to reach sample homogeneity cannot be achieved with conventional one-step purification protocols and cannot typically yield an adequate amount of material for robust detection of locus-bound proteins. Moreover, despite the recent major technological innovations, mass spectrometry can only identify specific peptides in complex mixtures in the low-femtomolar range (Vermeulen and Déjardin 2020). For a diploid locus, this means that the minimum amount of cell material required for proteomic characterization is estimated to be at least half-a-billion cells (Vermeulen and Déjardin 2020).

As our cellular platform to study latency harbors only one copy of the integrated HIV-1 5'LTR per cell, in our study we scaled up even further than this number, ultimately using at least 3 billion cells per condition; an enormous experimental undertaking in technical complexity and costs. Another caveat in locus-specific proteomics techniques is that there is typically a large fraction of the exogenously expressed bait that is present diffusely in the cells and that is not exclusively bound to the locus of interest. This fraction of the bait, which is nevertheless captured during the purification pipeline, significantly contributes to the background signal, affecting sensitivity. A common strategy for background elimination in these types of experiments is a subtraction from the final dataset using a robust set of negative control and multiple replicates (Liu et al. 2017). While this approach effectively eliminates some background and has successfully led to the identification of several locus-specific proteins, it does not, however, address the fact that the detection of a large amount of background inevitably reduces sensitivity.

In this work, we presented a partial solution to this problem and have removed the unspecific background associated with the non-locus bound dCas9 molecules biochemically, rather than by subtraction. We have made use of a sequential, two-step affinity purification pipeline, consisting of a dCas9, V5 epitope-based, immunoprecipitation followed by histone antibodies-based immunoprecipitation that has allowed us to enrich for the chromatin-bound fraction of the dCas9 bait. This represents

an element of novelty in the field and has allowed for the removal of a large quantity of background signal originating from the non-targeted fraction of the bait. Another strength of this work is that to eliminate potential nonspecific interactors, we have used a control and isogenic cell line where the dCas9 bait has been guided to the same location and the HIV-1 5'LTR has been induced using PMA. We then have considered for our selection proteins that were differentially identified to be bound to the latent versus the transcriptionally activated HIV 5'LTR. This distinct profile has resulted in stringent elimination of factors bound to both conditions, allowing the identification of a list of factors significantly enriched or exclusively bound to the latent HIV-1 promoter. We have also verified the specificity of the dCas9 binding in our experimental system by ChIP-sequencing and found that the binding is highly specific for the targeted region at the HIV-1 promoter. The stringency of our purification is supported by our validation experiments, the identification, and characterization of IKZF1, and further demonstrated by the identification of a large number of previously published and verified HIV 5'LTR modulators (**Chapter 2, Figure 3F**).

We are confident that the Catchet-MS purification pipeline developed in this chapter is a step forward in the field and a useful discovery tool that has led to the identification of many bona fide locus-specific factors, including IKZF1. However, we are also aware that this work presents some of the technical limitations typical of locus-specific strategies, and that we are far from fully developing what would be the "holy grail" of chromatin biology. While techniques such as Catchet-MS can be very useful to identify some locus-specific factors, in fact, methodologies that allow a comprehensive description of the composition of a single locus are unfortunately still lacking in the field.

It has been estimated that unambiguous identification of a promoter region composition, to near purity, would require a 1 million-fold enrichment, which is far from what is typically achieved by locus-specific strategies using a single-step purification (Vermeulen and Déjardin 2020). By comparison, one of the landmark papers in the field had an estimated fold enrichment for the targeted single locus of 1000 fold (Liu et al. 2017).

A possible strategy for increasing the specificity of the purification could be the concomitant use, of multiple Cas9 variants (such as Cas X, CasY, Cas12a or SpCas9) with different sgRNA and targets specificity, or alternatively zinc fingers proteins, to be used as additional baits that would be simultaneously guided to different regions within the desired chromatin location. Those additional baits could be tagged with different synthetic tags, allowing for multiple rounds of ChIP-based purification, with different affinity reagents. Additionally, as many of the biologically relevant protein–chromatin associations are very dynamic and usually transient, the concomitant use of a proximity labeling strategy such as the long-range biotinylation offered by TurboID, could be very helpful to enrich for those transient interactors (Branon et al. 2018). Perhaps the use of a streptavidin mediated purification of the biotin-labeled proteins as the last step of a sequential, reverse-ChIP based, purification pipeline, would allow us to enrich for labeled proteins located at the desired chromatin, providing an additional level of specificity to the detection.

Additionally, as dynamic interactions contribute to a lesser extent to the complexity of the purified material, identification of more subtle differences in chromatin composition between different functional states may require a data-independent acquisition (DIA) method in MS, which would likely improve the capacity of detecting proteins present in minute amounts in a complex mixture (Venable et al. 2004; Searle et al. 2018). Moreover, when investigating different functional states, the use of multiplexed quantitative proteomics based on isobaric tagging, such as TMT or iTRAQ, may be more powerful at detecting subtle differences in the chromatin composition between the two different states than label-free, semi-quantitative approaches (Pappireddi, Martin, and Wühr 2019).

Importantly, in Chapter 2, using Catchet-MS we identified a number of hits that we functionally confirmed to be important for the maintenance of latency in the cellular models used. This list of validated interactors may represent an important resource in the field and contribute to a better understanding of the molecular regulation of the HIV-1 promoter. Moreover, the identification of IKZF1 as a novel DNA-bound transcriptional repressor, required for the recruitment of PRC2 and the establishment of a repressive chromatin environment is of particular importance. Despite numerous studies, the mechanisms of PRC2

recruitment to the HIV LTR were not yet fully established in the field and it is therefore very significant.

Of therapeutic relevance in the field, IKZF1 and related family member IKZF3 levels can be controlled by modulating ubiquitination levels. Immunomodulatory drugs (IMIDs) such as thalidomide, lenalidomide, pomalidomide and iberdomide promote ubiquitin-dependent proteasomal degradation of IKZF1 and IKZF3 by redirecting the substrate specificity of the $CRL4^{CRBN}$ ubiquitin ligase complex (G. Lu et al. 2014; Krönke et al. 2014). Among these drugs we identified the clinically advanced drug, iberdomide (CC-220), currently in phase 2 Clinical trial for Systemic lupus erythematosus (SLE) and Multiple Myeloma (MM), to be very effective at reducing IKZF1 levels in primary CD4+ T cells.

We demonstrated that iberdomide mediated depletion of IKZF1 leads to a significant reversal of HIV-1 latency, with no significant associated toxicity, in ex vivo infected primary CD4+ T cells and infected cells isolated from c-ART suppressed, aviremic individuals. BET inhibitors such as JQ1 are a well-established class of LRAs and are also a class of compounds previously reported to synergize with the activity of IMIDs in inhibiting the growth of refractory forms of MM (Díaz et al. 2017; Moros et al. 2014). We, therefore, examined the effect of combinatory treatment of JQ1 and iberdomide in latently infected cells. Remarkably, co-treatment of ex vivo infected primary CD4+ T cells and cells obtain from HIV infected cART suppressed aviremic patients resulted in strong and synergistic induction of HIV-1 transcription quantitated as an increase in cell-associated HIV-1 Gag RNA. Crucially as we did not observe any detrimental effect on cell viability, T cell activation, and the overall T cells functionality, Iberdomide can be considered a safe, thus promising, LRA candidate for combinatory approaches to latency reversal.

Other IMiDs such as thalidomide, lenalidomide, and pomalidomide are already widely used in the clinic and, in combination with proteasome inhibitors, steroids, and monoclonal antibodies, play a key role in the treatment of multiple myeloma (MM) (S. Gao, Wang, and Song 2020). Lenalidomide is also used in the treatment of other hematological malignancies such as myelodysplastic syndrome (MDS)

with deletion of chromosome 5q (del(5q)), mantle cell lymphoma (MCL) (Stahl and Zeidan 2017) and proven to be clinically active in a host of lymphoproliferative diseases, including chronic lymphocytic leukemia (CLL) (Itchaki and Brown 2017). Use of Iberdomide or related IMiDs could therefore be readily explored in future HIV-1 reactivation clinical trials, perhaps in combination with other LRAs acting on a different latency pathway,

Several lines of evidence suggest that, in latently infected cells, clonal expansion due to proliferation plays an important role, contributing to the prolonged maintenance of the latent reservoir (Cohn, Chomont, and Deeks 2020). Interestingly, and consistent with its role as an immunomodulatory treatment for lymphoid and myeloid malignancies (Fuchs 2019), we observed a reduction of T cell proliferative capacity after treatment with Iberdomide, alone or in combination with JQ-1. Being an antiproliferative drug, the use of Iberdomide as a novel LRA, possibly in combination with other LRAs and/or drug interventions aiming at restoring intrinsic cell immunity and apoptosis of the infected cells, may help not only for the reservoir mobilization but also for its reduction in size (Hosmane et al. 2017; Reeves et al. 2018).

In **Chapter 3** we have described another discovery approach that makes use of insertional mutagenesis in pseudo-haploid KBM7 cells, coupled to next-generation sequencing. With this methodology we were able to identify previously unknown genes whose depletion leads to latency reversal in cellular models of latency. Forward genetics in mammalian cells has always been hampered by the fact that in diploid cells, mutagenesis often produces heterozygous knockout cells which may not necessarily show a phenotype, thus resulting in false negatives. In this regard, the use of KBM7 cells, derived from chronic myelogenous leukemia, has offered offer the unique opportunity of conducting forward genetics in mammalian cells. A remarkable feature of this cell line is that it is near-haploid for most of its chromosomes, except for chromosome 8 and a 30 megabase fragment of chromosome 15 (Andersson et al. 1987; Kotecki, Reddy, and Cochran 1999). Importantly, the use of a forward genetic approach for the identification of novel targets has allowed the identification of genes and pathways that might modulate latency

indirectly, through genetic interaction, rather than physical association, with the HIV-1 5'LTR.

In this study, we generated a latently infected KBM7 cell line (Hap-Lat) harboring an integrated HIV-1 5'LTR that controls the expression of a GFP reporter gene. Hap-Lat cells were then subjected to gene trap (GT) insertional mutagenesis using a mCherry reporter GT virus. Following mutagenesis, cells effectively mutagenized and reactivated, as shown by the expression of mCherry and GFP, were selected by multiple rounds of fluorescence-activated cell sorting (FACS) and subjected to NGS for mapping of the integration sites. This strategy has successfully led to the identification of at least 10 novel genes confirmed to be important for the maintenance of latency in cellular models of latency, further expanding our knowledge over the cellular routes to latency. Of clinical relevance, the glutamate ionotropic receptor kainate type subunit 5 (GRIK5) inhibitor, Topiramate, was found to reverse latency in ex vivo infected primary CD4+ T cells, with limited associated toxicity and no effect on T cells activation. Topiramate can therefore be regarded as a novel candidate LRA, acting on a previously unknown pathway to latency, worth further investigation.

Despite the successes, this strategy also presents some limitations that, if addressed correctly, may further increase the discovery potential of forward genetics methods in pseudo-haploid mammalian cells. It is important to mention that at the time that this study was designed, CRISPR/Cas9 technology was still in its infancy. Nowadays, with the advent of CRISPR/Cas9 screenings, gene-trap based forward genetics screenings are losing popularity. A limitation of gene trap cassettes is that they have to be integrated downstream of an active promoter to disrupt a gene function, resulting in low efficiency of mutagenesis. Consequently, the generation of a gene-trap mutagenized library, covering the whole genome, requires a high number of starting cells (Cadiñanos and Bradley 2007). Additionally, only actively transcribing genes could be trapped in our screening as only an active promoter can lead to the adequate expression of the gene trap reporter. In contrast, CRISPR/Cas9 mutagenesis can mutagenize the region regardless of the transcriptional status of the gene and the integration site of the sgRNA vector, providing better coverage than gene trap mutagenesis. Interestingly, the use of

focused sgRNA libraries may even allow customized mutagenesis of a specific cellular pathway of interest (Zhu et al. 2016; Cao et al. 2017). Another significant advantage is mapping. While this study has required an inverse PCR coupled to cloning strategy, for subsequent mapping of the region by NGS; in CRISPR/Cas9 screenings, the mutated gene can be identified by direct sequence analysis of the integrated sgRNA vector (Zhu et al. 2019).

Another aspect with important implications for this screening is the stochastic nature of HIV-1 transcription (Dar et al. 2014). Due to stochasticity, we have noticed that a significant number of reactivated cells (GFP positive) in the first rounds of cell sorting, were reverting to a GFP negative state. Only after multiple rounds of FACS selection, we were finally able to enrich for a stable, double-positive population which we have then characterized. While it may be considerably challenging to identify molecules that can suppress transcriptional noise, due to its intrinsically low threshold; suppression of transcriptional noise could potentially be used as a strategy to limit spontaneous reactivation (Dar et al. 2014). This could potentially allow a more efficient selection of a stable, double-positive population.

In **Chapter 4** we have followed a complementary strategy in which, without any prior knowledge over the molecular target, we have used J-Lat 11.1 and J-Lat A2 cells as cellular reporters to screen for biologically active natural compounds capable of reactivating HIV-1 transcription.

It is important to note that biological systems represent an enormous source of functionally active molecules with high chemical diversity and biochemical specificity. Half of the novel small molecules introduced in the market between 1981 and 2018 are nature-derived (Newman and Cragg 2016). Fungi, in particular, secrete a plethora of extracellular secondary metabolites that represent a vast and largely unexplored source of small molecules with potential pharmaceutical properties (Sanchez et al. 2012). Importantly, secondary metabolites from fungal origins, such as GTX, constitute a very important resource also for the rational design of novel drugs as the molecules produced are of low

molecular weight and highly heterogeneous and may be used as essential building blocks (Leitão and Enguita 2014).

As a source of natural compounds, we have used a large collection of fungal extrolites of 115 different fungal species, belonging to 28 orders (43 families) of the fungal kingdom. By then using orthogonal mass spectrometry with repeated fractionation of the fungal supernatants we were able to determine the composition of the active fractions and identify Gliotoxin (GTX) as an essential component for latency reversal.

This source of small molecules is ideal for an academic setting like our lab where we could combine low- and medium-throughput cellular activity screenings with fractionation, purification and the biochemical characterization of the molecular mechanism of the compound activity. Crucially, in our study, we have used an extremely large and varied collection of fungal extrolites to diversify as much as possible the collection of secondary metabolites screened. Remarkably, this study did not only led to the identification of a novel candidate LRA, and potentially a building block for the design of a more specific drug, but also to the identification of transcriptional elongation as a druggable regulatory mechanism of latency. We have demonstrated that GTX, by inhibition of LARP7 assembly and subsequent destabilization of the 7SK RNA, can disrupt the 7SK snRNP complex. The 7SK snRNP complex is the inhibitory ribonucleoprotein scaffold of the positive transcription elongation factor P-TEFb, which sequesters P-TEFb leading to RNA pol II proximal promoter pausing. We have shown that GTX leads to the release of active P-TEFb from the 7SK snRNP complex. Active P-TEFb then phosphorylates the RNA pol II (Pol II) C-terminal domain (CTD), boosting HIV-1 transcription by stabilizing Pol II-dependent transcriptional elongation. GTX is the first known molecule, to date, to be able to induce direct and specific disruption of the 7SK snRNP complex, facilitating elongation. It has been recently established that transcriptional elongation is a crucial rate-limiting step to productive transcription in patients CD4+ T cells (Yukl et al. 2018). The identification of GTX as a small molecule able to induce a significant increase of cell-associated HIV-1 RNA, in all patients CD4+ T cells examined, is therefore a remarkable advancement in the field and a major addition to the broad

arsenal of LRAs available for combinatorial treatments (described in **Chapter 5**).

Interestingly, for combinatorial approaches to latency reversal, we found that the use of GTX strongly synergizes with LRAs that derepress the chromatin structure such as BAF and HDAC inhibitors. Conversely, in latently infected primary CD4+ T cells, cotreatment with GTX and BET inhibitors only resulted in an additive effect. This can be explained by the fact that BET inhibitors, by antagonizing Brd4 mediated inhibition of Tat transactivation, also target transcriptional elongation (Z. Li et al. 2013). Thus far, only simultaneous pharmacological targeting with drugs acting on markedly different regulatory steps is capable of synergizing (e.g, HDAC inhibitors with PKC inhibitors) (Zaikos et al. 2018).

It is important to note that the inhibitors identified in this thesis: Iberdomide (**Chapter 2**), Topiramate (**Chapter 3**), and Gliotoxin (**Chapter 4**), also act on markedly different routes to latency. It may be therefore interesting to explore their use in combination, in future studies, as it may result in synergistic effects on viral reactivation.

In the general introduction to this thesis (**Chapter 1**), we have provided a detailed overview of the known molecular mechanisms and cellular pathways that contribute to the establishment and maintenance of HIV-1 latency. In **Chapter 5**, based on this extensive foundational knowledge and the most recent discoveries in the field, we have reviewed what are the state of art therapeutic interventions that show significant latency reversal potential, in *in vitro* and *in vivo* models of latency. This chapter provides a comprehensive overview of latency reversal approaches available, classified into different functional categories based on their mechanism of action, that can be used in combinatorial approaches.

Histone post-transcriptional modification modulators and in particular, class I histone deacetylases (HDAC), are one of the most well-established classes of LRAs presented in this classification (Zaikos et al. 2018; Margolis 2011). Several HDAC inhibitors within this class, including romidepsin and vorinostat, have shown high potential in the cellular model of latency and have been investigated for their latency reversal ability in clinical trials (Rasmussen and Lewin 2016; Andersen, Ntie-Kang, and Tietjen 2018). However, while in some cases transient

latency reversal has been observed upon their administration, none of these studies has reported a significant reduction of the reservoir size in patients (Abner and Jordan 2019; Zerbato et al. 2019). Another class of LRAs, such as PMA, Bryostatin, prostratin, and ingenol derivatives, exploits the NF-kB pathway engagement through the protein kinase C (PKC) pathway, an essential component of reactivation of the latent HIV-1 promoter, Prolonged activation of NF-kB, however, contributes to the development of various autoimmune, inflammatory, and malignant disorders and has therefore raised important safety concerns in clinical settings (Abner and Jordan 2019; Zerbato et al. 2019). Other important chromatin modulators presented here are BET inhibitors (Abner et al. 2018; P. Lu et al. 2016; Banerjee et al. 2012) and BAF inhibitors (Stoszko et al. 2016; Marian et al. 2018), which have also been shown to have a low toxicity profile shown and to synergize well with other classes of LRAs such as PKC agonists and HDAC inhibitors. More recently, TLR agonists and SMAC mimetics have also emerged as a promising LRA category as they can engage non-canonical NF-kB signaling and induce activation of the latent reservoir without eliciting systemic T cells activation (Pache et al. 2015; Campbell et al. 2018; Macedo, Novis, and Bosque 2019; Pache et al. 2020).

Despite the promising results obtained in vitro and in cellular models of latency, finding the right latency reversal intervention has proven to be extremely challenging due to the dynamic and heterogeneous nature of the latent reservoir and patient variability (Bradley et al. 2018; Ait-Ammar et al. 2020). Evidence has shown that no single LRA is likely capable of inducing the entire latent proviral reservoir (Rato et al. 2017; Battivelli et al. 2018). Additionally, a study performed on independent, barcoded HIV-1 infection ensembles (B-HIVE) has revealed that single LRAs from different classes activate proviruses from distinct, unique integration sites and that no single compound is likely to reactivate latency from the total viral reservoir of a patient (Chen, Zorita, and Filion 2018). While those findings have partially challenged the concept of latency reversal followed by elimination of the virally reactivated cell reservoir, they have also reinforced the idea that a successful latency reversal strategy may only be achieved using a combinatorial approach in which cocktails of multiple LRAs ‘’Shocktails”, acting on different molecular

targets and cellular pathways, are used to elicit highly synergistic effects. Alternatively, sequential treatments with different LRAs may also be a viable option (Bouchat et al. 2016). As explained in chapter 5, successful combinatorial treatment with LRAs should provide not only a high magnitude of reactivation but a degree of specificity to the intervention and should be robust enough to overrule the patient's specificity and the heterogeneity of the latent reservoir. Several clinical trials using a combination of LRAs are ongoing (Abner and Jordan 2019; Stoszko et al. 2019).

To date, proof of concept that latency reversal followed by elimination of the virally reactivated cell reservoir represents a viable strategy for a functional HIV-1 cure comes from recent evidence showing that elite HIV-1 controllers harbor the vast majority of the integrated proviruses in gene desert regions and chromatin regions with limited gene activity; suggesting that more re-activatable infected cells pools, within the reservoir, may have been eliminated in those individuals (Jiang et al. 2020). In an attempt to replicate this naturally occurring phenomenon with pharmacological interventions, robust latency reversal may represent the first step towards the elimination of the highly reactivatable fraction of the reservoir while latency promoting interventions may be useful for stabilizing its refractory/quiescent part (**Chapter 5**).

In Chapter 2 and 3 and of this thesis we presented novel important discoveries that contribute to a better understanding of the routes to latency, expand the known repertoire of available LRAs and constitute an important resource for moving the field forward, towards the design of a more powerful strategy for latency disruption. It has become apparent during the course of our research, however, that chromatin and epigenetic silencing of the viral promoter, and a restricted rate of transcriptional initiation, are not the only mechanisms contributing to HIV-1 latency.

The large majority of replication-competent latent proviruses in cART suppressed HIV infected participant reservoirs have been shown to contain a block to expression, not only at transcription elongation but also at completion (polyadenylation) and vRNA splicing (Yukl et al. 2018; M. J. Pace et al. 2012; Telwatte et al. 2018). Following transcription, production of viral particles requires a carefully regulated and balanced

post-transcriptional processing of the newly synthesized HIV-1 vRNA template for its efficient splicing, export, and translation (Karn and Stoltzfus 2012a; Lassen et al. 2006; Rojas-Araya, Ohlmann, and Soto-Rifo 2015). Altered transcriptional completion can compromise viral RNA stability and lead to a block in HIV-1 vRNA nuclear export (Lassen et al. 2006) and translation (Rojas-Araya, Ohlmann, and Soto-Rifo 2015). Suboptimal splicing can also contribute to latency as efficient viral replication requires optimal regulation of vRNA and mRNA production, and a balanced expression of all the viral proteins (Karn and Stoltzfus 2012b). A block to one or more of these processes may hamper viral protein production thus negatively affecting the immunogenicity of reactivated cells. The field is therefore currently moving towards investigating therapeutic interventions that can modulate these processes (also reviewed in **Chapter 5**).

Importantly, as evidence points to transcription elongation and RNA processing as critical steps involved in HIV-1 latency in vivo (Yukl et al. 2018), in **Chapter 2** we chose to target our multiple epitopes tagged HA-V5-FLAG-dCas9 bait downstream of the HIV-1 transcriptional start site (TSS), in a transcribed areas. Consequently, we have observed that a significant number of factors identified by Catchet-MS are likely recruited to the locus co-transcriptionally through association with the nascent viral RNA. The list of RNA-bound factors presented in this chapter may represent an important resource of putative regulators post-transcriptional vRNA processing, worth further investigation.

Elimination of the virally reactivated cell reservoir also requires some urgent and special attention. Many clinical trials with LRAs have shown that, while in some cases it is possible to achieve a significant degree of viral reactivation in vivo, clearance of the reactivated cells is limited (Nancie M. Archin et al. 2017; N. M. Archin et al. 2012; Elliott et al. 2015; 2014; Gutiérrez et al. 2016; Rasmussen et al. 2014). There may be multiple reasons why LRAs alone cannot induce clearance of the reservoir.

First, it has been observed that latently infected cells have an increased expression of anti-apoptotic proteins and are therefore more resistant to apoptosis (López-Huertas et al. 2013; Timilsina et al. 2016;

Cummins and Badley 2013). Additionally, in infected cells, HIV-1 proteins have been shown to counteract intrinsic and innate immunity pathways (Bergantz et al. 2019). Administration of killing agents such as pro-apoptotic drugs (PADs) (Youry Kim, Anderson, and Lewin 2018; Hayes 2020) and the use of drugs interventions that can restore HIV-1 sensing and activate innate immunity may represent a strategy to induce death of the virally reactivated HIV-1 infected cells (Bergantz et al. 2019).

Secondly, immune escape mutations (Deng et al. 2015) and T cell exhaustion (Chew et al. 2016; Day et al. 2006) has been observed in chronic infection, thus reducing the cytotoxic T lymphocytes response. Another issue is that potent HDAC inhibitors, which are widely used in the field, such as vorinostat, panobinostat, and romidepsin, have been shown to directly inhibit CD8+ T-cell and natural killer (NK) cell function, in vitro, potentially compromising immune clearance (M. Pace et al. 2016).

Additionally, LRAs effects on non-T cell cellular reservoirs, such as macrophages and dendritic cells, may be limited as those cells are less affected by cytopathic effects of viral expression (Thorlund et al. 2017). The use of immune-boosting strategies such as therapeutic vaccines (Stephenson 2018), checkpoint inhibitors (Abbar et al. 2020), antibodies (Kumar et al. 2018) or immunotherapeutic, has therefore been proposed to strengthen and actively induce, immune system-mediated killing of the infected cells. Also reviewed in Chapter 5 (Stoszko et al. 2019), and expanded here.

Several pro-apoptotic drugs, developed for cancer treatment, have been tested for their capacity to induce apoptosis in latently infected cells. The second mitochondria-derived activator of caspase mimetics (SMAC mimetics) can bind to inhibitor of apotosis proteins (IAPs) to induce both their inhibition and degradation, hence promoting apoptosis (Z. Gao et al. 2007; Bertrand et al. 2008). SMAC mimetics such as Birinapant, embelin, and GDC-0152 were found to lead to selective killing of HIV-1 infected central memory T cells by the degradation of XIAP and BIRC2 (Campbell et al. 2018) with a moderate effect on latency reversal in patient cells, in combination with vorinostat (Pache et al. 2015). Those findings suggest that SMAC mimetics may be capable of inducing cell death and depletion of the reservoir in vivo, in combination with effective LRAs.

Other pro-apoptotic drugs have also shown to be promising such as BH3-mimetic, or Bcl-2 inhibitors, that by mimicking the binding domain of pro-apoptotic molecules can antagonize the anti-apoptotic Bcl-2 family proteins (Balakrishnan and Gandhi 2013; Cummins et al. 2016). An ex vivo study has shown that the BH3 mimetics Venetoclax and Navitoclax led to the depletion of latently infected central memory cells upon anti-CD3 and anti-CD28 antibodies costimulation (Cummins et al. 2016). Importantly, Venetoclax has also been shown to promote selective killing of infected cells during productive infections, in vitro (Cummins et al. 2017).

Activation of the P13k/Akt survival pathway also restricts apoptosis (Rodrik-Outmezguine et al. 2011). HIV-1 Nef activates PI3K signaling leading to inhibitory phosphorylation of the pro-apoptotic factor Bad, blocking apoptosis (Chugh et al. 2008). HIV-1 Tat interferes with P53 binding to PTEN, thus promoting its degradation and activation of Akt (Chugh et al. 2008; N. Kim et al. 2010). Importantly, P13K/Akt inhibitors have been found to predispose latently infected macrophages and microglia to cell death by upregulation of pro-apoptotic genes (Lucas et al. 2010; Yuri Kim et al. 2011).

Cells also have innate immune responses to invading viruses such as the pattern recognition receptors (PRRs), including toll-like receptors (TLR) and retinoic acid-inducible gene I (RIG-I) that can trigger apoptosis of infected cells (Mogensen 2009). Stimulation of TLRs may lead to dendritic cell (DC) maturation, activation of natural killer (NK) cell, enhanced antigen presentation, and adaptive immune responses (Iwasaki and Medzhitov 2004; Kawasaki and Kawai 2014).

In the context of HIV, TLR agonists have been shown to have a role both as LRAs and immune modulators. The TLR7 agonists GS-986 and GS-9260 have been reported to be capable of inducing viral production in SIV-infected rhesus macaques on ART and also induced activation of multiple immune cell population (Lim et al. 2018). The TLR9 agonist lefitolimod (MGN1703) has been shown to be able to induce a significant increase in plasma HIV RNA and activation of immune responses such as dendritic cells (DCs), NK cells, and T cells (Vibholm et al. 2017). The effect of TLR-mediated reactivation of latently infected cells appears to be mediated in large part by Dendritic cells activation and

subsequent stimulation of T cells by IFN-alpha (Martinsen et al. 2020). Other studies in non-human primates (NHP) have shown very promising data: in combination with a therapeutic vaccine or broadly neutralizing antibodies, administration of TRL agonists leads to an increase in the magnitude and breadth of immune responses to SIV, and some of these combinations are currently moving into clinical testing (Martinsen et al. 2020).

RIG-I is an RNA helicase that can sense viral RNA, including HIV-1, and induce antiviral signaling and apoptosis (Chow, Gale, and Loo 2018). It has been shown that RIG-I inducers such as retinoic acid (RA) and its derivatives (e.g Acitretin) can also trigger selective apoptosis of HIV-1 infected central memory T cells, in vitro (P. Li et al. 2016).

It has also been observed that in people living with HIV-1, chronically-activated, exhausted T cells overexpress immune check-points (ICPs) such as programmed-cell-death-1 (PD-1), cytotoxiclymphocyte-antigen-4 (CTLA4), T-cell-immunoglobulin and mucin-domain-containing-3 (TIM3), lymphocyte-activation-gene-3 (LAG3) and T-cell-immune-receptor with Ig and ITIM domains (TIGIT) (Fromentin et al. 2016; McGary et al. 2017). Importantly, expression of PD-1 and other ICPs inhibits T cells proliferation and function (Day et al. 2006; Parry et al. 2005) and restricts viral replication in infected cells (Evans et al. 2018; Fromentin et al. 2019). Use of Immune checkpoint inhibitors (ICPs) in the context of latency reversal has been shown to be capable of restoring HIV-specific CD8+ T cell functions, in vitro (Day et al. 2006; Kaufmann et al. 2007; Trautmann et al. 2006) and inducing HIV production from the latent reservoir (Evans et al. 2018; Fromentin et al. 2019). Clinical trials aimed at determining their feasibility and efficacy as anti-HIV therapy are ongoing (Cai et al. 2020).

Accumulating evidence is also pointing to NK cells as crucial for the control of HIV-1 infection by the immune system. Approaches that augment NK cells responses may also improve killing of the infected cells (Peppa 2019).

The use of CAR T cells targeting HIV-1 has also been proposed for a long time as a strategy for boosting cytotoxic T lymphocytes (CTL) responses before viral activation by LRAs. Studies have revealed that in

elite controllers, spontaneous control of viral levels is largely mediated by CD8+ T-cell response (Blankson 2010). Remarkably, elite controllers have higher than average functional avidity and broad cross-reactivity of their CTL responses that is able to deal with viral escape mutations (Mothe et al. 2012). Equipping CD8+ T cells with a CAR with broad antigen capacity could therefore be key to a cure. The first-generation CAR T cells, targeting the HIV glycoprotein (gp120) with a chimeric CD4 receptor have shown to be safe, leading to stable and prolonged engraftment in patients, however with no substantial effect on the viral reservoir (Deeks et al. 2002; Scholler et al. 2012). Multi specific anti-HIV CAR T cells, duoCARs (targeting both the gp120 CD4-binding site and the gp120 co-receptor–binding site) have been shown to be capable of eliminating HIV in a mouse model, suggesting that a multiantigen approach to targeting HIV may represent a more promising strategy (Anthony-Gonda et al. 2019). Broadly neutralizing antibodies, found in approximately 20% of infected individuals, have the ability to neutralize most circulating strains by targeting the envelope glycoprotein (Env) (Kwong, Mascola, and Nabel 2013). The development of bNAb-based CAR T has shown promising results in vitro as co-culturing of latently infected T cells with bNAb-based CARs led to specific activation and killing of the infected cells (Hale et al. 2017). Another possible avenue for cellular therapy is the use of autologous infusion of CCR5-modified CD4 T cells, or hematopoietic stem progenitor cells HSPCs, that cannot be infected and therefore persist longer in the blood of patients than unmodified cells (Tebas et al. 2014; Xu et al. 2019).

Therapeutic Vaccine research has also made important progress in educating the immune system of HIV-1 infected individuals. The aim is to stimulate the immune system to elicit broad immune responses that could help the killing of the infected cells or control of viral replication in the absence of cART (Stephenson 2018). While none of the strategies, thus far, has successfully led to long-term HIV remission in clinical trials, after cART interruption, several vaccine strategies, however, have been shown to be able to broaden the host immune responses to recognize a wide range of escape variants (Stephenson 2018). Nonhuman primate research suggests that therapeutic vaccines that are able to elicit broad immune responses may be useful, in combination with LRAs or immune

modulators, to induce long-term HIV remission in humans (Stephenson 2018; Martinsen et al. 2020).

The list of immune-boosting strategies and interventions to induce cell death or killing of infected cells, upon latency reversal, is rapidly expanding. We have not exhaustively examined here all the approaches but attempted to provide an overview of the most promising strategies that could be combined with the right latency reversal approach, for an effective cure. Several barriers still need to be effectively tackled but many different lines of research are offering potential pathways to an HIV-1 cure. Despite the scarce successes of shock and kill in clinical trials there are reasons to be optimistic. The rapidly expanding repertoire of LRAs, reviewed in **Chapter 5**, offers a multitude of combinatory therapeutic avenues that need to be explored in clinical settings. We now have a pretty solid understanding of what the roadblocks to viral reactivations are and what the strategies could be to overcome those barriers. Additionally, immunological approaches and kill strategies are also obtaining promising results, bringing us closer to the design of an effective strategy to deplete the latent HIV-1 reservoir. Among a plethora of possibilities and possible strategies; a pathway to a cure, either functional or sterilizing, should be safe, feasible, able to overrule individual variability, effective, durable, and scalable. Those criteria should guide our selection for moving the field forward in clinical settings.

REFERENCES

Abbar, Baptiste, Marine Baron, Christine Katlama, Anne-Geneviève Marcelin, Marianne Veyri, Brigitte Autran, Amélie Guihot, and Jean-Philippe Spano. 2020. "Immune Checkpoint Inhibitors in People Living with HIV: What about Anti-HIV Effects?" *AIDS (London, England)* 34 (2): 167–75. https://doi.org/10.1097/QAD.0000000000002397.

Abner, Erik, and Albert Jordan. 2019. "HIV 'Shock and Kill' Therapy: In Need of Revision." *Antiviral Research* 166: 19–34. https://doi.org/10.1016/j.antiviral.2019.03.008.

Abner, Erik, Mateusz Stoszko, Lei Zeng, Heng-Chang Chen, Andrea Izquierdo-Bouldstridge, Tsuyoshi Konuma, Eduard Zorita, et al. 2018. "A New Quinoline BRD4 Inhibitor Targets a Distinct Latent HIV-1 Reservoir for Reactivation from Other 'Shock' Drugs." *Journal of Virology* 92 (10). https://doi.org/10.1128/JVI.02056-17.

Ait-Ammar, Amina, Anna Kula, Gilles Darcis, Roxane Verdikt, Stephane De Wit, Virginie Gautier, Patrick W. G. Mallon, Alessandro Marcello, Olivier Rohr, and Carine Van Lint. 2020. "Current Status of Latency Reversing Agents Facing the Heterogeneity of HIV-1 Cellular and Tissue Reservoirs." *Frontiers in Microbiology* 10 (January). https://doi.org/10.3389/fmicb.2019.03060.

Andersen, Raymond J., Fidele Ntie-Kang, and Ian Tietjen. 2018. "Natural Product-Derived Compounds in HIV Suppression, Remission, and Eradication Strategies." *Antiviral Research* 158: 63–77. https://doi.org/10.1016/j.antiviral.2018.07.016.

Andersson, B. S., M. Beran, S. Pathak, A. Goodacre, B. Barlogie, and K. B. McCredie. 1987. "Ph-Positive Chronic Myeloid Leukemia with near-Haploid Conversion in Vivo and Establishment of a Continuously Growing Cell Line with Similar Cytogenetic Pattern." *Cancer Genetics and Cytogenetics* 24 (2): 335–43. https://doi.org/10.1016/0165-4608(87)90116-6.

Anthony-Gonda, Kim, Ariola Bardhi, Alex Ray, Nina Flerin, Mengyan Li, Weizao Chen, Christina Ochsenbauer, et al. 2019. "Multispecific Anti-HIV DuoCAR-T Cells Display Broad in Vitro Antiviral Activity and Potent in Vivo Elimination of HIV-Infected Cells in a Humanized Mouse Model." *Science Translational Medicine* 11 (504). https://doi.org/10.1126/scitranslmed.aav5685.

Archin, N. M., A. L. Liberty, A. D. Kashuba, S. K. Choudhary, J. D. Kuruc, A. M. Crooks, D. C. Parker, et al. 2012. "Administration of Vorinostat Disrupts HIV-1 Latency in Patients on Antiretroviral Therapy." *Nature* 487 (7408): 482–85. https://doi.org/10.1038/nature11286.

Archin, Nancie M., Jennifer L. Kirchherr, Julia A. M. Sung, Genevieve Clutton, Katherine Sholtis, Yinyan Xu, Brigitte Allard, et al. 2017. "Interval Dosing with the HDAC Inhibitor Vorinostat Effectively Reverses HIV Latency." *The Journal of Clinical Investigation* 127 (8): 3126–35. https://doi.org/10.1172/JCI92684.

Balakrishnan, Kumudha, and Varsha Gandhi. 2013. "Bcl-2 Antagonists: A Proof of Concept for CLL Therapy." *Investigational New Drugs* 31 (5): 1384–94. https://doi.org/10.1007/s10637-013-0002-4.

Banerjee, Camellia, Nancie Archin, Daniel Michaels, Anna C. Belkina, Gerald V. Denis, James Bradner, Paola Sebastiani, David M. Margolis, and Monty Montano. 2012. "BET Bromodomain Inhibition as a Novel Strategy for Reactivation of

HIV-1." *Journal of Leukocyte Biology* 92 (6): 1147–54. https://doi.org/10.1189/jlb.0312165.

Battivelli, Emilie, Matthew S. Dahabieh, Mohamed Abdel-Mohsen, J. Peter Svensson, Israel Tojal Da Silva, Lillian B. Cohn, Andrea Gramatica, et al. 2018. "Distinct Chromatin Functional States Correlate with HIV Latency Reactivation in Infected Primary CD4+ T Cells." *ELife* 7 (May). https://doi.org/10.7554/eLife.34655.

Bergantz, Louis, Frédéric Subra, Eric Deprez, Olivier Delelis, and Clémence Richetta. 2019. "Interplay between Intrinsic and Innate Immunity during HIV Infection." *Cells* 8 (8). https://doi.org/10.3390/cells8080922.

Bertrand, Mathieu J. M., Snezana Milutinovic, Kathleen M. Dickson, Wai Chi Ho, Alain Boudreault, Jon Durkin, John W. Gillard, James B. Jaquith, Stephen J. Morris, and Philip A. Barker. 2008. "CIAP1 and CIAP2 Facilitate Cancer Cell Survival by Functioning as E3 Ligases That Promote RIP1 Ubiquitination." *Molecular Cell* 30 (6): 689–700. https://doi.org/10.1016/j.molcel.2008.05.014.

Blankson, Joel N. 2010. "Effector Mechanisms in HIV-1 Infected Elite Controllers: Highly Active Immune Responses?" *Antiviral Research* 85 (1): 295–302. https://doi.org/10.1016/j.antiviral.2009.08.007.

Bouchat, Sophie, Nadège Delacourt, Anna Kula, Gilles Darcis, Benoit Van Driessche, Francis Corazza, Jean-Stéphane Gatot, et al. 2016. "Sequential Treatment with 5-aza-2′-deoxycytidine and Deacetylase Inhibitors Reactivates HIV-1." *EMBO Molecular Medicine* 8 (2): 117–38. https://doi.org/10.15252/emmm.201505557.

Bradley, Todd, Guido Ferrari, Barton F. Haynes, David M. Margolis, and Edward P. Browne. 2018. "Single-Cell Analysis of Quiescent HIV Infection Reveals Host Transcriptional Profiles That Regulate Proviral Latency." *Cell Reports* 25 (1): 107-117.e3. https://doi.org/10.1016/j.celrep.2018.09.020.

Branon, Tess C., Justin A. Bosch, Ariana D. Sanchez, Namrata D. Udeshi, Tanya Svinkina, Steven A. Carr, Jessica L. Feldman, Norbert Perrimon, and Alice Y. Ting. 2018. "Efficient Proximity Labeling in Living Cells and Organisms with TurboID." *Nature Biotechnology* 36 (9): 880–87. https://doi.org/10.1038/nbt.4201.

Cadiñanos, Juan, and Allan Bradley. 2007. "Generation of an Inducible and Optimized PiggyBac Transposon System." *Nucleic Acids Research* 35 (12): e87. https://doi.org/10.1093/nar/gkm446.

Cai, Huiming, Ge Liu, Jianfeng Zhong, Kai Zheng, Haitao Xiao, Chenyang Li, Xun Song, et al. 2020. "Immune Checkpoints in Viral Infections." *Viruses* 12 (9). https://doi.org/10.3390/v12091051.

Campbell, Grant R., Rachel S. Bruckman, Shayna D. Herns, Shweta Joshi, Donald L. Durden, and Stephen A. Spector. 2018. "Induction of Autophagy by PI3K/MTOR and PI3K/MTOR/BRD4 Inhibitors Suppresses HIV-1 Replication." *The Journal of Biological Chemistry* 293 (16): 5808–20. https://doi.org/10.1074/jbc.RA118.002353.

Cao, Qingyi, Jian Ma, Chen-Hao Chen, Han Xu, Zhi Chen, Wei Li, and X. Shirley Liu. 2017. "CRISPR-FOCUS: A Web Server for Designing Focused CRISPR Screening Experiments." *PLoS ONE* 12 (9). https://doi.org/10.1371/journal.pone.0184281.

Chen, Heng-Chang, Eduard Zorita, and Guillaume J. Filion. 2018. "Using Barcoded HIV Ensembles (B-HIVE) for Single Provirus Transcriptomics." *Current Protocols in Molecular Biology* 122 (1): e56. https://doi.org/10.1002/cpmb.56.

Chew, Glen M., Tsuyoshi Fujita, Gabriela M. Webb, Benjamin J. Burwitz, Helen L. Wu, Jason S. Reed, Katherine B. Hammond, et al. 2016. "TIGIT Marks Exhausted T Cells, Correlates with Disease Progression, and Serves as a Target for Immune Restoration in HIV and SIV Infection." *PLoS Pathogens* 12 (1): e1005349. https://doi.org/10.1371/journal.ppat.1005349.

Chow, Kwan T., Michael Gale, and Yueh-Ming Loo. 2018. "RIG-I and Other RNA Sensors in Antiviral Immunity." *Annual Review of Immunology* 36 (1): 667–94. https://doi.org/10.1146/annurev-immunol-042617-053309.

Chugh, Pauline, Birgit Bradel-Tretheway, Carlos M. R. Monteiro-Filho, Vicente Planelles, Sanjay B. Maggirwar, Stephen Dewhurst, and Baek Kim. 2008. "Akt Inhibitors as an HIV-1 Infected Macrophage-Specific Anti-Viral Therapy." *Retrovirology* 5 (January): 11. https://doi.org/10.1186/1742-4690-5-11.

Cohn, Lillian B., Nicolas Chomont, and Steven G. Deeks. 2020. "The Biology of the HIV-1 Latent Reservoir and Implications for Cure Strategies." *Cell Host & Microbe* 27 (4): 519–30. https://doi.org/10.1016/j.chom.2020.03.014.

Cummins, Nathan W., and Andrew D. Badley. 2013. "Anti-Apoptotic Mechanisms of HIV: Lessons and Novel Approaches to Curing HIV." *Cellular and Molecular Life Sciences* 70 (18): 3355–63. https://doi.org/10.1007/s00018-012-1239-3.

Cummins, Nathan W., Amy M. Sainski, Haiming Dai, Sekar Natesampillai, Yuan-Ping Pang, Gary D. Bren, Maria Cristina Miranda de Araujo Correia, et al. 2016. "Prime, Shock, and Kill: Priming CD4 T Cells from HIV Patients with a BCL-2 Antagonist before HIV Reactivation Reduces HIV Reservoir Size." *Journal of Virology* 90 (8): 4032–48. https://doi.org/10.1128/JVI.03179-15.

Cummins, Nathan W., Amy M. Sainski-Nguyen, Sekar Natesampillai, Fatma Aboulnasr, Scott Kaufmann, and Andrew D. Badley. 2017. "Maintenance of the HIV Reservoir Is Antagonized by Selective BCL2 Inhibition." *Journal of Virology* 91 (11). https://doi.org/10.1128/JVI.00012-17.

Dar, Roy D., Nina N. Hosmane, Michelle R. Arkin, Robert F. Siliciano, and Leor S. Weinberger. 2014. "Screening for Noise in Gene Expression Identifies Drug Synergies." *Science (New York, N.Y.)* 344 (6190): 1392–96. https://doi.org/10.1126/science.1250220.

Day, Cheryl L., Daniel E. Kaufmann, Photini Kiepiela, Julia A. Brown, Eshia S. Moodley, Sharon Reddy, Elizabeth W. Mackey, et al. 2006. "PD-1 Expression on HIV-Specific T Cells Is Associated with T-Cell Exhaustion and Disease Progression." *Nature* 443 (7109): 350–54. https://doi.org/10.1038/nature05115.

Deeks, Steven G., Bridget Wagner, Peter A. Anton, Ronald T. Mitsuyasu, David T. Scadden, Christine Huang, Catherine Macken, et al. 2002. "A Phase II Randomized Study of HIV-Specific T-Cell Gene Therapy in Subjects with Undetectable Plasma Viremia on Combination Antiretroviral Therapy." *Molecular Therapy: The Journal of the American Society of Gene Therapy* 5 (6): 788–97. https://doi.org/10.1006/mthe.2002.0611.

Deng, Kai, Mihaela Pertea, Anthony Rongvaux, Leyao Wang, Christine M. Durand, Gabriel Ghiaur, Jun Lai, et al. 2015. "Broad CTL Response Is Required to Clear Latent HIV-1 Due to Dominance of Escape Mutations." *Nature* 517 (7534): 381–85. https://doi.org/10.1038/nature14053.

Díaz, Tania, Vanina Rodríguez, Ester Lozano, Mari-Pau Mena, Marcos Calderón, Laura Rosiñol, Antonio Martínez, et al. 2017. "The BET Bromodomain Inhibitor CPI203 Improves Lenalidomide and Dexamethasone Activity in in Vitro and in Vivo Models of Multiple Myeloma by Blockade of Ikaros and MYC Signaling."

Haematologica 102 (10): 1776–84. https://doi.org/10.3324/haematol.2017.164632.

Elliott, Julian H., James H. McMahon, Christina C. Chang, Sulggi A. Lee, Wendy Hartogensis, Namandje Bumpus, Rada Savic, et al. 2015. "Short-Term Administration of Disulfiram for Reversal of Latent HIV Infection: A Phase 2 Dose-Escalation Study." *The Lancet. HIV* 2 (12): e520-529. https://doi.org/10.1016/S2352-3018(15)00226-X.

Elliott, Julian H., Fiona Wightman, Ajantha Solomon, Khader Ghneim, Jeffrey Ahlers, Mark J. Cameron, Miranda Z. Smith, et al. 2014. "Activation of HIV Transcription with Short-Course Vorinostat in HIV-Infected Patients on Suppressive Antiretroviral Therapy." *PLOS Pathogens* 10 (11): e1004473. https://doi.org/10.1371/journal.ppat.1004473.

Evans, Vanessa A., Renée M. van der Sluis, Ajantha Solomon, Ashanti Dantanarayana, Catriona McNeil, Roger Garsia, Sarah Palmer, et al. 2018. "Programmed Cell Death-1 Contributes to the Establishment and Maintenance of HIV-1 Latency." *AIDS (London, England)* 32 (11): 1491–97. https://doi.org/10.1097/QAD.0000000000001849.

Fromentin, Rémi, Wendy Bakeman, Mariam B. Lawani, Gabriela Khoury, Wendy Hartogensis, Sandrina DaFonseca, Marisela Killian, et al. 2016. "CD4+ T Cells Expressing PD-1, TIGIT and LAG-3 Contribute to HIV Persistence during ART." *PLoS Pathogens* 12 (7): e1005761. https://doi.org/10.1371/journal.ppat.1005761.

Fromentin, Rémi, Sandrina DaFonseca, Cecilia T. Costiniuk, Mohamed El-Far, Francesco Andrea Procopio, Frederick M. Hecht, Rebecca Hoh, et al. 2019. "PD-1 Blockade Potentiates HIV Latency Reversal Ex Vivo in CD4+ T Cells from ART-Suppressed Individuals." *Nature Communications* 10 (1): 814. https://doi.org/10.1038/s41467-019-08798-7.

Fuchs, Ota. 2019. "Treatment of Lymphoid and Myeloid Malignancies by Immunomodulatory Drugs." *Cardiovascular & Hematological Disorders Drug Targets* 19 (1): 51–78. https://doi.org/10.2174/1871529X18666180522073855.

Gao, Shaobing, Shichao Wang, and Yongping Song. 2020. "Novel Immunomodulatory Drugs and Neo-Substrates." *Biomarker Research* 8 (1): 2. https://doi.org/10.1186/s40364-020-0182-y.

Gao, Zhonghua, Yuan Tian, Junru Wang, Qian Yin, Hao Wu, Yue-Ming Li, and Xuejun Jiang. 2007. "A Dimeric Smac/Diablo Peptide Directly Relieves Caspase-3 Inhibition by XIAP. Dynamic and Cooperative Regulation of XIAP by Smac/Diablo." *The Journal of Biological Chemistry* 282 (42): 30718–27. https://doi.org/10.1074/jbc.M705258200.

Gauchier, Mathilde, Guido van Mierlo, Michiel Vermeulen, and Jérôme Déjardin. 2020. "Purification and Enrichment of Specific Chromatin Loci." *Nature Methods* 17 (4): 380–89. https://doi.org/10.1038/s41592-020-0765-4.

Gutiérrez, Carolina, Sergio Serrano-Villar, Nadia Madrid-Elena, Maria J. Pérez-Elías, Maria Elena Martín, Coral Barbas, Javier Ruipérez, et al. 2016. "Bryostatin-1 for Latent Virus Reactivation in HIV-Infected Patients on Antiretroviral Therapy." *AIDS (London, England)* 30 (9): 1385–92. https://doi.org/10.1097/QAD.0000000000001064.

Hale, Malika, Taylor Mesojednik, Guillermo S. Romano Ibarra, Jaya Sahni, Alison Bernard, Karen Sommer, Andrew M. Scharenberg, David J. Rawlings, and Thor A. Wagner. 2017. "Engineering HIV-Resistant, Anti-HIV Chimeric Antigen

Receptor T Cells." *Molecular Therapy* 25 (3): 570–79. https://doi.org/10.1016/j.ymthe.2016.12.023.

Hayes, Alexander M.L. 2020. "Future Approaches to Clearing the Latent Human Immunodeficiency Virus Reservoir: Beyond Latency Reversal." *Southern African Journal of HIV Medicine* 21 (1). https://doi.org/10.4102/sajhivmed.v21i1.1089.

Hosmane, Nina N., Kyungyoon J. Kwon, Katherine M. Bruner, Adam A. Capoferri, Subul Beg, Daniel I. S. Rosenbloom, Brandon F. Keele, Ya-Chi Ho, Janet D. Siliciano, and Robert F. Siliciano. 2017. "Proliferation of Latently Infected CD4+ T Cells Carrying Replication-Competent HIV-1: Potential Role in Latent Reservoir Dynamics." *The Journal of Experimental Medicine* 214 (4): 959–72. https://doi.org/10.1084/jem.20170193.

Itchaki, Gilad, and Jennifer R. Brown. 2017. "Lenalidomide in the Treatment of Chronic Lymphocytic Leukemia." *Expert Opinion on Investigational Drugs* 26 (5): 633–50. https://doi.org/10.1080/13543784.2017.1313230.

Iwasaki, Akiko, and Ruslan Medzhitov. 2004. "Toll-like Receptor Control of the Adaptive Immune Responses." *Nature Immunology* 5 (10): 987–95. https://doi.org/10.1038/ni1112.

Jiang, Chenyang, Xiaodong Lian, Ce Gao, Xiaoming Sun, Kevin B. Einkauf, Joshua M. Chevalier, Samantha M. Y. Chen, et al. 2020. "Distinct Viral Reservoirs in Individuals with Spontaneous Control of HIV-1." *Nature* 585 (7824): 261–67. https://doi.org/10.1038/s41586-020-2651-8.

Karn, Jonathan, and C. Martin Stoltzfus. 2012a. "Transcriptional and Posttranscriptional Regulation of HIV-1 Gene Expression." *Cold Spring Harbor Perspectives in Medicine* 2 (2): a006916. https://doi.org/10.1101/cshperspect.a006916.

Kaufmann, Daniel E., Daniel G. Kavanagh, Florencia Pereyra, John J. Zaunders, Elizabeth W. Mackey, Toshiyuki Miura, Sarah Palmer, et al. 2007. "Upregulation of CTLA-4 by HIV-Specific CD4+ T Cells Correlates with Disease Progression and Defines a Reversible Immune Dysfunction." *Nature Immunology* 8 (11): 1246–54. https://doi.org/10.1038/ni1515.

Kawasaki, Takumi, and Taro Kawai. 2014. "Toll-like Receptor Signaling Pathways." *Frontiers in Immunology* 5: 461. https://doi.org/10.3389/fimmu.2014.00461.

Kim, Nayoung, Sami Kukkonen, Sumeet Gupta, and Anna Aldovini. 2010. "Association of Tat with Promoters of PTEN and PP2A Subunits Is Key to Transcriptional Activation of Apoptotic Pathways in HIV-Infected CD4+ T Cells." *PLOS Pathogens* 6 (9): e1001103. https://doi.org/10.1371/journal.ppat.1001103.

Kim, Youry, Jenny L. Anderson, and Sharon R. Lewin. 2018. "Getting the 'Kill' into 'Shock and Kill': Strategies to Eliminate Latent HIV." *Cell Host & Microbe* 23 (1): 14–26. https://doi.org/10.1016/j.chom.2017.12.004.

Kim, Yuri, Joseph A. Hollenbaugh, Dong-Hyun Kim, and Baek Kim. 2011. "Novel PI3K/Akt Inhibitors Screened by the Cytoprotective Function of Human Immunodeficiency Virus Type 1 Tat." *PLOS ONE* 6 (7): e21781. https://doi.org/10.1371/journal.pone.0021781.

Kotecki, M., P. S. Reddy, and B. H. Cochran. 1999. "Isolation and Characterization of a Near-Haploid Human Cell Line." *Experimental Cell Research* 252 (2): 273–80. https://doi.org/10.1006/excr.1999.4656.

Krönke, Jan, Namrata D. Udeshi, Anupama Narla, Peter Grauman, Slater N. Hurst, Marie McConkey, Tanya Svinkina, et al. 2014. "Lenalidomide Causes Selective Degradation of IKZF1 and IKZF3 in Multiple Myeloma Cells." *Science (New York, N.Y.)* 343 (6168): 301–5. https://doi.org/10.1126/science.1244851.

Kumar, Rajesh, Huma Qureshi, Suprit Deshpande, and Jayanta Bhattacharya. 2018. "Broadly Neutralizing Antibodies in HIV-1 Treatment and Prevention." *Therapeutic Advances in Vaccines and Immunotherapy* 6 (4): 61–68. https://doi.org/10.1177/2515135518800689.

Kwong, Peter D., John R. Mascola, and Gary J. Nabel. 2013. "Broadly Neutralizing Antibodies and the Search for an HIV-1 Vaccine: The End of the Beginning." *Nature Reviews. Immunology* 13 (9): 693–701. https://doi.org/10.1038/nri3516.

Lassen, Kara G, Kasra X Ramyar, Justin R Bailey, Yan Zhou, and Robert F Siliciano. 2006. "Nuclear Retention of Multiply Spliced HIV-1 RNA in Resting CD4+ T Cells." *PLoS Pathogens* 2 (7). https://doi.org/10.1371/journal.ppat.0020068.

Leitão, Ana Lúcia, and Francisco J. Enguita. 2014. "Fungal Extrolites as a New Source for Therapeutic Compounds and as Building Blocks for Applications in Synthetic Biology." *Microbiological Research* 169 (9–10): 652–65. https://doi.org/10.1016/j.micres.2014.02.007.

Li, Peilin, Philipp Kaiser, Harry W. Lampiris, Peggy Kim, Steven A. Yukl, Diane V. Havlir, Warner C. Greene, and Joseph K. Wong. 2016. "Stimulating the RIG-I Pathway to Kill Cells in the Latent HIV Reservoir Following Viral Reactivation." *Nature Medicine* 22 (7): 807–11. https://doi.org/10.1038/nm.4124.

Li, Zichong, Jia Guo, Yuntao Wu, and Qiang Zhou. 2013. "The BET Bromodomain Inhibitor JQ1 Activates HIV Latency through Antagonizing Brd4 Inhibition of Tat-Transactivation." *Nucleic Acids Research* 41 (1): 277–87. https://doi.org/10.1093/nar/gks976.

Lim, So-Yon, Christa E. Osuna, Peter T. Hraber, Joe Hesselgesser, Jeffrey M. Gerold, Tiffany L. Barnes, Srisowmya Sanisetty, et al. 2018. "TLR7 Agonists Induce Transient Viremia and Reduce the Viral Reservoir in SIV-Infected Rhesus Macaques on Antiretroviral Therapy." *Science Translational Medicine* 10 (439). https://doi.org/10.1126/scitranslmed.aao4521.

Liu, Xin, Yuannyu Zhang, Yong Chen, Mushan Li, Feng Zhou, Kailong Li, Hui Cao, et al. 2017. "In Situ Capture of Chromatin Interactions by Biotinylated DCas9." *Cell* 170 (5): 1028-1043.e19. https://doi.org/10.1016/j.cell.2017.08.003.

López-Huertas, María Rosa, Elena Mateos, María Sánchez Del Cojo, Francisco Gómez-Esquer, Gema Díaz-Gil, Sara Rodríguez-Mora, Juan Antonio López, et al. 2013. "The Presence of HIV-1 Tat Protein Second Exon Delays Fas Protein-Mediated Apoptosis in CD4+ T Lymphocytes: A Potential Mechanism for Persistent Viral Production." *The Journal of Biological Chemistry* 288 (11): 7626–44. https://doi.org/10.1074/jbc.M112.408294.

Lu, Gang, Richard E. Middleton, Huahang Sun, MarkVic Naniong, Christopher J. Ott, Constantine S. Mitsiades, Kwok-Kin Wong, James E. Bradner, and William G. Kaelin. 2014. "The Myeloma Drug Lenalidomide Promotes the Cereblon-Dependent Destruction of Ikaros Proteins." *Science (New York, N.Y.)* 343 (6168): 305–9. https://doi.org/10.1126/science.1244917.

Lu, Panpan, Xiying Qu, Yinzhong Shen, Zhengtao Jiang, Pengfei Wang, Hanxian Zeng, Haiyan Ji, et al. 2016. "The BET Inhibitor OTX015 Reactivates Latent HIV-1 through P-TEFb." *Scientific Reports* 6 (April). https://doi.org/10.1038/srep24100.

Lucas, Amanda, Yuri Kim, Omayra Rivera-Pabon, Sunju Chae, Dong-Hyun Kim, and Baek Kim. 2010. "Targeting the PI3K/Akt Cell Survival Pathway to Induce Cell Death of HIV-1 Infected Macrophages with Alkylphospholipid Compounds." *PLoS ONE* 5 (9). https://doi.org/10.1371/journal.pone.0013121.

Macedo, Amanda B., Camille L. Novis, and Alberto Bosque. 2019. “Targeting Cellular and Tissue HIV Reservoirs With Toll-Like Receptor Agonists.” *Frontiers in Immunology* 10 (October). https://doi.org/10.3389/fimmu.2019.02450.

Margolis, David M. 2011. “Histone Deacetylase Inhibitors and HIV Latency.” *Current Opinion in HIV and AIDS* 6 (1): 25–29. https://doi.org/10.1097/COH.0b013e328341242d.

Marian, Christine A., Mateusz Stoszko, Lili Wang, Matthew W. Leighty, Elisa de Crignis, Chad A. Maschinot, Jovylyn Gatchalian, et al. 2018. “Small Molecule Targeting of Specific BAF (MSWI/SNF) Complexes for HIV Latency Reversal.” *Cell Chemical Biology* 25 (12): 1443-1455.e14. https://doi.org/10.1016/j.chembiol.2018.08.004.

Martinsen, Janne Tegder, Jesper Damsgaard Gunst, Jesper Falkesgaard Højen, Martin Tolstrup, and Ole Schmeltz Søgaard. 2020. “The Use of Toll-Like Receptor Agonists in HIV-1 Cure Strategies.” *Frontiers in Immunology* 11 (June). https://doi.org/10.3389/fimmu.2020.01112.

McGary, Colleen S., Claire Deleage, Justin Harper, Luca Micci, Susan P. Ribeiro, Sara Paganini, Leticia Kuri-Cervantes, et al. 2017. “CTLA-4+PD-1- Memory CD4+ T Cells Critically Contribute to Viral Persistence in Antiretroviral Therapy-Suppressed, SIV-Infected Rhesus Macaques.” *Immunity* 47 (4): 776-788.e5. https://doi.org/10.1016/j.immuni.2017.09.018.

Mogensen, Trine H. 2009. “Pathogen Recognition and Inflammatory Signaling in Innate Immune Defenses.” *Clinical Microbiology Reviews* 22 (2): 240–73, Table of Contents. https://doi.org/10.1128/CMR.00046-08.

Moros, A., V. Rodríguez, I. Saborit-Villarroya, A. Montraveta, P. Balsas, P. Sandy, A. Martínez, et al. 2014. “Synergistic Antitumor Activity of Lenalidomide with the BET Bromodomain Inhibitor CPI203 in Bortezomib-Resistant Mantle Cell Lymphoma.” *Leukemia* 28 (10): 2049–59. https://doi.org/10.1038/leu.2014.106.

Mothe, Beatriz, Anuska Llano, Javier Ibarrondo, Jennifer Zamarreño, Mattia Schiaulini, Cristina Miranda, Marta Ruiz-Riol, et al. 2012. “CTL Responses of High Functional Avidity and Broad Variant Cross-Reactivity Are Associated with HIV Control.” *PloS One* 7 (1): e29717. https://doi.org/10.1371/journal.pone.0029717.

Newman, David J., and Gordon M. Cragg. 2016. “Natural Products as Sources of New Drugs from 1981 to 2014.” *Journal of Natural Products* 79 (3): 629–61. https://doi.org/10.1021/acs.jnatprod.5b01055.

Pace, Matthew J., Erin H. Graf, Luis M. Agosto, Angela M. Mexas, Frances Male, Troy Brady, Frederic D. Bushman, and Una O’Doherty. 2012. “Directly Infected Resting CD4+T Cells Can Produce HIV Gag without Spreading Infection in a Model of HIV Latency.” *PLoS Pathogens* 8 (7). https://doi.org/10.1371/journal.ppat.1002818.

Pace, Matthew, James Williams, Ayako Kurioka, Andrew B. Gerry, Bent Jakobsen, Paul Klenerman, Nneka Nwokolo, Julie Fox, Sarah Fidler, and John Frater. 2016. “Histone Deacetylase Inhibitors Enhance CD4 T Cell Susceptibility to NK Cell Killing but Reduce NK Cell Function.” *PLoS Pathogens* 12 (8). https://doi.org/10.1371/journal.ppat.1005782.

Pache, Lars, Miriam S. Dutra, Adam M. Spivak, John M. Marlett, Jeffrey P. Murry, Young Hwang, Ana M. Maestre, et al. 2015. “BIRC2/CIAP1 Is a Negative Regulator of HIV-1 Transcription and Can Be Targeted by Smac Mimetics to Promote Reversal of Viral Latency.” *Cell Host & Microbe* 18 (3): 345–53. https://doi.org/10.1016/j.chom.2015.08.009.

Pache, Lars, Matthew D. Marsden, Peter Teriete, Alex J. Portillo, Dominik Heimann, Jocelyn T. Kim, Mohamed S. A. Soliman, et al. 2020. “Pharmacological Activation of Non-Canonical NF-KB Signaling Activates Latent HIV-1 Reservoirs In Vivo.” *Cell Reports Medicine* 1 (3): 100037. https://doi.org/10.1016/j.xcrm.2020.100037.

Pappireddi, Nishant, Lance Martin, and Martin Wühr. 2019. “A Review on Quantitative Multiplexed Proteomics.” *Chembiochem: A European Journal of Chemical Biology* 20 (10): 1210–24. https://doi.org/10.1002/cbic.201800650.

Parry, Richard V., Jens M. Chemnitz, Kenneth A. Frauwirth, Anthony R. Lanfranco, Inbal Braunstein, Sumire V. Kobayashi, Peter S. Linsley, Craig B. Thompson, and James L. Riley. 2005. “CTLA-4 and PD-1 Receptors Inhibit T-Cell Activation by Distinct Mechanisms.” *Molecular and Cellular Biology* 25 (21): 9543–53. https://doi.org/10.1128/MCB.25.21.9543-9553.2005.

Peppa, Dimitra. 2019. “Entering a New Era of Harnessing Natural Killer Cell Responses in HIV Infection.” *EBioMedicine* 44 (June): 26–27. https://doi.org/10.1016/j.ebiom.2019.05.045.

Rasmussen, Thomas A., and Sharon R. Lewin. 2016. “Shocking HIV out of Hiding: Where Are We with Clinical Trials of Latency Reversing Agents?” *Current Opinion in HIV and AIDS* 11 (4): 394–401. https://doi.org/10.1097/COH.0000000000000279.

Rasmussen, Thomas A., Martin Tolstrup, Christel R. Brinkmann, Rikke Olesen, Christian Erikstrup, Ajantha Solomon, Anni Winckelmann, et al. 2014. “Panobinostat, a Histone Deacetylase Inhibitor, for Latent-Virus Reactivation in HIV-Infected Patients on Suppressive Antiretroviral Therapy: A Phase 1/2, Single Group, Clinical Trial.” *The Lancet. HIV* 1 (1): e13-21. https://doi.org/10.1016/S2352-3018(14)70014-1.

Rato, Sylvie, Antonio Rausell, Miguel Muñoz, Amalio Telenti, and Angela Ciuffi. 2017. “Single-Cell Analysis Identifies Cellular Markers of the HIV Permissive Cell.” *PLoS Pathogens* 13 (10). https://doi.org/10.1371/journal.ppat.1006678.

Reeves, Daniel B., Elizabeth R. Duke, Thor A. Wagner, Sarah E. Palmer, Adam M. Spivak, and Joshua T. Schiffer. 2018. “A Majority of HIV Persistence during Antiretroviral Therapy Is Due to Infected Cell Proliferation.” *Nature Communications* 9 (1): 4811. https://doi.org/10.1038/s41467-018-06843-5.

Rodrik-Outmezguine, Vanessa S., Sarat Chandarlapaty, Nen C. Pagano, Poulikos I. Poulikakos, Maurizio Scaltriti, Elizabeth Moskatel, José Baselga, Sylvie Guichard, and Neal Rosen. 2011. “MTOR Kinase Inhibition Causes Feedback-Dependent Biphasic Regulation of AKT Signaling.” *Cancer Discovery* 1 (3): 248–59. https://doi.org/10.1158/2159-8290.CD-11-0085.

Rojas-Araya, Bárbara, Théophile Ohlmann, and Ricardo Soto-Rifo. 2015. “Translational Control of the HIV Unspliced Genomic RNA.” *Viruses* 7 (8): 4326–51. https://doi.org/10.3390/v7082822.

Sanchez, James F., Amber D. Somoza, Nancy P. Keller, and Clay C. C. Wang. 2012. “Advances in Aspergillus Secondary Metabolite Research in the Post-Genomic Era.” *Natural Product Reports* 29 (3): 351–71. https://doi.org/10.1039/c2np00084a.

Scholler, John, Troy L. Brady, Gwendolyn Binder-Scholl, Wei-Ting Hwang, Gabriela Plesa, Kristen M. Hege, Ashley N. Vogel, et al. 2012. “Decade-Long Safety and Function of Retroviral-Modified Chimeric Antigen Receptor T-Cells.” *Science Translational Medicine* 4 (132): 132ra53. https://doi.org/10.1126/scitranslmed.3003761.

Searle, Brian C., Lindsay K. Pino, Jarrett D. Egertson, Ying S. Ting, Robert T. Lawrence, Brendan X. MacLean, Judit Villén, and Michael J. MacCoss. 2018. "Chromatogram Libraries Improve Peptide Detection and Quantification by Data Independent Acquisition Mass Spectrometry." *Nature Communications* 9 (1): 5128. https://doi.org/10.1038/s41467-018-07454-w.

Siliciano, Janet M., and Robert F. Siliciano. 2015. "The Remarkable Stability of the Latent Reservoir for HIV-1 in Resting Memory CD4+ T Cells." *The Journal of Infectious Diseases* 212 (9): 1345–47. https://doi.org/10.1093/infdis/jiv219.

Stahl, Maximilian, and Amer M. Zeidan. 2017. "Lenalidomide Use in Myelodysplastic Syndromes: Insights into the Biologic Mechanisms and Clinical Applications." *Cancer* 123 (10): 1703–13. https://doi.org/10.1002/cncr.30585.

Stephenson, Kathryn E. 2018. "Therapeutic Vaccination for HIV: Hopes and Challenges." *Current Opinion in HIV and AIDS* 13 (5): 408–15. https://doi.org/10.1097/COH.0000000000000491.

Stoszko, Mateusz, Elisa De Crignis, Casper Rokx, Mir Mubashir Khalid, Cynthia Lungu, Robert-Jan Palstra, Tsung Wai Kan, et al. 2016. "Small Molecule Inhibitors of BAF; A Promising Family of Compounds in HIV-1 Latency Reversal." *EBioMedicine* 3 (January): 108–21. https://doi.org/10.1016/j.ebiom.2015.11.047.

Stoszko, Mateusz, Enrico Ne, Erik Abner, and Tokameh Mahmoudi. 2019. "A Broad Drug Arsenal to Attack a Strenuous Latent HIV Reservoir." *Current Opinion in Virology* 38: 37–53. https://doi.org/10.1016/j.coviro.2019.06.001.

Tebas, Pablo, David Stein, Winson W. Tang, Ian Frank, Shelley Q. Wang, Gary Lee, S. Kaye Spratt, et al. 2014. "Gene Editing of CCR5 in Autologous CD4 T Cells of Persons Infected with HIV." *The New England Journal of Medicine* 370 (10): 901–10. https://doi.org/10.1056/NEJMoa1300662.

Telwatte, Sushama, Sulggi Lee, Ma Somsouk, Hiroyu Hatano, Christopher Baker, Philipp Kaiser, Peggy Kim, et al. 2018. "Gut and Blood Differ in Constitutive Blocks to HIV Transcription, Suggesting Tissue-Specific Differences in the Mechanisms That Govern HIV Latency." *PLOS Pathogens* 14 (11): e1007357. https://doi.org/10.1371/journal.ppat.1007357.

Thorlund, Kristian, Marc S. Horwitz, Brian T. Fife, Richard Lester, and D. William Cameron. 2017. "Landscape Review of Current HIV 'Kick and Kill' Cure Research - Some Kicking, Not Enough Killing." *BMC Infectious Diseases* 17 (1): 595. https://doi.org/10.1186/s12879-017-2683-3.

Timilsina, Uddhav, Dibya Ghimire, Bivek Timalsina, Theodore J. Nitz, Carl T. Wild, Eric O. Freed, and Ritu Gaur. 2016. "Identification of Potent Maturation Inhibitors against HIV-1 Clade C." *Scientific Reports* 6 (June). https://doi.org/10.1038/srep27403.

Trautmann, Lydie, Loury Janbazian, Nicolas Chomont, Elias A. Said, Sylvain Gimmig, Benoit Bessette, Mohamed-Rachid Boulassel, et al. 2006. "Upregulation of PD-1 Expression on HIV-Specific CD8+ T Cells Leads to Reversible Immune Dysfunction." *Nature Medicine* 12 (10): 1198–1202. https://doi.org/10.1038/nm1482.

Venable, John D., Meng-Qiu Dong, James Wohlschlegel, Andrew Dillin, and John R. Yates. 2004. "Automated Approach for Quantitative Analysis of Complex Peptide Mixtures from Tandem Mass Spectra." *Nature Methods* 1 (1): 39–45. https://doi.org/10.1038/nmeth705.

Vermeulen, Michiel, and Jérôme Déjardin. 2020. “Locus-Specific Chromatin Isolation.” *Nature Reviews. Molecular Cell Biology* 21 (5): 249–50. https://doi.org/10.1038/s41580-020-0217-0.

Vibholm, Line, Mariane H. Schleimann, Jesper F. Højen, Thomas Benfield, Rasmus Offersen, Katrine Rasmussen, Rikke Olesen, et al. 2017. “Short-Course Toll-Like Receptor 9 Agonist Treatment Impacts Innate Immunity and Plasma Viremia in Individuals With Human Immunodeficiency Virus Infection.” *Clinical Infectious Diseases: An Official Publication of the Infectious Diseases Society of America* 64 (12): 1686–95. https://doi.org/10.1093/cid/cix201.

Xu, Lei, Jun Wang, Yulin Liu, Liangfu Xie, Bin Su, Danlei Mou, Longteng Wang, et al. 2019. “CRISPR-Edited Stem Cells in a Patient with HIV and Acute Lymphocytic Leukemia.” *The New England Journal of Medicine* 381 (13): 1240–47. https://doi.org/10.1056/NEJMoa1817426.

Yukl, Steven A., Philipp Kaiser, Peggy Kim, Sushama Telwatte, Sunil K. Joshi, Mai Vu, Harry Lampiris, and Joseph K. Wong. 2018. “HIV Latency in Isolated Patient CD4+ T Cells May Be Due to Blocks in HIV Transcriptional Elongation, Completion, and Splicing.” *Science Translational Medicine* 10 (430). https://doi.org/10.1126/scitranslmed.aap9927.

Zaikos, Thomas D., Valeri H. Terry, Nadia T. Sebastian Kettinger, Jay Lubow, Mark M. Painter, Maria C. Virgilio, Andrew Neevel, et al. 2018. “Hematopoietic Stem and Progenitor Cells Are a Distinct HIV Reservoir That Contributes to Persistent Viremia in Suppressed Patients.” *Cell Reports* 25 (13): 3759-3773.e9. https://doi.org/10.1016/j.celrep.2018.11.104.

Zerbato, Jennifer M., Harrison V. Purves, Sharon R. Lewin, and Thomas A. Rasmussen. 2019. “Between a Shock and a Hard Place: Challenges and Developments in HIV Latency Reversal.” *Current Opinion in Virology* 38: 1–9. https://doi.org/10.1016/j.coviro.2019.03.004.

Zhu, Shiyou, Zhongzheng Cao, Zhiheng Liu, Yuan He, Yinan Wang, Pengfei Yuan, Wei Li, Feng Tian, Ying Bao, and Wensheng Wei. 2019. “Guide RNAs with Embedded Barcodes Boost CRISPR-Pooled Screens.” *Genome Biology* 20 (1): 20. https://doi.org/10.1186/s13059-019-1628-0.

Zhu, Shiyou, Wei Li, Jingze Liu, Chen-Hao Chen, Qi Liao, Ping Xu, Han Xu, et al. 2016. “Genome-Scale Deletion Screening of Human Long Non-Coding RNAs Using a Paired-Guide RNA CRISPR–Cas9 Library.” *Nature Biotechnology* 34 (12): 1279–86. https://doi.org/10.1038/nbt.3715.

APPENDIX

Summary

Samenvatting

Resume

PhD Portfolio

Acknowledgments

SUMMARY

Since the discovery of HIV-1 as the causative agent of acquired immunodeficiency syndrome (AIDS), in 1983/1984, significant advances have been made in understanding the molecular pathogenesis of the infection. While the virus constantly mutating nature has made it impossible to develop an effective vaccine, the development of highly effective antiviral drugs and the advent of combination antiretroviral therapy (cART) has allowed the reduction of AIDS-associated mortality and prevented transmission to uninfected individuals. Despite these successes, the quest for an HIV-1 cure remains a global priority as cART is not curative, has side effects, and must be taken lifelong. Additionally, the global roll-out of cART, particularly in resource-limited countries, remains an ongoing challenge.

HIV-1 persists because, following infection, the provirus can establish latent infection in resting CD4+ T cells and other long-lived immune cell populations. Due to this reservoir of long-lived latently HIV-1 infected cells, interruption of cART leads to a rapid rebound of unrestricted viral replication, necessitating life-long treatment. Therapeutic strategies for HIV-1 cure aim to eliminate, inactivate, or reduce the pool of latently infected cells such that the patient's immune system can control viral replication upon cessation of cART. A popular strategy is to induce viral production in latently infected cells, using drug interventions referred to as latency reversal agents (LRAs), to render the infected cell recognizable to the immune system or susceptible to viral cytopathic effects for elimination.

In this thesis, we developed three different and complementary discovery tools that have led to the identification of novel molecular targets, critical for HIV-1 latency and novel small molecule latency reversal agents (LRAs) that can be exploited for therapeutic interventions aiming at reversing latency. This work further expands the known repertoire of factors and cellular pathways that determine viral latency (described in the general introduction: **Chapter 1**) and contributes to a better understanding of the mechanisms and routes that can be targeted by latency reversal strategies.

In **Chapter 2** (Ne et al. 2021) of this thesis we designed a locus-specific proteomic strategy to identify, in an unbiased way, host proteins physically associated with the latent and active, integrated proviral promoter. We made use of a nuclease deficient Cas9 bait tagged by multiple epitopes (HA-V5-FLAG-dCas9) to purify the region of interest and introduced a histone enrichment step in the purification pipeline to enrich for the chromatin-bound fraction of the dCas9 associated complexes. Importantly, this work resulted in the establishment of a locus specific proteomic purification pipeline that we named "dCas9 targeted chromatin and histone enrichment for mass spectrometry'' (Catchet-MS), which can be of great interest in the field of chromatin regulation.

Catchet-MS resulted in the identification of multiple novel (and several previously characterized) host factors, physically associated with the latent and active HIV-1 promoter and represent an invaluable resource of putative regulators of its activity. We found that IKZF1 is a novel HIV-1 5'LTR bound transcriptional repressor, required for the recruitment of the Polycomb repressive complex 2 (PRC2) to the region and for the establishment of a repressive chromatin environment characterized by the H3K27me3 mark. Of therapeutic interest, we also show that the clinically advanced thalidomide derived drug iberdomide, which targets IKZF1 for degradation, reverses latency in ex vivo HIV-1 infected primary CD4+ T cells and results in significantly increased levels of cell-associated HIV-1 Gag RNA in cells isolated from cART suppressed, HIV-1 infected participants.

In **Chapter 3** (Roling et al. 2021) we presented an alternative and unique approach by which, using a two-color insertional mutagenesis screening in pseudo-haploid KBM7 cells, we were able to identify previously unknown genes whose disruption leads to upregulation of HIV-1 expression. Here, as a cellular platform for the screening, we generated a latently infected KBM7 cell line (Hap-Lat) harboring an integrated transcriptionally silent HIV-1 5'LTR that controls expression of a GFP reporter gene. Hap-Lat cells were then subjected to gene trap (GT) insertional mutagenesis using an mCherry reporter GT virus. Upon mutagenesis, Hap-Lat cells expressing GFP as a reporter of HIV-1 reactivation, and mCherry, confirming the presence of a GT virus, were

selected by multiple rounds of fluorescence activated cell sorting (FACS) and subjected to NGS mapping of the integration sites.

Using this methodology, we have identified a list of 69 candidate genes, of which, we could confirm 10 to be required for HIV latency in different cellular models of latency, thus representing an important resource for future studies. Importantly, for 3 of the novel candidates identified we tested different small molecule inhibitors of which, the glutamate ionotropic receptor kainate type subunit 5 (GRIK5) inhibitor, Topiramate, was found to have potential clinical relevance. Among the factors identified we also identified CHD9 to be a 5'LTR bound chromatin associated factor that is removed upon viral reactivation in cellular models of latency.

In **Chapter 4,** without any a priori knowledge of the targeted molecular effector, we screened a library of growth supernatants from selected fungal species in search of novel compounds capable of reversing HIV-1 latency. Here as a cellular platform for the screening we used latently HIV-1 infected J-Lat 11.1 and A2 cells harboring GFP as a reporter for LTR activity. We identified the supernatant from the species Aspergillus Fumigatus to display latency reversal activity. Coupling our bioassay to orthogonal mass spectrometry (MS) and fractionation of the Aspergillus Fumigatus growth supernatant, we identified Gliotoxin (GTX), as a novel candidate LRA. Experiments on primary cells subsequently confirmed that GTX is a novel LRA capable of inducing HIV-1 activation in ex vivo infected CD4+ T cells and cells isolated from cART suppressed HIV-1 infected participants, with limited toxicity. We then used transcriptome analysis, biochemical assays and molecular modelling to unravel the molecular mechanism of GTX mediated HIV-1 induction.

Our data suggest that GTX targets the LARP7 component of the 7SK snRNP complex, which sequesters P-TEFb and disrupts it, causing release of P-TEFb. This results in enhanced availability of the free or active P-TEFb fraction, which then is recruited by the Tat-TAR axis to phosphorylate RNA pol II in its C-terminal domain, hence stabilizing transcriptional elongation and increasing the rate of productive HIV-1 transcription.

In **Chapter 5**, we present the state-of-the-art therapeutic interventions available to attack, mobilize and even permanently silence a reservoir of HIV-1 latently infected cells which has proven to be strenuous and very persistent in infected individuals. The novel drug interventions examined in this thesis may extend this list further. Importantly, this review also offers new perspectives into HIV-1 cure strategies.

In the general discussion of the thesis (**Chapter 6**) we cover the strengths and limitations of the research tools used and offer potential improvements. We then review our findings and put them in a broader context, examining the implications and future directions in the development of unbiased screens for the identification of molecular targets and putative latency reversal agents. Lastly, we thoroughly discuss the limitations of the latency reversal strategy followed by elimination of the latent HIV-1 reservoir, propose a revision to this strategy, and discuss the opportunities for development of combinatory interventions towards an HIV-1 cure.

SAMENVATTING

Sinds de ontdekking van HIV-1 als de veroorzaker van het verworven immunodeficiëntiesyndroom (AIDS), in 1983/1984, is er aanzienlijke vooruitgang geboekt bij het begrijpen van de moleculaire pathogenese van de infectie. Hoewel het virus dat voortdurend muteert het onmogelijk heeft gemaakt om een effectief vaccin te ontwikkelen, heeft de ontwikkeling van zeer effectieve antivirale geneesmiddelen en de komst van antiretrovirale combinatietherapie (cART) de aan aids gerelateerde mortaliteit verminderd en de overdracht naar niet-geïnfecteerde personen voorkomen. Ondanks deze successen blijft de zoektocht naar een HIV-1 remedie een wereldwijde prioriteit, aangezien cART niet genezend is, bijwerkingen heeft en levenslang moet worden ingenomen. Bovendien blijft de wereldwijde uitrol van cART, met name in landen met beperkte middelen, een voortdurende uitdaging.

HIV-1 blijft aanwezig omdat het provirus na de infectie een latente infectie kan veroorzaken in rustende CD4+ T-cellen en andere langlevende immuun cellen. Vanwege dit reservoir van langlevende, latente met HIV-1 geïnfecteerde cellen, leidt onderbreking van cART tot een snelle opleving van ongeremde virale replicatie, wat een levenslange behandeling noodzakelijk maakt. Therapeutische strategieën voor de genezing van HIV-1 zijn gericht op het elimineren, inactiveren of verminderen van de poel van latent geïnfecteerde cellen, zodat het immuunsysteem van de patiënt na stopzetting van cART de virale replicatie kan controleren. Een populaire strategie is om virale productie in latent geïnfecteerde cellen te induceren, met behulp van medicamenteuze interventies die latentie omkeer middelen (LRA's) worden genoemd, zodat de geïnfecteerde cel herkenbaar wordt voor het immuunsysteem of vatbaar wordt voor virale cytopathische effecten wat resulteert in eliminatie.

In dit proefschrift hebben we drie verschillende en complementaire onderzoeksmethoden ontwikkeld die hebben geleid tot de identificatie van nieuwe moleculaire doelwitten die cruciaal zijn voor de latentie van HIV-1, en nieuwe kleine moleculen (LRA's) die kunnen worden benut voor therapeutische interventies gericht op het omkeren van latentie. Dit werk breidt het bekende repertoire van factoren en cellulaire routes die virale latentie bepalen verder uit (beschreven in de algemene inleiding:

Hoofdstuk 1), wat bijdraagt aan een beter begrip van de mechanismen en signaleringsroutes waarop latentie-omkeerstrategieën gericht kunnen zijn.

In **Hoofdstuk 2** (Ne et al. 2021) van dit proefschrift hebben we een locus-specifieke proteomische strategie ontworpen om op een onbevooroordeelde manier gastheereiwitten te identificeren die fysiek geassocieerd zijn met de latente of actieve, geïntegreerde provirale promotor. We maakten gebruik van een nuclease-deficiënte en met meerdere epitopen gelabeld Cas9 (HA-V5-FLAG-dCas9) om het gebied van interesse te zuiveren en introduceerden een extra histon-verrijkingsstap in de zuiveringspijplijn om te verrijken voor de chromatine-gebonden fractie van de dCas9-geassocieerde complexen. Belangrijk is dat dit werk resulteerde in het opzetten van een locus-specifieke proteomische zuiveringspijplijn die we 'dCas9 gerichte chromatine- en histon verrijking voor massaspectrometrie' noemden (Catchet-MS), welke van grootte interesse kan zijn voor het chromatine-regulering vakgebied.

Catchet-MS resulteerde in de identificatie van meerdere nieuwe (en verschillende eerder gekarakteriseerde) gastheerfactoren, welke fysiek geassocieerd zijn met de latente of actieve HIV-1-promotor en vormen een onschatbare bron van potentiele regulatoren van zijn activiteit. We ontdekten dat IKZF1 een nieuwe HIV-1 5'LTR-gebonden transcriptionele repressor is, vereist voor de rekrutering van het Polycomb-repressieve complex 2 (PRC2) naar de regio en voor de totstandbrenging van een repressieve chromatine-omgeving die wordt gekenmerkt door de H3K27me3 modificatie. Van therapeutisch belang is dat we ook aantonen dat het van thalidomide afgeleide medicijn iberdomide, dat in ontwikkeling is voor klinisch gebruik, zorgt voor afbraak van IKZF1 en de latentie in ex vivo met HIV-1 geïnfecteerde primaire CD4 + T-cellen omkeert en in cellen geïsoleerd uit cART-onderdrukte, met HIV-1 geïnfecteerde deelnemers, resulteert in significant verhoogde niveaus van cel-geassocieerd HIV-1 Gag RNA.

In **Hoofdstuk 3** (Roling et al. 2021) presenteren we een alternatieve en unieke benadering waarmee we, met behulp van een tweekleurige insertie-mutagenesescreening in pseudo-haploïde KBM7-cellen, voorheen onbekende genen konden identificeren waarvan de verstoring leidt tot op-regulatie van HIV-1 expressie. Wij hebben als cellulair platform voor de screening een latent geïnfecteerde KBM7-cellijn (Hap-Lat) gegenereerd

dat een geïntegreerd transcriptioneel inactieve HIV-1 5'LTR bevat die de expressie van een GFP-reporter gen regelt. Hap-Lat-cellen werden vervolgens onderworpen aan gene trap (GT) insertiemutagenese met behulp van een mCherry reporter GT-virus. Na mutagenese werden Hap-Lat-cellen die als een reporter van HIV-1-reactivering GFP tot expressie brengen, en mCherry, die de aanwezigheid van een GT-virus bevestigt, vervolgens geselecteerd door middel van meerdere ronden van fluorescentie-geactiveerde cel sortering (FACS) waarna vervolgens de integratie plekken in kaart worden gebracht door middel van NGS.

Met behulp van deze methodologie hebben we een lijst van 69 kandidaat-genen geïdentificeerd, waarvan we van 10 in verschillende cellulaire latentiemodellen hebben bevestigd dat die nodig zijn voor HIV-latentie en die vormen daarom een belangrijke uitgangspunt voor toekomstige studies. Belangrijk is dat we voor 3 van de geïdentificeerde nieuwe kandidaten verschillende moleculaire remmers hebben getest, waarvan de glutamaationotrope receptorkainaat-type subeenheid 5 (GRIK5) -remmer, Topiramaat, potentiële klinische relevantie bleek te hebben. Onder de geïdentificeerde factoren bevind zich ook CHD9, een in latente cellen 5'LTR-gebonden chromatine-geassocieerde factor maar die niet meer bindt na virale reactivering in cellulaire latentiemodellen.

In **Hoofdstuk 4** hebben we, zonder enige a priori kennis van de beoogde moleculaire effector, een verzameling supernatanten van geselecteerde schimmelsoorten gescreend als manier om nieuwe verbindingen te identificeren die de latentie van HIV-1 kunnen omkeren. Als een cellulair platform voor de screening gebruikten we latent met HIV-1 geïnfecteerde J-Lat 11.1- en A2-cellen die GFP herbergen als een reporter voor LTR-activiteit. We identificeerden het supernatant van de soort Aspergillus Fumigatus als latentie-omkeeractiviteit vertonend. Door onze bio assay te koppelen aan orthogonale massaspectrometrie (MS) en fractionering van het Aspergillus Fumigatus-supernatant, identificeerden we Gliotoxine (GTX) als een nieuwe kandidaat-LRA. Experimenten met primaire cellen bevestigden vervolgens dat GTX een nieuwe LRA is die in staat is om HIV-1-activering te induceren in ex vivo geïnfecteerde CD4+ T-cellen en cellen geïsoleerd uit cART-onderdrukte HIV-1-geïnfecteerde deelnemers, terwijl het beperkte toxiciteit vertoond. Vervolgens hebben we transcriptoom analyse, biochemische assays en moleculaire modellering gebruikt om het moleculaire mechanisme van GTX-gemedieerde HIV-1-inductie te ontrafelen.

Onze gegevens suggereren dat GTX zich richt op de LARP7-component van het 7SK snRNP-complex, dat P-TEFb rekruteert en dit proces verstoort, waardoor P-TEFb vrijkomt. Dit resulteert in een verbeterde beschikbaarheid van de vrije of actieve P-TEFb-fractie, die vervolgens wordt gerekruteerd door de Tat-TAR-as om RNA pol II in zijn C-terminale domein te fosforyleren, waardoor transcriptionele extensie wordt gestabiliseerd en de snelheid van productieve HIV-1 transcriptie wordt verhoogd.

In **Hoofdstuk 5** presenteren we de state-of-the-art therapeutische interventies die beschikbaar zijn om een reservoir van latente HIV-1 geïnfecteerde cellen aan te vallen, te mobiliseren en zelfs permanent tot zwijgen te brengen, waarvan bewezen is dat het zeer persistent is bij geïnfecteerde individuen. De nieuwe medicamenteuze interventies die in dit proefschrift worden onderzocht, kunnen deze lijst verder uitbreiden. Belangrijk is dat dit overzicht ook nieuwe perspectieven biedt op de behandelingsstrategieën voor HIV-1.

In de algemene discussie van het proefschrift (**Hoofdstuk 6**) behandelen we de sterke punten en beperkingen van de gebruikte onderzoeksinstrumenten en bieden we suggesties voor mogelijke verbeteringen. Vervolgens bekijken we onze bevindingen en plaatsen ze in een bredere context, waarbij we de implicaties en toekomstige richtlijnen onderzoeken met betrekking tot de ontwikkeling van onbevooroordeelde screeningsmethoden voor de identificatie van moleculaire doelwitten en mogelijke latentie omkeermiddelen. Ten slotte bespreken we grondig de beperkingen van de latentie-omkering strategie gevolgd door eliminatie van het latente HIV-1-reservoir, stellen we een herziening van deze strategie voor en bespreken we de mogelijkheden voor de ontwikkeling van gecombineerde interventies voor HIV-1-genezing.